Tecnología de biorreactores de membrana como tratamiento terciario de aguas residuales domésticas

Autor:
Oliver Díaz López

Directores:
Luisa María Vera Peña
Juan Manuel Rodríguez Sevilla

Universidad de La Laguna
Departamento de Ingeniería Química
y Tecnología Farmacéutica

2016

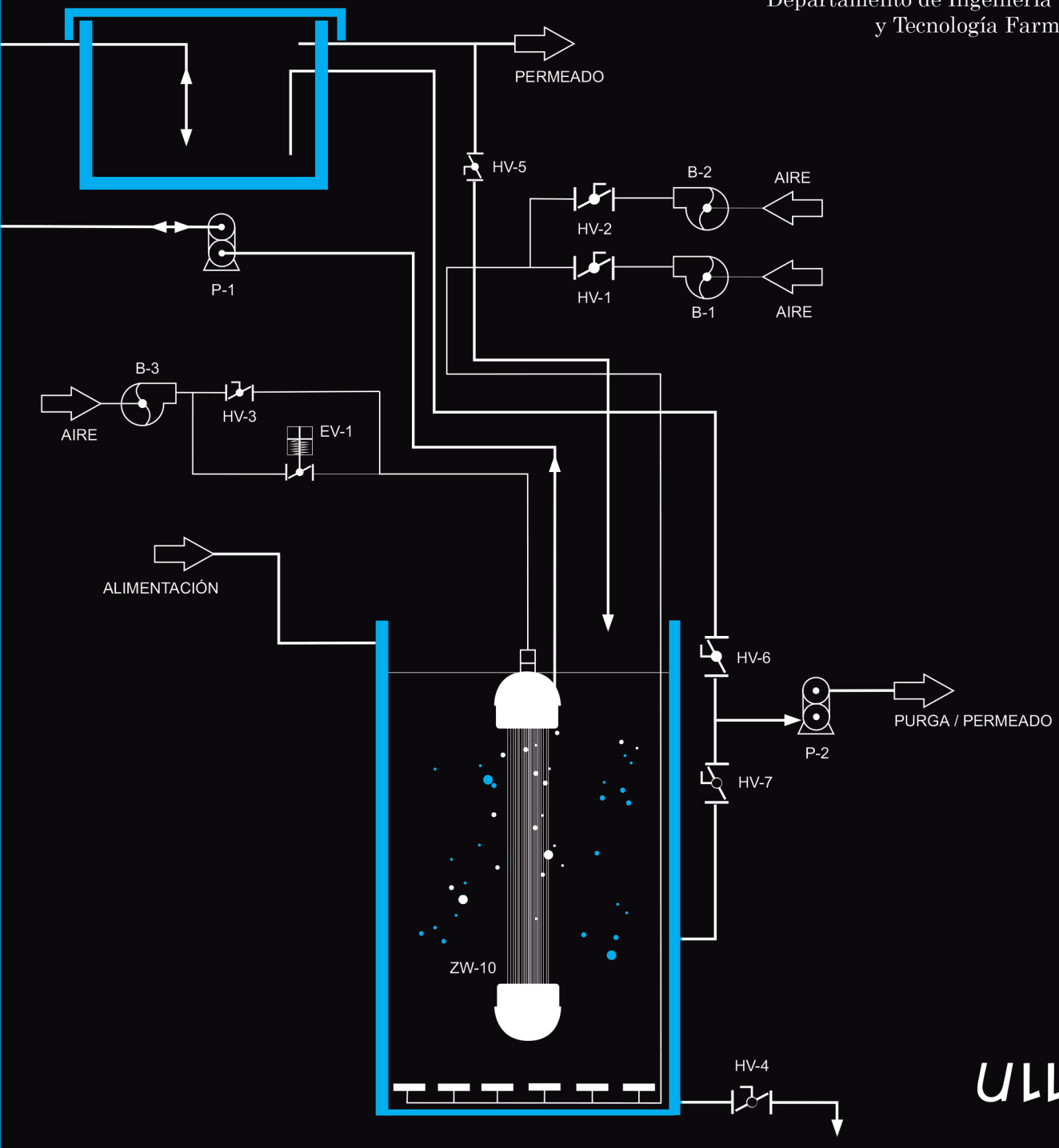

ULL | Universidad de La Laguna

Dña. Luisa María Vera Peña, Doctora en Química, Profesora Ayudante a Doctor de la Universidad de La Laguna y D. Juan Manuel Rodríguez Sevilla Profesor Titular de la Universidad de la Laguna,

CERTIFICAN

1. Que D. Oliver Díaz López, Ingeniero Químico por la Universidad de La Laguna, ha realizado bajo su dirección el trabajo de Tesis Doctoral que lleva por título "Tecnología de biorreactores de membrana como tratamiento terciario de aguas residuales domésticas".
2. Que revisado el trabajo, expresan su conformidad para que éste sea sometido a defensa frente al Tribunal correspondiente, ya que consideran que la presentación del mismo reúne los requisitos necesarios para optar al grado de Doctor.
3. Que habiéndose realizado la Memoria de Tesis por la modalidad de compendio de publicaciones, declaran que el doctorando ha sido responsable del trabajo experimental, participando interactivamente con ellos en su diseño, en el análisis de los resultados, extracción de las conclusiones, y en la redacción de los trabajos publicados.
4. Que ninguna de las publicaciones compendiadas en esta Tesis ha sido, ni será utilizada por otros para la realización de una Tesis Doctoral.
5. Que los indicadores de calidad de las publicaciones recogidas en esta Tesis son los siguientes:
    - CLEAN-Soil, Air, Water (1 publicación) índice de impacto 1,945 según el JCR (Thomson Reuters 2015).
    - Environmental Science Pollution Research (1 publicación) índice de impacto 2,828 según el JCR (Thomson Reuters 2015).
    - Journal of Membrane Science (4 publicaciones, 3 publicadas y 1 enviada) índice de impacto 5,056 según el JCR (Thomson Reuters 2015).

San Cristóbal de La Laguna, a 7 de Junio de 2016

Fdo. Luisa María Vera Peña

Fdo. Juan Manuel Rodríguez Sevilla

Tecnología de biorreactores de membrana como tratamiento terciario de aguas residuales domésticas

Autor:
Oliver Díaz López

Directores:
Luisa María Vera Peña
Juan Manuel Rodríguez Sevilla

Universidad de La Laguna
Departamento de Ingeniería Química
y Tecnología Farmacéutica

2016

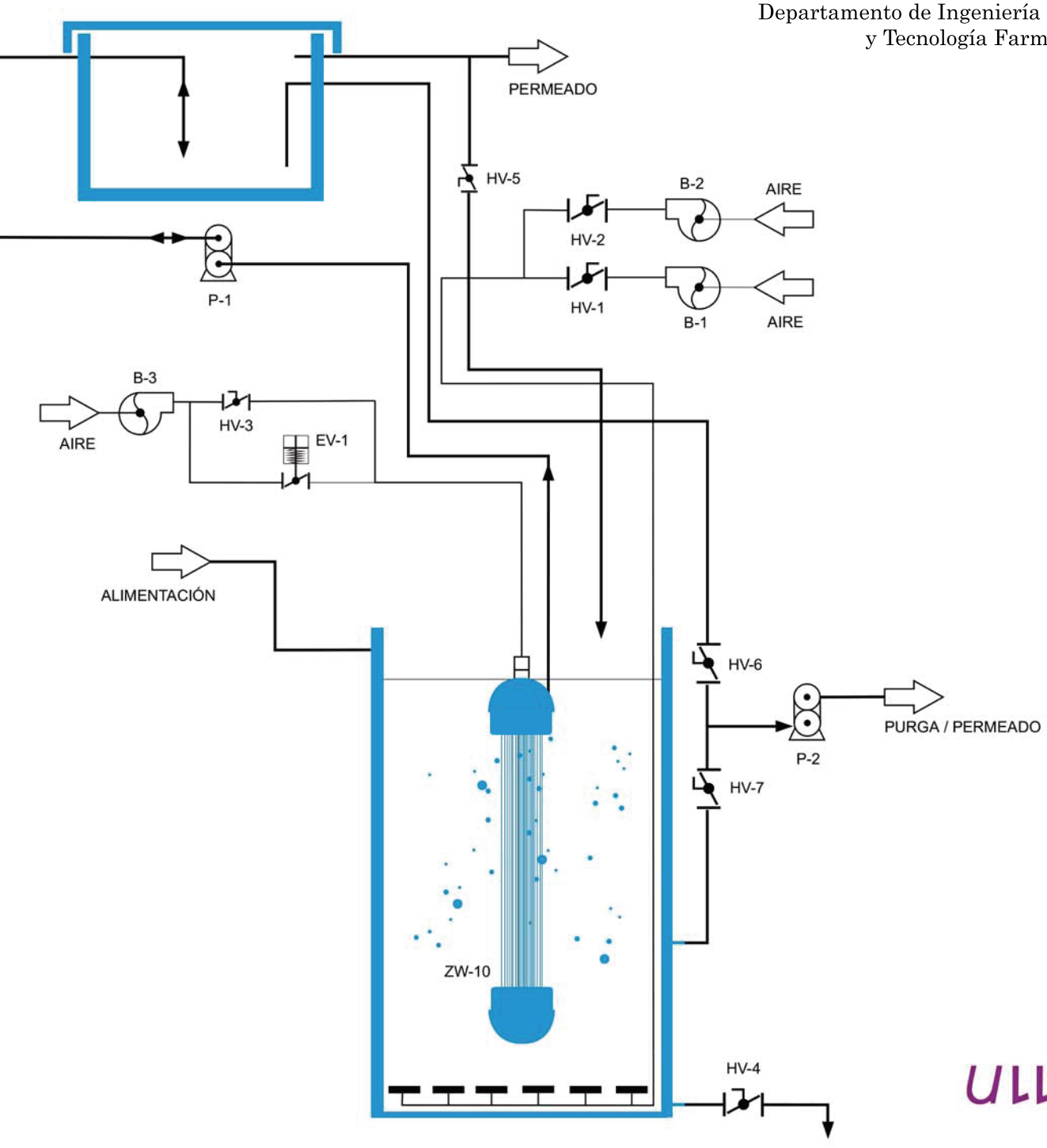

ULL Universidad de La Laguna

Agradecimientos

A lo largo de éstas breves líneas me gustaría expresarles mi gratitud a todas las personas que de manera directa o indirecta han colaborado en el desarrollo de esta tesis, así como resaltar desde un punto de vista humano lo que ha supuesto este proceso para mí.

En primer lugar me gustaría darle las gracias a la financiación concedida a la ULL por la Consejería de Economía, Industria, Comercio y Conocimiento, cofinanciada en un 85% por el Fondo Social Europeo

Al organismo autónomo local "Balsas de Tenerife, BALTEN", por el apoyo prestado durante todo el desarrollo de esta investigación. En especial a D. Escolástico Aguiar y a D. Juan Antonio Media por su siempre colaboración e interés en los estudios llevados a cabo por el grupo de investigación. A D. Juan Francisco López, por su continuo interés y apoyo demostrado durante toda la fase experimental.

Al Consejo Insular de Aguas de Tenerife, por su interés y colaboración con todos los trabajos que se llevan a cabo en la Línea de Investigación de "Tratamientos y Reutilización de aguas". En especial a D. Óscar Campos por su siempre interés y sobre todo, por las oportunidades que me ha brindado.

A Suez-Degremont, porque en los últimos tiempos me han permitido compatibilizar el desarrollo de esta Tesis con mi trabajo. En especial a D. Jose Garcia y D. Javier Santaella, por su especial interés y también a todos mis compañeros.

A mis tutores los cuales no tengo las palabras suficientes para transmitirles las gracias. A la Dra. Dña Luisa Mª Vera Peña, por su dedicación, consejo, apoyo e indicaciones que han permitido que esta tesis sea lo que es hoy, gracias por entregarte tanto siempre. Al Dr. D. Juan Manuel Rodríguez Sevilla, por su siempre punto de vista crítico, por su entrega y por sus consejos.

Al Dr. D. Enrique González Cabrera, gracias por vivir tan intensamente la investigación, pienso que si escribo todo lo que te debo esta tesis debería tener el doble de páginas. Gracias por actuar como un co-director, un compañero y un amigo.

A Cristina Afonso, Zoraida Sosa y Jose Juan Santana por su colaboración en la determinación de contaminantes emergentes.

A Raquel Díaz, gracias por su colaboración con la microscopía óptica y ayudarme a entender ese mundo desconocido de los microorganismos. Al Servicio de Apoyo a la Investigación de la Universidad de La Laguna (SEGAI) por todos los servicios prestados.

A todo el personal del Departamento de Ingeniería Química y Tecnología Farmacéutica por brindarme su apoyo en el momento que lo necesite, en especial a Paco y a Margarita por toda su colaboración. A todos mis compañeros de la línea de investigación de "Tratamiento y Reutilización de Aguas", así como de "Catalisis heterogénea"; por soportar mis quejas y ayudarme en todo lo que estuviese en su mano.

A todos los alumnos y alumnas que ha colaborado en esta Tesis mediante el desarrollo de su Proyecto Fin de Carrera o Trabajo Fin de Grado, a Elisa García, Laura Porlan, Rafael Bohorque y Rubén Sánchez. Gracias por soportar mis exigencias y comprender que de su trabajo dependía el mío.

A mis amigos, Laura, Eli, Eira, Alicia, Flavia y Denis, gracias por aguantarme durante tanto tiempo, gracias por animarme en tiempos bajos y por mostrarme que hay más vida fuera de las aguas residuales. A Diego, que se ha convertido en la persona más importante en mi vida, gracias por ayudarme, animarme, apoyarme, entenderme y acompañarme siempre en todo lo que hago.

A mi familia, que me han entendido y acompañado durante toda mi vida. Gracias por entender mi mal humor y mi estrés. En especial a Cristina e Irene, gracias por iluminarme la vida.

A todas aquellas personas que, directa o indirectamente, han participado en esta Tesis, dándome consejos, teniéndome paciencia, acompañándome en los buenos y malos momentos; y que en estas breves líneas he podido omitir.

A todos, muchas gracias.

Índice

CAPÍTULO 1: Introducción

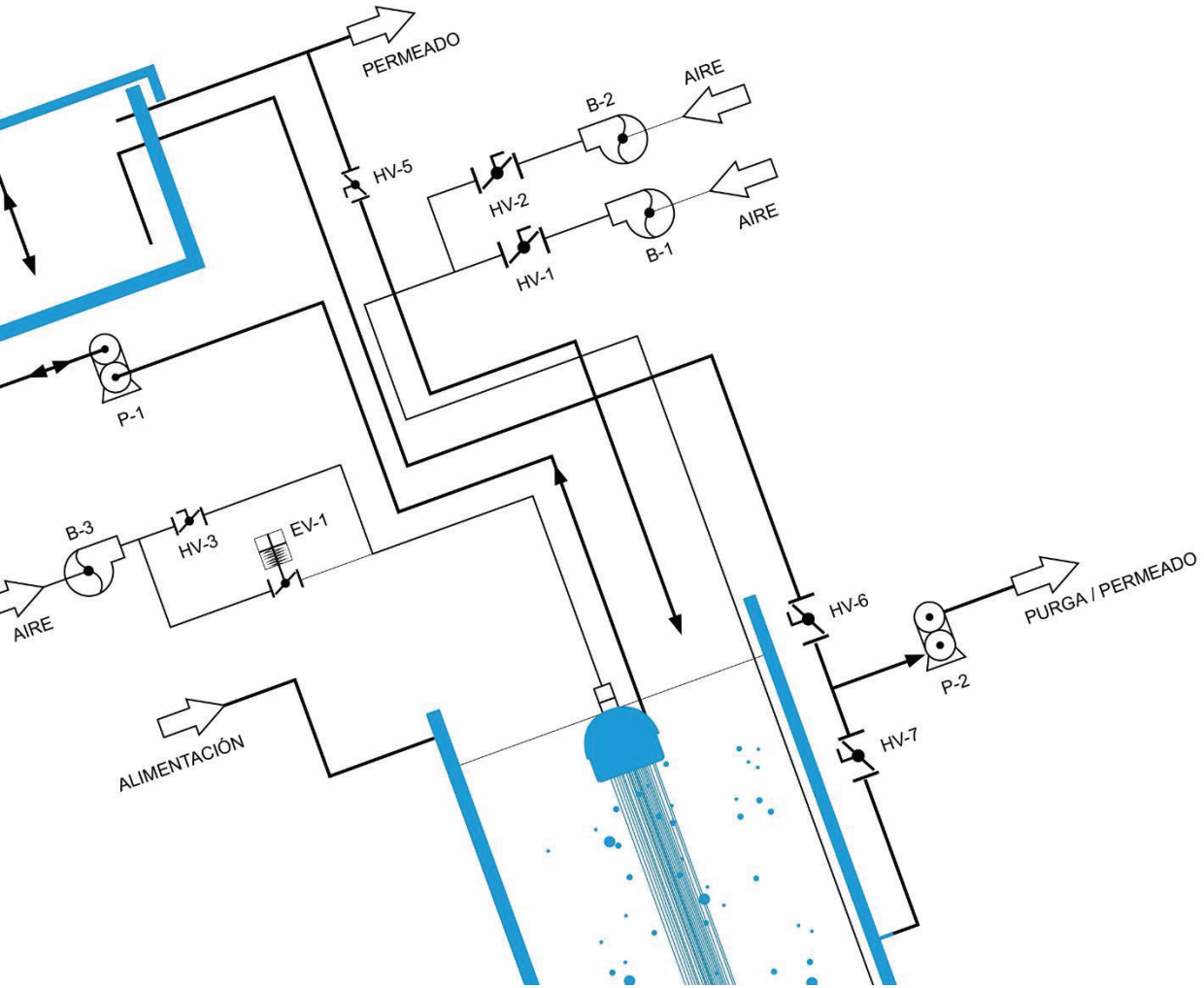

Capítulo 1
Introducción

1. Reutilización y regeneración de aguas residuales

El agua es una de las principales sustancias necesarias para el desarrollo de la vida, y por tanto, su disponibilidad se ha convertido en uno de los grandes problemas de la humanidad. Durante los últimos años, el gran desarrollo demográfico e industrial de los países más desarrollados ha generado un desequilibrio hídrico en todo el planeta Tierra, existiendo lugares con exceso y otros con escasez de agua.

En España las fuentes hídricas naturales, entendiéndose por éstas las subterráneas y superficiales, alcanzan los 111.000 hm^3/año (Ministerio de Agricultura, Alimentación y Medio Ambiente, 2015). Sin embargo, el sector agrícola español consume en torno a un 80% de la capacidad hídrica disponible (Montoya et al., 2016). Por tanto, la necesidad de incrementar la eficiencia en el uso del agua en el sector agrícola se ha convertido en el centro de la política nacional de aguas para garantizar el suministro de agua en todo el territorio nacional (Ministerio de Agricultura, Alimentación y Medio Ambiente, 2015).

La Directiva Marco del Agua (UE, 2000) supone un reto para la gestión del agua, ya que obliga a proteger y conservar los ecosistemas acuáticos promoviendo un uso sostenible de los recursos hídricos. Por tanto, no sólo se trata de proteger las aguas superficiales y subterráneas, sino también de cambiar el modelo de gestión, de forma que se fomente el ahorro y el del uso eficiente del agua. En este sentido, la regeneración de las aguas depuradas, que consiste en tratar éstas hasta alcanzar la calidad requerida en función del uso final que se les desee dar, alcanzando incluso, grado de potabilidad, es fundamental.

La legislación española (BOE, 2007) establece en el Real Decreto (RD) 1620/2007, del 7 de diciembre, la calidad requerida para cada uno de los usos permitidos: riego agrícola, usos urbano, industrial, recreativo y ambiental, y prohíbe su uso como agua potable, en industrias

alimentarias e instalaciones hospitalarias, entre otras. El RD 1620/2007 establece los criterios de calidad atendiendo principalmente, a las concentraciones de nematodos intestinales, *Escherichia coli*, sólidos en suspensión y turbidez. Por ejemplo, para el uso en riego agrícola de cultivos que permitan el contacto directo del agua regenerada con las partes comestibles, el agua debe cumplir los niveles de calidad estipulados en la Tabla 1.1.

Tabla 1.1. Calidad del agua regenerada para el uso en riego agrícola (uso 2.1, adaptado del RD 1620/2007)

PARÁMETRO	VALOR	UNIDAD
Nematodos intestinales	1	Huevo/10L
Escherichia coli	100	UFC/100mL
Legionella spp.	1000	UFC/L
Sólidos en suspensión	20	mg/L
Turbidez	10	NTU

En Canarias, el recurso hídrico tradicional ha sido las aguas subterráneas. Sin embargo, a pesar de su importante papel en el conjunto de las islas, durante las últimas décadas estas aguas han experimentado un significativo descenso tanto en cantidad, como en calidad. Este hecho se debe principalmente a dos causas antrópicas: la sobreexplotación de los acuíferos y la infiltración de vertidos.

La calidad de una parte importante de las masas de agua subterráneas en el archipiélago es deficiente, y en ocasiones los requisitos normativos para el abastecimiento a poblaciones (BOE, 2003) o la calidad necesaria para riego agrícola se cumplen con dificultades. Así, en las islas donde el balance hídrico natural es positivo (La Palma y La Gomera), con unos recursos superiores a la demanda, se limita la extracción de agua de los acuíferos. Por el contrario, en las islas deficitarias en recursos (Tenerife, Gran Canaria, Hierro, Lanzarote y Fuerteventura) se han instalado plantas desalinizadoras que permiten satisfacer las necesidades de agua de abasto.

Canarias ha sido una región pionera a nivel europeo, en la desalinización de agua de mar. Desde 1964, tras la puesta en marcha de la primera desalinizadora en Lanzarote, este recurso hídrico se viene utilizando de manera masiva, para el abastecimiento urbano y el riego de cultivos agrícolas.

Desde las décadas de los 80 y 90 del siglo pasado, Canarias ha sido pionera también en el ámbito de la reutilización de las aguas depuradas con la implantación de los primeros sistemas de aprovechamiento, principalmente con fines agrícolas. En la actualidad, es la cuarta comunidad autónoma en porcentaje de reutilización respecto al volumen de agua depurado (INE, 2016). La Figura 1.1. muestra el porcentaje del total de agua depurada que es reutilizada en cada comunidad autónoma según los últimos datos publicados por el Instituto Nacional de Estadística, correspondientes al año 2013 (INE, 2016). El porcentaje volumétrico de agua depurada que es reutilizada en la comunidad canaria representa un 27%, valor muy alejado del 62% que presenta la región de Murcia pero muy superior a la media nacional situada en un 10%.

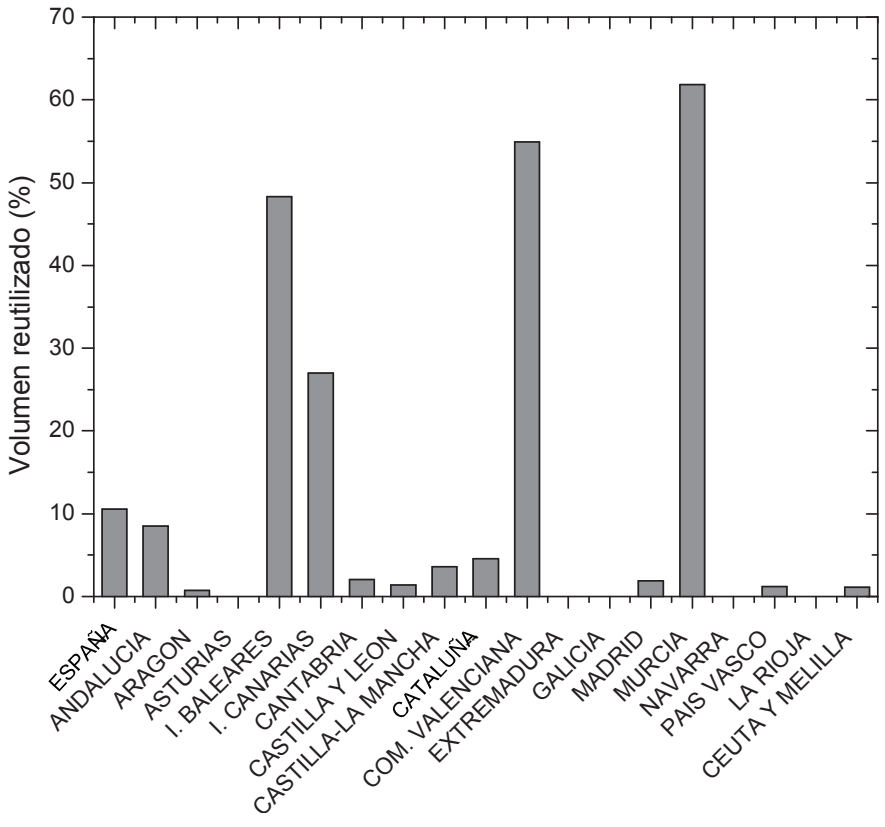

Figura 1.1. Porcentaje de volumen reutilizado en España para el año 2013 (Fuente INE, 2016)

Según los últimos datos publicados por el Instituto Nacional de Estadística en el año 2013, en Canarias, el volumen de depuración diario y por habitante alcanzó los 157 L mientras que el reutilizado fue de tan solo 43 L, lo que implica que un 73% de las aguas residuales no son aprovechadas y podrían suponer una solución parcial al estrés hídrico local. La Figura 1.2. muestra la evolución experimentada en los últimos años por los volúmenes medios de agua residual depurada y reutilizada por habitante y día en Canarias (INE, 2016). Se puede observar que si bien en los últimos años se ha realizado una labor importante para aumentar el caudal de agua residual depurado no ha ocurrido lo mismo con el volumen que es reutilizado. Por tanto, es necesario impulsar más la reutilización para que el ahorro de recursos convencionales sea el deseado y lograr la transformación de un vertido potencial: las aguas depuradas, en un recurso válido para determinados usos.

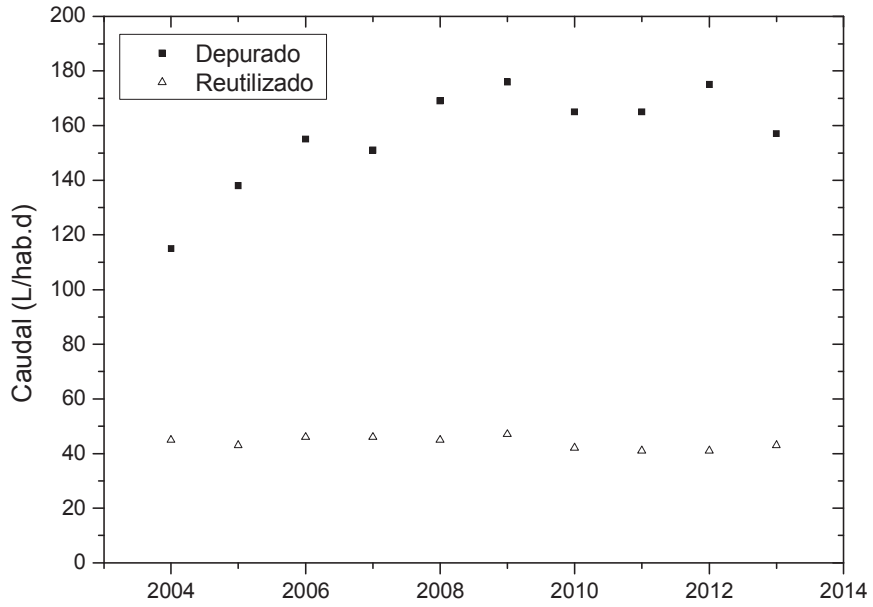

Figura 1.2. Evolución temporal del caudal depurado y reutilizado en Canarias (Fuente INE, 2016)

Por otra parte, dado que la agricultura es el sector productivo que demanda mayor volumen de agua, la regeneración-reutilización de aguas residuales puede jugar un papel fundamental como fuente de recursos hídricos para este sector. Especialmente si se tiene en cuenta que las aguas regeneradas pueden aportar nutrientes valiosos para la agricultura, como el nitrógeno o el fósforo. Por tanto, se puede afirmar que la regeneración de aguas residuales constituye una de las grandes alternativas para paliar el problema de escasez hídrica.

2. Sistema de reutilización de la isla de Tenerife

En la isla de Tenerife, la reutilización de aguas residuales procedentes de la estación depuradora de aguas residuales de Santa Cruz comenzó en torno a 1980. Entonces, se pretendía abastecer las necesidades de riego de los cultivos de plátano del sur de la isla, cuya demanda llegó a alcanzar el 62% de los recursos totales disponibles para la agricultura. Para ello, se diseñó y construyó el sistema general de reutilización de la isla de Tenerife (Delgado, 2003).

Figura 1.3. Esquema del sistema de reutilización de la Isla de Tenerife

El sistema global (Figura 1.3.) se compone de los siguientes elementos:

- **Estación depuradora (EDAR)**: Se trata de un sistema convencional de lodos activos, dimensionada para un caudal teórico de 90.000 m^3/d, para tratar las aguas residuales domésticas procedentes de los municipios de San Cristóbal de La Laguna y Santa Cruz de Tenerife. El esquema de depuración no contempla la eliminación de nutrientes.

- **Estación de bombeo**: El efluente de la EDAR se conduce hasta un depósito de hormigón armado de dos vasos que permite almacenar el agua para que esta sea bombeada en las horas de menor coste energético. A este elemento se le considera el primer eslabón de la reutilización de agua depurada, gestionada por la Entidad Pública Empresarial BALTEN (Balsas de Tenerife).

- **Depósito regulador de El Tablero**: Consiste en un recipiente que permite almacenar el agua depurada procedente de la estación de bombeo situada a una cota de 305

metros sobre el nivel del mar y desde el cual comienza la conducción que transporta el agua depurada por gravedad hasta el Valle de San Lorenzo.

- **Conducción**: El sistema de conducción de 60 km de longitud, formado por una tubería de fundición dúctil de 600 mm de diámetro y con presiones de trabajo que llegan a las 30 atmósferas, discurre paralelamente a la Autopista TF-1, con un perfil irregular en dientes de sierra que permite la colocación de más de 70 ventosas y desagües. En los puntos kilométricos 18 y 50 existen derivaciones hacia depósitos para la distribución de pequeños volúmenes de agua en La Ladera de Güimar y en San Isidro.

- **Balsa de San Lorenzo**: Se trata de una balsa de forma troncopiramidal de planta hexagonal regular (Figura 1.4), conformada con tierras e impermeabilizada con una geomembrana de polietileno de alta densidad de 2 mm de espesor y 28.000 m^2 de superficie, con una capacidad de 250.000 m^3. En este sistema se consigue homogenizar la calidad del agua residual, así como adecuar la calidad del agua depurada a la normativa. Entre los procesos de afino de la calidad que se realizan en Valle San Lorenzo, destacan las estaciones de filtrado y desinfectado; así como, la estación de desalación. Cabe destacar, que la balsa recibe también agua depurada procedente de la EDAR de Adeje-Arona.

Figura 1.4. Vista área de la Balsa de San Lorenzo

Uno los grandes problemas de la reutilización de aguas reside en que la producción de agua residual se puede encontrar a kilómetros del punto de reutilización, como en el caso del sistema de Tenerife. En la conducción de trasporte, la velocidad es una variable de gran importancia, pues si es demasiado baja, sobre 0,5 m/s, se produce la sedimentación de sólidos suspendidos

sobre las paredes de la tubería, formándose una biopelícula que lleva aparejada transformaciones químicas y bioquímicas (Delgado et al, 1999). Además, la ausencia de oxígeno y las altas temperaturas en la conducción pueden llevar a la producción de sulfuro de hidrógeno (H_2S). Si en determinadas zonas de la conducción se dan estas condiciones, el proceso generaría problemas de olores pestilentes y corrosión, además, el H_2S es un gas peligroso y tóxico a concentraciones relativamente bajas. La producción de sulfuro depende de varios factores como el pH, la temperatura, los nutrientes, el tiempo de contacto, la formación de biopelícula sobre las paredes de la tubería, la presencia de inhibidores de la reducción del sulfato y el potencial de reducción-oxidación (Delgado et al, 1999).

Desde la puesta en marcha de la conducción de agua depurada, el grupo de investigación "Tratamiento y Reutilización de Aguas" del Departamento de Ingeniería Química y Tecnología Farmacéutica de la Universidad de La Laguna ha mantenido convenios de manera regular, con la empresa gestora del tratamiento y conducción de agua depurada para su reutilización, BALTEN, para el estudio, control y minimización de la producción de H_2S durante el transporte del agua depurada.

Para poder solventar el inconveniente de la generación de sulfuros durante la conducción, inicialmente se analizó el comportamiento estándar de la tubería (Elmaleh et al., 1998; Delgado et al., 1999). Estos trabajos concluyeron que la tubería presentaba distintas zonas de trabajo: una pequeña zona aerobia inicial donde ocurre un fenómeno de nitrificación, tal y como se constata por la reducción de la concentración de amonio y posteriormente, tiene lugar un fenómeno de desnitrificación que se confirma por la reducción de nitritos y nitrógeno total.

Así, cuando la relación DQO/N-NO_x no es la adecuada, se producen condiciones anaerobias en la conducción, marcadas por la aparición de sulfuros. Este fenómeno tiene lugar en torno al kilómetro 10 de la misma, donde se inicia la desaparición del oxígeno disuelto, con valores del ORP (potencial de oxidación-reducción) inferiores a -100 mV (Elmaleh et al., 1998). Estos estudios indicaron también, que la concentración de sulfuros a la salida podía oscilar desde 18 mg/L hasta valores inferiores a 1 mg/L, debido a que la generación del compuesto no fue constante sino variable, en función de las condiciones de la conducción. Además, se estableció el espesor medio de la biopelícula creada sobre las paredes interiores de la tubería entre los 2 a 6 mm (Delgado et al., 2001).

Una de las vías para evitar la formación del sulfhídrico es la inyección de óxidos de nitrógeno al inicio de la conducción, ya que estos inhiben el proceso de desnitrificación. En base a esto, se ensayó la inyección de nitrato de calcio en el depósito del Tablero con concentraciones de 2,5 y 5 mg/L. Con la primera concentración ensayada se alcanzó una mejoría notable debido a que las condiciones anaerobias se retrasaban aproximadamente hasta el kilómetro 20, reduciendo por tanto la producción de sulfuros. En cambio, la concentración de 5 mg/L consiguió mejores resultados, ya que la tubería no presentaba condiciones anaerobias en todo su recorrido y por tanto, la producción de sulfuros fue nula (Rodríguez-Gómez et al., 2005). Es evidente que la dosificación de nitratos llevaba aparejado un gasto económico de 0,01-0,023 €/m^3, teniendo en cuenta el coste de instalación y operación de un sistema dosificador con las condiciones óptimas obtenidas (Monteagudo et al., 2007).

Evidentemente, si la EDAR de Santa Cruz pudiera producir un efluente secundario con concentraciones de nitrato próximas a los 5 mg/L se obtendría el mismo efecto inhibidor, sin el coste asociado a la inyección de químicos. Por todo ello en 2004, la depuradora modificó su línea de proceso incluyendo dos reactores en serie aireados que permitían tener una concentración de nitratos en el efluente de 0,4 mg/L y 8,2 mg/L de nitritos. En esta nueva situación, la tubería se comportó inicialmente como en los casos anteriores, con un gran consumo de oxígeno disuelto y una concentración de nitritos constantes. Cuando el oxígeno desaparecía totalmente tenía lugar la reducción de nitratos a lo largo de toda la tubería, y la presencia de este compuesto inhibía totalmente la producción de sulfuros al comportarse el sistema como un reactor anóxico (Delgado et al., 2004).

Otra de las posibilidades analizadas para evitar la producción de sulfhídrico en la tubería fue la inyección de oxígeno en torno al kilómetro 16 que es donde comenzaban las condiciones anaerobias en la conducción (Rodríguez-Gómez et al., 2009). Con una inyección de 30 mg O_2/L el sistema alcanzó una alta nitrificación, la cual inhibió completamente las condiciones anaerobias en la conducción (Rodríguez-Gómez et al., 2011).

Desde 2009, la instalación de un tratamiento terciario mediante filtros de arena de doble etapa tipo DUALSAND, ha permitido inhibir las condiciones anaerobias en la conducción del sistema de reutilización de la isla de Tenerife.

3. Biorreactores de membrana

El termino biorreactor de membrana (en inglés, *membrane bioreactor*-MBR) se usa para designar al proceso de tratamiento de aguas residuales que integra una membrana permeselectiva con un proceso biológico.

Esta tecnología modifica los sistemas de lodos activados tradicionales, sustituyendo el clarificador o sedimentador secundario por una membrana, produciendo un efluente clarificado y desinfectado. Este reactor consigue concentrar la biomasa y en consecuencia, reducir el tamaño del tanque y aumentar la eficacia del tratamiento biológico (Cote et al., 2012).

La normativa cada vez más exigente en cuanto a calidad de los recursos hídricos y el desarrollo de la industria de las membranas, han propiciado el desarrollo exponencial de los sistemas MBR en los últimos años, con índices de crecimiento e implantación que varía dependiendo de las infraestructuras y entornos económicos. Lugares como China, Japón, Corea, Europa o Norte América, han apostado por esta tecnología y disponen de numerosas plantas en funcionamiento (Judd, 2011). En el caso concreto de España, existen varias instalaciones en diferentes puntos de la geografía como las de San Pedro del Pinatar, Sabadell y Gava con capacidades de 20.000 a 50.000 m^3/d y plantas de 10.000-20.000 m^3/d en Alcoy, Arenales y Tamaraceite (Judd, 2011). Además, se puede encontrar pequeñas instalaciones que procesan caudales inferiores a los 500 m^3/d en Agulo, Agaete, Valldemossa y El Campello (Judd, 2011).

Pese a que la tecnología MBR ha experimentado un incremento significativo en términos de cuota de mercado, con una tasa de crecimiento entre el 10-15% (Marketsandmarkets, 2014), el ensuciamiento de las membranas sigue siendo el principal factor que condiciona la aplicación de esta tecnología, ya que éste fenómeno incrementa los costes de operación (Fenu et al., 2010). A pesar de ello, la elevada calidad del efluente producido, que cumple con los requisitos establecidos para la reutilización de las aguas residuales, ha favorecido su implantación frente a otras tecnologías de depuración.

Los biorreactores de membrana se componen de dos partes principales: un reactor que contiene la biomasa encargada de producir la biodegradación de los principales compuestos presentes en el agua residual, y un módulo de membrana cuya función es separar físicamente la biomasa del agua tratada. En el diseño de los MBR existen fundamentalmente dos tipos de configuraciones:

- En la denominada comúnmente como configuración externa o *side-stream*, los módulos de membrana se ubican en el exterior del biorreactor. Históricamente, esta configuración fue la primera en ser implantada y se utiliza sobre todo en el tratamiento de aguas residuales industriales. Requiere un alto consumo energético (2-10 kWh/m^3), y operar a presiones comprendidas entre los 0,5-5 bar, alcanzado las membranas de ultrafiltración flujos de permeado del orden de 70 L/hm^2.

- En la configuración sumergida, los módulos se encuentran sumergidos dentro del biorreactor. Esta configuración es relativamente más reciente que la de membrana externa y opera a un flujo menor de permeado que oscila normalmente, entre 20 y 35 L/hm^2. Cabe destacar que se ha conseguido disminuir de manera significativa los consumos energéticos de operación para esta configuración hasta 0,8-1,0 kWh/m^3 (Gil et al., 2010), de manera que los menores consumos energéticos y la aparición de nuevas membranas menos caras, han potenciado que esta configuración sea actualmente, la más instalada para plantas de gran capacidad, como en el caso del tratamiento de aguas residuales urbanas.

4. Biorreactores de membrana terciarios

Las plantas convencionales de tratamientos de aguas residuales están constituidas generalmente por un sistema de tratamiento de lodos activados que, en muchos casos, no contempla la nitrificación del efluente de salida. Además, es habitual que tengan lugar episodios frecuentes de des-floculación, debido al bajo rendimiento de los clarificadores secundarios. Todo ello da lugar a efluentes sin nitrificar, con concentraciones relativamente altas de sólidos suspendidos y materia orgánica. En este escenario, resulta necesario incorporar algún tipo de tratamiento terciario que mejore la calidad del efluente de las EDARs y que permita alcanzar la calidad exigida por el RD 1620/2007.

Tratamientos como la coagulación, la filtración en lecho de arena, la cloración o la desalación son utilizados habitualmente, para adecuar la calidad del efluente de un sistema convencional de depuración. Sin embargo, en el caso de que se produzcan problemas de floculación en los clarificadores, estos tratamientos terciarios pueden presentar problemas operativos como: la generación de grandes cantidades de residuos, altos consumos de reactivos químicos, y en el caso de la desalinización, dificultades asociadas a la carga orgánica residual (Delgado et al., 1999)

En los últimos años, la introducción de tecnologías de membrana de ultrafiltración y microfiltración ha sido una alternativa muy extendida (Haberkamp et al., 2008; Zheng et al., 2014). Sin embargo, su aplicación puede verse restringida si el agua procedente del tratamiento secundario presenta una cantidad relativamente alta de materia orgánica disuelta (Haberkamp et al., 2008). En estos casos, donde se requiere la mejora de la calidad de efluentes de tratamiento secundario y su nitrificación para garantizar un transporte seguro, la utilización de un MBR como tratamiento terciario parece ser una buena opción tecnológica. Esta aplicación ha sido poco estudiada a escala piloto (Delgado et al., 2002, Delgado et al., 2010), pese a que el mayor proyecto de reutilización de aguas residuales del hemisferio sur incluye la tecnología MBR como tratamiento terciario (Koch Membrane).

La operación de un MBR terciario está ligada al desarrollo de una biomasa de características y propiedades presumiblemente diferentes a las presentes en un MBR clásico, operado como tratamiento secundario. En el caso del MBR terciario, la suspensión biológica se encuentra en una situación de "limitación de sustrato" (Delgado et al., 2010). Este fenómeno conduce al "mantenimiento celular" (Pirt, 1965), donde el crecimiento neto de la biomasa es prácticamente nulo y por ende, el tiempo de residencia celular es prácticamente infinito. Estas condiciones no solo mejoran la productividad del proceso ya que no se generan lodos residuales, sino que además, permiten reducir la concentración de biopolímeros, sustancias consideradas entre las principales causantes del ensuciamiento de las membranas (Lin et al., 2014). La operación sin purga de lodos en un MBR clásico se traduce en elevadas concentraciones de biomasa (12-24g/L) lo que genera un impacto negativo sobre la transferencia de oxígeno disuelto y un incremento en los costes de operación (Rosenberger et al., 2002). Sin embargo, los MBR terciarios (tMBR) ofrecen la posibilidad de operar con una retención total de lodos y una concentración moderada de MLSS, debido a la moderada carga orgánica de la alimentación (Delgado et al., 2010).

Por otro lado, se sabe que las condiciones de operación pueden ser determinantes en la operación de un MBR terciario, ya que afectan a la filtrabilidad de la biomasa, por lo que han de ser evaluadas para establecer las condiciones idóneas de filtrabilidad. Hasta el momento son pocos los estudios que han analizado la influencia de las características de una suspensión nitrificante sobre el ensuciamiento de las membranas (Gao et al., 2004; Fan et al., 2006; Delrue et al., 2011; Johir et al., 2012). Por otra parte, Delgado et al., (2010) demostraron que un sistema

MBR terciario puede operar con flujos moderados (30-32 L/hm^2) y baja frecuencia de limpieza física de la membrana.

5. Proceso biológico

Los procesos biológicos se basan en la conversión de materia orgánica e inorgánica en productos inocuos debido a la acción de microorganismos. Las principales especies degradadoras de materia orgánica son las bacterias. No obstante, los protozoos y rotíferos juegan un papel crucial en la reducción de materia orgánica soluble y especies más evolucionadas, como nematodos y larvas de insectos, contribuyen al consumo de materia orgánica particulada. Existen evidencias que indican que los microorganismos superiores como protozoos, organismos filamentosos, nematodos y ciliados están presentes en concentraciones inferiores en los MBR, en comparación con los sistemas convencionales (Wei et al., 2003). Por otro lado, se sabe que organismos superiores como protozoos y metazoos son depredadores de bacterias, y contribuyen a la reducción de biomasa (Wei et al., 2003; Ratsak et al., 1996).

El crecimiento microbiano requiere el control de determinadas condiciones como son el pH, la temperatura y la concentración de biomasa. El control eficaz del tratamiento biológico se basa en el conocimiento de los principios básicos del crecimiento de los microorganismos, que se compone de cuatro fases:

- Fase de retardo: los organismos se aclimatan a las condiciones ambientales.
- Fase de crecimiento: los microorganismos degradan el sustrato y se reproducen.
- Fase estacionaria: los microorganismos han agotado el sustrato y la población se mantiene estacionaria.
- Fase de muerte: la tasa de muerte supera la de producción.

Es importante observar que la discusión anterior se refiere a una única población de microorganismos, pero las unidades de tratamiento biológico se componen de complejas mezclas de poblaciones biológicas interrelacionadas, en las que cada tipo de microorganismos tiene su propia curva de crecimiento, que depende del alimento y de los nutrientes disponibles,

la temperatura o el pH; dificultando de esta manera, el estudio y el análisis de la suspensión biológica.

La materia orgánica presente en el agua de alimentación sirve como sustrato a las bacterias heterótrofas presentes en la suspensión biológica, para la síntesis celular que puede ser expresada de forma genérica mediante la expresión [1.1]

$$MO + O_2 + C_5H_7NO_2 + \text{nutrientes} \longrightarrow CO_2 + NH_3 + C_5H_7NO_2 \qquad [1.1]$$

Donde MO representa la materia orgánica y $C_5H_7NO_2$ la nueva biomasa formada. Por otro lado, las bacterias heterótrofas utilizan el oxígeno disuelto para la producción de energía mediante la expresión genérica [1.2]

$$C_5H_7NO_2 + 5\ O_2 \longrightarrow 5\ CO_2 + 2\ H_20 + NH_3 + \text{energía} \qquad [1.2]$$

La nitrificación biológica es un proceso microbiológico en el que tiene lugar la oxidación de compuestos nitrogenados reducidos a especies oxidadas, nitritos y nitratos. La reacción se lleva a cabo en dos etapas en serie; una primera donde ocurre la oxidación del ion amonio a nitrito, y una segunda en la que el nitrito es oxidado a nitrato.

La primera etapa es realizada principalmente por una familia de bacterias denominada bacterias oxidantes de amonio (AOB), según la ecuación:

$$NH_4^+ + 1{,}5\ O_2 \longrightarrow NO_2^- + 2\ H^+ + H_2O \qquad [1.3]$$

El proceso de oxidación de amoniaco, a su vez, comprende varios compuestos intermedios, siendo una reacción por etapas como se muestra a continuación:

$$NH_4^+ \longrightarrow NH_2OH \longrightarrow [NOH] \longrightarrow NO_2^-$$

La segunda etapa de la nitrificación, es la oxidación del nitrito a nitrato según se muestra en la ecuación [1.4] y es realizada principalmente, por las bacterias denominadas bacterias oxidantes de nitrito (NOB).

$$NO_2^- + 0{,}5\ O_2 \longrightarrow NO_3^- \qquad [1.4]$$

Estas bacterias autótrofas, en sus procesos anabólicos toman el CO_2 de la atmósfera como fuente de carbono. Dicho carbono tiene que ser reducido antes de formar parte de su propia estructura y, si el agente reductor es el ion amonio, la reacción es la siguiente:

$$15\ CO_2 + 13\ NH_4^+ \longrightarrow 10\ NO_2^- + 3\ C_5H_7NO_2 + 23\ H^+ + 4\ H_2O \qquad [1.5]$$

Cuando el agente reductor es el NO_2^- , la reacción es:

$$5\ CO_2 + NH_4^+ + 10\ NO_2^- + 2\ H_2O \longrightarrow 10\ NO_3^- + C_5H_7NO_2 + H^+ \qquad [1.6]$$

Combinando las expresiones [1.3], [1.5] y la reacción del equilibrio del bicarbonato, se tiene la siguiente expresión general:

$$55\ NH_4^+ + 76\ O_2 + 109\ HCO_3^- \longrightarrow C_5H_7NO_2 + 54\ NO_2^- + 104\ H_2CO_3 + 57\ H_2O \qquad [1.7]$$

De manera que se producen 113 g de bacterias ($C_5H_7NO_2$) por oxidación de 80,7 g NH_4^+ o 1.129,8 g de N-NH_4^+, dando lugar a un rendimiento de 0,10 g VSS/g N-NH_4^+. Por otro lado, se tiene que el consumo de oxígeno teórico según la estequiometría de la reacción, es de 3,24 g O_2/ g N-NH_4^+.

Asimismo, combinando las expresiones [1.4], [1.6] y la reacción del equilibrio del bicarbonato, se tiene la expresión general para las NOB:

$$400 NO_2^- + NH_4^+ + 195\ O_2 + HCO_3^- + 4H_2CO_3 \longrightarrow C_5H_7NO_2 + 400\ NO_3^- + 3H_2O \qquad [1.8]$$

En este caso, se producen 113 g de bacterias por oxidación de 134,5 g de NO_2, dando un rendimiento de 0,06 g VSS/g N-NO_2^-. El consumo de oxígeno teórico es de 1,1 g O_2/ g N-NO_2^-. Otro aspecto a tener en cuenta es la disminución del pH, que tiene lugar en la primera etapa del proceso de nitrificación. En resumen, se puede decir que el proceso de nitrificación se caracteriza por un crecimiento lento de las bacterias, alto consumo de oxígeno y un descenso del pH, si el medio no está tamponado.

En los tratamientos de aguas residuales aerobios, el suministro de oxígeno se realiza mediante el aporte de aire atmosférico al biorreactor. Para ello se suelen usar difusores de

burbuja fina, los cuales permiten además, mantener agitada la suspensión biológica. Los requerimientos de oxígeno para mantener la comunidad microbiana, degradar la materia orgánica y permitir una nitrificación del efluente puede ser determinado mediante balances de masa en el sistema (Judd, 2011). En los últimos años, numerosas estrategias han sido investigadas con el fin de reducir el consumo de aireación en el proceso biológico (Dalmau et al., 2014; Capodici et al., 2015). A bajas concentraciones de oxígeno disuelto, el proceso biológico se ve notablemente afectado por el incremento de las sustancias extrapoliméricas (EPS) y los productos solubles microbianos (SMP) (Gao et al., 2011). Por otro lado, la concentración de oxígeno disuelto afecta al estado de biofloculación del lodo, que en el caso de que el biorreactor en cuestión, sea un biorreactor de membranas, es un parámetro que influye directamente, en ensuciamiento de la membrana (Faust et al., 2014).

6. Ensuciamiento de la membrana

El termino de ensuciamiento o *fouling* (Figura 1.5) en los sistemas MBR para tratamiento de aguas residuales hace referencia al proceso que tiene lugar durante la filtración, por el cual se retienen contaminantes que normalmente se acumulan en la superficie de la membrana, produciendo fenómenos como la reducción del caudal de permeado y el aumento de la presión transmembrana (TMP), y por ende, el aumento de la resistencia hidráulica (Judd, 2011). Se puede afirmar que el ensuciamiento es el principal inconveniente de la tecnología MBR, ya que cuando no está controlado, la demanda energética aumenta considerablemente.

Figura 1.5. Efecto del ensuciamiento sobre membranas sumergidas de fibra hueca (Delgado et al., 2011).

En los procesos de filtración con membranas, la resistencia total de la misma al flujo del fluido aumenta por los siguientes mecanismos:

- La concentración de solidos rechazados en la superficie de la membrana.
- La precipitación de macromoléculas poliméricas solubles e inorgánicas.
- La acumulación de solidos retenidos sobre la membrana.

Los primeros mecanismos son producidos por la "concentración de polarización", este concepto describe la tendencia de los sólidos a acumularse en las inmediaciones de la membrana. A medida que el permeado atraviesa la misma, los solutos que contenía la suspensión se quedan en las proximidades de la superficie de la membrana formando una capa de líquido cuya velocidad tiende a cero, es decir, esta próxima al estancamiento. En ese caso, el único modo de transporte dentro de esta capa es la difusión, en este caso retrodifusión, ya que el soluto es arrastrado bajo las condiciones de flujo tangencial. De esta manera, se genera un gradiente de concentración que se denomina como polarización de la membrana y al aumento de la concentración que sufre la solución en contacto con la misma, concentración de polarización (Figura 1.6).

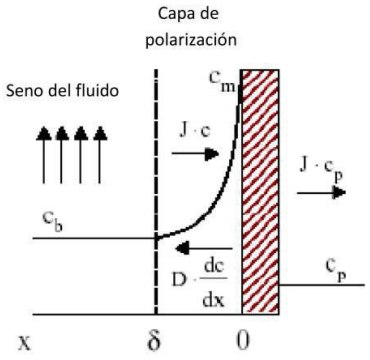

Figura 1.6. Concentración de polarización (adaptado de Judd, 2011).

Este fenómeno produce un descenso del flujo de permeado en los primeros instantes de la filtración, para luego estabilizarse y generar un flujo estacionario. Si se produjera un ensuciamiento considerable se observaría una disminución del flujo mucho mayor, pero ya debida al ensuciamiento o *fouling* (Figura 1.7).

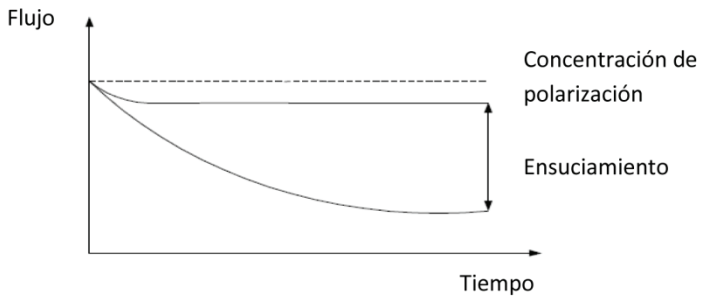

Figura 1.7. Efecto del ensuciamiento (adaptado de Judd, 2011).

Para evitar el fenómeno de la polarización se puede aumentar la velocidad tangencial o la turbulencia en la zona del rechazo, ya que de esta manera se consigue reducir el gradiente de concentración producido cerca de la superficie de la membrana.

El flujo límite es uno de los conceptos más usados en filtración tangencial y representa el flujo máximo de permeado que se puede conseguir al aumentar la presión transmembrana para una determinada solución o suspensión (Bacchin et al., 2006). A partir de este valor de flujo límite, el incremento de la TMP no produce ningún efecto sobre el flujo, ya que las incrustaciones o deposiciones saturan la capacidad de filtración de la membrana. En el extremo opuesto, en cuanto a condiciones de trabajo, se encuentra el flujo crítico, definido como el primer flujo que produce ensuciamiento. Por tanto, podemos decir que el flujo crítico es la transición entre la concentración de polarización y el fenómeno del ensuciamiento.

El ensuciamiento tiene lugar por diferentes mecanismos fisicoquímicos o biológicos, que se relacionan entre sí, aumentando la deposición no uniforme de materiales sobre la superficie de la membrana debido a la interacción del licor mezcla con el material de fabricación. Dicha interacción es difícil de definir, debido a que el licor mezcla es una combinación compleja y cambiante de especies orgánicas, como productos metabólicos, sustrato parcialmente degradado, células y microorganismos, además de sólidos inertes y sustancias inorgánicas.

La clasificación de distintos tipos de ensuciamiento se puede llevar a cabo atendiendo a la fuerza de atracción que exista entre el material y la membrana, o al método usado para recuperar la permeabilidad de la misma (Wang et al., 2014). Atendiendo a esta clasificación se define ensuciamiento reversible como la atracción leve de materiales sobre la superficie de la

membrana, los cuales pueden ser eliminados mediante limpiezas físicas. En general, éste ensuciamiento se produce por la construcción de una torta (Figura 1.8).

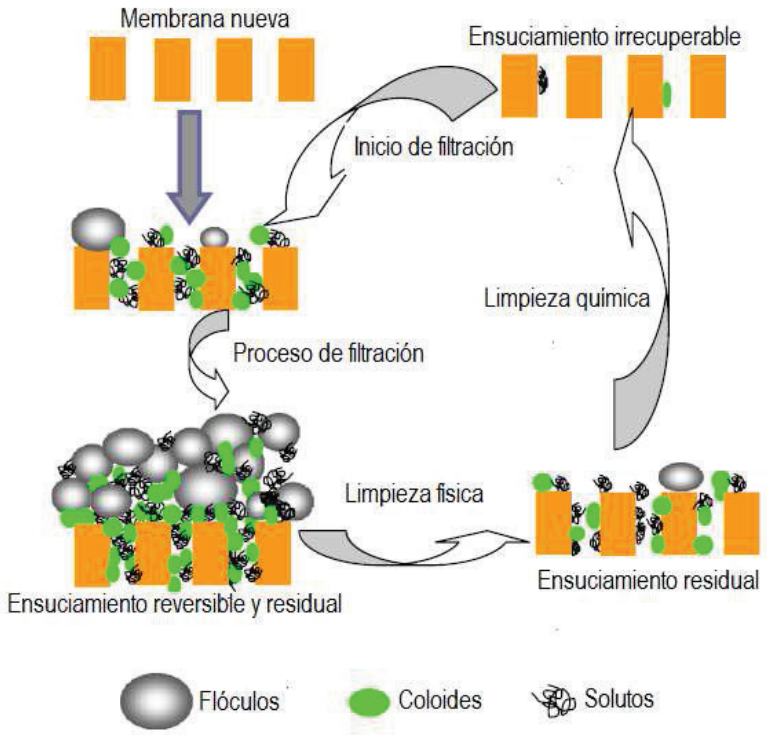

Figura 1.8. Tipos de ensuciamiento (adaptado Judd, 2011)

El ensuciamiento irreversible o residual es aquel que no puede ser eliminado de la superficie de la membrana mediante limpiezas físicas. Su formación se debe a una relación fuerte entre el ensuciamiento y la membrana, que tradicionalmente se asocia al bloqueo de poros o a la formación de un gel (Wang et al., 2014). Por último, el ensuciamiento irrecuperable se define como la resistencia remanente de la membrana tras las limpiezas químicas (Figura 1.8). Por tanto, se trata de un ensuciamiento permanente de la membrana, que además determina la vida útil de la misma (Wang et al., 2014).

7. Modelización del ensuciamiento

En los últimos años, el desarrollo de modelos predictivos del ensuciamiento ha cobrado importancia en los procesos de filtración, puesto que son una importante herramienta para predecir y simular el comportamiento de la membrana. Por otro lado, permiten una mejora del rendimiento del proceso, optimizar el diseño y especialmente, comprender los fenómenos relacionados con el ensuciamiento.

Los MBR operan normalmente mediante una filtración a flujo constante, por tanto, a medida que la membrana comienza a ensuciarse, la presión trasmembrana (TMP) aumenta para mantener el flujo de permeado. La evolución de la TMP se puede utilizar para la caracterización del ensuciamiento, considerando la ley de Darçy modificada:

$$TMP = J\mu R_t \quad [1.9]$$

donde J es el flujo de permeado, μ es la viscosidad del agua y R_t representa la resistencia hidráulica total. De acuerdo con el modelo de resistencias en serie, R_t toma la forma:

$$R_t = R_m + R_f \quad [1.10]$$

donde R_m es la resistencia de la membrana limpia y R_f es la resistencia asociada al ensuciamiento de la membrana en un instante de tiempo t. El ensuciamiento de la membrana suele dividirse en dos tipos: reversible y residual (Drews, 2010), y por tanto la resistencia asociada el ensuciamiento de la membrana se suele dividir en dos componentes:

$$R_f = R_{rdf} + R_{rvf} \quad [1.11]$$

En la ecuación anterior, R_{rdf} es la resistencia generada por el ensuciamiento residual, mientras que R_{rvf} se relaciona con el ensuciamiento reversible. La evolución de la R_{rvf} se ha descrito por diversos modelos que interpretan el ensuciamiento de la membrana. La Tabla 1.2 muestra los modelos clásicos propuestos por Hermia (1982), donde la presión trasmembrana asociada a la resistencia, debido al ensuciamiento reversible, se expresa en función del tiempo. Cada modelo corresponde con un tipo característico de ensuciamiento (Figura 1.9) y con una forma característica de la evolución de la TMP.

Tabla 1.2. Modelos clásicos de interpretación del ensuciamiento de membranas

MODELO	PARAMETROS	EXPRESIÓN	
Torta	K_c (s/m^2)	$\frac{TMP}{TMP_o} = 1 + K_c J^2 t$	[1.12]
Bloqueo intermedio	K_i (s/m^2)	$\frac{TMP}{TMP_o} = exp(K_i J t)$	[1.13]
Bloqueo completo	K_b(s^{-1})	$\frac{TMP}{TMP_o} = \frac{1}{1 - K_b t}$	[1.14]
Bloqueo estándar	K_s (m^{-1})	$\frac{TMP}{TMP_o} = \left(1 - \frac{K_s J t}{2}\right)^{-2}$	[1.15]

Debido a la complejidad del ensuciamiento, los modelos clásicos han sido modificados con el fin de entender, modelizar y predecir dicho proceso. Este es el caso de los modelos combinados donde se establecen relaciones entre los modelos descritos anteriormente (Bolton et al., 2006).

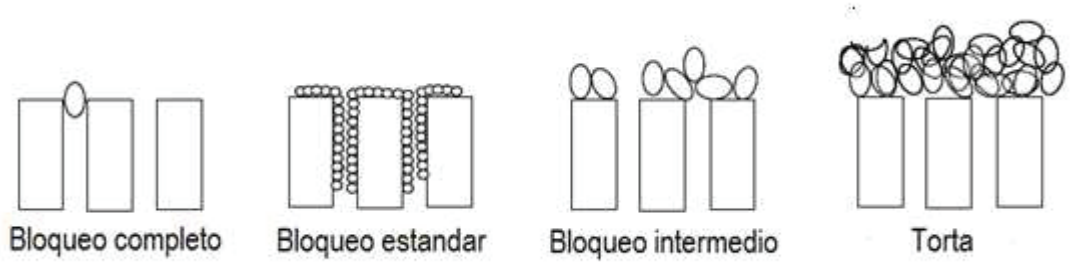

Figura 1.9. Modelos clásicos de ensuciamiento (Adaptado de Judd, 2011)

El modelo clásico de construcción de la torta ha sido modificado atendiendo a la compresibilidad del depósito sobre la membrana, obteniéndose el modelo de torta compresible (Sørensen & Sørensen, 1997; Foley 2006). En este modelo la evolución de la presión transmembrana durante un ciclo de filtración puede ser definida mediante la expresión [1.16]

$$TMP = TMP_0 + \mu\alpha\omega J^2 t \qquad [1.16]$$

Donde, TMP_0 es la presión asociada al ensuciamiento residual, μ es la viscosidad el permeado, ω es la concentración de sólidos en la torta por unidad de volumen filtrado y α es la resistencia específica de la torta. Para partículas compresibles, α aumenta con la presión transmembrana. Para la modelización de este ensuciamiento se han propuesto varias expresiones (Rushton et al.1996, McCarthy et al. 1999, Foley 2006), aunque para la filtración de suspensiones microbianas, se acepta la expresión [1.17]

$$\alpha = \alpha_0 \left(1 - \frac{\Delta TMP}{P_a}\right) \qquad [1.17]$$

donde α_0 corresponde a la resistencia específica de la torta a presión cero, ΔTMP es la caída de presión a través de la membrana y P_a es el factor de compresibilidad del ensuciamiento. La compresibilidad de la torta se ve afectada por las propiedades de las partículas y por la hidrodinámica de la formación de la torta.

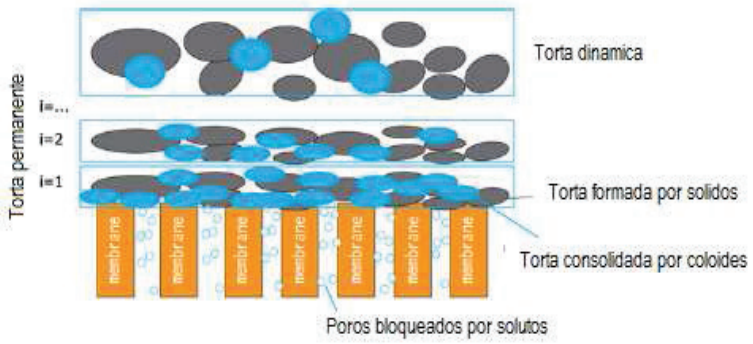

Figura 1.10. Modelos de ensuciamiento en base a la presencia de capas colmatante (Adaptado de Wu et al., 2012)

En los últimos años, con el fin de integrar en los modelos de ensuciamiento las diversas propiedades de la suspensión biológica, como pueden ser la concentración de sólidos o el contenido en materia orgánica disuelta y coloidal, han surgido modelos que explican el ensuciamiento como la sucesión de capas que se depositan sobre la membrana (Figura 1.10).

Una de estas capas es dinámica y eliminable mediante limpiezas físicas (ensuciamiento reversible) y otra es permanente y se relaciona con el ensuciamiento residual (Wu et al., 2012). No obstante, los modelos clásicos son simples y dan una explicación al ensuciamiento bastante completa, lo que les hace ventajosos frente a los nuevos modelos, que presentan una alta dificultad matemática y requieren la caracterización de la suspensión biológica.

8. Parámetros que afectan al ensuciamiento

El ensuciamiento se ve afectado por una multitud de variables, entre las que destacan:

- *Tipo de alimentación*: en los MBR, el ensuciamiento está asociado principalmente, a las interacciones entre la membrana y la suspensión biológica. Así, la alimentación influye sobre las condiciones de operación en que tienen lugar las transformaciones biológicas. En particular, el nivel de biodegradabilidad del carbono afecta a las características de la biomasa y al ensuciamiento. De hecho, los altos valores de glucosa, proteínas y carbohidratos generan una suspensión con flóculos de mayor tamaño (Le Clech et al., 2006).

- *Hidrofobicidad de la membrana*: debido a las interacciones hidrofóbicas que ocurren entre los solutos, las células microbianas y la membrana, el ensuciamiento de la membrana se espera que sea más severo en membranas hidrofóbicas que en las hidrofílicas.

- *Concentración de solidos suspendidos*: desde los inicios de los MBR, la concentración de biomasa se ha considerado el principal parámetro del ensuciamiento. Sin embargo, muchos estudios han revelado que este parámetro por si sólo es un indicador pobre del ensuciamiento (Meng et al., 2009; Drews, 2010; Van der Broeck et al., 2011). En general, se ha observado una correlación en función del rango de concentraciones estudiado, que afecta a otras propiedades, como la viscosidad o la morfología.

- *Concentración de Sustancias Poliméricas Extracelulares* (EPS): el ensuciamiento de la membrana ha sido atribuido por muchos autores, en gran parte, a los EPS (Le Clech et al., 2006; Drews, 2010): Este término general abarca diversas clases de macromoléculas como carbohidratos, proteínas, ácidos nucleicos, lípidos y otros polímeros que se encuentran en la superficie de la célula y en el espacio intercelular de los agregados microbianos (Le Clech et al.,

2006; Drews, 2010). Los EPS forman un gel hidratado en el que las células microbianas se ven integradas y producen una barrera notable a la transferencia de materia (biopelícula) que disminuye la permeabilidad.

- *Concentración de Productos Moleculares Solubles* (SMP): los SMP comprenden los componentes solubles celulares producidos en la lisis celular (Le Clech et al., 2006; Drews, 2010). Se considera que estos materiales son adsorbidos sobre la superficie de la membrana, bloqueando los poros.

- *Morfología de la suspensión:* de manera general se considera a los flóculos y a las bacterias libres mayores al tamaño del poro de la membrana, por tanto, la distribución de tamaños en la suspensión tiene un papel importante en los mecanismos de consolidación de la torta. Muchos autores han indicado que suspensiones con un menor tamaño de partículas producen una torta más densa que incrementa la resistencia de acuerdo a la ecuación de Carman-Kozeny (Lin et al., 2011).

El ensuciamiento se ve afectado también por variables de operación, como el flujo de filtración, las condiciones de las limpiezas físicas y la aireación tangencial de las membranas, que son analizadas en apartados posteriores.

9. Control y reducción del ensuciamiento

El control del ensuciamiento se puede llevar a cabo aplicando las siguientes estrategias (Judd, 2011):

- La aplicación de pretratamiento apropiado a la alimentación.

- El empleo de protocolos adecuados de limpiezas químicas y físicas.

- El incremento de la turbulencia en la proximidad de la membrana, por medio del aumento de la velocidad tangencial o de la aireación.

- Modificaciones bioquímicas del licor mezcla.

En todos los sistemas MBR el control del pretratamiento es clave para el adecuado funcionamiento de la instalación, de ahí la importancia de la instalación de rototamices de al menos 0,5 mm (Frenchen et al., 2008), que permiten la eliminación de fibras y cabellos.

La modificación de la suspensión biológica se puede realizar mediante la adición de coagulantes, floculantes, adsorbentes, etc.; que permiten mejorar la calidad del licor mezcla.

Las operaciones llevadas a cabo habitualmente para mantener la permeabilidad de la membrana son las limpiezas físicas y químicas. La frecuencia de estas debe ser analizada y estudiada previamente para conseguir la combinación óptima de filtración y control del ensuciamiento. A parte de estas operaciones, el ensuciamiento se puede reducir aumentando la turbulencia en el lado del rechazo, mediante un sistema de aireación en las inmediaciones de la membrana.

9.1. Limpiezas físicas y químicas

Los métodos más habituales de limpiezas físicas automáticas de la membrana son el retrolavado y la relajación. Con estas técnicas se consigue eliminar parcialmente el ensuciamiento generado sobre la membrana, produciendo ciclos de limpieza que permiten mantener la TMP en un determinado rango y así se consigue prolongar su operatividad durante más tiempo, antes de ejecutar una limpieza química.

Los principales parámetros de la limpieza física son generalmente la duración y la frecuencia. Se ha demostrado que el retrolavado es más eficiente si es de corta duración y se realiza con una alta frecuencia (Chen et al., 2003). El retrolavado consiste en invertir el flujo de permeado a través de la membrana para limpiar los poros y eliminar las partículas que se pudieran haber adherido a la superficie. Durante el retrolavado la filtración se para y las bombas de succión de permeado se utilizan para invertir el flujo a través de la membrana. Para poder llevar a cabo esta operación, parte del permeado se almacena en un depósito hasta el momento de su utilización, siendo este uno de los inconvenientes que presenta el retrolavado, ya que se produce una pérdida en la producción neta de permeado.

La Figura 1.8 muestra como a medida que tiene lugar la filtración, la membrana sufre ensuciamiento. Tras un retrolavado se consigue recuperar parcialmente la permeabilidad de la membrana, pero no totalmente, apareciendo un ensuciamiento irreversible o residual. Este

ensuciamiento es crítico en la operación con un MBR, ya que su eliminación solo es posible con limpiezas químicas.

Las limpiezas químicas se llevan a cabo con ácidos orgánicos o inorgánicos, sosa cáustica o hipoclorito sódico (Judd, 2011), siendo lo más habitual hipoclorito sódico con una composición del 0,1- 0,5 % en peso para eliminar la materia orgánica. Los ácidos orgánicos como por ejemplo, el cítrico o el oxálico se utilizan para eliminar las incrustaciones inorgánicas.

Los protocolos de limpieza química pasan por sumergir la membrana un determinado tiempo en la solución de limpieza o realizar un retrolavado con una baja concentración del agente químico, consiguiendo así eliminar todo el ensuciamiento irreversible. No obstante, la permeabilidad de la membrana puede que no se recupere totalmente quedando un ensuciamiento irrecuperable imposible de eliminar por estos medios, teniéndose que llevar a cabo limpiezas manuales de la membrana.

9.2. Aireación de la membrana

La inyección de aire en la proximidad de la membrana permite el aumento de la turbulencia y del esfuerzo de cizalladura sobre la superficie de la misma, consiguiendo así, disminuir la capa de ensuciamiento que se haya podido formar, sin presentar efecto sobre el ensuciamiento residual (Delgado et al., 2008).

La aireación de la membrana constituye uno de los parámetros clave en el diseño y la operación de los sistemas MBR, de manera que la frecuencia e intensidad de dicha aireación suele ser analizada para optimizar el sistema.

El flujo de permeado aumenta linealmente con la tasa de aireación hasta un valor umbral a partir del cual no hay aumento significativo de la permeabilidad (Judd, 2011), consiguiéndose mejores resultados con burbujas grandes porque producen una mayor turbulencia y un mayor esfuerzo de cizalladura.

La evaluación de la intensidad de aireación se mide habitualmente con el parámetro SAD_m, que se define como el caudal de aire aplicado en condiciones normales por unidad de superficie de membrana. La Tabla 1.3 muestra los valores típicos de SAD_m para los principales distribuidores comerciales de biorreactores de membrana. La tendencia generalizada de los suministradores en los últimos años, es disminuir esta demanda específica, experimentándose

una optimización en el consumo de aire que reduce por tanto, los costes de operación de los sistemas MBR.

Tabla 1.3. Valores típicos del SAD_m (adaptado Judd, 2011)

CASA COMERCIAL	J (L/hm^2)	SAD_m (Nm^3/m^{2}h)
Kubota	24	0,83
GE Zenon	27	0,44
Norit-Pentair	46	0,35
Koch- Puron	23	0,39

La aireación de la membrana es considerada como el principal demandante de energía por parte de los sistemas MBR, excediendo habitualmente el 50% del consumo energético total (Krezeminski et al., 2012). Por tanto, la operación en modo frontal se presenta como una gran alternativa puesto que significaría una elevada reducción de los costes de operación de los MBR. En éste caso el sistema opera sin esfuerzo cortante sobre la membrana lo que se traduce en un incremento del ensuciamiento.

9.3. Avances en el modo de operación

Todos los avances que se realizan en la tecnología MBR están encaminados a la reducción de costes de operación y éstos a su vez, están relacionados con las estrategias para reducir o evitar el ensuciamiento. En los últimos años se han desarrollado modos alternativos de operación que permiten controlar o reducir el ensuciamiento. Casi todas las estrategias se basan en limpiar la membrana para recuperar la resistencia inicial de la misma. La Figura 1.11 muestra distintas estrategias propuestas para modificar las limpiezas físicas y químicas convencionales.

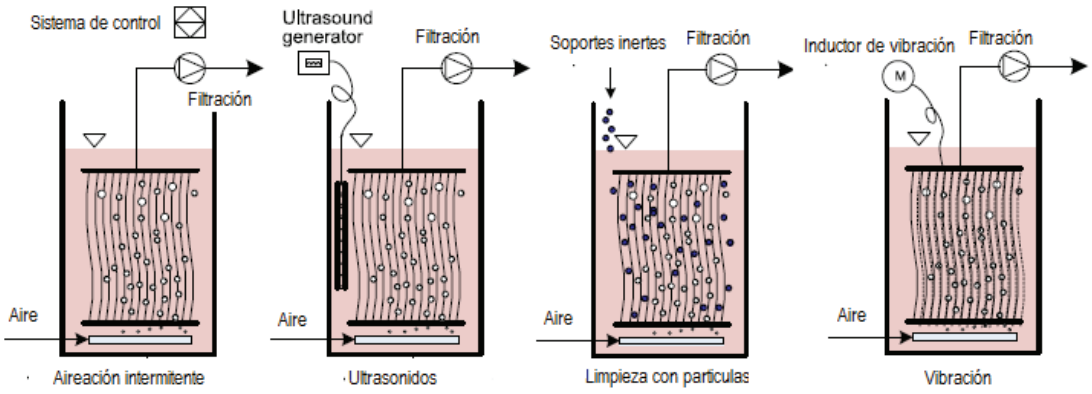

Figura 1.11. Distintos modos de operación alternativos (adaptado Wang et al., 2014).

Una de las primeras modificaciones realizadas a la operación convencional de los MBR fue sustituir la aireación continua por aireación intermitente, estableciendo ciclos de filtración tangencial y frontal, que reducen el ensuciamiento. En los últimos años se han establecido ciclos de alta/baja intensidad de aireación, pues con aireación de baja intensidad no se consigue eliminar las grandes partículas colocadas sobre la membrana que pueden actuar como un pre-filtro y proteger la capa activa de la membrana del bloqueo de poros (ensuciamiento residual o irreversible). Por otro lado, la aireación de alta intensidad permite eliminar la torta formada por las grandes partículas debido al elevado esfuerzo cortante. La combinación de los dos tipos de aireación, con ciclos largos de baja intensidad y cortos de alta intensidad, permite reducir considerablemente el ensuciamiento (Wang et al., 2014).

La adición de soportes inertes a la suspensión biológica parece tener efectos positivos sobre el ensuciamiento, ya que la materia coloidal tiende a absorberse sobre su superficie, y por tanto se reduce el ensuciamiento residual (Wang et al., 2014). Se ha demostrado una alta efectividad del carbón activo como soporte inerte en MBR, en cuanto a la reducción de SMP y EPS (Johir et al., 2011, Johir et al., 2013). No obstante, no se sabe con seguridad los efectos secundarios que puede presentar la incorporación de soportes inertes sobre la superficie de la membrana (Alresheedi et al., 2014).

La vibración o rotación de la membrana puede ser una alternativa a los sistemas convencionales en los que se ejerce un esfuerzo tangencial sobre la membrana. La utilización de ultrasonidos en MBR parece ser una buena práctica, ya que se consigue reducir la concentración de polarización y la torta sobre la membrana (Wang et al., 2014). No obstante, la vibración está

bastante limitada por el bajo rango de frecuencias y la amplitud de la vibración (Bilad et al, 2012). En cambio, la rotación de la membrana parece ser un método más acertado para la reducción del ensuciamiento, debido a la alta turbulencia generada. Se ha demostrado que con giros de 60 rpm se alcanza una alta eficacia de limpieza, que es mejorable cuando esta velocidad se incrementa (Zuo et al., 2010). No obstante, parece que su implantación se enfoca a MBR anaerobios, debido al consumo energético que implica.

Por otro lado, parece bastante intuitivo que una de las mejores alternativas al modo de operación convencional de un MBR es la aplicación de un sistema de control que permita controlar el ensuciamiento y únicamente realizar las limpiezas físicas y/o químicas cuando el sistema alcance un determinado ensuciamiento predeterminado. Este modo de operación alternativo se ha denominado de "presión de consigna" y se basa en iniciar el retrolavado de manera automática, cuando una determinada presión trasmembrana es alcanzada (Villarroel et al., 2013).

10. Modo de operación por presión de consigna

El principal inconveniente de los sistemas MBR es el ensuciamiento de la membrana, que condiciona notablemente los costes de instalación (CAPEX) y los costes de operación (OPEX). El principal parámetro para controlar los CAPEX y OPEX es la selección de un adecuado flujo de filtración. Altos flujos de permeado producen una reducción del área de filtración requerida y por tanto, unos menores CAPEX. Sin embargo, el ensuciamiento de la membrana se ve incrementado al operar a elevados flujos, lo que conlleva un incremento de la frecuencia del retrolavado o un incremento en la aireación de la membrana, y por tanto, un aumento en los OPEX.

Por lo general para evitar el ensuciamiento incontrolado de las membranas y el consiguiente incremento de costes, las plantas MBR a escala industrial, se diseñan y operan en condiciones altamente conservativas. Un reciente estudio comparativo entre grandes instalaciones de MBR en Europa (Lesjean et al., 2009), muestra las diferencias entre las diversas configuraciones. Así, en sistemas con membranas planas se consigue un flujo medio de 32 L/hm^2, mientras que para los sistemas de fibra hueca se alcanza un valor medio de 29 L/hm^2. Sin embargo, en ambos casos se consigue un flujo neto similar, de 18 L/hm^2.

La pérdida de flujo neto está asociada a operaciones de limpieza física (retrolavado o relajación) que son prefijadas en duraciones de 30 a 130 segundos cada 10 ó 25 minutos (Judd, 2011). Además, la tendencia general es operar con bajos flujos, por debajo del flujo crítico, para evitar cualquier posibilidad de ensuciamiento severo de la membrana. Estas dos circunstancias llevan a realizar limpiezas físicas cuando el sistema no lo requiere y por tanto, a perder flujo neto y al aumento de los consumos energéticos derivados de esta operación.

Por otro lado, el modo de operación conservativo, pre-establecido, favorece el envejecimiento de la membrana, ya que en la mayoría de las ocasiones se realizan limpiezas químicas de mantenimiento para evitar el ensuciamiento irreversible cuando todavía, ni siquiera existe ensuciamiento reversible.

La mejora de los modos de operación se debe realizar atendiendo a un control de la filtración ya sea mediante la regulación del aire, la mejora de ciclos de filtración, los retrolavados, la relajación o la adición de reactivos (Ferrero et al., 2012). Atendiendo a esto, una gran alternativa es un control *feedback* que permita establecer el inicio del retrolavado mediante un seguimiento de la permeabilidad, ajustando automáticamente la frecuencia de retrolavado en función del aumento de la presión transmembrana, alcanzando en determinados casos, reducciones de un 40% del agua necesaria para el retrolavado (Smith et al., 2006).

Por tanto, el modo por presión de consigna se propone como un modo alternativo de operación basado en el seguimiento del ensuciamiento de la membrana (Villarroel et al., 2013). En este caso, el retrolavado sólo se inicia cuando una determinada presión transmembrana de consigna es alcanzada. De esta manera los ciclos de filtración son variables ajustándose al ensuciamiento dinámico de la membrana. En el caso de un bajo ensuciamiento, el tiempo de filtración se incrementará, sin embargo, cuando el ensuciamiento sea rápido y alto, la frecuencia del retrolavado se incrementará.

El ensuciamiento de la membrana, en este modo de operación, depende considerablemente de la presión de consigna (TMP_{sp}) seleccionada para el inicio del retrolavado, ya que los mayores flujos netos son alcanzados con TMP_{sp} moderadas (Villarroel et al., 2013).

Sin embargo, los experimentos llevados a cabo con el modo de operación por presión de consigna hasta ahora, han sido de corta duración y a escala de laboratorio, haciendo necesaria la validación de este modo de operación en ensayos de larga duración y en planta piloto.

11. Estructura y justificación de la unidad temática de la tesis

El formato de la presente tesis es por compendio de publicaciones, con seis capítulos de Resultados que se corresponden cada uno, con una publicación. De acuerdo con lo establecido por el Reglamento de Enseñanzas Oficiales de Doctorado de la Universidad de La Laguna, los capítulos de resultados van precedidos de esta introducción para el conjunto del trabajo, un capítulo de objetivos globales de la Tesis y un resumen general de la técnica experimental que se ha seguido durante el desarrollo de todos los capítulos de resultados.

Tras los capítulos de resultados se recoge una discusión global que permite el análisis en conjunto de todas las publicaciones, seguido de un capítulo de conclusiones generales de esta Tesis.

Las seis publicaciones utilizadas para el compendio de publicaciones están englobadas en el análisis y estudio de los biorreactores de membrana como tratamientos terciarios de un efluente convencional de lodos activos. Todos los trabajos comparten el mismo tipo de alimentación y una metodología conjunta que permite el análisis del ensuciamiento de la membrana y la optimización de las variables de operación para un biorreactor de membrana terciario (tMBR).

En el Capítulo 4, que corresponde a la publicación titulada "*Effect of sludge characteristics on membrane fouling during star-up of a tertiary submerged membrane bioreactor*", se analiza la puesta en marcha de un tMBR, poniéndose el foco de atención en la evolución de las características de la suspensión biológica y como éstas afectan al ensuciamiento de la membrana.

Una vez puesto en marcha y estabilizado el MBR como tratamiento terciario, se comparó esta tecnología con un sistema de ultrafiltración directa. El Capítulo 5, que se corresponde con la publicación titulada "*The role of pretreatment of nonofiltration/reverse osmosis for water reuse: Ultrafiltration versus tertiary MBR*", versa sobre un estudio comparativo que analiza en profundidad, el ensuciamiento desarrollado en membranas de baja porosidad o densas, por el permeado procedente de tecnologías de ultrafiltración.

El estudio detallado del ensuciamiento así como, la optimización de los parámetros de operación del tMBR se desarrolla en los Capítulos 6, 7, 8 y 9. En todos estos capítulos se ha

utilizado el modo alternativo de operación basado en la presión transmembrana de consigna para limitar el ensuciamiento de la membrana.

En el Capítulo 6, que se corresponde con la publicación "*Performance of tertiary submerged membrane bioreactor operated at supra-critical fluxes*", se valida el modo alternativo de operación por presión de consigna. Además, se evalúa la operación de un tMBR a flujos supra-críticos en filtración tangencial, analizando la influencia de los principales parámetros de operación: caudal de aireación y flujos de filtración y retrolavado.

El Capítulo 7, que se corresponde con la publicación "*Application of backwashing stratergy based on trasnmembrane pressure set-point in a tertiary submerged membrane bioreactor*", analiza en profundidad el principal parámetro del modo de operación alternativo, la presión transmembrana de set-point o consigna. Por otro lado, se realiza un análisis en profundidad del ensuciamiento de la membrana en un tMBR producido por los fenómenos de consolidación del ensuciamiento.

En el Capítulo 8, que se corresponde con la publicación "*Fouling analysis of a tertiary submerged membrane bioreactor operated in dead-end mode at high fluxes*", se analiza la viabilidad de la operación de un tMBR en filtración frontal. Por otro lado, se analiza la influencia del flujo de filtración y las condiciones del retrolavado sobre el ensuciamiento, lo que ha permitido el desarrollo de un modelo empírico para describir el ensuciamiento residual. Además, la caracterización y modelización del ensuciamiento permite la estimación de las condiciones óptimas de operación.

Por último, el Capítulo 9, que se corresponde con la publicación "*Fouling analysis and mitigation in a tertiary MBR operated under restricted aeration*", estudia y analiza la operación de un tMBR con bajas concentraciones de oxígeno disuelto y con filtración frontal. En este capítulo se evalúa las condiciones óptimas de operación que permitan reducir los costes de operación e instalación. Además, se realiza un estudio del ensuciamiento de la membrana, centrando la atención en los efectos que tienen las condiciones de operación (flujo de filtración y concentración de oxígeno disuelto) sobre la compresibilidad de la torta y el fenómeno de consolidación del ensuciamiento.

Las copias de los artículos ya publicados se encuentran como anexos de la presente Tesis Doctoral, y dentro de cada Capítulo de resultados se encuentran los manuscritos de cada publicación con el formato de general de la Tesis.

En conclusión, todos las publicaciones incluidas en esta tesis por compendio están dentro de la misma unidad temática y conforman en su conjunto una visión globalizada de la tecnología de biorreactores de membrana como tratamiento terciario, analizando en profundidad el ensuciamiento de la membrana como aspecto primordial en la operación de estos sistemas.

12. Referencias

Alresheedi M.T., Basu O.D., Support media impacts on humic acid, cellulose, and kaolin clay in reducing fouling in a submerged hollow fiber membrane system. *Journal of Membrane Science,* 450, (2014), 282-290.

Bacchin, P., Aimar, P., & Field, R. W., Critical and sustainable fluxes: Theory, experiments and applications. *Journal of Membrane Science,* 281(1–2), (2006) 42-69.

Bilad M.R., Mezohegyi G., Deckerck P., Vankelecom I.F.J., Novel magnetically induced membrane vibration (MMV) for fouling control in membrane bioreactors. *Water Research*, 46(1), (2012) 63-72.

Boletin Oficial del Estado, Real Decreto 140/2003 de 7 de febrero, por el que se establecen los criterios sanitarios de la calidad del agua de consumo humano.

Boletin Oficial del Estado, Real Decreto 1620/2007 del 7 de diciembre, por el que se establece el régimen jurídico de la reutilización de las aguas depuradas.

Bolton G., LaCasse D., Kurriyel R., Combined models of membrane fouling: Development and application to microfiltration and ultrafiltration of biological fluids, *Journal of Membrane Science*, 277, (2006), 75-84.

Capodici M., Di Bella G., Di Trapani D., Torregrossa M., Pilot scale experiment with MBR operated in intermittent aeration condition: Analysis of biological performance. *Bioresource Technology* 102 (2011) 5626-5633

Chen, J. P., Kim, S. L., & Ting, Y. P., Optimization of membrane physical and chemical cleaning by a statistically designed approach. *Journal of Membrane Science,* 219, (1–2), (2003) 27-45.

Cote P., Alam Z., Penny J., Hollow fiber membrane life in membrane bioreactors (MBR). *Desalination,* 288, (2012), 145-151

Dalmau M., Monclús H., Gabarrón S., Rodriguez-Roda I., Comas J.. Towards integrated operation of membrane bioreactors: Effects of aeration on biological and filtration performance. *Bioresource Technol*ogy, 171, (2014) 103-112.

Delgado S., Alvarez M., Rodriguez-Gomez L.E.; Aguilar E., H2S Generation in a Reclaimed. Urban Wastewater Pipe. Case study: Tenerife (Spain), *Water Research*, 33 (2), (1999), 539-547.

Delgado S., Álvarez M. , Rodríguez-Gómez L.E., Elmaleh S., Aguilar E., How partial nitrification could improve reclaimed wastewater transport in log pipes. *Water Science and Technology*, 43 (10), (2001), 133-138.

Delgado S., Díaz F., Villarroel R., Vera L., Díaz R., Elmaleh S., Nitrification in hollow-fiber membrane bioreactor. *Desalination*, 146, (2002) 445-449.

Delgado, S., Tendencias en la reutilización de aguas. El caso de Tenerife, T*ecnología del Agua*, nº 236 (2003) 30-42.

Delgado S., Álvarez M., Rodríguez-Gómez L.E., Elmaleh S., Transportation of reclaimed wastewater through a long pipe: Inhibition of sulphide production by nitrite from the secondary treatment. *Enviromental Techology*, 25, (2004), 365-371.

Delgado S., Villarroel R., González E., Effect of the shear intensity on fouling in submerged membrane bioreactor for wastewater treatment. *Journal of Membrane Science,* 311, (2008) 173–181.

Delgado S., Villaroel R., González E., 2010. Submerged membrane bioreactor at substrate-limited conditions: Activity and biomass characteristics. *Water Enviromental Research*, 82 (2010), 202-208

Delgado S., Villarroel R., González E., Morales M., (2011), Aerobic membrane bioreactor for wastewater treatment performance under substrate limited conditions". Darko Matovic (Eds.). Biomass-Detection, Production and Usage. (265-288) Croatia. InTech.

Delrue, F., Stricker, A.E., Mietton-Peuchot M., Recaoult Y. Relationships between mixed liquor properties, operation conditions and fouling on two full-scale MBr plants, *Desalination,* 272, (2011), 9-19.

Drews A., Membrane fouling in membrane bioreactors-Characterization, contradictions, cause and cures. *Journal of Membrane Science*, 363, (2010), 1-28.

Elmaleh S., Delgado S., Alvarez M., Rodríguez-Gómez L.E., Aguilar E., Forecasting of H2O build-up in a reclaimed wastewater pipe. *Water Science and Technology*, 38 (10), (1998) 241-248.

Fan, F., Zhou, H., Husain, H. Identification of wastewater sludge characteristics to predict critical flux for membrane bioreactor processes. *Water Research*, 40, (2006), 205-2012.

Faust L., Temmink H., Zwijnenburg A., Kemperman A.J.B., Rijnaarts H.H.M., Effect of dissolved oxygen concentration on the bioflocculation in high loaded MBRs. *Water Research,* 66, (2014) 199-207.

Fenu A., Roels J., Wambecq T., De Gussem K., Thoeye C., De Gueldre G., Van De Steene B., Energy audit of a full scale MBR system. *Desalination,* 262, (2010), 121-128.

Ferrero G., Rodríguez-Roda I., Comas J., Automatic control systems for submerged membrane bioreactors: A state-of-the-art review. *Water Research*, 46, (2012) 3421-3433.

Foley G., A review of factor affecting filter cake properties in dead-end microfiltration of microbial suspensions. *Journal of Membrane Science*, 274, (2006), 38-46.

Frechen, F. B., Schier, W., & Linden, C., Pre-treatment of municipal MBR applications. *Desalination,*231 (1–3), (2008) 108-114.

Gao, M., Yang, M., Li, H., Wang, Y., Pan, F. Nitrification and sludge characteristics in a submerged membrane bioreactor on syntetic inorganic wastewater. *Desalination.* 170, (2004), 177-185.

Gao D., Fu Y., Tao Y., Li X., Xing M., Gao X., Ren N., Linking microbial community structure to membrane biofouling associated with varying dissolved oxygen concentrations. *Bioresour. Technol.,* 102, (2011) 5626-5633.

Gil J.A., Túa L., Rueda A., Montaño B., Rodríguez M., Prats D. Monitoring and analysis of the energy cost of a MBR. *Desalination,* 350, (2010) 997-1001.

Haberkamp, J., Ernst, M., Böckelmann, U., Szewzyk, U., Jekel, M.. Complexity of ultrafiltration membrane fouling caused by macromolecular dissolved organic compounds in secondary effluents. *Water research,* 42, (2008), 3153-3161.

Hermia J., Constant pressure blocking filtration laws-application to power-law now-newtonian fluids, *Institution of chemical Engineers,* 60 (1982), 183-187

Instituto Nacional de Estadística 2016, (http://www.ine.es/)

Johir, M.A.H., Aryal R., Vigneswatran S., Kandasamy J., Grasmick A.. Influence of supporting media in suspension on membrane fouling reduction in submerged membrane bioreactor, *Journal of Membrane Science*, 374, (2011) 121-128.

Johir, M.A.H., Vigneswaran, S., Sathasivam, A., Handasamy, J., Chang, C.Y., Effect of organic loading rate on organic matter and foulant characteristics in membrane bio-reactor*, Bioresource Technology*, 113, (2012) 154-160.

Johir M.A., Shanmuganathan S., Vigneswaran S., Kandasamy J., Performance of submerged membrane bioreactor (SMBR) with and without the addition of the different particles sizes of GC as suspended medium. *Bioresource Technology,* 141, (2013) 13-18.

Judd S., The MBR Book, 2nd edition, 2011. Principles and Applications of Membrane Bioreactors for Water and Wastewater Treatment. Elsevier, Oxford.

Koch Membrane, Case Study. Aquapolo Ambienal Water Reuse Project, (2004). (http://www.kochmembrane.com/PDFs/Case-Studies/KMS-Sao-Paulo-Brazil-Case-Study.aspx)

Krzeminski P., Van der Graff J.H.J.M., van Lier J.B., Specific energy consumption of membrane bioreactor (MBR) for sewage treatment. *Water Science Technology*, 65 (2012), 380-392.

Le Clech P., Chen V., Fane T.A.G., Fouling in membrane bioreactor used in wastewater treatment. *Journal of Membrane Science*, 284 (2006), 17-53.

Lesjean B., Tazi-Pain A., Thaure D., Moeslang H., Buisson H.,Ten persistent myths and the realities of membrane bioreactor technology for municipal applications. *Water Sci. Technol*. 63, (2011) 32-39.

Lin H.J., Gao W.J., Leung K.T., Liao B.Q., Characteristis of different fractions of microbial flocs and their role in membrane fouling. *Water Science Technology* 63 (2011), 262-269.

Lin, H., Zhang, M., Wang, F., Meng, F., Liao, B.Q., Hong, H., Chen, J., Gao, W. A critical review of extracellular polymeric substances (EPSs) in membrane bioreactors: Characteristics, roles in membrane fouling and control strategies, *Journal of Membrane Science*, 460, (2014), 110-125.

Marketsandmarkets, Membrane bioreactor systems market by application (municipal wastewater treatment and industrial wastewater treatment), by type (hollow fiber, flat sheet, and multi tubular), by configuration (internal/submerged and external/side stream), and by region-trend & forescast to 2019, *Report CH 2651* (2014)

McCarthy A.A., Gilboy P., Walsh P.K., Foley G., Characterization of cake compressibility in dead-end microfiltration of microbial suspensions, *Chemical Engineering Community*, 173 (1999),79-90.

Meng F., Chae S.R., Drews A., Kraume M., Shin H.S., Yang F., Recent advances in membrane bioreactors (MBRs): membrane fouling and membrane material, *Water research*, 43 (2009), 1489-1512.

Ministerio de Agicultura, Alimentación y Medio Ambiente, Memoria anual del Magrama 2014, (http://www.magrama.gob.es/es/ministerio/servicios/publicaciones/Memoria2014_cap.aspx).

Monteagudo Pérez-Machado, T., Rodríguez-Gómez, L.E. Álvarez M., Sistema de dosificación de nitrato en una conducción de trasporte de agua depurada para evitar la generación de sulfuro. Tecnología del Agua, 286, (2007), 44-49.

Montoya F.G., Baños R., Meroño J.E., Manzano-Agugliaro F.M., The research of water use in Spain, *Journal of Cleaner Production,* 112 (2016) 4719-4732

Pirt, S., (1965). The maintenance energy of bacteria in growing cultures. Proc R Soc London, 163B, 224-231.

Rastak C.H., Maarsen K.A., Kooijman S.A.L.M. Effects of protozoa on carbon mineralization in activated sludge. *Water Research*. 30(1), (1996), 1-12.

Rodríguez-Gómez L.E., Delgado S., Álvarez M., Elmaleh S., Inhibition of Sulfide Generation in a Reclaimed WasteWater Pipe by Nitrate Dosage and Denitrification Kinetics. *Water Envirometal Research,* 77 (22), (2005), 193-198.

Rodríguez-Gómez L.E., Álvarez M., Rodríguez-Sevilla J., Marrero M.C., Hernández A., Nitrogen trasnformation of reclaimed wastewater in a pipeline by oxygen injection. *Environmental Technology*, 30 (7), (2009), 715-723.

Rodríguez-Gómez L.E., Álvarez M., Rodríguez-Sevilla J., Marrero M.C., Hernández A., Reclaimed wastewater quality enhancement by oxygen injection during transportation. *Water Science & Technology* 63.4, (2011), 641-648.

Rosenberger S., Kruger U., Witzig R., Manz W., Szewzyk U., Kraume M., Performance of a bioreactor with submerged membrane for aerobic treatment of municipal wastewater. *Water Research*, 36 (2002), 413-420

Rushton A., Ward A.S., Holdich R.G., Solid-Liquid filtration and separation technology. VCH: Weinheim, Germany (1996), 538pp ISBN 3-527-28613-6.

Smith P.J., Vigneswaran S., Ngo H.N., Ben-Aim R., Nguyen H., A new approach to backwash initiation in membrane systems. *Journal of Membrane Science*. 278, (2006) 381-389.

Sørensen B.L., Sørensen P.B., Structure compression in cake filtration, *Journal Environmental Engineering*, 123, (1997) 345-353.

Union Europea, Directiva 2000/60/CE del Parlamento Europeo y del Consejo de 23 de octubre de 2000 por la que se establece un marco comunitario de actuación en el ámbito de la política de aguas.

Van der Broeck R., Krseminski P., Van Dierdonck J., GinsG., Lousada-Ferreira M., Van Impre J.F.M., Van der Graaf J.H.J.M., Smets I.Y., Van Lier J.B., Activated sludge characteristic affecting sludge filterability in municipal and industrial MBRs: unraveling correlations using multi-component regression analysis. *Journal of Membrane Science*, 378 (2011), 330-338.

Villarroel R., Delgado S., González E., Morales M., Physical cleaning initiation controlled by trasnmembrane pressure set-point in a submerged membrane bioreactor, *Separation and Purification Technology* 104, (2013) 55-63.

Wang Z., Ma J., Tang C.Y., Kimura K., Wang Q., Han X., Membrane cleaning in membrane bioreactor: A review. *Journal of Membrane Science*. 468, (2014), 276-307.

Wei Y., Van Houten R., Borger A., Eikelboom D.H., Fan Y. Minimization of excess sludge production for biological wastewater treatment. *Water Research*. 37, (2003), 4453-4467.

Wu J., He C., Zhang Y., Modeling membrane fouling in a submerged membrane bioreactor by considering the roll of solids, colloidal and soluble components. *Journal of Membrane Science*, 397-398 (2012), 102-111.

Zheng, X., Khan, M.T., Croué, J.P. Contribution of effluent organic matter (EfOM) to ultrafiltration (UF) membrane fouling: Isolation, Characterization, and fouling effect of EfOM fraction. Water Research, 65, (2014), 414-424.

CAPÍTULO 2: Introducción

1. Objetivo general
2. Objetivos específicos

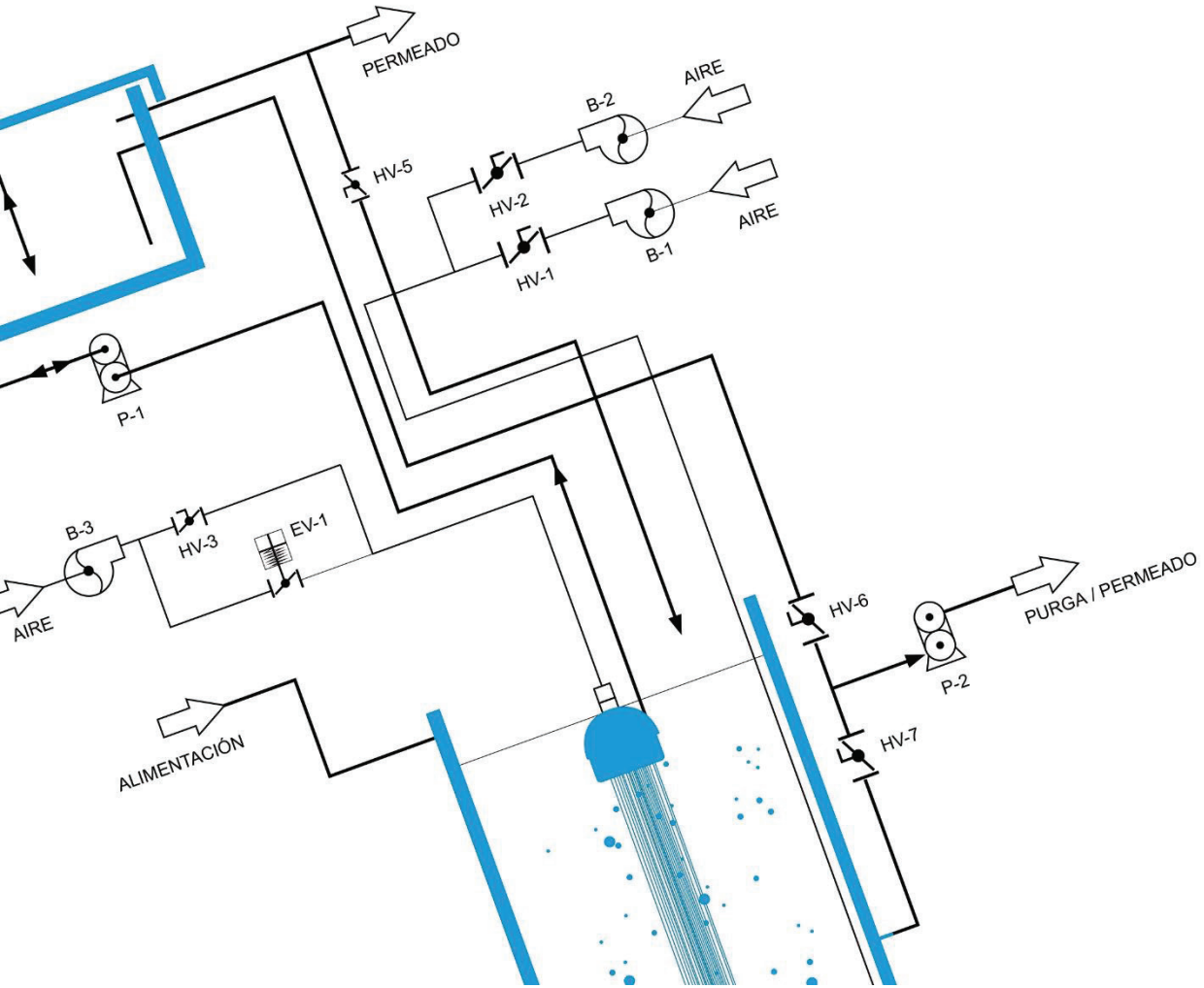

Capítulo 2

Objetivos

1. Objetivo general

El objetivo general de esta tesis es evaluar la viabilidad de la tecnología de biorreactores de membranas sumergidas como tratamiento terciario de un sistema convencional de depuración de aguas residuales domésticas. Concretamente, el foco de atención se ha centrado en estudiar el ensuciamiento experimentado por las membranas y en optimizar las variables de operación que influyen en dicho ensuciamiento, con el fin de minimizarlo y poder así reducir los costes de explotación. En el desarrollo de esta tesis se ha evaluado un modo de operación de los biorreactores, alternativo al modo de operación temporizado, basado en establecer previamente el ensuciamiento permitido en la membrana.

2. Objetivos específicos

Para alcanzar el cumplimiento del objetivo general se han planteado los siguientes objetivos específicos:

- Analizar las condiciones de operación óptimas de un biorreactor de membrana sumergidas terciario operado a escala piloto, alimentando con agua real, en función de la calidad del influente recibido y las características de la suspensión biológica (Capítulo 4).

- Realizar un estudio comparativo del ensuciamiento de las membranas, el rendimiento de depuración y la reducción de contaminantes emergentes alcanzado por dos sistemas de membrana sumergida, operados en paralelo: un biorreactor de membrana terciario y una ultrafiltración directa (Capítulo 5).

- Analizar la influencia de las características de la suspensión biológica desarrollada en el biorreactor de membrana sobre el ensuciamiento (Capítulos 4, 5, 6, 7, 8 y 9).

- Analizar y desarrollar correlaciones matemáticas entre las características de la suspensión, el agua de alimentación y el ensuciamiento experimentado por las membranas (Capítulos 4 y 9).

- Estudiar la influencia relativa de las distintas fracciones constitutivas de la suspensión biológica sobre el ensuciamiento global de las membranas sumergidas (Capítulos 5 y 6).

- Evaluar la viabilidad de un modo alternativo de operación de biorreactores de membrana sumergida, basado en el inicio automático del retrolavado en función del ensuciamiento permitido a la membrana, a partir de los principales parámetros de operación: flujos de filtración y retrolavado, presión trasmembrana de consigna y modo de filtración (tangencial o frontal) (Capítulos 6, 7, 8 y 9).

- Analizar el efecto del retrolavado sobre la re-dispersión del ensuciamiento logrado durante el retrolavado y su re-deposición (Capítulos 7 y 8).

- Estudiar el ensuciamiento reversible, profundizando en el estudio de la compresibilidad de la torta y su dependencia tanto de los parámetros de operación como de las características de la suspensión (Capítulo 8 y 9).

- Desarrollar modelos matemáticos para la predicción del ensuciamiento residual cuando el sistema opera con el modo por presión de consigna (Capítulos 8 y 9).

- Efecto de las limpiezas químicas de recuperación sobre la membrana (Capítulos 4, 7 y 8).

- Analizar la concentración óptima de oxígeno disuelto en el proceso biológico, para permitir la nitrificación de la alimentación sin afectar a la productividad del biorreactor de membranas (Capítulo 9).

CAPÍTULO 3: Técnica experimental

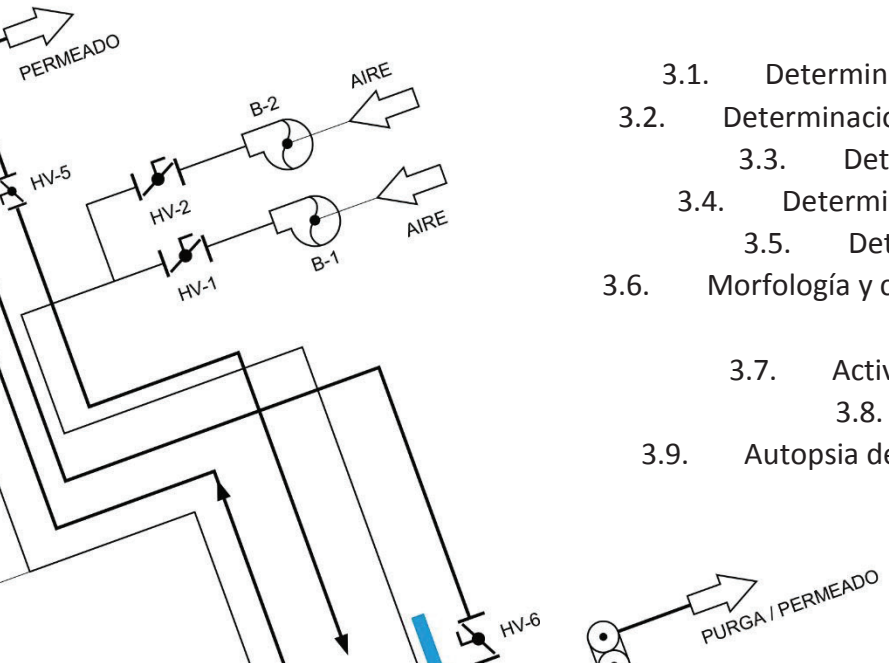

Capítulo 3

Técnica experimental

1. Instalaciones y procedimiento experimental a escala piloto

La experimentación realizada en el marco de la presente Tesis Doctoral ha sido realizada en instalaciones a escala piloto ubicadas en la estación de bombeo de aguas depuradas de Santa Cruz de Tenerife, gestionada por la Entidad Pública Empresarial-Balsas de Tenerife-BALTEN. Las instalaciones reciben directamente el efluente depurado en la Estación Depuradora de Aguas Residuales-EDAR de lodos activos de S/C de Tenerife, sin ningún tipo de pretratamiento.

1.1. Instalación experimental ZW-10

1.1.1. Descripción del sistema

La unidad piloto ZeeWeed®-10 (ZW-10) es una instalación comercial suministrada por GE Water & Process Tecnologies (GE, EEUU). Las Figuras 3.1 y 3.2 corresponden a una fotografía de las instalaciones y un diagrama general de la planta piloto, respectivamente.

Figura 3.1. Fotografía de las instalaciones a escala piloto

La instalación permite dos configuraciones: Filtración con “Recirculación parcial” (ZenoGem® System) o “Filtración directa“(Direct Filtration System). En la primera configuración se elimina sólo una parte del permeado y el resto se recircula al depósito de membrana (biorreactor), además no se genera corriente de rechazo, es decir, se opera sin purga de lodos.

Por el contrario, en “Filtración directa” se extrae todo el permeado y se genera una línea de rechazo. Cada configuración se regula mediante las válvulas manuales HV-5, HV-6 y HV-7, como se puede observar en la Figura 3.2.

Los Capítulos de resultados 4 y 5 se llevaron a cabo con la configuración de “Filtración directa”, cerrando la válvula HV-5 y HV-6; y manteniendo abierta la HV-7, en el caso de realizar extracción de rechazo o purga de lodos. Por el contrario, el resto de Capítulos de resultados se realizaron con la configuración de “Recirculación parcial”, cerrando HV-7 y manteniendo abiertas las válvulas HV-5 y HV-6. Con esta última configuración se consigue independizar el tiempo de retención hidráulico de las condiciones de filtración.

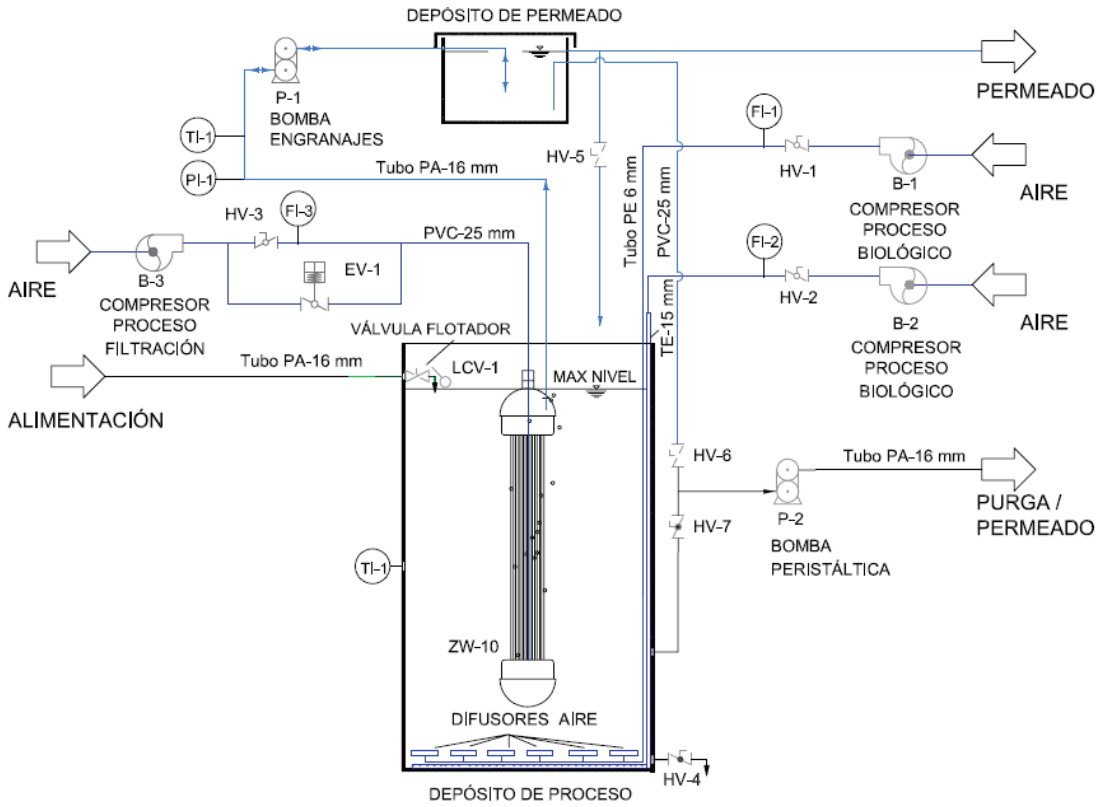

Figura 3.2. Diagrama de la instalación ZW-10

El agua clarificada procedente del tratamiento secundario de la EDAR de S/C de Tenerife, accede al depósito de proceso o biorreactor a través de una válvula de flotador (LCV-1).En dicho depósito tiene lugar la depuración biológica. Una vez depurado, el efluente se extrae a través de la membrana mediante una microbomba de engranajes (P-1) y se conduce hasta el depósito de permeado. En la configuración "Recirculación parcial", una bomba peristáltica (P-2) regula la salida de una parte del permeado del sistema y el resto se retorna al depósito de proceso por gravedad. Por el contrario, mediante la configuración de "Filtración directa" la bomba P-2 extrae el rechazo del depósito de proceso mientras que el permeado es eliminado por gravedad. El sistema presenta un sistema de aireación para el proceso biológico compuesto por dos compresores y sus correspondientes sistemas de control. Por otro lado, el sistema permite mantener aireadas las fibras para reducir el ensuciamiento de la membrana, mediante el compresor (B-3) y su sistema de control. Por último, la bomba de engranajes P-1 admite la inversión del flujo que permite el retrolavado de la membrana, permitiendo controlar el ensuciamiento de la misma.

1.1.2. Elementos principales y especificaciones

En este apartado se detallan los principales elementos y las especificaciones de la instalación experimental.

Depósito de proceso o biorreactor, es un recipiente de polietileno con una capacidad máxima de 254 L y un volumen útil de 220 L, que alberga el bastidor de membranas ligeramente suspendido sobre el fondo del tanque. El control del nivel superior del líquido en el depósito se ejerce mediante la válvula de flotador (LCV-1). Las fibras del módulo de membranas deben permanecer cubiertas, por lo tanto, cuando el sistema alcanza un nivel de seguridad mínimo debido a un fallo en la alimentación, la bomba peristáltica P-2 se para y el sistema comienza a operar en circuito cerrado. Una vez que se recupera un nivel de líquido aceptable, el sistema comienza a operar con normalidad. La aireación para el proceso biológico se realiza mediante compresores que suministran un caudal constante para poder conseguir la depuración biológica, además, generan turbulencia que permite mantener el licor mezcla en suspensión. El compresor RESUN LP-60 (B-1 en la Figura 3.2) con una potencia de 60W, se encuentra conectado a una tubería perforada que abarca todo el perímetro del fondo del depósito de proceso y cuya misión es proporcionar burbujas gruesas que favorezcan la agitación del sistema. El caudal suministrado es regulado por una válvula manual (HV-1) y un rotámetro (FI-1). El segundo compresor BIBUS SV-50 (B-2) con una potencia de 118W se encuentra conectado a difusores de burbuja fina, los cuales

favorecen la transferencia de oxígeno. Al igual que en caso anterior, el caudal de aire se regula con una válvula manual (HV-2) y un rotámetro (FI-2).

La bomba de permeado (P-1), MICROPUMP® I-DRIVE, permite generar el vacío necesario para poder realizar la filtración del licor mezcla a través de la membrana. Además, permite obtener un flujo constante de permeado que es regulado mediante el sistema de automatización de la instalación experimental. La bomba es un sistema de impulsión de desplazamiento positivo rotatorio que permite realizar además, los retrolavados. El vacío o sobrepresión generado por la bomba se mide con un manómetro DMP 331 de la casa comercial SENSOTEC (PI-1).

Depósito de permeado y bomba de purga, el depósito de permeado está fabricado en polietileno y tiene una capacidad máxima de 27 L. Parte del permeado se utiliza para el retrolavado de las membranas. En el caso de que el volumen de permeado extraído sea superior a la capacidad máxima del depósito, el permeado retornará por gravedad al biorreactor o se extraerá. La bomba de purga de permeado (P-2) es una bomba modelo ALPB04 (220V/3f) que se controla de manera manual y permite establecer el caudal de permeado que se extrae del sistema y por tanto, establece el tiempo de residencia hidráulico. De esta manera podemos mantener este parámetro independiente del flujo de permeado, permitiendo mayor versatilidad de la instalación.

Compresor de aire para el proceso de filtración (B-3), MEDO LA-120 (B-2) con una potencia de 118W, proporciona el aire necesario para la limpieza de la membrana durante la filtración. Dicho compresor está conectado directamente al sistema de automatización, en donde se regula su funcionamiento. De esta manera el sistema permite trabajar con distintas frecuencias de aireación que son predefinidas por el usuario. El caudal suministrado es regulado por una válvula manual (HV-3) y un rotámetro (FI-3). Además, el sistema de automatización permite la activación del compresor B-3 y la electroválvula EV-1 durante el retrolavado, para mejorar la eficacia de la limpieza física. En este caso el sistema opera con el máximo caudal que permite el compresor (SAD_m = 3,1 Nm^3/hm^2).

Sistema de automatización, el sistema está controlado y monitorizado mediante un ordenador, el cual registra los datos de presión y flujos de la unidad utilizando un dispositivo de adquisición de datos Labjack U12. Además, permite establecer todas las variables del sistema, así como controlar la bomba de permeado o la aireación de la membrana, mediante un software realizado en el entorno de desarrollo DAQ Factory Express 5.79A (Figura 3.3).

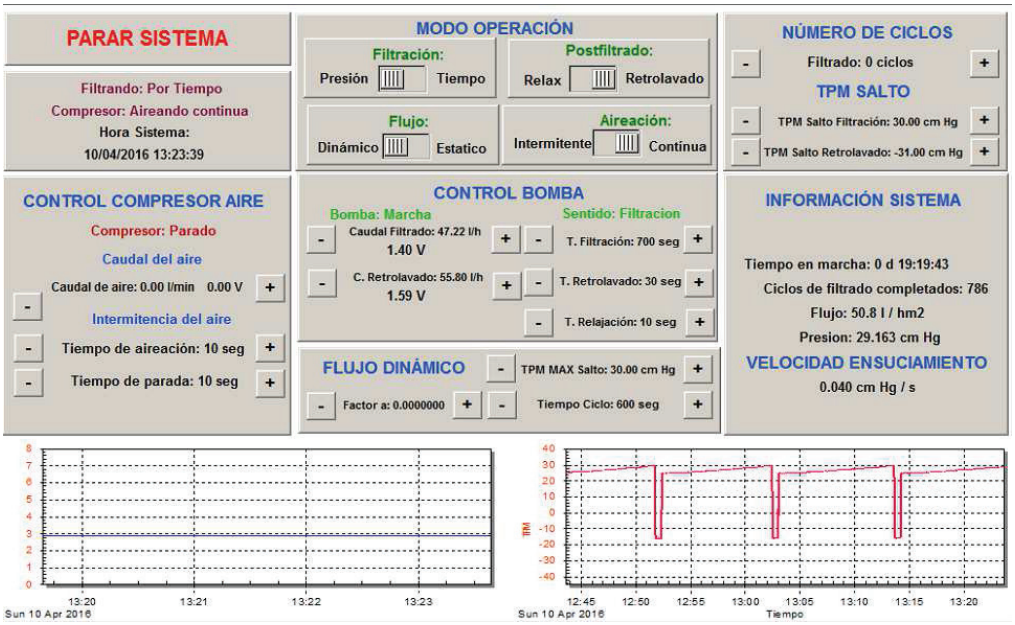

Figura 3.3. Detalle de las variables controladas y monitorizadas mediante el software

1.1.3. Módulo de membranas

El módulo de membrana (Figura 3.4) utilizado es el ZeeWeed-10 (ZW-10), que posee un haz de fibras huecas poliméricas, asimétricas, hidrófilas, con capa activa externa de polivinildifloruro (PVDF) y con un diámetro medio de poro de 0,033 µm. El módulo está compuesto por 150 fibras huecas dispuestas verticalmente, de unos 60 cm de longitud, lo que le confiere una superficie activa de 0,93 m^2.

El sistema opera con el módulo sumergido en el interior del biorreactor y la filtración tiene lugar desde el exterior al interior de las fibras mediante el vacío generado por la bomba de permeado. Entre los dos cabezales que soportan las fibras existe un tubo de aireación que dispone de perforaciones en su zona inferior para la formación de burbujas gruesas de aire, las cuales actúan como promotores de turbulencia para reducir el ensuciamiento de las fibras. El permeado se extrae sólo por el cabezal superior.

La Tabla 3.1 muestra los límites de operación del módulo, indicados por el fabricante.

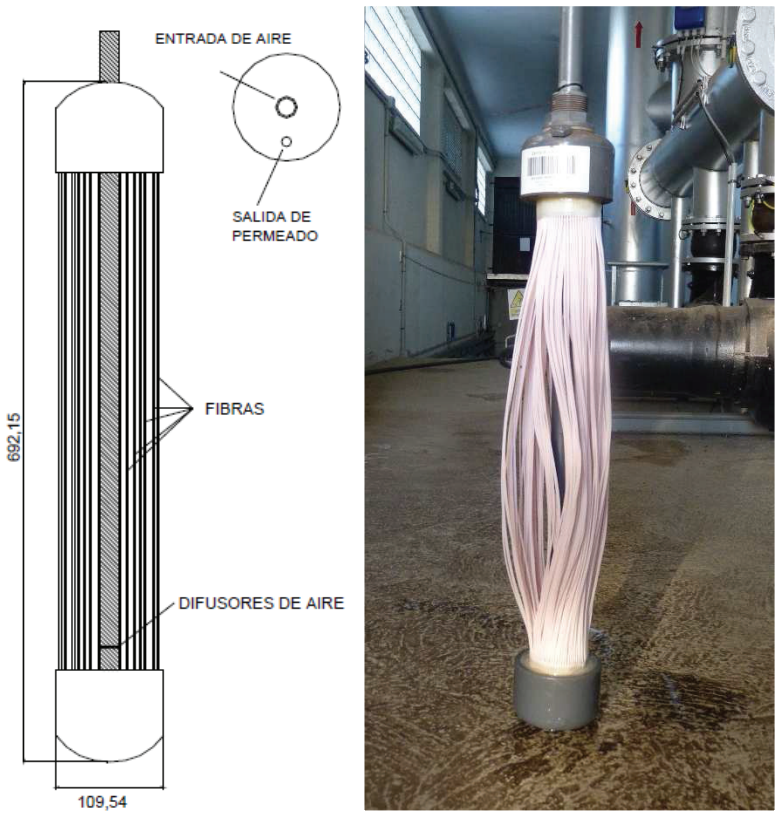

Figura 3.4. Módulo de membrana ZW-10.

Tabla 3.1. Límites de operación del módulo ZW-10

PARAMETRO	UNIDAD	VALOR
Máximo valor de TMP	kPa	62
Rango de operación de TMP	kPa	10-50
Máximo valor de TMP de retrolavado	kPa	55
Máximo valor de Temperatura	^{0}C	40
Rango de operación de pH	-	5-9
Máxima concentración de hipoclorito	mg/L	1000

1.2. Metodología

1.2.1. Caracterización de la membrana

La resistencia que ofrece la membrana al flujo de un fluido es uno de los parámetros que permiten caracterizarla, puesto que está relacionado con las características y naturaleza del material de la misma, el diámetro de poro, la porosidad superficial y el espesor de la membrana. La ley de Darcy (ecuación 3.1) relaciona la resistencia de la membrana con el flujo de filtración, la viscosidad del fluido permeado y la presión transmembrana aplicada.

$$R_m = \frac{TMP}{\mu \cdot J} \qquad [3.1]$$

Donde R_m es la resistencia de la membrana, TMP es la presión trasmembrana, μ es la viscosidad del permeado y J es el flujo de filtración.

El ensuciamiento de la membrana provoca la modificación de sus propiedades y la pérdida de permeabilidad que obliga a la regeneración de la misma. Para poder comparar distintos ensayos, es necesario conocer el grado de regeneración alcanzado y por tanto, definir un estado de referencia de la membrana. Cabe destacar que el estado de referencia no es el de la membrana nueva, sino aquel estado al que se llega sistemáticamente después de sucesivas regeneraciones. Para el desarrollo de esta Tesis se utilizaron dos membranas ZW-10, que ya fueron estandarizadas en ensayos previos no incluidos en esta Tesis Doctoral. Para facilitar el estudio se han codificado las dos membranas como ZW-10A y ZW-10B. Cada una de ellas tras un proceso de regeneración, fue sometida a un ensayo de caracterización, el cual se basa en filtrar agua blanca a distintos flujos de filtración y analizar la presión transmembrana (TMP) alcanzada.

La Figura 3.5 muestra los valores de TMP encontrados para distintos flujos de filtración en los ensayos de caracterización correspondientes. Como se puede observar cada membrana posee una resistencia estándar, la membrana ZW-10A presenta una resistencia estándar de $4{,}9 \cdot 10^{11}$ m^{-1}, en cambio la resistencia de la membrana ZW-10B es de $9{,}5 \cdot 10^{11}$ m^{-1}. Los estudios llevados a cabo en los Capítulos 4 y 5 fueron desarrollados con la membrana ZW-10B mientras que la membrana ZW-10A fue la utilizada en los ensayos correspondientes a los Capítulos 6, 7, 8 y 9.

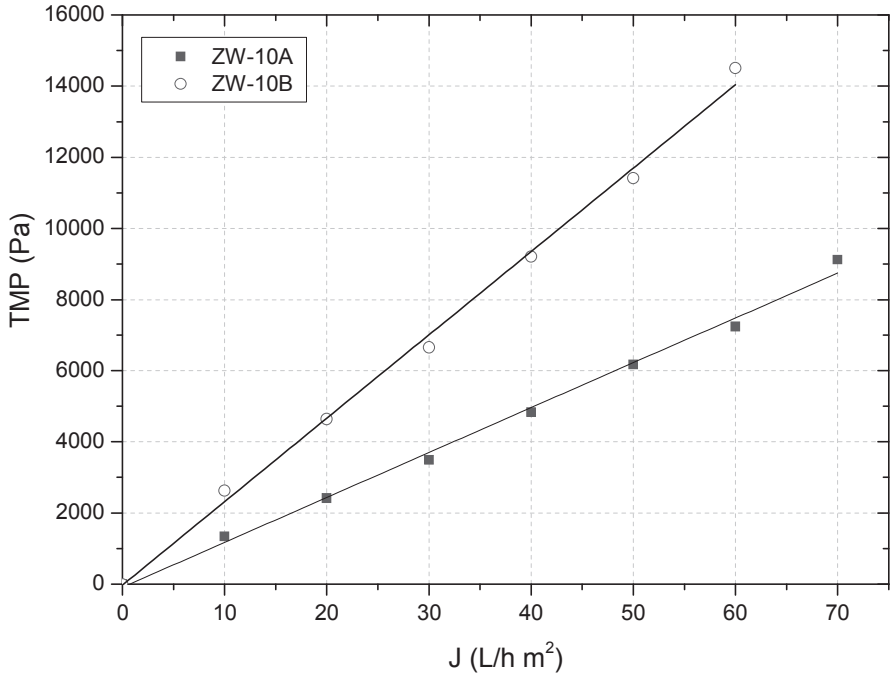

Figura 3.5. Caracterización de las membranas ZW-10A y ZW-10B

1.2.2. Experimentos de corta duración. Determinación del flujo crítico

La determinación del flujo crítico se ha llevado a cabo mediante la realización de experimentos escalonados. Estos ensayos de corta duración se basan en aplicar sucesivos incrementos de flujo hasta un máximo, tal y como se describe en Le-Clech et al. (2003). Para reducir la influencia del ensuciamiento histórico se han introducido, antes de cada incremento de flujo, un corto periodo de relax que permite la eliminación parcial del mismo (Van der Marel et al., 2009). Sin embargo, el método modificado propuesto en la presente Tesis sustituye los cortos periodos de relax por retrolavados. Este tipo de limpieza física permite asemejar los experimentos de corta duración con la operación convencional de un MBR.

En cada experimento de corta duración se fijaron las siguientes variables:

- Flujo inicial y final de filtración
- Incremento de flujo en cada escalón
- Duración de cada escalón
- Caudal de aireación

- Presión de seguridad
- Condiciones del retrolavado
    - Flujo
    - Duración
    - Aireación

El estudio del flujo crítico conlleva el seguimiento de la velocidad de ensuciamiento dentro de cada escalón de flujo así como de la presión transmembrana inicial en cada escalón. Finalmente, la descripción del procedimiento experimental seguido en cada capítulo se encuentra desarrollada en el apartado de "materiales y métodos" del mismo.

1.2.3. Experimentos de larga duración

Los experimentos de larga duración fueron llevados a cabo aplicando dos modos de operación distintos: el modo temporizado y el modo por presión de consigna. El primero se basa en prefijar la frecuencia de la limpieza física de la membrana, de esta manera el retrolavado o relax se lleva a cabo siempre, tras un tiempo predeterminado de filtración. Por el contrario, el modo de operación por presión de consigna establece un ensuciamiento máximo permitido, iniciando la limpieza física (retrolavado o relax) cuando este es alcanzado. Es decir, se predetermina una presión transmembrana de consigna (TMP_{sp}) y el retrolavado se inicia inmediatamente después de que esta es alcanzada. Por tanto, se trata de un modo de operación que permite ajustar automáticamente la frecuencia del retrolavado en función del ensuciamiento de la membrana.

Para cada serie experimental se fijaron y midieron las siguientes variables:

- Proceso biológico
    - Edad de lodo (SRT)
    - Tiempo de residencia hidráulico (TRH)
    - Concentración de oxígeno disuelto (DO)
- Proceso de filtración
    - Caudal de aireación o intermitencia durante la filtración
    - Flujo de permeado (J)
    - Condiciones de retrolavado: Flujo y duración (J_b y t_b, respectivamente)
    - Tiempo de filtración (t_f), para el modo de operación temporizado

- Presión transmembrana de consigna (TMP_{sp}) para el modo de operación por presión de consigna.

Asimismo, durante cada serie experimental se hizo seguimiento de la evolución de la presión transmembrana (TMP) con el tiempo. Además, se analizaron periódicamente los parámetros descritos en la Tabla 3.2, para las tres corrientes indicadas, con el fin de estudiar el proceso de depuración y caracterizar la suspensión biológica o licor mezcla.

Tabla 3.2. Seguimiento analítico a las distintas corrientes (siendo: A, alimentación; LM, licor mezcla o suspensión biológica; P, permeado)

PARAMETRO	A	LM	P
Demanda química de oxigeno total y soluble (COD)	x	x	x
Carbono orgánico disuelto (DOC)	x	x	x
Demanda biológica de oxígeno (BOD_5)	x		
Solidos suspendidos totales (TSS o MLSS)	x	x	
Solidos suspendidos volátiles (VSS o MLVSS)	x	x	
Turbidez	x		x
Nitrógeno total	x		x
Nitrógeno amoniacal	x		x
Nitratos	x		x
Nitritos	x		x
Color	x		x
Distribución de tamaño de partículas		x	
Turbidez del sobrenadante		x	
Viscosidad		x	
Actividad biológica		x	
“Time to filter “ (TTF)		x	

Por último, indicar que la descripción del procedimiento experimental seguido en cada capítulo se encuentra desarrollada en los correspondientes apartados de "materiales y métodos" de cada uno de ellos.

1.2.4. Protocolo de limpieza de la membrana

Las limpiezas de regeneración se han realizado al concluir cada ensayo o bien, cuando se alcanza, durante la operación normal de la instalación, valores de la TMP cercanos al máximo permitido (66 kPa). En el desarrollo de esta Tesis se han llevado a cabo dos tipos de limpiezas de regeneración: las de recuperación de la membrana y las de caracterización del ensuciamiento.

A.- LIMPIEZAS DE RECUPERACIÓN: Este tipo de limpieza se llevó cabo en el marco de los Capítulos 4 y 5; y después de cada experimento de flujo escalonado. Esta limpieza requiere una eliminación previa de todos aquellos sólidos más gruesos que se hayan depositado en la superficie de las fibras, mediante la inyección a presión de agua de red. A continuación, el módulo se sumerge en una disolución de NaClO (500 mg/L) durante 24 horas y a temperatura ambiente. Una vez transcurridas las 24 horas y tras un enjuague en agua de red, se realiza un ensayo de caracterización de la membrana filtrando agua blanca, para evaluar la resistencia de la misma y determinar si la limpieza ha sido efectiva.

B.- CARACTERIZACIÓN DEL ENSUCIAMIENTO: Este tipo de limpieza se realizó en el marco de los Capítulos 7, 8 y 9. Esta limpieza de regeneración requiere de las siguientes etapas:

I- Enjuague con agua Milli-Q

II- Retrolavado con agua Milli-Q a un flujo de 90 L/hm^2 durante 15 minutos.

III- Limpieza química con NaOH (ph=11) durante 24 horas

IV- Limpieza química con NaClO (500 mg/L) durante 24 horas

Después de cada una de las etapas descritas, se caracterizó la membrana para evaluar la resistencia remanente tras cada limpieza. Las soluciones resultantes del enjuague, retrolavado y limpiezas químicas fueron asimismo, analizadas en términos de carbono orgánico disuelto (DOC) y sólidos suspendidos totales (TSS). En el caso de que la membrana no consiguiera regenerarse adecuadamente se han incluido dos etapas adicionales al protocolo de limpieza:

V- Limpieza química con ácido cítrico (6000 mg/L) durante 24 horas

VI- Limpieza química con NaClO (500 mg/L) durante 24 horas

No obstante, las condiciones de la limpieza de recuperación aplicadas en cada ensayo se encuentran descritas con mayor grado de detalle, en los apartados "materiales y métodos" de los correspondientes capítulos.

2. Instalaciones y procedimiento experimental a escala laboratorio

2.1. Instalación experimental ZW-1

2.1.1. Descripción del sistema

La instalación ZW-1 es una unidad de filtración a escala de laboratorio que permite operar con la membrana ZeeWeed®-1 (ZW-1) y que se ha utilizado para estudiar las contribuciones relativas de las distintas fracciones presentes en el licor mezcla: materia particulada, coloidal y soluble, sobre el ensuciamiento global de la membrana. Esta instalación permite operar con el mismo sistema de control y monitorización utilizado en la planta piloto. En las figuras 3.6 y 3.7 se muestra una imagen de la instalación y el diagrama general de la misma, respectivamente.

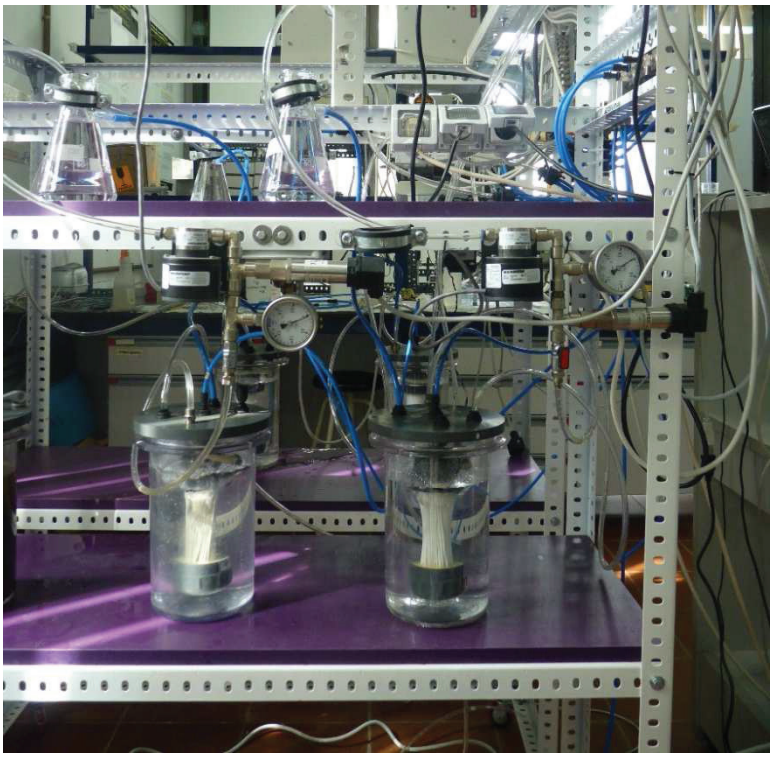

Figura 3.6. Instalación a escala de laboratorio ZW-1

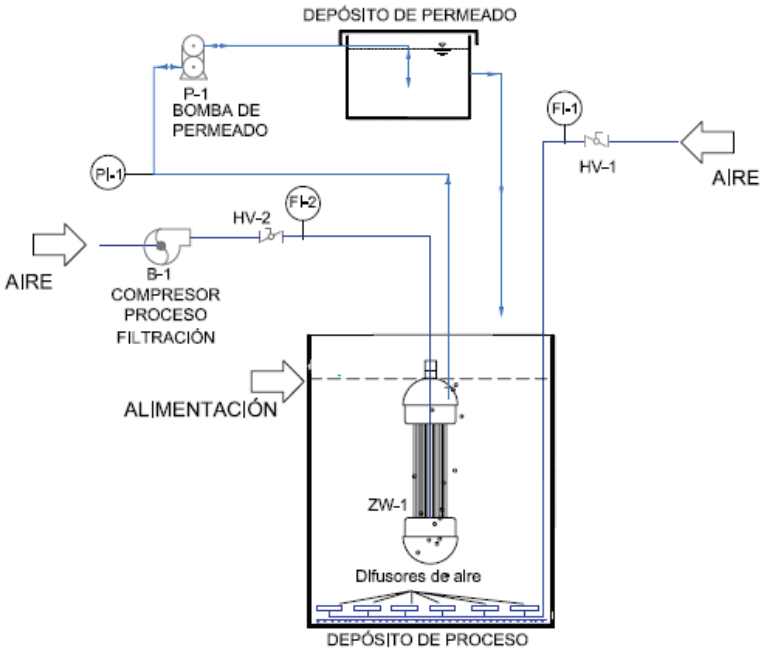

Figura 3.7. Diagrama general de la instalación de laboratorio ZW-1

La suspensión objeto de estudio se introduce en el depósito de proceso de 1,5L de volumen y una altura de columna de agua de 21 cm. El depósito está fabricado en polietileno de alta densidad y se ubica sobre una placa agitadora que permite mantener la homogeneidad de la suspensión. El sistema, además, presenta una tubería perforada de polietileno, que abarca todo el perímetro del fondo del depósito de proceso, con la finalidad de proporcionar burbujas finas que permiten mantener las condiciones aerobias durante el experimento. Este aire suministrado por el sistema externo de aire comprimido, se regula mediante una válvula manual (HV-1) y un rotámetro (FI-1). El suministro de aire para las limpiezas de la membrana se realiza mediante un compresor MK-10 (Secoh Shangai MEC LTD) activado por medio del sistema de automatización de la instalación. El caudal proporcionado es regulado mediante una válvula manual (HV-2) y un rotámetro (FI-2).

El efluente se extrae a través de la membrana mediante una microbomba de engranajes (P-1) y se conduce hasta el depósito de permeado. Se trata de una bomba MICROPUMP® I-DRIVE que permite generar el vacío necesario para poder realizar la filtración a través de la membrana. Además, permite obtener un flujo constante de permeado que es regulado mediante el sistema de automatización de la instalación experimental. La bomba consiste en un sistema de impulsión de desplazamiento positivo rotatorio. El vacío o sobrepresión generado por la bomba se mide con

un manómetro DMP 331 de la casa comercial SENSOTEC (PI-1). La filtración se realiza en circuito cerrado es decir, el permeado se recircula en su totalidad al depósito de proceso.

La instalación experimental está controlada mediante un ordenador que también registra los datos de presión y flujos de la unidad utilizando un dispositivo de adquisición de datos Labjack U12. Además, permite establecer todas las variables del sistema, así como controlar la bomba de permeado o la aireación de la membrana, mediante un software realizado en el entorno de desarrollo DAQ Factory Express 5.79A, idéntico al utilizado en la planta piloto ZW-10.

2.1.2. Módulo de membrana

El módulo de membranas utilizado es el ZW-1, el cual posee fibras con características idénticas a las del módulo ZW-10. La principal diferencia es la escala del módulo, ya que el ZW-1 presenta una superficie filtrante de 0,047 m^2. Al igual que el módulo a escala piloto, las fibras se disponen de forma vertical en torno a un eje central cuya función es conducir el aire hasta la base del módulo. El rango de condiciones de operación es idéntico al del módulo ZW-10 (ver Tabla 3.1).

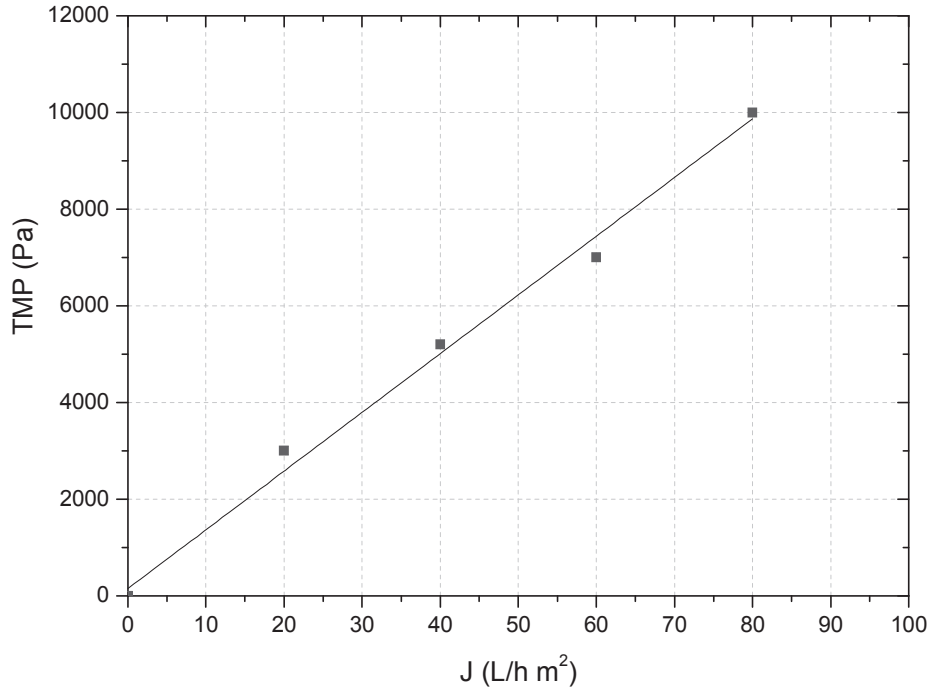

Figura 3.8. Caracterización de la membrana ZW-1

2.1.3. Caracterización de la membrana

Como ya se ha indicado anteriormente, el estado de referencia de la membrana es aquel estado al que se llega sistemáticamente después de sucesivas regeneraciones de la membrana. Los ensayos realizados en el laboratorio fueron llevados a cabo con una membrana ZW-1 ya estandarizada en ensayos previos no incluidos en la presente memoria. La Figura 3.8 muestra los valores obtenidos de presión transmembrana al filtrar agua de red a distintos valores de flujo de permeado. La resistencia de la membrana de referencia, obtenida de forma análoga a la ZW-10, es de $5{,}2 \cdot 10^{11}$ m^{-1}. Al iniciar cada experimento se ha caracterizado la membrana con el fin de evaluar el grado de recuperación alcanzado al aplicar el protocolo de limpieza.

2.1.4. Procedimiento experimental. Fraccionado de la suspensión o licor mezcla

La instalación de laboratorio ZW-1 fue utilizada para ensayos cortos que permiten analizar la contribución relativa de las distintas fracciones que componen la suspensión filtrante sobre el ensuciamiento global de la membrana. La suspensión ha sido divida en tres fracciones: particulada, coloidal y soluble, tal y como se resume en la Tabla 3.3.

Tabla 3.3. Fraccionado de la suspensión

	CAPITULO 5	**CAPITULO 6**
Suspensión a estudio	Partículas	Sedimentables
		No sedimentables(>1,5µm)
	Macro-coloides	Coloides entre 0,45 µm y 1,5 µm
	Micro-coloides y solutos	Coloides entre 0,22 µm y 0,45 µm
		Solutos y coloides < 0,22µm

En el Capítulo 5 la suspensión se divide en tres fracciones claramente diferenciadas: las partículas, los macro-coloides y los micro-coloides y solutos. Por el contrario, en el Capítulo 6 esas tres fracciones se dividen en cinco: partículas sedimentables, no sedimentables (>1,5 µm), coloides entre 0,45 µm y 1,5 µm, coloides entre 0,22 µm y 0,45 µm y solutos y coloides menores a 0,22 µm. Para llevar a cabo el fraccionamiento de los distintos componentes de la suspensión se realizaron dos procedimientos bastante similares. En el primer caso, la suspensión fue fraccionada

mediante filtros de microfibra (Millipore) de diferente tamaño de poro nominal, 1,5 µm y 0,45 µm, que permite obtener las tres fracciones.

En el Capítulo 6, la suspensión es sometida inicialmente, a un ensayo de sedimentación en un cilindro de 3L durante 30 minutos, según el método normalizado 2710 C (ALPHA, 2005), de esta manera se puede obtener una fracción sin los sólidos sedimentables. Posteriormente, esta fracción es filtrada sucesivamente por filtros de microfibra (Millipore) de un tamaño de poro nominal de 1,5 µm, 0,45 µm y 0,22 µm, para obtener las fracciones detalladas en la Tabla 3.3.

A cada una de las fracciones se le somete a un ensayo de filtración en la unidad de laboratorio ZW-1. Se trata de un experimento de 30 minutos donde se analiza la evolución de la presión transmembrana (TMP) con el tiempo. Para cada experimento se estableció el flujo de filtración y el modo de operación entre filtración frontal o tangencial. Para éste último caso, se estableció un caudal de aireación de la membrana.

Finalmente, la descripción del procedimiento experimental seguido en cada capítulo se encuentra desarrollada en el apartado de "materiales y métodos" del mismo

2.1.5. Protocolo de limpieza de la membrana

Al finalizar cada experimento la membrana es sometida a un protocolo de limpieza que permite su regeneración. Dicho protocolo requiere la eliminación previa de todos aquellos sólidos gruesos que se hayan depositado en la superficie de las fibras. Este proceso se lleva a cabo mediante la inyección de agua de red a presión. A continuación, el módulo se sumerge en una disolución de NaClO (500 mg/L) durante 24 horas, a temperatura ambiente. Después de cada etapa se caracteriza la membrana con agua de la red para evaluar la resistencia de la misma.

2.2. Instalación experimental SEPA CF II

2.2.1. Descripción del sistema

La celda de membranas SEPA CF II es una unidad a escala laboratorio que permite realizar operaciones de filtración en flujo cruzado. Su diseño, patentado por Sterlitech, simula la dinámica de flujo de los módulos de arrollamiento en espiral utilizados en el ámbito industrial y proporciona datos de rendimiento precisos para una cantidad mínima de producto. Mediante la combinación de una serie de separadores de acero inoxidable, espaciadores y membranas, pueden modificarse las condiciones de operación y la dinámica del flujo.

Las Figuras 3.9 y 3.10 muestran una fotografía de la instalación experimental y un diagrama general de la misma, respectivamente.

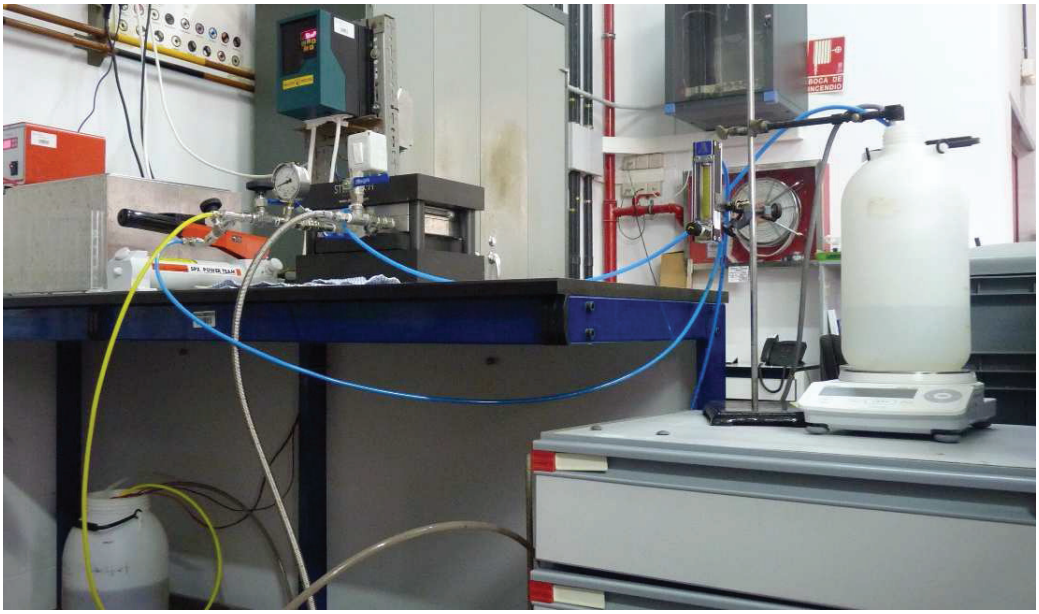

Figura 3.9. Celda de membranas SEPA CF II

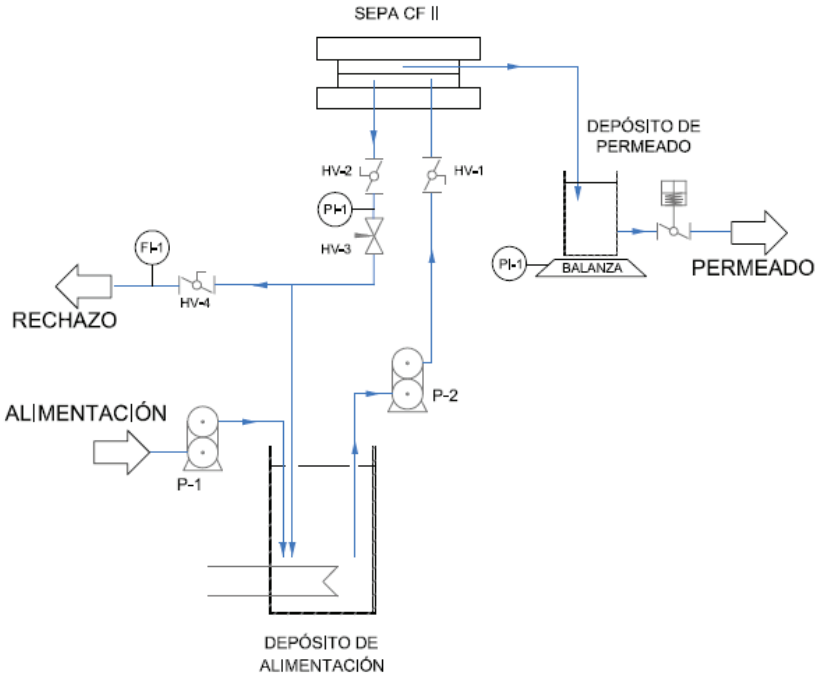

Figura 3.10. Diagrama general de la instalación SEPA CF II

El nivel del depósito de alimentación es controlado mediante un sistema de nivel que permite la activación de una bomba (P1) para mantener un volumen de agua de alimentación en el depósito de al menos 5L. La bomba P1 es un dispositivo de engranajes, modelo ALPb04 (220V/3f). El tanque de alimentación fabricado en polietileno, tiene una capacidad de 10 L y se encuentra termostatizado con el fin de mantener la temperatura constante en un rango de 20 ± 1^0C.

Mediante una bomba de engranajes de alta presión (P-2), modelo M-03S Hydracell Pump (220V/3f), provista de un variador de frecuencia (salida 230V, 3f, TBD) impulsa el influente desde el tanque de alimentación hacia la celda de membranas, obteniéndose a su salida dos corrientes: permeado y rechazo.

Parte del rechazo es recirculado al depósito de alimentación para poder asemejar los ensayos a un proceso de filtración industrial, a la vez que hace posible establecer distintos caudales de rechazo y así, analizar su influencia sobre el ensuciamiento de la membrana. El caudal de rechazo extraído del sistema se regula mediante una válvula manual (HV-4) y un rotámetro (FI-1).

La presión del sistema se regula mediante una válvula de aguja (HV-3) situada en la conducción de salida del rechazo de la celda de membranas SEPA CF II, lo que permite el control de la presión transmembrana. Para poder medir la presión local, se utiliza un manómetro analógico (PI-1).

La presurización de la celda de membranas se logra mediante una bomba hidráulica manual para aplicar una presión sobre la cubierta superior de la celda a la presión de operación a la que circula el fluido por el interior de la misma. Los experimentos se han realizado con una altura de espaciado de 1,2mm, que corresponde a una velocidad tangencial de 0,35 m/s.

El sistema de cuantificación del caudal de permeado consta de una balanza digital (carga máxima de 4.200 gr y una precisión de 0,1 gr), un depósito de polietileno, un controlador de nivel y un ordenador. La balanza se encuentra conectada al ordenador y mediante un programa almacena datos de diferencia de pesada cada 30 s, lo que permite obtener el flujo de permeado. Un controlador de nivel evita que se supere un nivel de líquido máximo en el depósito, lo que se traduce en no superar la carga máxima de la pesa. El caudal de permeado extraído del sistema se regula mediante una electroválvula (EV-1) accionada por el controlador de nivel.

2.2.2. Módulo de membrana

Los ensayos realizados en la unidad SEPA CF II han sido desarrollados con dos tipos de membranas, atendiendo a los distintos procesos de filtración utilizados: nanofiltración (GE Desal DK) y ósmosis inversa (TriSep X201). El área efectiva de cada módulo de membrana fue de 142 cm^2 y se trata de módulos planos cuyas características principales se resumen en la Tabla 3.4.

Tabla 3.4. Fraccionado de la suspensión

PARAMETRO	GE Desal DK	TriSep X201
Material	Poliamida	Poliamida-urea (copolímero)
Rango de operación de pH	1-11	2-11
Peso molecular de corte (MWCO)	200-300 Da	-
Tasa de rechazo	98 % (como $MgSO_4$)	99,5 % (como NaCl)

2.2.3. Acondicionamiento de la membrana

Las membranas de alta presión requieren de un acondicionamiento previo, éstas deben ser lavadas, siguiendo las recomendaciones del fabricante, hasta retirar por completo la capa de gel protector que las recubre. Posteriormente, la membrana es sometida a un proceso de compactación durante 2 horas, a una presión de 12,5 bar con una disolución de agua desionizada. En el transcurso de este tiempo se realizan mediciones de flujo de permeado, hasta observar que se ha alcanzado el régimen estacionario.

2.2.4. Caracterización de la membrana

Como ya se ha indicado anteriormente, el estado de referencia de la membrana es aquel estado al que se llega sistemáticamente después de sucesivas regeneraciones de la membrana. La Figura 3.11 y 3.12 muestran los valores obtenidos de flujo al filtrar agua de red para distintos valores de presión tanto para la membrana de nanofiltración como para la de ósmosis inversa, respectivamente. La resistencia de la membrana de referencia, obtenida de forma análoga a la ZW-10 y ZW-1, es de $4{,}9 \cdot 10^{13}$ m^{-1} y $2{,}0 \cdot 10^{14}$ m^{-1} para las membranas de nanofiltración y ósmosis inversa, respectivamente. Al iniciar cada experimento se caracteriza cada membrana para evaluar el grado de recuperación alcanzado con el protocolo de limpieza.

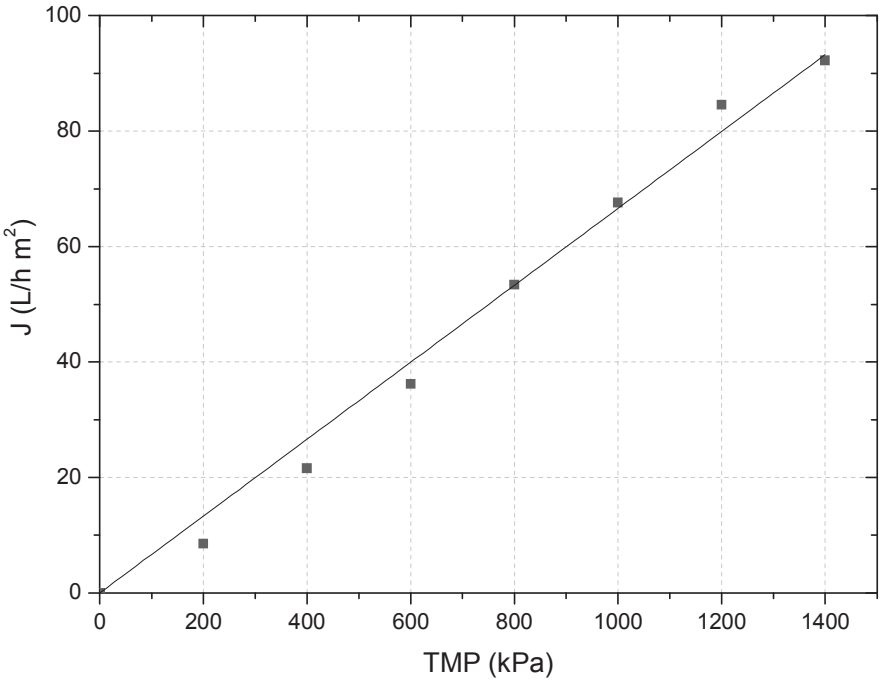

Figura 3.11. Caracterización de la membrana de nanofiltración GE Desal DK

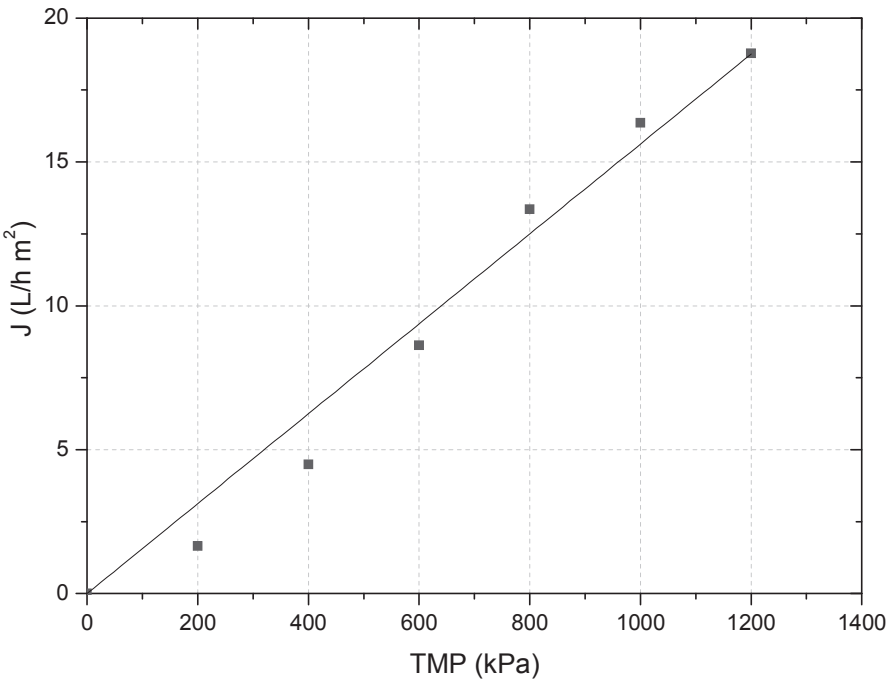

Figura 3.12. Caracterización de la membrana de ósmosis inversa TriSep X201

2.2.5. Procedimiento experimental

Se analizó la influencia del tipo de agua de alimentación y el factor de recuperación o "*recovery*" sobre el rendimiento global de un proceso de nanofiltración y ósmosis inversa. Para cada tipo de membrana y agua de alimentación se planteó una serie experimental con una duración total de 92 horas. Inicialmente el "*recovery*" se estableció en un 30 % y cada 24 horas se incrementó hasta un 50, 70 y 90%. Al finalizar cada serie experimental se sometió a la membrana a un protocolo de limpieza. La presión de operación se estableció en 7 y 12 bar para la nanofiltración y ósmosis inversa, respectivamente. Durante el desarrollo de todo el experimento se siguió la evolución de flujo de permeado con el tiempo.

Para cada serie experimental se fijaron y midieron las siguientes variables:

- Tipo de agua de alimentación
- Presión transmembrana
- Tasa de rechazo a "recovery"

Las corrientes de alimentación, permeado y rechazo fueron caracterizadas mediante el seguimiento de los siguientes parámetros:

- Conductividad
- Carbono orgánico disuelto (DOC)
- Bicarbonatos
- Cloruros
- Nitratos
- Fosfatos
- Sulfatos
- Sodio
- Potasio
- Magnesio
- Calcio
- Amonio
- Color

Finalmente, la descripción del procedimiento experimental seguido en cada capítulo se encuentra desarrollada en los apartados "materiales y métodos" correspondientes.

2.2.6. Protocolo de limpieza de la membrana

Las limpiezas de regeneración de la membrana se han llevado a cabo después de cada serie experimental. El protocolo de limpieza se realizó atendiendo a las especificaciones del fabricante y fue llevado a cabo “in situ”. La limpieza de regeneración consta de los siguientes pasos

I- Enjuague con agua destilada durante 15 minutos
II- Limpieza química con NaOH (pH=10) durante 2 horas
III- Limpieza química con HCl (pH=2) durante 2 horas

Entre cada etapa del protocolo de limpieza se procedía a circular agua destilada por toda la instalación, durante 5 minutos, con la finalidad de realizar un enjuague a la unidad. Una vez finalizada la limpieza de regeneración se somete a la membrana a un ensayo de caracterización para analizar la resistencia y por tanto, el grado de recuperación.

2.2.7. Autopsia de la membrana

La autopsia de las membranas se ha llevado a cabo después de finalizar las series experimentales con cada tipo de membrana, nanofiltración y ósmosis inversa. El protocolo de limpieza es el mismo que el descrito en el apartado anterior, con la principal diferencia que en este caso la limpieza se realiza “ex situ”. Para ello se introduce la membrana en un baño de ultrasonidos de la casa comercial SELECTA modelo ULTRASONS H-D.

Antes de realizar el protocolo de limpieza se toma una muestra de membrana (15 cm^2 de manera aproximada) para su posterior análisis. Por último, la descripción del procedimiento experimental desarrollado en cada capítulo, se describe en el apartado "materiales y métodos" correspondiente.

3. Métodos analíticos

La descripción de los métodos analíticos realizados en el desarrollo de la presente Tesis, se ha resumido en el siguiente apartado. La descripción detallada seguida en cada capítulo se incluye en el apartado "materiales y métodos" correspondiente.

3.1. Determinación del contenido en carbono

Demanda química de oxígeno total (COD), se ha llevado a cabo mediante el método 5220 D (ALPHA, 2005). La medida de la COD se realiza por colorimetría en un espectrofotómetro HACH DR5000.

Demanda química de oxígeno soluble (COD_S), el método utilizado es el método 5220 D (ALPHA, 2005). Se realiza el mismo procedimiento descrito para la COD con la diferencia que la muestra ha sido previamente filtrada por una membrana de nitrocelulosa (Millipore) de 0,45 µm de diámetro nominal de poro.

Demanda biológica de oxígeno (BOD_5), el método utilizado ha sido el manométrico, 5210 B (ALPHA, 2005), con un equipo digital WTW modelo Oxitop, que mide la presión de oxígeno dentro de la botella hermética cada día. El proceso de incubación se realiza a temperatura de 20 ^{0}C.

Carbono orgánico disuelto (DOC), se ha llevado a cabo el método 5310 B, Método de combustión - infrarrojo (ALPHA, 2005) donde la muestra se inyecta en una cámara de reacción caliente rellena con un catalizador oxidante. Las interferencias generadas por los carbonatos y bicarbonatos se eliminan acidificando inicialmente la muestra. La determinación se ha llevado a cabo con el medidor automático SHIMADZU, modelo TOC-VCSH/TOC-VCSN.

Productos solubles microbianos (SMP), cuantificados mediante la medida de carbono orgánico disuelto, filtrando previamente la muestra de suspensión biológica por un filtro nitrocelulosa (Millipore) de 0,45 µm de diámetro nominal de poro.

Materia orgánica del efluente (EfOM), se estima como la concentración de carbono orgánico disuelto filtrando previamente la muestra de influente por un filtro nitrocelulosa (Millipore) de 0,45 µm de diámetro nominal de poro.

"Biopolymer clusters" (BPC), se determina mediante la diferencia entre la concentración de SMP y carbono orgánico disuelto del permeado.

3.2. Determinación del nitrógeno total y Kjeldhal

Nitrógeno total, su determinación es mediante el método colorimétrico LCK 138 (HACH), NT_b, que oxida el nitrógeno inorgánico y orgánico a nitrato mediante la digestión con peroxidisulfato. La medida se realiza usando el espectrofotómetro DR-5000 de la casa comercial HACH.

Nitrogeno Kjeldhal, su estimación se realiza mediante la diferencia entre la concentración de nitrógeno total y la correspondiente de nitritos y nitratos, en la muestra en cuestión.

3.3. Determinación aniónica y catiónica

Conductividad, se determina según el método normalizado 2510 (ALPHA, 2005). El conductímetro empleado es inLab Cond 720.

pH, se determina según el método electrométrico 4500-H^+ (ALPHA, 2005). El pH-METHROM consta de un potenciómetro, un electrodo de vidrio, un electrodo de referencia y un dispositivo para compensar la temperatura.

Bicarbonatos, su determinación se realizó por el método de titulación 2320 (ALPHA, 2005). El equipo usado es un valorador automático de la marca METHROM modelo Citrino DMS 716, usando como agente valorador ácido clorhídrico con una concentración de 0,1 mol/L.

Nitrógeno amoniacal, fue llevado a cabo mediante el Método Nessler (método 8038, HACH). La medida se realiza usando el espectrofotómetro DR-5000 de la casa comercial HACH.

Determinación aniónica y catiónica (Cl^-, NO_2^-, NO_3^-, PO_4^{3-}, SO_4^{2-}, Na^+, K^+, Mg^{2+}, Ca^{2+}), se llevó a cabo mediante el método 4110 C (ALPHA, 2005) y se empleó el cromatógrafo iónico de METROHM Profesional IC 882. Este equipo está compuesto por una bomba de propulsión, un detector de conductividad y las columnas intercambiables aniónica y catiónica.

3.4. Determinación del contenido en sólidos

Sólidos suspendidos totales (TSS), su determinación se llevó a cabo mediante el método 2540 D (ALPHA, 2005). Los filtros usados en este ensayo son de un diámetro nominal de poro de 0,45µm de nitrocelulosa (MIllipore).

Sólidos suspendidos totales en el licor mezcla (MLSS), se determina mediante el mismo procedimiento descrito para los TSS, con la diferencia que en este caso la muestra procesada es la suspensión filtrante.

Sólidos suspendidos volátiles (VSS), su determinación se llevó a cabo mediante el método 2540 D (ALPHA, 2005) Los filtros usados en este ensayo son de un diámetro nominal de poro de 0,45µm de nitrocelulosa (MIllipore).

Sólidos suspendidos volatiles en el licor mezcla (MLVSS), se determina mediante el mismo procedimiento descrito para los VSS, con la diferencia que en este caso la muestra procesada es la suspensión filtrante.

3.5. Determinación del color y turbidez

Color, se determina mediante el método 2120 (ALPHA, 2005). La medida se realiza usando el espectrofotómetro DR-5000 de la casa comercial HACH.

Turbidez, su determinación se realiza con el turbidímetro HACH 2100D (HACH), que expresa su resultado directamente en NTU (Unidades Nefelométricas de Turbidez), según el método 2130 (ALPHA, 2005).

3.6. Morfología y caracterización de la suspensión biológica

"Time to filter" (TTF), su determinación se realiza mediante una modificación del método estándar 2710 H (ALPHA, 2005) debido al uso de un filtro de 9 cm WHATMAN 934 AH glass fibre.

Turbidez del sobrenadante, se ha realizado mediante el método propuesto por Ng et al. (2005), que consiste en centrifugar la muestra a 1300 g durante 2 minutos y medir la turbidez del sobrenadante.

Distribución de tamaño de partículas, el análisis del tamaño del flóculo se lleva a cabo mediante la determinación de la distribución de tamaño de partículas en el licor mezcla. Este procedimiento se realizó en el Servicio General de Apoyo a la Investigación de la ULL (SEGAI), mediante el uso del Mastersizer (MALVERN INSTRUMENTS), que determina el tamaño de partículas hasta 0,02µm, mediante la dispersión de la luz láser.

Viscosidad, fue determinada mediante viscosímetro rotacional cilíndrico (Visco Star plus, FungiLab), con una velocidad de giro de 100 rpm.

3.7. Actividad biológica de la suspensión

Método de Kristensen et al., 1992, la actividad biológica de la suspensión es cuantificada mediante ensayos individuales que permiten establecer la velocidad de consumo de amonio, nitrito, nitrato y oxigeno (AUR, NIUR, NUR y $SOUR_e$, respectivamente). En el caso de la determinación del AUR y NIUR, la muestra es saturada en oxígeno y alimentada con sustratos, con una concentración 10 mg N/L. A distintos tiempos se retira un volumen de muestra y se somete a

centrifugación (3000 g durante 2 minutos) para analizar selectivamente el ion a estudio. La determinación del NUR, se lleva a cabo en ausencia de oxígeno y la suspensión es alimentada con un sustrato de nitrato a una concentración de 10mg N/L. En el caso de la determinación del NUR, además se añade N-aliltiurea (ATU) a una concentración 86µM. Como en los casos anteriores se toman muestras a distintos tiempos y se determina la concentración de nitrato. En el caso del $SOUR_e$, la muestra es saturada en oxígeno. Una vez alcanzado el grado de saturación se elimina la aireación y se registra la evolución del consumo de oxígeno con el tiempo mediante una sonda HQ40d (HACH). Para todos los casos se encuentra una relación lineal entre la concentración de sustrato a estudio y el tiempo, lo que permite determinar la actividad biológica como una relación entre la cantidad de sustrato consumido y la concentración de biomasa por unidad de tiempo.

Método de Ginestet et al., 1998, este procedimiento permite un análisis rápido para la determinación de la velocidad de consumo de amonio, nitrito, acetato y oxígeno (SOUR AOB, SOUR NOB, SOUR OHO, $SOUR_{endogenous}$; respectivamente). El método consiste en la saturación de oxígeno en el licor mezcla para posteriormente eliminar la aireación, y medir el consumo de oxígeno disuelto. Tras un tiempo, se añade una mezcla de sustratos (10 mg $N\text{-}NH_3$/L; 10 mg $N\text{-}NO_2^-$/L y 10 mg de C-acetato/L), registrando el consumo de oxígeno disuelto y posteriormente, se suministra la Aliltiurea, que inhibe selectivamente la oxidación de amoniaco. Tras otro periodo de tiempo, se procede a la adición de Azida que inhibe la reducción del nitrato. De esta manera se puede determinar la actividad de cada uno de los microorganismos presentes en el biorreactor. La evolución de la concentración de oxígeno disuelto se determina mediante el uso del medidor HQ40d (HACH).

3.8. Determinación de fármacos

La técnica para la determinación de fármacos ha sido la cromatografía líquida de alta resolución acoplada a un detector de espectrometría de masas de triple cuadrupolo con ionización de “electrospray” (LC-ESI-MS7MS). La técnica empleada para la extracción y pre-concentración de las muestras fue la extracción en fase sólida de manera “off-line”. Esta técnica ha sido realizada en el Departamento de Química de la Universidad de Las Palmas de Gran Canaria.

3.9. Autopsia de la membrana: SEM-EDX y FTIR

Microscopía electrónica (SEM), este procedimiento se realizó en el Servicio General de Apoyo a la Investigación de la ULL (SEGAI), mediante el uso del equipo Jeol JSM 6300.

Espectroscopía de infrarrojo por transformada de Fourier (FTIR), este procedimiento se realizó en el Servicio General de Apoyo a la Investigación de la ULL (SEGAI), mediante el uso del equipo IFS 28/55.

4. Referencias

American Public Association/Water Environment Federation, Standard Methods for the examination of Water and Watewater, 21st ed., Washington, DC, USA, 2005.

Ginestet P., Audic JM., Urbain V., Block JC, Estimation of nitrifying bacterial activities by measuring oxygen uptake in the presence of the metabolic inhibitors allylthiourea and azide. *Application Environmental Microbiologic,* 64(6), (1998), 2266-2268.

Hg H., Hermanowicz S., Membrane bioreactor operation at short solids retention time: performance and biomass characteristics, *Water Research,* 39, (2005), 981-992.

Kristensen G. H., Jørgensen P. H., Henze M., Characterization of functional microorganism groups and substratate in activated sludge and wastewater by AUR, NUR, and OUR. *Water Science Technology*, 25(6), (1992), 193-199

Le-Clech P., Jefferson B., Chang J., Judd S., Critical flux determination by the flux-step method in a submerged membrane bioreactor. *Journal of Membrane Science*, 227, (2003), 83-91.

Van der Marel P., Zwijnenburg A., Kemperman A., Wessling M., Temmink H., Van der Meer W., An improved flux-stepmethod to determine the critical flux and the critical flux for irreversibility in a membrane bioreactor. *Journal of Membrane Science*, 332, (2009), 24-2

CAPÍTULO 4: Efecto de las características del lodo sobre el ensuciamiento de la membrana durante la puesta en marcha de un biorreactor de membrana sumergida terciario

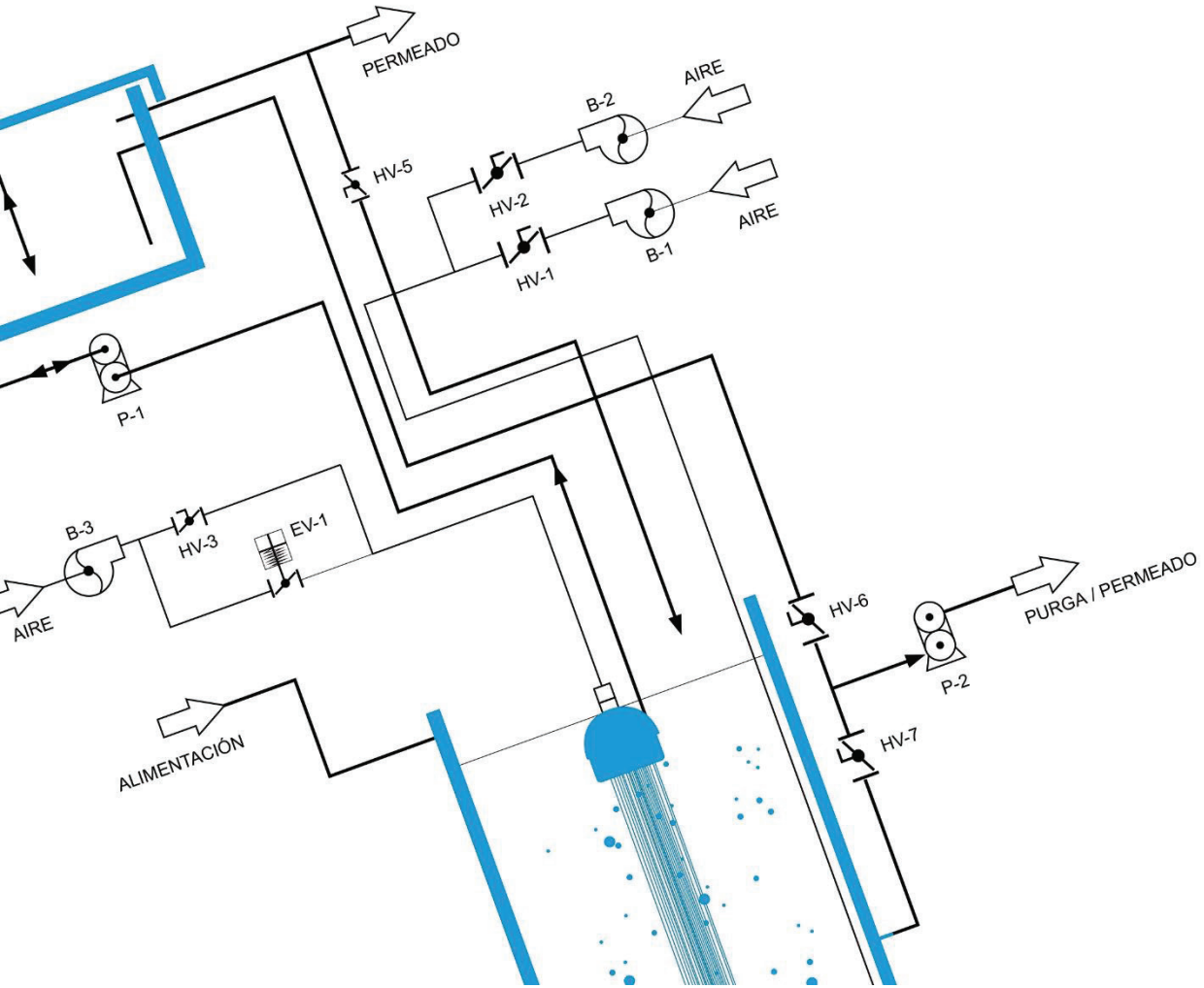

Capítulo 4

Efecto de las características del lodo sobre el ensuciamiento de la membrana durante la puesta en marcha de un biorreactor de membrana sumergida terciario

Effect of sludge characteristics on membrane fouling during star-up of a tertiary submerged membrane bioreactor

Oliver Díaz, Luisa Vera, Enrique González, Elisa García, Juan Rodríguez-Sevilla

Environmental Science Pollution Research
23(9), (2016) 8951-8962

Factor de impacto: 2,828 (JCR®, Thomson Reuters 2015)

Highlights

- Tertiary MBR applied for advanced treatment of secondary effluent from a conventional WWTP
- Better understanding of influence of microbial parameters on membrane bioreactors performance
- Determination of critical concentration of suspended solids for minimal membrane fouling
- Biopolymer Clusters (BPCs) as indicator of fouling potential from sludge
- Definition of strategies for membrane fouling mitigation based on sludge properties

Keywords

Secondary effluent reclamation, Tertiary submerged membrane biorreactor, Fouling, Biopolymer clusters, Sludge properties, Biological nitrification

Resumen:

Durante las últimas décadas, los biorreactores de membrana han experimentado un gran desarrollo. Sin embargo, el ensuciamiento de la membrana sigue siendo el principal inconveniente para la aplicación generalizada de esta tecnología. En éste Capítulo, un biorreactor de membrana sumergida para tratamiento terciario, fue operado a escala piloto en continuo alrededor de 200 días con el objetivo de evaluar el desarrollo experimentado por la biomasa. Se analizó la relación entre el estado fisiológico de la biomasa y el estrés ambiental, y su influencia en el rendimiento del proceso.

La planta piloto fue operada con un tiempo de retención hidráulico de 7,2 horas sin purga de lodos, exceptuando el muestreo de la suspensión biológica. La puesta en marcha se llevó a cabo sin inoculo de lodo, por tanto, la biomasa desarrollada en el reactor procedía de los microorganismos presentes en el agua de alimentación. El sistema experimentó una completa nitrificación y un alto rendimiento de eliminación de DQO (COD en inglés) tras los primeros días de operación.

La concentración de solidos suspendidos en el licor mezcla (MLSS) fue inferior a los 3,000 mg/L, durante los primeros días de operación. En estas condiciones la biomasa fue altamente sensible al estrés ambiental generado por incrementos en el caudal de aireación o por picos de contaminación orgánica en la corriente de alimentación. Estas condiciones generaron des-floculación de la biomasa que provocó un aumento de los agregados de biopolímeros (BPC-*biopolymer clusters* en inglés) presentes en la suspensión y en consecuencia, un incremento del ensuciamiento de la membrana que requirió la aplicación de limpiezas químicas para mantener la operatividad del sistema.

Por el contrario, la operación a concentraciones de sólidos suspendidos (MLSS en inglés) superiores a los 3,000 mg/L se caracterizó por provocar un bajo ensuciamiento de la membrana, baja concentración de BPCs y presentar moderada bioactividad. Durante el periodo de crecimiento estable de la biomasa, los microorganismos fueron sometidos a unas condiciones severas de limitación de sustrato. Debido a las condiciones de inanición, la biomasa no utilizó el sustrato disponible para actividades relacionadas con la biosíntesis, dando lugar a una baja producción neta de lodo.

La operación con limitación de sustrato ha condicionado considerablemente las características de la biomasa en el biorreactor de membrana terciario. Una vez alcanzado el régimen de crecimiento estable, la suspensión biológica presentó un elevado estado de biofloculación y los BPCs en el medio fueron biodegradados/adsorbidos por la biomasa. La reducción de estos biopolímeros generó la disminución del ensuciamiento de la membrana hasta valores adecuados para la operación del biorreactor. Sin embargo, al aumentar los tiempos de operación, el sistema experimentó un ligero incremento del ensuciamiento residual, posiblemente debido al incremento de la concentración de MLSS y de la viscosidad de la suspensión.

Se ha logrado establecer una correlación entre la concentración de MLSS con la viscosidad, el SOUR endógeno y la concentración de BPC de la suspensión. Por el contrario, no se ha encontrado relación entre los MLSS y el "*Time to Filter*-TTF", por tanto, los resultados parecen indicar que la concentración de biomasa no afecta directamente, a la filtrabilidad de la suspensión. En cambio, los ensayos de filtrabilidad llevados a cabo mediante el TTF, muestran una correlación con la turbidez del sobrenadante, lo que revela el considerable efecto de la biofloculación sobre la filtrabilidad de la suspensión.

Asimismo, el análisis del ensuciamiento reversible experimentado por la membrana reveló una alta influencia de la concentración de BPC (r^2=0,868). A moderados valores de MLSS (<3.000 mg/L), se observó una correlación negativa entre la concentración de biomasa y el ensuciamiento reversible. Por el contrario, se encontró una correlación positiva entre ambos parámetros a concentraciones de sólidos superiores a los 5.000 mg/L.

En conclusión, las condiciones óptimas de operación para un MBR terciario corresponden a concentraciones en la suspensión biológica: inferiores a 5 mg/L de BPC y de MLSS comprendidas entre 3.000 a 5.000mg/L. Estos resultados son similares a los encontrados por otros autores en MBR operados como tratamiento secundario de aguas residuales domésticas.

Por último, indicar que el ensuciamiento de la membrana en las condiciones de estudio está asociado a la formación de una torta incompresible, donde la concentración de BPC presenta un papel fundamental, en comparación con otras propiedades de la suspensión, como indicador del ensuciamiento.

Abstract

In membrane bioreactors applied to wastewater treatment, fouling is typically a complex function of sludge characteristics. A pilot-scale tertiary submerged membrane bioreactor (tMBR) was continuously operated for over 200 d to assess the effect of biomass physiological state and environmental stress on process performance. Sludge characteristics were evaluated in terms of suspended solids concentration (MLSS and MLVSS), apparent viscosity, bioflocculation state, filterability, bioactivity, biopolymeric clusters (BPCs) and soluble microbial products. During the initial period of the tMBR start-up, when MLSS was below 3000 mg/L, the biomass was found to be very sensitive to environmental stress by sudden oxygen increase or organic shock loading, resulting in temporary biomass deflocculation and BPC release, and consequently, severe induced membrane fouling. However, at higher MLSS values, low stable biomass growth (0.04±0.002 kg MLVSS/kg COD) was measured, regardless of organic overloading shocks or feeding failures. This period was also characterised by low bioactivity, BPC content and membrane fouling. Statistical analysis showed that BPCs have an important role when compared with other sludge properties as indicators of its fouling potential.

1. Introduction

Over the last two decades, membrane bioreactor (MBR) technology has attained a significant market share in municipal wastewater treatment, increasing its value at a compound annual growth rate of 10-15% (Marketsandmarkets, 2014). This technology combines suspended biomass, similar to the conventional activated sludge process, with microfiltration or ultrafiltration membranes that replace gravity sedimentation and clarify the wastewater effluent. Among the commercially available process configurations and membrane modules of MBRs, the submerged hollow-fibre type is the most widely used in municipal wastewater treatment owing to lower operation costs (Judd, 2010). The rapid market penetration of MBRs has principally been driven by superior effluent quality, suitable for unrestricted irrigation and other industrial applications. Such quality permits a significant reduction of total plant footprint compared to conventional activated sludge plant (Cote et al., 2012). However, despite considerable progress over the past two decades, membrane fouling is still the main factor limiting widespread application of this technology. This drawback leads to increased operating expenditure (OPEX), due to the cost of membrane aeration, cleaning requirements and membrane replacement (Fenu et al., 2010).

Fouling can be defined as the alteration in the membrane caused by specific physical and/or chemical interactions between the membrane and components of the microbial suspension, leading to membrane permeability loss. Several mechanisms have been proposed to explain this phenomenon, including pore clogging, adsorption of foulants, gel or cake formation, cake layer consolidation and osmotic pressure effects (Lin et al., 2014). Conventional filtration strategies to reduce fouling largely involve air scouring to induce favourable hydrodynamics in the vicinity of the membrane surface and physical cleaning through backwashing (i.e. permeate is used to flush the membrane backwards) or relaxation (when no filtration takes place), supplemented with periodic chemical cleaning in place (CIP) (Judd, 2010). The rate and extent of fouling is typically a complex function of membrane properties, hydrodynamic and operating conditions, feedwater nature and microbial suspension characteristics (Le-Clech et al., 2006). Therefore, for a given system (i.e. feedwater and membrane) and favourable hydrodynamics, an appraisal of the impact operating parameters have on microbial suspension characteristics is necessary, in order to select the best operating conditions. Several authors have tried to identify the characteristics of the suspensions that have the greatest influence on fouling, among which are concentration of suspended solids in the mixed liquor (MLSS), viscosity, particle size distribution (PSD), biomass activity and biopolymer content (Le-Clech et al., 2006; Meng et al., 2009). Biopolymers are organic substances of microbial origin, consisting mainly of polysaccharides and proteins, which can be in the microbial flocs (extracellular polymeric substances - EPS_s), or in the liquid phase as soluble microbial products (SMP_s) and colloidal biopolymer clusters (BPC_s). Based on the concept of utilisation and biomass associated products (Aquino and Stuckey, 2008), biopolymer content is related to various microbial processes including substrate degradation, biomass decay, EPS hydrolysis and soluble biopolymer degradation.

Since MBR use began, MLSS has been considered one of the main foulant parameters. Nevertheless, most studies indicate that the MLSS concentration, considered alone, is a poor indicator of the fouling tendency of suspensions (Meng et al., 2009, Drews, 2010; Van den Broeck et al., 2011). In general, the relationship between MLSS concentration and fouling appears to depend on the MLSS concentration range; below 6 g/L an inverse relationship is often reported while a direct relationship is generally found above 15 g/L (Le-Clech et al., 2006). A greater MLSS effect may have an influence on sludge viscosity, so affecting the hydrodynamics of the filtration process (Trussell et al., 2007). In addition to MLSS, other factors such as sludge morphology (i.e. particle-size distribution) and BPCs are expected to cause membrane fouling (Wang and Li, 2008). Since sludge flocs and free bacteria are considerably larger than membrane

pores, particle size distribution (PSD) has an influence on the explanations of fouling focussed on cake-layer and consolidation mechanisms. Many authors report that cake layers formed by small flocs were denser than those by large ones, probably due to a higher specific cake resistance according to the Carman–Kozeny equation (Lin et al., 2011). In addition, small flocs have a greater tendency to settle on the membrane due to their lower back-transport velocity (Zeman and Zydney, 1996). Meanwhile, it is widely reported that biopolymer matter strongly affected membrane fouling in an MBR. Soluble/colloidal biopolymers could enter into the membrane pores causing pore blocking; they form a gel layer, enhance floc attachment to the membrane, affect cake structure and induce osmotic effect (Lin et al., 2014).

Despite extensive research efforts to understand the effect of operating conditions on biomass characteristics and membrane fouling propensity, the variety of installations and feedwater characteristics sometimes lead to contradictory results, as in the case of sludge retention time (SRT) (Sabia et al., 2013; Villain and Marrot et al., 2013). Moreover, determination of the actual membrane fouling rate is significantly affected by the fouling history of the membrane (Drews, 2010). For this reason, several ex situ filterability tests such as the time-to-filter (TTF) or Delft filtration characterization method (DFC_m) have been introduced. Nevertheless, these tests may not accurately reflect the real operating conditions in MBRs and the correlation between the test methods and membrane fouling rates must be checked case by case (Drews, 2010). In addition, the interconnection between sludge characteristics adds a particular complication in ascertaining which component of the suspension is the primary cause of membrane fouling (Van den Broeck et al., 2013). Therefore, pilot tests are generally required to characterise the suspensions with greatest influence on fouling under particular MBR operating conditions.

Recent studies have shown the capability of tertiary submerged membrane bioreactors (tMBRs) for treatment of secondary effluents from old plants with poor performance by secondary clarifiers (e.g. Vera et al., 2014). These clarifier malfunctions can compromise the economic feasibility of other tertiary treatments. In fact, growing interest in this technology has been seen recently in the Aquapolo project (Sao Paulo, Brazil), the largest wastewater reuse project in the Southern Hemisphere, which includes a tMBR in the treatment scheme (Koch, 2014). One of the most attractive points of tMBR is its capability to operate under complete solid retention (without a waste sludge purge) due to extremely low sludge production in the substrate-limited conditions imposed. This advantage significantly reduces operating costs (Vera

et al., 2014). There are several experiments with MBRs treating raw municipal wastewater that have demonstrated their capability to operate under complete sludge retention time limitations without drawbacks in biodegradation activity (e.g., Rosenberger et al., 2002). In these experiences, high biomass concentrations were required (12 to 24 g/L) in order to operate under substrate-limited conditions, which had a negative impact on oxygen transfer efficiency and hence, on operating costs. In addition, Pollice et al. (2008) found that sludge filterability deteriorated under complete sludge retention, probably due to excessive increments in MLSS and sludge viscosity. In contrast, tMBRs offer the capability to operate under complete sludge retention time and moderate MLSS concentration, due to low organic content in the feedwater. However, the consequences of complete sludge retention for morphology, bioactivity, soluble biopolymer content and filterability of the microbial suspension must be studied in detail in order to optimise process performance.

The aim of this study is to assess biomass development in a tMBR and its relationship with membrane fouling. For this purpose, a pilot tMBR operated with complete sludge retention was continuously fed with a secondary effluent for 195 days. Biomass development was assessed by following the evolution of MLSS, MLVSS, viscosity, particle size distribution, TTF, bioactivity (heterotrophic and nitrifying activity), and colloidal and soluble biopolymers content (BPC_s and SMP_s). The relationships between membrane fouling rate and each property of the sludge were further analysed statistically, to assess the role and significance of each.

2. Materials and methods

2.1. Feedwater

The tMBR was fed with secondary effluent from a conventional activated sludge wastewater treatment plant, designed only for carbon removal (Table 4.1). This effluent exhibited a high variable chemical oxygen demand (COD = 559 mg/L, on average), mainly as particulate matter (COD_s/COD = 0.14 and COD/SST = 1.35), with a low readily biodegradable fraction (5-day biochemical oxygen demand BOD_5-to-COD ratio was approximately 0.22). This high particulate content was attributed to the short SRT (< 4 days) and oxygen deficiency in the activated sludge process, which frequently resulted in episodes of sludge deflocculation. Nitrogen compounds were mainly in the form of ammonium (43 mg/L, on average). In terms of

the total COD, this feedwater is comparable to a moderate loaded wastewater, but mainly composed of suspended slowly biodegradable organic matter.

Table 4.1. Main feedwater characteristics.

		PHASE I (N= 17)		PHASE II (N=28)		PHASE III (N=15)		PHASE IV (N=27)		PHASE V (N=10)	
PARAMETERS	UNITS	MEAN	RANGE	MEAN	RANGE	MEAN	RANGE	MEAN	RANGE	MEAN	RANGE
COD	mg/L	438	150-1510	810	106-2320	461	318-1800	216	110-494	264	130-640
COD_S	mg/L	83	56-120	88	54-136	86	62-132	75	14-220	71	34-90
DOC	mg/L	20	11-30	25	14-138	20	16-26	22	15-36	21	17-27
$N\text{-}NH_3$	mg/L	45	28-60	43	15-90	47	35-57	39	28-61	43	35-53
$N\text{-}NO_3^-$	mg/L	0.15	0.12-0.22	0.18	0.02-0.53	0.28	0.02-0.94	0.45	0.02-1.7	0.22	0.01-1.25
TSS	mg/L	281	62-1220	534	28-1708	647	220-1395	149	32-530	173	94-900

2.2. MBR

A cylindrical 220 L deposit was equipped with ZeeWeed® ZW-10 (GE Water & Process Technologies) hollow-fibre membranes with a 0.04 µm rated pore diameter, 1.9 mm external diameter and 0.9 m^2 of filtering surface area, assembled vertically (see Vera et al., 2014). ZeeWeed® consists of a woven reinforcing braid on which a PVDF membrane is cast. The effluent (permeate) was extracted from the top header of the module under slight vacuum. Throughout the experimental time ultrafiltration was carried out at constant permeate flux (J = 35 L/h m^2), registering transmembrane pressure as a function of time. Furthermore, backwashing was applied each 7 min at constant conditions (J_B = 60 L/h m^2 and t_B = 30 s) for fouling removal. Although air sparging was not supplied during the filtration phase, constant air scouring at 3.1 $Nm^3/h\ m^2$ was applied during backwashing, to improve its efficiency. The process tank was stirred by air bubbling from the bottom, at a flowrate of 1.2 Nm^3/h. A compressor also supplied additional air (0.3 Nm^3/h) for the biological processes. The bioreactor was run at a hydraulic retention time of 7.6 h without sludge removal except for sampling. During the experimental time, the biological suspension was routinely characterised to analyse the influence of microbial

suspension characterisation on membrane fouling. Membrane chemical cleaning was carried out by soaking with NaOCl (1,000 ppm) for 12 h.

2.3. Analytical methods

Total and soluble chemical oxygen demand (COD and COD_s, respectively), 5-day biochemical oxygen demand (BOD_5), total suspended solids (TSS), mixed liquor suspended solids (MLSS), mixed liquor volatile suspended solids (MLVSS), time to filter (TTF) and turbidity were determined in conformity with the Standard Methods (2005). The analyses of ammonium-nitrogen ($N\text{-}NH_3$) were carried out by the Nessler method using a DR-5000 Hach spectrophotometer. Dissolved organic carbon (DOC) concentration was measured with a TOC-meter (TOC-5000A, Shimadzu). The difference in DOC concentration between the filtrated suspension through a 0.45 µm nitrocellulose membrane filter (HA, Millipore) and the MBR permeate was assigned as biopolymer clusters (BPC). Nitrate-nitrogen ($N\text{-}NO_3^-$) and nitrite-nitrogen ($N\text{-}NO_2^-$) were analysed through ion chromatography using a Compact IC plus 882 device supplied by Metrohm. Microbial floc size distribution was measured using a Malvern Mastersizer 2000 instrument with a detection range of 0.02-2000 µm. To quantify supernatant turbidity, the biomass samples were centrifuged at 1300 g for 2 min. The biological activities was evaluated by respirometric measurement described in Ginestet et al., (1998) using allylthiourea (86µM) and azide (24µM) as selective inhibitors of ammonia and nitrite oxidation, respectively. The sludge viscosity was determined by using the concentric cylinder rotational viscosimeter Visco Star plus (FungiLab, Spain), with a rotational speed of 100 rpm.

3. Results and discussion

3.1. Evolution of sludge characteristics and process performance

The pilot plant was operated continuously for 195 days under similar operating conditions (HRT = 7.2 h and complete retention time), to study biomass development. To facilitate analysis, the experimental period has been divided into five phases according to process stability: initial biomass growth (phase I, 1st-21st day), unsteady operation (phase II, 22nd-60th day) and steady biomass growth (phase III, 61st-84th day; phase IV, 85th-157th day; phase V, 158th-195th day).

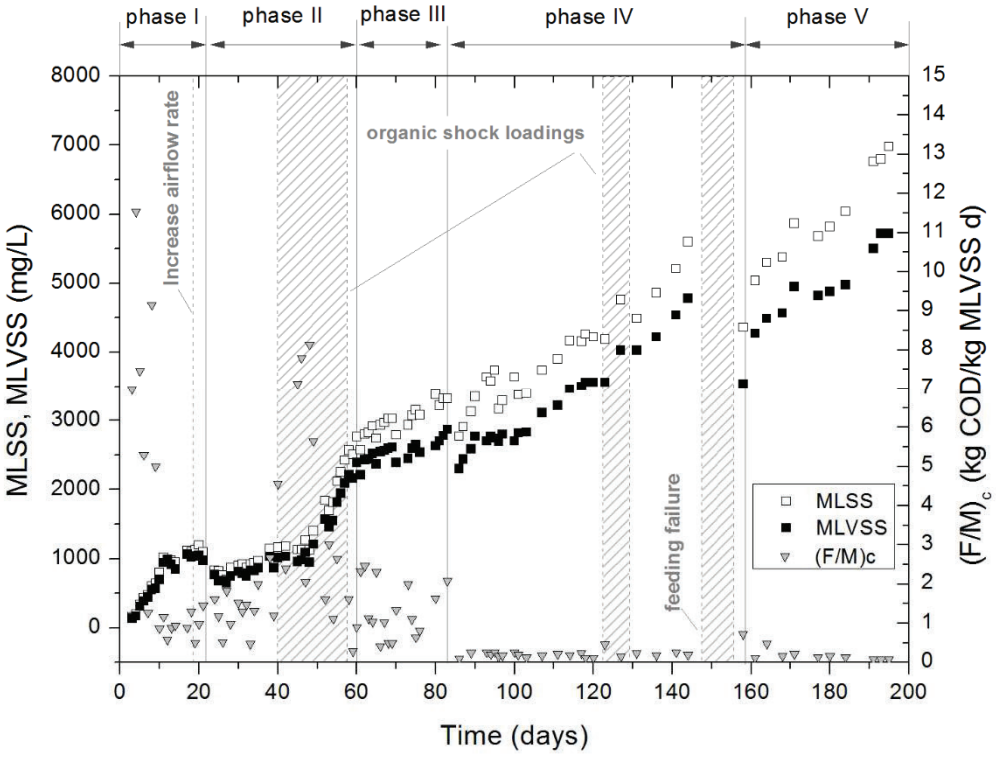

Figure 4.1. MLSS, MLVSS and $(F/M)_C$ evolution during the different experimental phases

The plant started without any sludge inoculum, so the biomass developed from the microorganisms entered with feedwater (i.e. secondary effluent). As shown in Fig.4.1, MLSS and MLVSS rapidly increased during phase I due to microorganism retention and growth, resulting from the high $(F/M)_C$ imposed (11.5-5.0 kg COD_s/kg MLVSS d). Nevertheless, at the end of phase I, to maintain complete nitrification with a proper dissolved oxygen concentration, air flow-rate to the bioreactor was increased to 1.5 Nm^3/h, producing a shock to the microorganisms, which started to produce BPCs and generate white foam (Fig. 4.4b). This relationship between intense biopolymer production and foam is commonly observed in MBRs and attributed to proteins that have properties as surface-active agents (Di Bella et al., 2011). This foam disappeared after the 40th day. In addition, from the 44th to 57th day, the tMBR suffered sporadic events of organic overloading shocks, and feedwater COD increased from 670 to 2,230 mg COD/L due to temporary malfunction of the WWTP. This significantly increased suspended solid concentration in the tMBR. The unstable period was identified as phase II. After that, biomass started to grow continuously during a 135 day period (phases III-V), with the exception of another shock load (123rd - 127th day) and a period of feeding failure (146th - 157th day). During this period of stable growth, microorganisms were progressively subjected to severe substrate limitation (from

0.26 to 0.10 kg COD/kg MLVSS d), which may justify the low sludge-yield coefficient (Y_{obs}) of 0.04±0.002 kg MLVSS/kg COD. Due to the starvation conditions, it was expected that available substrate was mainly utilised by microorganisms for non-growth activities rather than biosynthesis, which reduced net sludge production (Rosenberger et al., 2002). In addition, previous studies in similar conditions have demonstrated the existence of predator species in the tMBR, especially sessile ciliates and free-swimming ciliates, which are known to be responsible for a reduction in the population of smaller bacteria (Wang et al., 2013). The sludge yield was within the typical range of those reported for secondary MBRs operated with complete sludge retention (0.03-0.12 kg MLVSS/kg COD (e.g., Pollice et al., 2004). It was also consistent with predicted values (0.05-0.1 kg MLVSS/kg COD) of ASM-based models considering the concepts of endogenous respiration and slow hydrolysis at long SRTs (> 100 d) (Amanatidou et al., 2015). At the same time, the MLVSS/MLSS ratio decreased from 0.85 of day 60 to 0.82 of day 195 (phases III-V), which indicated a slight inert solids accumulation in the sludge. This is in accordance with previous studies, suggesting that MBRs operated for long SRTs develop slow-growing bacteria that may degrade inert substances and avoid significant accumulation in the sludge (van Loosdrecht and Henze, 1999).

Table 4.2 shows the evolution of sludge bioflocculation, viscosity and filterability. During phases I-II, results revealed an increase in bioflocculation, detected in supernatant turbidity and mean particle size behaviour, due to biomass development. It should also be noted that unsteady conditions (phase II) greatly affected sludge characteristics, as seen from the variability of turbidity measurements. Once the steady biomass growth period was achieved (phases III-V), average turbidity slightly increased from 16 to 27 NTU. As expected, the small flocs content (i.e. d10, 10% of the volume distribution being below this value) decreased from 44 to 29 µm during the same period. These results indicated some degree of sludge deterioration after long operation times. Probably, the main reason for the observed behaviour is the progressive substrate limitation imposed, which decreased biomass activity. Wilén et al. (2000) studied the effect of microbial activity on floc stability and concluded that the bacterial metabolism was important in maintaining the strength of the flocs. Nevertheless, this slight deflocculation did not have a significant impact on process performance, since no significant decrease in the substrate consumption rate nor appreciable release of SMPs was observed. Regarding rheological properties, apparent viscosity seems to be related to MLSS, as previously reported (Trussell et al., 2007). Based on this approach, a critical MLSS value can be identified (~ 3,000-3,500 mg/L); over it apparent viscosity significantly increased (phases IV-V, from 2.0 to 4.0 mPa

s). Finally, the results presented in Table 4.2 also underline the link between bioflocculation and sludge filterability, measured as TTF. Similar results have been reported by Van den Broeck et al. (2011), reflecting the key role of small floc size in filterability.

Table 4.2. Main characteristics of microbial suspension for each experimental phase. The reported data are expressed as min-max.

		phase I		phase II		phase III		phase IV		phase V	
PARAMETERS	**UNITS**	**RANGE**	**N**	**RANGE**	**N**	**RANGE**	**N**	**RANGE**	**N**	**RANGE**	**N**
Supernatant turbidity	NTU	42-106	6	13-116	22	6.6-27	16	17-38	17	19-35	4
PSD											
$D_{(v,0.1)}$	µm	15-23	3	15-61	5	44	1	30-34	2	29	1
$D_{(v,0.5)}$	µm	51-66	3	86-198	5	119	1	94-97	2	86	1
$D_{(v,0.9)}$	µm	125-153	3	266-449	5	327	1	242-265	2	227	1
Apparent viscosity	mPa s	1.7-2.0	6	1.5-2.0	22	1.6-2.0	16	1.8-3.2	17	3.0-4.0	4
TTF	s	330-2122	6	5-4620	22	6-58	16	69-135	17	69-135	4

As expected, high COD removal and complete nitrification were obtained after the first days of operation, corresponding with the rapid biomass growth observed in phase I (Fig. 4.2). However, there was considerable variability in COD removal efficiencies during the whole experimental period, between 79% and 97%. This range may be attributable to influent COD fluctuations (110-960 mg/L), since permeate COD values decreased from 81 mg/L (on average) in the initial phase to less than 35 mg/L during phases III-V. Nitrifying biomass followed the typical trend, always achieving ammonium removal rates higher than 98% after the first 20 days, with stable behaviour after increasing airflow rate (17th day). In phases III-V, average concentrations for nitrogen compounds in the permeate were 0.53 mg N/L, 50.3 mg N/L and 0.03 mg N/L for NH_4^+, NO_3^- and NO_2^-, respectively.

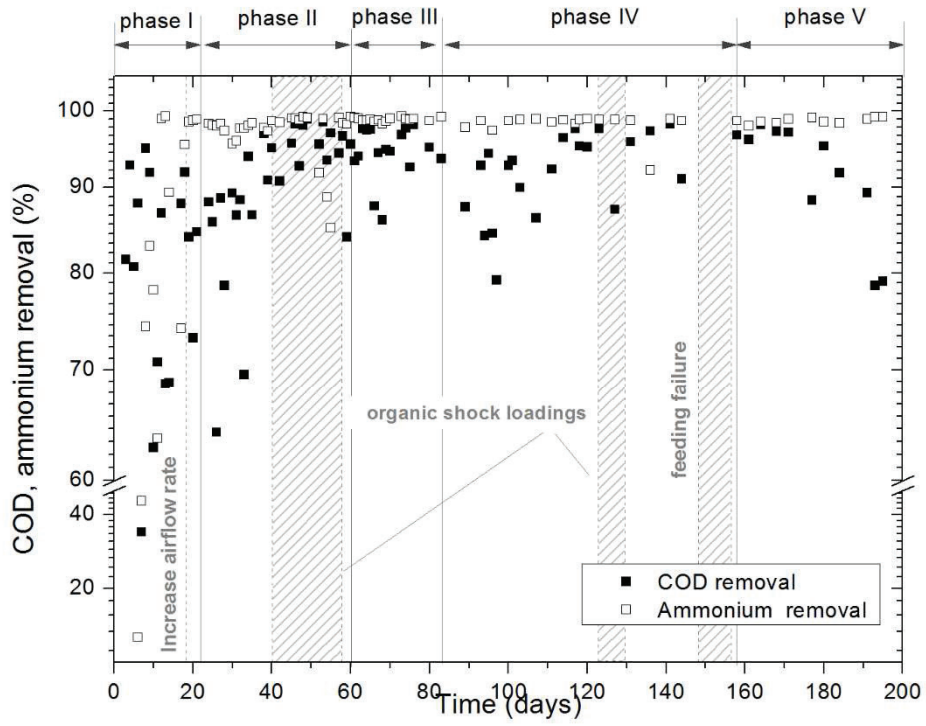

Figure 4.2. COD and ammonium removal during the different experimental phases

3.2. Biomass activity and colloidal/soluble biopolymer content

Respiration tests with various substrates were periodically carried out to elucidate the physiological state and activity of the microbial community. Endogenous specific uptake rate (SOUR endogenous) is defined as oxygen consumption of the microbial population in the absence of external substrates. It mainly consists of the maintenance energy requirement. In addition, heterotrophic, ammonium-oxidising (AOB) and nitrite-oxidising bacteria (NOB) were examined by adding potassium acetate, ammonium chloride and sodium nitrite, respectively, and measuring respiration consumption after dosing these substrates in excess. Fig. 4.3 shows that endogenous SOUR continuously decreased with operation time. Similar trends have been reported by many authors, revealing the influence of MLSS (i.e. $(F/M)_C$ ratio) on microbial activity (Pollice et al., 2004). During the stable biomass growth period (phases III-V), low average SOUR values were observed (from 4.9 to 2.8 mg O2/g MLVSS h), similar to those usually reported for MBRs operated in endogenous conditions (Pollice et al., 2004). This is consistent

with the low biomass growth observed. In addition, $SOUR_{OHO}$ behaved the same, decreasing with operation time. It is notable that the endogenous uptake rate was approximately 60% of that with a carbon substrate, confirming the substantial organic carbon limitation imposed on the microorganisms in the tMBR.

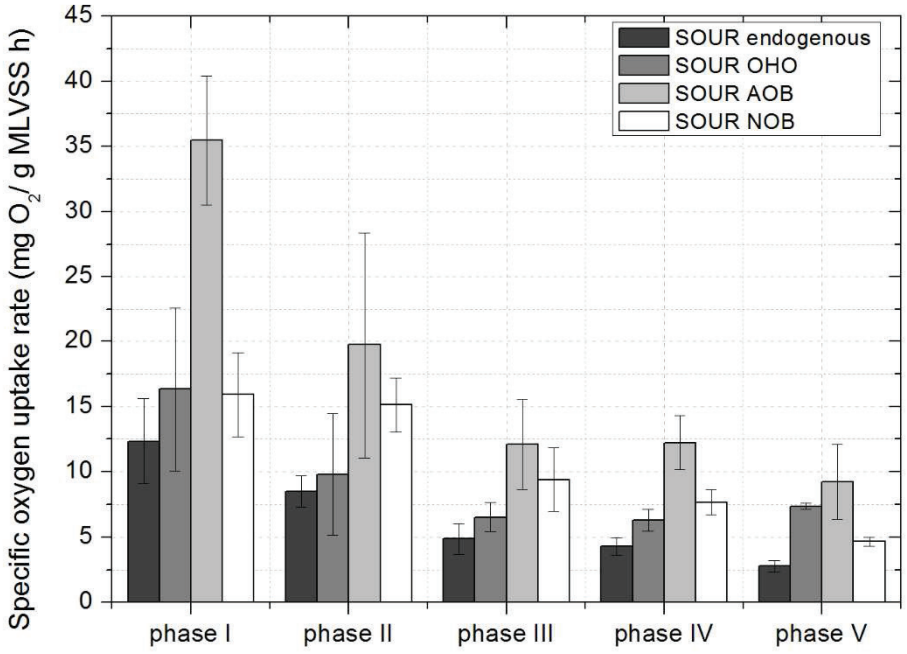

Figure 4.3. Specific oxygen uptakes rates for the different experimental phases in endogenous conditions and with addition of substrates: acetate ($SOUR_{OHO}$), ammonium ($SOUR_{AOB}$) and nitrite ($SOUR_{NOB}$)

Autotrophic activity is here expressed as specific oxygen uptake rate of ammonia oxidation bacteria, $SOUR_{AOB}$, and nitrite oxidation bacteria, $SOUR_{NOB}$. Both rates tended to decrease with operation time, a trend similar to the ammonium feed to microorganism ratio ($(F/M)_N$) in the tMBR. Assuming a theoretical factor for oxygen consumption of 4.57 (Metcalf and Eddy, Inc., 2003) and subtracting the endogenous consumption for recalculation of $SOUR_{AOB}$, ammonia uptake rates declined from 5.1±1.5 to 1.4±0.7 mg N/g MLVSS h, corresponding to a $(F/M)_N$ drop from 6.0 to 1.2 mg N/g MLVSS h. Similarly, based on a factor of 1.1 for $SOUR_{NOB}$, nitrite uptake rates reached 3.2±0.8 mg N/g MLVSS h at the end of phase I, increased to 6.0±1.2 mg N/g MLVSS h during phase II and then decreased to 1.7±0.9 mg N/g MLVSS h (phase V). Consistent with this, complete nitrification was continuously observed after 20 days of operation.

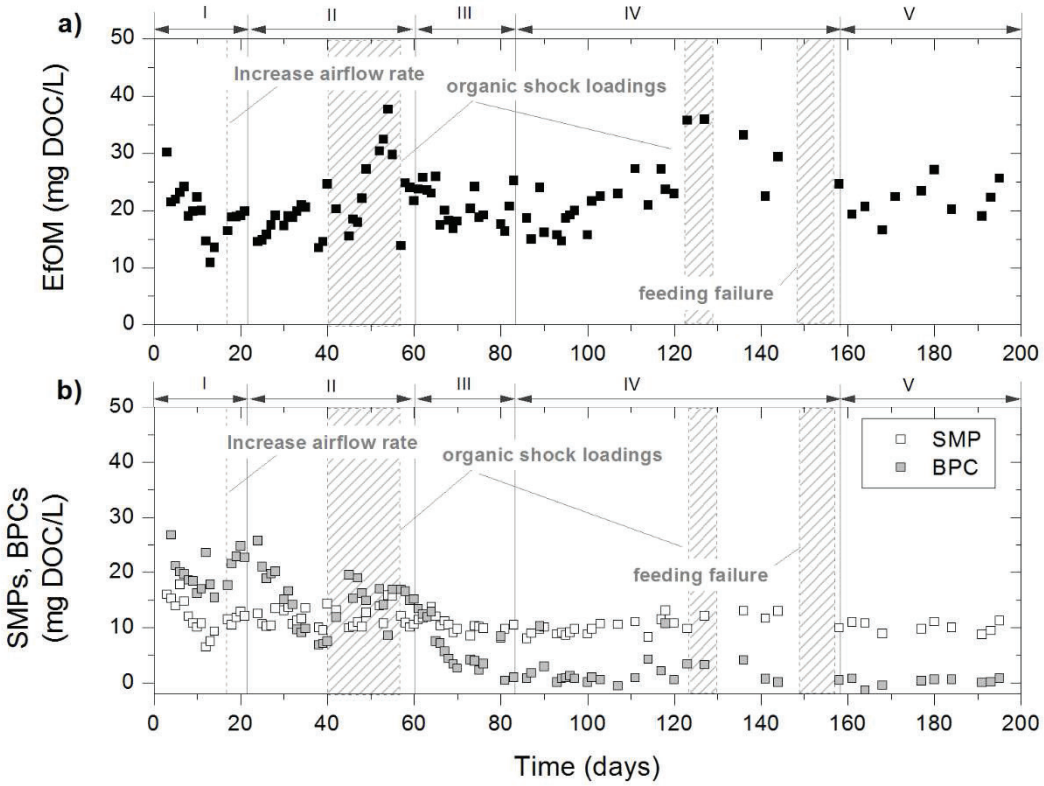

Figure 4.4. Evolution of secondary effluent organic matter (i.e. soluble organic feedwater concentration) and supernatant BPCs and permeate SMPs during the different experimental phases.

Many researchers have suggested that colloidal and soluble biopolymers (BPCs and SMPs) play an important role in membrane fouling (Meng et al., 2009; Lin et al., 2014). For this reason, biopolymer content was routinely analysed (Fig. 4.4b). BPC in the tMBR was estimated from the difference between DOC concentrations in the suspension supernatant and the permeate. SMP concentration was assumed to be the DOC concentration in the permeate. Secondary effluents are mainly composed of organic matter (EfOM) of different origins, where biopolymers represent an important part. Therefore, feedwater DOC concentration was also measured in order to assess biopolymer production and degradation by the microorganisms in the tMBR. During the experimental period, EfOM ranged between 10.9 and 37.7 mg DOC/L, with an average of 21.3±5.1 mg DOC/L (Fig. 4a). As shown in Fig. 4b, BPCs tended to accumulate in tMBR, following the same trend as EfOM during the first 17 days of phase I. In addition, corresponding with the increasing airflow rate, BPCs rapidly increased while white foam appeared. Net BPC release is a common response of microorganisms to environmental stresses, which cause release of proteins and polysaccharides due to sludge deflocculation (Lin et al., 2014). This deflocculation process is consistent with the high supernatant turbidity (Table 4.2)

and the presence of white foam, attributed to some proteins with surface-active properties (Di Bella et al., 2011). From day 24, BPCs started to decrease until day 40, when concentration reached 7.5 mg/L. At this point, the sum of BPC and SMP concentrations was similar to EfOM concentration; it was thus assumed that deflocculation had ceased. Nevertheless, an organic shock load in the feedwater again led to a significant rise in BPCs. After that, during the biomass stable-growth period (phases III-V), BPCs were progressively biodegraded/adsorbed by the biomass until a very low stable concentration was reached (1.85 mg/L, on average). Furthermore, given the low microbial activity reached in this period, lower biopolymer production was expected because of the low substrate utilization.

On the other hand, SMPs remained nearly constant throughout the experimental study, with an average of 11.1±2.0 mg DOC/L (Fig. 4.4b). During stable biomass conditions (phases III-V), a mass balance between EfOM and SMPs revealed a net removal of 52±7 %. Therefore, feedwater fluctuations and microbial processes appear to only affect BPC concentration, which in turn correlates with the biopolymer fraction retained by the membrane. Consequently, it is expected that BPC evolution affects membrane fouling, consistently with previous studies (Wang and Li, 2008).

3.3. Correlation between different biomass characteristics

Table 4.3 shows the multicollinearity (expressed by Pearson´s coefficient r) of the sludge parameters previously discussed. As expected, MLSS was highly correlated with the apparent viscosity (r = 0.852). This correlation is frequently reported in many studies. For example, Wu and Huang (2009) obtained a similar correlation coefficient in different sludges from MBRs. MLSS also correlated (r = -0.826) with endogenous SOUR, confirming its influence on microbial activity, in agreement with previous studies (Pollice et al., 2004). The low coefficient (r = -0.557) obtained for nitrification activity ($SOUR_{AOB}$) should be attributed to the considerable variability associated with unstable conditions in phases I-II. It should be noted that the autotrophic population shows a lower growth rate and therefore requires more time to become accustomed to the new conditions. Results also highlighted a moderate correlation (r = -0.735) between MLSS and BPC. This may be related principally to the development of the slow-growing population after a long operation time, which are able to degrade the biopolymers, as proposed by other authors [e.g. Sabia et al., 2013].

Table 4.3. Pearson´s correlation coefficient between suspension characteristics.
p significance in brackets

PARAMETERS	N	BPC	MLSS	Supernatant turbidity	d_{10}	Apparent viscosity	SOUR Endogenous	$SOUR_{AOB}$	TTF
BPC	58	1							
MLSS	51	-0.735 ($1.4\cdot10^{-7}$)	1						
Supernatant turbidity	65	0.581 ($6.3\cdot10^{-6}$)	-0.473 ($1.6\cdot10^{-3}$)	1					
$D_{(v,0.1)}$	13	-0.442 ($1.7\cdot10^{-1}$)	0.171 ($6.3\cdot10^{-1}$)	-0.668 ($2.4\cdot10^{-2}$)	1				
Apparent viscosity	65	-0.378 ($1.9\cdot10^{-2}$)	0.852 ($3.0\cdot10^{-14}$)	-0.129 ($4.2\cdot10^{-1}$)	-0.112 ($7.5\cdot10^{-1}$)	1			
SOUR endogenous	37	0.699 ($1.4\cdot10^{-4}$)	-0.826 ($2.1\cdot10^{-7}$)	0.493 ($5.7\cdot10^{-3}$)	0.258 ($6.7\cdot10^{-1}$)	-0.618 ($5.8\cdot10^{-4}$)	1		
$SOUR_{AOB}$	37	0.429 ($2.9\cdot10^{-2}$)	-0.557 ($2.1\cdot10^{-2}$)	0.403 ($2.0\cdot10^{-2}$)	0.890 ($4.3\cdot10^{-3}$)	-0.402 ($3.7\cdot10^{-2}$)	0.588 ($2.5\cdot10^{-4}$)	1	
TTF	65	0.522 ($7.8\cdot10^{-4}$)	-0.413 ($2.5\cdot10^{-3}$)	0.775 ($1.7\cdot10^{-9}$)	-0.634 ($4.7\cdot10^{-2}$)	-0.138 (0.35)	0.310 (0.12)	0.216 (0.27)	1

Among the parameters affecting suspension filterability, expressed by TTF, only supernatant turbidity presented a moderate correlation (r = 0.775), revealing a considerable effect of bioflocculation on sludge filterability. In contrast, results indicated that MLSS did not directly correlate to sludge filterability.

3.4. Membrane performance

Submerged hollow-fibre MBRs are frequently operated under temporised filtration/backwashing cycles (Judd, 2010). This operation mode was applied in the present work. During a filtration cycle, transmembrane pressure (TMP) linearly increased with elapsed

time. This behaviour can be explained by the incompressible cake model (Vera et al., 2014), where TMP within a filtration cycle can be expressed in terms of the initial transmembrane pressure (TMPi), fouling rate (r_f) and elapsed time (t) (Eq. [4.1]):

$$TMP(t) = TMP_i + r_f\, t \qquad [4.1]$$

Based on this approach, r_f can be used as a quantification parameter of reversible fouling and TMP_i as another parameter associated with residual fouling phenomena after backwashing.

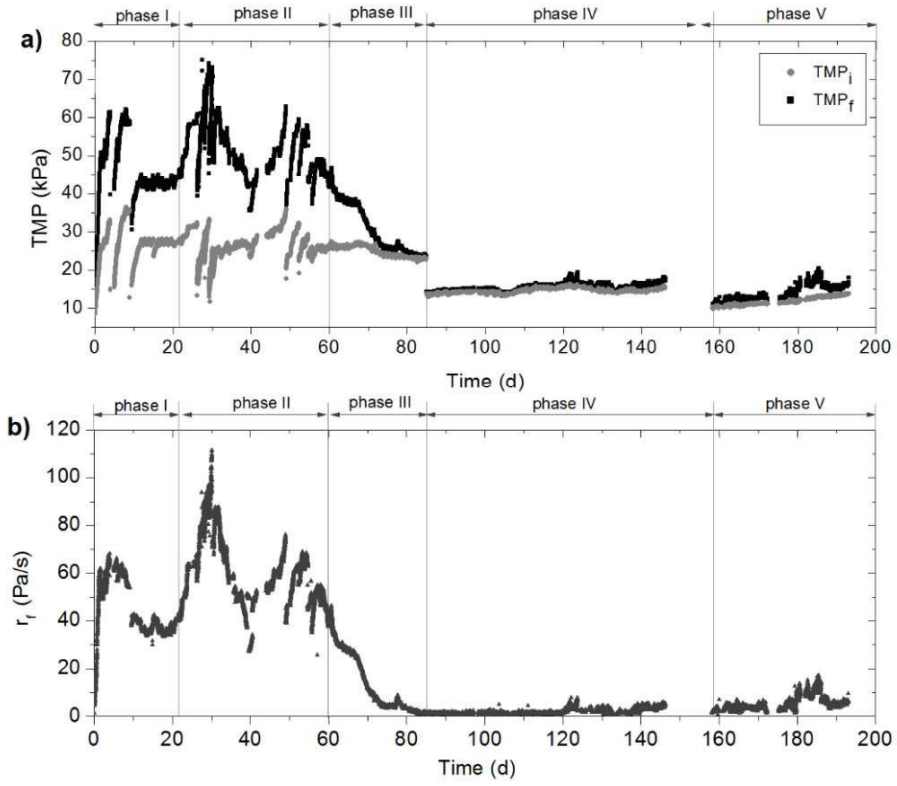

Figure 4.5. Evolution of membrane performance during the different experimental phases: **a** initial and final transmembrane pressure within cycles; **b** fouling rates during each cycle

The evolution of membrane performance, expressed in terms of TMP_i and TMP_f (transmembrane pressure at the end of the filtration cycle), is shown in Fig. 4.5a. During phase I, TMP_i tended to rapidly increase up to 28-36 kPa (higher than the technical operating values), despite two chemical cleanings performed on days 4 and 8. Identical TMP_i trends were observed between chemical cleanings, where most of the fouling was observed on the first day of operation. A theoretical explanation for this behaviour has been proposed, considering a specific

deposited mass remaining on the membrane surface after backwashing (Charfi et al., 2015). Therefore, residual fouling depends on backwashing effectiveness, and the properties and quantity of the mass deposited after backwashing (i.e. r_f and filtration time). For given backwashing conditions and a fixed filtration time (7 min), TMP_i is expected to depend on r_f. Consistently, r_f followed a similar trend to TMP_i, suddenly increasing to 35-65 Pa/s, which is 20-40 times higher than typically found in full-scale MBRs (Fig. 4.5b) (Drews, 2010). After increasing airflow rate on day 17, r_f suddenly rose to impractical levels (> 65 Pa/s), resulting in numerous plant shutdowns due to the high TMP reached. For membrane recovery, several chemical cleanings were periodically performed on days 18, 20 and 22 and 23. On the 27th day, the system started to recover its normal operation due to r_f decline. Nevertheless, the high organic loads in the feedwater from the 44th to 57th day significantly increased r_f again, leading to another unstable period which lasted until the end of phase II. These results suggest that environmental stresses due to raised oxygen concentration and organic load have a profound effect on membrane fouling. Both environmental factors have been identified as causes for biopolymer release and fouling propensity in MBRs (Le-Clech et al., 2006). In accordance with this, r_f showed a similar trend to that observed for BPCs during phase II (Fig. 4b). After that, during phase III (61st-84th day), r_f gradually dropped to operative values (~1 Pa/s) (Drews, 2010). During the same period, TMP_i slightly decreased from 26 to 23 kPa confirming the linkage between reversible fouling rate and residual fouling. Yet again, r_f decline coincided with a similar BPC decay. Thus, the results indicate that biomass progressively acclimatised after a couple of days, decreasing its BPC levels and fouling potential. Subsequent phases (III and IV) were characterised by stable membrane performance. Phase IV (85th-157th day) started with a chemical cleaning which removed most of the residual fouling. TMP_i and r_f remained at nearly constant and low values. Another chemical cleaning was performed in phase V, achieving a TMP value similar to that at the beginning of the experimental period. Although r_f showed some variability during phase V, it remained between operative values. However, this variability induced a slow TMP_i increase at a constant rate of 0.10 Pa/s. This fouling cannot be directly related to BPCs, since their concentration remained very low during this phase (Fig. 4.4b). This behavior can be justified by other factors such as a slight sludge deflocculation and the rise in MLSS and apparent viscosity with operation time (see Table 2).

3.5. Influence of biomass characteristics on membrane fouling rate

As previously reported in many studies, no single biomass parameter can explain membrane fouling, and thus its origin must be explored in combination with several parameters (Van den Broeck et al., 2011). For this reason, four parameters (BPCs, MLSS, supernatant turbidity and TTF) that describe key suspension properties such us colloidal biopolymer content, suspended solids concentration, bioflocculation state and sludge filterability, were assessed. Table 4.4 summarises the Pearson's coefficient of the parameters derived from the fouling rate data obtained during all experimental phases. Fig. 4.6 also shows how the fouling rates change with these parameters.

Table 4.4. Pearson´s correlation coefficient between selected parameters and r_f.

PARAMETERS	N	*min*	*max*	*r*
BPC (mg DOC/L)	97	-0.54	28.2	0.868 ($<1\cdot10^{-9}$)
MLSS (mg/L)	100	153	6,980	-0.765 ($<1\cdot10^{-9}$)
TTF (s)	65	5	4,620	0.233 (0.080)
Supernatant turbidity (NTU)	65	6.6	116	0.250 (0.032)

p significance in brackets

The highest correlation for r_f was found for BPCs, with a coefficient of 0.868, where they ranged from 0.54 to 28.2 mg DOC/L (Fig. 4.6a). This high correlation is in agreement with some previous studies (Wu and Huang, 2009) and differs with others considering components of BPCs such as polysaccharides or proteins (Drews, 2010). Discrepancies may be due to the complexity of fouling phenomenon at different operation parameters and hydrodynamic conditions. In subcritical flux operation, where TMP often shows a three-stage profile, the colloidal biopolymers have often been identified as the main foulants during the second stage, corresponding to a prolonged TMP rise (Charfi et al., 2015). During this period, fouling rate increases with foulant load (i.e. permeate flux and biopolymer concentration) but very low fouling rates are commonly reported (Le-Clech et al., 2006). In contrast, supracritical flux operation leads to high fouling rates due to rapid deposition of suspended solids on membrane surfaces, forming a cake layer. Colloidal biopolymers can influence caking by enhancing sludge floc attachment to the membrane (Lin et al., 2014), reducing cake-layer porosity (Charfi et al.,

2015) and increasing specific cake resistance due to an osmotic pressure mechanism (Chen et al., 2012). Biopolymers are commonly considered as a whole, without distinguishing soluble and colloidal fractions. However, soluble biopolymers should pass through the membrane with the effluent and thus not significantly contribute to fouling. In fact, membrane pore constriction can also be induced by this soluble fraction but many studies have shown that internal fouling is less than surface fouling in MBRs (Shen et al., 2015). In the present study, the results revealed that colloidal biopolymers (i.e. BPCs) were a crucial factor that regulated membrane fouling. On the other hand, since the membrane was operated at high permeate flux and low shear rates (i.e. without air scouring at the membrane surface), a major contribution from MLSS was expected in contrast with previous studies (Bae and Tak, 2005) that remark the importance of colloidal/soluble biopolymers rate. Nevertheless, the level of MLSS appeared not to have a significant effect on membrane fouling, since a negative correlation (r = -0.765) between MLSS and rf was calculated (Table 4.4). This trend is in fact inconsistent with the cake filtration model in dead-end conditions (i.e. without shear rate), where the solid concentration of the cake tends to rise with MLSS concentration (Le-Clech et al., 2006). A deeper analysis showed different trends according to the MLSS range (Fig. 4.6b). At low to moderate values (<3,000 mg/L), a negative correlation was clearly observed, while slight positive correlation resulted from increasing MLSS above ~5,000 mg/L. Therefore, results seem to indicate that the low shear rate due to bioreactor mixing was enough to induce some back-transport of suspended solids from the membrane. It is known that back-transport due to shear-induced diffusion and inertial lift increases with shear rate and particle size (Zeman and Zydney, 1996), which justifies a selective deposition of colloidal biopolymers onto the membrane, as previously reported (Pan et al, 2010). This explains the importance of BPCs for membrane fouling at MLSS lower than 3,000 mg/L. On the other hand, as discussed in section 3.1 apparent viscosity significantly increased when MLSS became higher than 3,500 mg/L. Since shear rate decreases with viscosity (Trussell et al., 2007), this may be reason for the slight rise in r_f when MLSS are above 5,000 mg/L. From the results it can be deduced that optimum operating conditions involve concentrations of BPC below ~5 mg/L and MLSS approximately within the range between 3,000 and 5,000 mg/L. It should be noted that similar results have been reported with secondary MBRs treating raw municipal wastewater. Several studies have suggested that low F/M ratios may result in a low metabolic activity, suitable sludge morphology and low soluble biopolymer concentration, which was correlated to a less fouling potential (Meng et al., 2009, R. Van den Broeck et al., 2012, Sabia et al., 2013).

The sludge filterability, measured by TTF, did not show a significant correlation with fouling rate (Table 4.4 and Fig. 4.6c). As TTF is based on cake filtration in dead-end regime, this trend is consistent with some degree of suspended solids back-transport during filtration in the tMBR. However, supernatant turbidity showed a similar trend to that obtained for TTF, revealing a poor correlation with fouling rate (Table 4 and Fig. 6d). It can thus be concluded that BPCs have a predominant role when compared with other sludge properties as indicators of its fouling potential.

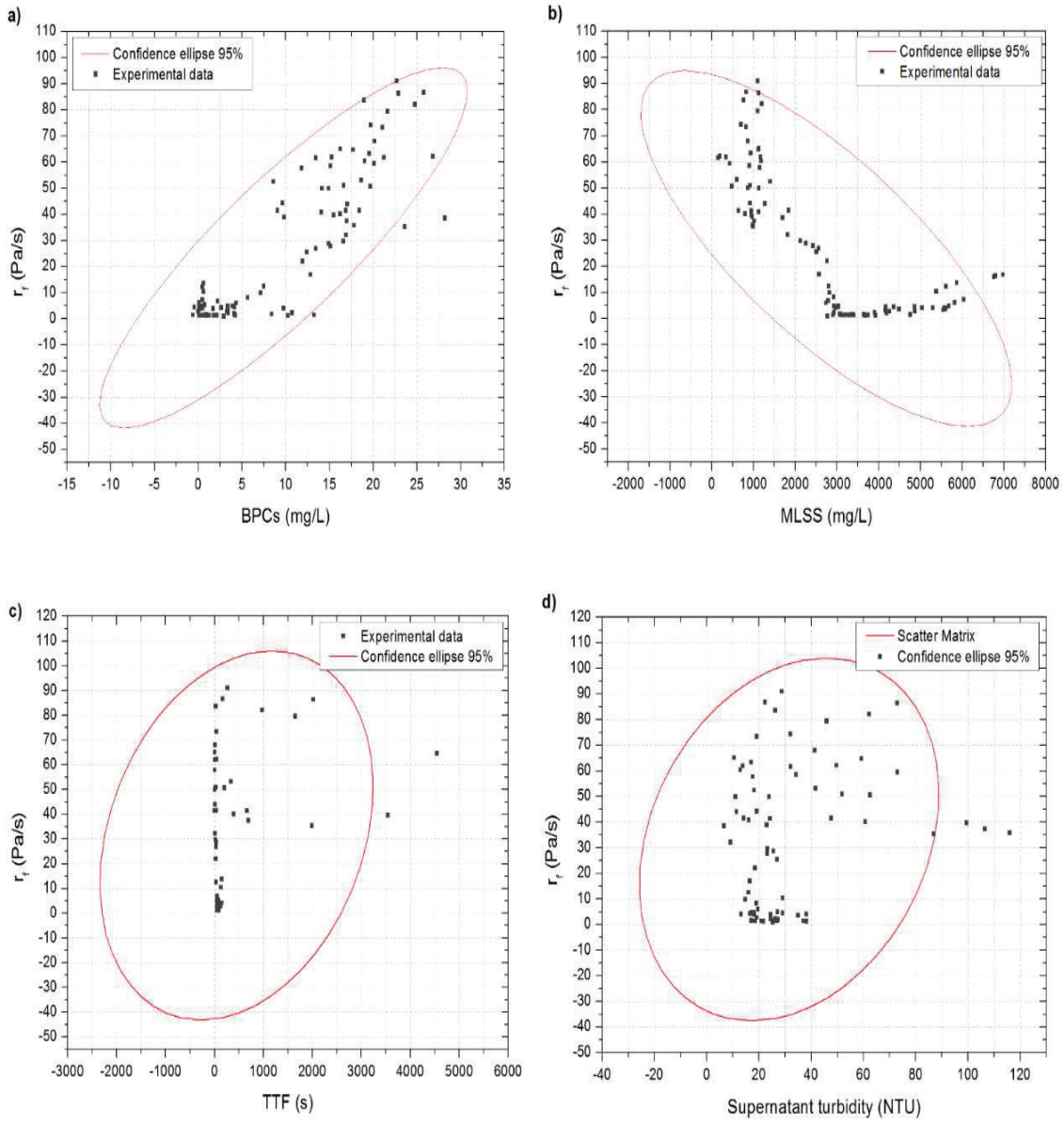

Figure 4.6. Relationship of fouling rate with several biomass characteristics: a BPCs, b MLSS, c TTF and d supernatant turbidity

4. Conclusions

The effect of sludge characteristics on membrane fouling in a tMBR was assessed in this study; the following may be concluded:

- Environmental stress affected sludge characteristics and thus membrane fouling. A sudden oxygen increase resulted in temporary biomass deflocculation, BPC release and consequently, severe induced membrane fouling. Organic shock loads also increased BPC content but their effect on membrane fouling seemed to depend on MLSS range. While at MLSS lower than 3,000 mg/L the effect was significant, at higher concentrations it was not noticeable. This behaviour was attributed to the development of the slow-growing microbial population able to degrade BPCs.

- At MLSS higher than 3,000 mg/L, a low stable biomass growth (0.04±0.002 kg MLVSS/kg COD) was observed, regardless of organic shock loads or feeding failures. This stable growth period was characterised by low bioactivity, BPC content and membrane fouling.

- Statistical multicollinearity of the sludge characteristics showed a significant correlation between MLSS and a set of parameters (endogenous SOUR, apparent viscosity and BPCs). In contrast, results indicated that MLSS were not directly correlated to sludge filterability, measured as TTF.

- In the hydrodynamic conditions assessed (J =35 L/h m^2 without air scouring in the filtration phase), incompressible cake-layer formation was found to be the predominant fouling mechanism. In these conditions, it was demonstrated that BPCs have a predominant role, compared with other sludge properties, as indicators of its fouling potential.

5. References

Amanatidou, E., Samiotis, G., Bellos, D., Pekridis, G., Trikoilidou, E., Net biomass production under complete solids retention in high organic load activated sludge process, *Bioresource Technology,* 182, (2015), 193-199.

Aquino, S.F., Stuckey, D.C., Integrated model of the production of soluble microbial products (SMP) and extracellular polymeric substances (EPS) in anaerobic chemostats during transient conditions, *Biochem. Eng. J.,* 38, (2008), 138-146.

Bae, T.H., Tak, T.M., Interpretation of fouling characteristics of ultrafiltration membranes during the filtration of membrane bioreactor mixed liquor, *J. Membr. Sci.,* 264, (2005), 151–160.

Charfi, A, Yang, Y., Harmand, J., Ben Amar, N., Heran, M., Grasmick, A., Soluble microbial products and suspended solids influence in membrane fouling dynamics and interest of punctual relaxation and/or backwashing. *J. Membr. Sci.,* 475, (2015), 156-166.

Chen, J., Zhang, M., Wang, A., Lin, H., Hong, H., Lu, X., Osmotic pressure effect on membrane fouling in a submerged anaerobic membrane bioreactor and its experimental verification. *Bioresour. Technol.*, 125, (2012), 97–101.

Cote, P., Alam, Z., Penny, J., Hollow fiber membrane life in membrane bioreactors (MBR). *Desalination* 288, (2012), 145-151.

Di Bella, G., Torregrossa, M., Viviani, G., The role of EPS concentration in MBR foaming: analysis of a submerged pilot plant. *Bioresour. Technol.*, 102, (2011), 1628-1635.

Drews, A., Membrane fouling in membrane bioreactors—Characterisation, contradictions, causes and cures*. J. Membr. Sci.,* 363, (2010), 1–28.

Fenu, A., Roels, J., Wambecq, T., De Gussem, K., Thoeye, C., De Gueldre, G., Van De Steene, B.,. Energy audit of a full-scale MBR system. *Desalination*, 262, (2010), 121-128.

Gineset, P., Audic, J.M., Urbain, V., Block, J.C., Estimation of Nitrifying bacterial activities by measuring oxygen uptake in the presence of the metabolic inhibitiors allythiourea and azide, *Appl. and Environ. Microbiol.*, 64 (6), (1998), 2266-2268.

Judd, S., The MBR Book, Principles and Applications of Membrane Bioreactors for Water and Wastewater Treatment, 2nd edition. Elsevier. (2010)

Koch Membrane, (2014). Case Study. Aquapolo Ambiental Water Reuse Project. (http://www.kochmembrane.com/PDFs/Case-Studies/KMS-Sao-Paulo-Brazil-Case-Study.aspx)

Le-Clech, P., Chen, V., Fane, A.G., Fouling in membrane bioreactors used in wastewater treatment. *J. Membr. Sci.*, 284, (2006), 17-53.

Lin, H., Zhang, M., Wang, F., Meng, F., Liao, B., Hong, H., Chen, J., Gao, W., A critical review of extracellular polymeric substances (EPSs) in membrane bioreactors: Characteristics, roles in membrane fouling and control strategies. *J. Membr. Sci.*, 460, (2014), 110-125.

Lin, H.J., Gao, W.J., Leung, K.T., Liao, B.Q., Characteristics of different fractions of microbial flocs and their role in membrane fouling. *Water Sci. Technol.,* 63, (2011), 262-269.

Marketsandmarkets, (2014). Membrane Bioreactor Systems Market by Application (Municipal Wastewater Treatment and Industrial Wastewater Treatment), by Type (Hollow Fiber, Flat Sheet, and Multi Tubular), by Configuration (Internal/Submerged and External/Side stream), and by Region - Trends & Forecasts to 2019. Report CH 2651.

Meng, F., Chae. S.R., Drews, A., Kraume, M., Shin, H.S., Yang, F., Recent advances in membrane bioreactors (MBRs): Membrane fouling and membrane material. *Water Res.* 43, (2009), 1489-1512.

Metcalf and Eddy, Inc.,. Wastewater Engineering: Treatment and Reuse. McGraw-Hill, New York (2003).

Pan, J.R., Su, Y.C., Huang, C., Lee, H.C., Effect of sludge characteristics on membrane fouling in membrane bioreactors. *J. Membr. Sci.,* 349, (2010), 287–294.

Pollice, A., Laera, G., Blonda, M., Biomass growth and activity in a membrane bioreactor with complete sludge retention. *Water Res.*, 38, (2004), 1799-1808.

Pollice, A., Laera, G., Saturno, D., Giordano, C., Effects of sludge retention time on the performance of a membrane bioreactor treating municipal sewage. *J. Membr. Sci.,* 317, (2008), 65-70.

Rosenberger, S., Kruger, U., Witzig, R., Manz, W., Szewzyk, U., Kraume, M., Performance of a bioreactor with submerged membranes for aerobic treatment of municipal wastewater. *Water Res*., 36, (2002), 413–420.

Sabia, G., Ferraris, M., Spagni, A., Effect of solid retention time on sludge filterability and biomass activity: Long-term experiment on a pilot-scale membrane bioreactor treating municipal wastewater. *Chem. Eng. J.,* 221, (2013), 176-184.

Shen, L.G. Lei, Q., Chen, J.R., H.C. Hong, H.C., He, Y.-M., Lin, H.J., Membrane fouling in a submerged membrane bioreactor: Impacts of floc size. *Chem. Eng. J.,* 269, (2015), 328–334.

Standard Methods for the examination of Water and Wastewater, American Public Health Association/Water Environment Federation, 21st ed. Washington DC, USA. (2005)

Trussell, R.S., Merlo, R., Hermanowicz, S.W., Jenkins, D., Influence of mixed liquor properties and aeration intensity on membrane fouling in a submerged membrane bioreactor at high mixed liquor suspended solids concentrations. *Water Res.,* 41, (2007), 947-958.

Van den Broeck, R., Krzeminski, P., Van Dierdonck, J., Gins, G., Lousada-Ferreira, M., Van Impe, J.F.M., van der Graaf, J.H.J.M., Smets, I.Y., van Lier, J.B., Activated sludge characteristics affecting sludge filterability in municipal and industrial MBRs: Unraveling correlations using multi-component regression analysis. *J. Membr. Sci.*, 378, (2011), 330-338.

Van Loosdrecht, M., Henze, M., Maintenance, endogenous respiration, lysis, decay and predation. *Water Sci. Technol.*, 39, (1999), 107–117.

Vera, L. González, E., Díaz, O., Delgado, S., Performance of a tertiary submerged membrane bioreactor operated at supra-critical fluxes. *J. Membr. Sci.,* 457, (2014), 1-8.

Villain, M., Marrot, B., Influence of sludge retention time at constant food to microorganisms ratio on membrane bioreactor performances under stable and unstable state conditions. *Bioresour. Technol.,* 128, (2013), 134-144.

Wang, X.M., Li, X.Y., Accumulation of biopolymer clusters in a submerged membrane bioreactor and its effect on membrane fouling. *Water Res.,* 42(2008), 855-862.

Wang, Z., Yu, H., Ma, J., Zheng, X., Wu, Z., Recent advances in membrane bio-technologies for sludge reduction and treatment. *Biotechnology Advances*, 31, (2013), 1187-1199.

Wilén, B.M., Keiding, K., Nielsen, P.H., Anaerobic deflocculation and aerobic reflocculation of activated sludge. *Water Res.,* 34, (2000), 3933-3942.

Wu, J., Huang, X., Effect of mixed liquor properties on fouling propensity in membrane bioreactors. *J. Membr. Sci.,* 342, (2009), 88–96.

Zeman, L.J., Zydney, A.L., Microfiltration and ultrafiltration: principles and application. Marcel Dekker, Inc., New York. (1996)

CAPÍTULO 5: El papel de los pretratamientos de nanofiltración/ósmosis inversa para la reutilización de agua: Ultrafiltración versus MBR

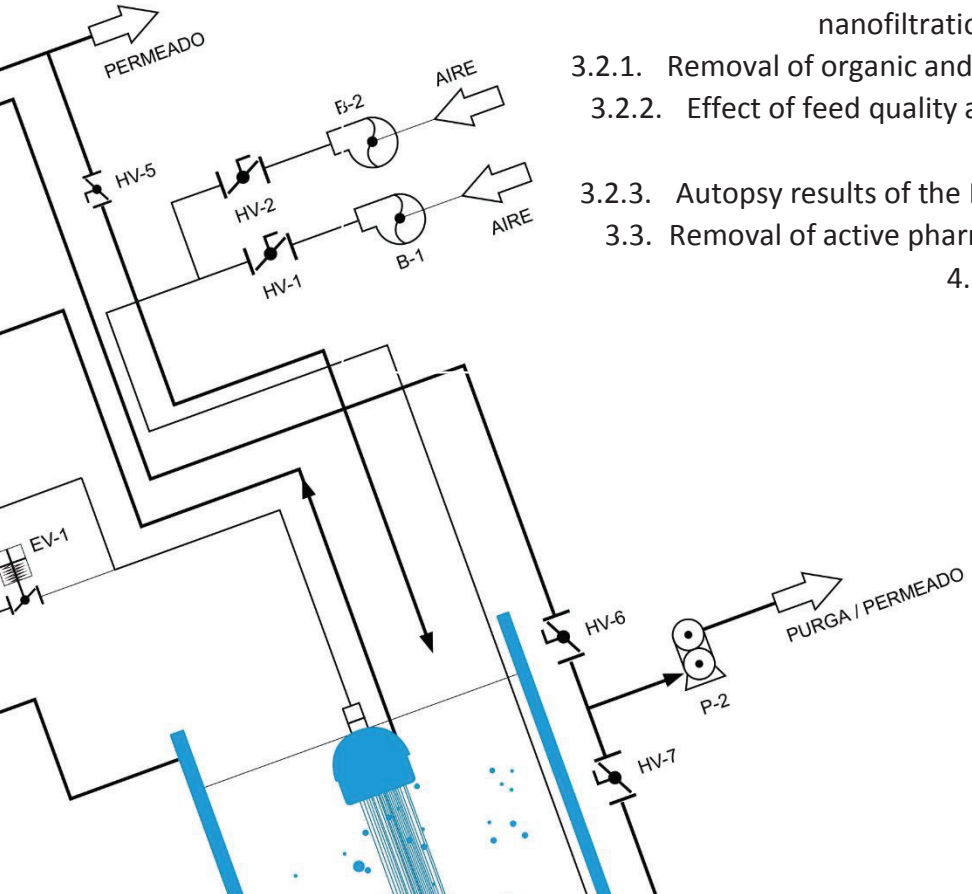

Capítulo 5

El papel de los pretratamientos de nanofiltración/ósmosis inversa para la reutilización de agua: Ultrafiltración versus MBR terciario

The role of pretreatment of nanofiltration/reverse osmosis for water reuse: Ultrafiltration versus tertiary MBR

Oliver Díaz, Enrique González, Luisa Vera, Laura Porlán, Juan Rodríguez-Sevilla, Cristina Afonso-Olivares, Zoraida Sosa-Ferrera, José Juan Santana-Rodríguez

Enviado a
CLEAN- Soil, Air, Water

Factor de impacto: 1,945 (JCR®, Thomson Reuters 2015).

Highlights

- Comparison of ultrafiltration and membrane bioreactor systems
- Influence of biopolymeric clusters on membranes fouling
- Advanced treatment trains for wastewater reuse without sanitary and chemical risks
- Improvement of wastewater reuse schemes for promoting secure irrigation
- High pressure membrane processes for domestic wastewater reuse applications

Keywords

Nanofiltration, Reverse Osmosis, Tertiary membrane bioreactor, Wastewater reuse, Pharmaceutical active compounds

Resumen:

En regiones con escasez de agua, la regeneración de aguas residuales constituye una práctica cada vez más extendida en el marco de la gestión de recursos hídricos. Las distintas legislaciones que regulan la reutilización de aguas residuales, son muy exigentes en cuanto a la calidad del agua regenerada y a la salvaguarda de la seguridad sanitaria asociada a su utilización,

por ello se hacen necesario la implantación de tratamientos avanzados que permitan alcanzar los requerimientos exigidos al agua regenerada. Las antiguas plantas de tratamiento de aguas residuales que presentan frecuentes episodios de des-floculación, y por tanto, un pobre rendimiento de los clarificadores secundarios, necesitan de tratamientos terciarios, como la ultrafiltración directa, para obtener un efluente con una calidad aceptable. Por otro lado, en zonas costeras donde los recursos hídricos subterráneos son sobre-explotados, el agua residual municipal presenta generalmente valores altos de salinidad, y por tanto, el proceso de reutilización requiere una etapa final de desalinización. En éste Capítulo se analiza el rendimiento alcanzado por un proceso de ultrafiltración directa (UF) y un biorreactor de membrana (MBR, en inglés) terciario como pretratamientos de efluentes depurados en depuradoras convencionales de lodos activos, antes de ser desalinizados en procesos de nanofiltración y ósmosis inversa.

La ultrafiltración directa y el MBR terciario operaron con membranas sumergidas del mismo tipo, alcanzando un grado de eliminación de materia orgánica, expresada como COD, del 87% y 93%, respectivamente. La diferencia de eficacia exhibida por ambos sistemas se debe a la degradación biológica de la materia orgánica y la nitrificación completa del influente experimentada en el MBR terciario. La concentración de materia orgánica en el agua de alimentación, expresada como COD, fue relativamente alta. El MBR terciario permitió la degradación biológica de estas sustancias hasta alcanzar concentraciones significativamente inferiores a las alcanzadas en el concentrado de la ultrafiltración directa.

El ensuciamiento de las membranas de ultrafiltración fue asociado a la construcción de una torta incompresible, en ambos sistemas. Sin embargo, el mecanismo de construcción de dicho ensuciamiento fue diferente en cada tratamiento. En el caso del MBR terciario, la construcción de la torta fue lenta, y además, su naturaleza fue reversible durante todo el periodo experimental. Esto puede ser debido a la baja concentración de BPC en el medio y al uniforme y moderado tamaño de los flóculos. De hecho, el ensuciamiento observado en el MBR fue debido principalmente, a la deposición de partículas de la suspensión. Para el caso de la ultrafiltración directa, el sistema experimentó una velocidad de ensuciamiento reversible y además, un mayor ensuciamiento residual. Éste comportamiento se ha atribuido a la alta concentración de BPC en el medio, y un ensuciamiento de la membrana debido principalmente, a los micro-coloides y sustancias disueltas.

La membrana de ósmosis inversa experimentó una alta tasa de rechazo de los principales constituyentes orgánicos e inorgánicos presentes en los efluentes producidos tanto por la UF como por el MBR. El carbono orgánico disuelto fue retenido entre un 98 y 100%, mientras que la conductividad fue reducida hasta 45-87 µS/cm. Por otro lado, la membrana de nanofiltración experimentó una alta retención de sustancias orgánicas disueltas (93-97%) y una moderada tasa de rechazo a los iones multivalentes. En el caso de los iones monovalentes, el sistema presento una retención parcial debida probablemente al efecto Donnan, lo que generó un permeado con alta conductividad (900-1.300 µS/cm).

Tanto la membrana de nanofiltración como la de ósmosis inversa sufrieron un mayor ensuciamiento al alimentar el efluente procedente de la ultrafiltración directa, debido al alto contenido de DOC presente en el permeado procedente de este pretratamiento. Por otra parte, el ensuciamiento de la membrana de nanofiltración fue mucho más acusado que el exhibido por la membrana de ósmosis inversa, debido a que esta última operó a flujos iniciales más moderados y por tanto, menos colmatantes.

La autopsia de la membrana de nanofiltración reveló la constitución de una estructura reticular densa cubriendo la superficie de la membrana, y eliminable sólo parcialmente, por medio de limpiezas físicas. El espectro EDX reveló que dicha estructura estaba formada principalmente por P, Fe, Ca; con una baja presencia de Mg y Na. Los resultados para la membrana de ósmosis fueron relativamente similares, sin embargo, el ensuciamiento de la membrana en éste caso se concentró en torno a los espaciadores. En ambos casos, el análisis FITR reveló que el ensuciamiento retirado por el enjuague se debió principalmente, a proteínas y polisacáridos.

El biorreactor de membrana terciario alcanzó una mayor eliminación de fármacos debido a que la biodegradación de estas sustancias se vio favorecida por las condiciones de operación endógenas aplicadas. Como era de esperar, el sistema de ósmosis inversa alcanzó una retención total de los fármacos estudiados, mientras la membrana de nanofiltración presento coeficientes de retención moderados: 94, 85, 70 y 27% para el atenolol, paraxantina, cafeína y ácido clofíbrico, respectivamente.

Abstract

The potential for nanofiltration (NF) and reverse osmosis (RO) in secondary effluent reclamation is noteworthy, but they require extensive pretreatment to prevent membrane fouling and promote system longevity. In this study, performance of direct ultrafiltration (UF) and tertiary membrane bioreactors (tMBRs) as feed pretreatments were assessed on a pilot scale. Both technologies achieved high organic matter removal (87% and 93% for UF and tMBR, respectively). Differences in efficiencies were related to suspended biomass in the tMBR, which enhanced degradation of the dissolved organic substances (<5 mg/L) and also stabilised process performance by minimising residual fouling. Whichever pretreatment was applied, RO reached higher rejection coefficients and low fouling levels. Nevertheless, lower normalised flux (12%) was achieved when UF effluent was due to high concentration of organic substances. Membrane autopsies by SEM-EDX and FTIR revealed that organic fouling appears to be predominant in both NF/RO membranes. The main organic foulants identified were polysaccharides and proteins. Inorganic foulants mainly consisted of calcium, phosphorus and iron. Complete removal of pharmaceutical active compounds was observed for RO, while NF presented moderate retention coefficients (94, 85, 70 and 27% for atenolol, paraxanthine, caffeine and clofibric acid, respectively).

1. Introduction

In regions with scarcity of natural water resources, wastewater reclamation and reuse is a widely extended practice. Legislation affecting reclaimed wastewater reuse is very demanding regarding quality and health safety, which has required the application of advanced technology. Among the technologies available to comply with the stringent standards, ultrafiltration (UF) is successfully applied for the treatment of secondary effluents in order to meet the requirements of increasingly stricter reclaimed water quality requirements (Wintgens et al., 2005). Alternatively, tertiary submerged membrane bioreactors (tMBR) have also been proposed for old wastewater treatment plants (WWTP) with poor performance of secondary clarifiers [http://www.kochmembrane.com/PDFs/Case-Studies/KMS-Sao-Paulo-Brazil-Case-Study.aspx].

By operating at maintenance energy level (i.e. minimal value for the carbon substrate utilisation rate), tMBR significantly reduces sludge production and minimises the concentration of organic soluble components (Delgado et al., 2010; Vera et al., 2014). Despite advances in both technologies, experience gained over recent decades from operating membranes has demonstrated that membrane fouling continues to be the main limitation halting its widespread

application (Filloux et al., 2012). Fouling is mainly caused by the organic matter present in secondary effluents, which can be adsorbed or deposited within membrane pores or on its surface, leading to membrane permeability decline. To maintain process productivity and mitigate membrane fouling in hollow-fibre membrane modules, backwashing (i.e. use of permeate to flush membrane backwards) has been incorporated as a standard operating strategy (Judd 2010).

On the other hand, although UF and tMBR have shown highly efficient removal of particle and colloidal matter, they do not completely remove dissolved organic matter and salts. These residual organics include trace organic micropollutants such as pharmaceutically active compounds, which accumulate in the environment, threatening water resources (Jurado et al., 2012). In addition, in some coastal areas where underground water resources have been over-exploited, municipal wastewaters are often generated with very high levels of salinity (electrical conductivity between 2,000 and 2,500 µS/cm). This pollution directly affects water reclamation schemes, requiring a final complementary desalination process to avoid compromising soil and crop integrity.

High-pressure membrane processes such as nanofiltration (NF) and reverse osmosis (RO) for brackish wastewater treatment show high potential in the framework of water reuse for crop irrigation. Because RO can achieve a high degree of removal of nearly all dissolved constituents from water, it is one the most popular tertiary treatments for wastewater reclamation. In fact, RO has also been considered for post-treatment of MBR permeate in treating wastewater to drinking water standards for water reclamation applications (Lutchmiah et al., 2014). Nanofiltration (NF) was introduced in the late 1980s, mainly combining softening and organic removal. Since then, the implementation of NF has extended widely. Nowadays this process is applied successfully to drinking water production, removing various pollutants including pesticides and endocrine disruptors, and also for partial desalination (Van der Bruggen et al., 2008).

The potential for these NF/RO processes in wastewater reclamation is noteworthy, but effective fouling control is necessary to increase cost effectiveness. Biofouling and colloidal material are not specific problems due to previous treatment with ultrafiltration membranes, in contrast to deposition or adsorption of small organic solutes and scaling. Organic fouling is a complex phenomenon that involves interactions between the feed solution, membrane

properties and operation conditions (Cobry et al., 2011). Scaling is a thermodynamic process involving a phase change and forms a scaling layer on the membrane surface. Classical solutions to fouling are the optimisation of pre-treatment methods and hydrodynamic conditions (crossflow velocity, permeate flux and transmembrane pressure).

The aim of this study was to assess the performance of UF and tMBR as pretreatments for NF/RO processes for removing salinity and pharmaceuticals from a secondary effluent. Comparison was carried out in terms of membrane fouling and permeate quality. In addition, four pharmaceuticals with molecular weights less than 300 g/mol and different physico-chemical properties were selected as model compounds. The propensity of NF/RO membranes to fouling was also assessed and related to the pretreatment process applied. Finally, complementary information was obtained from NF/RO autopsies, including characterisation of fouling layer components and its reversibility.

Table 5.1. Feedwater main characteristics (n = 14)

PARAMETERS	UNITS	MEAN	RANGE
COD_t	mg/L	450	72-695
COD_s	mg/L	90	29-120
DOC	mg/L	22	16-30
$N\text{-}NH_3$	mg/L	45	23-53
$N\text{-}NO_3^-$	mg/L	0.8	0.5-3
Turbidity	NTU	453	22.1-1,100
TSS	mg/L	596	62-1,400
Conductivity	mS/cm	1.76	1.30-2.10

2. Materials and methods

2.1. Feedwater

The tertiary unit was fed with secondary effluent from a conventional activated sludge wastewater treatment plant, whose average characteristics are given in Table 5.1. This is a conventional WWTP designed for carbon removal only. Due to the short sludge ages and oxygen deficiency in the activated sludge process, frequent episodes of sludge de-flocculation or not

enough sedimentation usually appear, resulting in high suspended solids and organic matter concentrations in the effluent.

2.2. Pilot tMBR/UF system.

A cylindrical 220 L deposit was equipped with ZeeWeed® ZW-10 (GE Water & Process Technologies) hollow-fibre membranes of 0.04 µm rated pore diameter, 1.9 mm external diameter and 0.9 m^2 of filtering surface area, assembled vertically (see Vera et al., 2014). ZeeWeed® consists of a woven reinforcing braid on which a PVDF membrane is cast. The effluent (permeate) was extracted from the top header of the module under slight vacuum. All experiments were carried out at constant permeate flux (J= 35 L/hm^2), registering transmembrane pressure as a function of time. Membrane fouling was controlled each 7 min by backwashing and their conditions (flux J_B and backwashing time t_B) were constant throughout the experimental period at J_B= 60 L/hm^2 and t_B= 30 s. The system was operated in dead-end filtration mode, although constant air scouring during the backwashing phase was applied at 3.1 $Nm^3/h\ m^2$ in order to improve fouling removal (Vera et al., 2014). Process tank stirring was carried out by air-bubbling at the bottom of the bioreactor. This unit was operated as tertiary membrane bioreactor and as ultrafiltration unit in order to compare their filterability and productivity.

In tMBR operation mode, the system was run without sludge removal. Additional air was also supplied by a biological compressor process to always maintain the dissolved oxygen concentration in the reactor above 1.5 mg/L. In contrast, when the pilot was operated as UF, the biological process compressor was turned off and a peristaltic pump was activated to continuously withdraw the concentrate stream from the process tank.

2.3. Fouling tests of biological suspension/concentrate fractions

In order to assess the relative contribution of different fractions to global fouling, both biological suspensions from tMBR (mixed liquor) and UF (concentrate) were separated in three components (particulate, colloidal and soluble). Fractionation was carried out using several microfiber filters (Millipore) of different nominal pore sizes: 1.50 and 0.45 µm. Each fractionated suspension was filtered in a bench-scale filtration unit at similar hydrodynamic conditions in order to estimate its fouling potential.

The laboratory unit for fouling tests was equipped with a ZeeWeed® ZW-1 hollow-fibre similar to that used in the pilot unit but with a smaller filtration area (0.047 m^2). ZW-1 was operated in a closed loop, through a stirred 1.5 L tank of 21 cm water height. A magnetic drive pump was used to withdraw permeate from the membrane module. All trials were run at constant permeate flux (J = 35 L/h·m^2), dead-end filtration mode and lasted 30 min.

2.4. Advanced treatment bench unit: NF/RO

2.4.1. Experimental protocol

The advanced treatment was assayed by a laboratory unit equipped with a SEPA II experimental module which allows cross-flow filtration. The cross-flow velocity was fixed at 0.35 m/s by a 1.2 mm spacer. Two commercial membranes were used, providing 142 cm^2 of filtering surface area: nanofiltration GE Desal_DK and reverse osmosis TriSep X201. The chosen NF membrane was a hydrophilic thin-film membrane (polyamide top layer) with a molecular weight cut-off at 200-230 Da. The RO was also via a thin-film membrane, featuring a polyamide-urea copolymer top layer, with a highly negatively charged surface.

All experiments were carried out at constant transmembrane pressure (7 and 12 bar for NF and RO, respectively), registering the permeate flux as a function of time by an automatic balance. Permeates from UF and tMBR were filtered at different recoveries: 30, 50, 70 and 90%. Retentate flow was controlled by a manual valve and excess was returned to the feed tank. Temperature of feed water was controlled and stabilised at 20±1^{0}C throughout the experimental time.

2.4.2. Membrane autopsy

Structural analysis and chemical characterisation of the fouled and cleaned membranes were achieved by scanning electron microscopy with dispersive X-ray (SEM-EDX) and Fourier transform infrared spectroscopy (FTIR). An *ex situ* cleaning procedure was applied: (1) soaking with Milli-Q water for 15 min; (2) chemical cleaning with a solution of NaOH (pH=10) for 2 h; and (3) chemical cleaning with a solution of HCl (pH=10) for 2 h. Membrane samples for SEM-EDX and FTIR analysis were taken after each step. FTIR was conducted using an IFS 28/55 Bruker spectrometer and SEM-EDX analysis with JEM 6300 supplied by JEOL Ltd.

2.5. Analytical methods

Dissolved oxygen was measured using a WTW 340i and conductivity with a WTW 720. Total and soluble chemical oxygen demand (COD_t and COD_s, respectively), total suspended solids (TSS), colour, and turbidity were determined in conformity with the Standard Methods (ALPHA, 2005). The analysis of ammonium-nitrogen ($N\text{-}NH_3$) was carried out by the Nessler method using a DR-5000 Hach spectrophotometer. Dissolved organic carbon (DOC) concentration was measured with a TOC-meter (TOC-5000A, Shimadzu). The difference in DOC concentration between the filtrate of the suspension obtained through a 0.45 µm nitrocellulose membrane filter (HA, Millipore) and the ZeeWeed permeate was assigned as biopolymer clusters (BPC). The analyses of nitrate-nitrogen ($N\text{-}NO_3^-$), chloride (Cl^-), phosphate(PO_4^{3-}), sulphate (SO_4^{2-}), sodium (Na^+), potassium (K^+) and magnesium (Mg^{2+}) were conducted through ion chromatography using a Compact IC plus 882 device supplied by Metrohm. Bicarbonate (HCO_3^-) and pH were measured by automatic volumetric titration using the 716 DMS titrino supplied by Metrohm. Microbial floc size distribution was measured using a Malvern Mastersizer 2000 instrument with a detection range of 0.02-2000 µm.

2.6. Pharmaceutical compounds determination

Solid Phase Extraction (SPE) procedure was used as extraction/preconcentration technique combined with Liquid Chromatography tandem Mass Spectrometry (LC-MS/MS) for the determination of the pharmaceutical compounds (atenolol, paraxanthine, caffeine and clofibric acid) after the treatment process using a previously optimised methodology (Afonso-Olivares et al., 2012). The SPE procedure was carried out using 250 mL of treated water sample at pH 8, which was passed through an Oasis HLB polymeric cartridge and subsequently 2 mL of methanol was used as an extracting solvent. The methanol extract was evaporated under a gentle nitrogen stream and reconstituted with 1 mL of water. Then, 10 µL of aqueous extract was analysed by LC-MS/MS triple quadrupole with an electrospray ionisation (ESI) interphase from Varian system (Varian Inc., Madrid, Spain) using a 3.0 mm x 100 mm, 3.5 µm particle SunFire™ C_{18}column. The mobile phase consisted of water (containing a 0.2% formic acid and 5mM ammonium formate, pH 2.6 mixture)/methanol at a flow rate of 200 $\mu L \cdot min^{-1}$. The gradient used began with 90:10 (v/v) and during 13 min it changed to 45:55 (v/v). Then, the mixture increased at 65% (v/v) of methanol during 1 min. Finally, it returned to initial condition using 16 min and then 5 min was employed to equilibrate the system. Limits of quantification (LOQs) of different compounds were calculated as the lowest concentration that gave a signal-to-noise ≥ 10 (Shrisvastava et al.,

2011). LOQs values were 0.16 $ng \cdot L^{-1}$, 264 $ng \cdot L^{-1}$, 32.5 $ng \cdot L^{-1}$ and 0.65 $ng \cdot L^{-1}$ to atenolol, paraxanthine, caffeine and clofibric acid, respectively.

3. Results and discussion

3.1. Performance of tertiary treatments: direct ultrafiltration and membrane bioreactor

3.1.1. Permeate quality and concentrate/biological suspension characteristics

The main characteristics of permeate and concentrate/biological suspension obtained from UF/tMBR are shown in Table 5.2. It can be seen that both systems achieved a high COD removal (87% and 93% for UF and tMBR, respectively), due to high particulate and colloidal fractions in the feedwater (see Table 5.1). The differences between the systems can be attributed to biological degradation of the soluble organic matter in the tMBR, consistent with the lower mean value of DOC measured in the corresponding permeate. As expected, a complete nitrification (97%) was observed in tMBR according to the high sludge retention and biological stabilisation attained. Similar values for the physico-chemical parameters not affected by biological degradation (turbidity, conductivity and colour) were also observed for both units.

Regarding concentrate/biological suspension characteristics, biopolymer clusters (BPC), total suspended solids (TSS) and mean particle diameter ($D_{(v,0.5)}$) were routinely measured due to their important role in membrane performance. BPC can be defined as a pool of non-filterable organic matter of microbial origin associated with fouling layer formation in membrane pores or on the surface (Sun et al., 2011). Although the BPC are mainly biodegradable, the conventional hydraulic times used in activated sludge processes are usually not long enough to degrade completely those BPC and thus the secondary effluents usually present a substantial concentration. In accordance to this, results show a high concentration of BPC (20 mg/L as DOC) in UF concentrate, while in the tMBR, due to biological degradation, the BPC concentration decreased to 3 mg/L. In addition, UF concentrate presented a high mean TSS concentration, in accordance with the highly loaded feedwater, mainly comprised of settleable particles ($D_{(v,0.5)}$ = 69 µm). On the other hand, the biological suspension in the tMBR, as is usual when operated as a tertiary treatment and without biomass purge, stabilised at a nearly constant TSS concentration (3,380 mg/L), according to a low carbon utilisation rate (0.09 kg COD/kg MLSS d) (Vera et al., 2014).

Table 5.2. Main characteristics of permeate and UF concentrate/tMBR suspension (n = 7)

PARAMETERS	UNITS	UF		tMBR	
		MEAN	RANGE	MEAN	RANGE
Permeate					
COD	mg/L	56	42-74	31	26-34
DOC	mg/L	16	14-17	9	7-10
$N\text{-}NH_3$	mg/L	47	40-53	0.5	0.4-0.6
$N\text{-}NO_3^-$	mg/L	0.3	0.1-0.5	37	32-40
Turbidity	NTU	0.5	0.4-0.6	0.4	0.3-0.5
Conductivity	µS/cm	1,915	1,810-2,010	1,929	1,580-1,710
Color	Units Pt/Co	115	114-121	120	109-132
Concentrate/Biological suspension					
Biopolymer clusters (BPC)	mg/L	20	15-24	3	1-4
TSS	mg/L	250	143-460	3,382	2,770-3,920
PSD					
$D_{(v,0.1)}$	µm	23	21-23	36	29-43
$D_{(v,0.5)}$	µm	69	65-76	103	94-119
$D_{(v,0.9)}$	µm	171	146-214	275	242-327

3.1.2. Membrane fouling analysis

Hydraulic resistance defined by Darcy's law was used to assess membrane performance. According to the 'resistance-in-series' model and disregarding the osmotic pressure term, the transmembrane pressure (*TMP*) can be described by Eq. 5.1:

$$TMP = J\mu R_t = J\mu(R_m + R_f) \quad [5.1]$$

where μ is the permeate viscosity, J is the permeate flux, R_t is the total hydraulic resistance, R_m is the clean membrane resistance and R_f is the fouling resistance.

In UF and tMBR with hollow-fibre modules, it is common to operate under frequent backwashing cycles for limiting membrane fouling (Judd, 2010). Therefore, fouling can be classified into two categories: reversible fouling (removed by backwashing) and residual fouling

(removed only through the use of chemicals). Accordingly, fouling resistance can be separated into reversible fouling (R_{rvf}) and residual fouling (R_{rdf}) resistances:

$$R_f = (R_{rvf} + R_{rdf}) \quad [5.2]$$

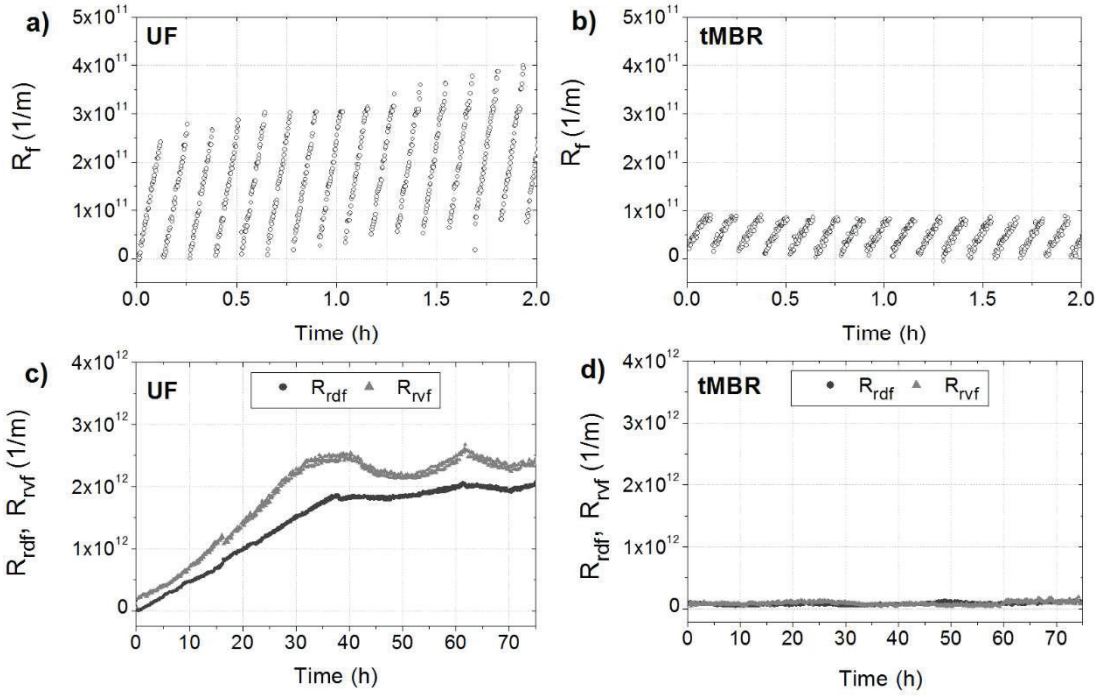

Figure 5.1. Fouling resitance (R_f) evolution during the first 2 h of operation: UF(a) and tMBR(b). Residual (R_{rdf}) and reversible (R_{rvf}) fouling resitances during the fouling test: UF (c) and tMBR(d)

Fig. 5.1a and 5.1b show the fouling resistance evolution with elapsed time under consecutive cycles, which linearly increased during the filtration phase for UF and tMBR. This linear trend is generally found in systems operated in dead-end mode when filtering high-particulate feedwater. It has been related to an incompressible cake/gel development mechanism against the membrane wall (Vera et al., 2014). However, significant differences between the two processes in residual and reversible fouling were observed (Fig. 5.1c and 5.1d). The tMBR membrane was fouled by deposition at a low rate ($1.3 \cdot 10^8$ 1/m s), which was also completely reversible throughout the experimental time. This result may be attributed to the particle size distribution of the microbial suspension, where uniform and large sized flocs were obtained (mean value of 103 µm), and the very low concentration of BPC (Table 5.2). In addition,

due to operating in dead-end regime where shear forces are absent, it is reasonable that large flocs build up into a porous cake layer with a low specific resistance. This cake layer should also be effectively removed by backwashing, accordingly with previous studies (Wu et al., 2012). In contrast, although the amount of foulants in the UF was lower than that in the tMBR, the fouling rate ($6.6 \cdot 10^9$ 1/m s) was much higher than for the tMBR. This confirms that the high BPC concentration contributed to the low porosity and high specific resistance, as recently reported by Poorasgari et al. (2015). Consistently, UF showed the typical trend for thin biopolymer (i.e. gel) layer formation where residual resistance linearly increased until reaching a critical mass deposited, corresponding to a residual fouling resistance of $1.85 \cdot 10^{12}$ 1/m (Charfi et al., 2015).

Table 5.3. Relative contribution of several fractions to the overall fouling rate for tMBR and UF. Lab-scale test carried out at unit ZW-1

	Relative contribution of fractions to fouling rate (%)		
SAMPLE	**Particles**	**Macro-colloids**	**Micro-colloids/dissolved substances**
UF (concentrate)	34.4	0.9	64.7
Tertiary MBR (mixed liquor)	84.8	6.0	9.2

To determine the 'foulest' fraction and therefore the most influential on filterability for both UF and tMBR systems, both suspensions, concentrate and mixed liquor were fractionated into several components. Then, these pre-filtered fractions were filtered in the lab-scale unit ZW-1 under the same hydrodynamic conditions as the pilot plant. Three fractions were studied: particles (>1.5 µm), macro-colloids (1.5-0.45µm), and micro-colloids/dissolved substances (<0.45µm). Table 5.3 shows the relative contributions of each fraction to the overall reversible fouling rate. Results confirmed that the particles were the dominant fraction in tMBR (84.8%), while in UF the micro-colloidal/dissolved substances performed the main role (64.7%). Macro-colloids did not make a significant contribution in either case. The low contribution of colloids in the tMBR (6.0% and 9.2% for macro and micro-colloids/ dissolved substances, respectively) is in accordance with the low BPC concentration, due to biological degradation.

3.2. Performance of advanced treatments: nanofiltration and reverse osmosis

As previously stated, several differences in dissolved organic concentration were observed between UF and tMBR permeates. This section assesses their influence on the subsequent performances of nanofiltration (NF) and reverse osmosis (RO) membranes.

3.2.1. Removal of organic and inorganic constituents

Retention coefficients for organic and inorganic constituents at different permeate recovery values (R=30% and R=90%) are given in Table 5.4. As expected, similar inorganic constituents were found for both different feedwaters (i.e. UF and tMBR permeates) except for the nitrogen compounds. In the UF, nitrogen was predominantly in the form of NH_4^+, while the nitrification process occurring in tMBR had mainly transformed NH_4^+ to NO_3^-.

Table 5.4. Effects of feed concentration on retention coefficient for each advanced treatment train assayed (n=2)

Advanced treatment train	**UF**				**tMBR**			
	NF		**RO**		**NF**		**RO**	
Parameters	R=30%	R=90%	R=30%	R=90%	R=30%	R=90%	R=30%	R=90%
Conductivity	60	48	97	97	41	39	95	98
DOC	97	97	98	99	93	94	100	98
HCO_3^-	76	61	97	97	62	54	96	98
Cl^-	26	16	98	94	21	17	98	98
NO_3^-	3	4	94	95	2	8	97	97
PO_4^{3-}	100	100	96	99	100	97	97	99
SO_4^{2-}	97	97	95	99	98	96	97	98
Na^+	58	41	97	97	26	30	96	98
K^+	61	49	96	97	33	26	96	97
Mg^{2+}	94	91	99	99	87	83	93	99
Ca^{2+}	88	83	99	99	74	67	90	98
NH_4^+	56	37	90	95	62	79	95	96

As expected, the capability of the RO membrane to reject organic constituents was higher than that of NF. On the other hand, inorganic retention was not influenced by feedwater quality. RO showed a high rejection for all ions (>90%), decreasing feed conductivity to as low as 40-87

µS/cm, supporting previous studies (Sachit et al., 2014). In contrast, NF presented a moderate to high retention for multivalent ions (67-100%) but monovalent ions were only partially retained (14-61%), as other authors previously reported (Van der Bruggen et al., 2008). Based on Kovács and Samhaber (2008), NF membrane (DK GE Osmonics) has a MWCO of 200-230 g/mol, corresponding to a pore radius of 0.39-0.44 nm. Monovalent cations such as NH_4^+, Na^+, and K^+ with a hydrated radius of 0.331, 0.276 and 0.201 nm, respectively, seem not to be rejected by steric exclusion (37-79%, 26-58% and 26-61%, respectively). Previous studies have reported that the DK membrane has an isoelectric point in the region of pH 3.5 to 4.1 (Oatley-Radcliffe et al., 2014). Therefore, this moderate retention may be due to a Donnan effect where only a small percentage of counter-ions (a different charge to the membrane, i.e. cations) can permeate (Azaïs et al., 2014). However, the high concentration of several monovalent cations in the feed water, mostly notably Na^+ (218-250 mg/L), may force a poor retention of monovalent anions like NO_3^- (0.335 nm) and Cl^- (0.324 nm) in order to maintain permeate electro-neutrality during the nanofiltration operation. As a result, NF only lowered feed conductivity to 900-1,300 µS/cm according to the recovery imposed.

3.2.2. Effect of feed quality and permeate recovery on membrane fouling

Fig. 5.2 shows normalised flux (J/J_0) declined as a function of permeate recovery for NF and RO membranes. Different fouling trends were observed for both processes. NF showed more severe flux decay during the trial (0.35-0.44 at 90% of recovery), probably due to the higher initial flux (J_0) promoting membrane fouling. Typically, at high J_0 values, two distinct phases can be observed: an initial period characterised by a pronounced flux decline and a second period in which permeate flux remained largely constant. This decline may be related to a liquid/solid transition caused by the accumulation of species in the boundary layer, which can lead to the formation of a fouling layer on the membrane surface or within the pores. Consistently, increasing the initial flux induced a more pronounced flux decline rate. After that, permeate flux reached a stationary value achieved when the system attains its equilibrium conditions. This occurs when the convective flux (permeate flux) is compensated by the dispersive fluxes of the solutes from the membrane. In these conditions, stationary flux values ranged between 28 and 9 L/h m^2 according to recovery value and the pretreatment process (i.e. UF or tMBR). According to these results, the operation should be carried out at lower *TMP* values (2.5 and 3 bar) which may result in low initial fluxes (~9-12 L/h m^2) and thus should not apparently produce a noticeable reduction in the permeate flux with operating time.

In contrast, RO operated at moderate initial fluxes (14.4-14.8 L/h m^2) achieving higher normalised fluxes of 0.76 and 0.86 at 90% recovery, for permeates from UF and tMBR, respectively. Differences between normalised fluxes of UF and tMBR around 78% may be attributed to high levels of DOC in UF permeate (Table 5.2), which led to different fouling behaviour according to previous studies (Cobry et al., 2011). From the results, fouling with organic matter is thought to be mainly associated with gel-layer formation, which could not be prevented by cross-flow shear force (Van der Bruggen et al., 2008). Several authors have observed that a feedwater with higher DOC concentration showed greater flux decline in RO membranes (Jacob et al., 2010; Wu et al., 2013; Mohammad et al., 2015). In long-term operation, the existence of organic matter in feed solution result in organic fouling and at the same time it will became the nutrient for microorganisms to grow and adhere to the membrane surface (Mohammad et al., 2015), and thus the biofouling may be controlled by reduction of organic matter in feed solution (Suwarno et al., 2014). In addition, some degree of inorganic fouling was also expected for both membranes, according to the high recovery values (Cobry et al., 2011).

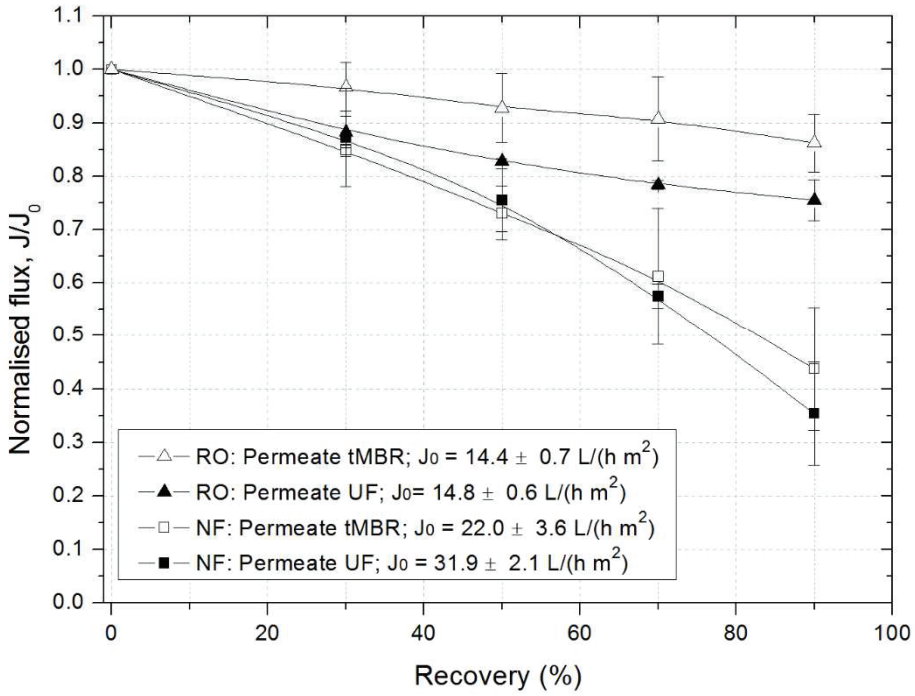

Figure 5.2. RO and NF normalized fluxes against permeate recovery for permates from UF and tMBR

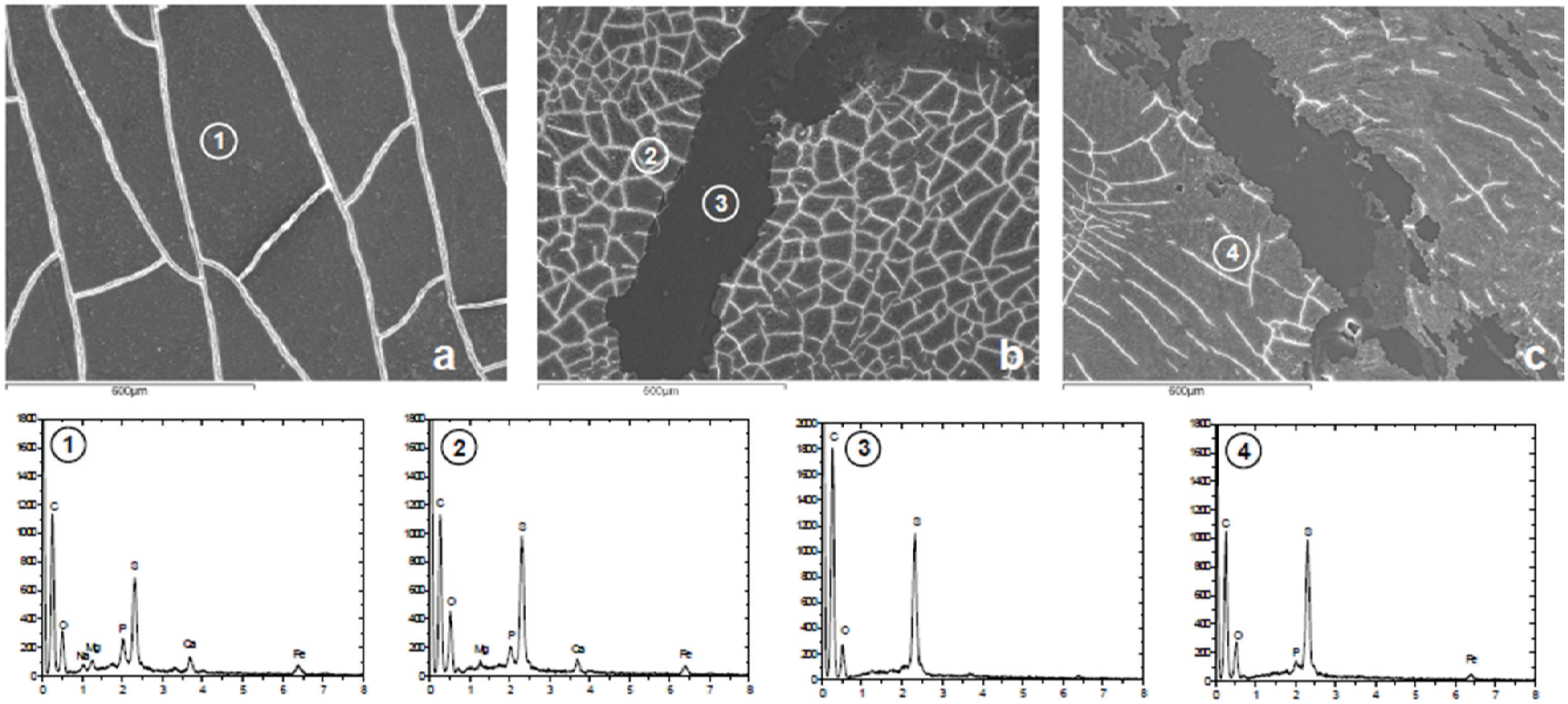

Figure 5.3. SEM micrographs of the NF fouled membrane (a), after water rising (b) and after chemical cleaning (c) and associated and EDX analysis. Micrographs of fouled and cleaned NF membrane samples were at 100 time magnification

3.2.3. Autopsy results of the NF and OI membranes

Several membrane samples were taken at the end of the trials and after successive steps of the specific cleaning protocol, in order to characterise the nature of fouling built up on NF and RO membranes during the experimental runs.

Fig. 5.3 displays SEM microphotographs of the fouled NF membrane at the end of the UF permeate filtration test (90% permeate recovery), after water rinsing and finally, after chemical cleaning (Fig. 5.3a, b and c, respectively). Fouled membrane showed a dense reticulated fouling layer covering the whole surface, where no crystalline or amorphous particles were visible. Results from EDX analysis indicated that the new membrane composition included C, S and O (data not shown), probably due to a polysulphone support layer (Cobry et al., 2011). EDX spectra of the fouling layer (area 1 in Fig. 5.3) showed significant quantities of P (10%), Fe (9%), Ca (7%) but relatively low levels of Mg (3%) and Na (3%). Previous analysis of fouled NF membranes applied to wastewater reclamation commonly include P and Ca as the main components of scalants, which may be related to the low solubility of calcium phosphate, with minor presence of Fe and Mg (Xu et al., 2010). In addition, metal ions, most notably Ca, can also augment organic membrane fouling by forming complexes with organic molecules (Li et al., 2004). It is important to note that relatively high levels of Fe have a significant impact on NF performance since it has been found associated with irreversible fouling in previous studies (Gwona et al., 2003). This dense fouling layer was partially detached by water rinsing, leaving uncovered the new membrane (area 3 in Fig. 5.3b). However, EDX analysis of the remaining fouling layer revealed a similar composition to that obtained before water rinsing (area 2 in Fig. 5.3b). Chemical cleaning by NaOH and HCl removed most of the inorganic foulants from the membrane surface (area 4 in Fig. 5.3c), where only traces of P and Fe could be detected. However, micrographs of the NF membrane revealed that the chemical cleaning did not remove the fouling layer. Therefore, it was evident that organic matter promoted the development of a compact gel-layer, which was only partially removed by physical means.

Similar results were obtained when analysing the RO membrane at the end of tMBR permeate filtration test (Fig. 5.4a, b and c), the main difference being an uneven distribution of deposits over the surface and a large accumulation in the regions near the spacer strands. This difference may be related to the lower initial flux applied to the RO membrane, corresponding to a lower surface organic load on the membrane. It known that the spacer may promote thick deposits in regions close to the strands (Tran et al., 2007).

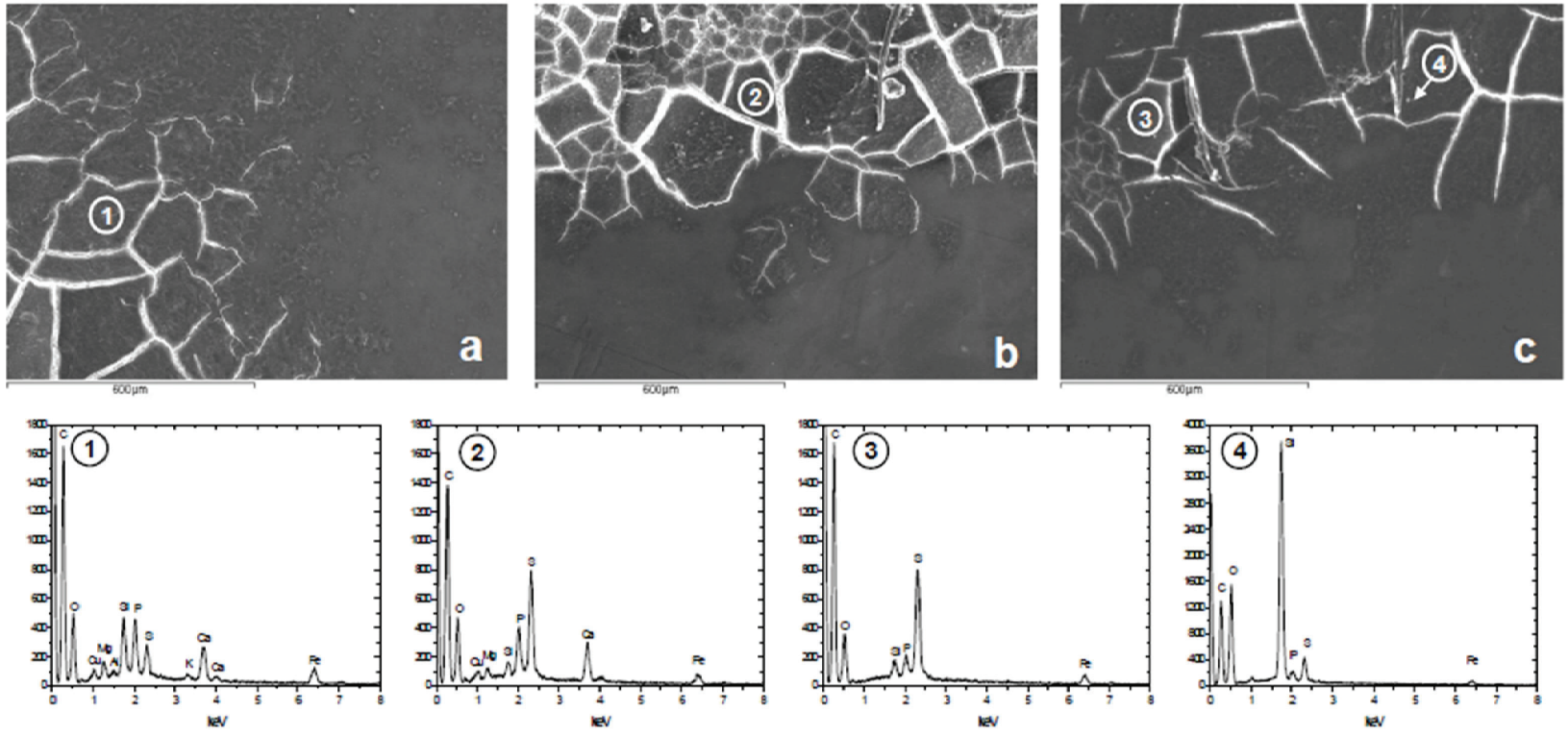

Figure 5.4. SEM micrographs of the RO fouled membrane (a), after water rising (b) and after chemical cleaning (c) and associated and EDX analysis. Micrographs of fouled and cleaned RO membrane samples were at 100 time magnification

In addition, silica deposits on the RO membrane (area 4 in Fig. 5.4c) can be clearly observed, even after cleaning protocol application.

In addition, the fouled membranes were analysed by FTIR (Fig. 5.5a and b) in order to identify the organic constituents of the compact gel-layer. For the NF membrane, the spectrum showed important new transmittance bands after fouling in the vicinity of 1,640-1,650 cm^{-1} (C=O stretching of amide I, quinone and ketone), 1,545-1,585 cm^{-1} (N-H deformation and C-N stretching of amide II) and 1,037-1,150 cm^{-1} (functional C-O) (Fig. 5.5a). The results suggest that the constituents of the fouling layer included proteins and polysaccharides (Tran et al., 2007, Melián-Martel et al., 2012, Moreno et al., 2013, Tang et al., 2014). After water rinsing, the bands associated with organic fouling seem to decrease and the partial elimination of fouling permitted the characteristic peaks of the new membrane to appear (1,095-1,280 cm^{-1}). When the fouled NF membrane was cleaned with chemicals, the FTIR spectrum was similar to that obtained after water rising, which confirms that the organic fouling was only partially removed by physical means.

Similar results were obtained when analysing the RO membrane (Fig. 5.5b), where bands associated with polysaccharides and proteins were detected in the fouled membrane (1,037, 1,545 and 1,640 cm^{-1}). As previously mentioned, due to the smaller gel-layer development compared with NF, a low cleaning efficiency was obtained and consequently FTIR spectra of the fouled membrane were similar throughout the cleaning protocol.

3.3. Removal of active pharmaceutical compounds

Four neutral and ionic compounds (atenolol, paraxanthine, caffeine and clofibric acid) with molecular weights ranging from 180 to 266 Da (similar to 200-230 MWCO of the NF membrane) were selected to assess removal capacities of NF and RO membranes. These compounds are representative of several therapeutic pharmaceutical categories (β-blockers, stimulants and lipid regulators) and are very common in effluents from wastewater treatment plants.

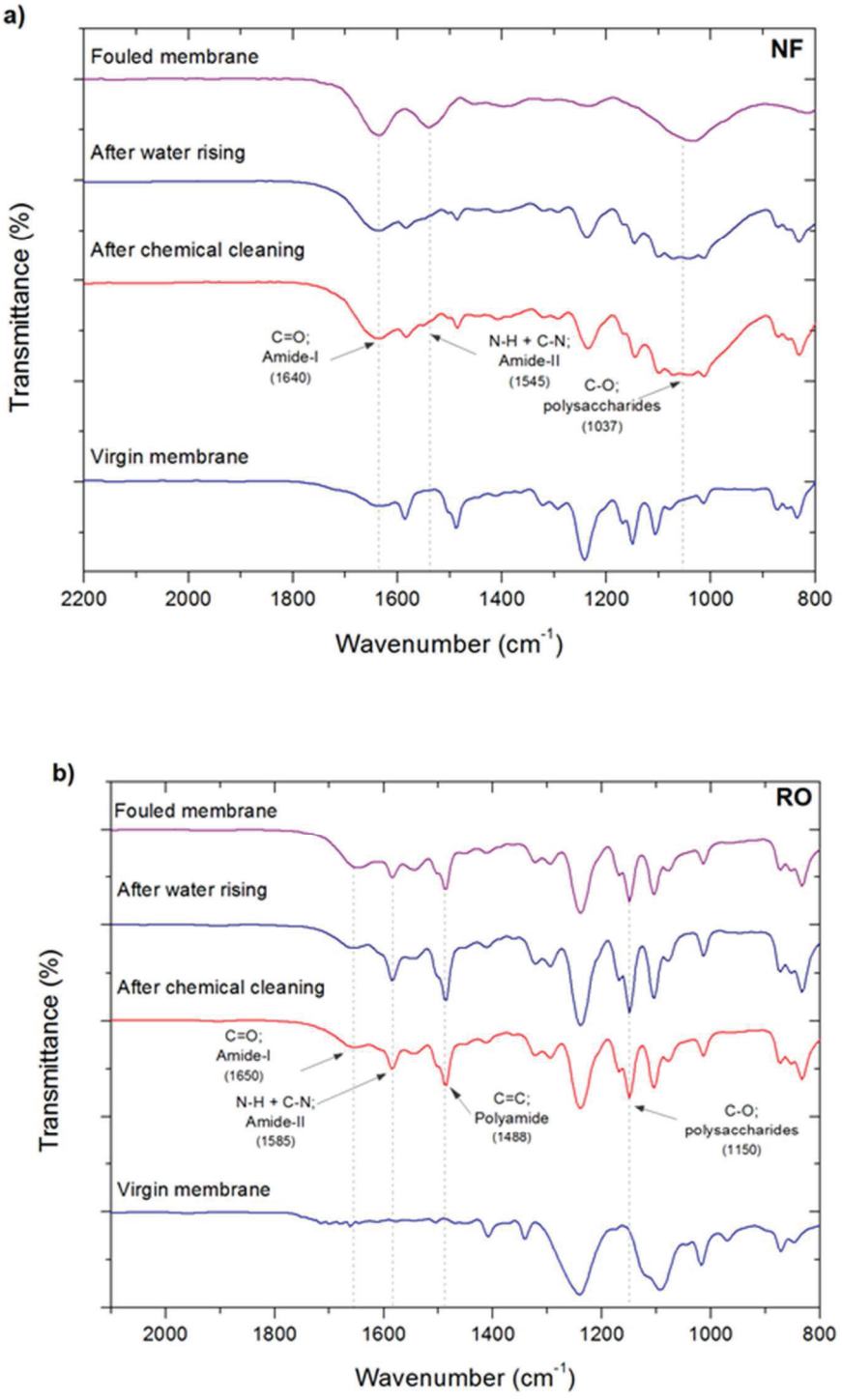

Figure 5.5. FTIR spectra of the new membranes and fouled NF (a) and RO (b) membranes

Fig. 5.6a and b show concentrations of the above-mentioned compounds in NF and RO retentates and permeates during the filtration tests of the feedwaters (i.e. UF and tMBR

permeates). In general, lower concentrations were detected in retentates from tMBR permeate compared to those obtained from UF, which may be due to biodegradation by the microorganisms in the tMBR (Dólar et al., 2012). The most prevalent compounds, paraxanthine and caffeine, showed an average reduction of 92% and 96%, respectively. High concentrations of these stimulants are commonly detected in raw wastewaters (20-100 µg/L) and biodegradation by conventional secondary treatments reaches 70-90% (Urtiaga et al., 2013). In the current tMBR, the high solid retention time and reduced feed-to-microorganism ratio may result improved removal of these stimulants (Radjenocic et al., 2009). A lesser removal efficiency of 65% was obtained for the atenolol (β-blocker), in accordance with the moderate biodegradability (44-71%) generally observed for β-blockers in conventional treatments or MBRs (Radjenocic et al., 2009). In contrast, the lipid regulator (clofibric acid) seems to be unaffected by biodegradation. This result is probably associated with the presence of chlorine in their molecular structure (Kikamura et al., 2005). Therefore, results confirm the limitations of a tertiary treatment by UF or tMBR for removing the selected pharmaceutically active compounds.

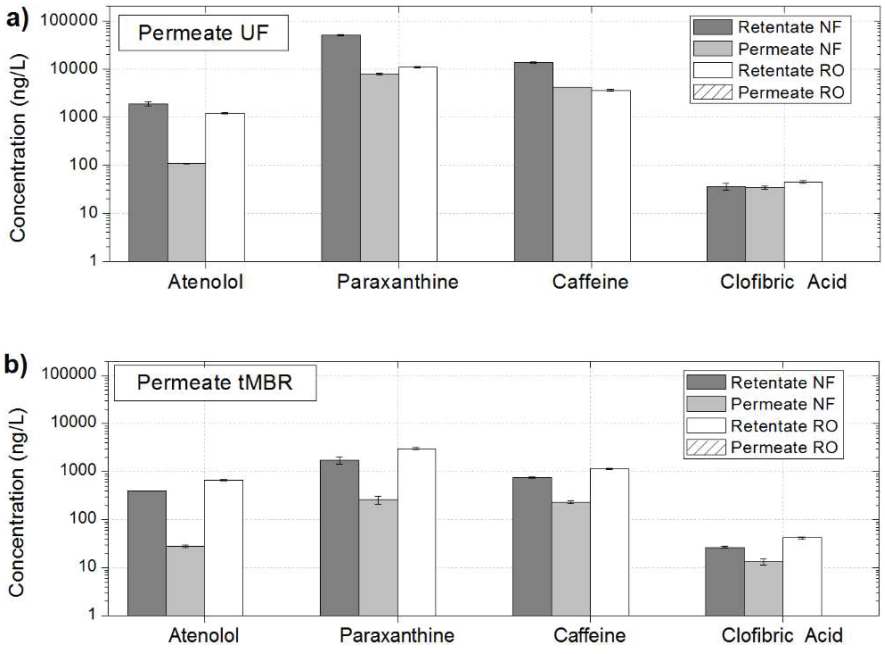

Figure 5.6. Pharmaceutic compounds concentration in NF and RO rententates and permeates during the filtration tests of the feedwaters (i.e. UF and tMBR permeates)

The rejection of the compounds by the NF/RO membranes was determined using the Equation [5.3]:

$$R = \frac{C_r - C_p}{C_r} \cdot 100 \qquad [5.3]$$

where C_r is the retentate concentration and C_p is the permeate concentration of a specific compound. As expected, these pharmaceutical compounds were completely removed or concentrations were below LOQs after RO filtration (Fig. 5.6a and b). This was due to a steric hindrance mechanism according to the low MWCO (Dólar et al., 2012). Similarly, Alturki et al. (Altuki et al., 2010) obtained rejection efficiencies greater than 99% for 40 trace organic contaminants, including atenonol and caffeine in a MBR/RO combined system. Urtiaga et al., (2013) also reported removal rates up to 99% for both compounds using a UF unit followed by a RO process. Thus, it was confirmed that RO membranes significantly reject the selected pharmaceuticals.

NF retained a significant amount of the compounds; although they were detected in permeate at trace levels. Average rejection coefficients were 94, 85, 70 and 27% for atenolol (MW= 266 Da), paraxanthine (180 Da), caffeine (194 Da) and clofibric acid (215 Da), respectively. The high rejection of atenolol, with the large molecular weight, seems to be governed by steric exclusion mechanism. Consistently, Fujioka et al. (2014) reported that for two NF membranes, the atenolol retention increased when decreasing the molecular weight cut-offs of the membrane tested. However, paraxanthine and caffeine presented moderate retention despite their low molecular weights and being hydrophilic. These results point to other effects, besides steric exclusion, determining the rejection efficiency of NF membrane. In fact, organic membrane fouling has been demonstrated to contribute to higher rejections of neutral pharmaceuticals in NF membranes (Comerton et al., 2008). According to Fujioka et al. (2014) caffeine is relatively hydrophilic at neutral pH. Due to this factor, this compound was not expected to be effectively adsorbed on the membrane. Conversely, high rejections were frequently observed when using the same NF membrane (DK GE Osmonics) as used in the current study, Acero et al. (2010) reported a removal efficiencies of 83.7 and 89.9% for the caffeine when filtering ultrapure water and secondary effluent, respectively. Although the mechanism for the caffeine rejection is unclear, it appears that feedwater composition do not have a significant effect upon the rejection. In addition, electrostatic interactions between charged solutes and the membrane have been frequently reported to be an important rejection

mechanism (Narbaitz et al., 2013). In the case of clofibric acid, the deprotonation of the molecule (pKa=3.2) within the pH range studied (8.1-8.4) and consequently its negative charge, should force it to be permeable in order to maintain permeate electroneutrality.

4. Concluding Remarks

In summary, the assessment of UF and tMBR performance as pretreatments to NF/RO processes for removing salinity and pharmaceuticals from a conventional secondary effluent allow conclude:

- UF and tMBR successfully retained most of the chemical oxygen demand of the secondary effluent (87% and 93% for UF and tMBR, respectively). Differences may be associated with biological degradation of soluble organic substances in the tMBR, according to the lower concentration of biopolymer clusters observed (20 mg/L and 3 mg/L for UF and tMBR, respectively).

- Evolution of fouling resistance in both pretreatments has been related with the development mechanism of an incompressible cake/gel on the membrane wall. However, for the tMBR, membrane fouling is suggested to occur by build-up of a deposit at low fouling rate, which was completely reversible throughout the experimental time. In contrast, the high BPC concentration in the UF seems to contribute to a gel layer formation. Consistently, lab-scale trials with sludge fractionation revealed different relative contribution of particle and colloidal/soluble fractions to the overall fouling in similar hydrodynamic conditions. While the dominant fraction in the tMBR was particulate, in the UF the micro-colloidal/dissolved substances played the main role.

- Whatever the pretreatment applied, RO obtained higher organic and inorganic rejection coefficients. Dissolved organic substances retention ranged between 98 and 100%, while feedwater conductivity decreased to 45-87 µS/cm. On the other hand, NF presented a high retention for dissolved organic substances (93-97%) and moderate to high for multivalent ions (67-100%). However, monovalent ions were only partially retained (14-61%), probably due to a Donnan effect, resulting in a higher permeate conductivity of 900-1,300 µS/cm.

- NF showed a severe normalised flux decay (0.35-0.44 at 90% recovery), possibly due to the higher initial fluxes. In contrast, RO operated at moderate initial fluxes, achieving higher

normalised fluxes of 0.76 and 0.86 at 90% recovery, for permeates from UF and tMBR, respectively. Differences may be attributable to high levels of dissolved organic substances in UF permeate (78% between UF and tMBR).

- Fouled membrane autopsies by SEM revealed a dense fouling layer for NF membrane covering the whole surface, which was partially detachable by physical means. EDX spectra showed significant quantities of P (10%), Fe (9%) and Ca (7%), with minor presence of Mg (3%) and Na (3%). Similar results were obtained when analysing the RO membrane but with uneven distribution over the surface with a large accumulation near the spacer strands. In addition, FTIR analysis suggested that the constituents of the gel fouling layer included proteins and polysaccharides for both NF/RO membranes.

- A complete removal of pharmaceutically active compounds was observed for RO, while NF presented moderate retention coefficients (94, 85, 70 and 27% for atenolol, paraxanthine, caffeine and clofibric acid, respectively).

5. References

Acero J., Benitez F., Teva F., Leal A., Retention of emerging micropollutants from UP water and a municipal secondary effluent by ultrafiltration and nanofiltration, *Chem. Eng. J.*, *163*, (2010), 264-272.

Afonso-Olivares C., Sosa-Ferrera Z.,. Santana-Rodríguez J.J, Analysis of anti-inflammatory, analgesic, stimulant and antidepressant drugs in purified water from wastewater treatment plants using SPE-LC tandem mass spectrometry, *J. Environ. Sci. Health A Tox Hazard Subst. Environ. Eng.*, *47(6)*, (2012)887-95.

ALPHA, American Public Health Association/Water Environment Federation, Standard Methods for the examination of Water and Wastewater, 21st ed., Washington DC, USA, 2005.

Altuki A.A., Tadkaew N., McDonald J.A., Khan S.J., Price W.E., Nghiem L.D., Combining MBR and NF/RO membrane filtration for the removal of trace organic in indirect potable water reuse applications, *J. Membr. Sci.*, *365*, (2010), 206-215.

Azaïs A., Mendret J., Gassara S., Petit E., Deratani A., Brosillon S., Nanofiltration for wastewater reuse: Counteractive effects of fouling and matrice on the rejection of pharmaceutical active compounds, *Sep. Pur. Technol.*, *133*, (2014), 313–327.

Charfi A., Yang Y., Harmand J., Amar N.B.,. Heran M, Grasmick A., Soluble microbial products and suspended solids influence in membrane fouling dynamics and interest of punctual relaxation and/or backwashing, *J. Membr. Sci.*, *475*, (2015), 156-166.

Cobry K.D., Yuan Z., Gilron J., Bright V.M., Krantz W.B., Greenberg A.R., Comprehensive experimental studies of early-stage membrane scaling during nanofiltration, *Desalination*, *283*, (2011), 40-51.

Comerton A.M., Andrews R.C., Bagley D.M., Hao C., The rejection of endocrine disrupting and pharmaceutically active compounds by NF and RO membranes as a function of compound and water matrix, *J. Membr. Sci.*, *313*, (2008), 323-335.

Delgado S.,. Villarroel R, González E., Submerged membrane bioreactor at substrate-limited conditions: Activity and biomass characteristics, *Water Environment Research*, *82 (3)*, (2010), 202-208.

Dólar D., Gros M., Rodríguez-Mozaz S., Moreno J., Comas J., Rodríguez-Roda I., Barceló D., Removal of emerging contaminants from municipal wastewater with an integrated membrane systems, MBR-RO, *J. Hazardous Materials*, *239-240*, (2012)64-69.

Filloux E., Labanowski J., Croue J. P., Understanding the fouling of UF/MF hollow fibres of biologically treated wastewaters using advanced EfOM characterization and statistical tools, *Bioresour. Technol.*, *118*, (2012), 460–468.

Fujioka T., Khan S. J., McDonald J.A., Nghiem L. D., Nanofiltration of trace organic chemicals: A comparison between ceramic and polymeric membranes, *Sep. Purifi. Technol.*, *136*, (2014) 258-264.

Gwona E.M., Yu M.J., Oh H.K., Ylee Y.H., Fouling characteristics of NF and RO operated for removal of dissolved matter from groundwater, *Water Res.*, *37*,(2003), 2989-2997

Jacob M., Guigi C., Cabassud C., Darras H., Performance of Ro and NF processes for wastewater reuse: tertiary treatment after a conventional activated sludge or a membrane bioreactor, *Desalination*, 250, (2010), 833-839.

Judd S., The MBR Book, Principles and Applications of Membrane Bioreactors for Water and Wastewater Treatment, 2nd edition, Elsevier, 2010.

Jurado A., Vàzquez-Suñé E., Carrera J., López de Alda M., Pujades E., Barceló D., Emerging organic contaminants in groundwater in Spain: A review of sources, recent occurrence and fate in a European context, *Sci. Total Environ.*, *440*, (2012), 82-94.

Kikamura K., Hara H., Watanabe Y., Removal of pharmaceutical compounds by submerged membrane bioreactors (MBRs), *Desalination*, *178*, (2005), 135-140.

Kovács Z., Samhaber W., Contributions of pH dependent osmotic pressure to amino acid transport through nanofiltration membranes, *Sep. and Purif. Technol.*, *61*, (2008), 243–248.

Li Q., Elimelech M., Organic fouling and chemical cleaning of nanofiltration membranes: measurements and mechanisms. *Environ. Sci. Technol.*, *38*, (2004), 4683-4693.

Lutchmiah K., Verliefde A.R.D., Roest K., Rietveld L.C., Cornelissen E.R., Forward osmosis for application in wastewater treatment: A review, *Water Res.*, *58*, (2014), 179-197.

Melián-Martel N., Sadhwani J.J., Malamis S., Ochsenkühn-Petropoulou M., Structural and chemical characterization of long-term reverse osmosis membrane fouling in a full scale desalination plant, *Desalination*, *305*, (2012), 44-53.

Mohammad A.V., Teow Y.H., Ang W.L., Chung Y.T., Oatley-Radcliffe D.L., Hilal N., Nanofiltration membrane review: recent advances and future prospects, *Desalination*, 356, (2015), 226-254.

Moreno J., Monclús H., Stefani M., Cortada E., Aumatell J., Adroer N., De Lamo-Castellví S., Comas J., Characterization of RO fouling in an integrated MBR/RO system for wastewater reuse, *Water Res. & Tech.*, *67.4*, (2013), 780-788.

Narbaitz R. M., Rana D., Dang H. T., Morrissette J., Matsuura T., Jasim S. Y., Tabe S., Yang P., Pharmaceutical and personal care products removal from drinking water by modified cellulose acetate membrane: Field testing, *Chem. Eng. J.*, *225*, (2013), 848-856.

Oatley-Radcliffe D., Williams S., Barrow M., Williams P., Critical appraisal of current nanofiltration modelling strategies for seawater desalination and further insights on dielectric exclusion, *Desalination*, *343*, (2014), 154–161.

Poorasgari E., Bugge T., Christensen M., Jørgensen M., Compressibility of fouling layers in membrane bioreactors, *J. Membr. Sci.*, *475*, (2015), 65–70.

Radjenović J., Petrović M., Barceló D., Fate and distribution of pharmaceuticals in wastewater and sewage sludge of the conventional activated sludge (CAS) and advanced membrane bioreactor (MBR) treatment, *Water Res.*, *43*, (2009), 831–841.

Sachit D.E., Veenstra J.N., Analysis of reverse osmosis membrane performance during desalination of simulated brackish surface waters, *J. Membr. Sci.*, *453*, (2014), 136-154.

Shrisvastava A., Gupta V.B., Methods for the determination of limit of detection and limit of quantitation of the analytical methods, *Chronicles of Young Scientists*, *2(1)*, (2011), 21-25.

Sun F.Y., Wang X. M., Li X.Y., Change in the fouling propensity of sludge in membrane bioreactors (MBR) in relation to the accumulation of biopolymer clusters, *Bioresour. Technol.*, *102*, (2011), 4718–4725.

Suwarno S. R., Chen X., Ching T.H., McDougald D., Cohen Y., Rice S.A., Fane A. G., Biofouling in reverse osmosis processes: The roles of flux, crossflow velocity and concentration polarization in biofilm development, *J. Membr. Sci.*, 467, (2014), 116-125.

Tang F., Hu H.Y., Sun L.J., Wu Q.Y., Jiang Y.M., Guan Y.T., Huang J.J., Fouling of reverse osmosis membrane for municipal wastewater reclamation: Autopsy results from a full-scale plant, *Desalination*, *349*, (2014), 73-79.

Tran T., Bolto B., Gray S., Hoang M., Ostarcevic E., An autopsy study of a fouled reverse osmosis membrane element used in a brackish water treatment, *Water Res.*, *41*, (2007), 3915-3923.

Urtiaga A. M., Pérez G., Ibañez R., Ortiz I., Removal of pharmaceuticals from a WWTP secondary effluent by ultrafiltration/reverse osmosis followed by electrochemical oxidation of the RO concentrate, *Desalination*, *331*, (2013), 26-34.

Van der Bruggen B., Manttari M., Nystrom M., Drawbacks of applying nanofiltration and how to avoid them: A review, *Sep. Purif. Tech.*, *63*, (2008), 251-263.

Vera L., González E., Díaz O., Delgado S., Performance of a tertiary submerged membrane bioreactor operated at supra-critical fluxes, *J. Membr. Sci.*, *457*, (2014), 1-8.

Wintgens T., Melin T., Schäfer A., Khan S., Muston M., Bixio D., Thoeye C., The role of membrane processes in municipal wastewater reclamation and reuse, *Desalination*, *178*, (2005), 1-11.

Wu B., Kitade T., Chiong T. H., Uemura T., Fane A. G., Impact of membrane bioreactor operating conditions on fouling behavior of reverse osmosis membrane in MBR-RO processes, *Desalination*, 311, (2013) 37-45.

Wu J., He C., Effect of cyclic aeration on fouling in submerged membrane bioreactor for wastewater treatment, *Water Res.*, *46(11)*, (2012), 3507-3515.

Xu P., Bellona C., Drewes J., Fouling of nanofiltration and reverse osmosis membranes during municipal wastewater reclamation: Membrane autopsy results from pilot-scale investigations, *J. Membr. Sci.*, *353*, (2010), 111-121.

CAPÍTULO 6: Rendimiento de un biorreactor de membrana sumergida terciario operado con flujos supra-críticos

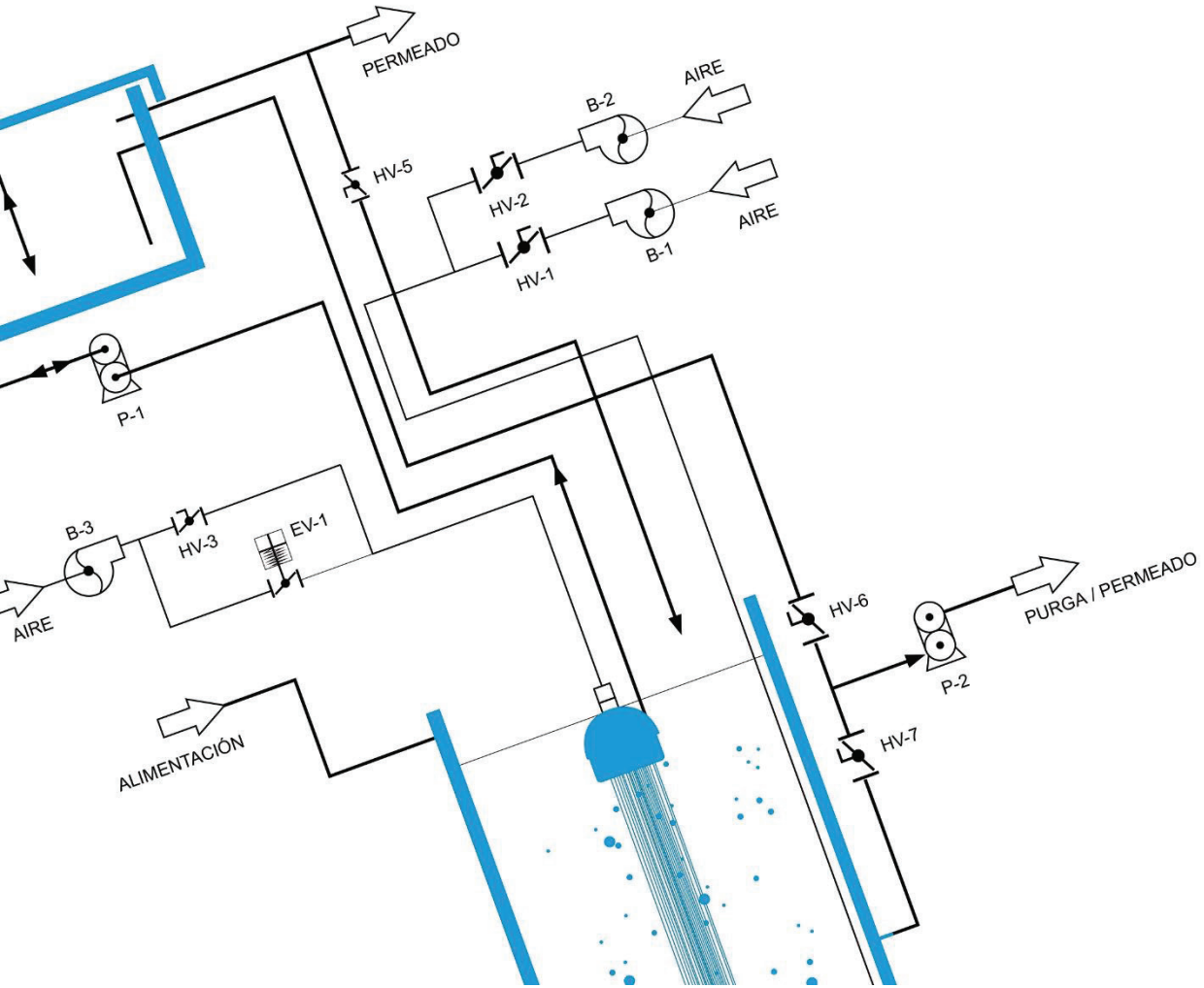

Capítulo 6

Rendimiento de un biorreactor de membrana sumergida terciario operado con flujos supra-críticos

Performance of a tertiary submerged membrane bioreactor operated at supra-critical fluxes

Luisa Vera, Enrique González, **Oliver Díaz**, Sebastián Delgado

Journal of Membrane Science
457, (2014) 1-8

Factor de impacto: 5,056 (JCR®, Thomson Reuters 2015).

Highlights

- Sustainability of an MBR operated at supra-critical fluxes
- Novel and promising operation mode for backwashing initiation
- Determination of residual fouling, reversible fouling rate and net permeate flux
- Applied for advanced treatment of secondary effluent from an WWTP
- Successfully operated without biomass purge resulting in a moderate MLSS

Keywords

Submerged membrane bioreactor; tertiary treatment; fouling; supra-critical fluxes; set-point trasmembrane pressure

Resumen:

La implantación de los biorreactores de membrana (MBR, en inglés) se ve limitada por los elevados costes de instalación y explotación. Uno de los principales factores que afectan a los costes de un MBR es la adecuada selección del flujo de filtración. De hecho, elevados flujos reducen los costes capitales o de instalación, mientras que incrementan los costes de operación. La tendencia general en plantas industriales de este tipo, a gran escala, es operar a bajos flujos de filtración incorporando retrolavados cuya frecuencia es predeterminada, lo que se denomina:

modo de operación temporizado. Sin embargo, la inflexibilidad que presenta este modo de operación genera la pérdida de la productividad y el incremento de la demanda energética. En éste Capítulo se presenta el estudio de un bioreactor de membrana sumergida a escala piloto, para tratamiento terciario de un sistema convencional de lodos activos, operado durante 2.200 horas a flujos supra-críticos. En este caso se aplicó un modo alternativo de operación basado en limitar el ensuciamiento de la membrana y que se ha denominado: modo de operación por presión de consigna.

El MBR logró un elevado grado de depuración del efluente secundario, con rendimientos medios de eliminación del 96%, 89% y 53% para el amonio, demanda química de oxígeno (COD) y carbono orgánico disuelto (DOC), respectivamente. Pese a operar sin purga de lodos y debido a las condiciones severas de limitación de sustrato, la concentración de MLSS se mantuvo constante, entre 4,1 y 7,1 g/L, según las fluctuaciones experimentadas por la alimentación. Las condiciones de inanición favorecieron la minimización de productos microbianos solubles (SMP, en inglés) en el licor mezcla. No obstante, la membrana retuvo una considerable fracción de estas sustancias solubles (21%), las cuales pueden bloquear los poros o adsorberse sobre la superficie de la membrana. Por su parte, los ensayos de filtrabilidad llevados a cabo a escala de laboratorio, revelaron que la principal contribución al ensuciamiento de la membrana cuando se operó con flujos supra-críticos, se debió a las partículas sedimentables y no sedimentables (77-84% y 6-12%, respectivamente).

La determinación del flujo crítico se realizó por medio de experimentos de corta duración, que se denominan experimentos escalonados. En dichos experimentos se aplicaron distintas frecuencias de aireación de la membrana. Las intermitencias de aireación 10s on/10s off y la aireación continua presentaron un comportamiento muy similar. Un incremento de la frecuencia de la aireación superior a 10 s on/50s off no presentó ningún efecto sobre el flujo crítico, que se mantuvo entre 45-50 L/hm^2. Por su parte, el análisis del ensuciamiento residual reveló que el flujo crítico para este tipo de ensuciamiento se encontraba en 55 L/hm^2, independientemente de las frecuencias de aireación aplicadas.

El modo de operación por presión de consigna permite establecer un ensuciamiento máximo permitido para la membrana iniciando el retrolavado inmediatamente después de que éste es alcanzado. La evolución de la presión trasmembrana durante cada uno de los consecutivos ciclos de filtración y retrolavado, sugirieron que el principal mecanismo de

ensuciamiento de la membrana era la construcción de una torta incompresible. La velocidad de ensuciamiento reversible pareció no verse afectada por el flujo de retrolavado impuesto, pero sí por el flujo de filtración. Como se esperaba, los valores encontrados para la velocidad de ensuciamiento fueron superiores a los típicos de plantas a gran escala operadas con bajos flujos.

En cuanto al ensuciamiento residual, tras estabilizarse el ensuciamiento inicial de la membrana, se observó que el retrolavado era capaz de eliminar el ensuciamiento residual de la membrana, permitiendo la operación durante 2.200 horas sin limpieza química. La velocidad de ensuciamiento residual fue significativamente inferior a la encontrada en plantas a gran escala (0,001-0,0033 Pa/s), lo que confirma que la operación a flujos supra-críticos permite la construcción de una torta que actúa como barrera secundaria e impide la adsorción y bloqueo de poros por parte de los SMP.

El modo alternativo de operación, mediante la imposición de una presión transmembrana de consigna (TMP_{sp}), ha permitido mantener controlado el ensuciamiento reversible de la membrana al ajustar la frecuencia del retrolavado para retirar la capa de torta depositada en la filtración durante 2.200 horas.

Abstract

A pilot-scale submerged aerobic membrane bioreactor (MBR) was run for over 3 months to assess the sustainability to operate at supra-critical fluxes. The MBR was applied as advanced treament of secondary effluent from a conventional wastewater treatment plant. The system was successfully operated without biomass purge at hydraulic retention time (HRT) of 8.8 h, resulting in a moderate liquor suspended solid concentrations range (MLSS = 4.1-7.1 g/L) in the bioreactor, according to the influent organic load fluctuations. Treatment performance was stable and achieved high conversion of ammonium to nitrate (96 %) and dissolved organic carbon removal (53 %). Short-term tests have been carried out according to a modified flux-step method to determine critical flux and evaluating optimum membrane cyclical aeration frequency. For the long-term tests, an alternative operation mode for backwashing initiation, based on a pre-selected transmembrane set-point, was applied. Under typical specific demand values (SAD_{pnet} = 13.7-18.3 Nm^3/m^3), continuous operation under different supra-critical filtration fluxes (J = 60-80 L/h m^2) and backwashing fluxes (40-80 L/h m^2) can be maintained without any chemical cleaning. Analysis by means of sludge fractionation in lab-scale tests, at

similar hydrodynamic conditions, indicated that the contribution of suspended solids to cake membrane fouling was estimated about 86-89%.

1. Introduction

It is widely known that in regions with water scarcity, wastewater reuse is a common practice and competent authorities have promoted many actions to encourage its reuse. In Tenerife island (Spain), since 1993 the secondary effluent obtained in the capital city's wastewater treatment plant (WWTP) is transported a long distance (60 km) by pipe, before being reused for crop irrigation. Biological treatment used in the plant is single-stage aeration and settling, which produces an effluent containing a significant and variable residual organic load and ammonium nitrogen (30-50 mg/L). Current scheme also includes a conventional tertiary treatment train (coagulation, sand filtration, chlorination and desalination). Some of the technical problems found in the treatment scheme have been the production of large quantities of residuals, high consumption of chemical reagents, sulfide generation during transport of the reclaimed water through a long pipe and decreased productivity in the downstream desalination plant due to the mentioned residual organic load (Delgado et al., 1999). Researching this issue provided some valuable technical solutions, indicating that anaerobic conditions inside the pipe can be inhibited by the presence of low nitrate concentration (Delgado et al., 2001).

Due to their well-known advantages (Judd, 2007), submerged membrane bioreactor (MBR) has turned out as an attractive option for replacing the current tertiary treatment. As it was stated in previous research, the WWTP effluent can be effectively treated in an MBR until it achieves a high dissolved organics removal and complete nitrification (Delgado et al., 2002). Particularly interesting could be operating at maintenance energy level of the biomass, which significantly reduces sludge production. Under these conditions, the soluble microbial product (SMP) concentration could be minimized and the system was operated successfully at moderate permeate fluxes and low cleaning frequency, without any fouling evidence (Delgado et al., 2010).

Notwithstanding the advantages of MBRs, their implementation is limited by the high costs, both in capital and operating expenditure (CAPEX and OPEX). A key issue regarding CAPEX and OPEX is the selection of the most appropriate permeate flux, which is determined by the classical trade-off problem: at higher fluxes CAPEX decreases while OPEX increases. High

fluxes are desirable to reduce the membrane area required (i.e. reduce CAPEX), however, membrane fouling increases with flux, which results in a higher membrane scouring demand and a more frequent cleaning to control membrane fouling (i.e. increase OPEX) (Judd, 2007). Verrecht et al. (2010) have concluded that higher sustainable fluxes lead to lower net present values (NPV), indicating that the higher OPEX are offset by lower CAPEX since less membrane area is required, based on the results of a cost sensitivity analysis for a full-scale hollow fibre MBR. Specifically, an increase in flux from 15 to 30 L/h m^2 decreases NPV by 9%. Nevertheless, the correlation between membrane fouling and flux is influenced by hydrodynamics, cleaning protocols, feedwater characteristics and biological conditions (Drews et al., 2010). The subsequent uncertainty has led to conservative plant designs and operation strategies. In addition, an analysis of design and operation of large MBR plants in Europe shows a broad difference between the design and operation flux (Lesjean et al., 2009). For flat-sheet systems, the net fluxes are designed at 14-48 L/h m^2 (mean at 32 L/h m^2) while for the hollow-fibre modules they are 20–37 L/h m^2 (mean at 29 L/h m^2). However, for both systems the operation net flux is of about 20 L/h m^2. Therefore, the general trend is to reduce operational risk by operating at low fluxes (below the critical flux) where fouling is limited (Bacchin et al., 2006). In addition, to maintain the process performance, strategies for fouling mitigation such as air scouring and physical cleaning techniques (i.e. backflushing and relaxation) have been incorporated as a standard (Le-Clech et al., 2006; Judd 2011). Air scouring, expressed as specific aeration demand per permeate volume unit (SAD_p), takes a typical value, for full-scale facilities, between 10 to 50 Nm^3/m^3 (Judd 2011). Relaxation and backflushing (only for hollow-fibre configuration) cycles with a pre-fixed duration are commonly applied for 30–130 seconds every 10–25 min of filtration (Le-Clech et al., 2006). However, inflexibility inherent of this time-based operation mode leads to a decrease in productivity when cleaning cycle is applied too often or it can promote irreversible fouling when applied too late (Drews, 2010).

Despite of the experience gained in the MBR operation over the last years, from a great variety of tested conditions, operation strategies are usually based on predetermined values of the key parameters (air scouring, filtration/physical cleaning sequences and permeate flux). However, these pre-set fixed values, based on general background or recommendations of membrane suppliers, lead to under-optimised systems and finally result in loss of permeate and high energy demand.

Special attention has been paid on feedback control to improve filtration process efficiency (Drews 2010). A comprehensive review of the achievements, including those related to the biological process, can be found in a recent paper (Ferrero et al., 2012). Among the control systems, Smith et al. (2006) have successfully validated a system for backwash initiation by permeability monitoring, automatically adjusting the backwashing frequency as a function of allowable transmembrane pressure increase in each filtration cycle, which results in a reduction of 40% in the required backwashing water. This control system was developed in a previous lab-scale study (Villarroel et al., 2013), which showed that membrane fouling can be significantly affected by the value of transmembrane pressure set-point (TMP_{sp}) selected and the cleaning method. However, a deeper investigation in long-term pilot experiments should be carried out in order to assess process sustainability, mainly focused on residual fouling development.

This paper assesses the sustainability of an MBR operated under controlled backwashing at supra-critical fluxes for treatment of secondary effluent. The role of backwashing flux was also investigated.

Table 6.1. Feedwater main characteristics

PARAMETERS	UNITS	MEAN	RANGE
COD	mg/L	280	13-2,520
DOC	mg/L	14	9-27
$N\text{-}NH_3$	mg/L	26	1-53
$N\text{-}NO_2^-$	mg/L	4	<1-13
$N\text{-}NO_3^-$	mg/L	2	<1-17
Turbidity	NTU	180	10-1,200
TSS	mg/L	280	33-1,100

2. Material and methods

2.1. Feedwater

The pilot MBR was fed with effluent from a conventional activated sludge wastewater treatment plant whose average characteristics are given in Table 6.1. This is an old WWTP designed only for carbon removal. Due to the short sludge ages and oxygen deficiency in the activated sludge process, frequent episodes of sludge deflocculation or not enough

sedimentation usually appear, which results in a high suspended solids concentration in the effluent.

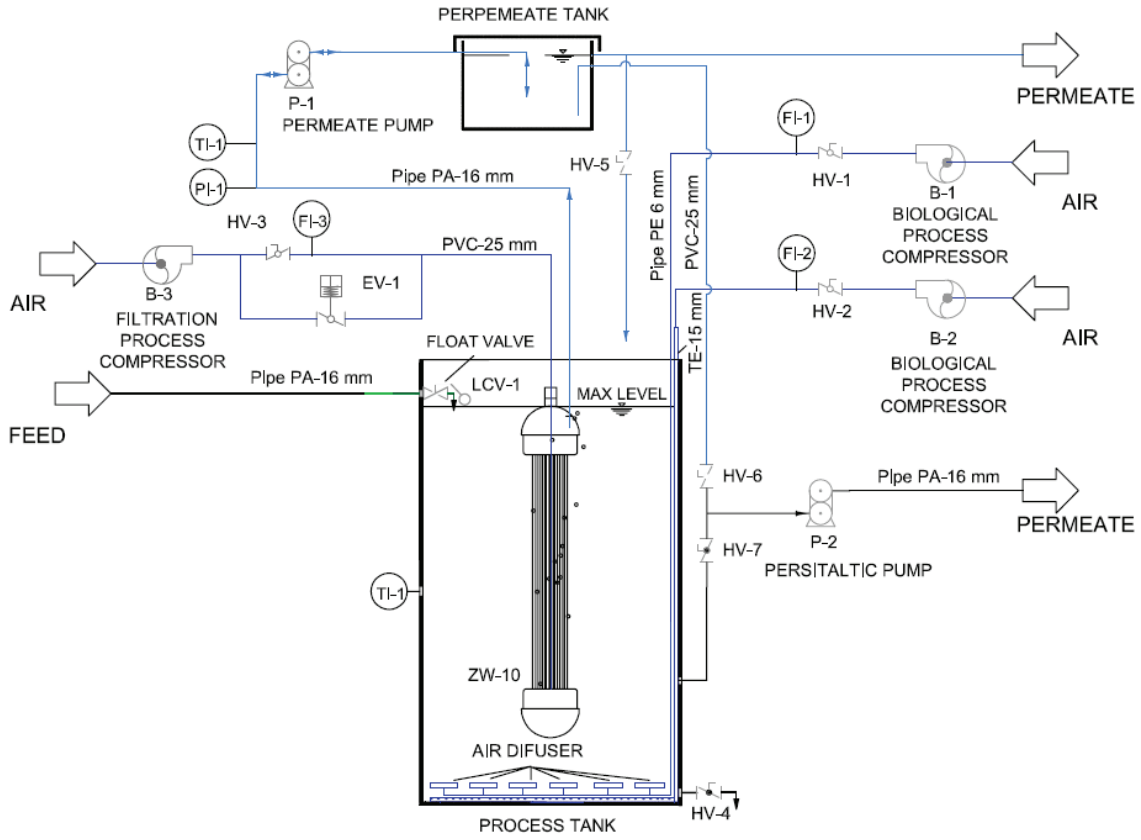

Figure 6.1. Configuration of the pilot-MBR system, ZW10

2.2. MBR

A cylindrical 220 liter MBR was equipped with ZeeWeed® ZW-10 (GE Water & Process Technologies) hollow-fiber membranes of 0.04 µm rated pore diameter and 1.9 mm outer diameter, assembled vertically, which provide 0.9 m^2 of filtering surface area (Figure 6.1). ZeeWeed® consists of a woven reinforcing braid on which a PVDF membrane is cast. The effluent (permeate) was extracted from the top header of the module under slight vacuum. All experiments were carried out at a constant permeate flux, registering transmembrane pressure as a function of time. Fouling was controlled by coarse bubbling of air flow and by intermittent backwashing. The unit operated in automatic cleaning initiated mode. Each filtration cycle was finished when a pre-established transmembrane pressure was reached (30 kPa), beginning the backwashing cycle immediately afterwards. A programmable logic controller (PLC) system was used to initiate and stop the backwashing by comparison of TMP set-point and instantaneous

pressure values. Continuous data logging and plotting of pressure profile evolution were also performed.

Before starting the experimental period, the pilot-scale MBR was seeded with sludge from the activated sludge reactor of the WWTP and operated for over 6 months to ensure that stationary conditions were reached. In this study, the bioreactor was run at HRT values of 8.8 h without sludge removal except for sampling. In order to maintain a constant HRT independent of the permeate flux, the excess of permeate was returned to the tank. Air was supplied through the bottom, providing oxygen and stirring. The dissolved oxygen concentration was always above 1.5 mg/l in the reactor operated at 23 ± 2 ºC. Suspensions were characterised by particle size, MLSS, MLVSS, biomass activity, non-flocculating microorganisms (Ng et al., 2005) and dissolved organic matter of the liquid phase. In order to determine fouling contribution of each sludge components, a filterability test in a lab filtration unit was carried out for the different sludge fractions.

2.3. Short-term flux step trials

The modified flux-step method is based on applying successive flux increments up to a maximum and back analogous, in accordance with the method of Le-Clech et al. (2003) and further improved by incorporating relaxation steps for reducing the influence of fouling history (Van der Marel et al., 2009). Nevertheless, the modified method proposed in this work substitutes the relaxation steps for short backwashing cycles (30 s) at a fixed flux value of 60 L/h m^2, to be more similar to the conventional operation of an MBR. The results are related to the reversible fouling rate (r_f), given by the change in TMP with time ($dTMP/dt$) at each J. Residual fouling was also assessed by measuring the transmembrane pressure after the backwashing cycle (TMP_0). The other experimental parameters were selected in accordance with (Guglielmi et al., 2007; Van der Marel et al., 2009): step duration of 15 min, flux-step height of 5 L/h m^2 and a maximum flux of 100 L/h m^2.

2.4. Filterability test unit

The experiments were made in a laboratory unit equipped with ZeeWeed® ZW 1 hollow fiber membrane module similar to that used in the pilot unit with a smaller filtration area (0.047 m^2). ZW1 was operated in a closed loop, through a stirred 1.5 liter tank of 21 cm water height. A magnetic drive pump was used to withdraw permeate from the membrane module. Membrane fouling was indicated by the increase of the transmembrane pressure measured by a pressure

sensor. To ensure membrane cleaning, air was intermittently supplied at a frequency of 10 s on/10 s off (SAD_{mnet} = 1.12 $Nm^3/h\ m^2$). Air flow-rate was controlled by a mass flow controller. The control system and the card interface were similar to the pilot system. Further details can be found elsewhere (Villarroel et al., 2013).

2.5. Analytical methods

Dissolved oxygen was measured using an oximeter WTW 340i. Chemical oxygen demand (COD), ammonium-nitrogen ($N\text{-}NH_3$), total suspended solids (TSS), mixed liquor suspended solids (MLSS), mixed liquor volatile suspended solids (MLVSS), time to filter (TTF) and turbidity were determined in conformity with the Standard Methods (ALPHA, 2005). Analyses of nitrite-nitrogen ($N\text{-}NO_2^-$) and nitrate-nitrogen ($N\text{-}NO_3^-$) were conducted through ion chromatography using a Compact IC plus 882 device supplied by Metrohm. Dissolved organic carbon (DOC) concentration was measured with a TOC-meter (TOC-5000A, Shimadzu). The oxygen uptake rate was measured by following the dissolved concentration with a membrane oxygen electrode, in a medium without substrate ($SOUR_e$, endogenous). Microbial floc size distribution was measured by using a Malvern Mastersizer 2000 instrument (Malvern Instruments Ltd.) with a detection range of 0.02-2000 µm. In order to quantify the amount of non-flocculating microorganisms, samples of biomass were centrifuged at 1300 g for 2 min and the supernatant turbidity was then measured (Ng et al., 2005). Sludge supernatant was obtained after settling in a 3 litre cylinder for 30 minutes. Fractionation of the supernatant was carried out using several dead-end cell (Millipore) microfibre filters of different nominal pore sizes: 1.50, 0.45 and 0.22 µm.

3. Results and discussion

3.1. Process performance and biomass characteristics

Table 6.2 summarises the COD, $N\text{-}NH_3$ and DOC removal efficiencies and main characteristics of the microbial suspension. Ammonia, COD and DOC removal efficiency were 96 %, 89 % and 53% on average. Despite operating in conditions of total sludge retention, MLSS concentration stabilised between 4.1 and 7.1 g/L according to influent fluctuations (33-1.100 mg TSS/L, see Table 6.1). In these conditions, the MLVSS/MLSS ratio remained constant throughout the experiment (77-80%), indicating no significant accumulation of inorganic matter. It is expected that microorganisms under severe substrate limitation should preferentially meet their maintenance energy requirements instead of producing additional biomass. Therefore, the "maintenance" concept introduced by Pirt (1965) may be the reason for the MLSS stabilisation in

the MBR operated without biomass purge. In addition, endogenous specific oxygen uptake rate ($SOUR_e$) was considerably lower than the typical values, which confirms a maintenance regime was achieved. Uniform and medium-sized flocs were also observed, with a mean $D_{(v,0.5)}$ value of 43 µm. Sludge filterability, quantified as TTF, was reasonably consistent at 3.7 ± 0.5 min. Furthermore, the low quantity of small non-floculating flocs, measured as supernatant turbidity (Ng et al., 2005), showed that the hydrodynamic stress due to membrane air scouring was sufficiently low to prevent sludge deflocculation.

Table 6.2. Bioreactor treatment performance and main characteristics of microbial suspension

PARAMETER	UNIT	MEAN VALUE	RANGE
Bioreactor treatment performance			
COD removal	%	89	
N-NH_3 removal	%	96	
DOC removal	%	53	
Permeate DOC	mg/L	6	3-16
Suspension characterisation			
MLSS	g/L	5.5	4.1-7.0
MLVSS	g/L	4.4	3.2-5.6
TTF	min	3.7	
PSD			
$D_{(v,0.1)}$	µm	17	
$D_{(v,0.5)}$	µm	43	
$D_{(v,0.9)}$	µm	92	
$SOUR_e$	mg O_2/g MLVSS h	1.66	
Supernatant turbidity	NTU	30	14-55
Supernatant DOC[a]	mg/L	9	5-34

[a] Samples were filtrated through microfibre filters with a nominal pore size of 0.45 µm

Finally, given the impact of soluble microbial products (SMP) on membrane fouling (Drews 2010), this was routinely analysed through the measurement of the dissolved organic carbon concentration (DOC), according to Lyko et al. (2008). Results showed that SMP was 36% (on average) lower in the sludge supernatant than in the influent (Table 6.1), resulting in a low and relative stable concentration, attributable to the biological degradation process. Based on the

concept of utilisation and biomass associated products (Lu et al., 2001), SMP production can be minimised at low substrate utilisation rates and biomass activity (i.e. maintenance conditions) while SMP biodegradation increases with sludge retention time (SRT). Nevertheless, it was found that the concentration of SMP in the supernatant was always slightly higher than that in the permeate. This confirms that the membrane retained a considerable fraction of the SMP (21%), which is expected to cause membrane fouling by entering into membrane pores or adsorbing onto the membrane surface. However, the operation at supra-critical fluxes with the associated cake layer formed on the membrane surface during filtration cycles could prevent partially this fouling, as it was reported in previous studies (Kuberkar and Davis, 2000).

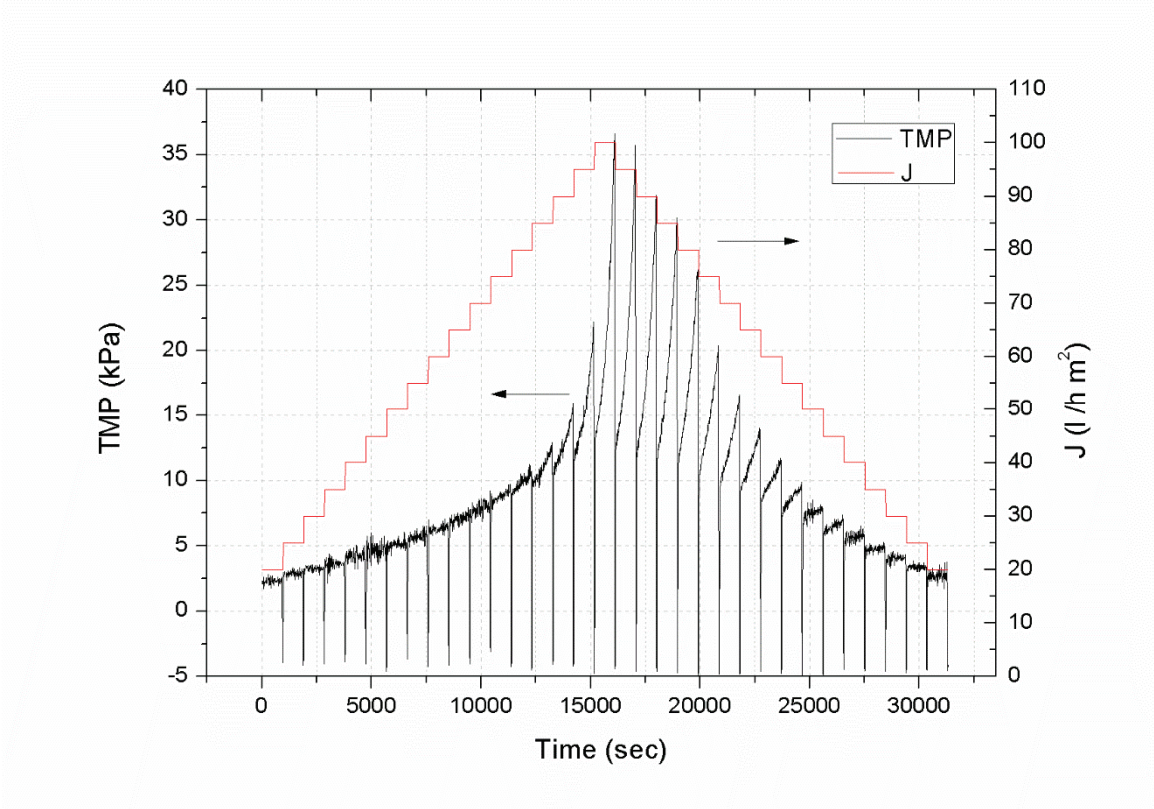

Figure 6.2. Flux and TMP profiles during short-term trials; aeration frequency (on/off)=10/50 s/s; aeration flow rate= 1.0 Nm^3/h; t_B=30s; and J_B=60 L/hm^2

3.2. Critical flux determination. Effect of cyclical aeration frequency

In Figure 6.2. typical flux (*J*) and *TMP* profiles during short-term trial for critical flux determination are shown. Figure 6.3a shows the reversible fouling rate (r_f) against *J* during the ascending phase. An increase of aeration frequency up to 10 s on/50 s off (net specific aeration demand, SAD_{mnet} = 0.18 $Nm^3/h\ m^2$) had no influence on the critical flux (J_c) of 45-50 $L/h\ m^2$. This

result is consistent with other studies suggesting a threshold aeration flow value after which no improvement is achieved (Le-Clech et al., 2003; Guglielmi et al., 2007). At the lowest frequency of 10 s on/100 s off (SAD_{mnet} = 0.10 $Nm^3/h\ m^2$), J_c decreased at 40-45 L/h m^2. If $J < J_c$, reversible fouling rates remained in the range of 0.04-0.06 mbar min^{-1} for any frequency selected, lower than the upper limit (0.1 mbar/min) proposed for the critical flux determination (Le-Clech et al., 2013). On increasing J at supra-critical values, r_f sharply increased: this could be explained by differences in particle deposition rates under diverse hydrodynamic conditions. The shear rate generated by air bubbling prevents the deposition of large particles on the membrane surface (Wu et al., 2012). Nevertheless, at high fluxes, permeate drag forces exceed the dispersive forces and particles can deposit on the membrane wall. A similar trend in reversible fouling rate was observed for continuous and intermittent aeration at 10 s on/10 s off (SAD_{mnet} = 0.55 Nm^3/m^2).

From the results of the residual fouling, measured by the transmembrane pressure after backwashing (TMP_0), a critical flux value with respect to residual fouling can be determined, where above it (55 L/h m^2), the TMP_0 starts to deviate from tap water behaviour (Figure 6.3b). This fact may be attributed to the severe cake fouling reached at high fluxes, which (for given conditions) cannot be effectively removed by backwashing. Instead of the limitations of short-term tests to predict long-term behaviour (Drews, 2010), this critical flux can be used as a practical guideline for pilot-plant operation. Therefore, three supra-critical fluxes were applied (60, 70 and 80L/h m^2) during the long-term trial.

3.3. Long-term test to assess process sustainability at supra-critical fluxes

Based on previous results (Villarroel et al., 2013), a value of 30 kPa was chosen for the *TMP* set-point in the long-term test. Supra-critical fluxes in the range 60-80 L/h m^2 and cyclical aeration with a frequency of 10 s on/10 s off were also selected. An important issue when operating at supra-critical fluxes is the capability of air scoring to re-disperse the cake layer detached from the membrane during the backwashing. Ye et al. (2011) have reported the improvement of backwashing efficiency with the aid of air scouring. The authors concluded that the fouling material is removed from the membrane with air, thus limiting re-deposition in the subsequent filtration cycle. Therefore, in order to maximise the process performance, air flow rate was slightly increased during the filtration phase (SAD_{mnet} = 1.1 $Nm^3/h\ m^2$) while a constant air sparging (SAD_m =3.1 $Nm^3/h\ m^2$) was applied during the backwashing phase. However, net specific aeration demand related to permeate volume (SAD_{pnet}) remained in 13.7-18.3 Nm^3/m^3, which is similar to the typical full-scale values (Judd, 2011).

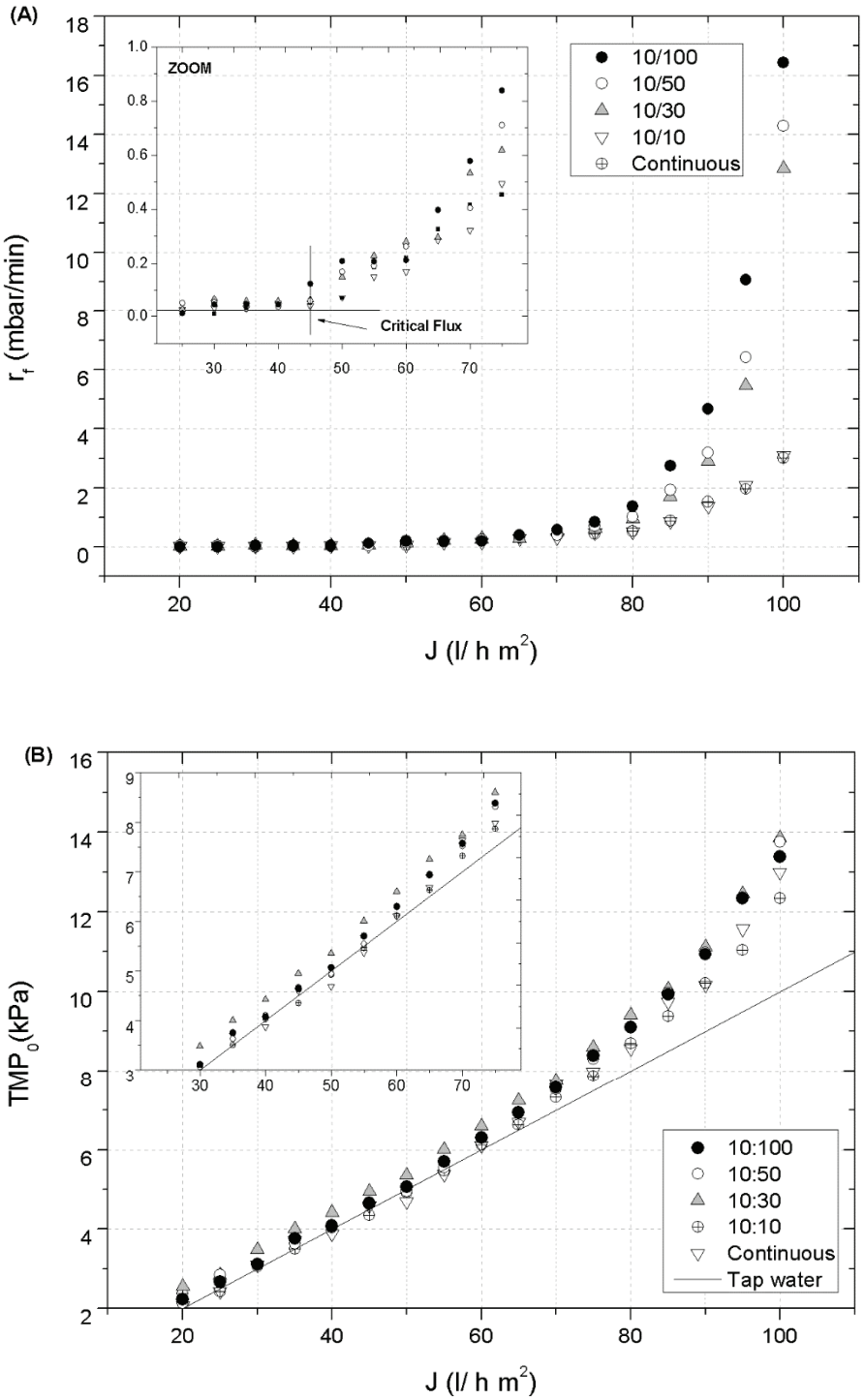

Figure 6.3. Fouling rate (A) and TMP_0 (B) against permeate flux during the ascending phase of short-term trials at different aeration frequencies; t_B=30 s and J_B=60 L/hm^2

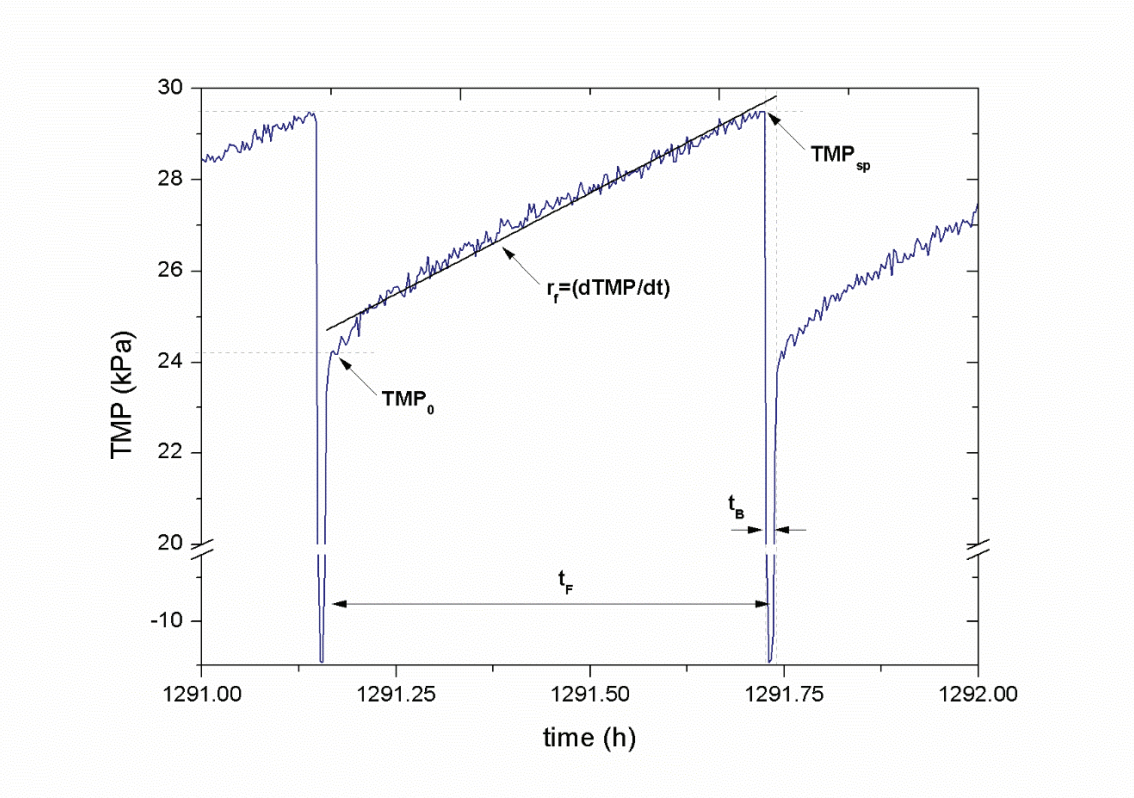

Figure 6.4. Typical TMP profile of consecutive filtration and backwashing cycles in a fraction of the long-term experiment; J=70L/hm^2; t_B=30 s; and J_B=60 L/hm^2

Figure 6.4 shows an example of the *TMP* evolution under consecutive filtration/backwashing cycles, where each filtration phase finished when the TMP_{sp} was reached. It can be observed that the *TMP* linearly increased with elapsed time. This behaviour suggests a cake development mechanism on the membrane wall. Then, the *TMP* evolution in each filtration phase can be described by the following equation (Delgado et al., 2008):

$$TMP = TMP_0 + r_f \cdot t \qquad [6.1]$$

where TMP_0 is the initial transmembrane pressure, r_f the reversible fouling rate and t the elapsed time.

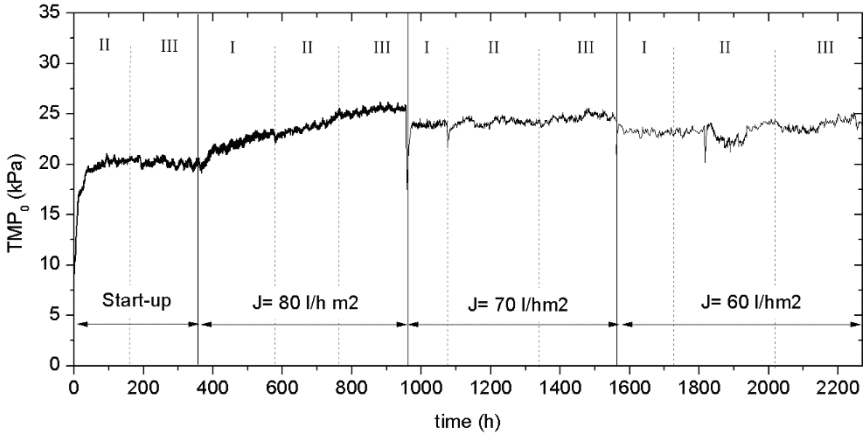

Figure 6.5. TMP_0 profile for different filtration and backwashing fluxes in long-term experiment; I: J_B=40 L/hm^2; II: J_B=60 L/hm^2 and III: J_B=80 L/hm^2

Resulting *TMP$_0$* profiles, related to irremovable residual fouling by backwashing, are shown in Figure 6.5. An initial sharp increase during the first 40 h (from 8.6 to 20 kPa) was followed by a slow and gradual *TMP$_0$* rise at *J* = 80 L/h m^2, which finally stabilised when lower fluxes (70 and 60 L/h m^2) were applied. This initial residual fouling may be due to a progressive particle accumulation in the deposit as a consequence of the experimental operating mode for backwash initiation. Accordingly, backwashing is only applied when significant fouling (significant mass deposited) is reached during the filtration phase, thus resulting in a growth in residual fouling which backwashing cannot effectively remove. This is consistent with other studies with fixed backwash intervals where increasing filtration time was observed to have a large effect on fouling resistance increase (Gui et al., 2003;Shoeberl et al., 2005). TMP_0 profile reflects, however, a dynamic behaviour during the first cycles, where residual fouling increased less with subsequent cycles until the amount of particle deposited and removed was balanced.

After this initial period, the backwashing was effective to remove the particle deposit during more than 2,200 h of operation, even applying high permeate fluxes. Also, the lowest backwashing flux (J_B, 40 L/h m^2) has revealed as enough to achieve the desired cleaning efficiency, while upper values did not improve membrane performance. The results have shown, therefore, that once the system reached steady-state conditions, backwashing efficiency was not significantly affected by operating conditions (permeate and backwashing fluxes) and influent fluctuations (Table 6.1). This may due to the fact that, with this alternative strategy, the system

automatically adjusts cleaning frequency to a preselected TMP_{sp}, which will determine the degree of membrane fouling allowed, and thus a stable backwashing efficiency can be achieved. In fact, it was observed a low TMP_0 increase rate (0.05-0.12 mbar/h) at the highest flux (80 L/h m^2), but significantly lower than typical ranges for residual fouling (0.6 mbar/h) reported for full-scale MBRs (Drews 2010). It is assumed that the low TMP_0 increase rate observed can be related to the formation of a cake layer on the membrane that might act as a secondary membrane. This secondary membrane could partially prevent SMPs from entering into the membrane pores or adsorbing onto the membrane surface. This behaviour is in agreement with Hwang et al. (2009) which reported that an extended filtration cycle time can increase backwashing efficiency, if the cake formed suppresses membrane pore blocking. Consistently, maintenance chemical cleanings were not necessary during the whole experimental period.

Regarding to the reversible fouling, which impacts on filtration phase duration and therefore in backwashing frequency, it is influenced by the permeate flux (Figure 6.6). As expected, the obtained values are slightly higher than those frequently observed in full-scale plants (0.1-1 mbar/min) operated at low fluxes (Drews 2010). Therefore, controlling backwashing by TMP_{sp} has revealed as an efficient control system which allows to operate at higher permeate fluxes and to optimise the length of the filtration time without any significant increase in residual fouling. It is noticeable the high value of r_f observed at J = 80 L/h m^2 and J_B= 40 L/h m^2 which clearly does not

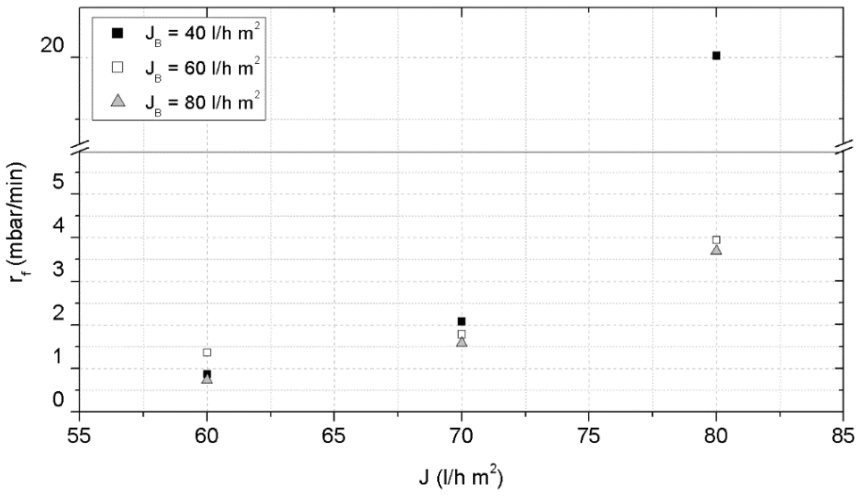

Figure 6.6. Mean reversible fouling rate against permeate flux at different backwashing fluxes (long-term experiment)

fit with the general trend. This could be related to a high accumulation of solids in the vicinity of the membrane due to the deficient cake dispersion during the backwashing, which produced a higher fouling rate. However, the system was capable to automatically adjust the backwashing frequency to obtain a reasonable filtration length (4.3 min) and effectively remove the particle deposit. This dynamic cleaning strategy can be also observed in Fig. 6.7 where the filtration phase length changed (between 17 and 152 min) as a function of the membrane fouling.

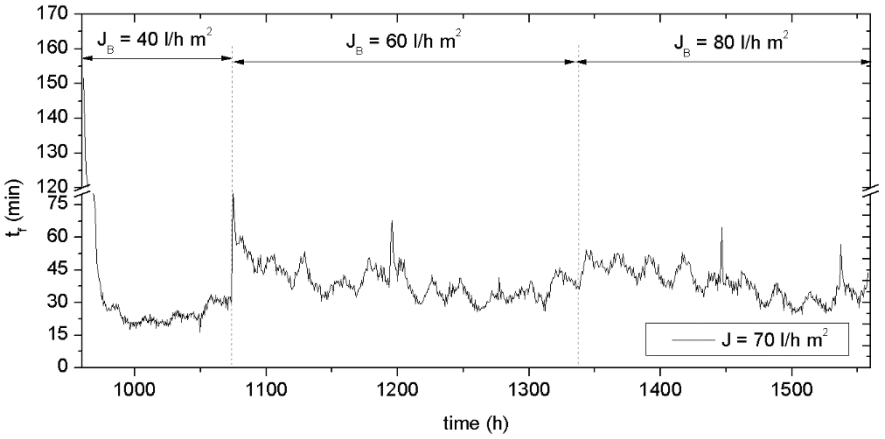

Figure 6.7. Profile of the duration filtration phase (t_f) for different backwashing fluxes at J=70L/hm^2

On the other hand, membrane performance was also assessed by the net permeate flux (J_{net}) calculated as:

$$J_{net} = \frac{t_F \cdot J - t_B J_B}{t_F + t_B} \qquad [6.2]$$

where t_B and t_F are the duration of the backwashing phase and the filtration phase, respectively. Figure 6.8 shows mean J_{net} as a function of the permeate flux. Although no significant effect of backwashing fluxes was found for the permeate flux, data suggest that J_{net} could be further improved by increasing J. This may be due to the larger filtration cycles obtained. The best result was obtained at the highest permeate flux (80 L/h m^2) and intermediate backwashing flux (60 L/h m^2), corresponding to a J_{net} = 76 L/h m^2. This net permeate flux represents a significant improve, of about 67% of the J_{net} obtained by a conventional temporised operation at critical filtration conditions (t_F = 12 min, t_B = 30 s, $J = J_c$ = 50 L/h m^2 and J_B =60 L/h m ^{2}). Also, the net flux of 76 L/h m^2 slightly improves (around 2%) the J_{net} corresponding to a temporised mode (t_F = 12 min, t_B = 30 s and J_B =60 L/h m ^{2}) at the same permeate flux of 80 L/ h m^2.

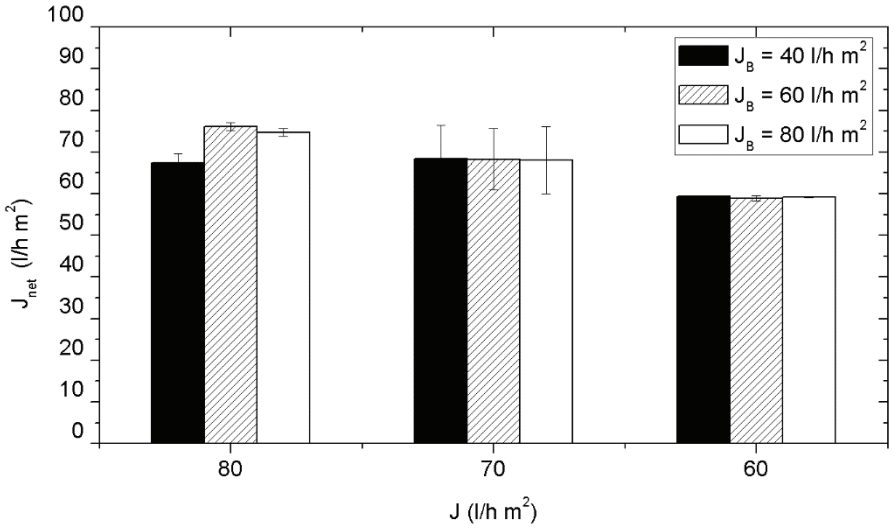

Figure 6.8. Net permeate flux (J_{net}) against permeate flux for different backwashing fluxes

3.4. Relative contribution of different sludge fractions to cake fouling

Microbial suspension was fractionated into five components: settling particles, non-settling particles (> 1.5 µm), large colloids (0.45-1.5 µm), medium colloids (0.22-0.45 µm), and fine colloids and solutes (< 0.22 µm). This approach has been applied to assess the relative contribution of individual microbial suspension fractions to the total fouling rate. The fouling rate of each fraction was measured in the lab-scale filtration unit at the same hydrodynamic conditions of the long-term experiments (Figure 6.9). Air sparging was also supplied at a similar specific air demand as that used in the pilot (SAD_{mnet} = 1.12 $Nm^3/h\ m^2$). Results revealed that the dominating fraction on cake membrane fouling was suspended particles (77-84% and 6-12% for settling and non-settling particles, respectively). Colloidal and soluble fractions did not have a relevant role on cake fouling (10-14%). This is because its low concentration (due to high degradation in the MBR) and the high fluxes applied, which jointly increased the particle contribution to the overall fouling. By contrast, several authors have identified colloids and solutes as the main contribution in MBRs treating raw domestic wastewater at subcritical fluxes (Le-Clech et al., 2006). Therefore, it is highlighted one of main advantages of the tertiary MBR operated at supra-critical fluxes: fouling control by this alternative operation mode appears to be a simple way for limiting deposition rate of suspended particles on membrane by the shear rate induced by air scouring. In addition, the deposit formed on the membrane, mainly by large particles, is effectively removed by backwashing.

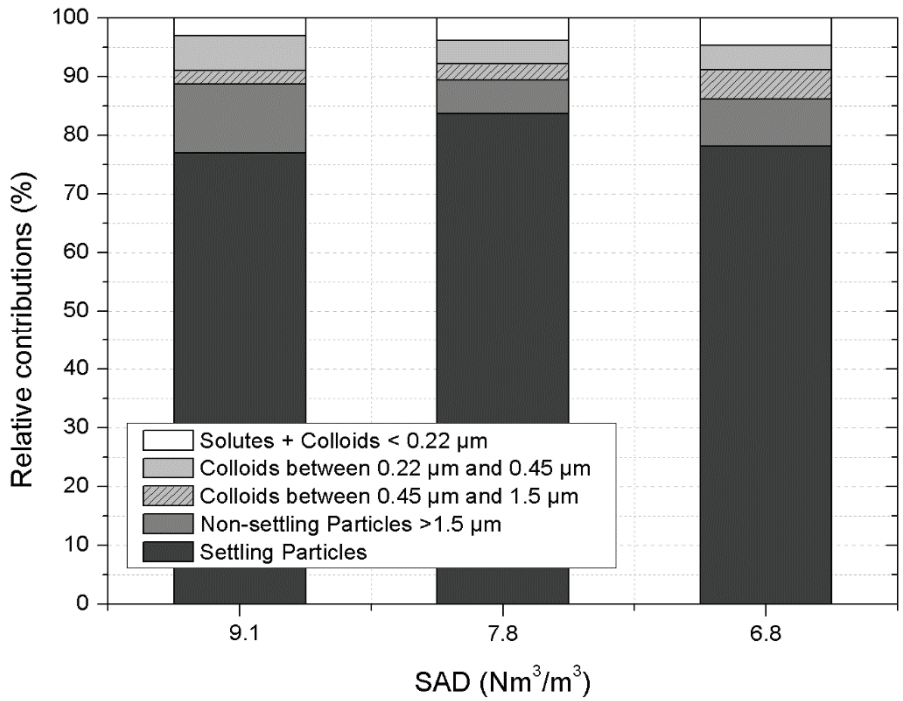

Figure 6.9. Relative contributions expressed as percentage, of the different sludge fractions to fouling

4. Conclusions

The sustainability of a pilot-scale submerged aerobic membrane bioreactor as advanced treatment for secondary treated wastewater, at supercritical fluxes, was evaluated. For this purpose, an alternative backwashing strategy based on transmembrane pressure set-point (TMP_{sp}) was implemented. From this study, the following may be concluded:

- As a result of carbon substrate limited conditions (i.e. maintenance conditions), the system was successfully operated with complete sludge retention achieving a high treatment performance with a moderate liquor suspended solid concentration. In addition, MBR technology has allowed an advanced treatment without sludge production. In these conditions, the soluble microbial products (SMP) concentration in the sludge supernatant was minimised.

- At supra-critical fluxes, an optimal membrane cyclical aeration frequency of 10 s on/ 10 s off was found, above which no improvement on membrane performance was observed.

- Sustainable process performance was observed at supra-critical fluxes (60-80 l/h m^2), providing high permeate net fluxes (59.4-76.1 l/h m^2) during more than 2,250 h of operation without chemical cleaning. In these conditions, fouling is mainly caused by a cake development mechanism on the membrane wall which was effectively removed by backwashing. This cake layer could act as a secondary membrane which prevents SMPs from entering into the membrane pores or adsorbing onto the membrane surface.

- Analysis by means of sludge fractionation in lab-scale tests at similar hydrodynamic conditions indicated that the contribution of suspended solids to cake membrane fouling was about 86-89%.

Maintenance conditions in tertiary MBR could be an attractive option in terms of operational costs, due to the reduction of sludge production and the minimisation of SMPs, which is considered as an important factor affecting residual membrane fouling. This fouling requires more frequent recovery/maintenance chemical cleanings of the membrane. Since fouling is mainly caused by suspended particles, an alternative backwashing strategy based in TMP_{sp} can be implemented allowing the operation at supra-critical fluxes, and thereby obtaining high water productivity. Nevertheless, it remains to be seen if this interesting operation mode is suited for MBRs used for treatment of municipal wastewaters, as it is the main application of this technology.

5. References

Bacchin P., Aimar P., Field R.W., Critical and sustainable fluxes: Theory, experiments and applications, *J. Membr. Sci.,* 281, (2006), 42-69.

Delgado S., Alvarez M., Aguiar E., Rodríguez-Gómez L.E., H_2S generation in a reclaimed urban wastewater pipe. Case study: Tenerife (Spain), *Water Res.*, 33(2), (1999), 539-547.

Delgado S., Alvarez M., Rodríguez-Gómez L.E., Elmaleh S., Aguiar E., How partial nitrification could improve reclaimed wastewater transport in long pipes, *Water Sci. Technol.*, 43 (10), (2001), 133-138.

Delgado S., Díaz F., Villarroel R., Vera L., López R., Elmaleh S., Nitrification in a hollow-fibre membrane bioreactor. *Desalination,* 146, (2002), 445-449.

Delgado S., Villarroel R., González E., Effect of the shear intensity on fouling in submerged membrane bioreactor for wastewater treatment. *J. Membr. Sci.*, 311, (2008), 173–181.

Delgado S., Villarroel R., González E., Submerged Membrane Bioreactor at Substrate-Limited Conditions: Activity and Biomass Characteristics, *Water Environ. Res.*, 82 (3), (2010), 202-208

Drews A., Membrane fouling in membrane bioreactors—Characterisation, contradictions, causes and cures, *J. Membr. Sci.,* 363, (2010), 1–28.

Ferrero G., Rodríguez-Roda I., Comas J., Automatic control systems for submerged membrane bioreactors: A state-of-the-art review, *Water Res.,* 46, (2012), 3421-3433

Guglielmi G., Chiarani D., Judd S.J., Andreottola G., Flux criticality and sustainability in a hollow fibre submerged membrane bioreactor for municipal wastewater treatment, *J. Membr.Sci.,* 289, (2007), 241-248.

Gui P., Huang X., Chen Y., Qian Y., Effect of operational parameters on sludge accumulation on membrane surfaces in a submerged membrane bioreactor, *Desalination*, 151, (2003), 185–194.

Hwang K., Chan C., Tung K., Effect of backwash on the performance of submerged membrane filtration, *J. Membr. Sci.,* 330, (2009), 349–356

Judd S., The status of membrane bioreactor technology, *Trends in Biotechnology*, 26, (2007), 165-171.

Judd S., The MBR Book, 2nd edition: Principles and Applications of Membrane Bioreactors for Water and Wastewater Treatment. Elsevier, Oxford (2011).

Kuberkar V., Davis R., Modeling of fouling reduction by secondary membranes, *J. Membr. Sci.*, 168, (2000), 243–258.

Le-Clech P., Jefferson B., Chang I., Judd S., Critical flux determination by the flux-step method in a submerged membrane bioreactor, *J. Membr. Sci.*, 227, (2003), 83-91.

Le-Clech P., Chen V., Fane A.G., Fouling in membrane bioreactors used in wastewater treatment, *J. Membr. Sci.,* 284, (2006), 17-53.

Lesjean B., Ferre V., Vonghia E., Moeslang H., Market and design considerations of the 37 larger MBR plants in Europe. *Desalination Water Treat*., 6, (2009), 227-233.

Lu S.G., Imai T., Ukita M., Sekine M., Higuchi T., Fukagawa M., A model for membrane bioreactor process based on the concept of formation and degradation of soluble microbial products, *Water Res.*, 35, (2001), 2038–2048.

Lyko S., Wintgens T., Al-Halbouni D., Baumgarten S., Tacke D., Drensla K., Janot A., Dott W., Pinnekamp J., Melin T., Long-term monitoring of a full-scale municipal membrane bioreactor—characterisation of foulants and operational performance, *J. Membr. Sci*., 317, (2008), 78–87.

Ng H., Hermanowicz S., Membrane bioreactor operation at short solids retention times: performance and biomass characteristics, *Water Res*., 39, (2005), 981–992.

Pirt S., The maintenance energy of bacteria in growing cultures. Proc R Soc London, 163B (1965) 224-231.

Schoeberl P., Brik M., Bertoni M., Braun R., Fuchs W., Optimization of operational parameters for a submerged membrane bioreactor treating dye house wastewater, *Sep. Pur. Tech*., 44, (2005), 61–68.

Smith P.J., Vigneswaran S., Ngo H.H., Ben-Aim R., Nguyen H., A new approach to backwash initiation in membrane systems, *J. Membr. Sci.,* 278, (2006), 381–389.

Standard Methods for the examination of Water and Wastewater, 21st ed. American Public Health Association/Water Environment Federation, Washington DC, USA (2005).

Van der Marel P., Zwijnenburg A., Kemperman A., Wessling M., Temmink H., van der Meer W., An improved flux-step method to determine the critical flux and the critical flux for irreversibility in a membrane bioreactor*, J. Membr. Sci*., 332, (2009), 24-29.

Verrecht B., Maere T., Nopens I., Brepols C., Judd S., The cost of a large-scale hollow fibre MBR, *Water Res*., 44, (2010), 5274-5283.

Villarroel R., Delgado S., González E., Morales M., Physical cleaning initiation controlled by transmembrane pressure set-point in a submerged membrane bioreactor, *Sep. Pur. Tech.,* 104, (2013), 55-63.

Wu J., He C., Zhang Y., Modelling membrane fouling in a submerged membrane bioreactor by considering the role of solid, colloidal and soluble components, *J. Membr. Sci.,* 397–398, (2012), 102–111.

Ye Y., Chen V., Le-Clech P., Evolution of fouling deposition and removal on hollow fibre membrane during filtration with periodical backwash, *Desalination*, 283, (2011), 198–205.

CAPÍTULO 7: Aplicación de una estrategia de retrolavado basada en la presión transmembrana de set-point en un biorreactor de membrana sumergida terciario

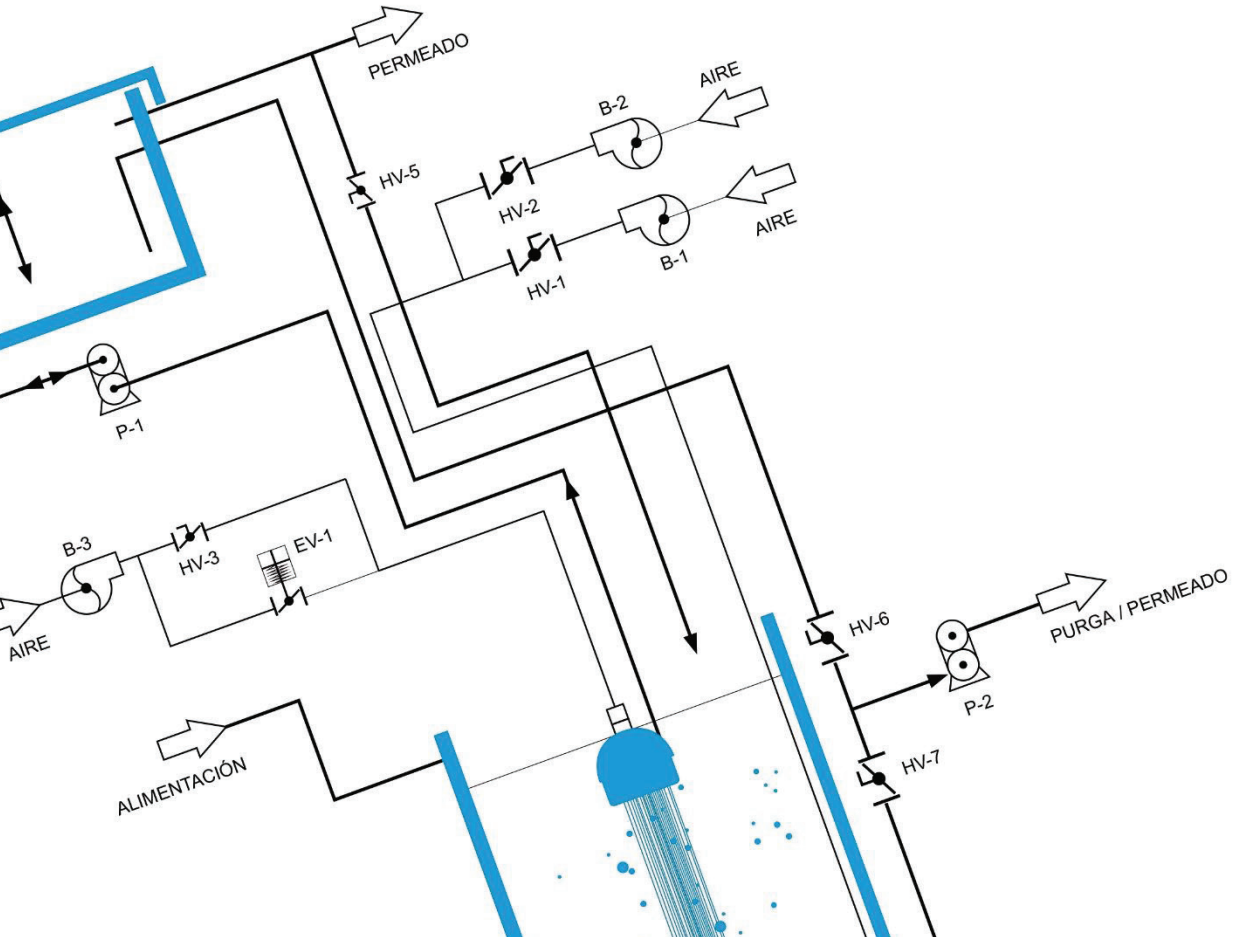

Capítulo 7

Aplicación de una estrategia de retrolavado basada en la presión transmembrana de set-point en un biorreactor de membrana sumergida terciario

Application of a backwashing strategy based on transmembrane pressure set-point in a tertiary submerged membrane bioreactor

Luisa Vera, Enrique González, **Oliver Díaz**, Sebastián Delgado

Journal of Membrane Science
470, (2014) 504-512

Factor de impacto: 5,056 (JCR®, Thomson Reuters 2015).

Highlights

- Sustainability of a MBR operated at supra-critical fluxes
- Novel and promising operation mode for backwashing initiation
- Automatic adjust of the degree of membrane fouling allowed and MBR productivity through backwashing frequency
- Applied for advanced treatment of secondary effluent from a WWTP
- Successfully operated without biomass purge resulting in a moderate MLSS

Keywords

Submerged membrane bioreactor; tertiary treatment; fouling; set-point transmembrane pressure; wastewater reclamation

Resumen:

El control del ensuciamiento en los biorreactores de membrana sumergida se lleva a cabo mediante frecuentes limpiezas físicas de la membrana, como por ejemplo el retrolavado o el relax. En el caso del retrolavado, el sentido del flujo en el interior del módulo de membrana se invierte con el fin de eliminar el ensuciamiento reversible. El rendimiento de esta limpieza física

depende de varios parámetros de operación como el flujo, la duración y la frecuencia con que se aplica. Debido a la complejidad del proceso, es habitual establecer valores predeterminados para las condiciones del retrolavado, lo que induce en la mayoría de los casos, operar con condiciones no optimizadas. En este Capítulo se profundiza en el estudio del modo de operación alternativo por presión de consigna para limitar el ensuciamiento, en el que el retrolavado es iniciado cuando se alcanza una determinada presión transmembrana de consigna (TMP_{sp}) asociada a un ensuciamiento máximo permitido. Concretamente, se analiza el efecto del principal parámetro de operación de este modo alternativo de operación: la presión transmembrana de consigna, sobre el ensuciamiento de la membrana y la productividad del MBR terciario para el tratamiento del efluente de un sistema convencional de lodos activos.

Debido a la calidad del agua de alimentación y a las condiciones de operación, la suspensión biológica se encontró, en el desarrollo del trabajo, en un régimen caracterizado por la limitación de sustrato, lo que se tradujo en una baja producción neta de biomasa y en una concentración constante de solidos suspendidos en el licor mezcla. Por otro lado, las condiciones de inanición favorecen la reducción de SMP en el licor mezcla, que presenta una baja concentración de microorganismos no floculados debido a la elevada presencia de protozoos, devoradores de bacterias dispersas.

Pese a las condiciones de limitación de sustrato, el sistema alcanzó un grado de nitrificación completo del efluente y una reducción considerable de materia orgánica (56 %, expresado como COD). Los resultados revelan que la presión transmembrana de consigna no influyó en la eliminación de materia orgánica, y la concentración de DOC en el permeado se mantuvo constante durante el estudio experimental.

El desarrollo del estudio implicó la realización de 6 series experimentales donde se impusieron distintos valores de TMP_{sp}. Al inicio de cada serie, el sistema experimentó un rápido ensuciamiento residual interno de la membrana que se manifestó por el incremento de la presión transmembrana inicial de cada ciclo de filtración. Al inicio de cada serie experimental se aumentó el ensuciamiento máximo permitido, es decir el valor de TMP_{sp}, lo que provocó un incremento del tiempo de filtración y por tanto, un fenómeno de consolidación del ensuciamiento.

El seguimiento de la presión transmembrana durante la filtración de los primeros ciclos reveló dos comportamientos durante la fase de filtración: un rápido crecimiento inicial de la

TMP seguido de un periodo con un crecimiento continuo. La primera fase se debe al fenómeno de recompresión del ensuciamiento residual externo que se produce cuando una parte del ensuciamiento, eliminado por el retrolavado, no es re-dispersado eficazmente en el medio y se deposita rápidamente sobre la membrana. La fase de crecimiento drástico del ensuciamiento se debió a la construcción de una torta incompresible sobre la membrana. A medida que tiene lugar el fenómeno de consolidación del ensuciamiento, el fenómeno de la recompresión se ve reducido hasta que el ensuciamiento formado es debido principalmente, a la construcción de una torta totalmente reversible, pues el aumento del ensuciamiento residual interno fue significativamente bajo.

El ensuciamiento residual interno se ve incrementado progresivamente con la presión transmembrana de consigna aplicada debido a la relevancia del fenómeno de consolidación que tiene lugar cuando se imponen grandes valores de TMP_{sp}. Por otra parte, el ensuciamiento residual externo y reversible muestran valores próximos entre sí, además a las mayores presiones transmembrana de consigna ambos tipos de ensuciamiento experimentaron un ligero descenso. No obstante, en todas las condiciones ensayadas el ensuciamiento residual interno resultó ser el principal responsable del ensuciamiento global de la membrana (58-96%).

En todas las series experimentales, los tiempos de filtración experimentaron un comportamiento cíclico: durante las primeras horas de la mañana se observaron tiempos de filtración bajos, que fueron aumentando progresivamente hasta un máximo durante la tarde, comenzando posteriormente su descenso. Este comportamiento parece deberse a las fluctuaciones ambientales del proceso, sin embargo, lo más destacable es que el modo de operación por presión de consigna permitió ajustar la limpieza física de manera automática en función del ensuciamiento puntual de la membrana.

Las condiciones de operación optimas del MBR se correspondieron a presiones transmembrana de consiga moderadas (30, 35 y 40 kPa) que permitieron alta productividad, en términos de flujo neto, y un alto rendimiento del retrolavado.

Abstract

An alternative backwashing strategy to enhance water productivity in a tertiary submerged membrane bioreactor (MBR) was assayed. This strategy is based on automatically adjustment of the backwashing frequency as a function of the membrane fouling, which is expected to increase

the net permeate flux produced. The effect of the key operational parameter (transmembrane pressure set-point, TMP_{sp}) on membrane fouling and process productivity was evaluated on a pilot-scale tertiary MBR. The system was successfully operated for over 4 months with complete sludge retention achieving a high treatment performance with a moderate liquor suspended solid concentration, as a result of carbon substrate limited conditions. The analysis of the membrane fouling at supra-critical filtrate flux of 70 L/(h·m^2) with a specific aeration demand identical to that usual at full-scale (SAD_{pnet} = 17 Nm^3/m^3) showed that backwashing efficiency (described in terms of residual fouling resistance) was significantly affected by the selected TMP_{sp} value. At high TMP_{sp}, the efficiency decreased and chemical cleaning was necessary for membrane recovery. Nevertheless, moderate set-point values (30-40 kPa) provided high permeate net fluxes of 65-67 L/(h·m^2) for more than 2000 h of operation, while the reversible fouling rate was not considerably influenced by TMP_{sp}. This was also confirmed by flux steps trials.

1. Introduction

Due to their well-known advantages (Judd, 2007; Judd 2010), aerobic membrane bioreactors (MBRs) have become an attractive option for wastewater reuse, being very compact and efficient systems for achieving the highest effluent quality standards. The considerable popularity of the MBRs in the wastewater treatment market, the numerous suppliers, and the upward trend in plant size now reflect the maturity reached by this technology (Santos and Judd, 2010). In fact, MBRs have been implemented in more than 200 countries (Icon 2008). Nevertheless, the main limitation to more widespread application is their high energy demand, besides awaiting new strategies to mitigate membrane fouling (Verrecht et al., 2008). In addition, the uncertainty associated with fouling has led to conservative plant designs where the main operating parameters are far from being optimised (Judd 2010).

As described in a previous research, aerobic MBRs can be effectively applied as an advanced treatment of secondary effluent from a wastewater treatment plant (Delgado et al., 2010;Lin et al., 2011). Delgado et al. (2010) demonstrated a high conversion of ammonium to nitrate and constant COD removal efficiency in their system, regardless of the influent fluctuations. As a result of carbon substrate limited conditions, a minimal value for the carbon substrate utilization rate was found and the system successfully operated at moderate

permeate fluxes (30-32 L/(h·m^2)) and low physical cleaning frequency. In these conditions, the production of soluble microbial products was minimized and higher organisms appeared.

For a submerged MBR, the operation strategy to control membrane fouling frequently includes physical cleaning through backwashing. During backwashing, permeate is used to flush the membrane backwards and it is routinely applied to hollow-fibre configuration. This technique has been successfully proved to remove reversible fouling caused by loosely packed sludge cake (Wu et al., 2008; Hwang et al., 2009). Several operating parameters such as frequency, duration and backwashing flux have been identified as crucial in fouling mitigation (Le-Clech et al., 2006). However, there is a gap in knowledge regarding the inter-relationships between those parameters and the permeate flux imposed. In fact, due to the complexity of the process, operation strategy is usually time-based and backwashing is commonly applied for 30-60 seconds every 5.8-15 min of filtration (Zsirai et al., 2012). As a consequence, the systems are not optimised during the whole operational period (Judd 2010).

Recently, special attention has been paid on feedback control for finding optimal operating conditions in MBRs (Ferrero et al., 2012). Busch and Marquardt (2009) introduced a run-to-run process control approach, in which the manipulated variables are optimised after each filtration cycle. The manipulated variables include the permeate and backwashing fluxes, and the filtration and backwash durations. Smith et al. (2006) have proposed a control system for backwash initiation by permeability monitoring, adjusting the backwashing frequency automatically as a function of the permissible increase of transmembrane pressure for each filtration cycle. This operation strategy was capable of achieving higher water productivity than the temporised mode with fixed intervals. The allowable TMP increase was fixed at 3% (1.5 kPa) of the maximum permissible value of 50 kPa, which is defined as the point where the fouling can still be removed by backwashing. Vargas et al. (2008) used a similar strategy in which backwash is initiated when the flux drops below a predetermined fraction of the maximum value in a sequential membrane bioreactor operated at a constant *TMP*. This approach has been further developed at lab-scale in order to assess the effect of transmembrane pressure set-point (TMP_{sp}) on membrane fouling and water productivity (2013). This backwashing strategy was also validated on pilot-scale, showing that continuous operation can be maintained at supra-critical filtration fluxes without chemical cleaning at moderate TMP_{sp} (30 kPa) (Vera et al., 2014). It is therefore desirable to identify the optimal TMP_{sp} value and its effect on membrane fouling over long-term periods in a MBR operated

under real feed parameters and temperature fluctuations. This paper continues the discussion about the applicability of this alternative operation strategy, in which backwashing initiation is controlled by the TMP_{sp}. Additional flux step trials have also been carried out in order to assess the effect of TMP_{sp} on reversible fouling and threshold flux.

2. Material and methods

2.1. Feedwater

The MBR was fed with the effluent from a conventional activated sludge wastewater treatment plant. The feed water was analysed three times a week through the whole experimental period and the average characteristics are summarised in Table 7.1. This is a conventional WWTP designed only for carbon removal. Due to the short sludge ages and oxygen deficiency in the activated sludge process, frequent episodes of sludge de-flocculation or insufficient sedimentation usually appear, resulting in a high suspended solids concentration in the effluent.

Table 7.1. Feedwater main characteristics (n= 63)

Parameters	Units	Mean	Range
COD	mg/L	55	12-205
DOC	mg/L	23	10.5-125.0
$N\text{-}NH_3$	mg/L	15	1.4-22.7
$N\text{-}NO_2^-$	mg/L	6	<1-12.8
$N\text{-}NO_3^-$	mg/L	9	<1-18.5
Turbidity	NTU	69	14-177
TSS	mg/L	156	27-316

2.2. MBR

A cylindrical 220 liter MBR was equipped with ZeeWeed® ZW-10 hollow-fibre membranes (GE Water & Process Technologies) of 0.04 µm rated pore diameter, 1.9 mm external diameter and 0.9 m^2 of filtering surface area, assembled vertically (Fig. 7.1). ZeeWeed® consists of a woven reinforcing braid on which a PVDF membrane is cast. The effluent (permeate) was extracted from the top header of the module under slight vacuum. All experiments were carried

out at constant permeate flux (70 L/(h·m^2)), registering transmembrane pressure as a function of time. Membrane fouling was controlled by backwashing based on an automatic cleaning initiation mode. Each filtration phase finished when a pre-established TMP_{sp} was reached, beginning the backwashing immediately afterwards. The system was operated at 6 different TMP_{sp} (25, 30, 35, 40, 45 and 50 kPa). A programmable logic controller system was used to initiate and stop the backwashing by comparison of TMP_{sp} and instantaneous pressure values. Pressure profiles were continuously data logged and plotted. Filtration flux (J) and backwashing conditions (flux J_B and backwashing time t_B) were constant throughout the experimental period with J = 70 L/(h·m^2), J_B = 60 L/(h·m^2) and t_B = 30 s.

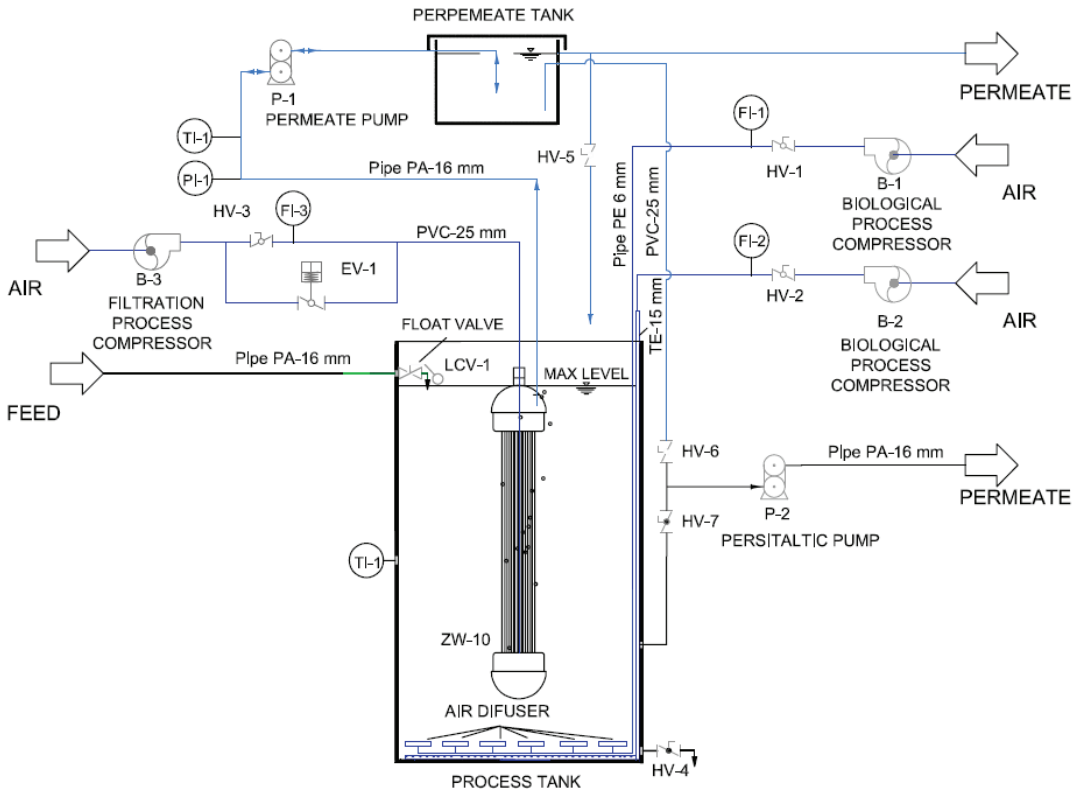

Figure 7.1. Configuration of the pilot-MBR system, ZW10

Fouling was also controlled by intermittent coarse bubbling of air (10 s on/ 10 s off) supplied at 1.1 Nm^3/h m^2 during the filtration phase, expressed as net aeration rate per membrane area (SAD_{mnet}). Nevertheless, constant air scouring during the backwashing phase was fixed at 3.1 Nm^3/h m^2 in order to improve the fouling removal, on the basis of previous results (Vera et al., 2014).

The bioreactor was run at hydraulic retention time (HRT) of 8.8 h without sludge removal except for sampling. The excess of permeate was returned to the tank in order to maintain a constant HRT independent of the permeate flux. Additional air was supplied at the bottom of the bioreactor, providing oxygen and stirring. The dissolved oxygen concentration in the reactor was always above 1.5 mg/L, operated at 25 ± 2 ºC. Suspensions were routinely characterised by particle size distribution, time-to-filter (TTF), MLSS, MLVSS, non-flocculating microorganisms and dissolved organic matter of the liquid phase.

Previous studies were carried out in this pilot-plant for over 3 months in order to evaluate the influence of permeate flux on membrane fouling produced with this novel operation mode based upon TMP_{sp} (Vera et al., 2014), consequently prior biomass acclimation was not required.

2.3. Short-term flux step trials

The effect of TMP_{sp} on critical flux was assessed by flux-step modified tests. The modified method is based on applying successive flux increments up to a maximum, in accordance with the method of Le-Clech et al. [18] and further improved by incorporating relaxation steps for reducing the influence of fouling history, as described by Van der Marel et al. (2009). The modified method proposed in this work substitutes the relaxation for short backwashing steps along 30 s at a fixed flux of 60 L/(h·m^2). These established values are similar to those in conventional operation of MBRs. Intermittent air bubbling (10 s on/ 10 s off) for membrane scouring was also supplied at SAD_{mnet} = 1.1 Nm^3/h m^2. The other experimental parameters were selected in accordance with previous studies (Van de Marel et al., 2009; Gublielmi et al., 2007): step duration of 15 min, flux-step height of 5 L/(h·m^2)and a maximum flux of 70 L/(h·m^2).

Results were related to reversible fouling rate (r_f), given by the derivative of the transmembrane pressure (d*TMP*/d*t*). On the other hand, residual fouling was assessed by measuring the transmembrane pressure after each backwashing (TMP_{if}).

2.4. Membrane cleaning protocol

After the long-term test, the fouled membrane was cleaned by a specific protocol that includes the following steps: (1) rinsing with Milli-Q water; (2) backwashing with Milli-Q water at a flux of 60 L/(h·m^2); (3) chemical cleaning with a solution of sodium hypochlorite (500 mg/l) for 24 h; (4) chemical cleaning with a solution of citric acid (6,000 mg/L) for 24 h; and (5) chemical

cleaning with sodium hypochlorite (500 mg/L) for 24h. After each step, tap water filtration test was applied to measure the remaining resistance.

2.5. Membrane fouling characterisation

TMP evolution can be used for membrane fouling characterisation. According to the "resistance-in-series" model and disregarding the osmotic pressure term, the *TMP* can be described by:

$$TMP = J \cdot \mu \cdot R_t = J \cdot \mu \cdot \left(R_m + R_{rdf} + R_{rvf}\right) \quad [7.1]$$

where μ is the permeate viscosity, J is the permeate flux, R_t is the total hydraulic resistance, R_m is the clean membrane resistance, R_{rdf} is the residual fouling resistance and R_{rvf} is the reversible fouling resistance.

Residual fouling is that which is not removed by backwashing. Its resistance can be separated into internal fouling resistance (R_{if}), related to internal membrane pore blocking (Jiang et al., 2003) and gel or compacted particle layer that is not detached during backwashing (McAdam and Judd 2008), and an external fouling resistance (R_{ef}) linked to fouling layer recompression [23]:

$$R_{rdf} = R_{if} + R_{ef} \quad [7.2]$$

During the filtration, this external layer compresses, increasing the residual resistance, and during backwashing this layer relaxes, yielding a lower residual resistance. Therefore, just at the beginning of the filtration cycle, the initial *TMP* (TMP_i) can be described by Eq. (3):

$$TMP_i = J \cdot \mu \cdot \left(R_m + R_{if}\right) \quad [7.3]$$

In contrast, reversible fouling resistance R_{rvf} is generally associated with a cake development mechanism on the membrane wall (Meng et al., 2009). According to the cake model, *TMP* linearly increases with filtration time and the slope of the straight line, the fouling rate r_f, can be used as a quantification parameter of reversible fouling (Delgado et al., 2008; Drews 2010). Therefore, *TMP* evolution with elapsed time t can be described by Eq. (4):

$$TMP = TMP_0 + r_f \cdot t \quad [7.4]$$

where TMP_0 is the transmembrane pressure related to the residual fouling and can be defined as:

$$TMP_0 = J \cdot \mu \cdot (R_m + R_{rdf}) \quad [7.5]$$

and the difference between TMP_i and TMP_0 called ΔTMP, is linked to the external residual fouling, R_{ef}.

Finally, another important parameter for membrane fouling characterisation can be considered, the backwashing efficiency η, which can be defined as (Jeison and van Lier, 2007):

$$\eta = \frac{R_{sp} - R_m - R_{rdf}}{R_{sp} - R_m} \cdot 100 \quad [7.6]$$

where R_{sp}, is the total hydraulic resistance at the TMP_{sp} (i.e. before backwashing), that can be estimated as the addition of several resistances: membrane itself, residual fouling and reversible cake fouling:

$$R_{sp} = R_m + R_{rdf} + (R_{rvf})_{t=t_f} \quad [7.7]$$

where t_F is duration of the filtration phase to reach the TMP_{sp}.

2.6. Analytical methods

Dissolved oxygen was measured using a WTW 340i. Chemical oxygen demand (COD), ammonium-nitrogen ($N\text{-}NH_3$), total suspended solids (TSS), mixed liquor suspended solids (MLSS), mixed liquor volatile suspended solids (MLVSS), time to filter (TTF) and turbidity were determined in conformity with the Standard Methods (ALPHA, 2005). The analyses of nitrite-nitrogen ($N\text{-}NO_2^-$) and nitrate-nitrogen ($N\text{-}NO_3^-$) were conducted through ion chromatography using a Compact IC plus 882 device supplied by Metrohm. Dissolved organic carbon (DOC) concentration was measured with a TOC-meter (TOC-5000A, Shimadzu). Microbial floc size distribution was measured by using a Malvern Mastersizer 2000 instrument with a detection

range of 0.02-2000 µm. To quantify the amount of non-flocculating microorganisms, the samples of biomass were centrifuged at 1300 g for 2 min and the supernatant turbidity was then measured (Ng et al., 2005). The microorganism population was observed by Binocular microscopy (CME, Leica).

3. Results and discussion

3.1. Biomass characteristics and permeate quality

Table 7.2 summarises the main characteristics of the microbial suspension developed in the bioreactor. Despite operating with total sludge retention, moderate MLSS concentration was obtained (3.7-6.6 g/L), which is attributable to the low organic load in the feedwater (Table 7.1). The MLVSS/MLSS ratio remains nearly constant (69-79 %) throughout the experimental period, indicating a low accumulation of inorganic particulate matter. At substrate-limited conditions, according to cellular "maintenance" concept (Pirt, 1965) microorganisms utilise available substrates mainly for maintenance purposes instead of producing additional biomass. As a consequence, the low organic substrate utilisation rate (<0.05 kg COD/kg MLVSS d) and the long sludge retention time improved soluble microbial products (SMP) biodegradation (65% on average). This was attributable to an increase in microbial diversity, including slow-growing microorganisms (Lu et al., 2001). As a result, a low concentration of SMP in the supernatant was observed (8.0 mg/L, expressed as equivalent DOC).

Table 7.2. Characteristics of microbial suspension

PARAMETER	UNIT	MEAN VALUE	RANGE
MLSS	g/L	5.5	3.7-6.6
MLVSS	g/L	4.2	2.9-5.2
TTF	s	257	40-330
PSD			
$D_{(v,0.1)}$	µm	17	
$D_{(v,0.5)}$	µm	47	
$D_{(v,0.9)}$	µm	102	
Supernatant turbidity	NTU	28.4	14-55
Supernatant DOC[a]	mg/L	8.0	6.2 -14.4

[a] Samples were filtrated through microfibre filters with a nominal pore size of 0.45 µm

In general, the suspension also showed good filterability, quantified as TTF (270 s), with uniform and medium-sized flocs ($D_{(v,0.5)}$= 47 µm). In addition, the suspension presented low quantity of small non-floculating flocs, measured as supernatant turbidity. This could be due to the presence of higher organisms like heterotroph protozoa (Figure 7. 2), which predate on dispersed bacteria (Wei et al., 2003).

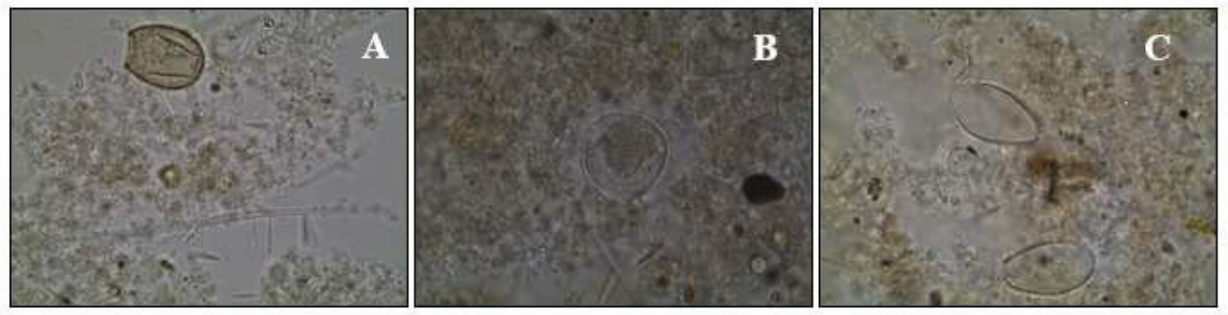

Figure 7.2. Protozoan population in sludge samples (100x)

Permeate quality is presented in Table 7.3, where results are classified into six experimental periods according to the values of TMP_{sp} applied. Regardless of the TMP_{sp}, the permeate turbidity remained in the range 0.3-0.7 NTU, thus confirming the membrane integrity throughout the experimental period. As expected, considerable organic matter removal (56% on average for COD) and complete nitrification was always obtained in the bioreactor. Regarding SMP retention by the membrane and the associated cake layer, no considerable effect of the TMP_{sp} on the permeate DOC concentration was observed.

Table 7.3. Permeate main characteristics

		TMP_{sp}											
		25 kPa		30 kPa		35 kPa		40 kPa		45kPa		50kPa	
Parameters	Units	Mean	Range	Mean	Range	Mean	Range	Mean	Range	Mean	Range	Mean	Range
COD	mg/L	20	15-25	32	17-42	28	18-43	25	19-36	26	12-33	23	21-25
$N\text{-}NH_3$	mg/L	0.3	0.3-0.4	0.4	0.4-0.6	0.5	0.4-0.6	0.6	0.4-1.0	0.5	0.5-0.6	0.5	0.4-0.5
$N\text{-}NO_3^-$	mg/L	36	26-43	35	24-60	36	22-42	27	5-42	27	24-30	31	29-33
Turbidity	NTU	0.5	0.4-0.6	0.6	0.4-0.7	0.5	0.4-0.7	0.4	0.3-0.5	0.6	0.5-0.6	0.5	0.4-0.5
DOC	mg/L	5.7	4.8-6.8	7.3	6.8-7.7	7.4	6.9-7.7	6.5	6.3-7.0	6.6	6.0-7.0	5.8	5.7-6.2

3.2. Effect of TMP set-point on membrane residual fouling and process productivity

In the present study, structured into six periods according to the selected *TMP_{sp}*, the pilot plant was run for more than 2.750 h without any severe problems. However, there were two events of power shortage during the second period (912-930 h) and the fifth one (2.610-2.658 h).

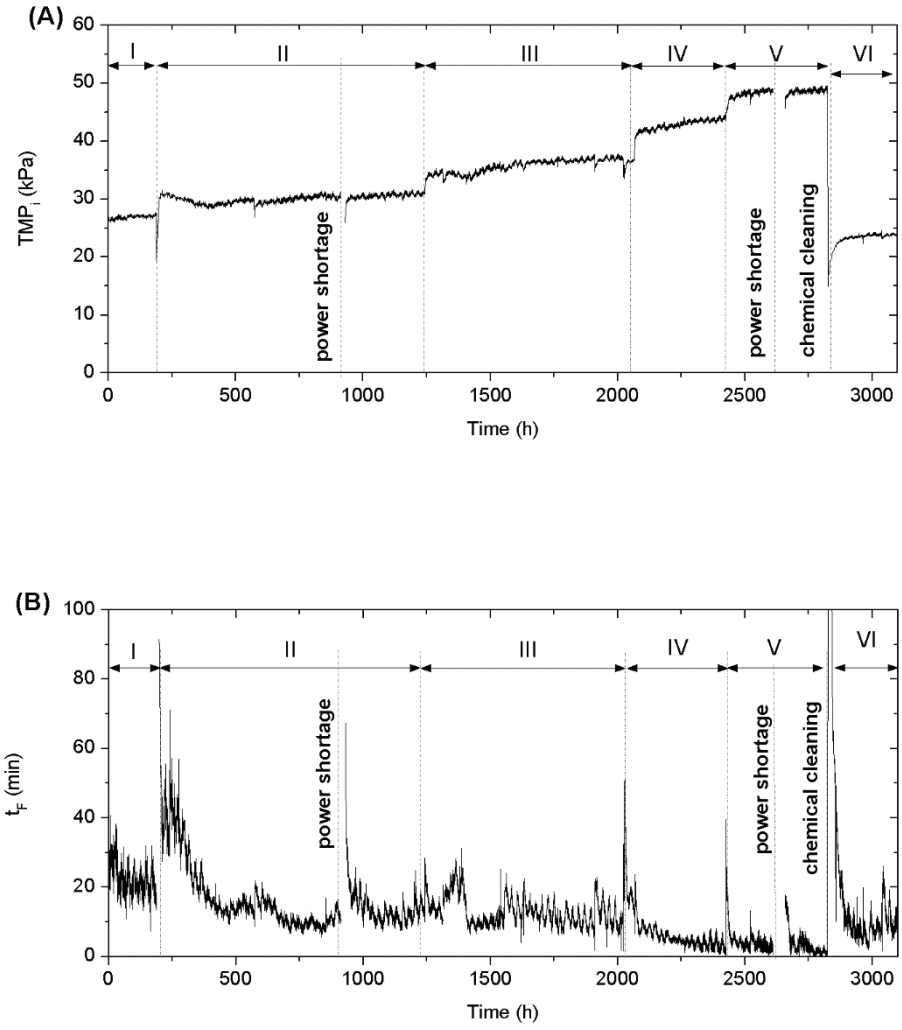

Figure 7.10. TMP_i (A) and t_f (B) profile at different TMP_{sp} throughout the experimental time: (I) TMP_{sp}=30kPa; (II) TMP_{sp}=35kPa; (III) TMP_{sp}=40kPa; (IV) TMP_{sp}=45kPa; (V) TMP_{sp}=50kPa; (VI) TMP_{sp}=25kPa;

Figure 7.3A displays TMP_i profiles the residual fouling rate for each period. The general trend indicates that TMP_i increased as a function of TMP_{sp}. Each period was characterised by a sudden increase of TMP_i followed by a slower and gradual rise. This initial TMP_i increase can be related to the operating mode for backwashing initiation, which starts when the pre-fixed TMP_{sp} value (i.e. significant membrane fouling) is reached during the filtration phase. It should be noted that air scouring was continuously supplied at SAD_{mnet} of 3.1 $Nm^3/h\ m^2$ during the backwashing, thus increasing this parameter by a factor of 2.8 with respect to filtration phase. Ye et al. (2011) highlighted the importance of enhancing backwashing efficiency with air scouring to avoid fouling layer recompression and favouring its re-dispersion. However, this strategy seems inefficient to prevent external residual layer at the tested conditions in the present study. These results suggest a progressive consolidation of the deposit as the TMP_{sp} rises, leading to growth of internal residual fouling that cannot be removed by physical cleaning. Increasing TMP_{sp} between phases should result in longer filtration times in the first cycles, where the sharp increase in internal fouling was observed (Figure 7.3B). A similar behaviour was observed after the mentioned power shortages, which can be considered as a long relaxation of the fouling layer. In fact, TMP_i rapidly increased until achieve the previous values after both power outage (Figure 7.3A). Therefore, a prolonged relaxation could remove partially this fouling layer that appears during the normal operation when transmembrane pressure set-point strategy is applied. Hence, the results would support a significant part of the internal residual fouling being related to compacted particle layer. McAdam and Judd (2008) indicated that the cake consolidation only occurs when the critical value of the mass deposited is reached, thus resulting in a linear increase of residual fouling with filtration duration beyond this critical value. Instead, after the initial TMP_i growth at the beginning of each period, the effectiveness of the backwashing tended to stabilise the TMP_i value for each phase. This fact is reflected by the slow rates of TMP_i rise (1.8 to 7.2 Pa/h) which were found to be independent of the TMP_{sp}.

The TMP_{sp} increase led to a longer filtration phase (t_F) during the early cycles of each period, as previously mentioned (Figure 7.3B). Then, a stabilised filtration phase length was achieved, which was significantly affected by inherent fluctuations in ambient conditions.

For the lower TMP_{sp} (25 kPa), as a consequence of the low value of the set-point, shorter stabilised filtration cycles were obtained (12 min on average). Sustainable t_F were observed at the moderate TMP_{sp} range: 22, 14 and 13 min for 30, 35 and 40 kPa, respectively. However, increasing TMP_{sp} up to 40 kPa showed a negative impact on t_F, decreasing its value below to a

non-operative level (5 and 3 min on average for 45 and 50 kPa, respectively). This indicates that the backwashing efficiency to prevent the sudden increase of TMP_i at the beginning of the period, declined with TMP_{sp}. This can be attributed to the rise in fouling load to the membrane. Similar effect on backwashing efficiency has been reported by other authors after extending the filtration length (i.e. increasing the amount of fouling) with fixed backwashing intervals (Gui et al., 2003; Schoeberl et al., 2005). To illustrate it, averages net permeate fluxes $(J_{net})_{ave}$ and backwashing efficiencies $(\eta)_{ave}$ were calculated (Eq. [7.8] and Eq. [7.9], respectively):

$$(J_{net})_{ave} = \frac{(t_F)_{ave} \cdot J - t_B \cdot J_B}{(t_F)_{ave} + t_B} \quad [7.8]$$

where $(t_F)_{ave}$ is the average filtration length, t_B is the duration of the backwashing phase, J is the permeate flux and J_B is the backwashing flux.

$$(\eta)_{ave} = \frac{R_{sp} - R_m - (R_{rdf})_{ave}}{R_{sp} - R_m} \cdot 100 \quad [7.9]$$

where $(R_{rdf})_{ave}$ is the average residual fouling resistance.

Figure 7.4 shows average $(J_{net})_{ave}$ in each period as a function of the TMP_{sp}. At 25 kPa, the higher backwashing frequency imposed due to the low TMP_{sp} selected did not result in a high value of the backwashing efficiency. These results suggest a permanent residual fouling which cannot be completely removed by backwashing, even operating a low TMP_{sp}. Consequently, moderate set-point values (30, 35, 40 kPa) provided high water productivity (67, 66, 65 L/(h·m^2)), respectively. On the other hand, increasing the selected set-point up to 40 kPa produced a significant decrease in $(J_{net})_{ave}$ due to a significant decline in average backwashing efficiency under 10%.

Finally, another aspect to analyse was the effect of the backwashing strategy on TMP_i and t_F profile during a day. Figure 7.5 shows an example of the typical trend: whilst TMP_i seems to be nearly constant (varying on a 0.8% range with a mean value 36.8 kPa) (Figure 7.5.A), t_F showed a cyclic pattern over 24 h (Figure 7.5.B). Lower t_F (7-9 min) were always observed during the early hours of the early morning (0:30-7:30) which gradually increased until reaching a maximum (12-15 min) in the afternoon (12:30- 19:30) starting to decline afterwards. This behaviour may be

related to significant changes in sludge filterability according to fluctuations of ambient conditions. Nevertheless, a deeper research is necessary to conclude the causes for this repetitive dairy evolution.

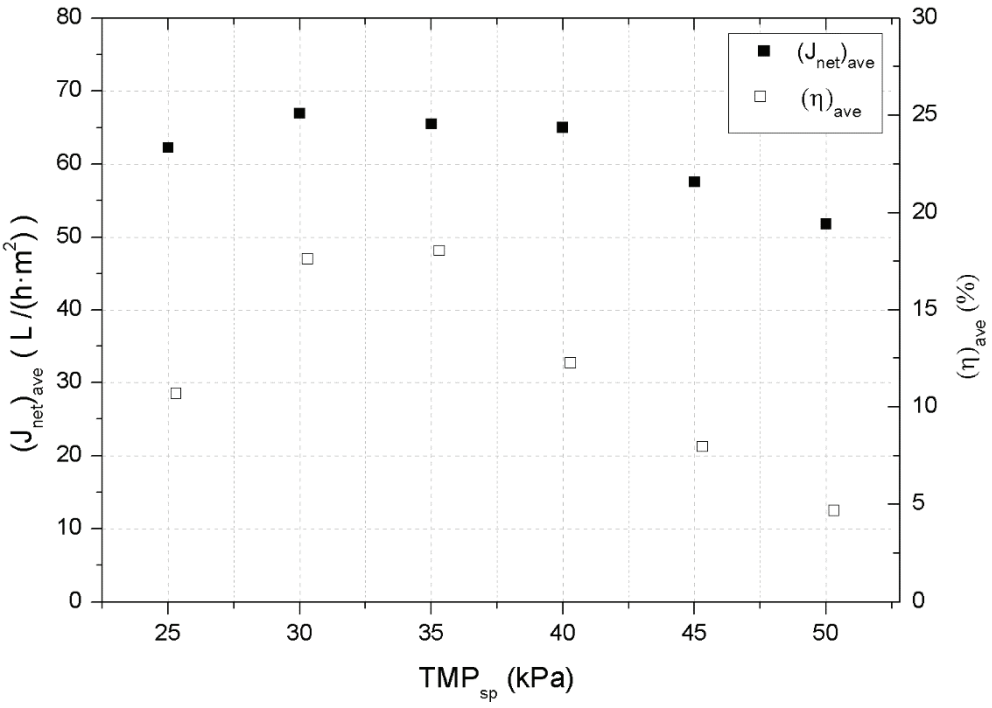

Figure 7.4. $(J_{net})_{ave}$ and $(\eta)_{ave}$ against TMP_{sp}

In summary, it may be concluded that the main advantage of this backwashing strategy is that the system automatically adjusts the degree of membrane fouling allowed through backwashing frequency (i.e. filtration length) for a preselected TMP_{sp}. This allows to operate at high permeate fluxes and to optimise the length of the filtration time. Permeate net fluxes obtained at moderate TMP_{sp} represents a significant improve, of about 60-65% of the J_{net} obtained by a conventional temporised operation at critical filtration conditions (t_F=12 min, t_B=30 s, J=45 L/(h·m^2) and J_B=60 L/(h·m^2)) (Judd, 2010).

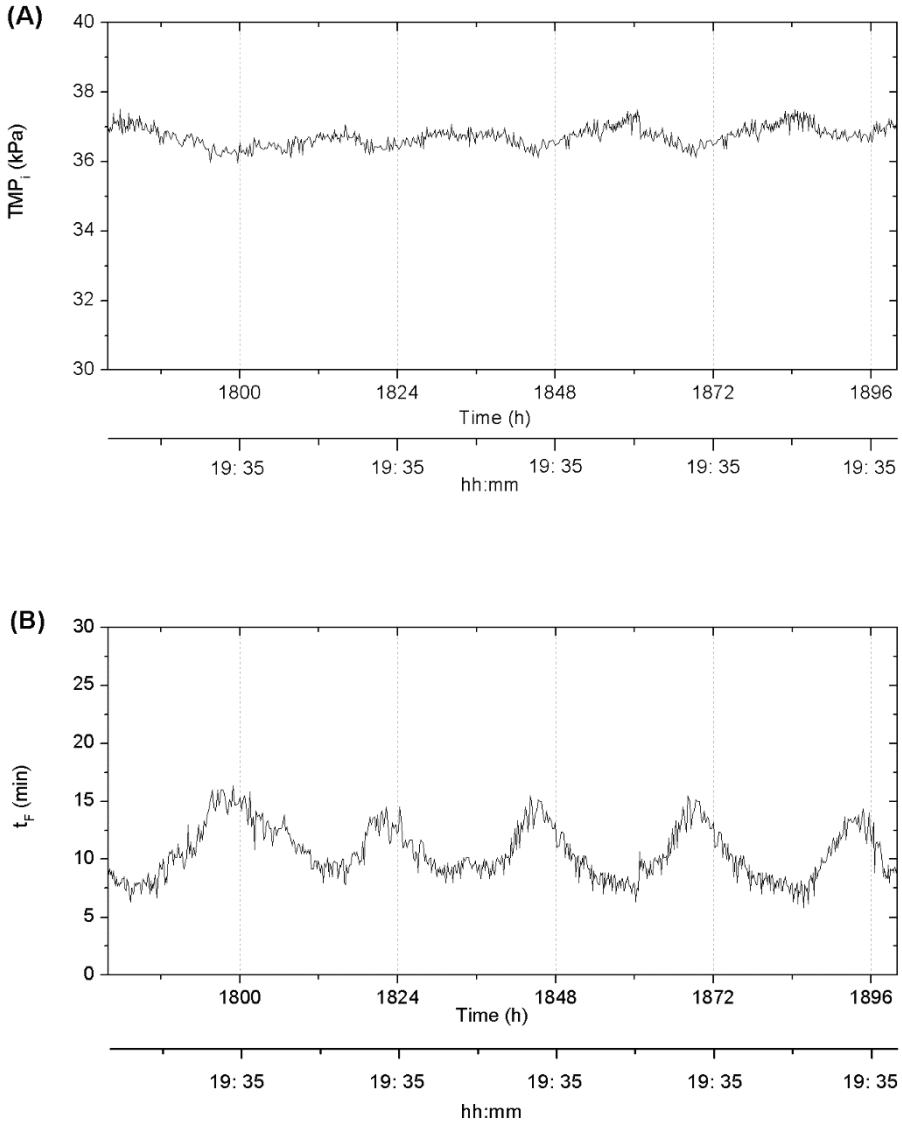

Figure 7.5. TMP_i (A) and t_F (B) profile during several consecutive days; Period III: TMP_{sp}=40 kPa

3.3. Proposed fouling mechanisms

According to the exposition developed in 2.5 and the results presented in previous section, a mechanism for fouling development in long-term experiments can be proposed.

As filtration proceeds, a two-step phenomenon was typically observed: a sudden increase in *TMP* followed by a linear rise (Figure 7.6). A sharp fouling increase may be due to a recompression process, as it was stated in the previous section. After this transient phase, the linear *TMP* rise was assumed to be caused by a cake development mechanism on the membrane surface. As supra-critical flux was applied, it can be expected that this cake layer was mainly

formed by deposition of large suspended solids which can be effectively removed by backwashing (Wu et al., 2008). Therefore, it can be distinguished a TMP_0, corresponding to the value of *TMP* at which it starts to increase linearly, which separates reversible cake formation and residual fouling.

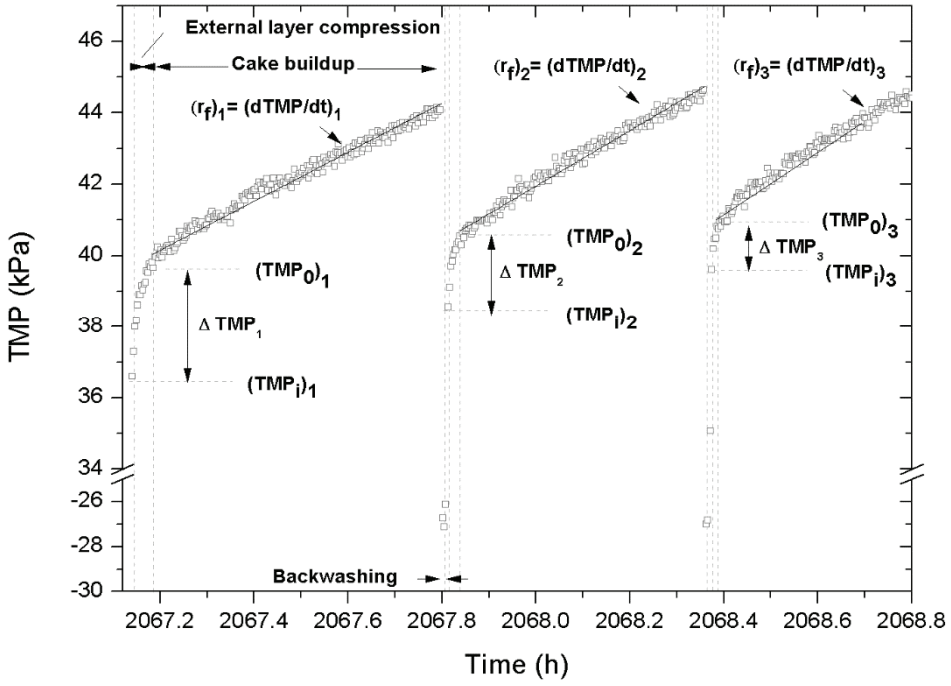

Figure 7.6. TMP profile of consecutive filtration and backwashing cycles at the beginning of the period IV (TMP_{sp}=45kPa)

Also, a dynamic behaviour with consecutive filtration/backwashing cycles was typically observed at the beginning of each experimental period defined through the pre-fixed TMP_{sp} value (45 kPa in Figure 7.6). An initial growth of TMP_i was observed, which was less in subsequent cycles. Accordingly, the duration of the recompression phase (associated with *ΔTMP*) decreased with successive cycles. This behaviour may be due to a progressive consolidation of the deposit which backwashing cannot remove. In these conditions, it is assumed that the cake layer is mainly reversible (i. e. amount of particle deposition and removal was balanced) and the resulting TMP_i increase rates were significantly lower (0.018-0.072 mbar/h) than typical ranges for residual fouling reported for full-scale MBRs (0.6 mbar/h) (Drews, 2010). A reason for this finding is that the cake layer might act a secondary membrane

that prevents pore blocking by SMP (Kuberkar and Davis, 2000). In addition, this hypothesis is in accordance with the relatively stable SMP concentration attributable to the degradation process, attained in the MBR due to the maintenance conditions applied. This behaviour is in agreement with Hwang et al. (2009), who reported that an extended filtration cycle time can increase backwashing efficiency if the cake formed suppresses membrane pore blocking. Consistently, maintenance chemical cleanings were not necessary during the whole experimental period.

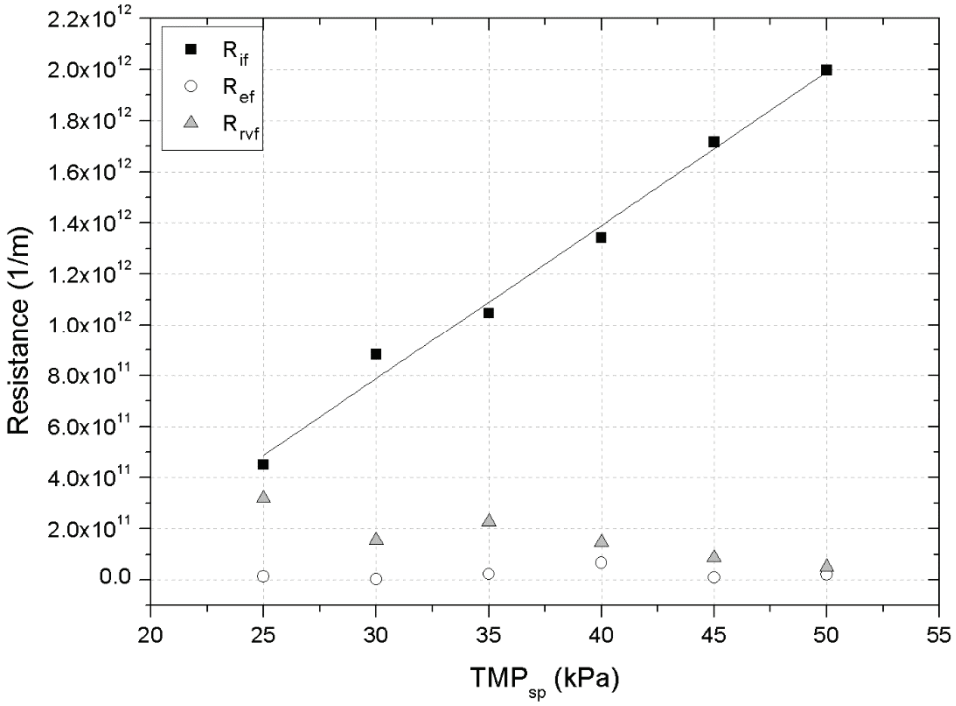

Figure 7.7. Fouling resistances against TMP_{sp}; R_{if} residual internal fouling resistance; R_{ef} residual external fouling resistance; R_{rvf} reversible fouling resistance

On the other hand, the effect of successive TMP_{sp} increase between steps was assessed in terms of residual fouling and reversible resistances (determined according to section 2.5). Figure 7.7 shows average fouling resistances against TMP_{sp}. It can be observed that internal fouling resistance R_{if} linearly increased with TMP_{sp} at the tested conditions. These results suggest a progressive consolidation of the deposit as the TMP_{sp} becomes higher. Both reversible resistance R_{rvf} and residual external fouling resistance R_{ef} showed near values and tended to decrease at high TMP_{sp} values (Figure 7.7). This is attributable to the high level of internal fouling achieved, at 45 and 50 kPa which was able to significantly reduce the average duration of the filtration

length within a cycle (5 and 3 min, respectively) and therefore, the amount of particles deposited onto the membrane. At the same time, by increasing the residual internal fouling, the pressure drop over the external layer and the cake deposit during the filtration phase was also reduced, which decreased the compression effect (Jørgensen et al., 2012).

The results revealed that the main contribution to the overall fouling at the end of the filtration phase (i.e. at TMP_{sp}) was from internal residual fouling (varying from 58 to 96% of the total resistance), its contribution increasing with TMP_{sp}. In contrast, external residual fouling due to recompression was irrelevant (0-4%) and it only had a relevant role to the cake layer at low to moderate TMP_{sp} of 25-40 kPa (41-9%).

3.4. Effect of TMP_{sp} on filterability of the suspension

An issue to be considered during the operation at different TMP_{sp} is the propensity to changes in reversible fouling that could be produced. In order to determine in situ the effect of the residual fouling achieved at different TMP_{sp} on critical fluxes, flux step trials were carried out for MBR monitoring. Figure 7.8A represents TMP_i as a measure of the initial pressure observed at the beginning of each step, which consistently increased proportionally to TMP_{sp}. Figure 7.8B shows the reversible fouling rates ($r_f = dTMP/dt$) against J. An exponential relationship is seem, as reported in many other studies (Le-Clech et al., 2003; Zsairai et al., 2012). Results also showed an identical critical flux of ~ 45 L/(h m^2) instead of the TMP_{sp} that might be an indication for the stability of the membrane performance regardless of the residual fouling history. Additionally, the identical trend suggested that particle deposition rate suggested it was not significantly affected by a compression process on the experimental conditions. Apparently, this is contrary to the results of previous studies (Bugge et al., 2012; Robles et al., 2013). The difference may be due to the high internal residual fouling levels reached in the present work, which significantly reduced the pressure drop over the cake (Jørgensen et al., 2012).

3.5. Membrane recovery cleaning

A specific protocol that combines physical and chemical cleaning methods was developed to evaluate the nature of the residual fouling achieved at the end of the 5^{th} period (TMP_{sp}= 50 kPa). The remaining resistance after each cleaning step was evaluated by clean water tests (Figure 7.9).

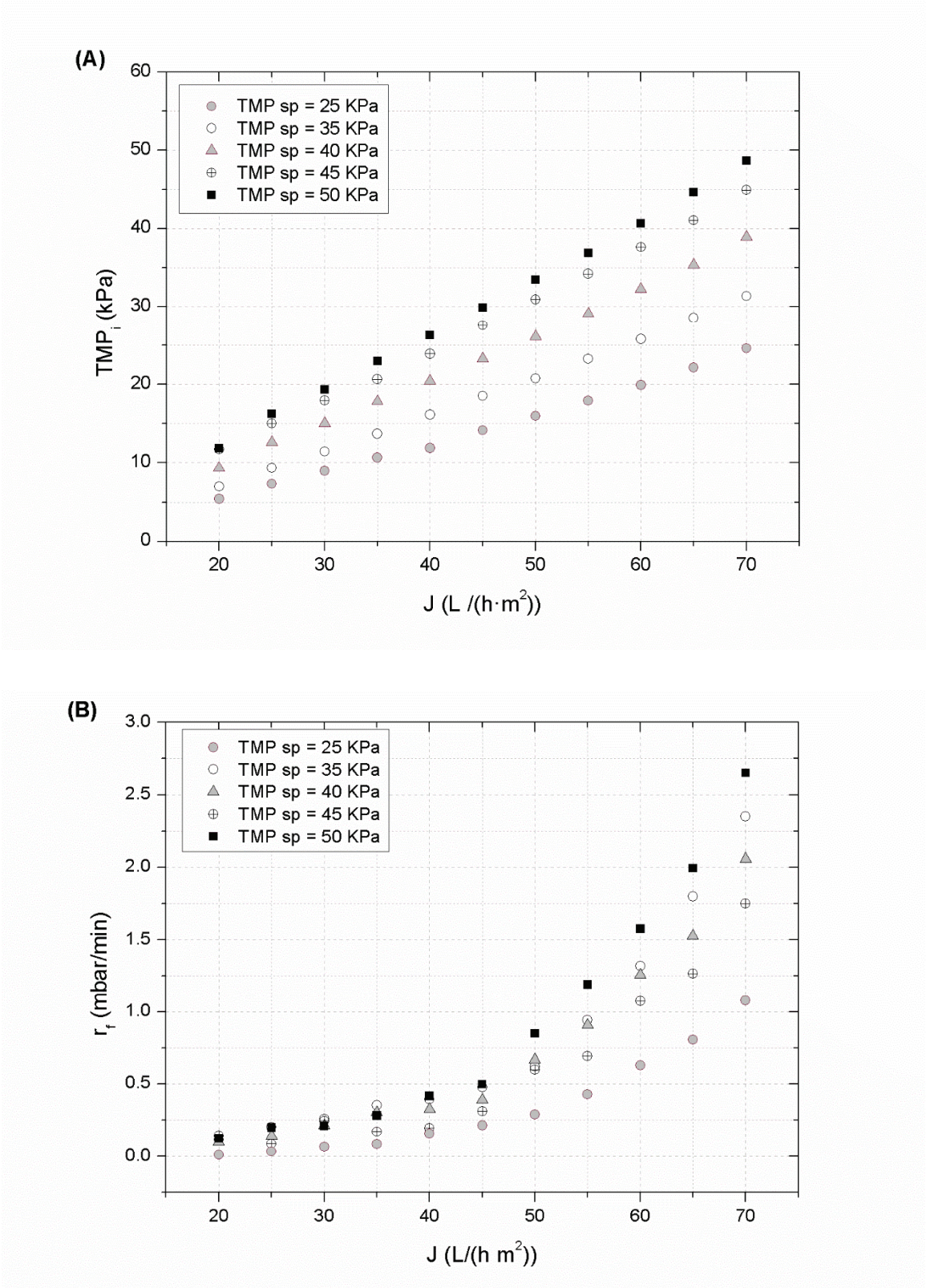

Figure 7.8. TMP_i (A) and reversible fouling rate r_f (B) against permeate flux at different TMP_{sp} in the flux-step test

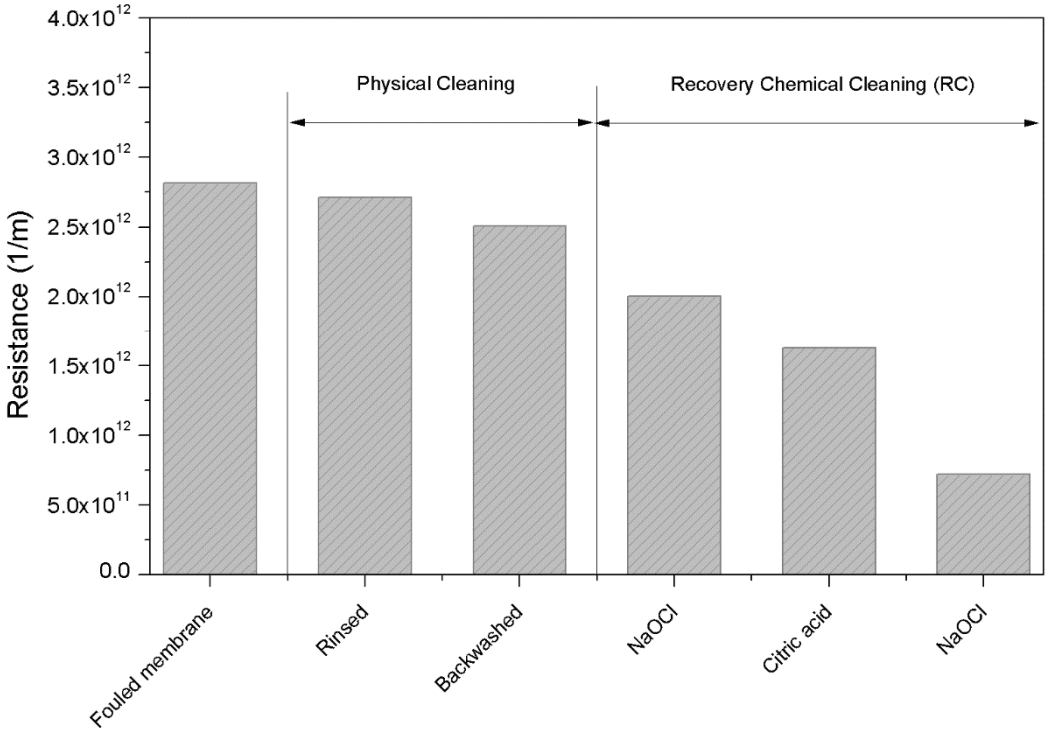

Figure 7.9. Evolution of membrane resistance during the cleaning protocol

The resistance of the fouled membrane was initially measured. It was observed some amount of particulate matter between fibres during the visual inspection (Figure 7.10A). This is a frequent operational problem (often cited as “sludging”) related to local failure of membrane scouring by aeration and the subsequent dewatering of biomass within the fibres (Judd, 2007; Judd, 2010; Lesjean et al., 2011). Nevertheless, after applying successive steps of physical methods (rinsed and backwashing with Milli-Q water) accompanied both by manual agitation to remove the clogged material, clean water tests revealed that the contribution to the fouled membrane resistance was low (13%) instead of the severe operating conditions imposed.

The recovery chemical cleaning (RC) included 3 sequential steps where membrane was soaked in three solutions: hypochlorite (500 mg/L), citric acid (6,000 mg/ L) and hypochlorite (500 mg/ L). Although conventional RC sequence includes only the first two steps (hypochlorite-citric) (Judd, 2010), it seemed to be insufficient for a proper membrane cleaning (Figure 7.10B), and an additional step of hypochlorite soaking was required. This can be attributed to the low hypochlorite concentration used in this case (Judd, 2007; Judd, 2010). RC removed 79% of

fouling resistance with a significant effect of the oxidant agents (Figure 7.9). After this cleaning, clean membrane resistance was successfully recovered (Figure 7.10C).

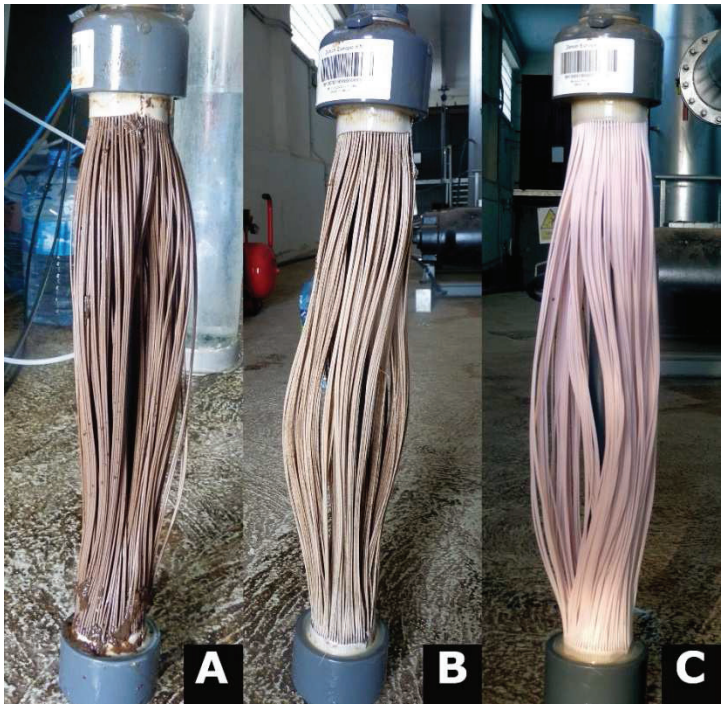

Figure 7.10. Membrane before physical cleaning methods (A), after first RC with hypochlorite (B) and finished the cleaned protocol (C).

4. Conclusions

- The main advantage of this backwashing strategy is that the system automatically adjusts the backwashing interval (i.e. filtration length) to a preselected transmembrane pressure set-point (TMP_{sp}), which will determine the degree of membrane fouling allowed. However, high TMP_{sp} values (> 40 kPa) during the MBR operation should be avoided in order to maintain competitive process productivity and limit residual fouling development.

- Sustainable process performance was observed at supra-critical permeate flux, with moderate TMP_{sp} (30-40 kPa), providing high permeate net fluxes J_{net} (65-67 l/h m^2). These are significantly higher than that usually obtained in conventional (temporised) operation at critical filtration conditions.

- The reversible fouling rate r_f was not significantly influenced by TMP_{sp}, as observed during *in situ* flux-steps trials. Therefore, an identical critical flux could be identified (~ 45 l/h m^2) as an indicator of the stable membrane performance instead of the residual fouling history.

- The analysis of the relative contribution of each mechanism to the overall fouling showed that the main contribution was the internal residual fouling, increasing its contribution with TMP_{sp}. In contrast, external residual fouling was insignificant and cake layer had only a relevant role at low to moderate $TMP_{sp.}$

- As a result of carbon substrate limited conditions, the system was successfully operated with complete sludge retention, achieving a high treatment performance with a moderate liquor suspended solid concentration. In these conditions, the soluble microbial products SMP concentration, which is considered to be an important factor affecting residual membrane fouling, was minimised.

5. References

American Public Health Association/Water Environment Federation, Standard Methods for the examination of Water and Wastewater, 21st ed., Washington DC, USA (2005).

Bugge T. V., Jørgensen K., Christensen M. L., Keiding K., Modeling cake buildup under TMP-step filtration in a membrane bioreactor: Cake compressibility is significant, *Water Res.,* 46, (2012), 4330–4338.

Busch J., Marquardt W., Model-based control of MF/UF filtration processes: pilot plant implementation and results. *Water Sci. Technol.,* 59, (2009), 1713–1720.

Delgado S., Villarroel R., González E., Effect of the shear intensity on fouling in submerged membrane bioreactor for wastewater treatment. *J. Membr. Sci.,* 311,(2008), 173–181.

Delgado S., Villarroel R., González E., Submerged Membrane Bioreactor at Substrate-Limited Conditions: Activity and Biomass Characteristics, *Water Environ. Res.*, 82, (2010), 202–208.

Diez V., Ezquerra D., Cabezas J.L., García A., Ramos C., A modified method for evaluation of critical flux, fouling rate and in situ determination of resistance and compressibility in MBR under different fouling conditions, *J. Membr. Sci.*, 453, (2014), 1-11.

Drews A., Membrane fouling in membrane bioreactors—Characterisation, contradictions, causes and cures, *J. Membr. Sci.* 363, (2010), 1–28.

Ferrero G., Rodríguez-Roda I., Comas J., Automatic control systems for submerged membrane bioreactors: A state-of-the-art review*, Water Res.,* 46, (2012), 3421-3433.

Guglielmi G., Chiarani D., Judd S.J., Andreottola G., Flux criticality and sustainability in a hollow fibre submerged membrane bioreactor for municipal wastewater treatment, *J. Membr.Sci.,* 289, (2007), 241-248.

Gui P., Huang X., Chen Y., Qian Y., Effect of operational parameters on sludge accumulation on membrane surfaces in a submerged membrane bioreactor, *Desalination*, 151, (2003), 185–194.

Hwang K. J., Chan C.S., Tung K.L., Effect of backwash on the performance of submerged membrane filtration, *J. Membr. Sci*., 330, (2009), 349–356.

Icon Group Publications, The 2009-2014 world outlook for membrane bioreactor (MBR) systems for wastewater treatment (2008).

Jeison D., van Lier J.B., Cake formation and consolidation: main factors governing the applicable flux in anaerobic submerged membrane bioreactors (AnSMBR) treating acidified wastewaters, *Sep. Purif. Technol.,* 56, (2007), 71–78.

Jiang T., Kennedy M.D., Van der Meer W.G.J., Vanrolleghem P.A., Schippers J.C., The role of blocking and cake filtration in MBR fouling, *Desalination*, 157, (2003), 335–343.

Jørgensen M. K., Bugge T. V., Christensen M. L., Keiding K., Modeling approach to determine cake buildup and compression in a high-shear membrane bioreactor, J. Membr. Sci. 409–410 (2012) 335–345.

Judd S., The MBR Book, Principles and Applications of Membrane Bioreactors for Water and Wastewater Treatment, 2nd edition, Elsevier (2010).

Judd S., The status of membrane bioreactor technology, Trends in Biotechnology 26 (2007) 165–171.

Kuberkar V., Davis R., Modeling of fouling reduction by secondary membranes, *J. Membr. Sci*., 168, (2000) 243–258.

Le-Clech P., Chen V., Fane A.G., Fouling in membrane bioreactors used in wastewater treatment, *J. Membr. Sci.*, 284, (2006), 17–53.

Le-Clech P., Jefferson B., Chang I., Judd S., Critical flux determination by the flux-step method in a submerged membrane bioreactor*, J. Membr. Sci.,* 227, (2003), 83-91.

Lesjean B., Tazi-Pain A., Thaure D., Moeslang H., Buisson H., Ten persistent myths and the realities of membrane bioreactor technology for municipal applications*. Water Sci. Technol*., 63, (2011), 32-39.

Lin H., Wang F., Ding L., Hong H., Chen J., Lu X., Enhanced performance of a submerged membrane bioreactor with powdered activated carbon addition for municipal secondary effluent treatment, *Journal of Hazardous Materials*, 192, (2011), 1509–1514.

Lu S.G., Imai T., Ukita M., Sekine M., Higuchi T., Fukagawa M., A model for membrane bioreactor process based on the concept of formation and degradation of soluble microbial products, *Water Res.,* 35, (2001), 2038–2048.

McAdam E. J., Judd S. J., Optimisation of dead-end filtration conditions for an immersed anoxic membrane bioreactor, *J. Membr. Sci.,* 325, (2008), 940–946.

Meng F., Chae S-R., Drews A., Kraume M., Shin H-S., Yang F., Recent advances in membrane bioreactors (MBRs): Membrane fouling and membrane material. *Water Res*., 43, (2009), 1489-1512.

Ng H., Hermanowicz S., Membrane bioreactor operation at short solids retention times: performance and biomass characteristics, *Water Res*., 39, (2005), 981–992.

Pirt S., The maintenance energy of bacteria in growing cultures. Proc R Soc London, 163B (1965) 224-231.

Robles A., Ruano M.V., Ribes J., Seco A., Ferrer J., Mathematical modeling of filtration in submerged anaerobic MBRs (SanMBRs): Long-term validation, *J. Membr. Sci*., 446, (2013), 303–309.

Santos A., Judd S., The commercial status of membrane bioreactor for municipal wastewater, *Separation Science and Technology*, 45, (2010), 850–857.

Schoeberl P., Brik M., Bertoni M., Braun R., Fuchs W., Optimization of operational parameters for a submerged membrane bioreactor treating dyehouse wastewater, *Sep. Pur. Tech.*, 44, (2005), 61–68.

Smith P.J., Vigneswaran S., Ngo H.H., Ben-Aim R., Nguyen H., A new approach to backwash initiation in membrane systems, *J. Membr. Sci.,* 278, (2006), 381–389.

Van der Marel P., Zwijnenburg A., Kemperman A., Wessling M., Temmink H., van der Meer W., An improved flux-step method to determine the critical flux and the critical flux for irreversibility in a membrane bioreactor, *J. Membr. Sci.*, 332, (2009), 24-29.

Vargas A., Moreno-Andrade I., Buitrón G., Controlled backwashing in a membrane sequencing batch reactor used for toxic wastewater treatment. *J. Membr. Sci*., 320, (2008), 185–190.

Vera L., González E., Díaz O., Delgado S., Performance of a tertiary submerged membrane bioreactor operated at supra-critical fluxes, *J. Membr. Sci*, 457 (2014)1-8.

Verrecht B., Judd S., Guglielmi G., Mulder J.W, Brepols C., An aeration energy model for an immersed membrane bioreactor, *Water Res*., 42, (2008), 4761–4770.

Villarroel R., Delgado S., González E., Morales M., Physical cleaning initiation controlled by transmembrane pressure set-point in a submerged membrane bioreactor, *Sep. Pur. Tech*., 104, (2013), 55–63.

Wei Y., van Houten R., Borger A., Eikelboom D.H., Fan Y., Minimization of excess sludge production for biological wastewater treatment, *Water Res*., 37, (2003), 4453-4467.

Wu J., Le-Clech P., Stuetz R.M., Fane A.G., Chen V., Effects of relaxation and backwashing conditions on fouling in membrane bioreactor, *J. Membr. Sci.*, 324, (2008), 26–32.

Ye Y., Chen V., Le-Clech P., Evolution of fouling deposition and removal on hollow fibre membrane during filtration with periodical backwash, *Desalination*, 283, (2011), 198–205.

Zsirai T., Buzatu P., Aerts P., Judd S., Efficacy of relaxation, backflushing, chemical cleaning and clogging removal for an immersed hollow fibre membrane bioreactor, *Water Res*., 46, (2012), 4499–4507.

CAPÍTULO 8: Análisis del ensuciamiento de un biorreactor de membrana sumergido terciario operado en modo frontal con altos flujos

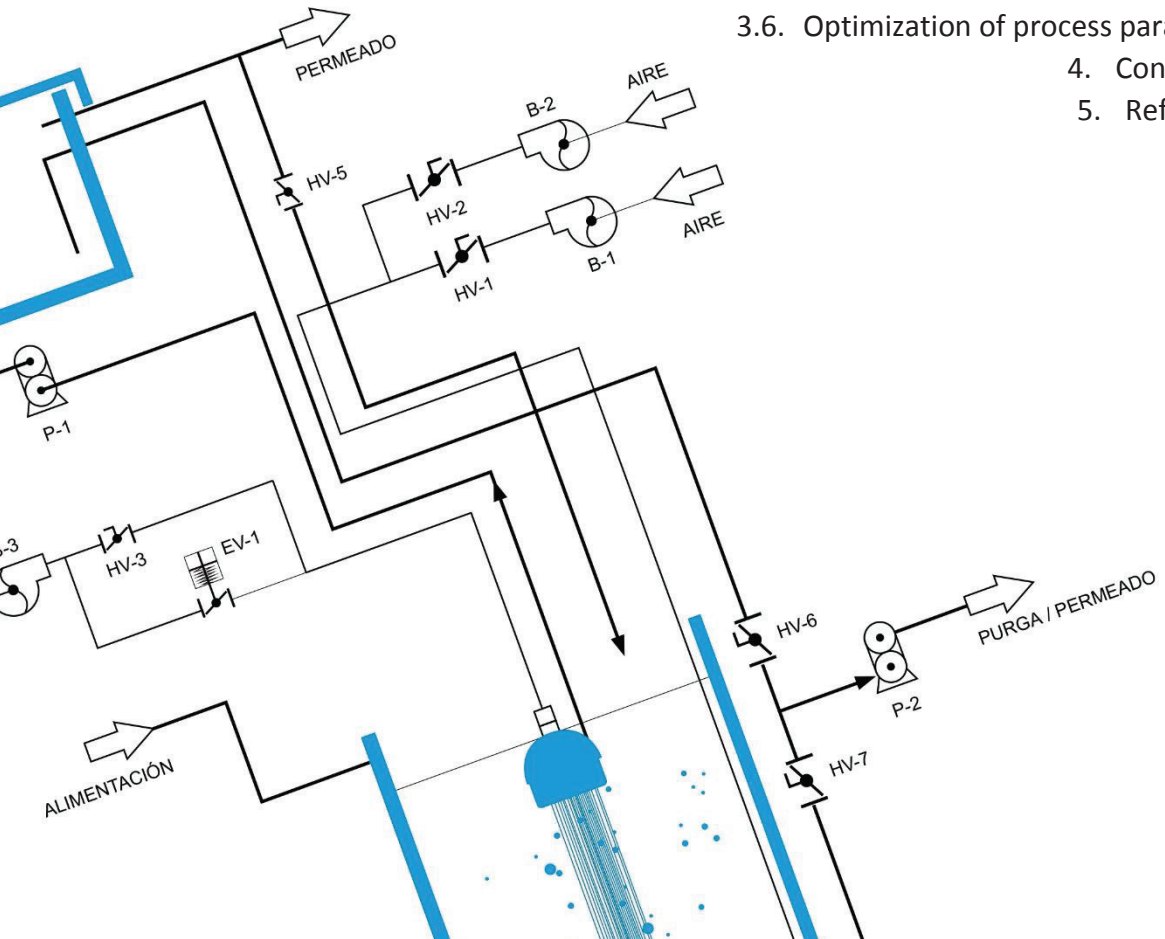

Capítulo 8

Análisis del ensuciamiento de un biorreactor de membrana sumergido terciario operado en modo frontal con altos flujos

Fouling analysis of a tertiary submerged membrane bioreactor operated in dead-end mode at high-fluxes

Luisa Vera, Enrique González, **Oliver Díaz**, Rubén Sánchez, Rafael Bohorque, Juan Rodríguez-Sevilla

Journal of Membrane Science
493, (2015) 8-18

Factor de impacto: 5,056 (JCR®, Thomson Reuters 2015).

Highlights

- Sustainability of an high-flux MBR operated at dead-end mode
- Novel and promising operation mode for backwashing initiation
- Analysis of the role of the compression process and backwashing conditions in membrane fouling reversibility
- Modelling of residual fouling by a non-linear expression
- Applied for advanced treatment of secondary effluent from an WWTP

Keywords

Submerged membrane bioreactor; tertiary treatment; set-point transmembrane pressure; filtration without air scouring; empirical model of residual fouling

Resumen:

Uno de las estrategias más aplicadas al control del ensuciamiento de las membranas en biorreactores de membrana sumergida es la inyección de aire. El objetivo es aplicar un caudal de aire determinado en las inmediaciones de la membrana para limitar la deposición de especies

colmatantes, actuando como promotor de turbulencias al mover las membranas lateralmente y provocar una cizalladura sobre la superficie de las mismas. Sin embargo, esta estrategia influye directamente en la demanda energética del proceso, lo que ha llevado al desarrollo de estrategias para reducir el consumo de aire. La filtración frontal es un modo de reducir los costes asociados a la aireación, pero la ausencia de turbulencia provoca un incremento considerable del ensuciamiento de la membrana. En este caso, para lograr la operación sostenible del MBR, es necesario reducir el flujo de filtración y aumentar la frecuencia de las limpiezas físicas. En el presente Capítulo se analiza la viabilidad de operar un MBR terciario con filtración frontal aplicando retrolavados únicamente al alcanzar el valor preestablecido de presión de consigna. Asimismo, se estudia la construcción del ensuciamiento, su consolidación y reversibilidad con el fin de optimizar la productividad de la membrana y la demanda específica de aireación.

Como era de esperar, el MBR logró la completa nitrificación y un alto rendimiento de eliminación de materia orgánica del efluente secundario de la estación depuradora convencional. Al igual que en los capítulos anteriores, el MBR operó en condiciones endógenas, que minimizan la concentración de productos solubles microbianos y el tamaño medio de flóculo presenta una distribución estrecha y unimodal. La calidad del permeado no se vio afectada por las fluctuaciones de calidad de la alimentación, pero éstas, sí afectaron al desarrollo de la suspensión biológica. Durante los episodios de alta carga de materia orgánica, el sistema experimentó un rápido crecimiento de solidos suspendidos, si bien una vez finalizado el vertido, el sistema fue capaz de asimilar la punta de carga alcanzando una concentración moderada y estable de MLSS en el reactor.

La determinación del flujo crítico, mediante experimentos escalonados, permitió analizar la reversibilidad del ensuciamiento en función de la duración del retrolavado apoyado con inyección de aire. El retrolavado permite despegar el ensuciamiento de la membrana y su dispersión en el seno de la suspensión biológica. Si además, el retrolavado se apoya con la inyección de aire simultánea, la re-dispersión se ve incrementada considerablemente, con lo cual los materiales que podrían colapsar la membrana en el escalón siguiente son alejados más eficazmente de las inmediaciones de la misma. Por todo ello, el flujo crítico aumentó al inyectar aire durante el retrolavado y al incrementar los tiempos de duración del mismo.

Al comienzo de cada experimento de larga duración, se presentan dos fases diferenciadas en la construcción del ensuciamiento de la membrana: una fase inicial en que la TMP crece

rápidamente, seguida por un incremento menos acusado. La primera etapa es característica de del fenómeno de recompresión, mientras que la segunda corresponde a la construcción de una torta compresible totalmente reversible. Una vez alcanzado el régimen estacionario, el ensuciamiento residual interno atribuido al proceso de consolidación del ensuciamiento aumentó considerablemente. Durante los primeros ciclos, la torta compresible era totalmente reversible, pero en los ciclos de filtración/retrolavado siguientes, la estructura de la misma se modificó y se transformó en un ensuciamiento consolidado, incrementando el ensuciamiento residual interno. Las resistencias específicas de la torta durante los ciclos iniciales y al alcanzar el régimen estacionario son parecidas entre sí, sin embargo, la compresibilidad de la torta parece verse afectada por el tiempo de operación. Llegado al régimen estacionario, la compresibilidad de la torta se vio reducida principalmente, por el elevado flujo local.

La resistencia específica de la torta durante el régimen estacionario no se vio afectada, ni por el flujo de filtración, ni por la presión transmembrana aplicada. Los resultados revelan que este parámetro aumentó con el flujo de retrolavado, demostrando que la re-dispersión juega un papel importante en las propiedades de la torta. También se observó que el flujo de filtración no afecta el ensuciamiento residual interno debido a que el modo de operación por presión de consigna permite el ajuste de la frecuencia del retrolavado. Para interpretar la influencia de las condiciones de operación sobre el ensuciamiento residual se desarrolló un modelo empírico, mediante una ecuación no lineal, divida en dos términos: el primero, relativo al rápido crecimiento inicial del ensuciamiento debido a la consolidación de la torta y el segundo, relacionado con crecimiento de la resistencia del ensuciamiento residual interno. Este modelo empírico asume que el ensuciamiento residual interno reduce gradualmente el área disponible de membrana. Por otro lado, el análisis de las limpiezas reveló que el ensuciamiento se debió principalmente, a sólidos que pueden ser eliminados por medio de limpiezas físicas severas. La capa que se adsorbe en la superficie de la membrana no depende de las condiciones de operación, sino el contenido de SMP en la suspensión biológica.

El relax como método de limpieza física de la membrana, presentó una eficacia muy baja debido al elevado grado de consolidación experimentado por el ensuciamiento y que genera bajos tiempos de filtración, bajo flujo neto y elevado consumo de aire, expresado como SAD_p. Por otro lado, cuando se aplicó el retrolavado el sistema alcanzó unos moderados flujos netos y bajos consumos de aire comparados con MBR industriales.

De acuerdo con el modelo empírico desarrollado para el ensuciamiento residual interno, las condiciones óptimas de producción para la membrana se han establecido en un flujo de filtración de 40 L/hm^2 y un flujo de retrolavado de 27,5 L/hm^2, en base a la baja demanda específica de energía y al área de membrana requerida. Estas condiciones son las óptimas cuando el MBR opera en filtración frontal, con el modo de operación por presión de consiga y el retrolavado se efectúa durante 30 segundos apoyado con aireación.

Abstract

Fouling deposition, consolidation and reversibility were assessed in a tertiary submerged membrane bioreactor. The unit was operated in dead-end mode (i.e. without air scouring during the filtration) and with an alternative physical cleaning strategy based on *TMP* set-point initiation. Several operating parameters such as filtration and backwashing fluxes, backwash duration and the aid of air scouring during backwashing were studied. The aim of the work was to optimise membrane productivity, specific aeration demand and operative time between chemical cleanings. The membrane bioreactor was operated for over 4 months with complete sludge retention, achieving a high treatment performance with moderate suspended solids concentration (MLSS=4-8 g/L). Flux-step trials pointed to the important role of the compression process and backwashing conditions in membrane fouling reversibility. During long-term tests, while reversible fouling was described by the compressible cake build-up model, residual fouling was modelled by a non-linear expression, assuming that fouling gradually reduces the available membrane area. Based on this approach, residual fouling consistently decreased with the backwashing flux applied. Analysis of the relative contribution of the different fouling layers revealed that the fraction formed by suspended solids was the main contributor. According to the residual fouling model, optimal membrane production can be established at a filtration flux of 40 L/h m^2 and a backwashing flux of 27.5 L/h m^2, due to the low specific energy demand, low membrane area requirement and reasonable operative time (t_{op}) between chemical cleanings.

1. Introduction

Growing worldwide water supply demands and the protection of water bodies have both increased the interest in wastewater reclamation. Legislation affecting reclaimed wastewater reuse is very demanding regarding quality and health safety, which has required the application of advanced technology. Among such techniques, the use of membranes emerges as a highly efficient system to obtain high quality recycled water. In fact, low-pressure membrane filtration

(microfiltration or ultrafiltration) of biologically degraded secondary effluents has been widely applied for upgrading conventional wastewater treatment plants (Wintgens et al., 2005). However, in the case of old plants with poor performance of secondary clarifiers which often leads to sludge bulking, the relatively high concentration of suspended solids in secondary effluents can compromise the economic feasibility of the membrane filtration processes (Bourgeous et al., 2001). In this scenario, a tertiary submerged membrane bioreactor (MBR) appears to be an attractive option for advanced treatment of secondary effluent. As described in previous research (Vera et al., 2014a), the tertiary MBR has demonstrated its capability of achieving high organic carbon removal and complete nitrification, regardless of high variability in the feedwater. As a consequence of the substrate-limited conditions, the microbial suspension generated in the bioreactor has suitable filtration properties (i.e. large flocs, presence of higher organisms and a low concentration of soluble microbial products). The growing interest in this technology is to be seen recently in the Aquapolo project (Sao Paulo, Brazil), the largest wastewater reuse project in the Southern Hemisphere, which includes a tertiary MBR in the treatment scheme (Koch membrane, 2014).

As in all membrane processes, fouling is still the main drawback of MBRs, preventing wide application (Judd, 2010). Fouling can be defined as the alteration in the membrane caused by specific physical and/or chemical interactions between the membrane and the components of the microbial suspension, which leads to membrane permeability loss. The rate and extent of fouling is typically a complex function of membrane properties, operating conditions and microbial suspension characteristics (Le-clech et al., 2006). Microbial suspension is a heterogeneous system mainly composed of salts, organic substances, colloids, cells and microbial flocs. Several mechanisms have been proposed to explain this complex phenomenon, including pore clogging, adsorption of foulants, gel or cake formation, cake layer consolidation and osmotic pressure effects (Lin et al., 2014).

In order to maintain membrane permeability, strategies for fouling mitigation such as air scouring, physical cleaning techniques (i.e. relaxation and backwashing) and chemical cleaning have been incorporated into MBR designs (Judd, 2015). Based on permeability recovery by physical means, membrane fouling can be classified into two main types. The first one is known as reversible fouling (caused by loose cake deposit and possibly by pore clogging) and refers to fouling which can be removed by physical means. The second type is residual fouling, which is

related to foulant adsorption, gel formation, and possibly consolidated cake deposition, and can only be removed by chemical cleaning (Drews, 2010).

In spite of the significant impact of fouling on membrane productivity, module lifespan and energy requirements (Drews, 2010), strategies for fouling control are usually based on predetermined values of the operating parameters (air scouring flow-rate and frequency, and filtration/physical cleaning sequences), which lead to an under-optimised system (Judd, 2010). Air scouring has been extensively proven to be an efficient means to limit foulant deposition due to the enhancement of foulant back-transport, the shear stress induced at the membrane surface and the lateral fibre movement (in hollow fibre modules) (Wibisono et al., 2014). Because of its impact on energy demand, several strategies have been implemented, mainly focused on adjusting flow rate and/or frequency of coarse air bubbles (Ferrero et al., 2012). Typically, it takes a value of 12-13 Nm^3/m^3, expressed as specific aeration demand per permeate volume unit (SAD_p), for full-scale facilities (Krezeminski et al., 2012). Also, pulse scouring with large bubbles was recently introduced as a means to increase scouring efficiency (Cummin et al., 2011). However, air scouring is still considered the greatest energy consumer in these processes, often exceeding 50% of total energy consumption (Krezeminki et al., 2012). Therefore, the priority is to explore operation modes with lower energy consumption. An alternative approach could be to operate in dead-end filtration mode (i.e. without air scouring). In that case, due to absence of shear forces, foulants back-transport is significantly decreased (by ceasing the transport mechanisms of lateral migration and shear induced diffusion) and consequently, net foulants transport towards the membrane is increased. Hence, to maintain a sustainable process operation at reasonable fouling rate, filtration flux should be decreased and frequent physical cleanings should be applied. This disadvantage must be compensated by alternative physical cleaning strategies, as it is discussed below.

Conventional physical cleaning techniques include backwashing (i.e. permeate is used to flush backwards) or relaxation (ceasing filtration whilst continuing air scouring). For both methods, the key parameters generally identified are frequency and duration (Le-Clech et al., 2006). Additionally, another parameter influencing cleaning efficiency of backwashing is its intensity, which typically ranges between 1-3 times the filtration flux (Wang et al., 2014). According to several studies of backwashing, a higher cleaning efficiency is observed with increasing backwashing flux, frequency and duration (Zsirai et al., 2012). Nevertheless, given the impact of these parameters on process productivity, optimisation of backwashing

conditions is still needed (Schoeberl et al., 2005). In this direction, a recent review study has highlighted the variety of operating trends. This is attributable to the fact that selection of appropriate cleaning protocols for a sustainable operation depends on other process variables (i.e. filtration flux, air scouring, temperature, etc.) and suspension filterability (Wang et al., 2014). As a consequence, pre-set values of these parameters are often selected in full-scale plants (Zsirai et al., 2012), where the operating trend is to perform a very frequent backwashing cycle (once every 3.3-8.3 min of filtration) (Itokawa et al., 2008). In recent years, several feedback control systems have been developed for physical cleaning optimisation (Ferrero et al., 2012). Among them, a system has been successfully implemented for physical cleaning initiation through transmembrane pressure (*TMP)* monitoring. This automatically adjusts the backwashing frequency to a preselected *TMP* set-point, which results in a significant increase in process productivity (Villarroel et al., 2013). Additionally, by selecting a moderate *TMP* set-point (30-40 kPa), effective fouling control has been achieved, allowing operation under less conservative conditions (supra-critical fluxes) (Vera et al., 2014a and 2014b).

As previously stated, dead-end operation could be an attractive option due to its lower energy demand. In fact, it has been widely used in direct ultrafiltration of secondary effluents (Asano et al., 2007). Nevertheless, the higher quantity of suspended solids in the MBR (several orders of magnitude higher than that of a secondary effluent) significantly increases the fouling rate and limits its applicability. However, fouling rate not only depends on cake solids concentration (ω) but also on the specific cake resistance (α), which is determined by the geometrical properties of the deposit (porosity, particle diameter, etc.) (Foley, 2006). Recent studies have reported significantly lower values of α for cake layers formed by microbial flocs (10^{12}-10^{13} m/kg) than that (10^{14} m/kg) obtained for gel layers mainly composed of soluble microbial products (SMP), which are considered the most important foulant in secondary effluents (Hong et al., 2014). Therefore, highly porous aggregates with low resistances are expected to form during the filtration without air scouring of a microbial suspension. In addition, the cake layer may act as a secondary membrane that prevents residual fouling caused by pore blocking or adsorption due to SMP (Kuberkar et al., 2000). Another issue to be considered is the deposit reversibility, since it is known that increasing the fouling load on the membrane reduces the removal efficiency. In general, it is expected that high filtration *TMP* results in a more compact cake layer, harder to remove by physical cleaning (Liang et al., 2012). Nevertheless, cake compressibility also depends on other factors including particle

characteristics (morphology, size, etc.) and hydrodynamics of cake formation process. Accordingly, although physical cleaning strategy based on the *TMP* set-point seems to be a suitable approach to reduce residual fouling, the optimal value of TMP_{sp} is site specific. Therefore, for a given system, it is necessary an experimental evaluation of the effect of TMP_{sp} on fouling consolidation and reversibility.

The aim of this study was to investigate fouling deposition, its consolidation and reversibility in a tertiary submerged membrane bioreactor operating in dead-end mode (i.e. filtration without air scouring) during long-term trials. An alternative physical cleaning strategy based on *TMP* set-point initiation was applied. Several operating parameters such as filtration and backwashing fluxes, backwashing duration and the aid of air scouring during the backwashing were studied in order to optimise membrane productivity and the specific energy demand.

2. Material and methods

2.1. Feedwater

The pilot MBR was fed with effluent from a conventional activated sludge wastewater treatment plant whose average physico-chemical characteristics are given in Table 8.1. The conventional WWTP was originally designed for only carbon removal. Due to the short sludge ages and oxygen deficiency in the activated sludge process, frequent episodes of sludge de-flocculation or insufficient sedimentation usually appear, resulting in higher suspended solids and organic material concentration in the effluent.

Table 8.1. Main feedwater characteristics (n=54)

PARAMETERS	UNITS	MEAN	RANGE
COD	mg/L	230	50-770
DOC	mg/L	20	11-39
$N\text{-}NH_3$	mg/L	37	16-57
$N\text{-}NO_2^-$	mg/L	2	<1-13
$N\text{-}NO_3^-$	mg/L	2	<1-4
Turbidity	NTU	137	6-1,100
TSS	mg/L	190	20-1,530

2.2. MBR

The pilot plant was the same as in previous studies (Vera et al., 2014a and 2014b), where a cylindrical 220 L MBR was equipped with ZeeWeed® ZW-10 (GE Water & Process Technologies) hollow-fibre membranes with 0.04 µm rated pore diameter and 1.9 mm outer diameter, assembled vertically, which provide 0.9 m^2 of filtering surface area. ZeeWeed® consists of a woven reinforcing braid on which a PVDF membrane is cast. The effluent (permeate) was extracted from the top header of the module under a slight vacuum. All experiments were carried out at a constant permeate flux, registering transmembrane pressure as a function of time. The unit was operated in automatic cleaning initiated mode. Membrane fouling was controlled by backwashing based on this mode. Each filtration phase finished when a pre-established TMP_{sp} was reached (30 kPa), beginning the backwashing immediately afterwards. A programmable logic controller (PLC) system was used to initiate and stop the backwashing by comparison of *TMP* set-point and instantaneous pressure values. Continuous data logging and plotting of pressure profile variations were also performed.

The MBR was operated without air scouring during the filtration phase. Nevertheless, constant air scouring during the backwashing phase was fixed at 3.1 $Nm^3/h\ m^2$, on the basis of previous results (Vera et al., 2014a), in order to improve fouling removal. The aim of the experiments was to assess the effect of filtration and backwashing flux on membrane fouling. For this purpose, twelve filtration tests of 250 h were carried out at different filtration fluxes (35, 45 and 55 $L/h\ m^2$) and backwashing fluxes (0, 20, 40 and 60 $L/h\ m^2$).

Before starting the experimental period, the pilot-scale MBR was seeded with sludge from the activated sludge reactor of the WWTP and operated for over 24 months. The bioreactor was run at HRT values of 8.8 h without sludge removal except for sampling. In order to maintain a constant HRT independent of the permeate flux, a fraction of permeate was returned to the tank. Additional air was supplied by fine bubble diffusers through the bottom (0.3 Nm^3/h), providing oxygen and stirring. The dissolved oxygen concentration was always above 1.5 mg/L in the reactor operated at 23 ± 2 ºC. Suspensions were characterised according to particle size, MLSS, MLVSS, biomass activity, non-flocculating microorganisms (Ng et al., 2005) and dissolved organic matter in the liquid phase.

2.3. Short-term flux step trials

The modified flux-step method is based on applying successive flux increments up to a maximum, in accordance with the method of Le-Clech et al. (2003) and further improved by incorporating relaxation steps for reducing the influence of fouling history (Van der Marel et al., 2009). In this study, a modified method is proposed and the relaxation steps are substituted by short backwashing cycles at a fixed flux value of 60 L/h m^2, to be more similar to the conventional operation of a MBR. Six flux step experiments were carried out at three backwashing times (15, 30 and 60 s) with and without air scouring at 3.1 Nm^3/h m^2 during the backwashing phase. The other experimental parameters were selected in accordance with previous studies (Guglielmi et al., 2007; Van der Marel et al., 2009): step duration of 15 min, flux-step height of 5 L/h m^2 and a maximum flux of 70 L/h m^2. In the flux-step trials, residual fouling can be characterized by the transmembrane pressure after each backwashing (TMP_i). A critical flux value can be established when TMP_i starts to raise respect to the tap water behaviour (Figure 8.1).

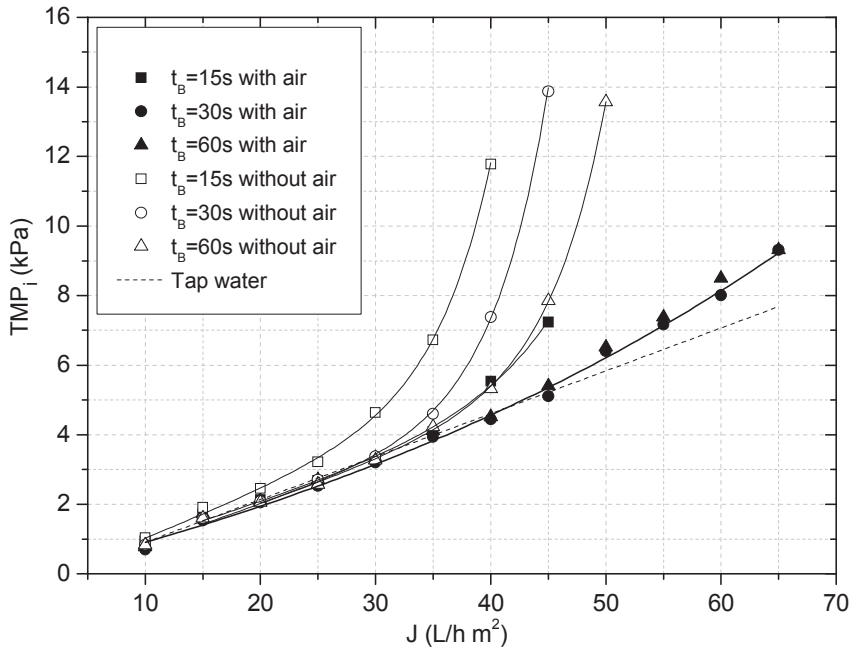

Figure 8.1. TMP_i against permeate flux at different backwash conditions during the flux steps trials; J_B=60 L/h m^2; t_F= 900 s.

2.4. Membrane cleaning protocol

After each long-term test, the fouled membrane was cleaned by a specific protocol that included the following steps: (1) rinsing with Milli-Q water; (2) backwashing with Milli-Q water at a flux of 90 L/(h·m^2) for 7 min and with air scouring; (3) chemical cleaning with a solution of NaOH (pH≈11) for 24 h; (4) chemical cleaning with sodium hypochlorite (500 mg/L) for 24h. After each step, a tap water filtration test was applied to measure the remaining resistance. The resulting solutions after rinsing, backwashing and desorption were collected and analysed in terms of dissolved organic carbon (DOC) and total suspended solids (TSS).

2.5. Analytical methods

Dissolved oxygen was measured using a portable dissolve oxygen meter (Oxi340i, WTW). Chemical oxygen demand (COD), total suspended solids (TSS), mixed liquor suspended solids (MLSS), mixed liquor volatile suspended solids (MLVSS), time to filter (TTF) and turbidity were determined in conformity with the Standard Methods (2005). Nitrite-nitrogen (N-NO_2^-) and nitrate-nitrogen (N-NO_3^-) were analysed by ion chromatography using a Compact IC plus 882 device supplied by Metrohm. Ammonium-nitrogen (N-NH_3) was analysed by the Nessler method using a DR-5000 Hach spectrophotometer. Dissolved organic carbon (DOC) concentration was measured with a TOC-meter (TOC-5000A, Shimadzu). The DOC concentration of the filtration suspension through a 0.45 µm nitrocellulose membrane filter (HA, Millipore) was assigned as the soluble microbial products (SMP). The oxygen uptake rate (SOUR) was measured in batch tests (250 ml stirred cells) by following the dissolved concentration with a membrane oxygen electrode, in a medium without substrate. Microbial floc size distribution was measured using a Malvern Mastersizer 2000 instrument with a detection range of 0.02-2000 µm. To quantify the amount of non-flocculating microorganisms, the samples of biomass were centrifuged at 1300 g for 2 min and the supernatant turbidity measured (Ng et al., 2005).

2.5. Membrane fouling characterisation

TMP evolution can be used for membrane fouling characterisation. According to the "resistance-in-series" model and neglecting the osmotic pressure term, the *TMP* can be described by:

$$TMP = J \cdot \mu \cdot R_t = J \cdot \mu \cdot \left(R_m + R_{rdf} + R_{rvf}\right) \quad [8.1]$$

where μ is the permeate viscosity, J is the permeate flux, R_t is the total hydraulic resistance, R_m is the clean membrane resistance, R_{rdf} is the residual fouling resistance and R_{rvf} is the reversible fouling resistance.

Residual fouling is that which is not removed by backwashing. Its resistance can be separated into internal fouling resistance (R_{if}), related to internal membrane pore blocking and gel or compacted particle layer that is not detached during backwashing (McAdam and Judd, 2008), and an external fouling resistance (R_{ef}), linked to fouling layer recompression:

$$R_{rdf} = R_{if} + R_{ef} \quad [8.2]$$

During the filtration, this external layer compresses, increasing the residual resistance, and during backwashing this layer relaxes, yielding a lower residual resistance. Therefore, just at the beginning of the filtration cycle, the initial *TMP* (TMP_i) can be described by Eq. [8.3]:

$$TMP = J \cdot \mu \cdot \left(R_m + R_{if}\right) \quad [8.3]$$

In contrast, reversible fouling resistance R_{rvf} is generally associated with a cake development mechanism on the membrane wall (Vera et al., 2014b). According to the cake model, *TMP* linearly increases with filtration time and the slope of the straight line. Therefore, *TMP* evolution with elapsed time *t* can be described by Eq. [8.4]:

$$TMP = TMP_0 + \mu\alpha\omega J^2 t \quad [8.4]$$

where TMP_0 is the transmembrane pressure related to the residual fouling, α is the specific cake resistance, ω is the solid concentration in the cake per unit filtrate volume and *t is* the elapsed time. TMP_0 can be defined as:

$$TMP_0 = J \cdot \mu \cdot \left(R_m + R_{rdf}\right) \quad [8.5]$$

and the difference between TMP_i and TMP_0 is linked to the external residual fouling, R_{ef}.

By considering the pressure drop over the cake layer (ΔTMP_c), Eq. [8.4] can be rewritten as Eq. [8.6] (Sørensen and Sørensen, 1997):

$$\Delta TMP_c = \mu\alpha\omega J^2 t \quad [8.6]$$

For compressible particles, α increases with *TMP.* To model it, several expressions have been proposed, including the well-known power-law expression (Rushton et al., 1996). While this expression has been found that generally represents accurately the pressure dependence of the specific resistance for most particles, its application to microbial suspensions has proved to be problematic (Foley, 2006). Alternatively, a linear relationship (Eq. [8.7]) has often been identified for compressible cakes when filtering microbial suspensions (McCarthy et al., 1999):

$$\alpha = \alpha_0 \left(1 + \frac{\Delta TMP_C}{P_a}\right) \quad [8.7]$$

where α_0 is the specific cake resistance at zero pressure and P_a is a characteristic pressure related to the compression effect, which usually ranges between 10 and 60 kPa for a MBR sludge, according to the studies of Jørgensen et al. (2012a, 2012b, 2014)

On the other hand, the consolidation process induced a progressive decrease in the available membrane area for filtration. Assuming the stationary conditions were reached after 200 h operation, the local flux $(J')_{t=200}$ increased accordingly with the loss of effective area by residual fouling (Eq.[8.8]):

$$(J')_{t=200} = \frac{(TMP_i)_{t=200}}{TMP_i} J \quad [8.8]$$

where $(TMP_i)_{t=200}$ is the *TMP* at the beginning of the filtration cycle after 200 h of operation.

3. Results and discussion

3.1. Microbial suspension characteristics and permeate quality

The bioreactor treatment performance and main characteristics of the microbial suspension are summarised in Table 8.2. As expected, complete nitrification (98%) and high organic material removal (87% on average for COD) were obtained throughout the experimental period, regardless of fluctuations in feedwater characteristics (see Table 8.1). Nevertheless, there were several episodes of high particulate organic load in the feedwater, which generated relatively high F/M ratios (>0.4 kg COD/kg MLSS d). These resulted in a sharp biomass increase (up to 8-8.6

g MLSS/L), since the system was operated with total sludge retention. Instead of these episodes, the system was able to assimilate these fluctuations obtaining a moderate concentration of biomass (6.2 g MLSS/L on average). Low accumulation of inorganic particulate matter was also found, since the MLVSS/MLSS ratio remained within the typical range of 77-89 %. It is known that the biomass stabilisation achieved in MBRs operated without biomass purge is related to the "maintenance concept" introduced by Pirt (1965), where microorganisms under severe substrate limitation should preferentially meet their maintenance energy requirements instead of producing additional biomass (Pollice et al., 2004). Maintenance conditions were also reflected by the low specific oxygen uptake rates ($SOUR_e$) obtained; significantly lower than the typical values of 20-40 mg O_2/g MLVSS h for a municipal activated sludge (Kristensen et al., 1992). In addition, due to the maintenance level, the soluble microbial products (SMP) were minimised in the supernatant (9 mg/L, expressed as equivalent DOC (Lyko et al., 2008)), consistently with previous studies (Vera et al., 2014a). Therefore, membrane fouling is expected to be mainly caused by suspended particles, and consequently soluble products should not play an important role. This is a key issue, since it is generally accepted that SMPs cause residual fouling by entering into the membrane pores (i.e. pore blockage) or adsorbing onto the membrane surface (Drews et al., 2010; Lin et al., 2014). In fact, by comparing supernatant and permeate SMP concentrations, it was seen that the membrane only retained a low fraction of the SMP (11% on average).

Regarding floc morphology, medium-sized flocs were observed (d_{50} = 63±6 µm) with a relatively narrow distribution (distribution spreading index of 1.29±0.13). Several authors have reported that suspensions with a narrow distribution of flocs tended to form cakes with high porosity and a low specific cake resistance (Su et al., 2013). In addition, non-flocculating particles in the 1-10 µm range only account for 4.5% of total sludge volume, which was also confirmed by the low values of supernatant turbidity observed (Ng et al., 2005). This can be partially attributed to the presence of higher organisms which predate on dispersed bacteria, according to previous studies (Vera et al., 2014b). Therefore, the suspension showed an excellent filterability (TTF = 8.9±2.9 s).

Table 8.2. Bioreactor treatment performance and main characteristics of microbial suspension

PARAMETER	UNIT	MEAN VALUE	RANGE
Bioreactor treatment performance			
COD removal	%	87	78-98[a]
N-NH_3 removal	%	98	94-99[a]
DOC removal	%	60	58-81[a]
Permeate DOC	mg/L	8	4-12[a]
Suspension characterisation			
MLSS	g/L	6.2	3.9-8.6[a]
MLVSS	g/L	5.3	3.1-7.4[a]
TTF	s	8.9	3.7-14[b]
PSD			
$D_{(v,0.1)}$	µm	20	18-22[c]
$D_{(v,0.5)}$	µm	63	55-68[c]
$D_{(v,0.9)}$	µm	183	137-204[c]
$SOUR_e$	mg O_2/g MLVSS h	1.51	0.92-2.03[b]
Supernatant turbidity	NTU	27	14-45[b]
Supernatant DOC[d]	mg/L	9	5-15[a]

[a] n=54; [b] n=18; [c] n=12; [d] Samples were filtered through microfibre with a 0.45µm nominal pore size.

3.2. Determination of critical flux for residual fouling: effect of backwash time and air scouring during backwash

Although the classical concept of critical flux for residual fouling is based on a mass balance between convection and diffusion transport, which leads to the formation of a residual deposit in cross-flow conditions (Bacchin etr al., 2006), the same phenomenon can be applied to the filtration without air scouring and backwashing. In these conditions, the critical flux for residual fouling is assumed to be related to the total mass deposited and the backwashing conditions imposed. In addition, the compression process, which depends on the *TMP* applied, can result in more cohesive deposits that affect fouling reversibility (Bugge at al., 2012).

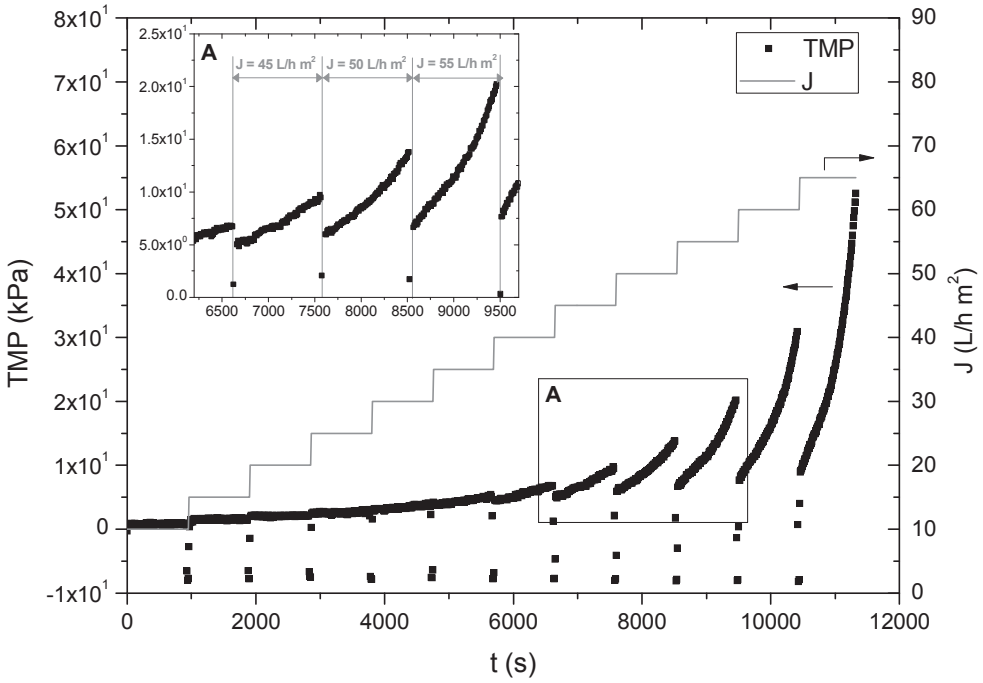

Figure 8.2. Flux and TMP profiles during flux step trials; backwash with air scouring; t_B=30 s; J_B=60 L/h m^2; t_F= 900 s.

Figure 8.2 shows the typical flux and *TMP* profiles during a short-term trial for critical flux determination. As it shows, at the end of each filtration step a backwash was applied (J_B = 60 L/h m^2 and t_B=30 s). The slope of the *TMP* against time (d*TMP*/dt) at each step represents the fouling rate due to fouling deposition, similar to that reported in many other studies (Le-Clech et al., 2003; Zsairai et al., 2012). For the test shown in Figure 8.2 (J_B = 60 L/h m^2 and t_B=30 s), different *TMP* profiles during the filtration steps can be observed below and above a critical flux, which can be identified at 40-45 L/h m^2. At sub-critical fluxes, constant and low fouling rates were obtained, while at supra-critical fluxes the fouling rate continuously increased with the elapsed time during each filtration step. Therefore it is evident that under these conditions, fouling not only depends on deposition rate (i.e. on filtration flux), but also on the mass previously deposited (filtration time) and on the actual *TMP* applied. McAdam and Judd (2008) have studied fouling behaviour in an immersed anoxic membrane bioreactor operated in dead-end mode. They described the effect of the filtration flux and duration on irreversible fouling in terms of a critical deposited mass that induced coagulation of the deposited cake layer. In accordance with previous studies (Bessiere et al., 2005), they identified the critical value at the

transition between an initial low *TMP*-rise region and a second period of sharp *TMP*-rise. Therefore, once a consolidated deposit is formed it is reasonable to assume that its reversibility is related to physical cleaning conditions. Consistently with this, Jørgensen et al. (2014) have reported that the critical flux for residual fouling depends on the cleaning time relative to the filtration time.

Analysing reversibility in the light of the critical flux concept, significant effects of backwashing duration and the application of air scouring during backwashing were found (Figure 8. 1). While tap water filtration (dotted line) shows a linear profile TMP_i vs flux, trials with microbial suspensions show a deviation from the straight-line at critical fluxes in the range of 10-45 L/h m^2, depending on backwash conditions. Without air injection during the backwash, the critical flux increased from 10 to 20 L/h m^2 while duration increased from 15 to 60 s, respectively. Higher critical values were found when air was applied (35-45 L/h m^2). Increasing backwash duration up to 60 s seems not to have a noticeable effect on the critical flux.

The higher critical fluxes observed with air scouring may be due to the lower mass deposited onto the membrane during the filtration steps. Backwash was expected to expand the deposit from the membrane and slightly disperse the expanded deposit into the bulk suspension (Le-Clech 2006). By applying air scouring during the backwash, this dispersion process is significantly enhanced (Ye et al., 2011). However during the flux steps without air scouring, the inefficient deposit re-dispersion induces an accumulation of mass in the convective zone near the membrane which rapidly collapses the membrane during the subsequent flux step. As a consequence, a consolidated deposit is formed. This process is expected to be more severe at high fluxes, which may explain the exponential relationship between TMP_i and filtration flux.

3.3. Fouling analysis during long-term trials.

3.3.1. Proposed fouling mechanisms based on TMP profiles

Process sustainability was investigated by assessing fouling deposition and reversibility at high filtration fluxes (35, 45 and 55 L/h m^2) with air-scouring aided backwash (t_B = 30 s). For each flux, four backwash fluxes were tested (0, 20, 40 and 60 L/h m^2). Based on previous results (Vera et al., 2014b), a moderate value of TMP_{sp} (30 kPa) was selected for these trials.

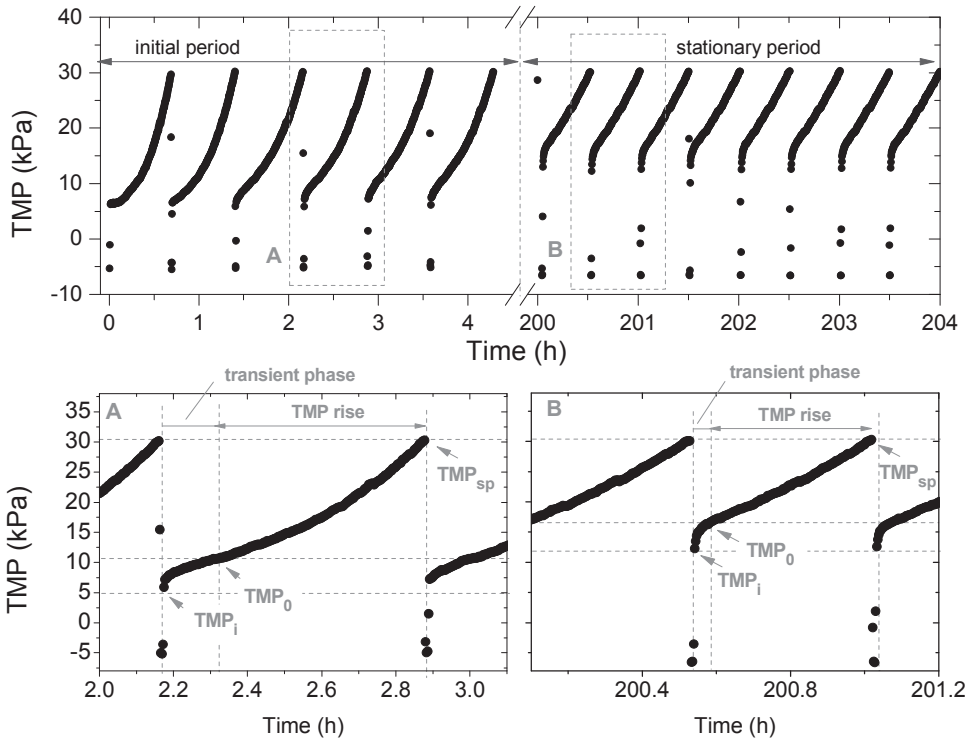

Figure 8.3. Typical TMP profiles during initial and stationary period. J= 35L/h m^2, J_B =20 L/h m^2 and t_B=30s

Figure 8.3 shows an example of the typical *TMP* evolution during a long-term test (J = 35 L/h m^2; J_B = 20 L/h m^2). It can be seen that the fouling pattern (i.e. *TMP* profiles within a filtration cycle) changed with successive filtration/backwashing cycles. During the first cycles (typically corresponding to the first 25-50 h of operation, depending on experimental conditions), two phases are clearly identifiable in the *TMP* profile: an initial transient phase followed by a non-linear (concave) *TMP* rise. The initial fouling has been also observed in systems operated under high fouling load conditions with periodic filtration/backwashing cycles (Ye et al., 2011). This behaviour has been related to a deposit recompression process in the external residual layer, which is expanded during the backwashing but not dispersed away from the convective zone of the membrane surface. Similar results have been reported by other authors on extending the filtration cycle length (i.e. increasing the amount of fouling) with fixed backwashing intervals (Schoeberl et al., 2005; Gui et al., 2003). Consistently, for an automatically initiated backwash, the amount of this fouling has been found to increase with the TMP_{sp} selected (Vera et al., 2014b). After the initial fouling phase, a nonlinear *TMP* rise was observed (Figure 8.3), which can be described by the compressible layer buildup model (Kim and DiGiano, 2009). In addition, this compressible layer seems to be mainly removed by the backwashing,

since TMP_i did not increase considerably during the first cycles. Consequently development, of a compressible cake layer on the membrane is assumed, made up mainly of large particles, which can be removed by backwashing (Zsirai et al., 2012; Wu et al., 2008). Other fouling phenomena, such as solute adsorption and pore blocking, seem to have a negligible role. Due to the filtration without air scouring and the high fluxes applied, the cake formation rate is particularly enhanced and this layer might act as a secondary membrane that prevents SMP entering the membrane pores, in accordance with previous studies (Kuberkar and Davis, 2000).

As previously mentioned, several changes were seen in the fouling pattern with successive filtration/backwashing cycles (Figure 8.3). In the stationary period, a considerable increment in TMP_i was observed, which can be attributed to a cake consolidation process. Consolidation affects the cake properties by reducing porosity and water content, and thus reversibility is also affected (Lin et al., 2014). Therefore, even though backwashing removed the cake layer during the initial cycles, the cake structure may have evolved to a more consolidated structure with subsequent cycles, increasing the residual fouling. Consolidation has often been observed during dead-end filtration of colloidal dispersions (Jönsson and Jönsson, 1996; Bessiere et al., 2005). A theoretical explanation has been proposed considering a critical deposited mass that induces consolidation (i.e. residual fouling) (Harmant and Aimar, 1998). Nevertheless, this approach does not explain the behaviour observed in the present study since the cake layer was initially completely reversible. The results suggest that cake consolidation is not only related to the deposited mass but also to the cake compressibility, which is known to be time- and *TMP*-dependent (McAdam and Judd, 2008; Jørgensen et al., 2012). Probably, the differences on comparison with other studies are due to the compressibility of the cake layer formed, which is greater for activated flocs than for colloids. In fact, stabilisation of the TMP_i (i.e. consolidation) occurred when a slightly linear *TMP* rise was observed in the stationary period, which can be attributed to a lesser compressibility of the cake layer (Delgado et al., 2004). This approach can be confirmed by assessing the accuracy of the compressible cake layer model (Eq. [8.3]).

Figure 8.4 shows the fit of α values obtained by Eq. [8.4] (assuming that ω is similar to suspended solid concentration in bulk suspension) to the linear expression (Eq.[8.7]) in both the initial and stationary periods. After the transient phase (> 3,000 Pa), data fitting gives an excellent correlation coefficient (R^2 = 0.99) for the initial period and a reasonable coefficient for the stationary period (R^2 = 0.77). Similar values of α_0 were found for both initial and stationary periods: $1.21 \cdot 10^{13}$ and $1.15 \cdot 10^{13}$ m/kg, respectively. These values are comparable with those

typically found in the literature (Bugge et al., 2012). However, results indicate that the compressibility of the cake layer decreases as the operation time increases. A reason for this finding could be the higher local flux obtained in the stationary period due to the consolidation process. As layer compressibility is a time-dependent process and filtration time was considerably reduced in the stationary conditions (Figure 8.3), it is reasonable to assume that the layer became less compressible. Similarly, Sioutopoulos and Karabelas (2015) observed that the layer compressibility decreased with permeate flux, during the dead-end filtration of alginate-model solutions.

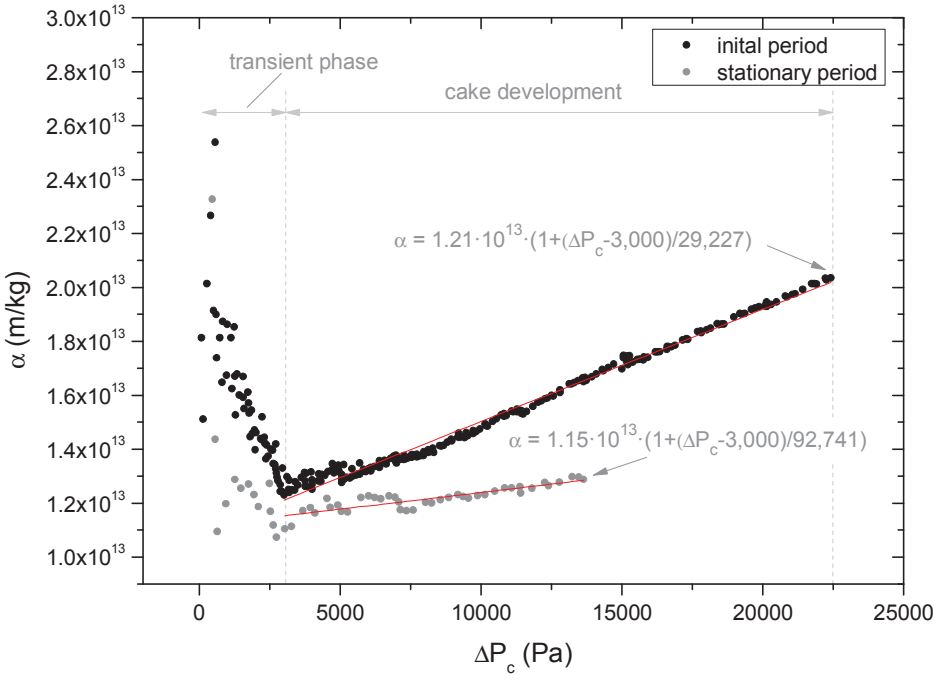

Figure 8.4. Evolution of specific cake resistance with increasing pressure drop across the cake during a cycle. J= 35L/h m^2, J_B =20 L/h m^2 and t_B=30s.

3.3.2. Effect of operating parameters on stationary reversible fouling

As also shown in Figure 8.3, within each filtration cycle once the stationary period was achieved, a short transient phase (0.5-2.7 min) was generally followed by a *TMP* linear rise. In these conditions, an incompressible cake development mechanism can be assumed where reversible fouling rate r_f = d*TMP*/d*t*, ranging between 26.0 and 63.5 kPa/h, increased its value

with filtration flux according to previous studies (Zsirai et al., 2012). However, the fouling rates obtained in this study were far higher than those often found in full-scale MBRs operating with air scouring (0.6-6 kPa/h) (Drews, 2010). This is to be expected, since aeration reduces the fouling rate by producing shear stress and lateral fiber movement (Drews, 2010). However, in spite of the high fouling rate observed, the backwashing was able to remove it and, thus, a sustainable operation was attained. In fact, the mean filtration cycle length was significantly high: 21-53, 14-22 and 136-17 min for 35, 45 and 55 L/h m^2, respectively.

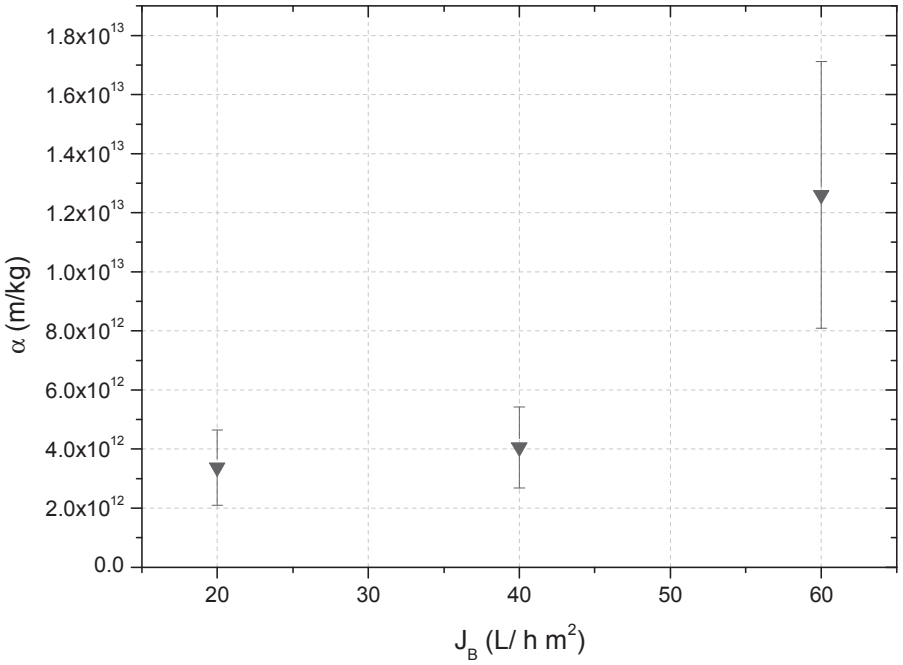

Figure 8.5. Specific cake resistance, α, against backwashing flux at different filtration fluxes

According to Eq. [8.4] and assuming *α* does not depend on *TMP* or *J* in the stationary period (i.e. incompressible cake model), *α* was determined under different backwashing conditions (Figure 8.5). It should be noted that when relaxation was used, due to the high cleaning frequency and low filtration cycle length (0.67-1.99 min), the linear *TMP* rise phase is too short to be considered, and therefore *α* cannot be accurately determined. The results also showed that the rise in backwashing flux increased the specific resistance, which suggests that re-dispersion plays an important role in cake properties. Several authors have recorded a higher specific resistance as the suspension concentration drops and commented that this reflects more orderly tighter deposits (McAdam and Judd, 2008; Kwon et al., 2000).

3.3.3. Effect of operating parameters on residual fouling

As mentioned before, the TMP_i increased significantly in the first few cycles, reflecting considerable residual fouling. This internal fouling, which is not removed by backwashing, can be related to internal pore blocking (Le-Clech et al., 2006) and a gel or compacted cake layer (Liang et al., 2012). Although pore blocking is expected to be caused by colloids and macromolecules, some authors have pointed out that cells adjacent to the membrane are exposed to a high compressive drag and will suffer great deformation (Foley, 2006; Wu et al., 2013). As a consequence, these cells will be capable of blocking membrane pores. In this sense, it seems that consolidation of the cake layer and membrane pore blocking are inseparably linked, particularly in the initial period, under the tested conditions.

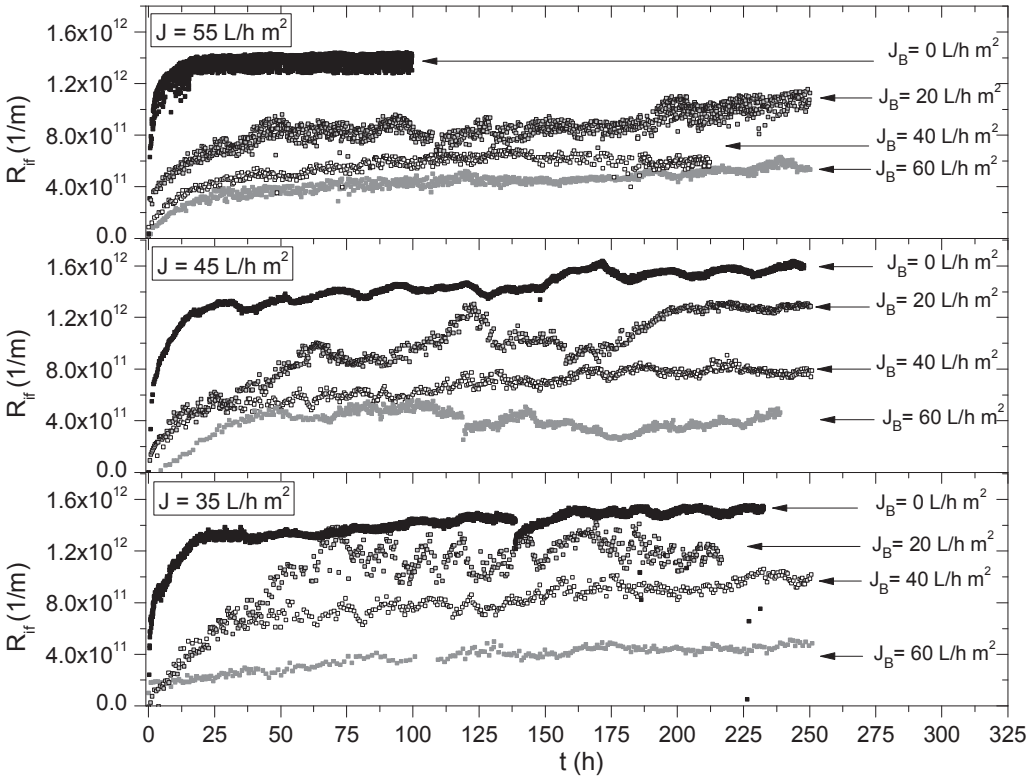

Figure 8.6. R_{if} evolution at different filtration and backwashing fluxes

Figure 8.6 shows the evolution of R_{if} under different operating conditions. Identical trends were observed for all filtration tests, where most of the fouling was detected in the first 25-50 h of operation followed by a slow rise. The observed variations may be related to significant changes in sludge filterability according to fluctuations in ambient conditions. It is obvious that relaxation was far less effective in preventing residual fouling than backwashing, which showed

similar values. In fact, backwashing flux (J_B) decreased the residual fouling resistance, consistently with previous studies (Wang et al., 2014; Zsirai et al., 2012). A roughly similar effect was observed at different filtration fluxes, where increasing J_B from 20 to 60 L/h m^2 resulted in a reduction in resistance of ~52%, ~62% and ~57%, for filtration fluxes of 55, 45 and 35 L/h m^2, respectively. Consequently, cleaning efficiency was mainly determined by backwashing flux, regardless of the imposed filtrate flux. This seems contrary to the results of previous studies where residual fouling increases with the filtrate flux applied (Wu et al., 2013). This may be due to the system automatically adjusting the cleaning frequency to a preselected TMP_{sp}, which determines the degree of fouling allowed. As the cake-layer reversibility may be closely related to its characteristics (i.e. density and compressibility) (Jeison and van Lier, 2007), by operating under TMP_{sp} control mode, a stable backwashing efficiency can be achieved.

To summarise the effects of the operating parameters on residual fouling resistance, an overall correlation can be established. The best results were obtained with a non-linear regression of R_{if} to an empirical equation (Eq. [8.9]). In all cases, a reasonable accuracy of the parameters (average R^2 of 0.84±0.09) was obtained. While the first term of the equation describes the sharp increase of residual fouling (i.e. initial period), the second considers the continuous R_{if} rise (i.e. stationary period).

$$R_{if} = \left(R_{if}\right)_{asym}[1 - exp(-k_C t)] + r_{if} t \qquad [8.9]$$

where $(R_{if})_{asym}$ is the asymptotic R_{if} value during the initial period (considered after 50 h of operation), k_c is a kinetic constant and r_{if} is the residual fouling rate in the stationary period. Assuming that residual fouling gradually reduces the available membrane area, Eq. [8.9] suggests that the decay rate is proportional to the actual available area and to the kinetic constant, k_c. It should be noted that this decay rate is expected to be closely related to the cake consolidation rate after several filtration/cleaning cycles. Figure 8.7A shows k_c against J_B at several applied J and different behaviour can be observed depending on the cleaning method used. The values for relaxation (J_B=0 L/h m^2) were significantly higher than those for backwashing, probably due to the severe fouling conditions imposed. However, the consolidation rate was not considerably affected by the filtration and backwashing fluxes under the tested conditions (k_c=0.083±0.015 1/h) when backwashing was applied. $(R_{if})_{asym}$ represents the maximum available area that can be reduced by residual fouling for the given backwashing conditions. Therefore, this value is

expected to depend on cleaning efficiency. Consistently, $(R_{if})_{asym}$ decreased linearly with J_B, regardless of the J imposed (Fig. 7B).

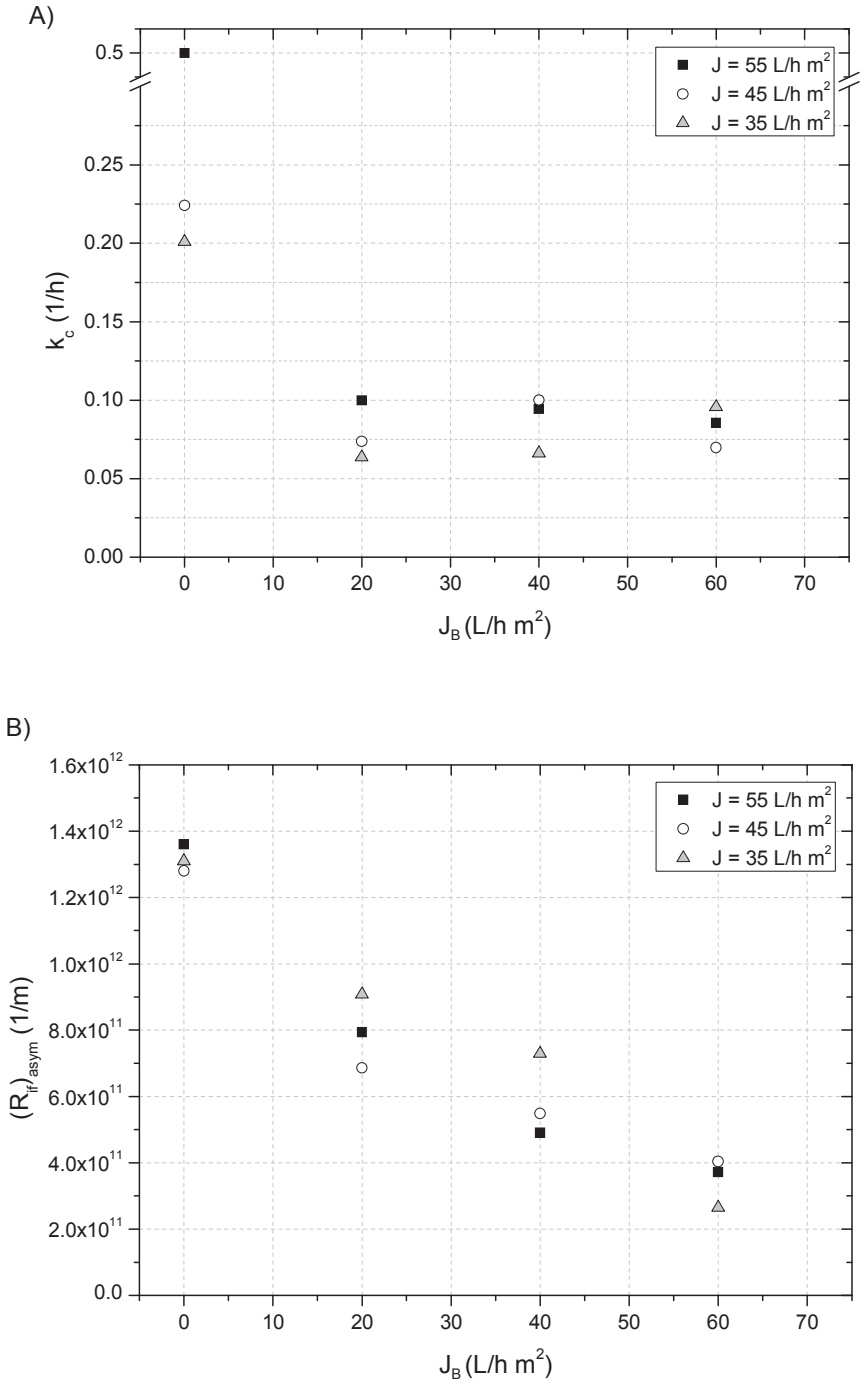

Figure 8.7. Empirical parameters in Eq. (6) against backwashing flux at different filtration fluxes: A) k_c and B) $(R_{if})_{asym}$

On reaching the stationary period, stable cleaning efficiencies were obtained which were not significantly affected by operating conditions (filtration and backwashing fluxes). In fact, a slight increase in the residual fouling rate (r_{if}) was noted, which ranged between $2.78 \cdot 10^8$ and $1.57 \cdot 10^9$ 1/m h. These values are significantly lower than those typically found for full-scale MBRs (Drews, 2010).

3.4. Process productivity and specific aeration demand

Process productivity was assessed by determining the net permeate flux (J_{net}), calculated as an average during the last 50 h of the stationary period:

$$J_{net} = \frac{t_F \cdot J - t_B \cdot J_B}{t_F + t_B} \qquad [8.10]$$

where t_B and t_F are the duration of the backwashing phase and the average duration of the filtration phase, respectively.

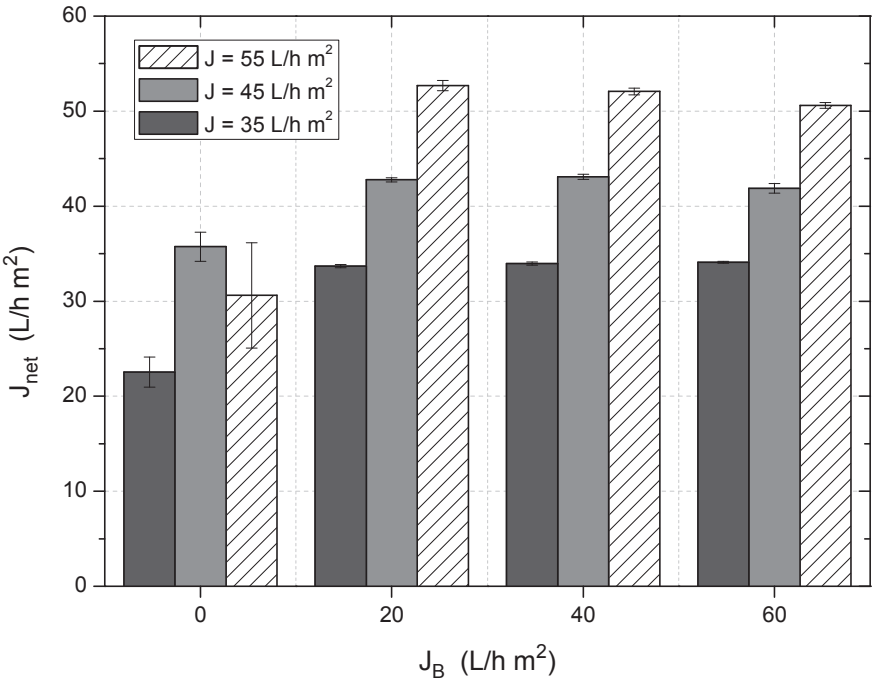

Figure 8.8. J_{net} against backwashing flux at different filtration fluxes in the stationary period.

Figure 8.8 shows J_{net} as a function of the assayed operating conditions. It is clear that relaxation (J_B=0 L/h m^2) yielded lower productivity than backwashing. This is due to the low efficiency in removing residual fouling, which resulted in a short filtration cycle length, as stated in previous sections. In contrast, backwashing obtained high productivities whose values mainly depended on the applied filtration flux. In fact, J_{net} was further improved by increasing the filtration flux (33.9 ± 0.2 L/h m^2, 42.6 ± 0.6 L/h m^2, 51.8 ± 1 L/h m^2 for 35, 45 and 55 L/h m^2, respectively). The long filtration cycles also explain the unimportant role of backwashing flux in the tested range of 20-60 L/h m^2.

Another important issue to be considered is the specific aeration demand linked to membrane cleaning (SAD_p). As previously mentioned, the system operated without air scouring and air is only supplied during the relaxation/backwashing. For relaxation, the high frequency of cleaning phases resulted in high values of SAD_p. For backwashing, SAD_p decreased with increasing J_B, achieving minimum values at 40 L/h m^2. In these conditions, SAD_p was significantly low (1-2 Nm^3_{air} /$m^3_{permeate}$) compared with those found in full-scale plants (Krzeminski et al., 2012).

Table 8.3. Percentage of SMP and TSS reported in the membrane fouling layers at different filtration conditions.

Filtration flux (L/h m^2)	Backwashing flux (L/h m^2)	TSS (%)		SMP (%)
		Cake	Adsorbed	Cake
35	60	98	2	85
	40	96	4	76
	20	91	9	65
	0	94	6	63
45	60	98	2	68
	40	97	3	78
	20	93	7	67
	0	80	20	76
55	60	94	6	76
	40	77	23	77
	20	86	14	86
	0	84	16	86

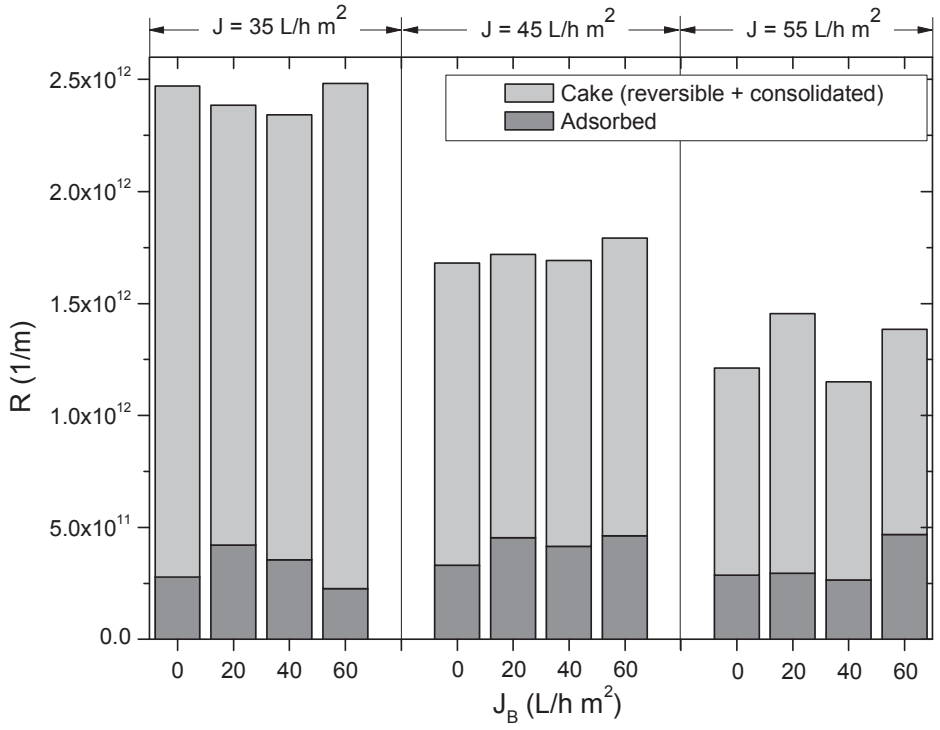

Figure 8.9. Fouling resistances due to the different fouling layers under several filtration conditions

3.5. Analysis of the different fouling layers.

At the end of each filtration test, a simplified analysis of the fouling layers was carried out. The cleaning procedure separates the layers into two main fractions: cake (removed by physical means), and adsorbed material (removed by chemical means). As expected, physical methods (i.e. rinsing in tap water and subsequent application of strong backwashing at 90 L/h m^2 for 15 min) were enough to remove most of the total solids from the membrane (Table 8.3). Therefore, it is assumed that the reversible and consolidated cake obtained during the filtration tests can largely be removed by physical means. Assessing the cleaning efficiency in terms of resistance (Figure 8.9), the cake fraction accounted for 85, 62 and 47% of the global resistance for filtration fluxes of 35, 45 and 55 L/h m^2, respectively. Also, the filtration and backwashing conditions did not have a significant effect on the adsorbed resistance, since it was practically constant under the different conditions (from $2.26 \cdot 10^{11}$ to $4.67 \cdot 10^{11}$ 1/m). Consistently, these values are similar to R_{if} values obtained during the filtration tests when a backwashing flux of 60 L/h m^2 was used (Figure 8.6). Therefore, results suggest that the absorbed fraction did not depend on the operating conditions and mainly comprised SMP, in accordance with previous studies (Wu et al.,

2012). However, the contribution of these foulants to the residual fouling was less, as also confirmed by the very low fouling rates observed in the stationary period (Figure 8.6). In addition, it was expected that the cake layer might act as a secondary membrane, retaining SMPs. As can be observed in Table 8.3, the cake fraction contained much more SMP than the adsorbed fraction, consistently with other studies (Wu et al., 2013).

3.6. Optimisation of process parameters.

It is generally accepted that the MBR implementation is limited by the high costs, both in capital and operating expenditure (CAPEX and OPEX). A key issue is the selection of the most appropriate filtration flux, which is determined by the classical trade-off problem: high fluxes are desirable to reduce membrane area requirement (i.e. CAPEX), however, membrane fouling increases with flux, which results in a higher energy demand and more frequent cleanings to control membrane fouling (i.e. increase OPEX).

The optimal conditions were assessed by simulating the effect of filtration and backwashing flux on specific energy demand (*SED*) (Figure 8.10). These values are calculated through the equations proposed for reversible and residual fouling rates (Eqs. [8.4-8.9]), after 120 days of operation, which was assumed as a sustainable operative time (t_{op}) between maintenance/recovery chemical cleanings. For *SED* determination, it is only considered the equipment related to filtration process: a blower and a permeate pump. Energy consumption of the blower (W_G) and the permeate pump (W_J) was calculated by applying Eqs. 8.11 and 8.12, respectively (Judd 2010):

$$W_G = \frac{R \cdot T \cdot \lambda}{1.63 \cdot 10^5 \cdot \zeta_c \cdot (\lambda - 1)} \cdot \left[\left(\frac{P_{A2}}{P_{A1}} \right)^{1-\frac{1}{\lambda}} - 1 \right] \cdot Q_A \qquad [8.11]$$

$$W_P = \frac{Q_p \cdot TMP}{1000 \cdot \zeta_p} \qquad [8.12]$$

where R is gas constant, T is the air temperature, P_{A1} is the absolute inlet pressure, P_{A2} is the absolute outlet pressure, λ is the adiabatic index, Q_A is the air volumetric flow rate, Q_P is the permeate volumetric flow rate, ζ_p is the pump efficiency and ζ_c is the blower efficiency.

Then, *SED* can be defined as Eq. [8.13]:

$$SED = \frac{W_J + W_G}{J_n \cdot A} \qquad [8.13]$$

where J_{net} is the net permeate flux and A is the membrane filtration area.

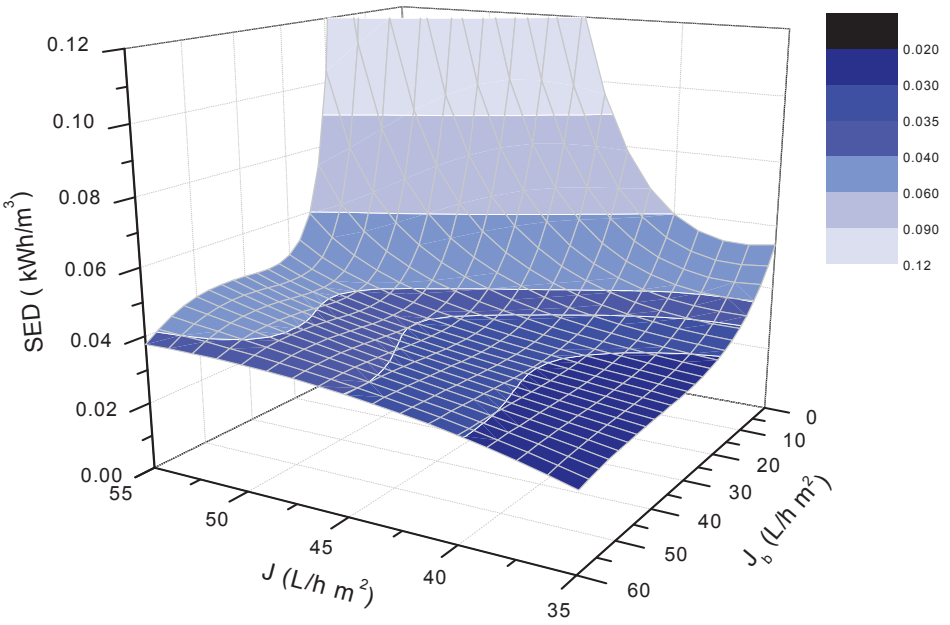

Figure 8.10. Estimated specific energy demand associated with permeate suction/backwashing and module aeration (SED) against different filtration conditions.

Simulation results indicated that low values of SED were achieved (0.02-0.03 kWh/m^3) when J was lower than 40-38.75 L/h m^2 and J_B was higher than 22.5-27.5 L/h m^2. For that reason it seems highly recommendable to operate at these conditions. Also, it should be noted the significant energy demand that arises from permeate pump (33-47% of total energy consumption), due to operation in dead-end filtration. When *J* increased above 40 L/h m^2, the significant increase of reversible fouling rate led to shorter filtration cycles and, thus, to more frequent backwashings, which both resulted in low J_{net} (Eq. [8.10]) and high W_G. On the other hand, it has been previously observed that backwashing flux affects the residual fouling (Section 3.3.3); this justifies the abrupt *SED* increase observed when decreasing J_B below 22.5 L/h m^2 at elevated *J* (0.06-0.12 kWh/m^3).

It should be noted that energy consumption depicted in Figure 8.10 does not account power consumption arising from other devices including bioreactor aeration, recirculation pumps, and compressors for valve switching. This can contribute to another 0.2-0.3 kWh/m^3, according to full-scale studies (Krzeminski et al., 2012).

Finally, another factor to be considered in order to optimize costs is the membrane area requirement. This area is inversely proportional to the net permeate flux. Hence, taken into account the operating conditions that minimize *SED* values to 0.02-0.03 kWh/m^3, a lower specific area demand (25.02 m^2 h/m^3) is obtained for the maximum J_{net} (39.97 L/h m^2, at J = 40 L/h m^2 and J_B = 27.5 L/h m^2). At optimum *SED* conditions, it is also observed that the specific area demand mainly depended on applied flux, while backwashing flux influence was irrelevant. Consistently, decreasing filtration flux from 40 to 35 L/h m^2 (~13%) at J_B = 27.5 L/h m^2 resulted in an increase of ~14% in the specific area demand, while varying backwashing flux from 60 to 20 L/h m^2 at J = 35 L/h m^2 lead to a less of 0.1% of variation in specific area demand.

4. Conclusions

- The tertiary membrane bioreactor demonstrated its capability to operate with complete sludge retention, achieving complete nitrification and high organic material removal (87 % on average for COD) with moderate suspended solids concentration (MLSS=4-8 g/L). The complete retention of sludge also induced a maintenance level for the microorganisms, where the concentration of soluble microbial products (SMP) in the supernatant was minimised. Consistently, membrane fouling was mainly caused by suspended particles, with a medium size (d_{50} = 63±6 µm) and a relatively narrow distribution (distribution spreading index of 1.29±0.13). As a result, the suspension showed an excellent filterability (TTF = 8.9±2.9 s).

- The *TMP* profiles during the flux-steps trials showed the important role of the compression process in cake fouling reversibility. Assessing this reversibility in terms of the critical flux, it was also found to be significantly affected by backwashing conditions (duration and application of air scouring).

- For the long-term tests, *TMP* profile can be described well by a compressible cake build-up model, where the compressibility decreased with successive filtration cycles until a stationary period was reached. During the initial period, a gradual residual fouling increase was also observed which can be attributed to cake consolidation and/or a pore-blocking mechanism.

- Evolution of residual fouling resistance was modelled by a non-linear expression, assuming that fouling gradually reduces the available membrane area. Based on this approach, the fouling resistance after the initial period decreased with the backwashing flux applied. Consistently, the relaxation was far less effective in preventing residual fouling than backwashing. In the stationary period, similar cleaning efficiency was obtained, which was not significantly affected by the operating conditions (filtration and backwashing fluxes).

- An analysis of the relative contribution of the fouling layers to the global fouling revealed that the cake fraction (mainly formed by suspended solids) accounted for 85-47%, decreasing with the filtration flux imposed. In contrast, resistance of the adsorbed fraction remained constant and low under the tested conditions.

- Simulation results indicated that the best conditions can be established at a filtration flux of 40 L/h m^2 and a backwashing flux of 27.5 L/h m^2, due to high net permeate flux and low specific energy demand.

5. References

American Public Health Association/Water Environment Federation, Standard Methods for the examination of Water and Wastewater, 21st ed., Washington DC, USA (2005).

Asano T., Burton F. L., Leverenz H.L., Tsuchihashi R., Tchobanoglous G., Water Reuse, Issues, Technologies, and applications, 1st editions, Metcalf & Eddy (2007).

Bacchin P., Aimar P., Field R.W., Critical and sustainable fluxes: Theory, experiments and applications, *J. Membr. Sci.*, 281, (2006), 42-69.

Bessiere Y., Abidine N., Bacchin P., Low fouling conditions in dead-end filtration: evidence for a critical filtered volume and interpretation using critical osmotic pressure, *J. Membr. Sci.*, 264, (2005), 37–47.

Bourgeous K. N., Darby J. L., Tchobanoglous G., Ultrafiltration of wastewater: effects of particles, mode of operation, and backwash effectiveness, *Water Res.*, 35, (2001), 77-90.

Bugge T. V., Jørgensen M. K., Christensen M. L., Keiding K., Modeling cake buildup under *TMP*-step filtration in a membrane bioreactor: Cake compressibility is significant, *Water Res*., 46, (2012), 4330–4338.

Cumin J., Behmann H., Hong Y., Bayly R., Gas sparger for an immersed membrane, (2011) U. S. Patent US/2011/0049047.

Delgado S., Díaz F., Vera L., Díaz R., Elmaleh S., Modelling hollow-fibre ultrafiltration of biologically treated wastewater with and without gas sparging, *J. Membr. Sci*., 228, (2004), 55-63.

Drews A., Membrane fouling in membrane bioreactors—Characterisation, contradictions, causes and cures, *J. Membr. Sci*., 363, (2010), 1–28.

Ferrero G., Rodriguez-Roda I., Comas J., Automatic control systems for submerged membrane bioreactors: A state-of-the-art review, *Water Res*., 46, (2012), 1-13

Foley G., A review of factors affecting filter cake properties in dead-end microfiltration of microbial suspensions, *J. Membr. Sci*., 274, (2006), 38-46.

Guglielmi G., Chiarani D., Judd S.J., Andreottola G., Flux criticality and sustainability in a hollow fibre submerged membrane bioreactor for municipal wastewater treatment, *J. Membr. Sci*., 289, (2007), 241-248.

Gui P., Huang X., Chen Y., Qian Y., Effect of operational parameters on sludge accumulation on membrane surfaces in a submerged membrane bioreactor, *Desalination,* 151, (2003), 185–194.

Harmant P., Aimar P., Coagulation of colloids in a boundary layer during cross-flow filtration, *Colloids and Surfaces A: Physicochemical and Engineering Aspects*, 138, (1998), 217-230.

Hong H., Zhang M., He Y., Chen J., Lin H., Fouling mechanisms of gel layer in a submerged membrane bioreactor, *Bioresour. Technol*. 166, (2014), 295–302.

Itokawa H., Thieming C., Pinnekamp J., Design and operating experiences of municipal MBRs in Europe, *Water Sci. Technol*. 58, (2008), 2319-2327.

Jeison D., van Lier J.B., Cake formation and consolidation: main factors governing the applicable flux in anaerobic submerged membrane bioreactors (AnSMBR) treating acidified wastewaters, *Sep. Purif. Technol*., 56, (2007), 71–78.

Jönsson A.S., Jönsson B., Ultrafiltration of colloidal dispersion—a theoretical model for the concentration polarization phenomena, *J. Colloid Interface Sci.,* 180, (1996), 504–518.

Jørgensen M. K., Bugge T. V., Christensen M. L., Keiding K., Modeling approach to determine cake buildup and compression in a high-shear membrane bioreactor, *J. Membr. Sci*., 409–410, (2012), 335–345.

Jørgensen M. K., Keiding K., Christensen M. L., On the reversibility of cake buildup and compression in a membrane bioreactor, *J. Memb, Sci*., 455, (2014), 152-161.

Judd S., The MBR Book, Principles and Applications of Membrane Bioreactors for Water and Wastewater

Kim J., DiGiano F.A., Fouling models for low-pressure membrane systems, *Sep. Purif. Technol*., 68, (2009), 293–304.

Koch Membrane, Case Study. Aquapolo Ambiental Water Reuse Project. (2014) (http://www.kochmembrane.com/PDFs/Case-Studies/KMS-Sao-Paulo-Brazil-Case-Study.aspx)

Kristensen G. H., JØrgensen P. E., Henze M., Characterization of functional microorganism groups and substrate in activated sludge and wastewater by AUR, NUR and OUR, *Water Sci. Technol*., 25, (1992) 43-57.

Krzeminski P., van der Graaf J.H.J.M., van J. B. Lier, Specific energy consumption of membrane bioreactor (MBR) for sewage treatment, *Water Sci. Technol*., 65, (2012), 380-392

Kuberkar V. T., Davis R. H., Modeling of fouling reduction by secondary membranes, *J. Membr. Sci*., 168, (2000), 243-258.

Kwon D.Y., Vigneswaran S., Fane A.G., Ben Aim R., Experimental determination of critical flux in cross-flow microfiltration, *Sep. Purif. Technol*., 19, (2000), 169–181.

Le-Clech P., Chen V., Fane A.G., Fouling in membrane bioreactors used in wastewater treatment, *J. Membr. Sci.,* 284, (2006), 17–53.

Le-Clech P., Jefferson B., Chang I., Judd S., Critical flux determination by the flux-step method in a submerged membrane bioreactor*, J. Membr. Sc*i., 227, (2003), 83-91.

Liang S., Zhao T., Zhang J., Sun F., Liu C., Song L., Determination of fouling-related critical flux in self-forming dynamic membrane bioreactors: Interference of membrane compressibility, *J. Membr. Sci.,* 390-391, (2012), 113-120.

Lin H., Zhang M., Wang F., Meng F., Liao B., Hong H., Chen J., Gao W., A critical review of extracellular polymeric substances (EPSs) in membrane bioreactors: Characteristics, roles in membrane fouling and control strategies, *J. Membr. Sci.,* 460, (2014), 110-125.

Lyko S., Wintgens T., Al-Halbouni D., Baumgarten S., Tacke D., Drensla K., Janot A., Dott W., Pinnekamp J., Melin T., Long-term monitoring of a full-scale municipal membrane bioreactor—characterisation of foulants and operational performance*, J. Membr. Sci*., 317, (2008), 78–87.

McAdam E. J., Judd S. J., Optimization of dead-end filtration conditions for an immersed anoxic membrane bioreactor*, J. Membr. Sci*., 325, (2008), 940-946.

McCarthy A.A., Gilboy P., Walsh P.K., Foley G., Characterisation of cake compressibility in dead-end microfiltration of microbial suspensions, *Chem. Eng. Commun*., 173, (1999), 79–90.

Meireles M., Molle C., Clifton M.J., Aimar O., The origin of high hydraulic resistance for filter cakes of deformable particles: cell-bed deformation or surface-layer effect?, *Chem. Eng. Sci*., 59, (2004),5819-5829.

Ng H., Hermanowicz S., Membrane bioreactor operation at short solids retention times: performance and biomass characteristics, *Water Res*., 39, (2005), 981–992.

Pirt S., The maintenance energy of bacteria in growing cultures. Proc. R. Soc. London, 163B (1965) 224-231.

Pollice A., Laera G., Blonda M., Biomass groth and activity in a membrane bioreactor with complete sludge retention. *Water Res*., 38, (2004), 1799-1808.

Rushton A., Ward A.S., Holdich R.G., Introduction to Solid–Liquid Filtration and Separation Technology, Wiley–VCH, 1995.

Schoeberl P., Brik M., Bertoni M., Braun R., Fuchs W., Optimization of operational parameters for a submerged membrane bioreactor treating dyehouse wastewater, *Sep. Purif. Technol*. 44, (2005), 61–68.

Sioutopoulos D.C., Karabelas A. J., The effect of permeation flux on the specific resistance of polysaccharide fouling layers developing during dead-end ultrafiltration, *J. Membr. Sci*., 473, (2015), 292-301.

Sørensen B.L., Sørensen P.B., Structure compression in cake filtration, *J. Environ. Eng*., 123, (1997), 345-353.

Su X., Tian Y., Li H., Wang C., New insights into membrane fouling based on characterization of cake sludge and bulk sludge: An especial attention to sludge aggregation *Bioresour. Technol*., 128, (2013), 586–592

Van der Marel P., Zwijnenburg A., Kemperman A., Wessling M., Temmink H., van der Meer W., An improved flux-step method to determine the critical flux and the critical flux for irreversibility in a membrane bioreactor, *J. Membr. Sci*., 332, (2009), 24-29.

Vera L., González E., Díaz O., Delgado S., Application of backwashing strategy based on transmembrane pressure set-point in a tertiary submerged membrane bioreactor, *J. Membr. Sci*, 470 (2014b)504-512.

Vera L., González E., Díaz O., Delgado S., Performance of a tertiary submerged membrane bioreactor operated at supra-critical fluxes, *J. Membr. Sci*, 457, (2014a),1-8.

Villarroel R., Delgado S., González E., Morales M., Physical cleaning initiation controlled by transmembrane pressure set-point in a submerged membrane bioreactor, *Sep. Purif. Technol*., 104, (2013), 55-63.

Wang Z., Ma J., Tang C. Y., Kimura K., Q. Wang, Membrane cleaning in membrane bioreactors: A review, J. *Membr. Sci.* 468, (2014), 276-307.

Wibisono Y., Cornelisse E.R. n, Kemperman A.J.B., van de Meer, W.G.J. Nijmeijer K., Two-phase flow in membrane processes: a technology with a future*, J. Membr. Sci.*, 463, (2014), 566-602.

Wintgens T., Melin T., Schäfer A., Khan S., Muston M., Bixio D., Thoeye C.. The role of membrane processes in municipal wastewater reclamation and reuse, *Desalination*, 178, (2005), 1-11.

Wu J., He C., Bi D., Yi J., Zhang Y., A bio-cake model for the soluble COD removal by the back-transport, adsorption and biodegradation processes in the submerged membrane bioreactor, *Desalination,* 322, (2013), 1-12.

Wu J., He C., Zhang Y., Modeling membrane fouling in a submerged membrane bioreactor by considering the role of solid, colloidal and soluble components, J. *Membr. Sci*., 397-398, (2012), 102-111.

Wu J., Le-Clech P., Stuetz R.M., Fane A.G., Chen V., Effects of relaxation and backwashing conditions on fouling in membrane bioreactor, J. *Membr. Sci*., 324, (2008), 26–32.

Ye Y., Chen V., Le-Clech P., Evolution of fouling deposition and removal on hollow fibre membrane during filtration with periodical backwash, *Desalination*, 283, (2011), 198–205.

Zsirai T., Buzatu P., Aerts P., S. Judd, Efficacy of relaxation, backflushing, chemical cleaning and clogging removal for an immersed hollow fibre membrane bioreactor, *Water Res*., 46, (2012), 4499–4507.

CAPÍTULO 9: Análisis y mitigación del ensuciamiento en un MBR operado con aireación restringida

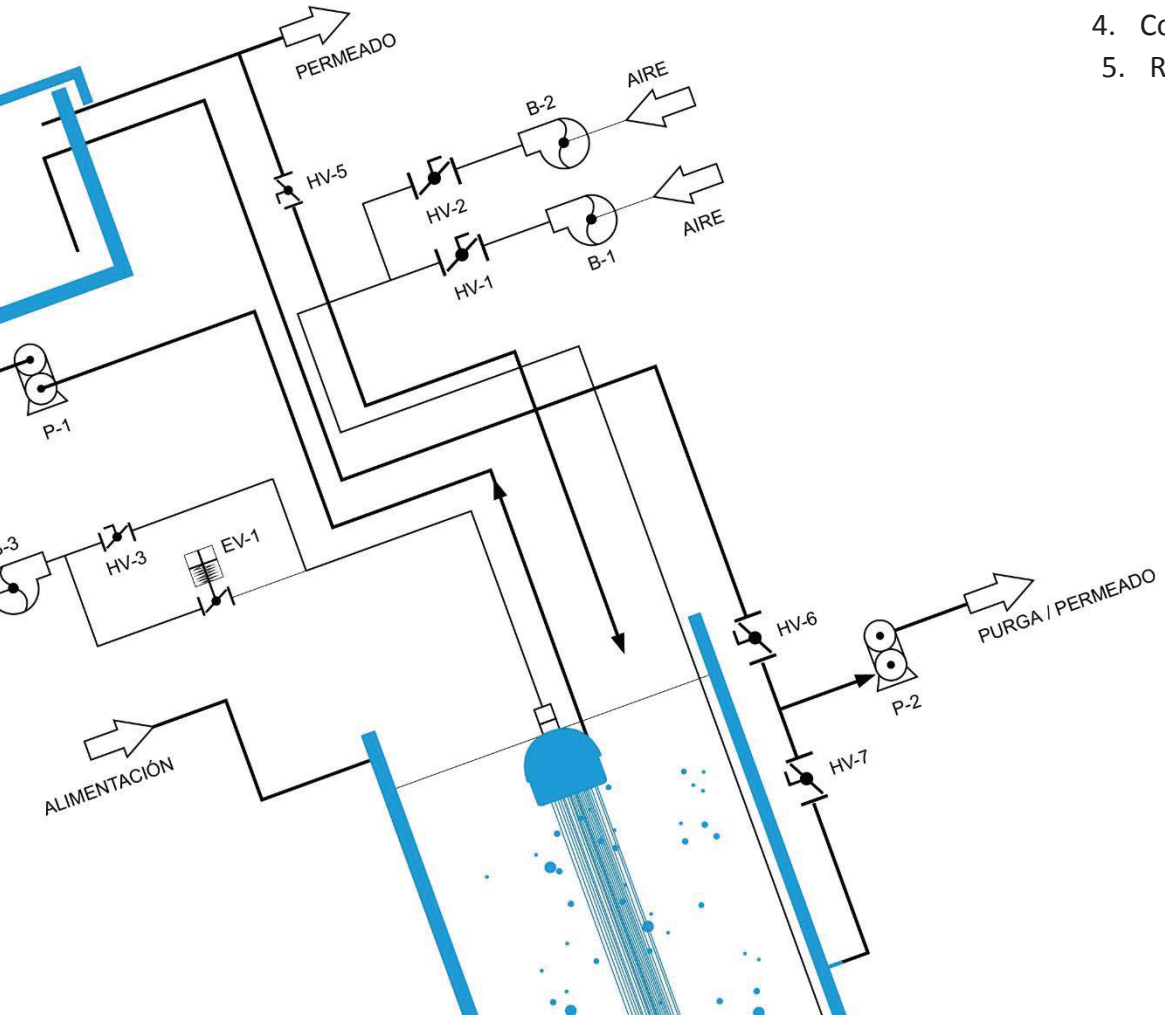

Capítulo 9

Análisis y mitigación en un MBR terciario operado con aireación restringida

Fouling analysis and mitigation in a tertiary MBR operated under restricted aeration

Oliver Díaz, Enrique González, Luisa Vera, José Juan Macías-Hernández, Juan Rodríguez-Sevilla

Enviado a
Journal of Membrane Science

Factor de impacto: 5,056 (JCR®, Thomson Reuters 2015).

Highlights

- Tertiary MBR applied for advanced treatment of secondary effluent from a conventional WWTP
- Better understanding of influence of biofflocculation on membrane bioreactors performance
- Determination of critical dissolved oxygen concentration for minimal membrane fouling
- Description of residual fouling membrane by an empirical model
- Biopolymer Clusters (BPCs) as regulator of the specific cake resistance associated with reversible fouling

Key-words: backwashing aided by air-scouring; compressible cake; sludge bioflocculation; residual fouling control, transmembrane pressure set-point

Resumen:

Los principales costes de operación de un MBR están asociados a los procesos de aireación necesaria para el proceso biológico como para la limitación del ensuciamiento de la membrana. Este último, corresponde a una práctica ampliamente instaurada como forma de mitigar el ensuciamiento de la membrana. En lo que se refiere a los costes relacionados con la aireación para el proceso biológico, estos son inevitables en un biorreactor aerobio, aunque podrían

minimizarse si se determina la concentración de oxígeno disuelto que permita desarrollar con garantías el proceso biológico, a la vez que permitir la operación a medio-largo plazo de la membrana. Por otra parte, la filtración en modo frontal sin promover turbulencia en las proximidades de la membrana permite reducir considerablemente los costes derivados de este proceso. En el presente Capítulo se analiza la sostenibilidad de un MBR terciario operado en filtración frontal a bajas concentraciones de oxígeno disuelto y además, con el modo alternativo de operación por presión de consigna.

El MBR terciario logró un elevado rendimiento de eliminación de materia orgánica, independientemente de la concentración de oxígeno disuelto impuesta. Además, a bajas tasas de aireación, el sistema logro mantener un rendimiento aceptable de eliminación de amonio, en torno al 38-46%. Por el contrario, las bajas concentraciones de oxígeno disuelto si afectaron negativamente a la biofloculación de la suspensión biológica, incrementando la concentración de BPCs y reduciendo significativamente, el tamaño del flóculo. Estas condiciones empeoraron la filtrabilidad de la suspensión, al aumentar el TTF, reduciendo significativamente el flujo crítico.

En éste Capítulo se ha introducido el concepto “masa crítica”, como la masa específica depositada sobre la membrana que induce la consolidación de la torta, relacionando el efecto de dicha consolidación con un valor crítico de compresibilidad que puede ser definido como el flujo crítico. A dicho flujo crítico existiría una transición entre un primer periodo caracterizado por bajo crecimiento de la TMP y una segunda etapa, de rápido crecimiento del ensuciamiento. Los resultados revelan un descenso significativo del flujo crítico, desde 55 a 15 L/hm^2, cuando la frecuencia de aireación se reduce desde 1 a 0. Sin embargo, la resistencia de la torta asociada a la presión transmembrana crítica es mantenida en torno al mismo valor, independientemente de la concentración de oxígeno disuelto impuesta. Éste comportamiento puede ser debido a que la resistencia crítica es proporcional a la resistencia específica de la torta formada y al contenido de sólidos por unidad de área de membrana, propiedades asociadas a la suspensión y no a las condiciones de operación.

El modo alternativo de operación ha resultado ser muy efectivo para limitar el ensuciamiento, incrementando la frecuencia del retrolavado cuando la biofloculación ha sido baja. Como consecuencia, el ensuciamiento residual parece no verse afectado por la concentración de oxígeno disuelto impuesta, ni por el flujo de filtración estudiado. Además, la tendencia del ensuciamiento residual interno puede ser descrita mediante el modelo empírico

propuesto en el capítulo anterior, donde el ensuciamiento reduce el área disponible de membrana hasta alcanzar un estado cuasi-estacionario.

En lo que se refiere al ensuciamiento reversible, éste es relacionado con la construcción de una torta compresible sobre la membrana, donde la resistencia específica de la torta está íntimamente relacionada con el estado de biofloculación, y concretamente con la concentración de BPC. Por el contrario, la compresibilidad de la torta se relaciona con las condiciones de filtrabilidad, puesto que a condiciones supra-criticas el sistema incrementa su compresibilidad. Por tanto, los resultados obtenidos en los experimentos de larga duración confirman los resultados de los experimentos escalonados.

Moderadas concentraciones de oxígeno disuelto ([O_2] =0,38 mg/L) han permitido la operación de un MBR terciario con elevada productividad, expresada como flujo neto y baja demanda energética asociada al proceso de filtración y la aireación biológica.

Abstract

Operation of tertiary membrane bioreactors at low dissolved oxygen concentration (DO) reduces energy consumption associated with biological aeration. However, low oxygen concentrations affect biological activity, sludge bioflocculation and fouling propensity. This study assesses the effectiveness of an alternative backwash initiation strategy for fouling control in a tertiary membrane bioreactor operated under restricted oxygenation. Long-term filtration tests were carried out at five DOs (0.09-1.23 mg/L) in a pilot-scale unit operated in dead-end filtration mode under a broad-range of permeate fluxes (25-65 L/h m^2). Bioflocculation was negatively affected at low DO ([O_2] ≤ 0.25 mg/L), resulting in relatively high values of biopolymeric clusters concentration (BPC ≥ 4.3mg DOC/L). This produced small floc sizes ($D_{(v,0.5)}$ ≤ 49 µm), poor filterability (TTF ≥ 573 s) and low critical fluxes (J_c ≤ 20 L/h m^2). However, above moderate oxygen concentrations ([O_2] ≥ 0.38 mg/L), sludge bioflocculation significantly increased, showing good filterability (TTF ≤ 173 s) and relatively high critical fluxes (J_c ≥ 45 L/h m^2). The filtration tests showed that the controlled backwashing initiation was effective in limiting the residual fouling even at a very low oxygen concentration, since it automatically increased backwashing frequency as sludge bioflocculation decreased. The reversible fouling, it can be described by the compressible cake model, with a specific cake resistance at zero pressure governed by the bioflocculation state, while the compressibility is determined by the filtration flux. Optimal sustainable conditions were established at moderate DO ([O_2] = 0.38 mg/L), which involves a low

specific energy demand for the filtration process and biological aeration (*SED* = 0.25 kWh/m^3), and a high net permeate flux (*J* = 42.2 L/h m^2).

1. Introduction

Membrane bioreactors (MBRs) combine the development of suspended biomass, similar to conventional activated sludge processes, with a permselective membrane (microfiltration or ultrafiltration membrane) that replaces gravity sedimentation and clarifies wastewater effluent. Focusing on protecting water resources against pollution, the new EU directives have promoted a stricter regulatory pressure on wastewater treatment in recent years (EU, 2000). This scenario has allowed MBR technology to attain a significant market share in municipal wastewater treatment, principally due to its superior effluent quality, suitable for unrestricted irrigation (Judd, 2011). In addition, MBRs permit a significant reduction in the total plant footprint compared to a conventional activated sludge plant (Cote et al., 2012). Moreover, secondary clarifier malfunctions in conventional wastewater treatment plants (WWTP) can cause numerous technical problems, such as large quantities of residuals, high consumption of chemical reagents, sulphide generation during reclaimed water transport through long pipes (Delgado et al., 1999). These require the implementation of tertiary treatments like coagulation, sand filtration or desalination. Recent studies have also shown the capability of MBRs in the tertiary treatment of secondary effluents from old plants with poor performance by secondary clarifiers. They can achieve high organic carbon removal and complete nitrification (Vera et al., 2015). In this case, MBR feedwater is mainly composed of suspended or colloidal organic matter, which is only slowly biodegradable (Díaz et al., 2016). Therefore, the system is usually operated under limited carbon substrate conditions, which significantly reduce sludge production. This is one of the most attractive points of tertiary membrane bioreactor (tMBR) application (Vera et al., 2015). In fact, the Aquapolo project (Sao Paulo, Brazil), the largest wastewater reuse project in the southern hemisphere includes a tMBR in the treatment scheme (Koch membrane, 2014), shows the growing worldwide interest in this technology.

The main drawbacks attributed to MBRs are due to fouling phenomena, which lower filtration efficiency and raise costs, both capital and operating expenditures (CAPEX and OPEX). Regarding both, a key issue is the selection of the suitable permeate flux. High fluxes are desirable to reduce the membrane area required, and thus limit CAPEX. Nevertheless, membrane fouling increases with flux and results in a higher membrane scouring demand and more frequent cleanings, and thus OPEX are raised. Membrane fouling is also influenced by

complex relationships between other parameters (such as hydrodynamics, cleaning protocols, feedwater characteristics and biological conditions) that involve conservative designs and operation strategies of MBR plants. So, pre-set or fixed values of selected parameters (based on the general background or recommendations of membrane suppliers) lead to an under-optimised system with high energy demand. In addition, the time-based operation mode drives to lower productivity when cleaning cycles are applied too often, or it can promote irreversible fouling when applied too late (Drews, 2007). In fact, the exact optimal backwash frequency and duration is impossible to pre-determine because membrane fouling can significantly fluctuate, even daily, due to the changing influent characteristics or operating conditions (such as temperature or peak flux) (Wang et al., 2014). Earlier work by our group showed that backwashing efficiency may be enhanced by monitoring the *TMP* profile during filtration. In this operation mode, when a pre-fixed *TMP* is reached (*TMP* set-point), backwashing begins immediately afterwards (Vera et al., 2015). This alternative operation mode permits operation at high filtration flux and control of membrane fouling, increasing the productivity of the process; however it has not yet been widely researched (Vera et al., 2015).

The principal contribution to OPEX in MBR is attributed to aeration (Krzeminski et al., 2012), however MBR aeration control is still rare in practice (Ferrero et al., 2012). Aeration is destined to cover two demands: physical (air scouring during filtration) and biological. Air scouring has been extensively proven to be an efficient means to limit foulant deposition, since it enhances foulant back-transport, shear stress at the membrane surface and lateral fibre movement (in hollow-fibre modules) (Wibisono et al., 2014). Membrane aeration is the largest energy consumer in the full-scale hollow-fibre MBR (Krzeminski et al., 2012). Although several strategies have been implemented to adjust flow rate and/or frequency of coarse air bubbles (Ferrero et al., 2012), this turbulence promoter has a high energy demand. In contrast, operation in dead-end filtration mode (i.e. without air scouring) allows significant energy savings. In this case, the absence of shear forces reduces foulant back-transport and consequently net foulant transport towards the membrane increases. Nevertheless, operation in dead-end filtration mode can operate at high fluxes when physical cleanings are automatically adjusted in response to membrane fouling (Vera et al., 2015). In these conditions, backwashing efficiency should be increased with the aid of punctual air scouring (Ye et al., 2011). So, air consumption in this case is significantly low compared with those in full-scale plants, where air is supplied during the filtration phase (Judd, 2011).

In recent years, several aeration strategies have been tested and applied for reducing the aeration required for biological processes (Dalmau et al., 2014; Capodici et al., 2015). At low DO, the biological process is affected and extracellular polymer substances (EPS) and soluble microbial products (SMP) increase in concentration (Gao et al., 2011). In fact, the DO is an important operational parameter for bioflocculation. Several mechanisms have been proposed in order to explain deflocculation behaviour at low DO (Faust et al., 2014). On the one hand, aerobic activity is reduced at low DO and this can result in slower production or faster anaerobic degradation of EPS (Faust et al., 2014). Meanwhile, other studies have been mainly focused on the proliferation of filamentous bacteria at low DO and their negative role in flocculation processes (Wilén et al., 1999).

This study assesses the sustainability of a tMBR operated under low DOs with an alternative operation mode for backwashing initiation in dead-end filtration. It is focused on the role of bioflocculation in membrane fouling, and the compression and reversibility of this phenomenon.

Table 9.1. Main feedwater characteristics for each A_R assayed

		AERATION RATIO									
		0 (n=5)		0.25 (n=5)		0.5 (n=4)		0.75 (n=6)		1 (n=5)	
Parameter	Unit	Mean	Range	Mean	Range	Mean	Range	Mean	Range	Mean	Range
COD	mg/L	363	306-420	252	195-346	277	131-345	269	130-604	237	50-766
COD_S	mg/L	46	45-48	91	62-118	52	44-65	71	22-95	74	34-90
DOC	mg/L	22	21-23	20	14-24	17	14-19	25	16-53	25	19-36
NH_4^+	mg N/L	51	42-57	52	44-55	51	47-55	42	35-65	39	37-46
N_T	mg N/L	62	52-78	70	64-68	54	48-66	55	46-65	57	48-62
SS	mg/L	234	204-286	155	102-238	151	80-265	179	68-326	126	32-287

2. Materials and methods

2.1. Feedwater

The pilot plant was fed with a secondary effluent from a conventional activated sludge wastewater treatment plant (WWTP), which was designed only for carbon removal. Table 9.1

summarises the main characteristics of feedwater in each experiment carried out at different frequencies of intermittent biological aeration. The secondary effluent exhibited high chemical oxygen demand, mainly as particulate matter (CODs/COD < 0.4 and COD/SST = 1.6). This high particulate content was attributed to the short SRT and oxygen deficiency in the activated sludge process, which frequently resulted in episodes of sludge deflocculation. Moreover, these operation parameters determine the absence of nitrification processes, and nitrogen compounds were mainly in the form of ammonium (NH_4^+/N_t = 0.8 on average).

2.2. MBR

The experimental study was carried out in a pilot plant equipped with ZeeWeed® ZW-10 (GE Water & Process Technologies) hollow-fibre membranes with a 0.04 µm-rated pore diameter, 1.9 mm external diameter and 0.9 m^2 of filtering surface area, assembled vertically in a cylindrical 220 L deposit. ZeeWeed® consists of a woven reinforcing braid on which a PVDF membrane is cast. The effluent (permeate) was extracted from the top header of the module under a slight vacuum. Fouling of the membrane was controlled by automatic backwashing based on an alternative operation mode. This mode ensured that each filtration phase finished when a pre-established TMP value (TMP_{sp}) was reached (30 kPa), initiating backwashing immediately afterwards. Backwashing conditions (flux and duration) were constant throughout the experimental time (J_B = 60 L/h m^2 and t_B = 30 s). Although air sparging was not supplied during the filtration phase, it was applied constantly at 3.1 Nm^3/h m^2 during backwashing to improve its efficiency [5].

The bioreactor tank was stirred by air bubbling from the bottom (2.8 Nm^3/h). A compressor also supplied additional air for the biological process, which was automatically controlled. Different aeration frequencies were applied to investigate the effect of DO. Before each test, an initial period of 30 days was necessary for biological acclimation. The aeration intermittence (on min/off min) and the resulting aeration ratios (A_R = aeration time/total cycle time) were 0/60 (A_R = 0), 15/45 (A_R=0.25), 15/15 (A_R = 0.5), 45/15 (A_R = 0.75) and 60/0 (A_R = 1).

2.3. Long-term studies

The effect of bioflocculation on membrane fouling was assessed after long-term tests (130 h) at a constant permeate flux (J = 45 L/h m^2) under different aeration ratios, registering transmembrane pressure as a function of time. Two additional filtration tests were conducted in

sub- and supra-critical conditions ($J = J_c \pm 10$ L/h m^2) at A_R values of 0 and 1, to study fouling mechanisms under different hydrodynamic conditions.

The bioreactor was run at a hydraulic retention time of 8.8 h, without sludge purge except for sampling. In order to keep this time constant and independent of permeate flux, a fraction of permeate was returned to the process tank. During the experimental time, the biological suspension was routinely characterised in order to analyse the influence of changes in microbial suspension on membrane fouling. After each experimental period, the membrane was chemically cleaned by soaking in NaOCl (500 ppm) for 24 h.

2.4. Short-term flux step trials

The modified flux-step method is based on applying successive flux increments up to a maximum, in accordance with the method of Le-Clech et al. (2013) and further improved by incorporating of relaxation steps to reduce the influence of fouling history (Van der Marel et al., 2009). In this study, a modified method is proposed, replacing the relaxation steps by short backwashing cycles at a fixed flux value of 60 L/h m^2, to resemble conventional MBR operation. The other experimental parameters were selected in accordance with previous studies (Gugliemi et al., 2007; Van der Marel et al., 2009): 15 min step duration, a flux-step height of 5 L/h m^2 and maximum flux 70 L/h m^2.

2.5. Analytical methods

Total and soluble chemical oxygen demand (COD and COD_s, respectively), total suspended solids (TSS), mixed-liquor suspended solids (MLSS), mixed-liquor volatile suspended solids (MLVSS), time to filter (TTF) and turbidity were determined in conformity with the Standard Methods (ALPHA, 2005). Ammonia-nitrogen ($N\text{-}NH_3$) analyses were carried out by Nessler's method using a DR-5000 Hach spectrophotometer. Dissolved organic carbon (DOC) concentration was measured with a TOC-meter (TOC-5000A, Shimadzu). The difference in DOC concentration between the filtrate resulting from passing the suspension through a 0.45 µm nitrocellulose membrane filter (HA, Millipore) and the permeate was assigned as biopolymer clusters (BPC). Nitrate-nitrogen ($N\text{-}NO_3^-$) and nitrite-nitrogen ($N\text{-}NO_2^-$) analyses were conducted through ion chromatography using a Compact IC plus 882 device supplied by Metrohm. Microbial floc size distribution was measured by using a Malvern Mastersizer 2000 instrument with a detection range of 0.02-2,000 µm. To quantify supernatant turbidity, biomass samples were centrifuged at 1,300 g for 2 min. Sludge viscosity was determined using the concentric

cylinder rotational viscosimeter Visco Star plus (FungiLab, Spain), at a rotational speed of 60 rpm. Biological activities were measured respirometrically, as described in Kristensen et al., (1992). DO in the bioreactor was measured with an on-line Hach HQ40d oximeter.

3. Results and discussion

3.1. Effect of biological aeration on process performance and sludge characteristics

Table 9.2 summarises process performance and the main sludge characteristics for each aeration ratio (A_R). It should be noted that DO was continuously measured in the tMBR, although only the average daily value has been included in the table. Obviously, a lower aeration ratio decreased average DO values. However, it must be noted that even at A_R = 0 the system presented a low DO which may be a due to air scouring of the membrane and tank stirring with coarse air bubbles.

Mixed-liquor suspended solids concentration (MLSS) remained within a moderate range, despite the system operating at complete sludge retention (i.e. without sludge purge). The reason for this may be related to the severe substrate limitation imposed ($(F/M)_C$ = 2.7-4.6 mg COD/g MLVSS h), whereby microorganisms should preferentially just meet their maintenance energy requirements instead of producing additional biomass (Amanodidou et al., 2015). At the same time, the MLVSS/MLSS ratio remained almost constant (84-86%), indicating there was no significant sludge mineralisation. This is consistent with previous studies, suggesting that MBRs operating for long SRTs develop slow-growing bacteria that can degrade inert substances and avoid significant accumulation in the sludge (Van Loosdrecht et al., 1999). These maintenance conditions were also reflected by the low endogenous specific oxygen uptake rates ($SOUR_e$) (1.1-1.3 mg O_2/g MLVSS h), which were much lower than the typical values of 20-40 mg O_2/g MLVSS h reported for municipal activated-sludge processes (Kristensen et al., 1992). It was also observed that the $SOUR_e$ values were nearly constant, regardless of the aeration ratio applied. This behaviour reveals a close relationship between $(F/M)_c$ and microbial activity, as reported in many studies (Pollice et al., 2004; Díaz et al., 2016). Despite the low bioactivities, the system achieved relatively high COD removal efficiencies (47.2-77.8%), resulting in low permeate COD values (17-48 mg/L). This is in accordance with previous experimental studies (Dalamu et al., 2014; Capodici et al., 2015), where high COD removal efficiencies in MBRs operating at low DO were reported. It should be noted that removal capacity of MBR is not only affected by biological

processes but also by the membrane, which completely retains the particulate and macro-colloidal fraction of the COD.

Table 9.2. Main characteristics of the microbial suspension and treatment performance for each experimental phase

		AERATION RATIO									
		0		0.25		0.5		0.75		1	
Parameter	**Unit**	**Value**	**n**	**Value**	**n**	**Value**	**n**	**Value**	**n**	**Value**	**n**
Biological parameters											
DO	mg O_2/L*	0.09 ± 0.09	-	0.25 ± 0.03	-	0.38 ± 0.18	-	0.62 ± 0.34	-	1.23 ± 0.30	-
F/M_C	mg COD/ g MLVSS h	4.6 ± 0.8	5	3.3 ± 0.7	5	3.2 ± 1.5	4	3.1 ± 0.8	6	2.7 ± 0.9	5
F/M_N	mg N-NH_4^+/g MLVSS h	0.70 ± 0.05	5	0.69 ± 0.1	5	0.71 ± 0.09	4	0.58 ± 0.08	6	0.70 ± 0.15	5
Bioreactor treatment performance											
COD	%	63.7 ± 8.3	5	47.2 ± 6.2	5	62.5 ± 6.6	4	71.2 ± 8.6	6	77.8 ± 6.5	5
NH_4^+	%	37.8 ± 3.3	5	46.1 ± 5.6	5	67.7 ± 2.3	4	97.3 ± 0.9	6	98.5 ± 1.2	5
N_T	%	36.9 ± 8.3	5	24.5 ± 2.3	5	13.0 ± 4.6	4	9.5 ± 0.6	6	8.3 ± 0.6	5
Suspension characterisation											
MLSS	g/L	10.2 ± 0.3	5	9.9 ± 0.7	5	9.7 ± 0.6	4	9.5 ± 0.2	6	6.8 ± 0.8	5
MLVSS/MLSS	%	86 ± 0.3	5	86 ± 0.4	5	86 ± 0.2	4	84 ± 0.9	6	85 ± 1	5
BPC	mg DOC/L	7.7 ± 1.1	5	4.3 ± 2.1	5	1.6 ± 0.4	4	0.5 ± 0.3	6	0.3 ± 0.2	5
Supernatant turbidity	NTU	128 ± 7	5	87 ± 14	4	75 ± 15	4	30 ± 7	4	27 ± 8	6
TTF	s	1,034 ± 66	4	573 ± 170	4	173 ± 25	4	118 ± 30	4	92 ± 36	4
PSD											
$D_{(v,0.1)}$	µm	17 ± 0.9	3	18 ± 1	3	25 ± 2	3	28 ± 1	3	21 ± 4	3
$D_{(v,0.5)}$	µm	48 ± 2	3	49 ± 3	3	72 ± 4	3	76 ± 4	3	86 ± 6	3
$D_{(v,0.9)}$	µm	97 ± 5	3	103 ± 12	3	153 ± 34	3	186 ± 12	3	201 ± 49	3
Apparent viscosity	mPa/s	9 ± 0.2	4	7 ± 0.5	4	6 ± 1	4	5 ± 0.5	4	5 ± 1	4
Biological activity											
$SOUR_e$	mg O_2/g MLVSS h	1.2 ± 0.2	3	1.1 ± 0.2	3	1.2 ± 0.2	3	1.3 ± 0.2	3	1.3 ± 0.1	3
AUR	mg N/g MLVSS h	1.8 ± 0.4	3	1.9 ± 0.2	3	1.3 ± 0.3	3	1.9 ± 0.1	3	1.4 ± 0.1	3
NIUR	mg N/g MLVSS h	3.4 ± 1	3	4.3 ± 0.4	3	3.8 ± 0.4	3	3.4 ± 0.8	3	5.6 ± 0.4	3
NUR	mg N/g MLVSS h	0.8 ± 0.4	3	0.5 ± 0.1	3	0.4 ± 0.1	3	0.3 ± 0.1	3	0.3 ± 0.1	3

(*): arithmetic mean of the average daily values

Regarding ammonia and nitrite/nitrate removal, different biological processes were observed according the A_R applied (Table 9.2). Whereas complete nitrification (<1.5 mg N-NH_4^+/L in the permeate) was observed at aeration ratios above 0.75, the lower ratios induced only partial nitrification and ammonia removal efficiencies decreased to 38-46 %. Furthermore, in these low DO conditions, nitrate concentration decreased below 30 mg N/L and hence a process of simultaneous nitrification and denitrification was most likely occurring (Dalamu et al., 2014). Maximum nitrification/denitrification activity was also evaluated by means of batch tests in the laboratory. However, the results revealed that the ammonia and nitrite uptake rates (AUR and

NIUR, respectively) were not significantly influenced by A_R. Therefore, it seems that AUR and NIUR are only related to the imposed ammonium feed to microorganism ratio, $(F/M)_N$. Moreover, denitrification capability (measured by maximum nitrate uptake rates, NUR) only slightly increased with decreasing A_R.

Sludge bioflocculation was evaluated in terms of biopolymeric clusters concentration (BPC), supernatant turbidity, floc size distribution, sludge filterability and viscosity (Table 9.2). During bioflocculation, microorganisms partly consume soluble biodegradable pollutants and excrete polymers that induce flocculation of colloidal and suspended feedwater particles (Faust et al., 2014). However, as reported in previous studies (e.g. Drews, 2007), low DO concentration may negatively affect the biomass flocculation ability. This was reflected in the BPC concentration, whose value increased with decreasing DO. In fact, net BPC release is a common response of microorganisms to environmental stresses such as a very low DO (Lin et al., 2014). This poor flocculation is consistent with the high supernatant turbidity detected at low aeration ratios. Furthermore, the sludge bioflocculation state can also be seen as a function of microbial floc size distribution. At high aeration ratios, the sludge was mainly composed of large flocs ($D_{(v,0.5)}$=86 µm) whose sizes tended to decrease with lowering A_R. Consistent with this, adequate sludge bioflocculation may enhance sludge filterability (as confirmed by TTF measurements) and lower the apparent viscosity.

3.2. Determination of critical flux for compressibility: effect of sludge bioflocculation

A widely accepted recommendation for determining design flux in the field of MBRs is the critical flux concept (J_C), generally considered as the flux level above which particles and colloids are deposited on the membrane surface (e.g. Bacchin et al., 2006). This approach is based on incompressible cake formation mechanism, assuming a constant fouling rate (i.e. *TMP* slope), which is also used to establish the critical flux (Le-Clech et al., 2003). However, a deeper analysis shows that under most operating conditions the fouling rate may increase with elapsed time, corresponding to the build-up of a compressible cake layer (Jørgensen et al., 2014; Bugge et al., 2012; Diez et al., 2014). It is evident that under these conditions, fouling not only depends on deposition rate (i.e. on filtration flux), but also on the cake previously deposited and the actual *TMP* applied. In this sense, the "critical mass" concept can be assumed valid, defined as the specific mass deposited onto the membrane that induces incipient cake consolidation, in accordance with previous studies (McAdam and Judd, 2008; Bessiere et al., 2005). As a result,

the cake compression effect is correlated with the critical value for compressibility, defined as the filtration flux when the transition takes place between an initial low *TMP*-rise region and a second period of sharp *TMP*-rise.

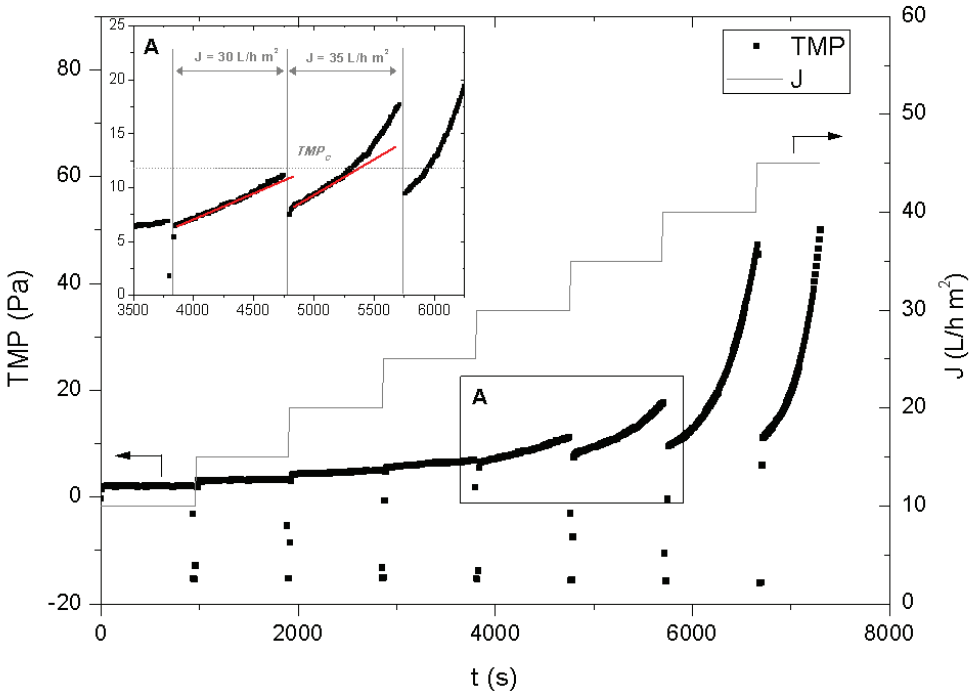

Figure 9.1. Flux and TMP profiles during flux step trials; A_R=0.5; t_B=30s; J_B=60L/hm^2; t_F=900s

Figure 9.1 shows the typical flux and *TMP* profiles during critical flux testing with intermediate backwashing steps. Different *TMP* profiles during the filtration steps can be observed below and above the critical flux for compressibility, which has been identified at 35 L/h m^2. At this flux, the transition between low and sharp *TMP*-rise regions defined a critical transmembrane pressure (TMP_{crit}). Similarly, for the different A_R applied, assessment of the critical fluxes for compressibility (J_c) indicated that sludge properties had a great influence on filtration performance (Figure 9.2). It can be seen that J_c increased from 15 to 55 L/h m^2 for an A_R increase from 0 to 1. However, while TMP_{crit} and J_c increased according to the selected value of A_R, a similar cake fouling resistance of $3.5 \cdot 10^{11} \pm 0.2 \cdot 10^{11}$ (5.9%) 1/m was obtained in all cases. This was calculated by using the resistance-in-series model (Eq. 9.1):

$$TMP_{cri} = J_c \cdot \mu \cdot R_t = J_c \cdot \mu \cdot \left(R_m + R_{fcri}\right) \quad [9.1]$$

where μ is the permeate viscosity, J_c is the critical flux, R_t is the total hydraulic resistance, R_m is the clean membrane resistance and R_{fcrit} is the cake fouling resistance at critical conditions.

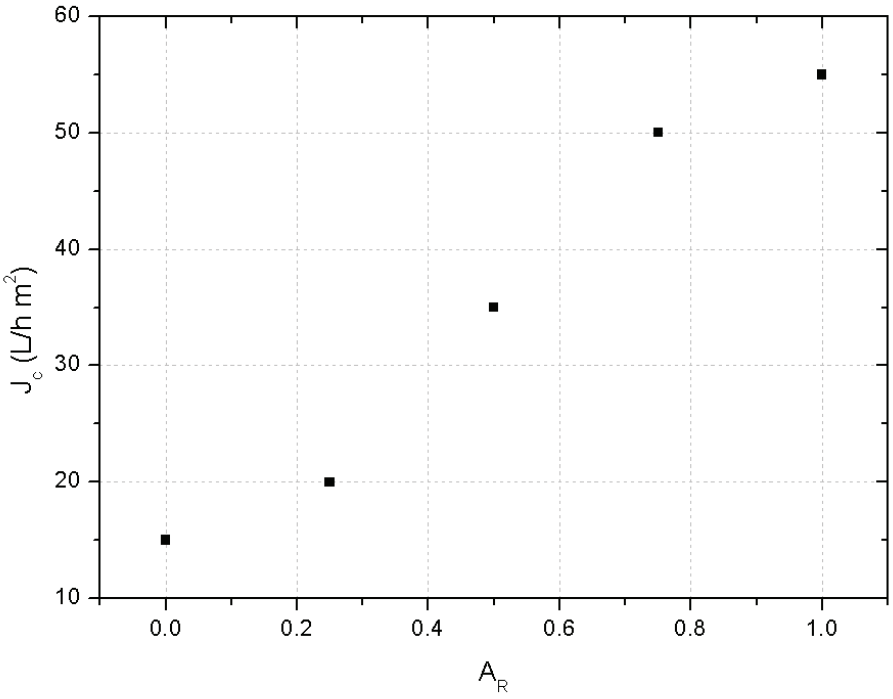

Figure 9.2. Critical flux against aeration ratio

Since cake resistance is proportional to the specific cake resistance and the solid content in the cake per unit membrane area (e.g. Kim et al., 2009), it is evident that the critical conditions not only depend on the mass deposited (i.e. permeate flux, bulk solids concentration and filtration time in dead-end operation) but also on its specific cake resistance. In fact, critical mass (M_{crit}=J_c·MLSS·t_{crit}) increased from 9.9 g/m^2 to 63.8 g/m^2 during an A_R increase from 0 to 1. In addition, results are consistent with those reported by Bessiere et al. (2005) which showed that the accumulated mass in critical conditions is directly related to the suspension characteristics. Consequently, since the specific resistance decreases with larger floc size and lower biopolymer content (Charfi et al., 2015; Meng et al., 2009), greater fluxes are required to reach the critical conditions as A_R rises.

3.3. Fouling analysis during long-term tests

Fouling deposition and reversibility were assessed for the different A_R values at sub- and supra-critical filtration fluxes (15, 25, 45 and 65 L/h m^2) in dead-end operation with backwashing aided by air-scouring (J_B=60 L/h m^2, t_B=30 s, SAD_m=3.1 Nm^3/h m^2). In order to investigate the dynamic behaviour of cake compression under consecutive filtration/backwashing cycles, a transmembrane pressure set-point (TMP_{sp}) of 30 kPa (corresponding to $3.5 \cdot 10^{12}$, $1.7 \cdot 10^{12}$ and $9.3 \cdot 10^{11}$ 1/m, for the respective applied filtration fluxes) was selected for these trials, higher than those for TMP_{crit} determination.

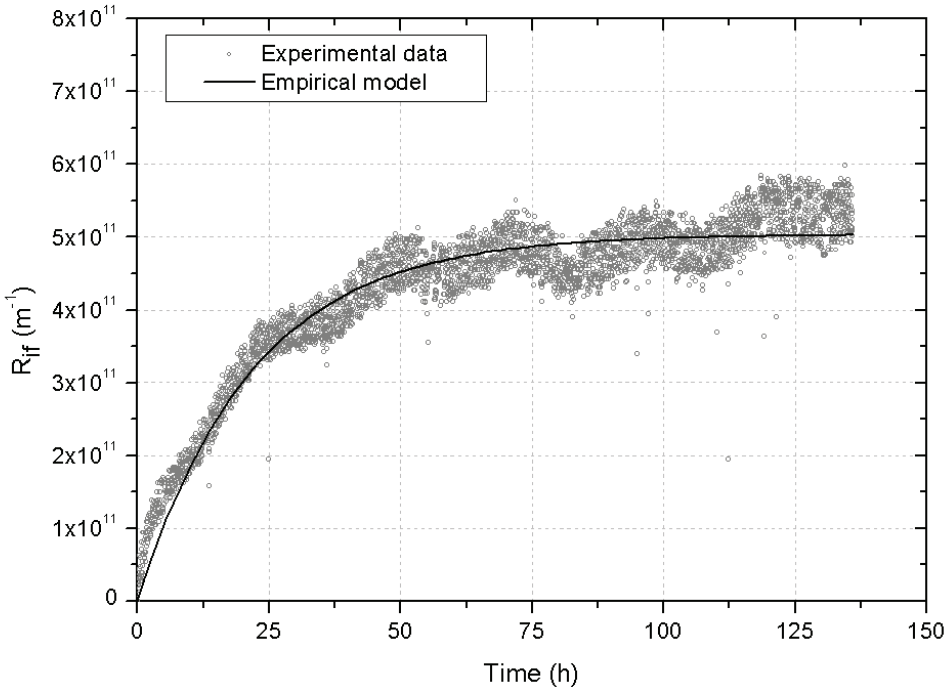

Figure 9.3. Adjustment of experimental data to the internal residual fouling resistance during a long-term test (A_R=0; J=45L/hm^2)

3.3.1. Influence of bioflocculation on residual fouling

Internal residual fouling has been defined as the fouling that is not completely detached from the membrane by physical means (Drews et al., 2010). Therefore, during membrane operation, the internal residual fouling resistance (R_{if}) is linked to the *TMP* at the beginning of the filtration phase after backwashing (TMP_i) (Vera et al., 2015):

$$TMP_i = J \cdot \mu \cdot \left(R_m + R_{if}\right) \quad [9.2]$$

Table 9.3. Empirical parameters of the residual fouling model under each set of filtration conditions assayed.

A_R	Flux (L/hm^2)	$(R_{if})_{asym}$ ·10^{-11} (m^{-1})	k_c ·10^{-2} (1/h)	r_{if} ·10^{-8} (1/m h)	R^2
0	15	5.10 ± 0.24	2.71 ± 0.29	20.1 ± 4.4	0.85
0	25	6.23 ± 0.67	3.37 ± 0.11	13.3 ± 3.8	0.85
0	45	5.03 ± 0.01	4.55 ± 0.03	14.7 ± 4.3	0.92
0.25	45	5.43 ± 0.06	4.40 ± 0.02	9.6 ± 2.7	0.91
0.5	45	5.83 ± 0.02	5.38 ± 0.14	5.0 ± 1.1	0.95
0.75	45	5.28 ± 0.03	4.50 ± 0.12	15.6 ±1.1	0.89
1	65	5.22 ± 0.02	2.24 ± 0.01	14.4 ± 4.2	0.87
1	45	5.56 ± 0.04	5.77 ± 0.31	4.3 ± 2.2	0.95

As an example, Figure 9.3 shows the typical variation in R_{if} during a long-term test (A_R=0 and J=45 L/h m^2). An identical trend was obtained for all the tests, where most of the fouling was observed during the first 25-50 h until reaching a similar asymptotic value $(R_{if})_{asym}$ (Table 9.3). Then, R_{if} increased at very slow rates (r_{if}), which seem to be independent of the filtration flux or the sludge bioflocculation. It should also be noted that this R_{if} profile is similar to that previously reported for MBRs with TMP_{sp} backwashing initiation (Vera et al., 2015, Vera et al., 2014). These studies supported the hypothesis that the internal residual fouling attained with this operation mode may be predominantly related to a consolidated cake layer formed during the initial filtration/backwashing cycles. Other fouling phenomena, such as solute adsorption and pore blocking, seem to have a negligible role. Consistently with this, the $(R_{if})_{asym}$ value obtained (5.5·10^{11}±0.4·10^{11} 1/m) is the same order of magnitude as the R_{fcrit} determined in flux-step trials. Hence, an empirical model can be applied to describe the fouling behaviour with reasonable accuracy (R^2 of 0.91±0.04) (Table 9.3). This model assumes the consolidation process is a partial reduction of the available membrane area at a rate proportional to its current value and a kinetic constant k_c, as seen in Eq. 9.3. While the first term of the equation describes the sharp

increase in internal residual fouling until reaching an asymptotic value (i.e. initial period), the second term considers the slow R_{if} rise (i.e. stationary period).

$$R_{if} = \left(R_{if}\right)_{asym}[1 - exp(-K_c t)] + r_{if} t \quad [9.3]$$

where *t* is the operation time.

The results shown that backwashing efficiency was not significantly affected by permeate flux or sludge bioflocculation. Hence, once the system reached steady-state conditions, the backwashing was effective in removing the particle deposit, even while filtering poorly flocculated suspensions. In addition, these values were significantly lower than those typically found for full-scale MBRs (Drews, 2010), reflecting a high backwashing efficiency. This seems contrary to the results of other studies where residual fouling increased with a reduction of DO in an MBR with temporised filtration/backwashing cycles (e.g. Dalmau et al., 2014). These discrepancies may be because the system automatically adjusts backwashing frequency to a preselected TMP_{sp}, which will determine the degree of membrane fouling allowed, regardless of sludge filterability. Therefore, this operation mode allows a stable backwashing efficiency to be achieved. Consequently, the experimental backwashing frequencies decreased from 0.76 to 0.06 1/min when A_R increased from 0 to 1. In addition, it is also assumed that the filtration conditions (dead-end and relatively high filtration fluxes) may be related to the formation of a cake layer on the membrane, which acts as a secondary membrane. This could prevent BPC from blocking membrane pores or adsorbing onto the membrane surface, thus enhancing backwashing efficiency (Hwang et a., 2009).

In the present study, the reported cake consolidation induced a progressive decrease in the available membrane area for filtration. Assuming stationary conditions were reached after 80 h operation, the local flux $(J')_{t=80}$ increased and can be related to the loss of effective area due to residual fouling, through the Eq. 9.4:

$$(J')_{t=80} = \frac{(TMP_i)_{t=80}}{TMP_i} \cdot J \quad [9.4]$$

where $(TMP_i)_{t=80}$ is the *TMP* at the beginning of the filtration cycle after 80 h of operation.

3.3.2. Effect of bioflocculation on reversible fouling and critical flux conditions

As previously mentioned, in the given conditions, reversible fouling is associated with mechanisms of cake development on the membrane wall, where the pressure drop over the cake layer (ΔTMP_C), can be written as Eq. 9.5 (Sørensen and Sørensen, 1997):

$$\Delta TMP_c = \mu \cdot \alpha \cdot \omega \cdot J^2 \cdot t \qquad [9.5]$$

where α is the specific cake resistance, ω is the solid concentration in the cake per unit filtrate volume and t is the elapsed time.

For compressible particles, α increases with *TMP.* Several expressions have been proposed to model it. A linear relationship (Eq. 9.6) has often been identified for compressible cakes when filtering microbial suspensions (Bugge et al., 2012):

$$\alpha = \alpha_0 \left(1 + \frac{\Delta TMP_c}{P_a}\right) \qquad [9.6]$$

where α_0 is the specific cake resistance at zero pressure and P_a is a characteristic pressure related to the compression effect.

Figure 9.4 shows *TMP* profiles during consecutive filtration/backwashing cycles for two different A_R values. For both conditions, filtration lengths suddenly decreased during the early cycles of the tests (first 25-50 h of operation), corresponding to the increase in the internal residual fouling. As cake consolidation reduces the available membrane area, residual fouling and filtration length may well be closely related. Once steady-state conditions were reached, a stabilised filtration length was achieved, which was significantly affected by aeration ratio. In fact, a sustainable value (16 min) was observed for the higher aeration ratio, whereas this value decreased to a non-operative level (1.3 min) for the lower ratio. Although it is generally accepted that the sludge particle size can influence specific cake resistance (e.g. Foley, 2006), different cake compressibility should be also expected (Jørgensen et al., 2014) and could explain the differences between the filtration length values. This approach was confirmed by assessing the experimental data in terms of the compressible cake layer model (Eqs. 9.5; 9.6). Figure 9.5 shows the plot of α values (assuming that ω is similar to suspended solids concentration in bulk

suspension) for different A_R values. Linearity of α data against ΔTMP_c for all conditions suggests a reasonable accuracy of the model.

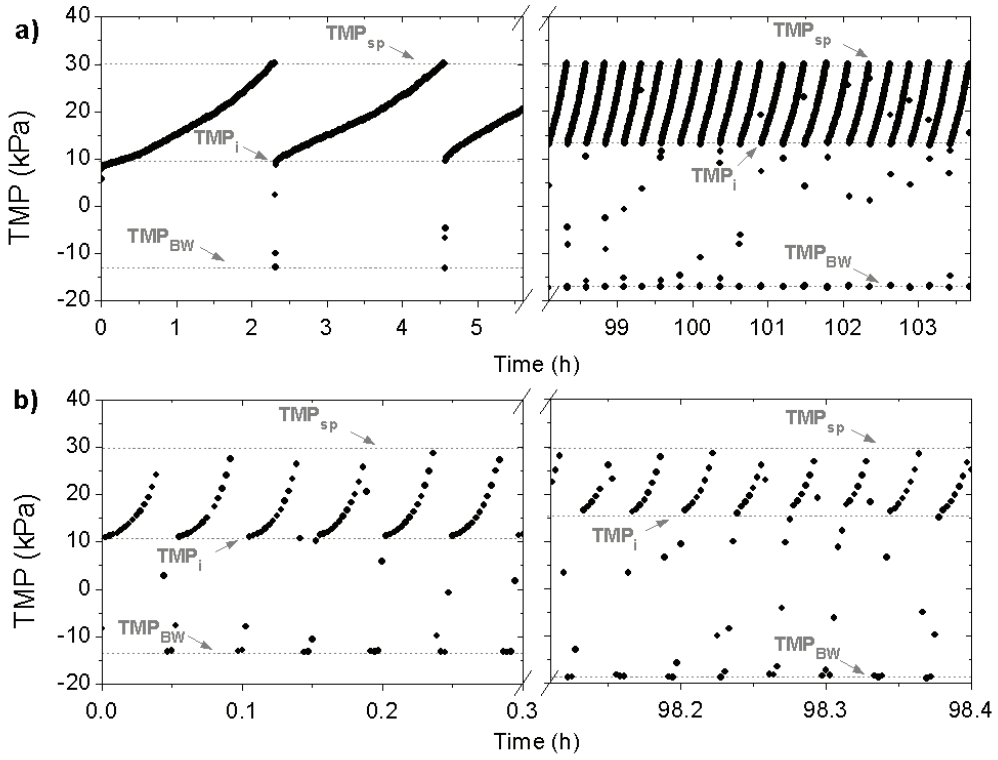

Figure 9.4. Typical TMP profiles during initial and stationary period: a) A_R=1; b) A_R=0. Experimental conditions: J=45 L/hm^2; J_B=60 L/hm^2; t_B=30s

Table 9.4 summarises specific cake resistances at zero pressure and characteristic pressures related to the compression effect for the different A_R. Specific cake resistances were within the typical range of 10^{12}-10^{13} m/kg reported for cake layers attached to the membrane, measured and subjected to a similar *TMP* range [32, 42]. However, decreasing A_R induced a severe cake resistance increase, about one order of magnitude. The small dispersed particles were expected to form a more closely packed structure offering strong resistance [17]. Indeed, α_0 decreased roughly linearly (R^2=0.65) against the square of $D_{(v,0.5)}$, as predicted from the Carman-Kozeny equation [41]. Nevertheless, a higher correlation (R^2=0.98) was found for biopolymeric clusters, a crucial factor regulating α_0. Two phenomena have been reported in the literature to characterise this behaviour: a reduction in cake-layer porosity (Charfi et al., 2015) and an increase in specific cake resistance due to an osmotic pressure mechanism (Chen et al., 2012).

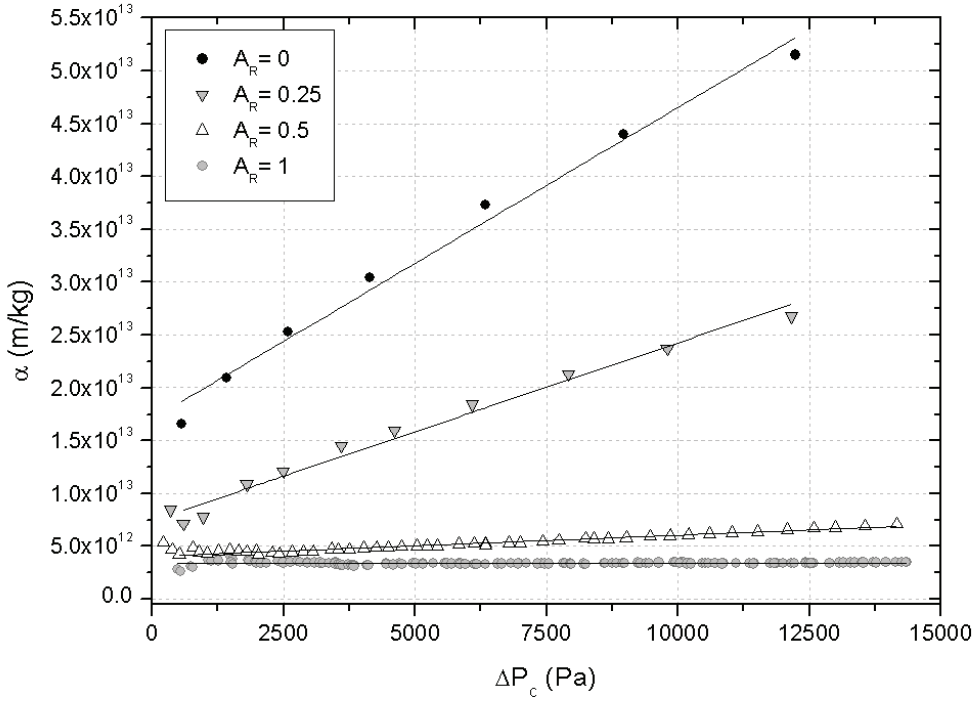

Figure 9.5. Evolution od specific cake resistance as function of pressure drop across the cake during a cycle of the stationary period at different aeration ratios, A_R. (J=45L/hm^2; J_B=60L/hm^2; t_B=30s)

In contrast, *BPC* and $D_{(v,0.5)}$ did not exert a significant influence on the characteristic pressure related to the compression effect. In fact, cake compressibility was closely linked with filtration conditions, where low P_a values (i.e. a noticeable compression effect) were obtained at supra-critical fluxes (Table 9.4). Therefore, the long-term tests confirmed the results reported in short-term flux step trials, where the compressibility of the cake layer increased at supra-critical conditions. Additional tests conducted for A_R values of 0 and 1 at different permeate fluxes confirmed this approach. At A_R=1, increasing permeate flux up to a supra-critical value of 65 L/h m^2 led to a similar value of α_0 but an abrupt decrease in P_a, reflecting a high degree of cake compressibility at this flux. Similarly, at A_R=0, a permeate flux decrease from a supra-critical to a critical value (15 L/h m^2) induced the formation of an incompressible cake layer. Therefore, the results show that bioflocculation may have a direct impact on cake resistance and an indirect effect—also depending on filtration conditions—on cake compressibility.

Table 9.4. Parameters of the compression model for cake build-up under each set of filtration conditions assayed.

A_R	Filtration conditions	Flux (L/h m^2)	$\alpha_o \cdot 10^{-12}$ (m/kg)	Pa (Pa)
0	Supra-critical	45	23.9 ± 0.9	11,622 ± 1000
0.25	Supra-critical	45	13.2 ± 0.2	10,265 ± 376
0.5	Supra-critical	45	4.6 ± 0.6	29,600 ± 634
0.75	Sub-critical	45	2.3 ± 0.3	406,000 ± 2,000
1	Sub-critical	45	3.4 ± 0.2	347,000 ± 3,000
1	Supra-critical	65	3.5 ± 0.6	2,210 ± 675
0	Supra-critical	25	11.4 ± 0.6	10,500 ± 400
0	Critical	15	32.1 ± 0.2	453,000 ±1,400

3.4. Optimisation of the biological aeration ratio

This section aims at selecting the most appropriate aeration ratio in terms of specific energy demand (*SED*). This is determined by a classic trade-off problem: high ratios are desirable to enhance process productivity by increasing the critical flux and decreasing membrane cleanings. However, this involves a higher energy demand associated with biological aeration. Process productivity was assessed by determining the net permeate flux (J_{net}), calculated as an average during the last 24 h of the stationary period:

$$J_{net} = \frac{t_F \cdot J - t_B \cdot J_B}{t_B + t_F} \quad [9.7]$$

where J_B is the backwashing flux, t_B and t_F are the duration of the backwashing phase and the average duration of the filtration phase, respectively.

It should be noted that the system was operated without air scouring, so air is only supplied during the backwashing. Therefore, the net specific aeration demand of membrane filtration

was only linked to the backwashing phase (SAD_{pnet}). Table 9.5 summarises t_F, J_{net} and SAD_{pnet} values for the different A_R applied. It can be seen that low aeration ratios ($A_R \leq 0.25$) led to short filtration lengths (i.e. high backwashing frequencies), which resulted in a loss of process productivity and high values of SAD_{pnet} (Table 9.5). Nevertheless, at moderate to high ratios, the system achieved high productivity (J_{net}>40 L/h m^2) and the SAD_{pnet} was significantly low (2.1–3.9 Nm^3 air/m^3 permeate), compared with those found in full-scale plants with intermittent aeration during the filtration phase (Krseminski et al., 2012).

Table 9.5. Filtration length, net permeate flux and specific aeration demand for each aeration ratio (J=45 L/h m^2).

Frequency	t_f (min)	J_{net} (L/h m^2)	SAD_{pnet} (Nm$^3_{air}$/Nm$^3_{permeate}$)
0	1.30 ± 0.09	15.9 ± 1.5	57.9 ± 0.1
0.25	2.09 ± 0.14	24.7 ± 1.1	25.9 ± 0.1
0.5	10.20 ± 0.51	40.1 ± 0.2	3.9 ± 0.5
0.75	15.35 ± 0.52	41.2 ± 0.3	2.5 ± 0.5
1	18.63 ± 0.53	42.2 ± 0.1	2.1 ± 0.5

The optimal conditions were assessed by specific energy demand (*SED*) determination. These values was calculated by the addition of the energy consumption of the air blowers (W_G) required for biological processes and backwashing, and for the permeate pump (W_J). Both energy consumptions were calculated by applying Eqs. 9.8-9.9 (Judd et al., 2011):

$$W_G = \frac{R \cdot T \cdot \lambda}{1.63 \cdot 10^5 \cdot \zeta_c \cdot (\lambda - 1)} \cdot \left[\left(\frac{P_{A2}}{P_{A1}} \right)^{1-\frac{1}{\lambda}} - 1 \right] \cdot Q_A \qquad [9.8]$$

$$W_P = \frac{Q_p \cdot TMP}{1000 \cdot \zeta_p} \quad [9.9]$$

where R is the gas constant, T is air temperature, P_{A1} is the absolute inlet pressure, P_{A2} is the absolute outlet pressure, λ is the adiabatic index, Q_A is the volumetric air flow rate for biological or membrane processes, Q_P is the volumetric permeate flow rate, ζ_p is the pump efficiency and ζ_c is the blower efficiency. Therefore, *SED* can be defined as Eq. 9.10:

$$SED = \frac{W_J + W_G}{J_n \cdot A} \quad [9.10]$$

where J_{net} is the net permeate flux and A is the membrane filtration area.

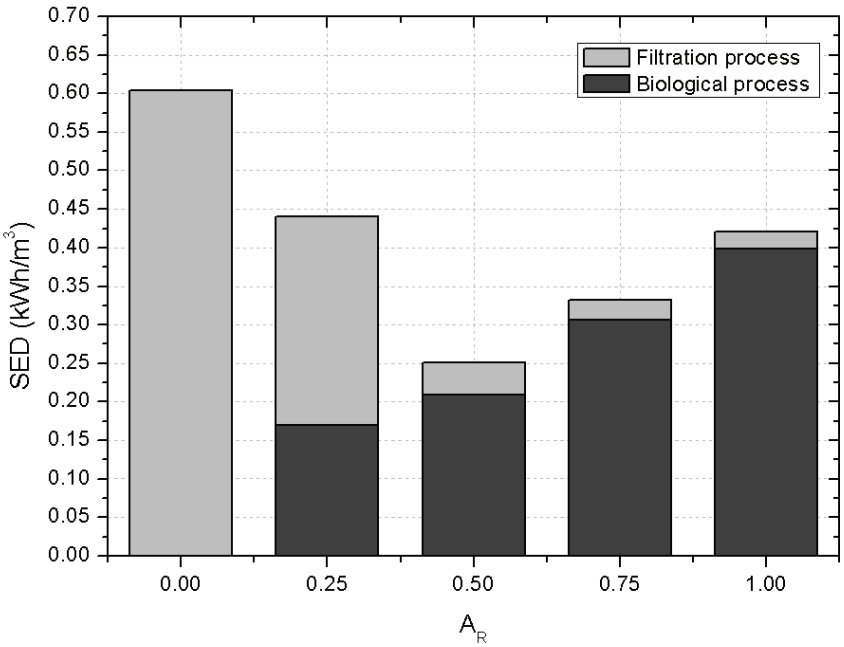

Figure 9.6. Estimated specific energy demand (SED) associated with aeration in biological and filtration process against different biological aeration frequency (J=45L/hm^2)

The results indicated the minimum value of *SED* (0.25 kWh/m^3) was achieved at moderate A_R (Figure 9.6). When the aeration ratio decreased below 0.5, the significant increase in reversible fouling led to more frequent backwashing, which resulted in a higher SED due to the

filtration process. In contrast, when the aeration ratio increased above 0.5, the energy demand associated with filtration became less significant (5-16%) compared with that of biological aeration.

4. Conclusions

This study has examined the effectiveness of a backwashing initiation strategy based on *TMP* set-point for fouling limitation in a tertiary membrane bioreactor operated at low DO, concluding the following:

- The tertiary MBR achieved high organic matter removal (47-78 % for COD) at low DOs (0.09-1.23 mg/L). In addition the nitrification process was maintained at a reasonable level with an ammonium removal rate ranging within 38-46%, even at very low values of DOs (0.09-0.25 mg/L). In contrast, bioflocculation was negatively affected at $[O_2] \leq 0.25$ mg/L, resulting in high values of biopolymeric clusters concentration (BPC ≥ 4.3mg DOC/L), small floc sizes ($D_{(v,0.5)} \leq 49$ µm), poor filterability (TTF ≥ 573 s) and low critical fluxes ($J_c \leq 20$ L/h m^2). However, above moderate concentrations ($[O_2] \geq 0.38$ mg/L), sludge bioflocculation significantly increased, showing good filterability (TTF ≤ 173 s) and relatively high critical fluxes ($J_c \geq 45$ L/h m^2)

- The backwashing mode based on transmembrane pressure set-point (TMP_{sp}) has shown to be highly effective in residual fouling control, automatically increasing backwashing frequency as sludge bioflocculation decreased. As a consequence, the residual fouling resistance observed was similar, regardless of the bioflocculation state or the permeate flux assayed. Furthermore, this trend has been well described by an empirical model that assumes that fouling gradually reduces the available membrane area until it reaches a quasi-stationary value.

- Analysis of the reversible fouling showed compressible cake build-up behaviour, where biopolymeric clusters were a crucial factor regulating the specific cake resistance at zero pressure. In contrast, compressibility was determined by filtration conditions, whereby the compressibility of the cake layer increased at supra-critical fluxes.

- Optimal conditions can be established at moderate DO ($[O_2] = 0.38$ mg/L) due to the low specific energy demand by the filtration process and biological aeration (SED = 0.25 kWh/m^3) and a high permeate net flux (J = 42.2 L/h m^2 on average).

5. References

Amanadidou E., Samiotis G., Bellos D., Pekridis G., Trikoilidou E., Net biomass production under complete solids retention in high organic load activated sludge process, *Bioresour. Technol*., 182, (2015), 193-199.

American Public Health Association, Water Environment Federation, Standard Methods for the examination of Water and Wastewater, 21stedition, Washington DC, USA, 2005.

Bacchin P., Aimar P., Field R.W., Critical and sustainable fluxes: Theory, experiments and applicaions, *J. Memb, Sci*., 281, (2006), 42-69.

Bessiere Y., Abidine N., Bacchin P., Low fouling conditions in dead-end filtration: evidence for a critical filtered volume and interpretation using critical osmotic pressure, *J. Membr. Sci*., 264, (2005), 37–47.

Bugge T.V., Jørgensen M.K., Christensen M. L., Keiding K., Modeling cake buildup under TMP-step filtration in a membrane bioreactor: Cake compressibility is significant. *Water Research*, 46, (2012), 4330-4338.

Capodici M., Di Bella G., Di Trapani D., Torregrossa M., Pilot scale experiment with MBR operated in intermittent aeration condition: Analysis of biological performance, *Bioresour. Technol*., 177, (2015), 398-405.

Charfi A., Yang Y., Harmand J., Ben Amar N., Heran M., Grasmick A., Soluble microbial products and suspended solids influence in membrane fouling dynamics and interest of punctual relaxation and/or backwashing, *J. Membr. Sci.,* 475, (2015), 156-166.

Chen J., Zhang M., Wang A., Lin H., Hong H., Lu X., Osmotic pressure effect on membrane fouling in a submerged anaerobic membrane bioreactor and its experimental verification, *Bioresour. Technol*., 125, (2012), 97-101.

Cote P. , Alam Z., Penny J., Hollow fiber membrane life in membrane bioreactors (MBR), *Desalination,* 288, (2012), 145-151.

Dalmau M., Monclús H., Gabarrón S., Rodriguez-Roda I., Comas J.. Towards integrated operation of membrane bioreactors: Effects of aeration on biological and filtration performance. *Bioresour. Technol.,* 171, (2014), 103-112.

Delgado S., Alvarez M., Aguiar E., Rodríguez-Gómez L. E., H_2S generation in a reclaimed urban waste water pipe. Case study: Tenerife (Spain), *Water Res.,* 33 (2), (1999), 539.

Díaz O., Vera L., González E., García E., Rodríguez-Sevilla J., Effect of sludge characteristics on membrane fouling during star-up of a tertiary submerged membrane bioreactor, *Environ. Sci. Pollut. Res*., 23(9), (2016), 8951-8962.

Diez V., Ezquerra D., Cabezas J.L., García A., Ramos C., A modified method for evaluation of critical flux, fouling rate and in situ determination of resistance and compressibility in MBR under different fouling conditions, *J. Membr. Sci.,* 453, (2014), 1-11.

Directive 2000/60/EC of the European Parliament and of the Council of 23 October 2000 establishing a framework for the Community action in the field of water policy, J. Eur. Communities (December (22)) (2000) 1–72.

Drews A., Mante J., Iversen V., Vocks M., Lesjean B., Kraume M., Impacts of ambient conditions on SMP elimination and rejection in MBRs, *Water Res*., 41, (2007), 3850-3858.

Drews A., Membrane fouling in membrane bioreactors—characterisation, contradictions, causes and cures, *J. Membr. Sci*., 363, (2010), 1–28.

Faust L., Temmink H., Zwijnenburg A., Kemperman A.J.B., Rijnaarts H.H.M., Effect of dissolved oxygen concentration on the bioflocculation in high loaded MBRs, *Water Res*., 66, (2014), 199-207.

Ferrero G., Rodriguez-Roda I., Comas J., Automatic control systems for submerged membrane bioreactors: a state-of-the-art review, *Water Res*. 46, (2012), 1–13.

Foley G., A review of factor affecting filter cake properties in dead-end microfiltration of microbial suspensions, *J. Membr. Sci*., 274, (2006), 38-46.

Gao D., Fu Y., Tao Y., Li X., Xing M., Gao X., Ren N., Linking microbial community structure to membrane biofouling associated with varying dissolved oxygen concentrations. *Bioresour. Technol*., 102, (2011), 5626-5633.

Guglielmi G., Chiarani D., Judd S. J., Andreottola G., Flux criticality and sustainability in a hollow fibre submerged membrane bioreactor for municipal wastewater treatment, *J. Membr. Sci*., 289, (2007), 241–248.

Hwang K., Chan C., Tung K., Effect of backwash on the performance of submerged membrane filtration, *J. Membr. Sci.*, 330, (2009), 349–356.

Jørgensen M. K., Keiding K., Christensen M. L., On the reversibility of cake buildup and compression in a membrane bioreactor, *J. Memb, Sci.*, 455, (2014), 152-161.

Judd S., The MBR Book: Principles and Applications of Membrane Bioreactors for Water and Wastewater Treatment, Elsevier, Oxford, 2011.

Kim J., DiGiano F.A., Fouling models for lo-pressure membrane system, *Sep. Purif. Technol*., 68, (2009), 293-304.

Koch Membrane, Case Study. Aquapolo Ambiental Water Reuse Project. (2014) (http://www.kochmembrane.com/PDFs/Case-Studies/KMS-Sao-Paulo-Brazil-Case-Study.aspx)

Kristensen G. H.., Jørgensen P. E., Henze M., Characterization of functional microorganism group and substrate in activated sludge and wastewater by AUR, NUR and OUR, *Wat. Sci. Technol*., 25 (6), (1992), 43-57.

Krzeminski P., van der Graaf J.H.J.M., van Lier J.B., Specific energy consumption of membrane bioreactor (MBR) for sewage treatment*, Water Sci. Technol*., 65, (2012), 380–392.

Le-Clech P., Jefferson B., Chang I., Judd S., Critical flux determination by the flux-step method in a submerged membrane bioreactor, *J. Membr. Sci*., 227, (2003), 83–91.

Lin H., Zhang M., Wang F., Meng F., Liao B., Hong H., Chen J., Gao W., A critical review of extracellular polymeric substances (EPSs) in membrane bioreactor: characteristics, roles in membrane fouling and control strategies. *J. Membr. Sci*., 460, (2014), 110-125.

McAdam E.J., Judd S.J., Optimization of dead-end filtration conditions for an immersed anoxic membrane bioreactor, *J. Membr. Sci.,* 325, (2008), 940–946.

Meng F., Chae S.R., Drews A., Kraume M., Shin H.S., Yang F., Recent advances in membrane bioreactors (MBRs): Membrane fouling and membrane material, *Water Res.,* 43, (2009), 1489-1512.

Pollice A., Laera G., Blonda M., Biomass growth and activity in a membrane bioreactor with complete sludge retention, *Water Res.*, 38, (2004), 1799–1808.

Sørensen B.L., Sørensen P.B., Structure compression in cake filtration, *J. Environ. Eng*., 123, (1997), 345-353.

Van der Marel P., Zwijnenburg A., Kemperman A., Wessling M., Temmink H., van der Meer W., An improved flux-step method to determine the critical flux and the critical flux for irreversibility in a membrane bioreactor, *J. Membr. Sci.,* 332, (2009), 24–29.

Van Loosdrecht M., Henze M., Maintenance, endogenous respiration, lysis, decay and predation, *Water Sci. Technol*., 39, (1999), 107–117.

Vera L., González E., Díaz O., Delgado S., Application of backwashing strategy based on transmembrane pressure set-point in a tertiary submerged membrane bioreactor, *J. Membr. Sci*., 470, (2014), 504-512.

Vera L., González E., Díaz O., Sánchez R., Bohorque R., Rodrígez-Sevilla J., Fouling analysis of a tertiary submerged membrane bioreactor operated in dead-end mode at high-fluxes, *J. Membr. Sci.,* 493, (2015), 8-18.

Wang X-M., Li X-Y., Huang X., Membrane fouling in a submerged membrane bioreactor (SMBR): Characterisation of the sludge cake and its high filtration resistance, *Sep. Purif. Technol*., 52, (2007), 439–445.

Wang Z., Ma J., Tang C.Y., Kimura K., Wang Q., Membrane cleaning in membrane bioreactors: a review, *J. Membr. Sci*., 468, (2014), 276–307.

Wibisono Y., Cornelissen E.R., Kemperman A.J.B., van de Meer W.G.J., Nijmeijer K., Two-phase flow in membrane processes: a technology with a future, *J. Membr. Sci*., 463, (2014), 566–602.

Wilén B-M., Balmé P., The effect of dissolved oxygen concentration on the structure, size and size distribution of activated sludge flocs, *Water Res.,* 33, (1999), 391-400.

Ye Y., Chen V., Le-Clech P., Evolution of fouling deposition and removal on hollow fibre membrane during filtration with periodical backwash, *Desalination*, 283, (2011), 198–205.

CAPÍTULO 10: Resultados y discusión general

1. Características de la biomasa y rendimiento de depuración en un biorreactor de membrana terciario
   1.1. Condiciones de operación con limitación de sustrato. Desarrollo de la biomasa
   1.2. Características de la biomasa. Influencia de las condiciones de operación
   1.3. Rendimiento de depuración
   1.4. Influencia de las características de la suspensión sobre el ensuciamiento de la membrana
2. Tratamientos terciarios con membranas sumergidas: Ultrafiltración directa versus Biorreactores de membrana
   2.1. Estudio comparativo de los distintos tratamiento terciarios
   2.2. Influencia del tipo de tratamiento terciario sobre los post-tratamientos de afino
   2.3. Eliminación de contaminantes emergentes
3. Estudio de las condiciones de operación para un ensuciamiento mínimo. Determinación del flujo crítico
   3.1. Análisis del flujo crítico en función de la velocidad y compresibilidad del ensuciamiento
   3.2. Análisis del flujo crítico en función de la reversibilidad del ensuciamiento
4. Control del ensuciamiento. Modo de operación por presión de consigna.
   4.1. Análisis comparativo entre el modo de operación por presión de consigna y el modo convencional temporizado
   4.2. Validación del modo de operación por presión de consigna a elevados flujos de operación
   4.3. El ensuciamiento máximo permitido. Influencia de la presión transmembrana de consigna
   4.4. Filtración frontal. Influencia de los flujos de filtración y retrolavado
   4.5. Influencia de la suspensión biológica sobre el modo de operación por presión de consigna
5. Análisis y caracterización del ensuciamiento reversible
6. Estudio y modelización del ensuciamiento residual
7. Estimación de las condiciones óptimas de operación de un biorreactor de membrana terciario

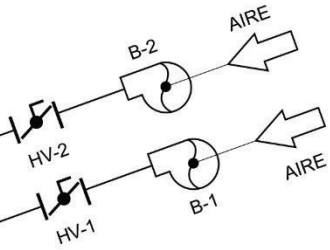

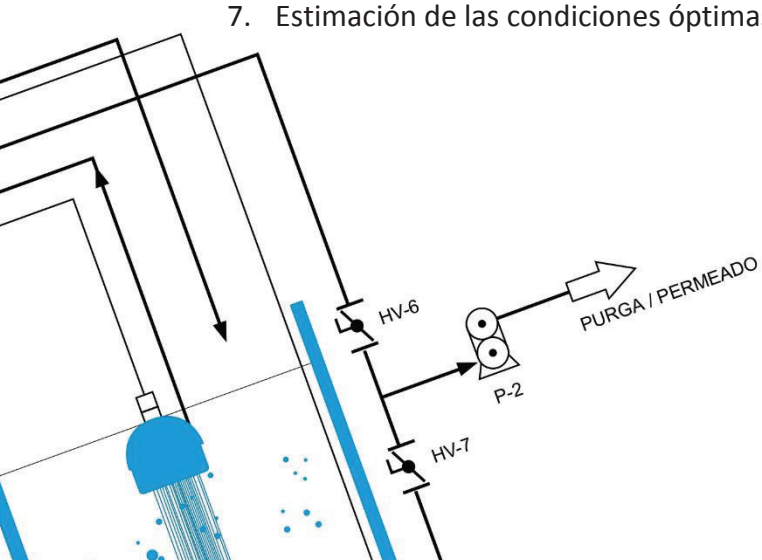

Capítulo 10
Resultados y discusión general

1. Características de la biomasa y rendimiento de depuración en un biorreactor de membrana terciario

1.1. Condiciones de operación con limitación de sustrato. Desarrollo de la biomasa

Uno de los objetivos fundamentales del Capítulo 4 es analizar la puesta en marcha de un biorreactor de membrana terciario (tMBR) sin ningún tipo de inoculo, permitiendo el libre desarrollo de los microorganismos presentes en el agua de alimentación. La figura 10.1 muestra la evolución experimentada por los sólidos suspendidos totales y volátiles en el licor mezcla durante el estudio experimental.

Inicialmente, el sistema experimentó un rápido crecimiento de la concentración de biomasa, debido a la elevada relación de "microorganismos/sustrato carbonoso" impuesta (F/M_C = 11,5-5,0 kg COD/kg MLVSS d). Las cargas puntuales de elevado contenido en carbono en la alimentación repercutieron directamente, en el crecimiento de la biomasa, tal y como se puede observar en la Figura 10.1. En condiciones normales de operación, el coeficiente de rendimiento del lodo fue significativamente bajo (Y_{obs}= 0,04 ± 0,002 Kg MLVSS/Kg COD) debido a las severas condiciones de limitación de sustrato impuestas en el biorreactor. La situación de inanición produce que los microorganismos utilicen el sustrato disponible principalmente, para su mantenimiento y no para actividades relacionadas con el desarrollo de nueva biomasa, lo cual reduce el crecimiento neto del lodo. Por otro lado, en los biorreactores de membrana terciarios operados con elevada edad de lodo, se observa una gran presencia de protozoos (Capítulo 7), los cuales son depredadores de bacterias dispersas que reducen por tanto, la población de pequeños microorganismos.

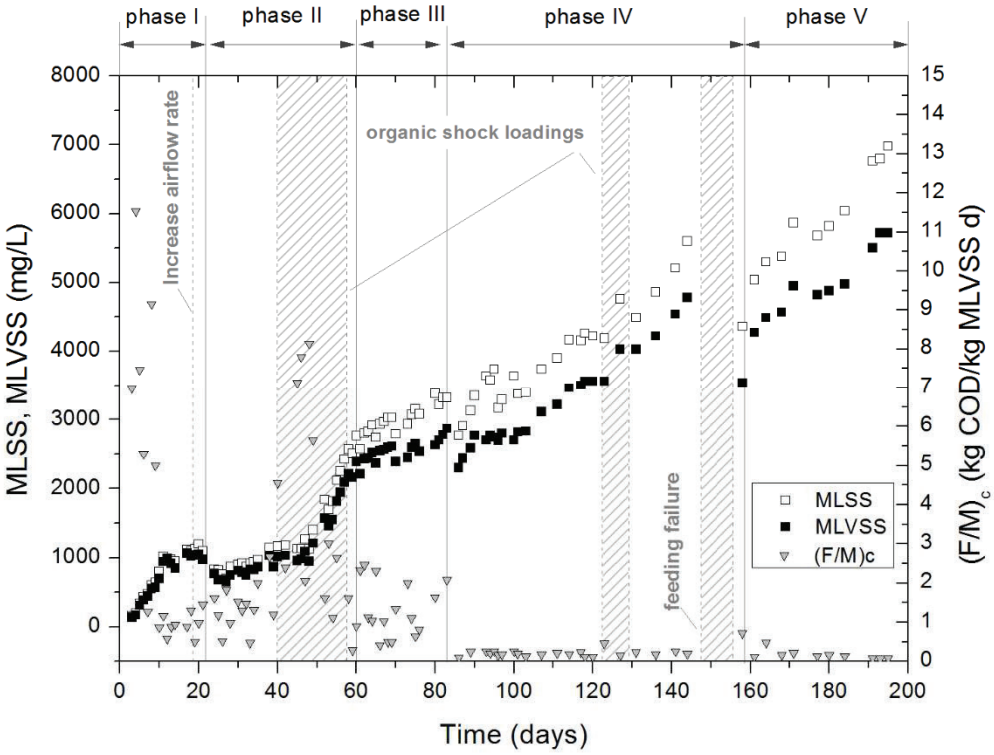

Figura 10.1 Evolución de los MLSS, MLVSS y $(F/M)_c$ durante la puesta en marcha de un tMBR

Los resultados obtenidos parecen indicar un lento crecimiento pero continuo de la biomasa. No obstante, tal y como ocurre en otros sistemas biológicos, con limitación de sustrato y elevadas edades de lodo, la concentración de biomasa tiende a estabilizarse en un valor, en función de la relación F/M_C impuesta. La Tabla 10.1 muestra la concentración de MLSS para el resto de estudios experimentales realizados. Como puede verse en dicha tabla, la concentración de biomasa se mantiene prácticamente constante pero presenta algunas fluctuaciones. Éstas variaciones de concentración que se han observado han sido producidas por los numerosos episodios de alta carga orgánica particulada en el agua de alimentación, la cual ha generado esporádicamente, elevadas relaciones F/M_c (>0,4 Kg COD/Kg MLSS d). Estos vertidos han producido un rápido crecimiento de la biomasa debido a la operación sin purga de lodos. Sin embargo, el sistema ha sido capaz de asimilar estas fluctuaciones y mantener estable la concentración de sólidos suspendidos. Por otro lado, durante todos los periodos experimentales se ha observado una baja mineralización del fango y la concentración de solidos suspendidos volátiles (MLVSS) se ha mantenido en torno a un 80% de los sólidos suspendidos totales.

Tabla 10.1. Concentración de la biomasa

	MLSS (mg/L)	
CAPITULO	**Promedio**	**Rango**
Capítulo 5	3.382	2.770-3.920
Capítulo 6	5.500	4.100-7.000
Capítulo 7	5.500	3.700-6.600
Capítulo 8	6.200	3.900-8.600
Capítulo 9	9.200	6.000-10.300

Las condiciones de limitación de sustrato son una de las principales ventajas de un tMBR debido a que el sistema opera sin purga de lodos, y por tanto, no existe una producción de residuos sólidos a tratar. No obstante, el análisis de la Tabla 10.1 muestra que en el reactor tiene lugar un lento crecimiento de la biomasa, aunque evidentemente, a mayor concentración menor es dicho crecimiento debido a la disminución de la relación F/M_C. Sin embargo, si se estableciera una purga de lodos a elevados tiempos de operación, esto se traduciría en tiempos de retención de lodos (SRT, en inglés) superiores a los 1.000 días, lo que operativamente se considera una edad de lodo infinita.

Durante el desarrollo de los trabajos enmarcados en la presente tesis, la suspensión ha experimentado una baja actividad biológica medida por medio de la velocidad de consumo de sustrato. Esto se ha debido a las severas condiciones de inanición impuestas. Además, la actividad biológica se ha visto muy influenciada por la relación microorganismos/sustrato carbonoso y nitrogenado (F/M_C y F/M_N, respectivamente), tal y como se explica en los Capítulos 4 y 9. No obstante, pese a la baja actividad biológica observada el MBR ha logrado elevados grados de depuración, tal y como se describirá más adelante.

Las condiciones endógenas y las elevadas edades de lodo incrementan la biodegradación/adsorción de los productos solubles microbianos (SMP) presentes en el licor mezcla. La Figura 10.2 muestra la evolución del contenido de agregados de biopolímeros (BPC)

en el licor mezcla, SMP en el permeado y la cantidad de materia orgánica disuelta en el agua de alimentación (EfOM).

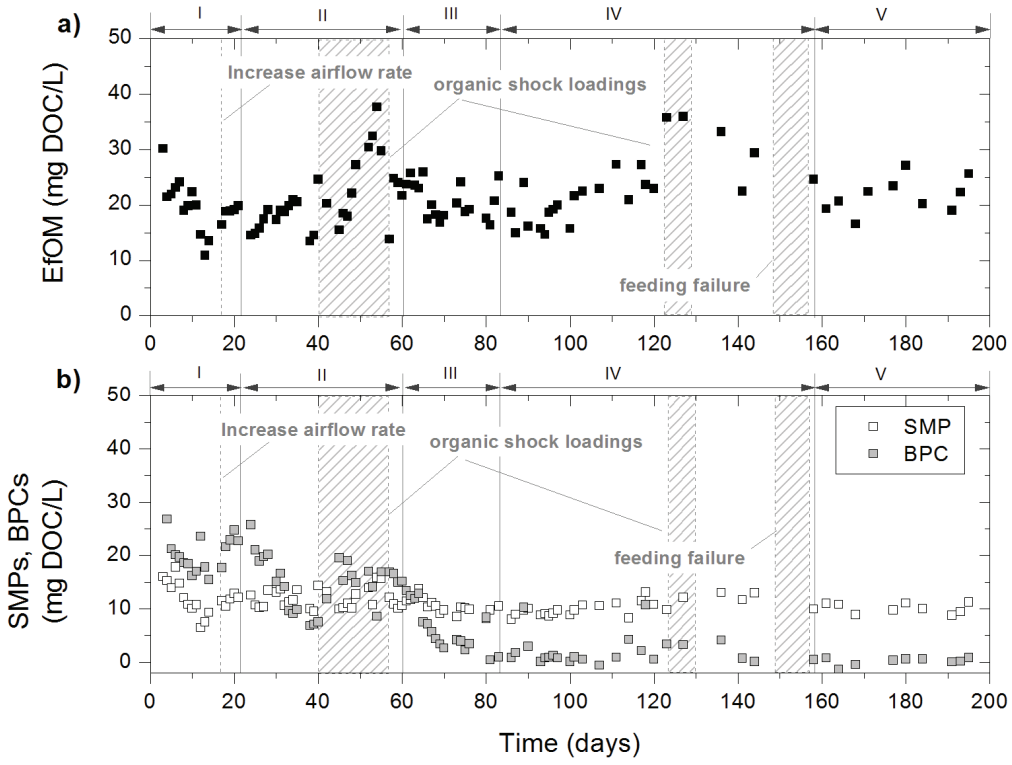

Figura 10.2. Evolución del contenido de EfOM, SMP y BPC durante la puesta en marcha de un tMBR

Inicialmente, debido a la baja concentración de biomasa en el biorreactor, se produjo una acumulación de BPC en el medio, y únicamente al alcanzarse las condiciones de limitación de sustrato y un crecimiento normal de la biomasa, dicho contenido en BPC se redujo y por ende, la concentración de SMP en el licor mezcla. Esta tendencia se ha mantenido en todos los estudios realizados donde la concentración de materia orgánica en el reactor se ha situado en torno a 8-9 mg DOC/L y 0,5-3 mg DOC/L expresada como SMP en el licor mezcla y BPC, respectivamente. Estos resultados revelan la escasa relevancia de las sustancias coloidales presentes en un tMBR, en relación al ensuciamiento de la membrana (establecida en torno a un 20%, ver Capítulos 5 y 6) debido a la baja concentración de estas sustancias en el medio.

La concentración de SMP en el permeado se ha mantenido prácticamente constante durante el proceso de desarrollo de la biomasa (Figura 10.2), y por tanto, cuando no se ha producido depuración biológica de la EfOM, la membrana ha sido capaz de retener parcialmente estas sustancias, pero a costa de experimentar un elevado ensuciamiento (Capítulos 4 y 5).

1.2. Características de la biomasa. Influencia de las condiciones de operación

Durante el desarrollo de la biomasa (Capítulo 4) se observó un incremento de la biofloculación, mediante el análisis de la turbidez del sobrenadante y de la distribución de tamaño de partículas. Sin embargo, una vez alcanzado el régimen estacionario, tras largos periodos de operación, el sistema experimentó un ligero empeoramiento de su estado de biofloculación, posiblemente debido a la reducción de la actividad biológica. No obstante, la suspensión resultante presentó baja turbidez del sobrenadante lo que se traduce en una pequeña concentración de microorganismos no floculados, además, de exhibir un tamaño medio y uniforme de flóculos con una buena filtrabilidad expresada como TTF. Estas características se han mantenido constantes a lo largo de todo el estudio, tal y como se observa en la Tabla 10.2, donde se muestra las principales características de la biomasa para el último periodo experimental a que se refiere el Capítulo 4 y el resto de los capítulos.

Tabla 10.2. Principales características de la biomasa

PARAMETRO	UNIDAD	CAP. 4	CAP. 5	CAP. 6	CAP. 7	CAP. 8
Turbidez del sobrenadante	NTU	25	--	30	28	27
$D_{(v,10)}$	µm	29	36	17	17	20
$D_{(v,50)}$	µm	86	103	43	42	63
$D_{(v,90)}$	µm	227	275	92	102	183
TTF	s	100	--	222	257	128

Los Capítulos 4, 5 y 8 fueron llevados a cabo en filtración frontal, mientras los Capítulos 6 y 7 se realizaron con un esfuerzo cortante sobre la superficie de la membrana mediante aireación. Los resultados revelan que bajo las condiciones estudiadas la filtración tangencial no afectó significativamente al estado de biofloculación de la suspensión. Sin embargo, puede observarse un ligero descenso del tamaño del flóculo debido a las posibles roturas que puede ocasionar la aireación de la membrana.

La biofloculación del lodo es influenciada notablemente, por la concentración de oxígeno disuelto para el proceso biológico, como reflejan los resultados encontrados en el Capítulo 9

(Tabla 10.3). Las bajas concentraciones de oxígeno disuelto afectan negativamente a la biofloculación, lo que resulta en un incremento de la concentración de BPCs producidos por el elevado estrés que sufre la biomasa. La pobre biofloculación también se reflejó en el incremento de la turbidez del sobrenadante, reducción del tamaño de partículas y por extensión, en el incremento del TTF.

Tabla 10.3. Principales características de la biomasa para cada ratio de aireación biológica estudiado

		RATIO DE AIREACIÓN (A_R)				
PARAMETRO	**UNIDAD**	**0**	**0,25**	**0,5**	**0,75**	**1**
BPC	mg COD/L	7,7	4,3	1,6	0,5	0,3
Turbidez del sobrenadante	NTU	128	87	75	30	27
$D_{(v,10)}$	µm	17	18	25	28	21
$D_{(v,50)}$	µm	8	49	72	76	86
$D_{(v,90)}$	µm	97	103	153	186	201
TTF	s	1.034	573	173	118	92

Los resultados encontrados en el Capítulo 4 permitieron analizar las relaciones existentes entre las distintas características de la biomasa. Como era de esperar, la concentración de MLSS se correlacionó linealmente con la viscosidad aparente (r=0,842) y con la velocidad de consumo de sustrato endógeno, SOUR (r=-0,826). Sin embargo, la concentración de biomasa no se correlaciona directamente con la filtrabilidad de la suspensión, medida como TTF. Por el contrario, el estado de biofloculación, medido como la turbidez del sobrenadante, mostró una moderada correlación con el TTF (r=0,775).

1.3. Rendimiento de depuración

El uso de los MBR como tratamientos terciarios permite adecuar la calidad del efluente, procedente de un sistema convencional de lodos activos con frecuentes episodios de des-floculación, para ser reutilizada con garantías.

Durante el desarrollo de la biomasa en un tMBR (Capítulo 4), el sistema alcanzó una alta eliminación de COD (79-81%) y una nitrificación completa (98%) desde los primeros días de operación. Los resultados indican que los rendimientos de depuración del sistema no se vieron afectado por las variables de filtración. La Tabla 10.4 muestra los rendimientos de depuración para el amonio, demanda química de oxígeno (COD), y carbono orgánico disuelto (DOC), en los distintos estudios realizados. La variación observable en términos de reducción de la COD es atribuible a las fluctuaciones en la concentración del agua de entrada, que oscila entre 20 y 2.520 mg/L, mientras que el permeado siempre presenta valores en torno a 20 - 30 mg/L.

Tabla 10.4. Rendimientos de depuración promedio obtenidos en cada estudio

	RENDIMIENTO DE DEPURACIÓN (%)			
PARAMETRO	**CAP 5**	**CAP 6**	**CAP 7**	**CAP8**
$N\text{-}NH_3^-$	97	96	98	98
COD	93	89	56	87
DOC	60	53	65	60

La concentración de oxígeno disuelto para el proceso biológico (Capitulo 9) parece no afectar a la eliminación de COD que se situó entre 47,2 – 77,8%, produciendo permeado con concentraciones de 17-48 mg/L. La eliminación de COD se produce debido a la acción combinada del proceso biológico y de la membrana. En el caso de que el sistema biológico no pueda biodegradar las partículas y los macro-coloides, es la membrana la que los retiene completamente, y por tanto, el rendimiento global de eliminación de COD no se ve afectado por la concentración de oxígeno disuelto

La nitrificación si se ve afectada notablemente, por la concentración de oxígeno disuelto (Capítulo 9) y cuando el sistema opera con concentraciones inferiores a 0,38 mg/L se observa una nitrificación parcial, con una reducción de amonio que oscila entre 38 y 46%.

1.4. Influencia de las características de la suspensión sobre el ensuciamiento de la membrana

Existe una compleja relación entre el ensuciamiento de la membrana y las características de la suspensión biológica. En el Capítulo 4 se consideraron distintos parámetros (BPC, MLSS, TTF y turbidez del sobrenadante) con el fin de correlacionarlos con el ensuciamiento reversible de la membrana, que en el caso del tMBR se corresponde al debido a la construcción de una torta incompresible, mediante la expresión [10.1].

$$TMP(t) = TMP_i + r_f t \qquad [10.1]$$

Que indica que la evolución temporal de la presión transmembrana (TMP) en un ciclo de filtración y que puede ser expresada en función del tiempo (t), la presión inicial del ciclo de filtración (TMP_i) y la velocidad de ensuciamiento (r_f). En base a esta aproximación, el ensuciamiento reversible puede cuantificarse mediante el seguimiento de r_f.

La Tabla 10.5 muestra los coeficientes de correlación de Pearson entre los parámetros seleccionados (BPC, MLSS, TTF y turbidez del sobrenadante) y la velocidad de ensuciamiento. Los resultados pusieron de manifiesto, la elevada relación entre el contenido en BPC del licor mezcla y la velocidad de ensuciamiento reversible, identificando el papel crucial de los biopolímeros coloidales (BPC) en la regulación del ensuciamiento de la membrana.

Tabla 10.5. Correlaciones de Pearson entre las características de la suspensión y la velocidad de ensuciamiento reversible (entre paréntesis el factor de significancia "p")

PARAMETRO	N	min	max	r
BPC (mg DOC/L)	97	-0,54	28.2	0,868 ($<1\cdot10^{-9}$)
MLSS (mg/L)	100	153	6980	-0,765 ($<1\cdot10^{-9}$)
TTF (s)	65	5	4620	0,233 (0.080)
Turbidez del sobrenadante (NTU)	65	6,6	116	0,250 (0.032)

La concentración de biomasa (MLSS) parece no tener una clara influencia sobre el ensuciamiento de la membrana, según los resultados mostrados en la Tabla 10.5. Sin embargo, a bajas concentraciones (<3.000mg/L), se observó una correlación negativa, mientras que un incremento de los MLSS por encima de 5.000mg/L se tradujo en una correlación positiva con el ensuciamiento, tal y como se observa en la Figura 10.3.

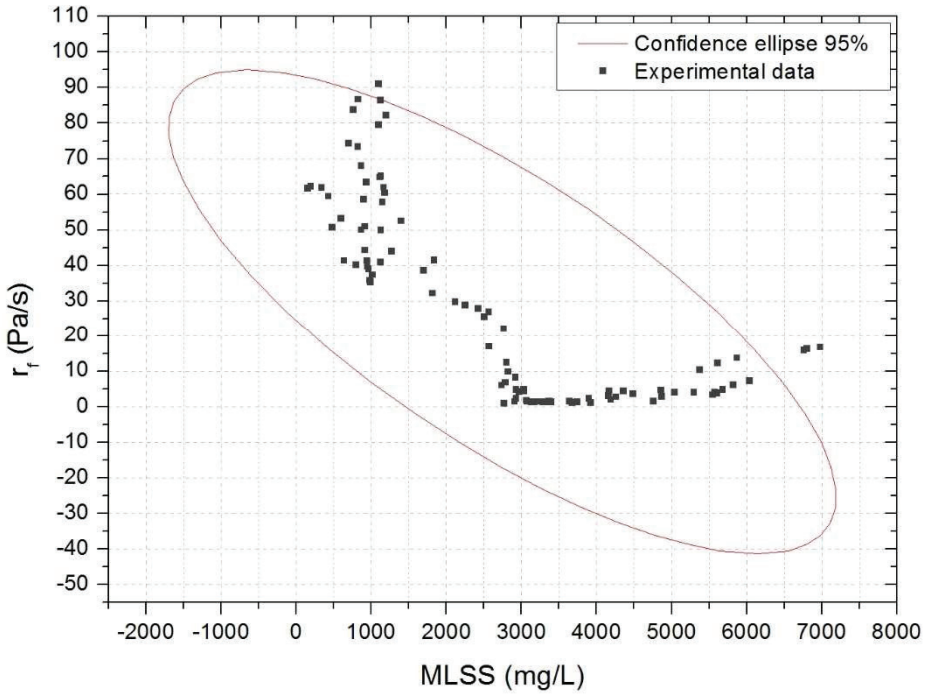

Figura 10.3. Relación entre el ensuciamiento reversible de la membrana y la concentración de biomasa

Los resultados revelan que las óptimas condiciones de operación para un tMBR involucran concentraciones de BPC inferiores a 5mg/L y concentraciones de MLSS entre los 3.000 y 5.000 mg/L.

La filtrabilidad del lodo medida como TTF parece no tener una influencia clara sobre el ensuciamiento reversible, al igual que la turbidez del sobrenadante (Tabla 10.5). Por lo tanto, puede concluirse que los BPC tienen un papel predominante en comparación a otras propiedades del lodo, como indicadores del ensuciamiento de la membrana.

2. Tratamientos terciarios con membranas sumergidas: Ultrafiltración directa versus Biorreactor de membrana

2.1. Estudio comparativo de distintos tratamientos terciarios

En el Capítulo 5 se presenta un estudio comparativo realizado bajo las mismas condiciones, de un sistema de ultrafiltración directa (UF) y un biorreactor de membrana terciario (tMBR). Ambos sistemas permitieron un alto rendimiento de depuración de COD (87% y 93% para la UF y tMBR, respectivamente). La diferencia entre ambas tecnologías es debido a la degradación biológica de materia orgánica soluble por parte del tMBR. En cambio en el caso de la UF el sistema sólo elimina la fracción coloidal y particulada presente en el agua de entrada. Además, tal y como ya se ha mencionado, el tMBR fue capaz de alcanzar la nitrificación completa del influente, y debido a las condiciones endógenas de operación, la concentración de biomasa se ha mantenido estable en 3.380 mg/L con un compacto y moderado tamaño de flóculo. Por otro lado, la UF no permitió la degradación de la cantidad de materia orgánica en la alimentación (EfOM), lo que se tradujo en una elevada cantidad de BPC en el concentrado (20 mg DOC/L).

Para el análisis del ensuciamiento de la membrana se consideró la ley de Darcy, que de acuerdo con el modelo de resistencias en serie puede ser expresada mediante la siguiente ecuación:

$$TMP = J\mu R_t = J\mu\left(R_m + R_f\right) \qquad [10.2]$$

donde J es el flujo de filtración, μ es la viscosidad del permeado y R_t es la resistencia hidráulica total al paso de un fluido por la membrana que, a su vez, puede ser expresada por la suma de la resistencia de la membrana limpia (R_m) y la resistencia asociada con el ensuciamiento (R_f). El ensuciamiento se puede clasificar como ensuciamiento reversible (eliminable mediante los retrolavados) y ensuciamiento residual (eliminable solo con limpiezas químicas). De acuerdo con esto, la resistencia ofrecida por el ensuciamiento se puede expresar mediante la ecuación [10.3].

$$R_f = R_{rvf} + R_{rdf} \qquad [10.3]$$

Siendo R_{rvf} y R_{rdf} las resistencias asociadas al ensuciamiento reversible y residual, respectivamente.

La Figura 10.4 muestra la evolución de la resistencia del ensuciamiento con respecto al tiempo durante los ciclos de filtración/retrolavado sucesivos. Como se presenta en el Capítulo 5, para ambos tratamientos terciarios el ensuciamiento reversible puede ser modelizado como la construcción de una torta/gel incompresible sobre la membrana (Figura 10.4 a y b).

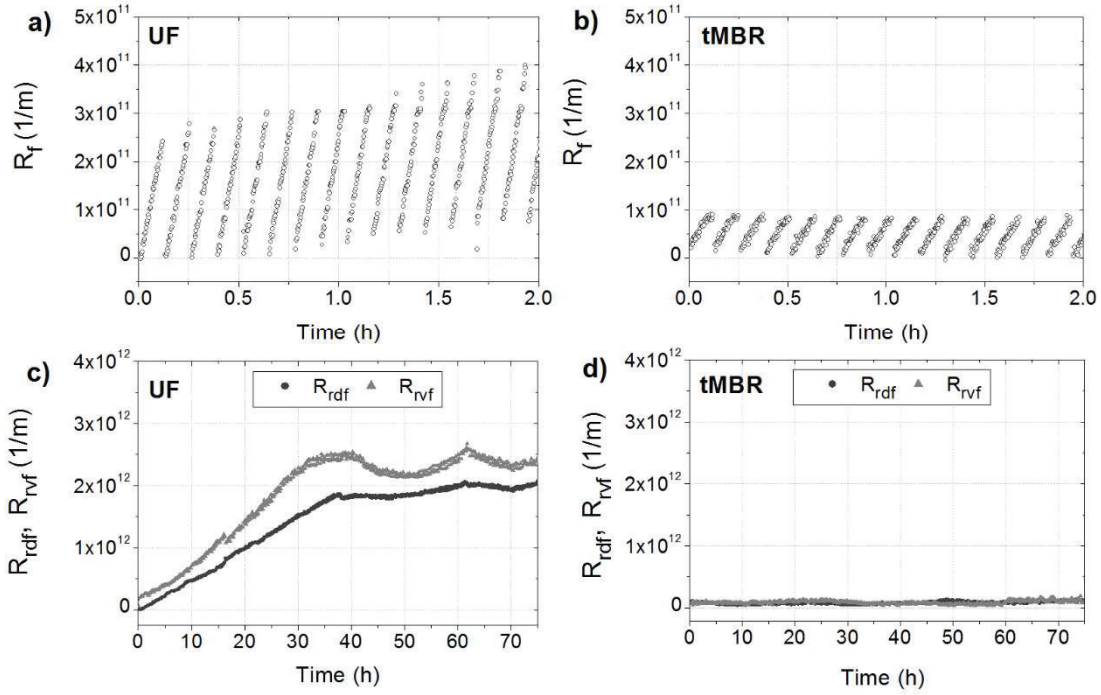

Figura 10.4. Evolución del ensuciamiento para la ultrafiltración directa y el biorreactor de membrana terciario.

En el caso del tMBR, el sistema experimentó una velocidad de construcción del ensuciamiento baja y totalmente reversible. Sin embargo, la UF experimentó una elevada velocidad de ensuciamiento reversible y residual (Figura 10.4 c). Este resultado se puede atribuir a la baja concentración de BPC en el tMBR, pues a concentraciones elevadas se produce una reducción de la porosidad de la torta y una elevada resistencia específica.

Por lo tanto, se puede concluir que los tMBR son un tratamiento terciario adecuado para efluentes con una elevada concentración de materia orgánica disuelta (EfOM) puesto que el ensuciamiento que se produce en la membrana presenta un componente reversible elevado.

2.2. Influencia del tipo de tratamiento terciario sobre los post-tratamientos de afino

En el Capítulo 5 se evaluaron dos post-tratamientos de afino: nanofiltración (NF) y ósmosis inversa (RO) para eliminar sales y contaminantes emergentes de los efluentes procedentes de la UF y del tMBR.

Como era previsible, la RO alcanzó una alta tasa de rechazo de todos los iones (>90%) independientemente del tipo de alimentación. De igual modo, la tasa de rechazo de los distintos iones para la NF no se vio afectada por el tipo de alimentación, sin embargo, las tasas de rechazo fueron inferiores: alta/moderada para los iones multivalentes (67-100%) y baja/moderada para los iones monovalentes (14-61%) debido posiblemente, al efecto Donnan.

El análisis del ensuciamiento observado en las membranas de NF y RO reveló un mayor ensuciamiento al ser alimentadas con el efluente de la UF, debido al elevado contenido orgánico, expresado como DOC, que da lugar a la formación de un gel difícilmente eliminable por la acción de la cizalladura. Por tanto, el tMBR parece ser mejor tratamiento que la ultrafiltración directa.

Las autopsias de las membranas revelaron un ensuciamiento muy similar para la NF y RO. En ambos casos se observaró ensuciamiento orgánico, producido por proteínas y polisacáridos, parcialmente eliminado mediante el enjuague de las membranas. El ensuciamiento inorgánico fue debido a incrustaciones de P, Fe, Ca, Mg y Na, en ambos casos.

2.3. Eliminación de contaminantes emergentes.

En el desarrollo de esta tesis se ha evaluado la eliminación de fármacos de efluentes procedentes de un tMBR y de una unidad de UF (Capítulo 5). La Figura 10.5 muestra la concentración de los cuatro fármacos estudiados en las corrientes de concentrado y permeado de las membranas de nanofiltración y ósmosis inversa

En general, se observó una menor concentración de fármacos en los concentrados de los post-tratamientos procedentes del tMBR comparados con los de la UF debido posiblemente, a la biodegradación de los mismos en el reactor biológico. El ácido clofíbrico fue el único que no presentó ésta tendencia debido a la presencia de cloro en su estructura y a la baja

biodegradabilidad del mismo. Los resultados ponen de manifiesto la deficiente eliminación de fármacos por ultrafiltración directa.

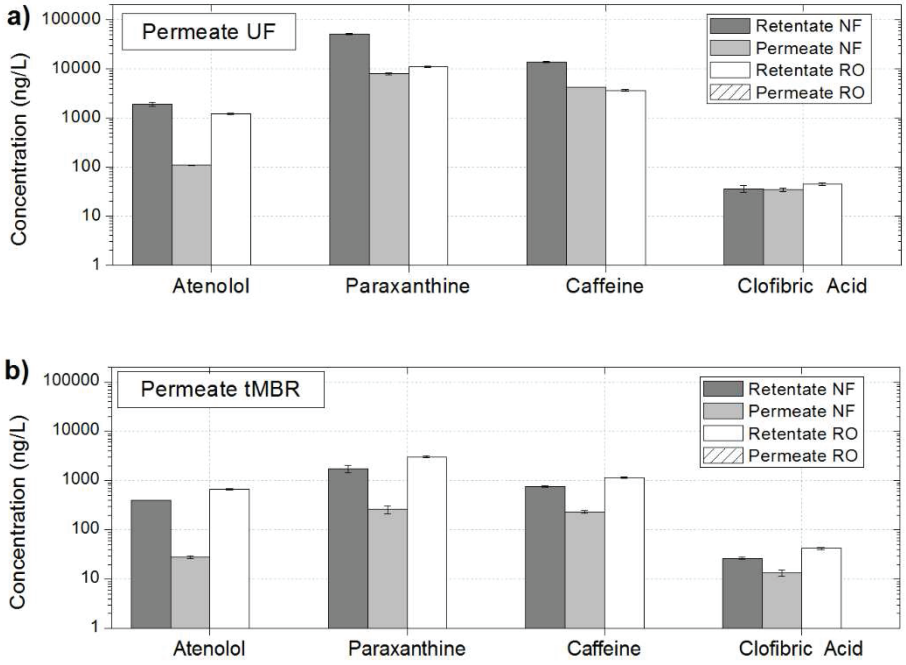

Figura 10.5. Concentración de fármacos presentes en el concentrado y rechazo para los distintos tratamientos estudiados.

Como era previsible la membrana de ósmosis inversa retuvo totalmente los fármacos analizados. Por el contrario, la membrana de NF presentó tasas de rechazo del 94, 85, 70 y 27% para el atenolol, paraxantina, cafeína y ácido clofíbrico, respectivamente.

3. Estudio de las condiciones de operación para un ensuciamiento mínimo. Determinación del flujo crítico.

3.1. Análisis del flujo crítico en función de la velocidad y compresibilidad del ensuciamiento

En el método de flujo escalonado aplicado para determinar el flujo crítico atendiendo a la velocidad de ensuciamiento en cada escalón, es posible atender a más de un criterio. De hecho existen varios modos alternativos para definir el flujo crítico.

En el Capítulo 6 se analiza la influencia del patrón de aireación aplicado a la membrana sobre el flujo crítico cuando se opera un tMBR. Para su determinación se estableció un valor crítico de velocidad de ensuciamiento reversible de 0,2 Pa/s o 0,1 mbar/min. La Figura 10.6 muestra la velocidad de ensuciamiento para cada escalón de flujo e intermitencia de aireación aplicada.

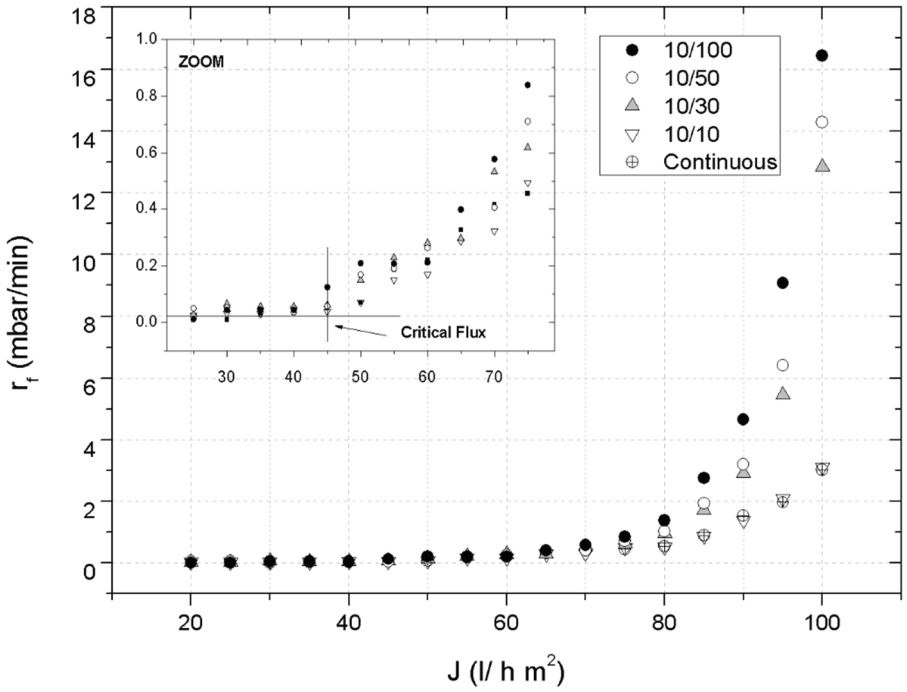

Figura 10.6. Velocidad de ensuciamiento en relación al flujo para distintas frecuencias de aireación aplicadas.

Los resultados indican una tendencia similar para el caso de aireación continua e intermitente 10/10 (10 “on” / 10 “off”), debido posiblemente a que el esfuerzo cortante o cizalladura sobre la membrana en ambas condiciones, es muy similar. Un incremento de la frecuencia de la aireación por encima de 10/50 (SAD_m=0,18Nm^3/hm^2) no parece tener efecto sobre el flujo crítico, el cual se establece en 45-50 L/hm^2. Sin embargo, las bajas frecuencias de aireación (10/100) se traducen en una reducción del flujo crítico (J_c) hasta 40-45 L/hm^2. En condiciones supra-criticas, las velocidades de ensuciamiento aumentan considerablemente para todas las intermitencias inferiores a 10/30. Éste comportamiento se debe a que la fuerza de

atracción ejercida por el flujo de filtración es superior a los esfuerzos cortantes y dispersivos de las burbujas de aireación, y por tanto, las partículas se depositan sobre la membrana.

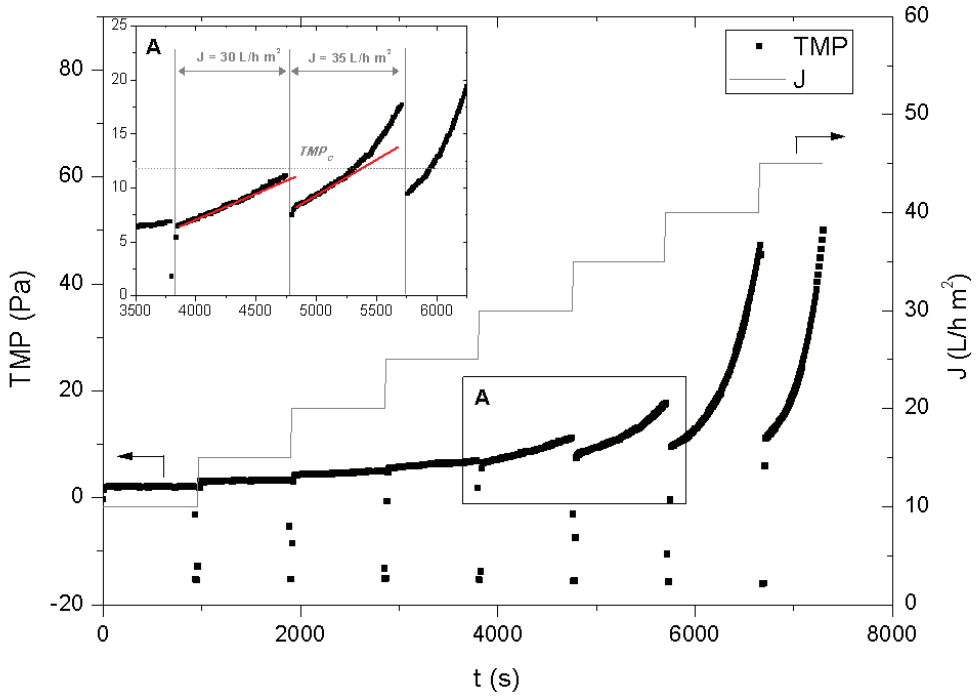

Figura 10.7. Perfiles de flujo y presión transmembrana obtenidos durante los experimentos escalonados; A_R=0,5; t_B=30 s; J_B=60 L/hm^2; t_F=900s

El análisis del ensuciamiento producido en cada escalón de flujo, desarrollado en los Capítulos 8 y 9, muestra diferentes perfiles de crecimiento de la TMP en función del flujo de filtración. A bajos flujos, el ensuciamiento experimentado por la membrana responde a un mecanismo de formación de torta incompresible, con una baja y constante velocidad de ensuciamiento. Sin embargo, a partir de un determinado valor del flujo, el ensuciamiento de la membrana comienza a desarrollarse a una velocidad que se incrementa con el transcurso del tiempo, y por tanto, se ajusta al modelo de torta compresible (Figura 10.7). Es evidente entonces, que bajo estas condiciones, el ensuciamiento no sólo depende de la velocidad del flujo de filtración, sino que también, está influenciada por la torta depositada previamente y la presión transmembrana actual aplicada. En conclusión, el flujo crítico atendiendo a la compresibilidad, puede ser definido como el flujo donde tiene lugar la transición entre el modelo de torta compresible e incompresible. Además, se introduce el concepto de "masa crítica", definida como la masa específica depositada sobre la membrana que induce una

incipiente consolidación del ensuciamiento. Asimismo, durante el escalón del flujo crítico, se define la presión transmembrana crítica (TMP_{cri}), como aquella que marca la transición entre el bajo y alto crecimiento de la TMP (Figura 10.7).

La concentración de oxígeno disuelto para el proceso biológico influye notablemente en las características de la suspensión biológica de un tMBR, y por tanto, en el flujo crítico (Capítulo 9). Atendiendo a la definición de flujo crítico (J_C) realizada anteriormente, en función de la compresibilidad, éste se incrementa desde 15 hasta 55 L/hm^2 para un aumento del ratio de aireación (A_R) desde 0 hasta 1. Sin embargo, la resistencia asociada a la presión transmembrana crítica se mantiene en $3{,}5\cdot10^{11}\pm0{,}2\cdot10^{11}$ 1/m, para todos los ratios de aireación estudiados.

La resistencia ofrecida por el ensuciamiento, si se opera en el modo de filtración frontal, es proporcional a la resistencia específica de la torta y al contenido de sólidos por unidad de área de membrana, que a su vez es proporcional al flujo de filtración, a la concentración de MLSS y al tiempo de filtración. La masa crítica se incrementa desde 9,9 g/m^2 hasta 63,8 g/m^2, cuando A_R pasa de 0 a 1. Sin embargo, la resistencia específica de la torta se ve significativamente reducida debido a la baja concentración de BPC y al elevado tamaño del flóculo en estas condiciones por lo que la resistencia crítica se mantiene siempre entorno a un mismo valor.

3.2. Análisis del flujo crítico en función de la reversibilidad del ensuciamiento

La definición del flujo crítico en función de la reversibilidad del ensuciamiento, se realiza atendiendo al primer flujo donde el ensuciamiento comienza la ser irreversible. Atendiendo a esta definición, el flujo crítico se puede identificar como el primer valor del flujo en el que la presión inicial de cada escalón se separa del comportamiento ideal encontrado para la filtración de agua blanca.

La aireación para la limpieza de las membranas parece no afectar la reversibilidad del ensuciamiento, según revelaron los resultados experimentales obtenidos en el Capítulo 6 y donde el flujo crítico se estableció en torno a 55 L/hm^2 para todas las intermitencias aplicadas.

La Figura 10.8 muestra la presión transmembrana inicial de cada escalón frente al flujo de filtración durante los escalonados llevados a cabo en el Capítulo 8, con el fin de analizar la influencia de las condiciones del retrolavado sobre el flujo crítico. El cambio de compresibilidad observado en los experimentos escalonados llevados a cabo en los Capítulos 8 y 9, resulta estar relacionado con la consolidación del ensuciamiento y por tanto, afecta directamente a la

reversibilidad del mismo. Los resultados del Capítulo 8 muestran que la definición del flujo crítico atendiendo a la compresibilidad y a la reversibilidad de la torta conducen al mismo valor oscilante entre 10 y 45 L/hm^2, dependiendo de las condiciones de retrolavado impuestas.

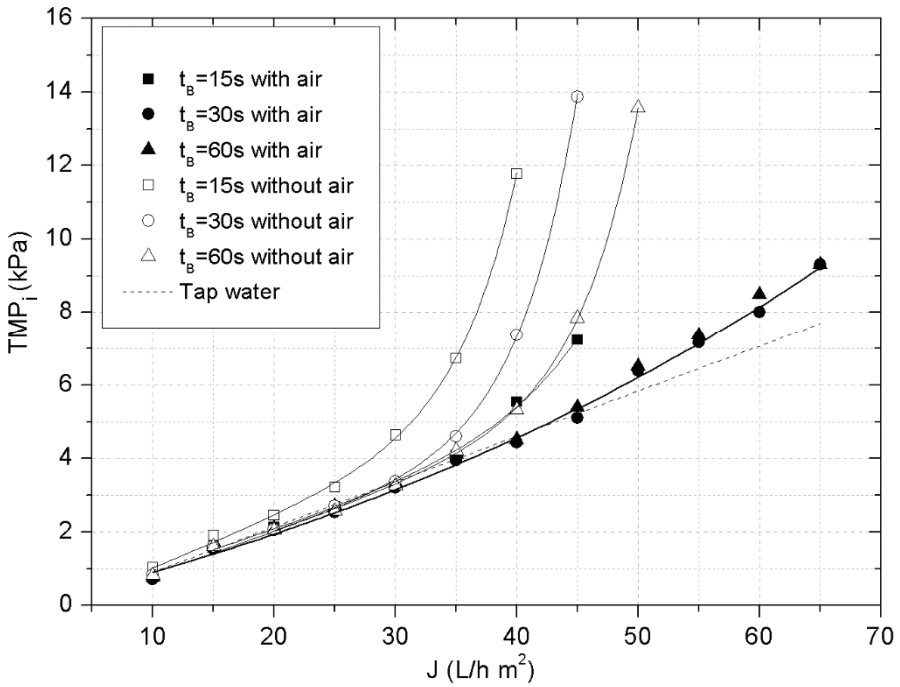

Figura 10.8. TMP$_i$ frente al flujo de filtración para las diferentes condiciones del retrolavado; J_B= 60L/hm^2; t_f=900s

Cuando el retrolavado fue aplicado sin aireación, el flujo crítico se estableció entre 10 y 20 L/hm^2, para un incremento en la duración de la aplicación desde 15 a 60s. Cuando se aplica aireación durante el retrolavado, el flujo crítico es más elevado, 35-45 L/hm^2, para un incremento de la duración desde 15 a 30s. Los resultados indican que un incremento de la duración por encima de 30 s, si se aplica aireación durante el retrolavado, no tiene un efecto notable sobre el flujo crítico.

En conclusión, los resultados del Capítulo 8 muestran que el retrolavado permite el despegue del ensuciamiento y su dispersión en el seno del fluido. La aireación durante el retrolavado logró aumentar significativamente la dispersión. Por el contrario, los experimentos llevados a cabo sin aireación sufrieron una ineficiente re-dispersión del ensuciamiento,

acumulando materia en las inmediaciones de la membrana que rápidamente la colapsaron en el siguiente escalón de flujo.

4. Control del ensuciamiento. Modo de operación por presión de consigna

4.1. Análisis comparativo entre el modo de operación por presión de consigna y el modo convencional temporizado

Para poder analizar cómo el modo de operación por presión de consigna permite mantener limitado el ensuciamiento de la membrana de un tMBR, se ha de recurrir a los experimentos mostrados en los Capítulos 4 y 8, realizados con las mismas condiciones de filtración. Los experimentos fueron llevados a cabo en filtración frontal, a un flujo de filtración de 35 L/hm^2 y el retrolavado con aireación a un flujo de 60L/hm^2 durante 30s. En el caso del modo de operación temporizado, el tiempo de filtración se fijó en 7 minutos, por el contrario, en el modo de operación la presión de consigna TMP_{sp} se estableció en 30kPa.

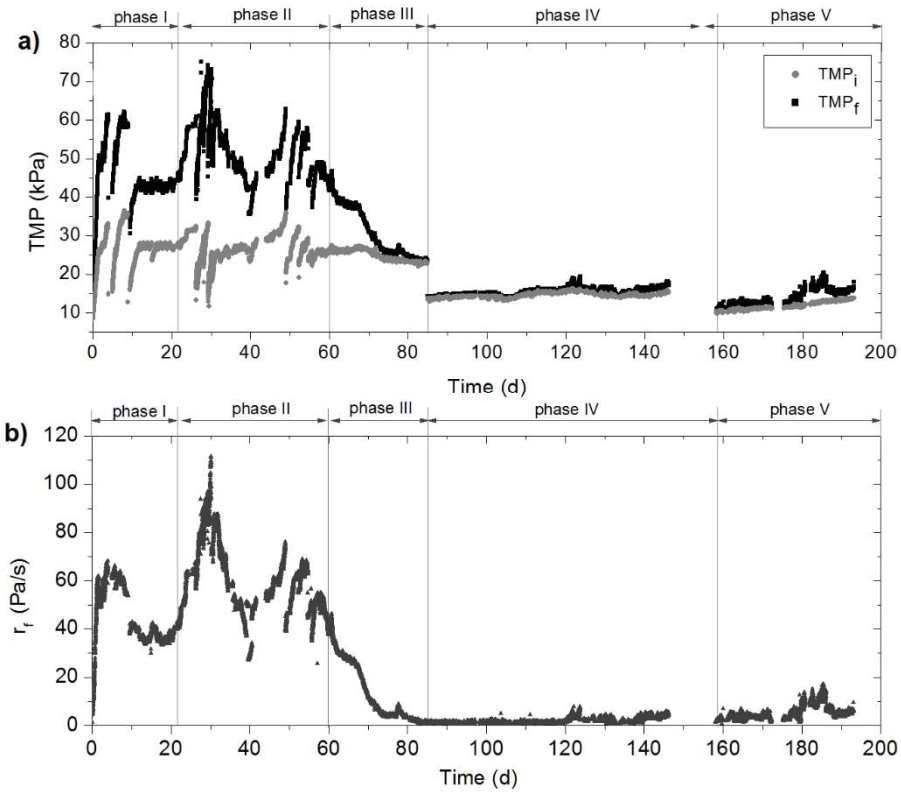

Figura 10.9. TMP_i y TMP_f (a); y la velocidad de ensuciamiento reversible (b) para cada ciclo de filtración durante el desarrollo de los ensayos mostrados en el Capítulo 4

La Figura 10.9 muestra la evolución de la presión inicial y final de cada ciclo de filtración, además de la velocidad de ensuciamiento reversible que tiene lugar durante las experiencias desarrolladas en el Capítulo 4 con el modo de operación temporizado.

Como se puede observar, el modo de operación temporizado no permitió controlar el ensuciamiento. Durante los primeros 60 días, la membrana experimentó un elevado ensuciamiento reversible que no fue controlado pues las limpiezas físicas se realizaban con una frecuencia demasiado baja, lo que provocó un elevado ensuciamiento y la necesidad de realizar limpiezas químicas. Por otro lado, cuando el tMBR alcanzo el régimen estacionario, la membrana experimentó un bajo ensuciamiento reversible y se realizaron limpiezas físicas cuando no eran necesarias. Éste comportamiento repercutió directamente en el rendimiento global del proceso puesto que el flujo neto se redujo hasta 29 L/hm^2 y las limpiezas físicas no se realizaron de manera optimizada.

Por el contrario, cuando se aplicó al tMBR el modo de operación por presión de consigna, en condiciones de operación similares (Capítulo 8) este fue capaz de ajustar la frecuencia del retrolavado en función del ensuciamiento experimentado. En estas condiciones, el flujo neto se estabilizó en 34 L/hm^2, lo que supuso un incremento de un 15% en la productividad del proceso. Por otro lado, el ensuciamiento alcanzado presentó una alta reversibilidad, pues la eficacia del retrolavado se mantuvo en un 86%.

En conclusión, el modo de operación por presión de consigna permite el control del ensuciamiento y un ajuste dinámico de la frecuencia del retrolavado, lo que se traduce en la optimización de la productividad del MBR, expresada como flujo neto.

4.2. Validación del modo de operación por presión de consigna a elevados flujos de filtración

Uno de los principales objetivos del Capítulo 6 fue analizar la viabilidad de un tMBR operado con altos flujos de filtración mediante el modo de operación por presión de consigna. La presión transmembrana de consigna (TMP_{sp}) fue establecida en 30kPa, se aplicó aireación intermitente (SAD_m=0,55 Nm^3/m^2) y el retrolavado apoyado con aireación fue llevado a cabo durante 30s. Durante todo el estudio experimental (>2.200 horas) se aplicaron tres flujos de filtración supra-críticos (80, 70 y 60 L/hm^2) y tres flujos de retrolavado (40, 60 y 80 L/hm^2). El análisis de la evolución de la TMP durante un ciclo de filtración corresponde a un ensuciamiento

de la membrana por construcción de una torta incompresible sobre la misma. La Figura 10.10 muestra la evolución de la presión transmembrana inicial durante todo el ensayo experimental. Los resultados muestran un incremento de la presión inicial cuando se aplica el mayor flujo de filtración (80L/hm^2), sin embargo para el resto de flujos la velocidad de ensuciamiento residual fue baja.

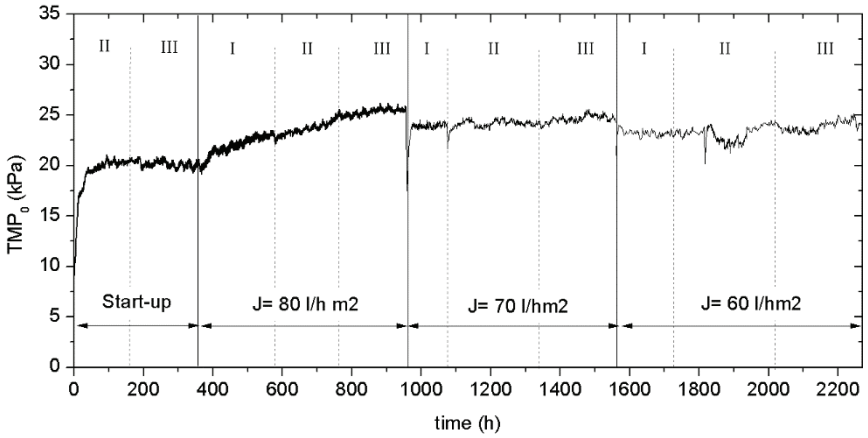

Figura 10.10. Perfil de la TMP_0 durante el ensayo experimental mostrado en el Capítulo 6; I: J_B=40 L/hm^2; II: J_B=60 L/hm^2; III: J_B=80 L/hm^2;

Después del periodo inicial, el retrolavado se mostró muy eficaz para eliminar el ensuciamiento durante más de 2.200 horas, pese a operar con elevados flujos de filtración. Independientemente del flujo de retrolavado, el sistema fue capaz de alcanzar el mismo rendimiento de retrolavado; por tanto, una vez que se alcanza el régimen estacionario parece que el flujo de filtración y el de retrolavado no afectan al ensuciamiento. Éste comportamiento se debe a que el sistema ajusta la frecuencia del retrolavado en función de la construcción del mismo. Cuando se aplican flujos de filtración altos, que producen una mayor velocidad de ensuciamiento reversible, el sistema aumenta la frecuencia del retrolavado y por tanto, mantiene el rendimiento de la limpieza física.

Los resultados experimentales permiten afirmar que el modo de operación por presión de consigna es capaz de operar un tMBR con altos flujos de filtración durante largos periodos de tiempo (<2.200 horas). Además, permite optimizar la frecuencia del retrolavado, estableciendo elevados flujos netos de operación, independientemente del flujo de retrolavado aplicado, en torno a 75, 68 y 59 L/hm^2 para los flujos de filtración de 80, 70 y 60 L/hm^2, respectivamente. Es

decir, el sistema logra aumentar la productividad del sistema, puesto que la reducción de flujo se encuentra en torno a un 3%, como valor promedio.

4.3. El ensuciamiento máximo permitido. Influencia de la presión transmembrana de consigna

La influencia de la presión transmembrana de consigna (TMP_{sp}), sobre la operación de un tMBR fue estudiada en el Capítulo 7, ensayando seis valores de TMP_{sp} a lo largo de más de 2.750 horas de operación, sin incidencias.

El ensuciamiento residual interno aumentó linealmente con la TMP_{sp} aplicada, en el rango de presiones considerado. Al comienzo de cada fase experimental, la membrana presentó un rápido crecimiento del ensuciamiento residual para luego seguir aumentando pero de forma más lenta, independiente de la TMP_{sp} aplicada. El rápido crecimiento inicial del ensuciamiento residual se debió a fenómenos de consolidación del ensuciamiento ligados a la larga duración de los primeros ciclos de filtración, dentro de cada fase experimental.

Para bajas presiones transmembrana de consigna (25kPa), el MBR operó de forma estable con ciclos de filtración cortos (t_F=12 min), debido a que la consolidación del ensuciamiento fue muy próxima al ensuciamiento máximo permitido. Para el caso de TMP_{sp} moderadas, los ciclos de filtración presentaron duraciones sostenibles de 22, 14 y 13 min para 30, 35 y 40 kPa, respectivamente. En cambio, la alta consolidación del ensuciamiento a las mayores TMP_{sp} ensayadas, 45 y 50 kPa provocó una reducción significativa del tiempo de operación a 5 y 3 minutos, respectivamente. La evolución mostrada en la duración del ciclo de filtración pone de manifiesto el bajo rendimiento del retrolavado cuando las presiones transmembrana de consigna fueron extremas (25, 45 y 50 kPa), dando lugar a fenómenos de consolidación del ensuciamiento (Figura 10.11).

La mayor productividad del proceso, medida como flujo neto, ha tenido lugar a presiones transmembrana de consigna moderadas, debido a que en esas condiciones, el ensuciamiento de la membrana exhibe baja consolidación (Figura 10.11).

En conclusión, la operación del tMBR bajo el modo por presión de consigna permite mayores rendimientos en término de producción neta de permeado y de eficacia del retrolavado si se establecen presiones de consigna moderadas.

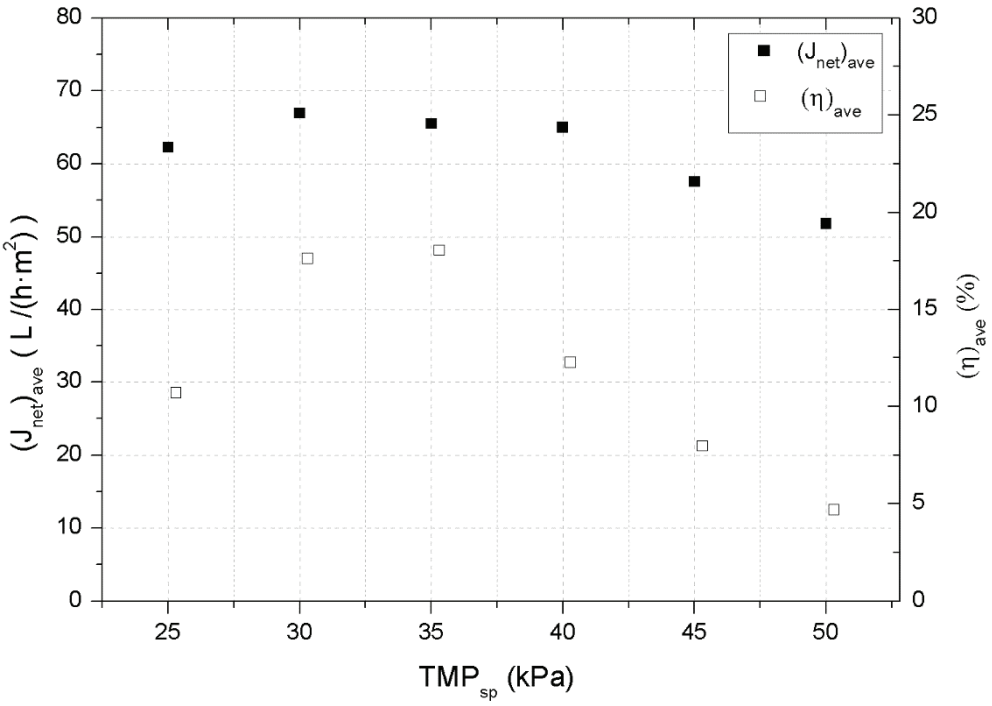

Figura 10.11. El flujo neto y el rendimiento del retrolavado en función de la presión transmembrana de consigna

4.4. Filtración en frontal. Influencia de los flujos de filtración y retrolavado.

La operación en filtración frontal permite la reducción de los costes operativos en un MBR, por ello se ha estudiado la viabilidad de operar el tMBR bajo este modo, fijando altos flujos de filtración y aplicando el retrolavado en base a una presión de consigna (Capitulo 8).

Como en el resto de capítulos anteriores, el modo de operación por presión de consigna permitió la filtración con elevados flujos (35, 45 y 55L/hm^2) y distintos flujos de retrolavado (0, 20, 40 y 60L/hm^2). La Figura 10.12 muestra la evolución de la resistencia asociada al ensuciamiento residual interno para todas las condiciones estudiadas. De forma análoga a lo observado en el Capítulo 7, durante el periodo inicial de cada experimento se observó una rápida construcción de ensuciamiento residual asociado a fenómenos de consolidación de los materiales colmatantes de la membrana. Como era de esperar, el flujo de retrolavado aplicado afectó al rendimiento del mismo, independientemente del flujo de filtración impuesto.

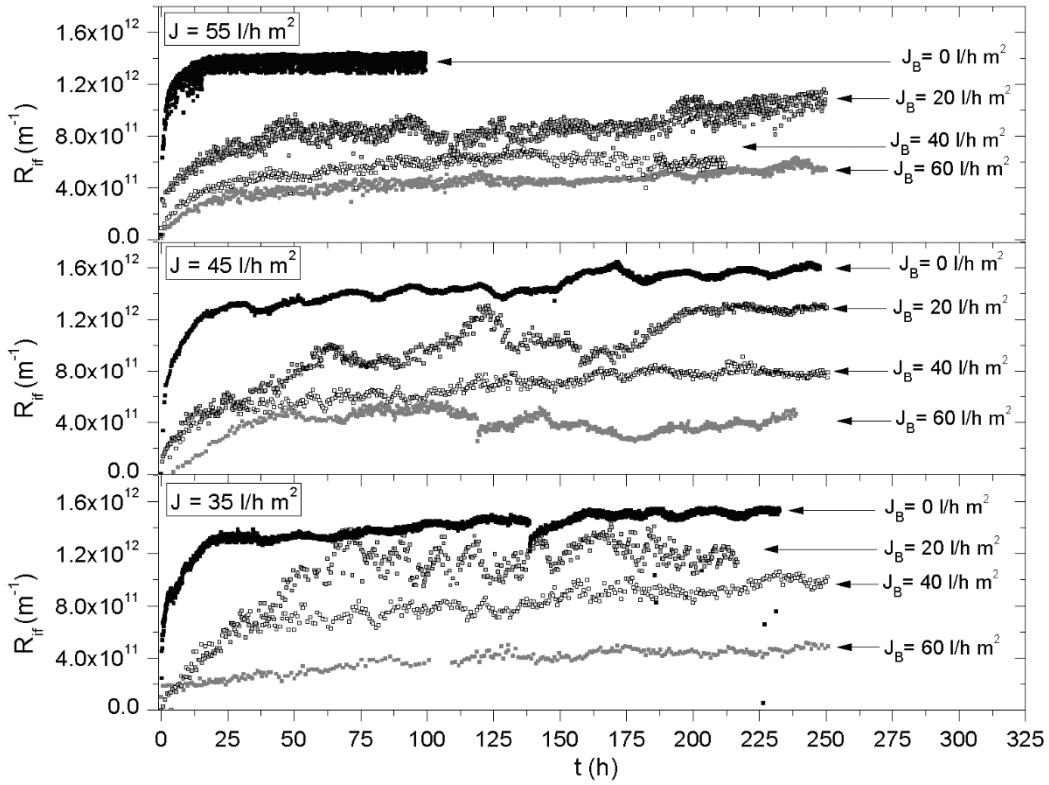

Figura 10.12. Evolución de la R_{if} para las diferentes condiciones de filtración estudiadas

El elevado ensuciamiento residual observado en los experimentos que aplicaron como limpieza física el relax, repercutió directamente en la operación del proceso reduciendo notablemente, el flujo neto. Por el contrario, la aplicación de retrolavado, independientemente de su flujo, favoreció la producción de flujos netos elevados: 33,9±0,2 L/hm^2, 42,6±0,6 L/hm^2 y 51,8±1 L/hm^2 para 35, 45 y 55 L/hm^2, respectivamente, debido a su efecto positivo en los tiempos de filtración.

En estos ensayos llevados a cabo en filtración frontal, las limpiezas físicas se apoyaron con aireación con el fin de mejorar el rendimiento de las mismas. La elevada frecuencia de las limpiezas, al aplicar relax obligó a incrementar considerablemente la aireación. Sin embargo, al aplicar retrolavados, la aireación fue significativamente baja (1-2 $Nm_{aire}^3/m_{permeado}^3$) respecto a los valores aplicados habitualmente en MBR industriales.

Por tanto, la aplicación del retrolavado por presión de consigna ha permitido operar un tMBR en filtración frontal a elevados flujos, limitando el ensuciamiento de la membrana y además, reduciendo significativamente los costes de operación.

4.5. Influencia de la suspensión biológica sobre el modo de operación por presión de consigna

La influencia de las características de la suspensión biológica en la efectividad del modo de operación por presión de consigna para mitigar el ensuciamiento de la membrana, se llevó a cabo aplicando diferentes concentraciones de oxígeno disuelto al proceso biológico, lo que conllevan estados de biofloculación de la suspensión diferentes (Capítulo 9).

Tabla 10.6. Tiempo de filtración, flujo neto y consumo de aireación para distintos ratios de aireación aplicados; J=45L/hm^2

A_R	t_F (min)	J_{net}(L/hm^2)	SADpnet ($Nm_{aire}^3/Nm_{permeado}^3$
0	1,39 ± 0,09	14,9 ± 1,5	57,9 ± 0,1
0,25	2,09 ± 0,14	24,7 ± 1,1	25,9 ± 0,1
0,5	10,20 ± 0,51	40,1 ± 0,2	3,9 ± 0,5
0,75	15,35 ± 0,52	41,2 ± 0,3	2,5 ± 0,5
1	18,63 ± 0,53	42,2 ± 0,1	2,1 ± 0,5

La Tabla 10.6 presenta el tiempo de filtración, el flujo neto y la aireación suministrada a la membrana para cada ratio de aireación ensayado. Como en capítulos anteriores, el retrolavado se aplicó con aireación, por tanto, y pese a que la filtración se realizó en frontal, se contabilizaron los consumos de aireación correspondientes. Al disminuir la frecuencia de retrolavado, el MBR ha presentado bajas tasas de aireación en comparación con MBRs industriales.

Los bajos ratios de aireación (A_R≤0,25) han producido un elevado ensuciamiento de la membrana por la baja biofloculación de la suspensión biológica, y por tanto, el rendimiento del MBR en términos de flujo neto fue bajo y los consumos de aireación para el proceso de membranas, altos. Por el contrario, los elevados ratios de aireación proporcionaron largos ciclos de filtración, y por tanto, elevados flujos netos y bajas tasas de aireación.

Un estudio económico preliminar reveló que las condiciones idóneas de operación corresponden a ratios de aireación moderados, que permiten tiempos de filtración altos, y por

tanto, un consumo bajo de aireación para los dos procesos, biológico y de membrana, además de, alcanzar una buena productividad en términos de flujo neto (Tabla 10.6).

Por último cabe destacar, que el modo de operación por presión de consigna incrementó automáticamente las frecuencias del retrolavado cuando la biofloculación resultó deficiente y en consecuencia, la evolución del ensuciamiento residual fue muy similar con independencia del flujo de permeado y del estado de biofloculación de la suspensión.

5. Análisis y caracterización del ensuciamiento reversible

El análisis y caracterización del ensuciamiento reversible de manera global, resulta complicado debido al gran número de variables que lo condicionan.

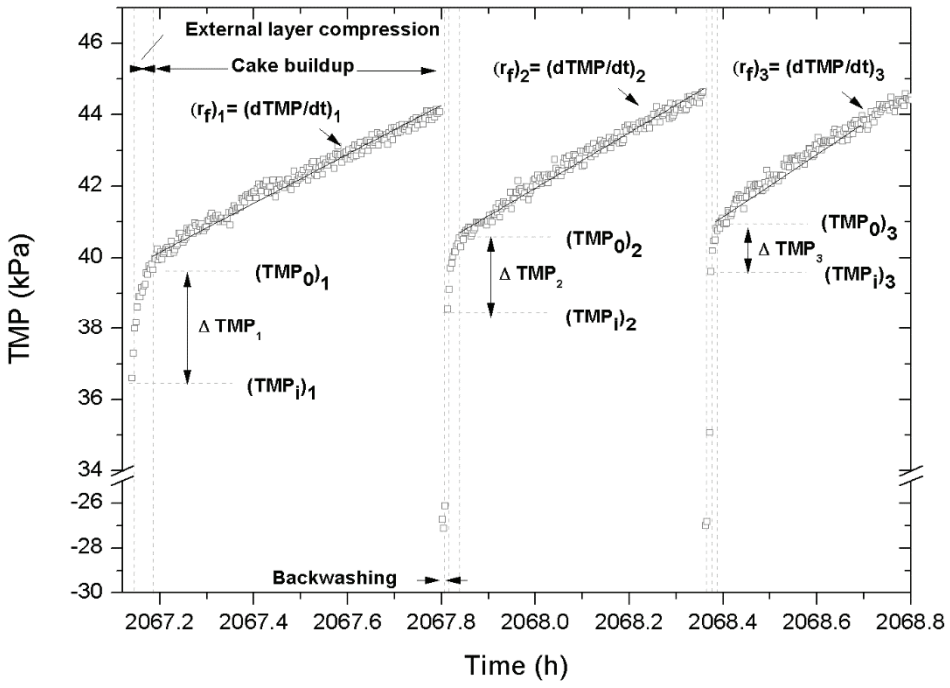

Figura 10.13. Perfil de TMP con los consecutivos ciclos de filtración/retrolavado al comienzo de la fase experimental en filtración tangencial para una presión transmembrana de consigna de 45kPa (Capítulo 7)

En el caso de los ensayos realizados en filtración tangencial (Capítulos 6 y 7) el ensuciamiento reversible observado se pudo interpretar por medio de un modelo de torta incompresible, definido por la ecuación [10.1]. La Figura 10.13 muestra el perfil típico de la TMP

con los consecutivos ciclos de filtración/retrolavado al establecer una presión transmembrana de consigna de 45 kPa (Capítulo 7). Durante la filtración se observaron dos fenómenos: un rápido crecimiento de la TMP, seguido de un crecimiento lineal. El periodo inicial puede ser debido al proceso de recompresión del ensuciamiento, mientras que el crecimiento lineal parece estar asociado al modelo de torta incompresible, tal y como ya se ha indicado. Por tanto, se puede distinguir la presión transmembrana inicial del ciclo de filtración (TMP_i) y la TMP_0 que es definida como el valor de TMP que separa el ensuciamiento residual externo del ensuciamiento reversible.

El fenómeno de recompresión se produce cuando parte del ensuciamiento eliminado por el retrolavado, permanece en las inmediaciones de la membrana, y se deposita rápidamente cuando se aplica de nuevo la fase de filtración. A este tipo de ensuciamiento se le denomina ensuciamiento residual externo, y se caracteriza por la caída de presión (ΔTMP) que tiene lugar durante su formación.

Al inicio de los ensayos correspondientes a los Capítulos 6 y 7, el MBR experimentó un incremento rápido de la TMP_i que fue disminuyendo en los siguientes ciclos (Figuras 10.10 y 10.13). El incremento del ensuciamiento residual interno viene acompañado de una reducción de la duración de la fase de recompresión (Figura 10.13). Éste comportamiento puede ser asociado a la consolidación del ensuciamiento residual externo que reduce la capacidad del retrolavado para eliminarlo, incrementándose el residual interno. Una vez que el proceso de consolidación del ensuciamiento residual termina, empieza a adquirir importancia la construcción de una torta incompresible totalmente reversible, tal y como confirma el bajo crecimiento experimentado por la TMP_i con el tiempo (0,018-0,072 mbar/h).

Los ensayos de filtrabilidad realizados en filtración frontal en el marco de los Capítulos 8 y 9, mostraron una evolución típica de la TMP, independiente del flujo de filtración y retrolavado impuestos o de la concentración de oxígeno disuelto disponible para el proceso biológico. La Figura 10.14 muestra, a modo de ejemplo, el perfil de la TMP en los ciclos sucesivos de filtración/retrolavado durante los ensayos enmarcados en el Capítulo 8, con un flujo de filtración de 35 L/hm^2 y un flujo de retrolavado de 20 L/hm^2.

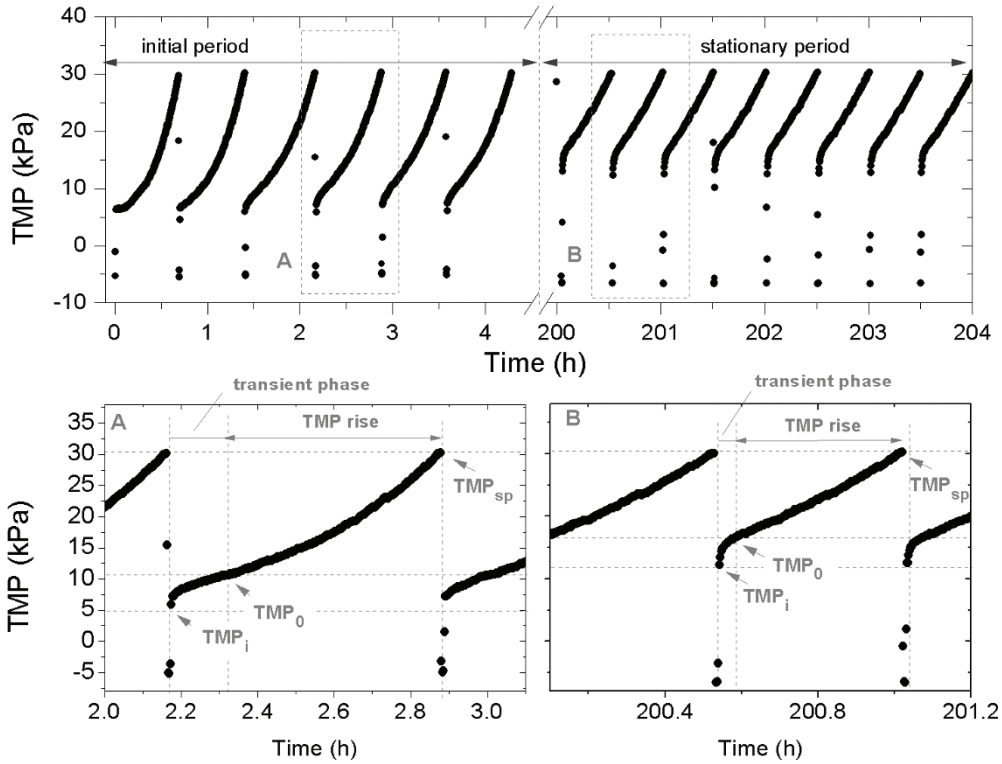

Figura 10.14. Perfil típico de TMP durante el periodo inicial y estacionario de los experimentos de filtración frontal; J=35 L/hm^2, J_B=20 L/hm^2 and t_B=30s

El análisis de los primeros ciclos de filtración (por lo general las primeras 25-50 horas, dependiendo de las condiciones) permite identificar claramente dos fenómenos de ensuciamiento, tal y como se observaba en los experimentos de filtración tangencial. La primera etapa se puede asociar a los fenómenos de recompresión del ensuciamiento residual externo, el cual se expulsa de la membrana debido al retrolavado pero no es dispersado suficientemente fuera de la zona convectiva de la membrana. Tras esta primera etapa, se observa un crecimiento no lineal de la TMP (Figura 10.14 A), que puede describirse considerando un modelo de construcción de una torta compresible. En este caso la caída de presión a través de la capa de ensuciamiento (ΔTMP_C) puede ser descrita mediante la expresión [10.4].

$$\Delta TMP_C = TMP - TMP_0 = \mu\alpha\omega J^2 t \qquad [10.4]$$

Donde α es la resistencia específica de la torta y ω la concentración de sólidos por unidad de volumen en la torta. Para partículas compresibles, α aumenta con TMP, que en el caso de suspensiones microbianas se ajusta a una expresión no lineal [10.5].

$$\alpha = \alpha_0 \left(1 + \frac{\Delta TMP_C}{P_a}\right) \qquad [10.5]$$

Donde α_0 es la resistencia específica de la torta a una presión cero y P_a es un parámetro que caracteriza el efecto de la compresibilidad.

La torta compresible en los primeros ciclos de filtración es completamente reversible, tal y como se puede deducir del bajo crecimiento de la TMP_i (Figura 10.14), debido a que la construcción de la torta compresible se debe principalmente, a grandes partículas que pueden ser eliminadas mediante el retrolavado. Sin embargo, se puede observar cambios importantes en la evolución de TMP_i cuando se realizan sucesivos ciclos de filtración/retrolavado. En el periodo estacionario se produjo un incremento considerable de la TMP_i, que puede ser atribuido a la consolidación del ensuciamiento. Aunque en los primeros ciclos la construcción de la torta fuera totalmente reversible, la estructura de la misma se vio modificada por los sucesivos ciclos, incrementando el ensuciamiento residual.

Una vez alcanzado el régimen estacionario, se observa un cambio de tendencia en la construcción de la torta (Figura 10.14) durante los experimentos de filtración frontal (Capítulos 8 y 9). El análisis de la compresibilidad reveló que para ambos periodos, la resistencia específica de la torta a presión cero (α_0) fue similar. Sin embargo, la compresibilidad, medida como P_a, disminuyó al aumentar el tiempo de operación, es decir, en el periodo estacionario la torta es más incompresible. Éste fenómeno parece estar asociado a la reducción de área disponible, debido a la consolidación del ensuciamiento, que incrementa el flujo local en el periodo estacionario.

La Figura 10.15 muestra la relación entre la resistencia específica de la torta y la caída de presión observada en los experimentos enmarcados en el Capítulo 9, mostrando el alto nivel de correlación entre los datos experimentales y el modelo matemático propuesto.

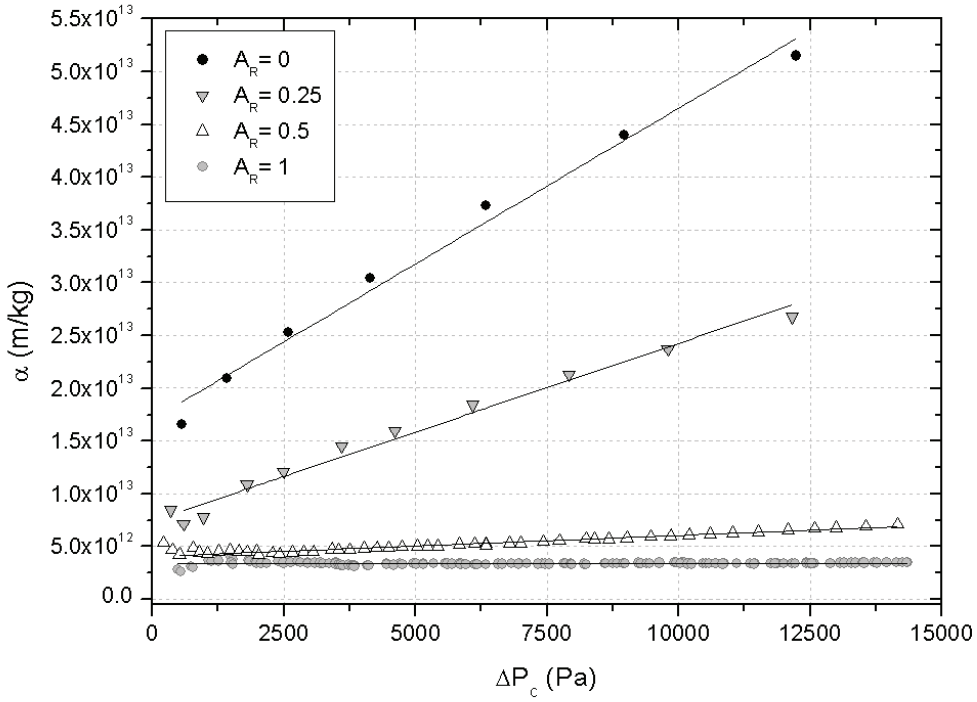

Figura 10.15. Evolución de la resistencia específica de la torta en función de la caída de presión durante un ciclo de filtración a diferentes ratios de aireación biológica; J=45 L/hm^2, J_B=60 L/hm^2 y t_B=30s

La Tabla 10.7 resume los valores de α_0 y P_a para las diferentes condiciones estudiadas en los ensayos correspondientes al Capítulo 9. La reducción de la concentración de oxígeno disuelto para el proceso biológico generó un incremento importante de la resistencia de la torta, debido principalmente a la presencia de partículas de menor tamaño y a la elevada concentración de BPC en el medio (Tabla 10.3). Además, los resultados experimentales indicaron una relación lineal entre el contenido de BPC y α_o (r^2=0,98). Por el contrario, ni el tamaño de las partículas, ni la concentración de BPC afectaron a la compresión.

El factor P_a resultó notablemente afectado por las condiciones de filtrabilidad (Tabla 10.7), así a flujos supra-críticos, el sistema presentó bajos valores de P_a, en sintonía con los resultados de los experimentos escalonados, donde la compresibilidad de la torta aumentó en condiciones supra-críticas. En el caso de operar en condiciones sub-críticas se favorece la construcción de una torta incompresible y la reducción de la concentración de BPC en el medio contribuye a una menor resistencia específica de la torta a presión cero.

Tabla 10.7. Parámetros del modelo de compresión para las condiciones estudiadas (Capítulo 9)

A_R	CONDICIONES DE FILTRACIÓN	Flujo (L/h m^2)	$\alpha_o \cdot 10^{-12}$ (m/kg)	P_a (Pa)
0	Supra-crítico	45	23,9 ± 0,9	11.622 ± 1.000
0.25	Supra-crítico	45	13,2 ± 0,2	10.265 ± 376
0.5	Supra-crítico	45	4,6 ± 0,6	29.600 ± 634
0.75	Sub-crítico	45	2,3 ± 0,3	406.000 ± 2.000
1	Sub-crítico	45	3,4 ± 0,2	347.000 ± 3.000
1	Supra-crítico	65	3,5 ± 0,6	2.210 ± 675
0	Sub-crítico	25	11,4 ± 0,6	10.500 ± 400
0	Crítico	15	32,1 ± 0,2	453.000 ±1.400

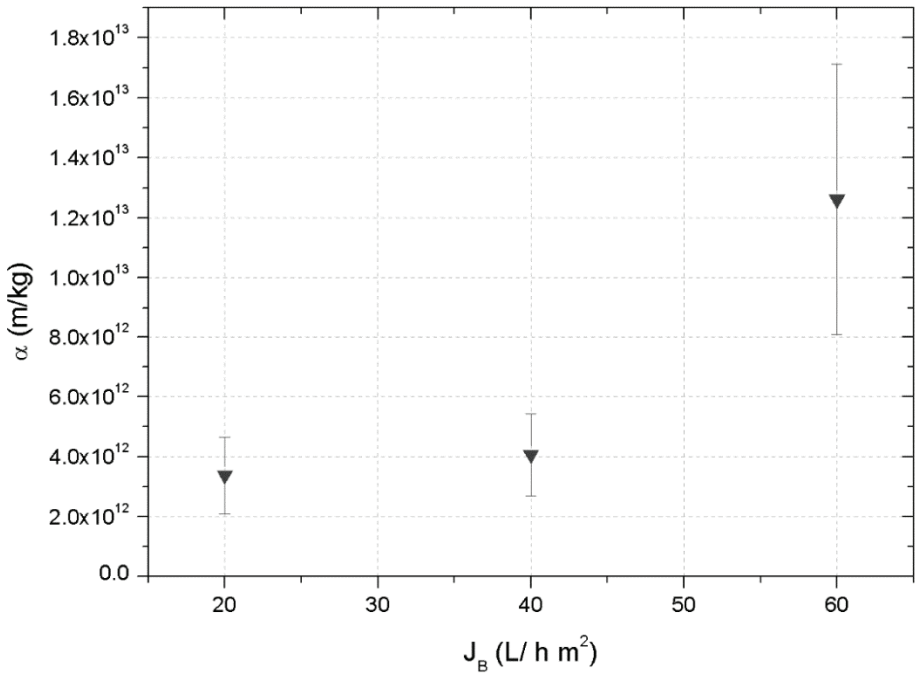

Figura 10.16. Evolución de la resistencia específica en función del flujo de filtración para las distintas condiciones de retrolavado evaluadas.

En los ensayos correspondientes al Capítulo 8, una vez alcanzado el régimen estacionario, la resistencia específica (α) no depende ni del flujo de filtración, ni de la presión aplicada, pues los

experimentos se realizan en condiciones sub-críticas (modelo de torta incompresible). La Figura 10.16 muestra la relación entre α y las condiciones del retrolavado. Los resultados obtenidos sugieren que la re-dispersión del ensuciamiento juega un papel relevante en las propiedades de la torta formada. Un incremento en el retrolavado parece incrementar la resistencia específica de la torta, debido posiblemente, a un incremento de la deposición de partículas de menor tamaño sobre la membrana.

6. Estudio y modelización del ensuciamiento residual

El ensuciamiento residual en un biorreactor de membrana terciario está caracterizado por un progresivo y lento crecimiento cuando se alcanza el régimen estacionario, tal y como revelan los datos experimentales presentados en la presente Tesis. Al inicio de cada estudio experimental se ha observado un rápido crecimiento de la presión transmembrana inicial (TMP_i) asociada al ensuciamiento residual interno (R_{if}) y que se justifica por la consolidación del ensuciamiento (Figuras 10.10, 10.12 y 10.14). Tradicionalmente, se asocia el ensuciamiento residual de la membrana con el bloqueo interno de poros o la compactación de la torta. Aunque el bloqueo de poros es causado por coloides y macromoléculas, se ha admitido que material adyacente a la membrana expuesto a grandes fuerzas compresivas puede sufrir deformación y como consecuencia, puede bloquear los poros. Por tanto, en los primeros ciclos de filtración, que presentan una larga duración, la consolidación y el bloqueo de poros parecen fenómenos inseparables, siempre que se opere con el modo alternativo por presión de consigna.

El Capítulo 7 analiza el efecto de la presión transmembrana de consigna (TMP_{sp}) sobre la consolidación del ensuciamiento de la membrana en un tMBR operado en filtración tangencial. La Figura 10.17 muestra las resistencias asociadas al ensuciamiento residual y reversible, en el estado estacionario en función de la TMP_{sp} impuesta.

El ensuciamiento residual interno aumenta linealmente con la TMP_{sp} en las condiciones estudiadas, debido a que la consolidación progresiva del ensuciamiento es mayor cuando el ensuciamiento máximo permitido es aumentado. Por otro lado, las resistencias asociadas al ensuciamiento residual externo y reversible han sido próximas entre sí, tendiendo a disminuir cuando se incrementa la TMP_{sp}. Por tanto, los resultados ponen de manifiesto que la principal contribución al ensuciamiento global de la membrana está asociado al ensuciamiento residual interno (en torno a un 58-96%).

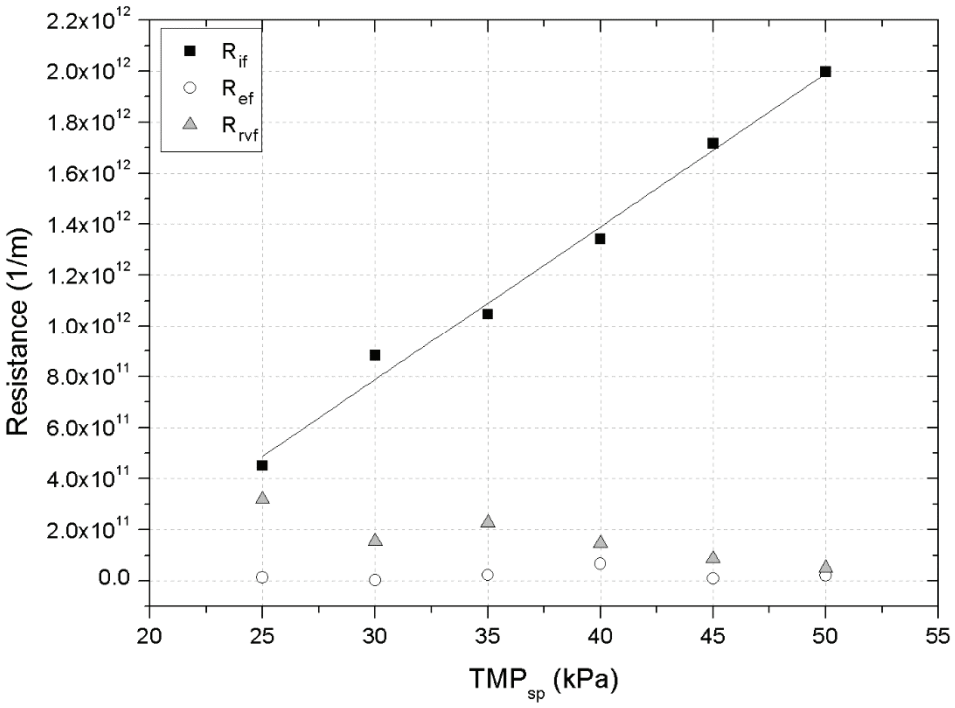

Figura 10.17. Resistencias asociadas a los diferentes tipos de ensuciamiento de la membrana frente a la TMP_{sp} aplicada (R_{if}: resistencia asociada al ensuciamiento residual interno; R_{ef}: resistencia relacionada con el ensuciamiento residual externo y R_{rvf}: resistencia debida al ensuciamiento reversible).

En el caso de filtración tangencial, el grado de consolidación del ensuciamiento residual parece no estar afectado por el flujo de retrolavado impuesto (Capítulo 6) tal y como se puede observar en la Figura 10.10, sin embargo cuando la filtración se realiza en modo frontal (Capítulo 8) el grado de consolidación se ve afectado por el flujo de retrolavado (Figura 10.12).

La Figura 10.18 muestra la evolución típica de la resistencia asociada al ensuciamiento residual interno ($J=45L/hm^2$; $J_B=60L/hm^2$; $t_B=30s$), donde el principal ensuciamiento fue observado en las primeras 25-50 horas, para continuar luego una evolución creciente más lenta. El crecimiento estable del ensuciamiento residual interno parece no estar afectado ni por el modo de filtración: frontal o tangencial, ni por el flujo de filtración o retrolavado y tampoco por las condiciones de filtración, puesto que parece que la consolidación del ensuciamiento actúa como una segunda membrana que podría prevenir el bloqueo de poros por parte de los BPC. Estos resultados son opuestos a los recogidos por otros estudios tal y como se analiza en el Capítulo 9, donde el ensuciamiento residual aumenta al empeorar las características de la

suspensión biológica (Capítulo 9). Estas discrepancias pueden ser atribuidas al ajuste automático de los retrolavados por el modo de operación por presión de consigna, que determina el grado máximo de ensuciamiento permitido sobre la membrana independientemente de su filtrabilidad.

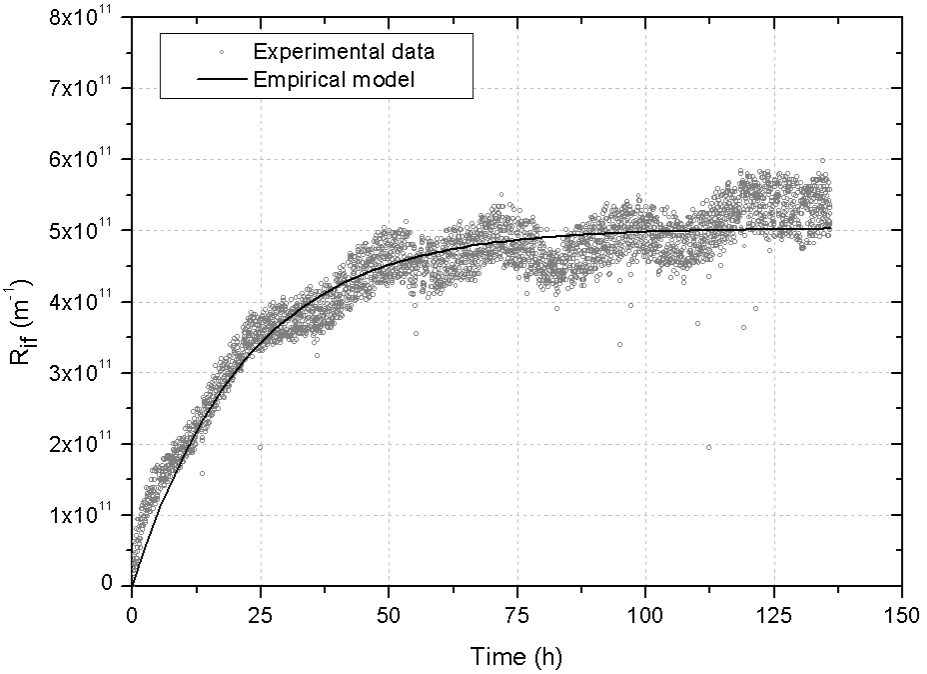

Figure 10.18. Evolución típica del ensuciamiento residual interno y ajuste de los datos experimentales al modelo empírico; A_R= 1; J=45L/hm^2; J_B=60L/hm^2; t_B=30s

El incremento del flujo de retrolavado permitió reducir el grado de consolidación del ensuciamiento, independientemente del flujo de filtración empleado (Figura 10.12, Capítulo 7), además el relax se ha presentado como una limpieza física con un bajo rendimiento. Las fluctuaciones observadas en las distintas condiciones (Figura 10.12 y 10.18) fueron producidas por los significativos cambios de filtrabilidad del lodo asociado a fluctuaciones en las condiciones ambientales. En conclusión, la eficacia de la limpieza física ha sido determinada principalmente, por el flujo de retrolavado, independientemente del flujo de filtración, debido al modo de operación por presión de consigna.

Con el objetivo de resumir el efecto de los diferentes parámetros de operación en el ensuciamiento residual, se ha propuesto un modelo empírico en el Capítulo 7, basado en que el ensuciamiento residual interno observado puede atribuirse principalmente, al proceso de

consolidación de la torta que tiene lugar en los primeros ciclos de filtración/retrolavado. Además, este mecanismo de ensuciamiento se asocia a la reducción del área de filtración disponible. El modelo empírico [10.6] presenta un primer término que describe el rápido crecimiento del ensuciamiento residual interno, mientras que el segundo considera el crecimiento más lento.

$$R_{if} = \left(R_{if}\right)_{asym}[1 - exp(-k_C t)] + r_{if} t \qquad [10.6]$$

Donde $(R_{if})_{asym}$ es el valor asintótico durante el periodo inicial, K_c es la constante cinética y r_{if} es la velocidad de ensuciamiento residual en el periodo inicial. La Figura 10.19A muestra la relación entre K_C y el flujo de retrolavado, para los distintos flujos de filtración ensayados (Capítulo 8). Los valores encontrados para el relax han sido significativamente altos debido posiblemente, al elevado grado de consolidación observado en estas condiciones. Sin embargo, cuando se aplica retrolavado, la constante cinética (K_C) parece no verse afectada ni por el flujo de retrolavado, ni por el de filtración. El valor de $(R_{if})_{asym}$ representa el área máxima que puede ser reducida mediante la consolidación, y como era de esperar éste valor decrece linealmente con el flujo de retrolavado, independientemente del flujo de filtración impuesto (Figura 10.19B). Además, este valor posee un orden de magnitud similar a la resistencia crítica encontrada en los experimentos de corta duración realizados para la determinación del flujo crítico (Capítulo 9).

Tabla 10.8. Parámetros del modelo empírico que describe el ensuciamiento residual bajo las distintas condiciones estudiadas

A_R	FLUJO (L/hm^2)	$(R_{if})_{asym}$ ·10^{-11} (m^{-1})	k_c ·10^{-2} (1/h)	r_{if} ·10^{-8} (1/m h)	R^2
0	15	5,10 ± 0,24	2,71 ± 0,29	20,1 ± 4,4	0,85
0	25	6,23 ± 0,67	3,37 ± 0,11	13,3 ± 3,8	0,85
0	45	5,03 ± 0,01	4,55 ± 0,03	14,7 ± 4,3	0,92
0.25	45	5,43 ± 0,06	4,40 ± 0,02	9,6 ± 2,7	0,91
0.5	45	5,83 ± 0,02	5,38 ± 0,14	5,0 ± 1,1	0,95
0.75	45	5,28 ± 0,03	4,50 ± 0,12	15,6 ±1,1	0,89
1	65	5,22 ± 0,02	2,24 ± 0,01	14,4 ± 4,2	0,87
1	45	5,56 ± 0,04	5,77 ± 0,31	4,3 ± 2,2	0,95

Como ya se ha mencionado, el ensuciamiento residual interno presenta el mismo comportamiento, independientemente del grado de bioflocculación que presente la suspensión biológica (Capítulo 9). La Tabla 10.8 resume los valores de los parámetros del modelo empírico propuesto para describir el ensuciamiento residual.

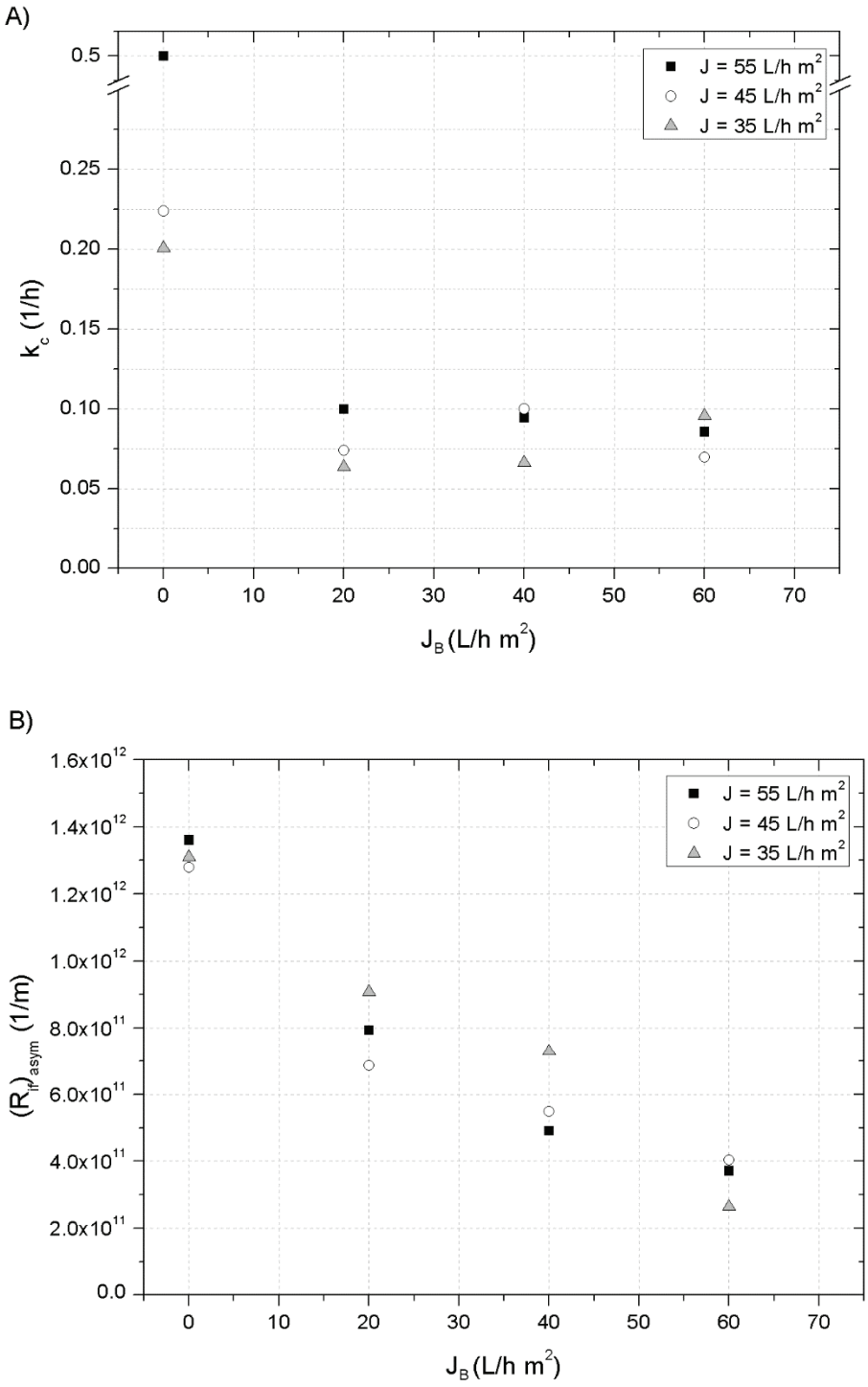

Figura 10.19. Relación de los parámetros empíricos de la ecuación [10.8] con el flujo de retrolavado para los distintos flujos de filtración estudiados; A K_C y B $(R_{if})_{asym}$

7. Estimación de las condiciones óptimas de operación de un biorreactor de membrana terciario

Para mantener el ensuciamiento de la membrana de un tMBR, este ha de ser operado con el modo alternativo por presión de consigna, que permite la operación en condiciones menos conservativas que el modo temporizado y por tanto, la reducción de costes de operación e instalación. Además, este modo de operación permite operar en filtración frontal sin poner en peligro la operación del MBR, reduciendo los costes de operación.

La modelización del ensuciamiento observado ha permitido realizar una estimación del consumo energético específico (SED) cuando el sistema opera en filtración frontal, con aireación durante el retrolavado, y bajo la máxima concentración de oxígeno disuelto para el proceso biológico. Además, esta estimación se realiza para una operación a 120 días, tiempo aceptable desde el punto de vista de la sostenibilidad del MBR, antes de efectuar una limpieza química de recuperación o mantenimiento. Para la determinación del SED sólo se ha considerado la energía consumida por el compresor y bomba de permeado (Capítulo 8). La Figura 10.20 muestra los resultados de la simulación realizada según las condiciones de filtración evaluadas.

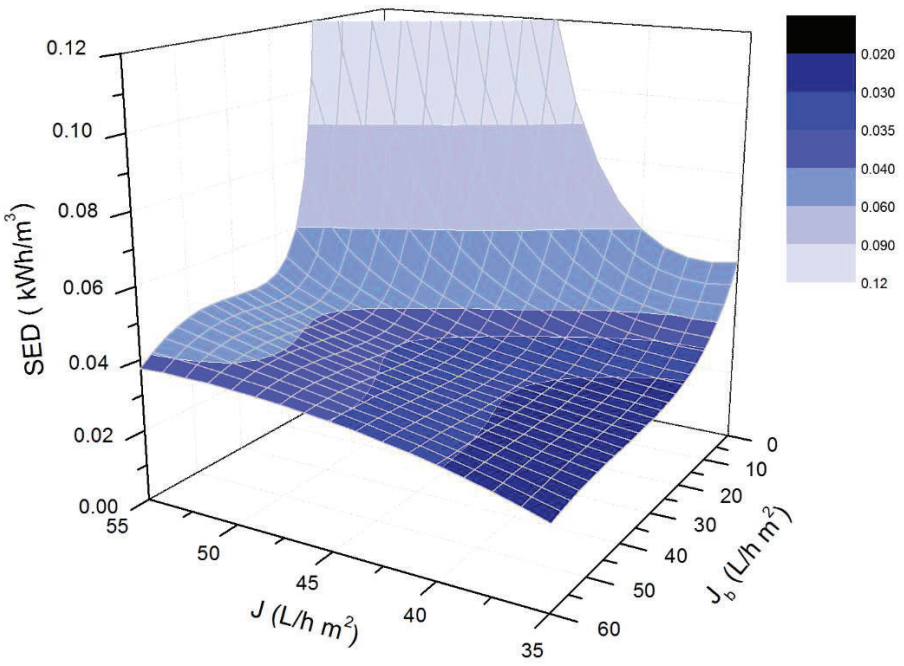

Figura 10.20. Estimación de la demanda específica de energía (SED) en función de distintas condiciones de operación

Un incremento del flujo de filtración por encima de 40 L/hm^2, implica un aumento de la velocidad de ensuciamiento y por tanto, una reducción de los ciclos de filtración, lo que se traduce en la necesidad de una mayor área de membrana y un aumento en la aireación para el proceso de filtración. Por otro lado, una reducción del flujo de retrolavado por debajo de 22,5 L/hm^2 genera un elevado grado de consolidación y por tanto, un incremento del SED. En conclusión, las mejores condiciones de operación pueden ser establecidas en: un flujo de filtración de 40 L/hm^2 y un flujo de retrolavado de 27,5 L/hm^2.

Para reducir los costes derivados de la aireación para el proceso biológico, las estimaciones de costes realizadas en el Capítulo 9 han revelado que la concentración de oxígeno disuelto debe mantenerse en 0,38 mg/L. En estas condiciones, el sistema alcanza bajos valores de SED (0,25 KWh/m^3) y una alta eliminación de materia orgánica (62,5 %), así como una nitrificación parcial del efluente (67,7%) que garantiza su transporte a largas distancias sin generación de especies tóxicas, ni corrosivas permitiendo además su reutilización inmediata.

CAPÍTULO 11: Conclusiones generales

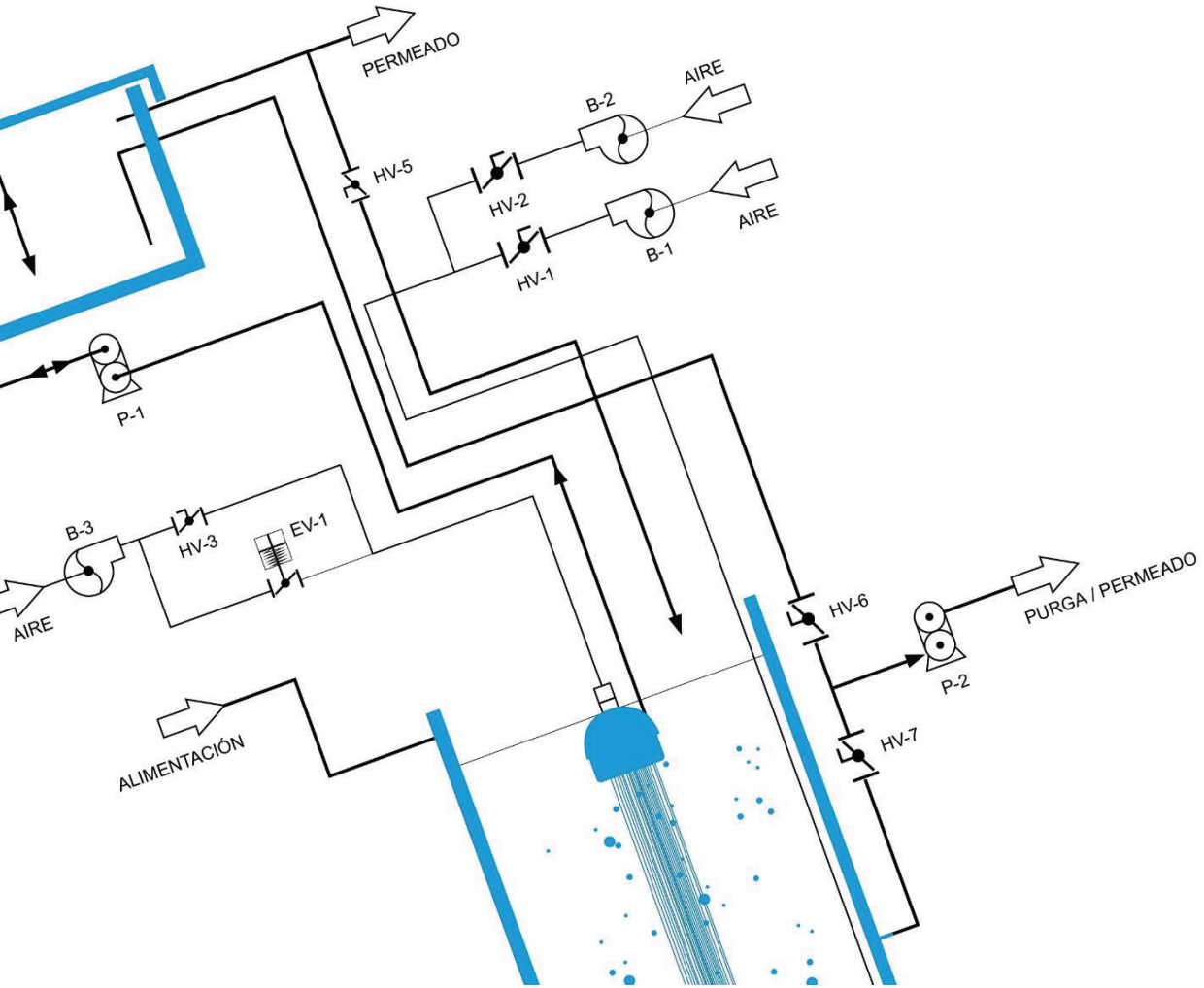

Capítulo 11

Conclusiones generales

El objetivo principal de la tesis ha sido evaluar la viabilidad de la tecnología de biorreactores de membranas sumergidas como tratamiento terciario de un sistema convencional de depuración de aguas residuales domésticas. De los resultados obtenidos se derivan las siguientes conclusiones generales:

1. El estrés ambiental afecta significativamente a las características del lodo y al ensuciamiento de la membrana. Las altas cargas orgánicas de la alimentación afectan al sistema en función de la concentración de sólidos suspendidos presentes en el licor mezcla. Mientras que el efecto de la carga ha sido más importante a concentraciones de sólidos inferiores a los 3.000mg/L, éste ha sido poco significativo al operar con concentraciones de biomasa superiores. Este comportamiento parece ser atribuible a la degradación/adsorción de agregados de biopolímeros (BPC) por parte de la biomasa.

2. El biorreactor de membrana terciario ha alcanzado una elevada reducción de materia orgánica independientemente de la concentración de oxígeno disuelto, si bien el grado de nitrificación logrado se ha visto afectado por este parámetro. En lo referente a la biofloculación, ha empeorado en el seno del biorreactor al operar con bajas concentraciones de oxígeno disuelto, alcanzando para ratios de aireación elevados un moderado tamaño del flóculo, una baja concentración de BPCs y una baja turbidez en el sobrenadante ligada, esta última, a la concentración de microorganismos no floculados.

3. La operación con limitación de sustrato del biorreactor de membrana terciario ha permitido un lento desarrollo de la biomasa y por tanto, evitar la purga de lodos y un elevado rendimiento de depuración asociado a la concentración moderada de sólidos suspendidos en el licor mezcla. Asimismo, la elevada edad de los lodos impuesta ha favorecido la reducción de productos solubles microbianos (SMP) y agregados de biopolímeros (BPC).

4. La concentración de sólidos suspendidos en la suspensión o licor mezcla (MLSS) presenta una correlación significativa con otros parámetros de dicha suspensión, como la actividad biológica endógena, la viscosidad aparente y el contenido en agregados de biopolímeros (BPC). Sin embargo, la concentración de MLSS no parece afectar de manera directa a la filtrabilidad medida en la suspensión expresada como TTF (*time to filter*). Por otro lado, la concentración de agregados de biopolímeros (BPC) si está muy relacionada con la velocidad de construcción del ensuciamiento asociado a torta incompresible y puede ser utilizado como indicador de la propensión de la suspensión a ensuciar la membrana.

5. La aplicación de biorreactores de membrana como tratamiento terciario ha permitido eliminar materia orgánica de forma más eficaz que la ultrafiltración directa, debido al proceso de degradación biológica. Además, ha permitido reducir la presencia de agregados de biopolímeros (BPC) en el medio, contribuyendo así a la construcción de un ensuciamiento lento y totalmente reversible sobre la superficie de la membrana.

6. Las membranas de nanofiltración y ósmosis inversa evaluadas como post-tratamientos de efluentes de procesos de membrana de ultrafiltración, presentaron ensuciamiento de naturaleza orgánica e inorgánica similar, según han revelado las autopsias realizadas a dichas membranas. Sin embargo, el permeado de la ultrafiltración directa provoca un ensuciamiento más severo por su alto contenido en carbono orgánico disuelto, en comparación con el efluente del biorreactor de membrana terciario.

7. El modo de activación del retrolavado por presión de consigna ha permitido operar con flujos supra-críticos en condiciones de filtración tangencial, sin llevar a cabo limpieza química. En estas condiciones, el mecanismo de ensuciamiento ha sido descrito por un modelo de construcción de torta incompresible, totalmente reversible, que actúa como una segunda membrana previniendo la adsorción de agregados de biopolímeros (BPC). La principal ventaja de este modo de operación es que permite limitar el ensuciamiento ajustando la frecuencia del retrolavado en función de la construcción de dicho ensuciamiento.

8. En el caso de la operación del biorreactor de membrana terciario en filtración frontal, el ensuciamiento de la membrana se ha descrito mediante un modelo de torta compresible donde la compresibilidad se reduce en los sucesivos ciclos de filtración/retrolavado. Por otro lado, la compresibilidad de la torta aumenta en condiciones de operación supra-críticas,

mientras que la resistencia específica de la torta a presión cero parece estar muy influenciada por las condiciones del retrolavado y por la concentración de agregados biopoliméricos (BPC) en el medio.

9. La operación del biorreactor cuando se han establecido valores elevados de presión de consigna (TMP_{sp}) ha dado lugar a una mayor consolidación del ensuciamiento y por tanto, a una reducción de la productividad del sistema. Los resultados experimentales han mostrado que las mejores condiciones de operación corresponden a valores moderados de presión de consigna. No obstante, el ensuciamiento residual externo y el reversible no se ven afectados por el valor de la presión de consigna establecido, pues la contribución de estos al ensuciamiento global de la membrana, es bajo.

10. El ensuciamiento residual está asociado principalmente, a la consolidación del ensuciamiento que se observa en los primeros ciclos de filtración. Este ha sido modelizado mediante una expresión no lineal, de carácter empírico que considera que el ensuciamiento reduce gradualmente el área de filtración disponible.

11. El flujo de retrolavado influye significativamente sobre el ensuciamiento residual interno de la membrana, mientras que el estado de biofloculación de la suspensión no parece tener la relevancia esperada por aplicar el retrolavado en función de la presión de consigna.

12. Las condiciones de operación más favorables del biorreactor de membranas para tratamiento terciario de aguas residuales domésticas han correspondido a la operación a concentraciones de agregados biopoliméricos (BPC) inferiores a 5mg/L y concentraciones de oxígeno disuelto en torno a 0,38 mg/L. La aplicación de retrolavado durante 30 s con inyección simultánea de aire cuando se opera con presiones de consigna pre-fijadas moderadas (30 kPa) permite optimizar la operación del biorreactor, en filtración frontal, con un flujo de filtración de 40 L/hm^2 y un flujo de retrolavado de 27,5L/hm^2. Estas condiciones han permitido producir un elevado flujo neto con una demanda de energía específica baja.

ANEXO A: Nomenclatura

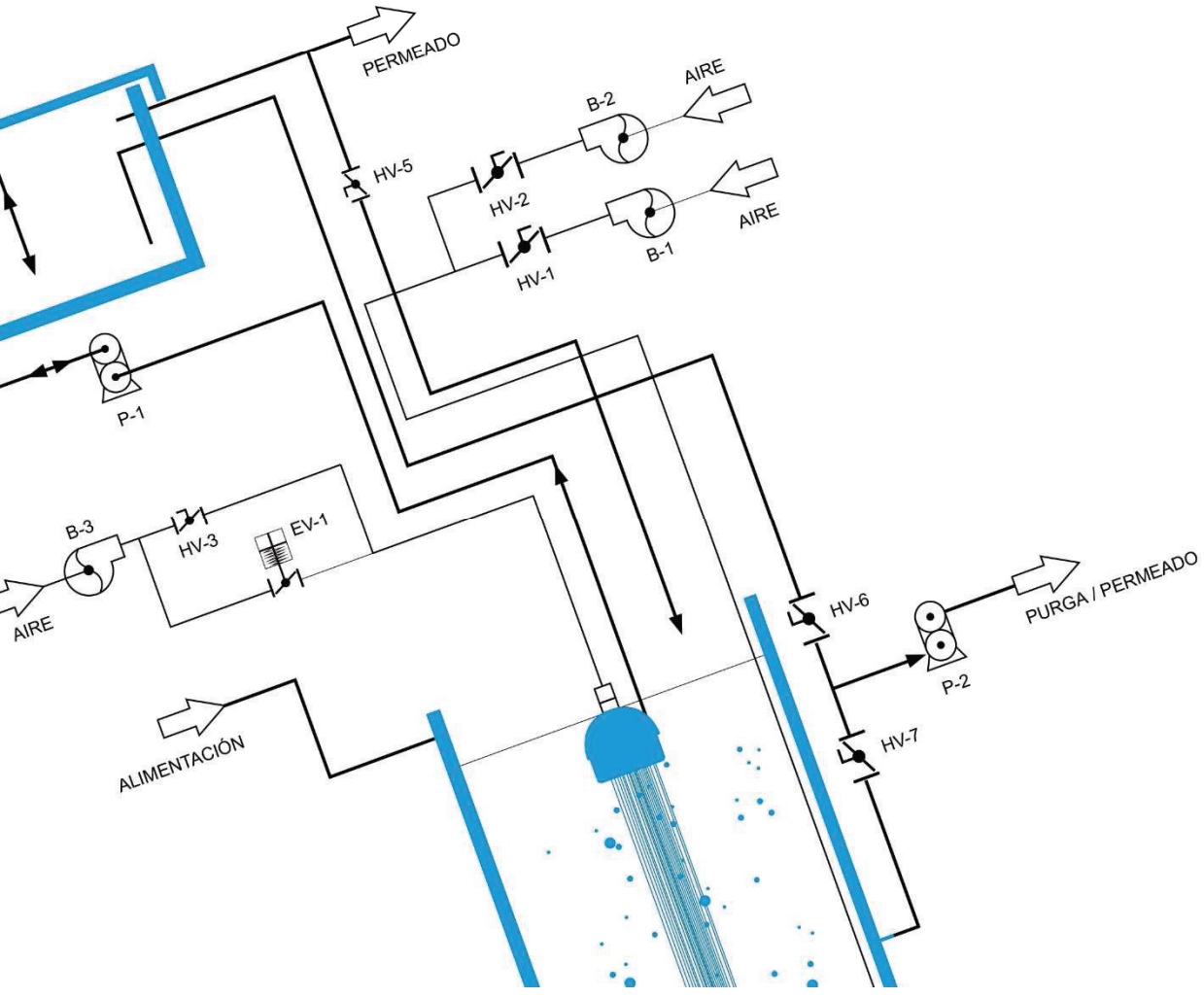

Nomenclatura

$(F/M)_C$, relación alimentación carbonosa/microorganismos, kg COD_s/kg MLVSS d

$(F/M)_N$, relación alimentación nitrogenada/microorganismos, kg N/kg MLVSS d

$(J')_t$, flujo de filtración local a tiempo t, L/h m^2

$(J_{net})_{ave}$, flujo neto medio, L/h m^2

$(R_{if})_{asym}$, resistencia asintótica asociada al ensuciamiento residual interno en el periodo inicial, 1/m

$(R_{rdf})_{ave}$, Resistencia media asociada al ensuciamiento residual, L/m

$(t_F)_{ave}$, duración de la fase de filtración media, min

$(TMP_i)_t$, presión transmembrana después de un retrolavado a un tiempo t, kPa

A, área de la membrana, m^2

AOB, bacterias oxidantes de amonio

A_R, ratio de aireación

AUR, velocidad de consumo máximo de amonio, mg N/g MLVSS h

BOD_5, demanda biológica de oxígeno a los 5 días mg/L

BPC, sustancias biopoliméricas, mg DOC/L

CAPEX, costes de instalación

CIP, limpiezas químicas in situ

COD_s, demanda química de oxígeno soluble mg/L

COD_t, demanda química de oxígeno total mg/L

$D_{(v,0.10)}$, tamaño medio de partículas para el 10% del volumen total, µm

$D_{(v,0.50)}$, tamaño medio de partículas para el 50% del volumen total, µm

$D_{(v,0.90)}$, tamaño medio de partículas para el 90% del volumen total, µm

DFC_m, método de caracterización de filtración frontal

DO, concentración de oxígeno disuelto, mg/L

DOC, carbono orgánico disuelto, mg/L

EfOM, materia orgánica presente en el efluente, mg DOC/L

EPS, sustancias extrapoliméricas celulares

F/M, relación alimentación/microorganismos, kg COD/kg MLSS d

HRT, tiempo de residencia hidráulico, h

J, flujo de filtración, l h/ m^2

J/J_0, flujo normalizado

J_0, flujo inicial, L/h m^2

J_B, flujo de retrolavado, l h/ m^2

J_c, flujo crítico, l h/ m^2

J_{net}, flujo neto, l h/ m^2

k_c, constante cinética del ensuciamiento residual, 1/h

LQOs, límite de cuantificación

MBR, biorreactor de membrana

M_{cri}, masa crítica, g/m^2

MLSS, solidos suspendidos en el licor mezcla, mg/L

MLVSS, solidos suspendidos volátiles en el licor mezcla, mg/L

MWCO, tamaño molecular de corte, Da

NF, nanofiltración

NIUR, velocidad máxima de consumo de nitrito, mg N/g MLVSS h

$N\text{-}NH_3$, nitrógeno en forma amoniacal, mg/L

$N\text{-}NO_2^-$, nitrógeno en forma de nitrito, mg/L

$N\text{-}NO_3^-$, nitrógeno en forma de nitrato, mg/L

NOB, bacterias oxidantes de nitrito

NPV, valor presente neto

NUR, velocidad máxima de consumo de nitrato, mg N/g MLVSS h

OPEX, costes operacionales

P_a, presión característica de la compresibilidad, kPa

P_{A1}, presión absoluta en el interior

P_{A2} , presión absoluta en el exterior

PLC, control lógico programable

PSD, distribución de tamaño de partículas

PVDF, fluoruro de polivinilo

Q_A caudal volumétrico de aire para el proceso de membranas, Nm^3/h

Q_P, caudal volumétrico de permeado neto, m^3/h

R, constante general de los gases

r, coeficiente de Pearson

R, recovery

R, resistencia del ensuciamiento total, 1/m

RC, limpieza química de recuperación

R_{ef}, resistencia asociada al ensuciamiento residual externo, L/m

R_f, resistencia del ensuciamiento, 1/m

r_f, velocidad de ensuciamiento reversible, kPa/h

R_{fcrti}, resistencia asociada a la presión transmembrana crítica, 1/m

R_{if}, resistencia asociada al ensuciamiento residual interno, 1/m

r_{if}, velocidad de ensuciamiento residual, 1/m h

R_m, resistencia hidráulica de la membrana limpia, 1/m

RO, ósmosis inversa

R_{rdf}, resistencia asociada al ensuciamiento residual, 1/m

R_{rvf}, resistencia asociada al ensuciamiento reversible, L/m

R_{sp}, resistencia asociada al ensuciamiento antes de un retrolavado, L/m

R_t, resistencia hidráulica total, L/m

SAD_{mnet}, demanda específica de aire con respecto al área de membrana, $Nm^3/h\ m^2$

SAD_p, demanda específica de aire con respecto al flujo de permeado, Nm^3/m^3

SAD_{pnet}, demanda específica de aire con respecto al flujo de permeado neto, Nm^3/m^3

SED, demanda energética específica, kWh/m^3

SMP, productos solubles microbianos

$SOUR_{endogenous}$, velocidad de consumo endógeno, mg O_2/g MLVSS h

$SOUR_{AOB}$, velocidad de consumo de oxígeno de las bacterias AOB, mg O_2/g MLVSS h

$SOUR_{NOB}$, velocidad de consumo de oxígeno de las bacterias NOB, mg O_2/g MLVSS h

$SOUR_{OHO}$, velocidad de consumo de oxígeno de las bacterias heterótrofas, mg O_2/g MLVSS h

SRT, edad de lodo, días

SST, sólidos suspendidos totales, mg/L

T, temperatura, K

t, tiempo, s

t_B, duración del retrolavado, s

t_{crit}, tiempo de operación crítico,

t_F, duración de la fase de filtración, min

tMBR, biorreactor de membrana terciario

TMP, presión transmembrana, kPa

TMP_0, presión transmembrana asociada a la construcción de la torta compresible o incompresible, kPa

TMP_{cri}, presión transmembrana crítica, kPa

TMP_{ef}, presión transmembrana asociada al ensuciamiento residual externo, kPa

TMP_f, presión transmembrana al final del ciclo de filtración, kPa

TMP_i, presión transmembrana al inicio del ciclo de filtración, kPa

TMP_{sp}, presión transmembrana de consigna, kPa

t_{op}, tiempo de operación estimado, d

TSS, sólidos suspendidos totales, mg/L

TTF, time to filter, min

UF, ultrafiltración directa

WWTP, planta de tratamiento de aguas residuales

Y_{obs}, coeficiente de crecimiento del lodo, kg MLVSS/kg COD

Letras griegas

$(\eta)_{ave}$, eficiencia media del retrolavado, %

η, eficiencia del retrolavado, %

α, resitencia específica del depósito, m/kg

α_0, resitencia específica del depósito a presión cero, m/kg

ΔTMP, caída de presión asociada al ensuciamiento residual externo, kPa

ΔTMP_c, caída de presión diferencial a través de la torta, kPa

ζ_c ,eficiencia del compresor

ζ_p , eficiencia de la bomba

λ, índice adiabático

μ, viscosidad del permeado, Pa s

ω, concentración de sólidos en la torta por unidad de permeado filtrada, kg/m^3

ANEXO B: Effect of sludge characteristics on membrane fouling during star-up of a tertiary submerged membrane bioreactor

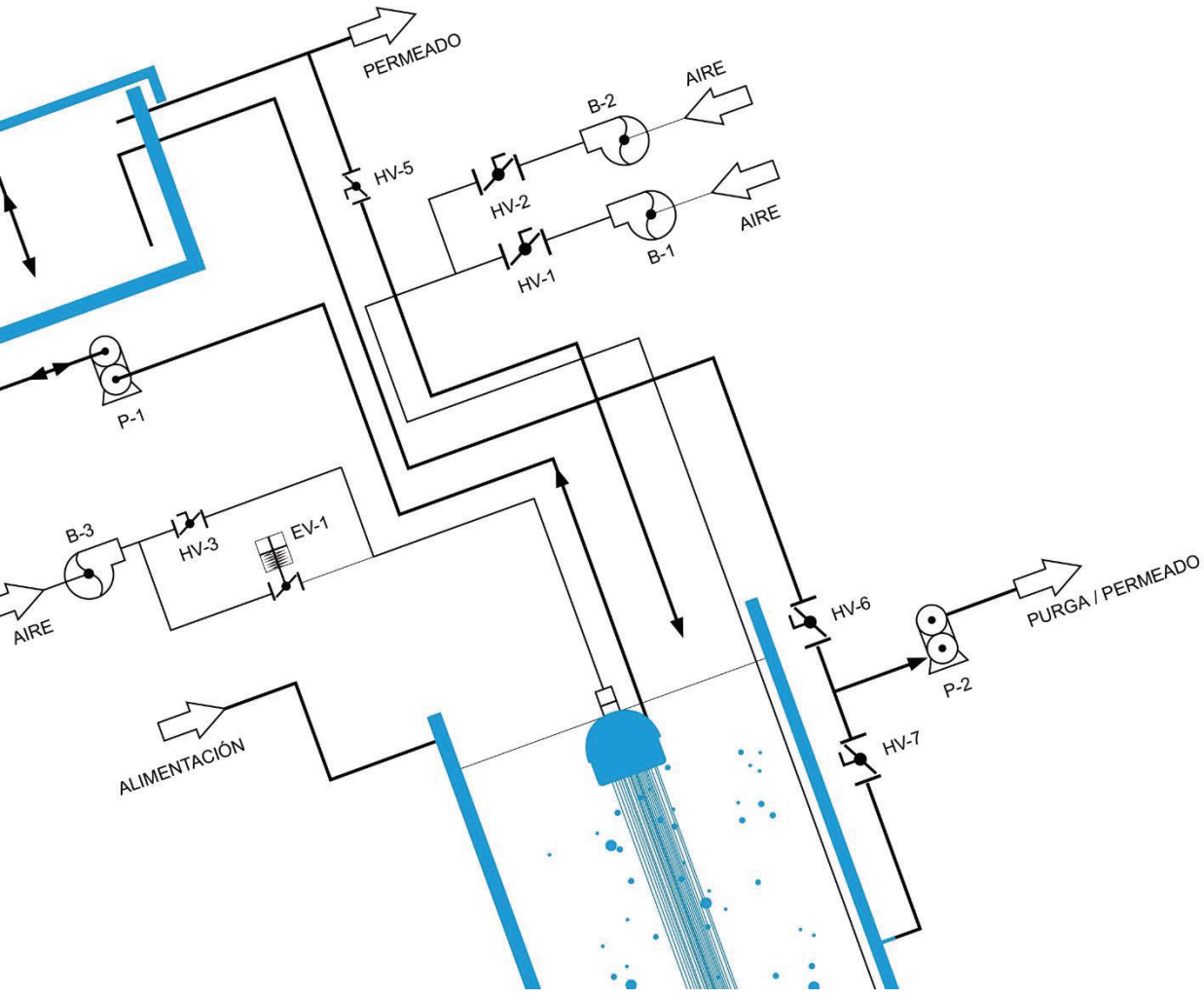

Environ Sci Pollut Res (2016) 23:8951–8962
DOI 10.1007/s11356-016-6138-y

RESEARCH ARTICLE

Effect of sludge characteristics on membrane fouling during start-up of a tertiary submerged membrane bioreactor

Oliver Díaz[1] · **Luisa Vera**[1] · **Enrique González**[1] · **Elisa García**[1] · **Juan Rodríguez-Sevilla**[1]

Received: 27 November 2015 / Accepted: 19 January 2016 / Published online: 29 January 2016

Abstract In membrane bioreactors applied to wastewater treatment, fouling is typically a complex function of sludge characteristics. A pilot-scale tertiary submerged membrane bioreactor (tMBR) was continuously operated for over 200 days to assess the effect of biomass physiological state and environmental stress on process performance. Sludge characteristics were evaluated in terms of suspended solid concentration (MLSS and MLVSS), apparent viscosity, bioflocculation state, filterability, bioactivity, biopolymeric clusters (BPCs) and soluble microbial products. During the initial period of the tMBR start-up, when MLSS was below 3000 mg/L, the biomass was found to be very sensitive to environmental stress by sudden oxygen increase or organic shock loading, resulting in temporary biomass deflocculation and BPC release, and consequently, severe induced membrane fouling. However, at higher MLSS values, low stable biomass growth (0.04 ±0.002 kg MLVSS/kg COD) was measured, regardless of organic overloading shocks or feeding failures. This period was also characterised by low bioactivity, BPC content and membrane fouling. Statistical analysis showed that BPCs have an important role when compared with other sludge properties as indicators of its fouling potential.

Responsible editor: Bingcai Pan

✉ Luisa Vera
luvera@ull.es

[1] Departamento de Ingeniería Química, Universidad de La Laguna (ULL), Av. Astrof. Fco. Sánchez s/n, 38200 La Laguna, Spain

Keywords Secondary effluent reclamation · Tertiary submerged membrane bioreactor · Fouling · Biopolymer clusters · Sludge properties · Biological nitrification

Introduction

Over the last two decades, membrane bioreactor (MBR) technology has attained a significant market share in municipal wastewater treatment, increasing its value at a compound annual growth rate of 10–15 % (Marketsandmarkets 2014). This technology combines suspended biomass, similar to the conventional activated sludge process, with microfiltration or ultrafiltration membranes that replace gravity sedimentation and clarify the wastewater effluent. Among the commercially available process configurations and membrane modules of MBRs, the submerged hollow-fibre type is the most widely used in municipal wastewater treatment owing to lower operation costs (Judd 2010). The rapid market penetration of MBRs has principally been driven by superior effluent quality, suitable for unrestricted irrigation and other industrial applications. Such quality permits a significant reduction of total plant footprint compared to conventional activated sludge plant (Cote et al. 2012). However, despite considerable progress over the past two decades, membrane fouling is still the main factor limiting widespread application of this technology. This drawback leads to increased operating expenditure (OPEX), due to the cost of membrane aeration, cleaning requirements and membrane replacement (Fenu et al. 2010).

Fouling can be defined as the alteration in the membrane caused by specific physical and/or chemical interactions between the membrane and components of the microbial suspension, leading to membrane permeability loss. Several mechanisms have been proposed to explain this phenomenon, including pore clogging, adsorption of foulants, gel or cake

formation, cake layer consolidation and osmotic pressure effects (Lin et al. 2014). Conventional filtration strategies to reduce fouling largely involve air scouring to induce favourable hydrodynamics in the vicinity of the membrane surface and physical cleaning through backwashing (i.e. permeate is used to flush the membrane backwards) or relaxation (when no filtration takes place), supplemented with periodic chemical cleaning in place (CIP) (Judd 2010). The rate and extent of fouling is typically a complex function of membrane properties, hydrodynamic and operating conditions, feedwater nature and microbial suspension characteristics (Le-Clech et al. 2006). Therefore, for a given system (i.e. feedwater and membrane) and favourable hydrodynamics, an appraisal of the impact operating parameters have on microbial suspension characteristics is necessary, in order to select the best operating conditions. Several authors have tried to identify the characteristics of the suspensions that have the greatest influence on fouling, among which are concentration of suspended solids in the mixed liquor (MLSS), viscosity, particle size distribution (PSD), biomass activity and biopolymer content (Le-Clech et al. 2006; Meng et al. 2009). Biopolymers are organic substances of microbial origin, consisting mainly of polysaccharides and proteins, which can be in the microbial flocs (extracellular polymeric substances—EPSs), or in the liquid phase as soluble microbial products (SMPs) and colloidal biopolymer clusters (BPCs). Based on the concept of utilisation and biomass associated products (Aquino and Stuckey 2008), biopolymer content is related to various microbial processes including substrate degradation, biomass decay, EPS hydrolysis and soluble biopolymer degradation.

Since MBR use began, MLSS has been considered one of the main foulant parameters. Nevertheless, most studies indicate that the MLSS concentration, considered alone, is a poor indicator of the fouling tendency of suspensions (Meng et al. 2009, Drews 2010; Van den Broeck et al. 2011). In general, the relationship between MLSS concentration and fouling appears to depend on the MLSS concentration range; below 6 g/L, an inverse relationship is often reported while a direct relationship is generally found above 15 g/L (Le-Clech et al. 2006). A greater MLSS effect may have an influence on sludge viscosity, so affecting the hydrodynamics of the filtration process (Trussell et al. 2007). In addition to MLSS, other factors such as sludge morphology (i.e. particle-size distribution) and BPCs are expected to cause membrane fouling (Wang and Li 2008). Since sludge flocs and free bacteria are considerably larger than membrane pores, particle size distribution (PSD) has an influence on the explanations of fouling focussed on cake-layer and consolidation mechanisms. Many authors report that cake layers formed by small flocs were denser than those by large ones, probably due to a higher specific cake resistance according to the Carman–Kozeny equation (Lin et al. 2011). In addition, small flocs have a greater tendency to settle on the membrane due to their lower back-transport velocity (Zeman and Zydney 1996). Meanwhile, it is widely reported that biopolymer matter strongly affected membrane fouling in an MBR. Soluble/colloidal biopolymers could enter into the membrane pores causing pore blocking; they form a gel layer, enhance floc attachment to the membrane, affect cake structure and induce osmotic effect (Lin et al. 2014).

Despite extensive research efforts to understand the effect of operating conditions on biomass characteristics and membrane fouling propensity, the variety of installations and feedwater characteristics sometimes lead to contradictory results, as in the case of sludge retention time (SRT) (Sabia et al. 2013; Villain and Marrot 2013). Moreover, determination of the actual membrane fouling rate is significantly affected by the fouling history of the membrane (Drews 2010). For this reason, several ex situ filterability tests such as the time-to-filter (TTF) or Delft filtration characterisation method (DFCm) have been introduced. Nevertheless, these tests may not accurately reflect the real operating conditions in MBRs and the correlation between the test methods and membrane fouling rates must be checked case by case (Drews 2010). In addition, the interconnection between sludge characteristics adds a particular complication in ascertaining which component of the suspension is the primary cause of membrane fouling (Van den Broeck et al. 2011). Therefore, pilot tests are generally required to characterise the suspensions with greatest influence on fouling under particular MBR operating conditions.

Recent studies have shown the capability of tertiary submerged membrane bioreactors (tMBRs) for treatment of secondary effluents from old plants with poor performance by secondary clarifiers (e.g. Vera et al. 2014). These clarifier malfunctions can compromise the economic feasibility of other tertiary treatments. In fact, growing interest in this technology has been seen recently in the Aquapolo project (Sao Paulo, Brazil), the largest wastewater reuse project in the southern hemisphere, which includes a tMBR in the treatment scheme (Koch 2014). One of the most attractive points of tMBR is its capability to operate under complete solid retention (without a waste sludge purge) due to extremely low sludge production in the substrate-limited conditions imposed. This advantage significantly reduces operating costs (Vera et al. 2014). There are several experiments with MBRs treating raw municipal wastewater that have demonstrated their capability to operate under complete sludge retention time limitations without drawbacks in biodegradation activity (e.g., Rosenberger et al. 2002). In these experiences, high biomass concentrations were required (12 to 24 g/L) in order to operate under substrate-limited conditions, which had a negative impact on oxygen transfer efficiency and hence on operating costs. In addition, Pollice et al. (2008) found that sludge filterability deteriorated under complete sludge retention, probably due to excessive increments in MLSS and sludge

viscosity. In contrast, tMBRs offer the capability to operate under complete sludge retention time and moderate MLSS concentration, due to low organic content in the feedwater. However, the consequences of complete sludge retention for morphology, bioactivity, soluble biopolymer content and filterability of the microbial suspension must be studied in detail in order to optimise process performance.

The aim of this study is to assess biomass development in a tMBR and its relationship with membrane fouling. For this purpose, a pilot tMBR operated with complete sludge retention was continuously fed with a secondary effluent for 195 days. Biomass development was assessed by following the evolution of MLSS, MLVSS, viscosity, particle size distribution, TTF, bioactivity (heterotrophic and nitrifying activity) and colloidal and soluble biopolymer content (BPCs and SMPs). The relationships between membrane fouling rate and each property of the sludge were further analysed statistically to assess the role and significance of each.

Materials and methods

Feedwater

The tMBR was fed with secondary effluent from a conventional activated sludge wastewater treatment plant, designed only for carbon removal (Table 1). This effluent exhibited a high variable chemical oxygen demand (COD = 559 mg/L, on average), mainly as particulate matter (CODs/COD = 0.14 and COD/SST = 1.35), with a low readily biodegradable fraction (5-day biochemical oxygen demand BOD_5 to COD ratio was approximately 0.22). This high particulate content was attributed to the short SRT (<4 days) and oxygen deficiency in the activated sludge process, which frequently resulted in episodes of sludge deflocculation. Nitrogen compounds were mainly in the form of ammonium (43 mg/L, on average). In terms of the total COD, this feedwater is comparable to a moderate loaded wastewater but mainly composed of suspended slowly biodegradable organic matter.

MBR

A cylindrical 220-L deposit was equipped with ZeeWeed® ZW-10 (GE Water & Process Technologies) hollow-fibre membranes with a 0.04-μm-rated pore diameter, 1.9-mm external diameter and 0.9 m^2 of filtering surface area, assembled vertically (see Vera et al. 2014). ZeeWeed® consists of a woven reinforcing braid on which a PVDF membrane is cast. The effluent (permeate) was extracted from the top header of the module under slight vacuum. Throughout the experimental time, ultrafiltration was carried out at constant permeate flux (J = 35 L/h m^2), registering transmembrane pressure as a function of time. Furthermore, backwashing was applied each 7 min at constant conditions (J_B = 60 L/h m^2 and t_B = 30 s) for fouling removal. Although air sparging was not supplied during the filtration phase, constant air scouring at 3.1 $Nm^3/h\ m^2$ was applied during backwashing, to improve its efficiency. The process tank was stirred by air bubbling from the bottom, at a flow rate of 1.2 Nm^3/h. A compressor also supplied additional air (0.3 Nm^3/h) for the biological processes. The bioreactor was run at a hydraulic retention time of 7.6 h without sludge removal except for sampling. During the experimental time, the biological suspension was routinely characterised to analyse the influence of microbial suspension characterisation on membrane fouling. Membrane chemical cleaning was carried out by soaking with NaOCl (1000 ppm) for 12 h.

Analytical methods

Total and soluble chemical oxygen demand (COD and COD_s, respectively), 5-day biochemical oxygen demand (BOD_5), total suspended solids (TSS), mixed liquor suspended solids (MLSS), mixed liquor volatile suspended solids (MLVSS), time to filter (TTF) and turbidity were determined in conformity with the standard methods (2005). The analyses of ammonium–nitrogen ($N–NH_3$) were carried out by the Nessler method using a DR-5000 Hach spectrophotometer. Dissolved organic carbon (DOC) concentration was measured with a TOC-meter (TOC-5000A, Shimadzu). The difference in DOC concentration between the

Table 1 Main feedwater characteristics

Parameters	Units	Phase I (n = 17)		Phase II (n = 28)		Phase III (n = 15)		Phase IV (n = 27)		Phase V (n = 10)	
		Mean	Range	Mean	Range	Mean	Range	Mean	Range	Mean	Range
COD	mg/L	438	150–1510	810	106–2320	461	318–1800	216	110–494	264	130–640
COD_s	mg/L	83	56–120	88	54–136	86	62–132	75	14–220	71	34–90
DOC	mg/L	20	11–30	25	14–138	20	16–26	22	15–36	21	17–27
$N–NH_3$	mg/L	45	28–60	43	15–90	47	35–57	39	28–61	43	35–53
$N–NO_3^-$	mg/L	0.15	0.12–0.22	0.18	0.02–0.53	0.28	0.02–0.94	0.45	0.02–1.7	0.22	0.01–1.25
TSS	mg/L	281	62–1220	534	28–1708	647	220–1395	149	32–530	173	94–900

filtrated suspension through a 0.45-μm nitrocellulose membrane filter (HA, Millipore) and the MBR permeate was assigned as biopolymer clusters (BPC). Nitrate–nitrogen ($N–NO_3^-$) and nitrite–nitrogen ($N–NO_2^-$) were analysed through ion chromatography using a Compact IC plus 882 device supplied by Metrohm. Microbial floc size distribution was measured using a Malvern Mastersizer 2000 instrument with a detection range of 0.02–2000 μm. To quantify supernatant turbidity, the biomass samples were centrifuged at 1300 g for 2 min. The biological activities were evaluated by respirometric measurement described in Ginestet et al. (1998) using allylthiourea (86 μM) and azide (24 μM) as selective inhibitors of ammonia and nitrite oxidation, respectively. The sludge viscosity was determined by using the concentric cylinder rotational viscosimeter Visco Star plus (FungiLab, Spain), with a rotational speed of 100 rpm.

Results and discussion

Evolution of sludge characteristics and process performance

The pilot plant was operated continuously for 195 days under similar operating conditions (HRT = 7.2 h and complete retention time) to study biomass development. To facilitate analysis, the experimental period has been divided into five phases according to process stability: initial biomass growth (phase I, 1st–21st day), unsteady operation (phase II, 22nd–60th day) and steady biomass growth (phase III, 61st–84th day; phase IV, 85th–157th day; phase V, 158th–195th day).

The plant started without any sludge inoculum, so the biomass developed from the microorganisms entered with feedwater (i.e. secondary effluent). As shown in Fig. 1, MLSS and MLVSS rapidly increased during phase I due to microorganism retention and growth, resulting from the high $(F/M)_C$ imposed (11.5–5.0 kg CODs/kg MLVSS day). Nevertheless, at the end of phase I, to maintain complete nitrification with a proper dissolved oxygen concentration, airflow rate to the bioreactor was increased to 1.5 Nm^3/h, producing a shock to the microorganisms, which started to produce BPCs and generate white foam (Fig. 4b). This relationship between intense biopolymer production and foam is commonly observed in MBRs and attributed to proteins that have properties as surface-active agents (Di Bella et al. 2011). This foam disappeared after the 40th day. In addition, from the 44th to 57th day, the tMBR suffered sporadic events of organic overloading shocks, and feedwater COD increased from 670 to 2230 mg COD/L due to temporary malfunction of the WWTP. This significantly increased suspended solid concentration in the tMBR. The unstable period was identified as phase II. After that, biomass started to grow continuously during a 135-day period (phases III–V), with the exception of another shock load (123rd–127th day) and a period of feeding failure (146th–157th day). During this period of stable growth, microorganisms were progressively subjected to severe substrate limitation (from 0.26 to 0.10 kg COD/kg MLVSS day), which may justify the low sludge-yield coefficient (Y_{obs}) of 0.04 ± 0.002 kg MLVSS/kg COD. Due to the starvation conditions, it was expected that available substrate was mainly utilised by microorganisms for non-growth activities rather than biosynthesis, which reduced net sludge production (Rosenberger et al. 2002). In addition, previous studies in similar conditions have demonstrated the existence of predator species in the tMBR, especially sessile ciliates and free-swimming ciliates, which are known to be responsible for a reduction in the population of smaller bacteria (Wang et al. 2013). The sludge yield was within the typical range of those reported for secondary MBRs operated with complete sludge retention (0.03–0.12 kg MLVSS/kg COD (e.g., Pollice et al. 2004)). It was also consistent with predicted values (0.05–0.1 kg MLVSS/kg COD) of ASM-based models considering the concepts of endogenous respiration and slow hydrolysis at long SRTs (>100 days) (Amanatidou et al. 2015). At the same time, the MLVSS/MLSS ratio decreased from 0.85 of day 60 to 0.82 of day 195 (phases III–V), which indicated a slight inert solid accumulation in the sludge. This is in accordance with previous studies, suggesting that MBRs operated for long SRTs develop slow-growing bacteria that may degrade inert substances and avoid significant accumulation in the sludge (van Loosdrecht and Henze 1999).

Table 2 shows the evolution of sludge bioflocculation, viscosity and filterability. During phases I–II, results revealed an increase in bioflocculation, detected in supernatant turbidity and mean particle size behaviour, due to biomass development. It should also be noted that unsteady conditions (phase II) greatly affected sludge characteristics, as seen from the variability of turbidity measurements. Once the steady biomass growth period was achieved (phases III–V), average turbidity slightly increased from 16 to 27 NTU. As expected, the small floc content (i.e. d_{10}, 10 % of the volume distribution being below this value) decreased from 44 to 29 μm during the same period. These results indicated some degree of sludge deterioration after long operation times. Probably, the main reason for the observed behaviour is the progressive substrate limitation imposed, which decreased biomass activity. Wilén et al. (2000) studied the effect of microbial activity on floc stability and concluded that the bacterial metabolism was important in maintaining the strength of the flocs. Nevertheless, this slight deflocculation did not have a significant impact on process performance since no significant decrease in the substrate consumption rate nor appreciable release of SMPs was observed. Regarding rheological properties, apparent viscosity seems to be related to MLSS, as previously reported (Trussell et al. 2007). Based on this approach, a critical MLSS value can be identified (~3000–3500 mg/L); over it, apparent viscosity significantly increased (phases IV–

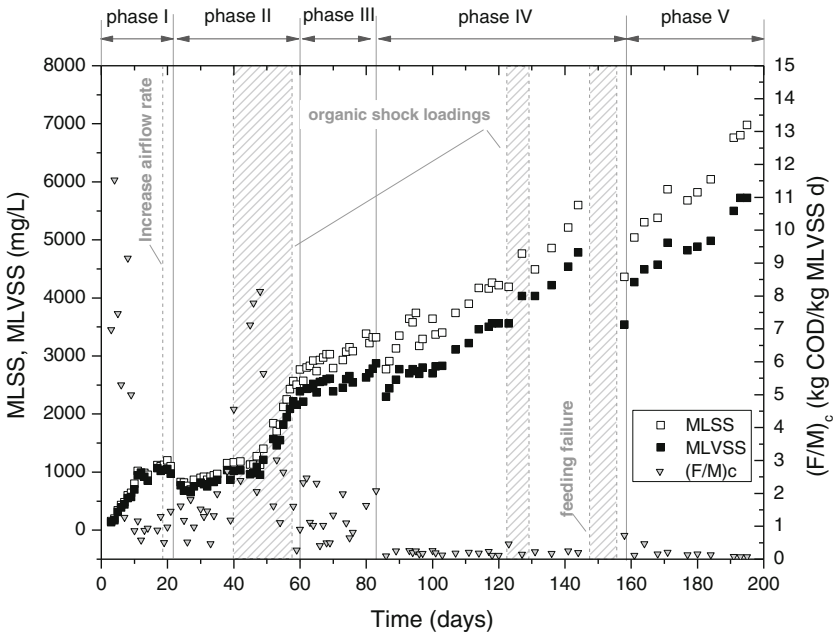

Fig. 1 MLSS, MLVSS and $(F/M)_C$ evolution during the different experimental phases

V, from 2.0 to 4.0 mPa s). Finally, the results presented in Table 2 also underline the link between bioflocculation and sludge filterability, measured as TTF. Similar results have been reported by Van den Broeck et al. (2011), reflecting the key role of small floc size in filterability.

As expected, high COD removal and complete nitrification were obtained after the first days of operation, corresponding with the rapid biomass growth observed in phase I (Fig. 2). However, there was considerable variability in COD removal efficiencies during the whole experimental period, between 79 and 97 %. This range may be attributable to influent COD fluctuations (110–960 mg/L) since permeate COD values decreased from 81 mg/L (on average) in the initial phase to less than 35 mg/L during phases III–V. Nitrifying biomass followed the typical trend, always achieving ammonium removal rates higher than 98 % after the first 20 days, with stable behaviour after increasing airflow rate (17th day). In phases III–V, average concentrations for nitrogen compounds in the permeate were 0.53, 50.3 and 0.03 mg N/L for NH_4^+, NO_3^- and NO_2^-, respectively.

Biomass activity and colloidal/soluble biopolymer content

Respiration tests with various substrates were periodically carried out to elucidate the physiological state and activity of the microbial community. Endogenous specific uptake rate (SOUR endogenous) is defined as oxygen consumption of the microbial population in the absence of external substrates. It mainly consists of the maintenance energy requirement. In addition, heterotrophic, ammonium-oxidising (AOB) and nitrite-oxidising (NOB) bacteria were examined by adding potassium acetate, ammonium chloride and sodium nitrite, respectively, and measuring respiration consumption after dosing these substrates in excess. Figure 3 shows that endogenous SOUR continuously decreased with operation time. Similar trends have been reported by many authors, revealing

Table 2 Main characteristics of microbial suspension for each experimental phase. The reported data are expressed as min–max

Parameters	Units	Phase I		Phase II		Phase III		Phase IV		Phase V	
		Range	*N*	Range	*N*	Range	*N*	Range	*N*	Range	*N*
Supernatant turbidity	NTU	42–106	6	13–116	22	6.6–27	16	17–38	17	19–35	4
PSD											
d_{10}	μm	15–23	3	15–61	5	44	1	30–34	2	29	1
d_{50}	μm	51–66	3	86–198	5	119	1	94–97	2	86	1
d_{90}	μm	125–153	3	266–449	5	327	1	242–265	2	227	1
Apparent viscosity	mPa s	1.7–2.0	6	1.5–2.0	22	1.6–2.0	16	1.8–3.2	17	3.0–4.0	4
TTF	s	330–2122	6	5–4620	22	6–58	16	69–135	17	69–135	4

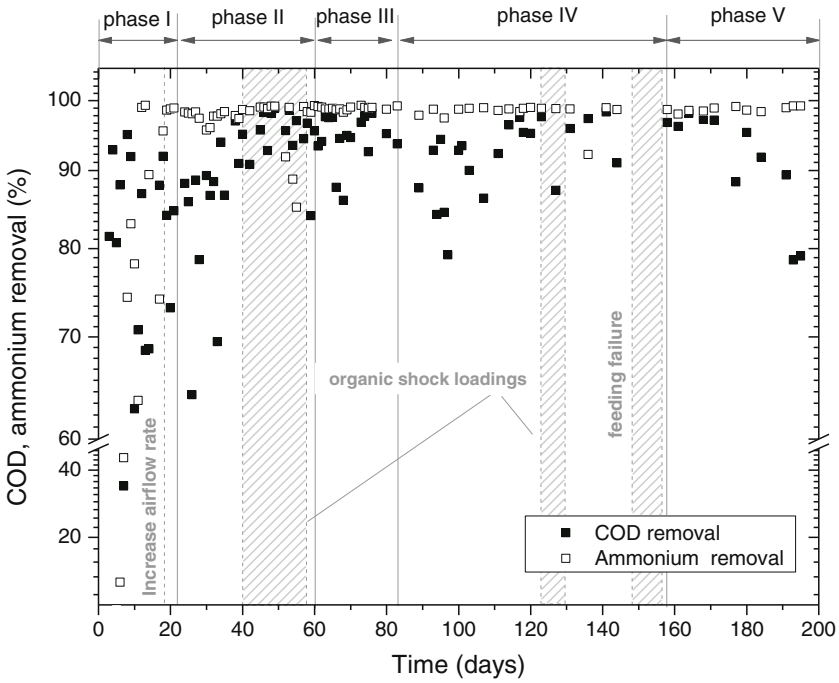

Fig. 2 COD and ammonium removal during the different experimental phases

the influence of MLSS (i.e. $(F/M)_C$ ratio) on microbial activity (Pollice et al. 2004). During the stable biomass growth period (phases III–V), low average SOUR values were observed (from 4.9 to 2.8 mg O_2/g MLVSS h), similar to those usually reported for MBRs operated in endogenous conditions (Pollice et al. 2004). This is consistent with the low biomass growth observed. In addition, $SOUR_{OHO}$ behaved the same, decreasing with operation time. It is notable that the endogenous uptake rate was approximately 60 % of that with a carbon substrate, confirming the substantial organic carbon limitation imposed on the microorganisms in the tMBR.

Autotrophic activity is here expressed as specific oxygen uptake rate of ammonia oxidation bacteria, $SOUR_{AOB}$, and nitrite oxidation bacteria, $SOUR_{NOB}$. Both rates tended to decrease with operation time, a trend similar to the ammonium feed to microorganism ratio ($(F/M)_N$) in the tMBR. Assuming a theoretical factor for oxygen consumption of 4.57 (Metcalf and Eddy, Inc. 2003) and subtracting the endogenous consumption for recalculation of $SOUR_{AOB}$, ammonia uptake rates declined from 5.1 ± 1.5 to 1.4 ± 0.7 mg N/g MLVSS h, corresponding to a $(F/M)_N$ drop from 6.0 to 1.2 mg N/g MLVSS h. Similarly, based on a factor of 1.1 for $SOUR_{NOB}$, nitrite uptake rates reached 3.2 ± 0.8 mg N/g MLVSS h at the end of phase I, increased to 6.0 ± 1.2 mg N/g MLVSS h during phase II and then decreased to 1.7 ± 0.9 mg N/g MLVSS h (phase V). Consistent with this, complete nitrification was continuously observed after 20 days of operation.

Many researchers have suggested that colloidal and soluble biopolymers (BPCs and SMPs) play an important role in membrane fouling (Meng et al. 2009; Lin et al. 2014). For this reason, biopolymer content was routinely analysed (Fig. 4b). BPC in the tMBR was estimated from the difference between DOC concentrations in the suspension supernatant and the permeate. SMP concentration was assumed to be the DOC concentration in the permeate. Secondary effluents are mainly composed of organic matter (EfOM) of different origins, where biopolymers represent an important part. Therefore, feedwater DOC concentration was also measured in order to assess biopolymer production and degradation by the microorganisms in the tMBR. During the experimental period, EfOM ranged between 10.9 and 37.7 mg DOC/L, with an average of 21.3

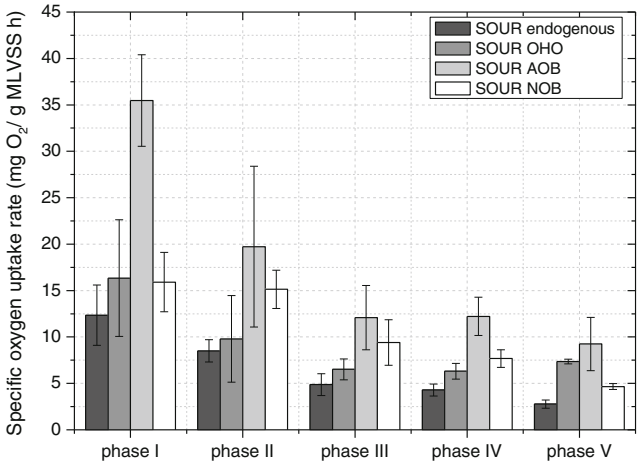

Fig. 3 Specific oxygen uptake rates for the different experimental phases in endogenous conditions and with addition of substrates: acetate (*SOUR OHO*), ammonium (*SOUR AOB*) and nitrite (*SOUR NOB*)

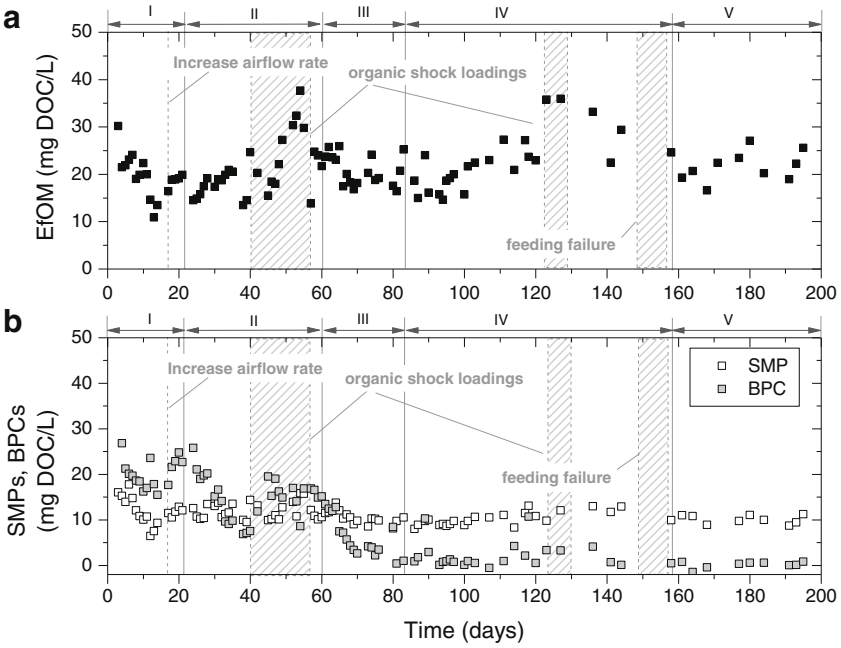

Fig. 4 Evolution of secondary effluent organic matter (i.e. soluble organic feedwater concentration) and supernatant BPCs and permeate SMPs during the different experimental phases

±5.1 mg DOC/L (Fig. 4a). As shown in Fig. 4b, BPCs tended to accumulate in tMBR, following the same trend as EfOM during the first 17 days of phase I. In addition, corresponding with the increasing airflow rate, BPCs rapidly increased while white foam appeared. Net BPC release is a common response of microorganisms to environmental stresses, which cause release of proteins and polysaccharides due to sludge deflocculation (Lin et al. 2014). This deflocculation process is consistent with the high supernatant turbidity (Table 2) and the presence of white foam, attributed to some proteins with surface-active properties (Di Bella et al. 2011). From day 24, BPCs started to decrease until day 40, when concentration reached 7.5 mg/L. At this point, the sum of BPC and SMP concentrations was similar to EfOM concentration; it was thus assumed that deflocculation had ceased. Nevertheless, an organic shock load in the feedwater again led to a significant rise in BPCs. After that, during the biomass stable-growth period (phases III–V), BPCs were progressively biodegraded/adsorbed by the biomass until a very low stable concentration was reached (1.85 mg/L, on average). Furthermore, given the low microbial activity reached in this period, lower biopolymer production was expected because of the low substrate utilisation.

On the other hand, SMPs remained nearly constant throughout the experimental study, with an average of 11.1 ±2.0 mg DOC/L (Fig. 4b). During stable biomass conditions (phases III–V), a mass balance between EfOM and SMPs revealed a net removal of 52±7 %. Therefore, feedwater fluctuations and microbial processes appear to only affect BPC concentration, which in turn correlates with the biopolymer fraction retained by the membrane. Consequently, it is expected that BPC evolution affects membrane fouling, consistently with previous studies (Wang and Li 2008).

Correlation between different biomass characteristics

Table 3 shows the multicollinearity (expressed by Pearson's coefficient r) of the sludge parameters previously discussed. As expected, MLSS was highly correlated with the apparent viscosity ($r=0.852$). This correlation is frequently reported in many studies. For example, Wu and Huang (2009) obtained a similar correlation coefficient in different sludges from MBRs. MLSS also correlated ($r=-0.826$) with endogenous SOUR, confirming its influence on microbial activity, in agreement with previous studies (Pollice et al. 2004). The low coefficient ($r=-0.557$) obtained for nitrification activity ($SOUR_{AOB}$) should be attributed to the considerable variability associated with unstable conditions in phases I–II. It should be noted that the autotrophic population shows a lower growth rate and therefore requires more time to become accustomed to the new conditions. Results also highlighted a moderate correlation ($r=-0.735$) between MLSS and BPC. This may be related principally to the development of the slow-growing population after a long operation time, which are able to degrade the biopolymers, as proposed by other authors [e.g. Sabia et al. 2013].

Among the parameters affecting suspension filterability, expressed by TTF, only supernatant turbidity presented a moderate correlation ($r=0.775$), revealing a considerable effect of bioflocculation on sludge filterability. In contrast, results indicated that MLSS did not directly correlate to sludge filterability.

Table 3 Pearson's correlation coefficient between suspension characteristics

Parameters	N	BPC	MLSS	Supernatant turbidity	d_{10}	Apparent viscosity	SOUR Endogenous	$SOUR_{AOB}$	TTF
BPC	58	1							
MLSS	51	$-0.735\ (1.4 \cdot 10^{-7})$	1						
Supernatant turbidity	65	$0.581\ (6.3 \cdot 10^{-6})$	$-0.473\ (1.6 \cdot 10^{-3})$	1					
d_{10}	13	$-0.442\ (1.7 \cdot 10^{-1})$	$0.171\ (6.3 \cdot 10^{-1})$	$-0.668\ (2.4 \cdot 10^{-2})$	1				
Apparent viscosity	65	$-0.378\ (1.9 \cdot 10^{-2})$	$0.852\ (3.0 \cdot 10^{-14})$	$-0.129\ (4.2 \cdot 10^{-1})$	$-0.112\ (7.5 \cdot 10^{-1})$	1			
SOUR endogenous	37	$0.699\ (1.4 \cdot 10^{-4})$	$-0.826\ (2.1 \cdot 10^{-7})$	$0.493\ (5.7 \cdot 10^{-3})$	$0.258\ (6.7 \cdot 10^{-1})$	$-0.618\ (5.8 \cdot 10^{-4})$	1		
$SOUR_{AOB}$	37	$0.429\ (2.9 \cdot 10^{-2})$	$-0.557\ (2.1 \cdot 10^{-2})$	$0.403\ (2.0 \cdot 10^{-2})$	$0.890\ (4.3 \cdot 10^{-3})$	$-0.402\ (3.7 \cdot 10^{-2})$	$0.588\ (2.5 \cdot 10^{-4})$	1	
TTF	65	$0.522\ (7.8 \cdot 10^{-4})$	$-0.413\ (2.5 \cdot 10^{-3})$	$0.775\ (1.7 \cdot 10^{-9})$	$-0.634\ (4.7 \cdot 10^{-2})$	−0.138 (0.35)	0.310 (0.12)	0.216 (0.27)	1

p significance in brackets

Membrane performance

Submerged hollow-fibre MBRs are frequently operated under temporised filtration/backwashing cycles (Judd 2010). This operation mode was applied in the present work. During a filtration cycle, transmembrane pressure (TMP) linearly increased with elapsed time. This behaviour can be explained by the incompressible cake model (Vera et al. 2014), where TMP within a filtration cycle can be expressed in terms of the initial transmembrane pressure (TMP_i), fouling rate (r_f) and elapsed time (t) (Eq. [1]):

$$\mathrm{TMP}(t) = \mathrm{TMP}_i + r_f t \quad (1)$$

Based on this approach, r_f can be used as a quantification parameter of reversible fouling and TMP_i as another parameter associated with residual fouling phenomena after backwashing.

The evolution of membrane performance, expressed in terms of TMP_i and TMP_f (transmembrane pressure at the end of the filtration cycle), is shown in Fig. 5a. During phase I, TMP_i tended to rapidly increase up to 28–36 kPa (higher than the technical operating values), despite two chemical cleanings performed on days 4 and 8. Identical TMP_i trends were observed between chemical cleanings, where most of the fouling was observed on the first day of operation. A theoretical explanation for this behaviour has been proposed, considering a specific deposited mass remaining on the membrane surface after backwashing (Charfi et al. 2015). Therefore, residual fouling depends on backwashing effectiveness and the properties and quantity of the mass deposited after backwashing (i.e. r_f and filtration time). For given backwashing conditions and a fixed filtration time (7 min), TMP_i is expected to depend on r_f. Consistently, r_f followed a similar trend to TMP_i, suddenly increasing to 35–65 Pa/s, which is 20–40 times higher than typically found in full-scale MBRs (Fig. 5b) (Drews 2010). After increasing airflow rate on day 17, r_f suddenly rose to impractical levels (>65 Pa/s), resulting in numerous plant shutdowns due to the high TMP reached. For membrane recovery, several chemical cleanings were periodically performed on days 18, 20 and 22 and 23. On the 27th day, the system started to recover its normal operation due to r_f decline. Nevertheless, the high organic loads in the feedwater from the 44th to 57th days significantly increased r_f again, leading to another unstable period which lasted until the end of phase II. These results suggest that environmental stresses due to raised oxygen concentration and organic load have a profound effect on membrane fouling. Both environmental factors have been identified as causes for biopolymer release and fouling propensity in MBRs (Le-Clech et al. 2006). In accordance with this, r_f showed a similar trend to that observed for BPCs during phase II (Fig. 4b). After that, during phase III (61st–84th day), r_f gradually dropped to operative values (~1 Pa/s) (Drews 2010). During the same period, TMP_i slightly decreased from 26 to 23 kPa confirming the linkage between reversible fouling rate and residual fouling. Yet again, r_f decline coincided with a similar BPC decay. Thus, the results indicate that biomass progressively acclimatised after a couple of days, decreasing its BPC levels and fouling potential. Subsequent phases (III and IV) were characterised by stable membrane performance. Phase IV (85th–157th day) started with a chemical cleaning which removed most of the residual fouling. TMP_i and r_f remained at nearly constant and low values. Another chemical cleaning was performed in phase V, achieving a TMP value similar to that at the beginning of the experimental period. Although r_f showed some variability during phase V, it remained between operative values. However, this variability induced a slow TMP_i increase at a constant rate of 0.10 Pa/s. This fouling cannot be directly related to BPCs since their concentration remained very low during this phase (Fig. 4b). This behaviour can be justified by other factors such as a slight sludge deflocculation and the rise in MLSS and apparent viscosity with operation time (see Table 2).

Influence of biomass characteristics on membrane fouling rate

As previously reported in many studies, no single biomass parameter can explain membrane fouling, and thus, its origin must be explored in combination with several parameters (Van den Broeck et al. 2011). For this reason, four parameters (BPCs,

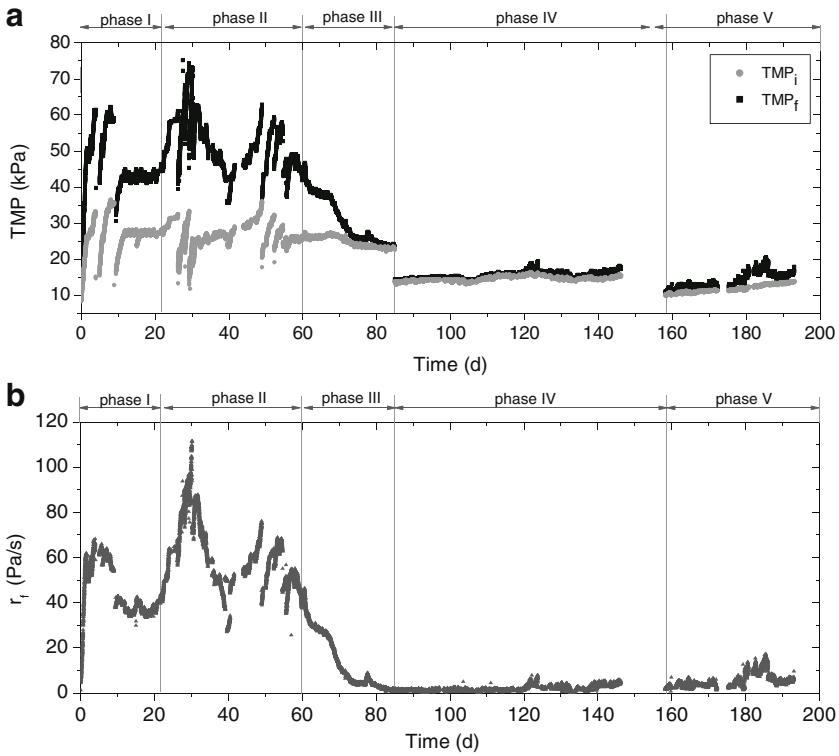

Fig. 5 Evolution of membrane performance during the different experimental phases: **a** initial and final transmembrane pressure within cycles; **b** fouling rates during each cycle

MLSS, supernatant turbidity and TTF) that describe key suspension properties, such us colloidal biopolymer content, suspended solid concentration, bioflocculation state and sludge filterability, were assessed. Table 4 summarises Pearson's coefficient of the parameters derived from the fouling rate data obtained during all experimental phases. Figure 6 also shows how the fouling rates change with these parameters.

The highest correlation for r_f was found for BPCs, with a coefficient of 0.868, where they ranged from 0.54 to 28.2 mg DOC/L (Fig. 6a). This high correlation is in agreement with some previous studies (Wu and Huang 2009) and differs with others considering components of BPCs such as polysaccharides or proteins (Drews 2010). Discrepancies may be due to the complexity of fouling phenomenon at different operation parameters and hydrodynamic conditions. In subcritical flux operation, where TMP often shows a three-stage profile, the colloidal biopolymers have often been identified as the main foulants during the second stage, corresponding to a prolonged TMP rise (Charfi et al. 2015). During this period, fouling rate increases with foulant load (i.e. permeate flux and biopolymer concentration) but very low fouling rates are commonly reported (Le-Clech et al. 2006). In contrast, supracritical flux operation leads to high fouling rates due to rapid deposition of suspended solids on membrane surfaces, forming a cake layer. Colloidal biopolymers can influence caking by enhancing sludge floc attachment to the membrane (Lin et al. 2014), reducing cake-layer porosity (Charfi et al. 2015) and increasing specific cake resistance due to an osmotic pressure mechanism (Chen et al. 2012). Biopolymers are commonly considered as a whole, without distinguishing soluble and colloidal fractions. However, soluble biopolymers should pass through the membrane with the effluent and thus not significantly contribute to fouling. In fact, membrane pore constriction can also be induced by this soluble fraction but many studies have shown that internal fouling is less than surface fouling in MBRs (Shen et al. 2015). In the present study, the results revealed that colloidal biopolymers (i.e. BPCs) were a crucial factor that regulated membrane fouling. On the other hand, since the membrane was operated at high permeate flux and low shear rates (i.e. without air scouring at the membrane surface), a major contribution from MLSS was expected in contrast with previous studies (Bae and Tak 2005) that remark the importance of colloidal/soluble biopolymer rate. Nevertheless, the level of MLSS appeared not to have a

Table 4 Pearson's correlation coefficient between selected parameters and *rf*

Parameters	*N*	Min	Max	*r*
BPC (mg DOC/L)	97	−0.54	28.2	0.868 ($<1 \cdot 10^{-9}$)
MLSS (mg/L)	100	153	6980	−0.765 ($<1 \cdot 10^{-9}$)
TTF (s)	65	5	4620	0.233 (0.080)
Supernatant turbidity (NTU)	65	6.6	116	0.250 (0.032)

p significance in brackets

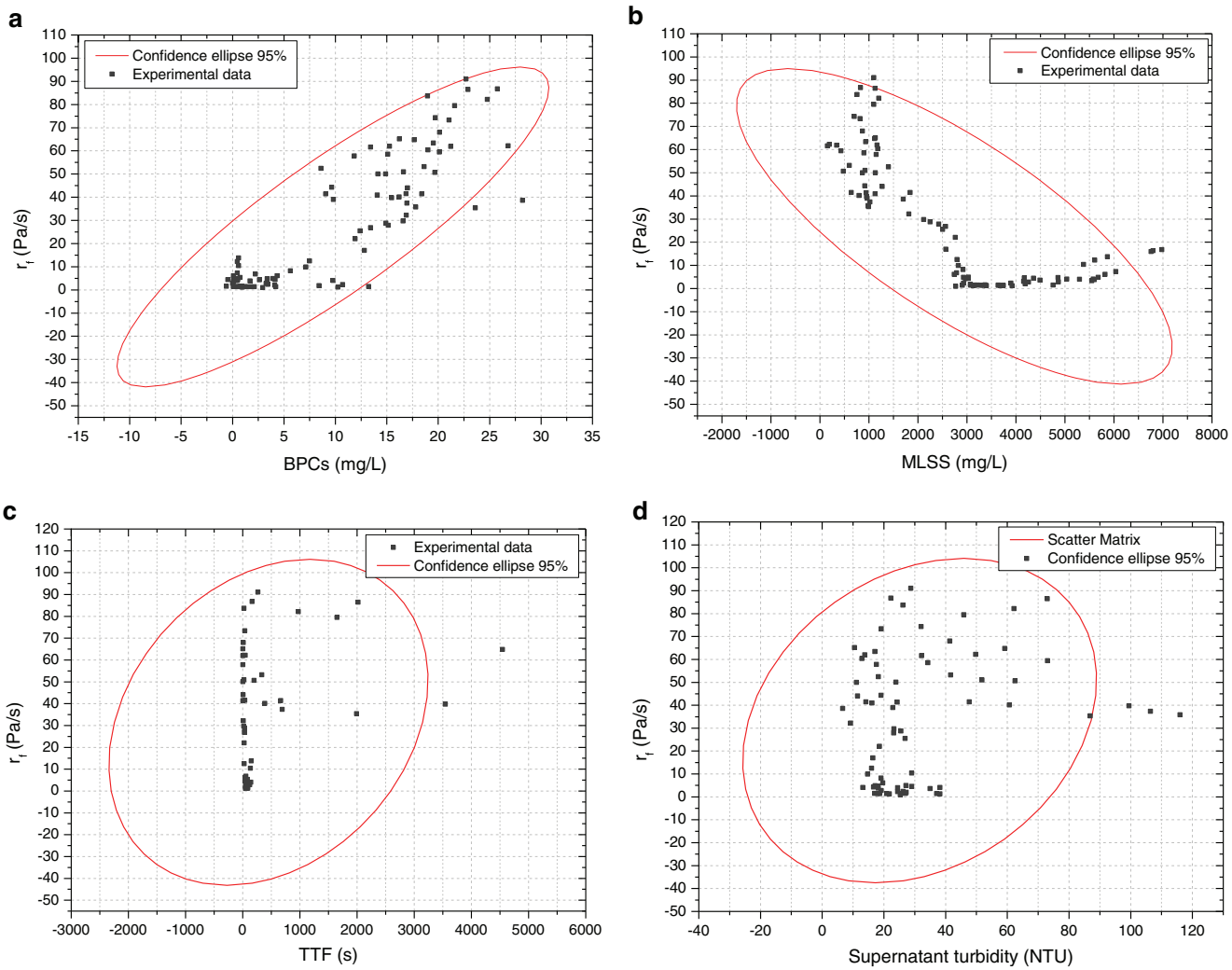

Fig. 6 Relationship of fouling rate with several biomass characteristics: **a** BPCs, **b** MLSS, **c** TTF and **d** supernatant turbidity

significant effect on membrane fouling since a negative correlation ($r = -0.765$) between MLSS and r_f was calculated (Table 4). This trend is in fact inconsistent with the cake filtration model in dead-end conditions (i.e. without shear rate), where the solid concentration of the cake tends to rise with MLSS concentration (Le-Clech et al. 2006). A deeper analysis showed different trends according to the MLSS range (Fig. 6b). At low to moderate values (<3000 mg/L), a negative correlation was clearly observed, while a slight positive correlation resulted from increasing MLSS above ~5000 mg/L. Therefore, results seem to indicate that the low shear rate due to bioreactor mixing was enough to induce some back-transport of suspended solids from the membrane. It is known that back-transport due to shear-induced diffusion and inertial lift increases with shear rate and particle size (Zeman and Zydney 1996), which justifies a selective deposition of colloidal biopolymers onto the membrane, as previously reported (Pan et al. 2010). This explains the importance of BPCs for membrane fouling at MLSS lower than 3000 mg/L. On the other hand, as discussed in "Evolution of sludge characteristics and process performance", apparent viscosity significantly increased when MLSS became higher than 3500 mg/L. Since shear rate decreases with viscosity (Trussell et al. 2007), this may be reason for the slight rise in r_f when MLSS are above 5000 mg/L. From the results it can be deduced that optimum operating conditions involve concentrations of BPC below ~5 mg/L and MLSS approximately within the range between 3000 and 5000 mg/L. It should be noted that similar results have been reported with secondary MBRs treating raw municipal wastewater. Several studies have suggested that low F/M ratios may result in a low metabolic activity, suitable sludge morphology and low soluble biopolymer concentration, which was correlated to a less fouling potential (Meng et al. 2009, Van den Broeck et al. 2011, Sabia et al. 2013).

The sludge filterability, measured by TTF, did not show a significant correlation with fouling rate (Table 4 and Fig. 6c). As TTF is based on cake filtration in dead-end regime, this trend is consistent with some degree of suspended solids back-transport during filtration in the tMBR. However, supernatant

turbidity showed a similar trend to that obtained for TTF, revealing a poor correlation with fouling rate (Table 4 and Fig. 6d). It can thus be concluded that BPCs have a predominant role when compared with other sludge properties as indicators of its fouling potential.

Conclusions

The effect of sludge characteristics on membrane fouling in a tMBR was assessed in this study; the following may be concluded:

- Environmental stress affected sludge characteristics and thus membrane fouling. A sudden oxygen increase resulted in temporary biomass deflocculation, BPC release and, consequently, severe induced membrane fouling. Organic shock loads also increased BPC content but their effect on membrane fouling seemed to depend on MLSS range. While at MLSS lower than 3000 mg/L, the effect was significant, at higher concentrations, it was not noticeable. This behaviour was attributed to the development of the slow-growing microbial population able to degrade BPCs.
- At MLSS higher than 3000 mg/L, a low stable biomass growth (0.04 ± 0.002 kg MLVSS/kg COD) was observed, regardless of organic shock loads or feeding failures. This stable growth period was characterised by low bioactivity, BPC content and membrane fouling.
- Statistical multicollinearity of the sludge characteristics showed a significant correlation between MLSS and a set of parameters (endogenous SOUR, apparent viscosity and BPCs). In contrast, results indicated that MLSS were not directly correlated to sludge filterability, measured as TTF.
- In the hydrodynamic conditions assessed (J = 35 L/h m^2 without air scouring in the filtration phase), incompressible cake-layer formation was found to be the predominant fouling mechanism. In these conditions, it was demonstrated that BPCs have a predominant role, compared with other sludge properties, as indicators of its fouling potential.

AOB, ammonium-oxidising bacteria; BOD_5, 5-day biochemical oxygen demand, mg/L; BPC, biopolymer clusters, mg DOC/L; CIP, chemical cleaning in place; COD, total chemical oxygen demand, mg/L; COD_s, soluble chemical oxygen demand, mg/L; d_{10}, measured particle size at 10 % of volume distribution, μm; d_{50}, measured particle size at 50 % of volume distribution, μm; d_{90}, measured particle size at 90 % of volume distribution, μm; DFC_m, Delft filtration characterisation method; DOC, dissolved organic carbon, mg/L; EfOM, organic matter present in secondary effluents, mg DOC/L; EPS, extracellular polymeric substances; $(F/M)_C$, carbon feed to microorganism ratio, kg COD_s/kg MLVSS day; $(F/M)_N$, nitrogen feed to microorganism ratio, kg N/kg MLVSS day; HRT, hydraulic retention time, h; J, filtrate flux, L/h m^2; J_B, backwashing flux, L/h m^2; MBR, membrane bioreactor; MLSS, mixed liquor total suspended solids, mg/L; MLVSS, mixed liquor volatile suspended solids, mg/L; N–NH_3, ammonium–nitrogen, mg/L; N–NO_2^-, nitrite–nitrogen, mg/L; N–NO_3^-, nitrate–nitrogen, mg/L; NOB, nitrite-oxidising bacteria; OPEX, operating expenditure; PSD, particle size distribution; PVDF, polyvinylidene fluoride; r, Pearson's coefficient; r_f, reversible fouling rate, Pa/s; SMP, soluble microbial products; $SOUR_{AOB}$, specific AOB oxygen uptake rate, mg O_2/g MLVSS h; $SOUR_{endogenous}$, specific endogenous oxygen uptake rate, mg O_2/g MLVSS h; $SOUR_{NOB}$, specific NOB oxygen uptake rate, mg O_2/g MLVSS h; $SOUR_{OHO}$, specific heterotrophic oxygen uptake rate, mg O_2/g MLVSS h; SRT, sludge retention time; t_B, backwashing phase duration, s; tMBR, tertiary submerged membrane bioreactor; TMP, transmembrane pressure, kPa; TMP_f, transmembrane pressure final filtration phase, kPa; TMP_i, transmembrane pressure initial filtration phase, kPa; TSS total suspended solids, mg/L; TTF time-to-filter, s; Y_{obs}, low sludge-yield coefficient, kg MLVSS/kg COD

Acknowledgments The control system, funded by the N.R.C. (MINECO project CTM2011-27307), was tested for long-term validation during the MBR operation described in this paper. The authors wish to express their gratitude to GE Water & Process Technologies and to BALTEN for their support and also to the staff of the Water Analysis Laboratory of the Chemical Engineering Department at Universidad de La Laguna (ULL) for their analytical advice. We greatly appreciate access to the multiparameter universal controller permitted by the CONVAGUA project of the Canary Agency-ACIISI, sponsored by the European Commission and the Canary Islands Regional Government. This study has been carried out in the framework of MBRgenera-AGUA01 project funded by Fundación Cajacanarias.

References

Amanatidou E, Samiotis G, Bellos D, Pekridis G, Trikoilidou E (2015) Net biomass production under complete solids retention in high organic load activated sludge process. Bioresour Technol 182:193–199

Aquino SF, Stuckey DC (2008) Integrated model of the production of soluble microbial products (SMP) and extracellular polymeric substances (EPS) in anaerobic chemostats during transient conditions. Biochem Eng J 38:138–146

Bae TH, Tak TM (2005) Interpretation of fouling characteristics of ultrafiltration membranes during the filtration of membrane bioreactor mixed liquor. J Membr Sci 264:151–160

Charfi A, Yang Y, Harmand J, Ben Amar N, Heran M, Grasmick A (2015) Soluble microbial products and suspended solids influence in membrane fouling dynamics and interest of punctual relaxation and/or backwashing. J Membr Sci 475:156–166

Chen J, Zhang M, Wang A, Lin H, Hong H, Lu X (2012) Osmotic pressure effect on membrane fouling in a submerged anaerobic membrane bioreactor and its experimental verification. Bioresour Technol 125:97–101

Cote P, Alam Z, Penny J (2012) Hollow fiber membrane life in membrane bioreactors (MBR). Desalination 288:145–151

Di Bella G, Torregrossa M, Viviani G (2011) The role of EPS concentration in MBR foaming: analysis of a submerged pilot plant. Bioresour Technol 102:1628–1635

Drews A (2010) Membrane fouling in membrane bioreactors—characterisation, contradictions, causes and cures. J Membr Sci 363:1–28

Fenu A, Roels J, Wambecq T, De Gussem K, Thoeye C, De Gueldre G, Van De Steene B (2010) Energy audit of a full scale MBR system. Desalination 262:121–128

Ginestet P, Audic JM, Urbain V, Block JC (1998) Estimation of nitrifying bacterial activities by measuring oxygen uptake in the presence of the metabolic inhibitors allythiourea and azide. Appl Environ Microbiol 64(6):2266–2268

Judd, S., (2010). The MBR book, principles and applications of membrane bioreactors for water and wastewater treatment, 2nd edition. Elsevier

Koch Membrane (2014) Case study. Aquapolo Ambiental Water Reuse Project., **http://www.kochmembrane.com/PDFs/Case-Studies/KMS-Sao-Paulo-Brazil-Case-Study.aspx**

Le-Clech P, Chen V, Fane AG (2006) Fouling in membrane bioreactors used in wastewater treatment. J Membr Sci 284:17–53

Lin H, Zhang M, Wang F, Meng F, Liao B, Hong H, Chen J, Gao W (2014) A critical review of extracellular polymeric substances (EPSs) in membrane bioreactors: characteristics, roles in membrane fouling and control strategies. J Membr Sci 460:110–125

Lin HJ, Gao WJ, Leung KT, Liao BQ (2011) Characteristics of different fractions of microbial flocs and their role in membrane fouling. Water Sci Technol 63:262–269

Marketsandmarkets (2014). Membrane bioreactor systems market by application (municipal wastewater treatment and industrial wastewater treatment), by type (hollow fiber, flat sheet, and multi tubular), by configuration (internal/submerged and external/side stream), and by region—trends & forecasts to 2019. Report CH 2651

Meng F, Chae SR, Drews A, Kraume M, Shin HS, Yang F (2009) Recent advances in membrane bioreactors (MBRs): membrane fouling and membrane material. Water Res 43:1489–1512

Metcalf and Eddy, Inc. (2003) Wastewater engineering: treatment and reuse. McGraw-Hill, New York

Pan JR, Su YC, Huang C, Lee HC (2010) Effect of sludge characteristics on membrane fouling in membrane bioreactors. J Membr Sci 349: 287–294

Pollice A, Laera G, Blonda M (2004) Biomass growth and activity in a membrane bioreactor with complete sludge retention. Water Res 38: 1799–1808

Pollice A, Laera G, Saturno D, Giordano C (2008) Effects of sludge retention time on the performance of a membrane bioreactor treating municipal sewage. J Membr Sci 317:65–70

Rosenberger S, Kruger U, Witzig R, Manz W, Szewzyk U, Kraume M (2002) Performance of a bioreactor with submerged membranes for aerobic treatment of municipal wastewater. Water Res 36:413–420

Sabia G, Ferraris M, Spagni A (2013) Effect of solid retention time on sludge filterability and biomass activity: long-term experiment on a pilot-scale membrane bioreactor treating municipal wastewater. Chem Eng J 221:176–184

Shen LG, Lei Q, Chen JR, Hong HC, He Y-M, Lin HJ (2015) Membrane fouling in a submerged membrane bioreactor: impacts of floc size. Chem Eng J 269:328–334

Standard methods for the examination of water and wastewater (2005). American Public Health Association/Water Environment Federation, 21st ed. Washington DC

Trussell RS, Merlo R, Hermanowicz SW, Jenkins D (2007) Influence of mixed liquor properties and aeration intensity on membrane fouling in a submerged membrane bioreactor at high mixed liquor suspended solids concentrations. Water Res 41:947–958

Van den Broeck R, Krzeminski P, Van Dierdonck J, Gins G, Lousada-Ferreira M, Van Impe JFM, van der Graaf JHJM, Smets IY, van Lier JB (2011) Activated sludge characteristics affecting sludge filterability in municipal and industrial MBRs: unraveling correlations using multi-component regression analysis. J Membr Sci 378:330–338

Van Loosdrecht M, Henze M (1999) Maintenance, endogenous respiration, lysis, decay and predation. Water Sci Technol 39:107–117

Vera L, González E, Díaz O, Delgado S (2014) Performance of a tertiary submerged membrane bioreactor operated at supra-critical fluxes. J Membr Sci 457:1–8

Villain M, Marrot B (2013) Influence of sludge retention time at constant food to microorganisms ratio on membrane bioreactor performances under stable and unstable state conditions. Bioresour Technol 128: 134–144

Wang XM, Li XY (2008) Accumulation of biopolymer clusters in a submerged membrane bioreactor and its effect on membrane fouling. Water Res 42:855–862

Wang Z, Yu H, Ma J, Zheng X, Wu Z (2013) Recent advances in membrane bio-technologies for sludge reduction and treatment. Biotechnol Adv 31:1187–1199

Wilén BM, Keiding K, Nielsen PH (2000) Anaerobic deflocculation and aerobic reflocculation of activated sludge. Water Res 34:3933–3942

Wu J, Huang X (2009) Effect of mixed liquor properties on fouling propensity in membrane bioreactors. J Membr Sci 342:88–96

Zeman LJ, Zydney AL (1996) Microfiltration and ultrafiltration: principles and application. Marcel Dekker, Inc., New York

ANEXO C: Performance of a tertiary submerged membrane bioreactor operated at supra-critical fluxes

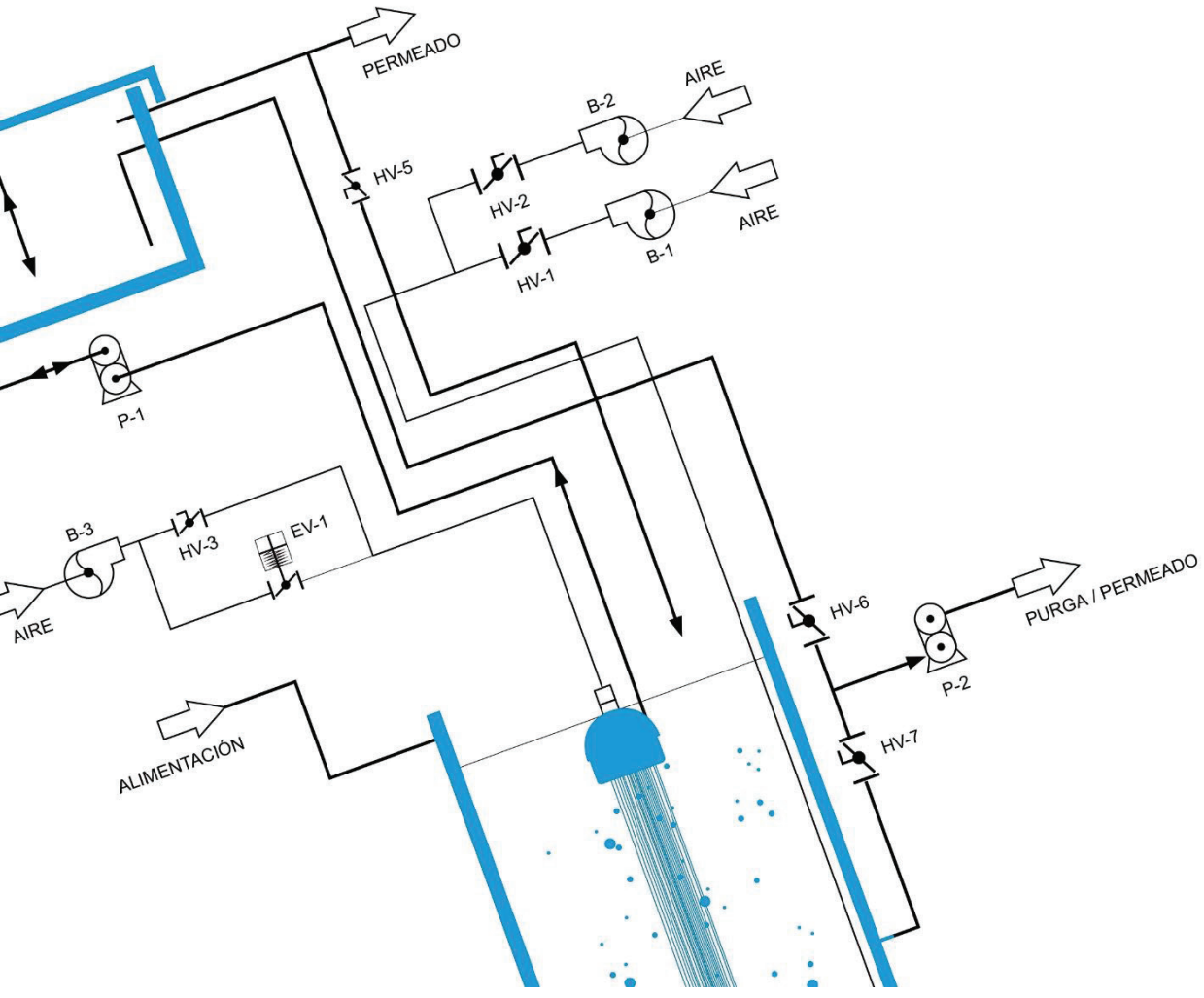

Journal of Membrane Science 457 (2014) 1–8

Contents lists available at ScienceDirect

Journal of Membrane Science

journal homepage: www.elsevier.com/locate/memsci

Performance of a tertiary submerged membrane bioreactor operated at supra-critical fluxes

L. Vera *, E. González, O. Díaz, S. Delgado

Department of Chemical Engineering, Faculty of Chemistry, Universidad de La Laguna, Av. Astrof. Fco. Sanchez s/n., 38200 La Laguna, Spain

ARTICLE INFO

Article history:
Received 2 August 2013
Received in revised form
23 December 2013
Accepted 12 January 2014
Available online 21 January 2014

Keywords:
Submerged membrane bioreactor
Tertiary treatment
Fouling
Supra-critical fluxes
Set-point trasmembrane pressure

ABSTRACT

A pilot-scale submerged aerobic membrane bioreactor (MBR) was run for over 3 months to assess the sustainability to operate at supra-critical fluxes. The MBR was applied as advanced treatment of secondary effluent from a conventional wastewater treatment plant. The system was successfully operated without biomass purge at hydraulic retention time (HRT) of 8.8 h, resulting in a moderate liquor suspended solid concentrations range (MLSS=4.1–7.1 g/l) in the bioreactor, according to the influent organic load fluctuations. Treatment performance was stable and achieved high conversion of ammonium to nitrate (96%) and dissolved organic carbon removal (53%). Short-term tests have been carried out according to a modified flux-step method to determine critical flux and evaluating optimum membrane cyclical aeration frequency. For the long-term tests, an alternative operation mode for backwashing initiation, based on a pre-selected transmembrane set-point, was applied. Under typical specific demand values (SAD_{pnet}=13.7–18.3 N m^3/m^3), continuous operation under different supra-critical filtration fluxes (J=60–80 l/h m^2) and backwashing fluxes (40–80 l/h m^2) can be maintained without any chemical cleaning. Analysis by means of sludge fractionation in lab-scale tests, at similar hydrodynamic conditions, indicated that the contribution of suspended solids to cake membrane fouling was estimated about 86–89%.

1. Introduction

It is widely known that in regions with water scarcity, wastewater reuse is a common practice and competent authorities have promoted many actions to encourage its reuse. In Tenerife island (Spain), since 1993 the secondary effluent obtained in the capital city's wastewater treatment plant (WWTP) is transported a long distance (60 km) by pipe, before being reused for crop irrigation. Biological treatment used in the plant is single-stage aeration and settling, which produces an effluent containing a significant and variable residual organic load and ammonium nitrogen (30–50 mg/l). Current scheme also includes a conventional tertiary treatment train (coagulation, sand filtration, chlorination and desalination). Some of the technical problems found in the treatment scheme have been the production of large quantities of residuals, high consumption of chemical reagents, sulphide generation during transport of the reclaimed water through a long pipe and decreased productivity in the downstream desalination plant due to the mentioned residual organic load [1]. Researching this issue provided some valuable technical solutions, indicating that anaerobic conditions inside the pipe can be inhibited by the presence of low nitrate concentration [2].

Due to their well-known advantages [3], submerged membrane bioreactor (MBR) has turned out as an attractive option for replacing the current tertiary treatment. As it was stated in previous research, the WWTP effluent can be effectively treated in an MBR until it achieves a high dissolved organics removal and complete nitrification [4]. Particularly interesting could be operating at maintenance energy level of the biomass, which significantly reduces sludge production. Under these conditions, the soluble microbial product (SMP) concentration could be minimised and the system was operated successfully at moderate permeate fluxes and low cleaning frequency, without any fouling evidence [5].

Notwithstanding the advantages of MBRs, their implementation is limited by the high costs, both in capital and operating expenditure (CAPEX and OPEX). A key issue regarding CAPEX and OPEX is the selection of the most appropriate permeate flux, which is determined by the classical trade-off problem: at higher fluxes CAPEX decreases while OPEX increases. High fluxes are desirable to reduce the membrane area required (i.e. reduce CAPEX), however, membrane fouling increases with flux, which results in a higher membrane scouring demand and a more frequent cleaning to control membrane fouling (i.e. increase OPEX) [3]. Verrecht et al. [6] have concluded that higher sustainable

* Corresponding author. Tel.: +34 922318054; fax +34 922318014.
E-mail address: luvera@ull.es (L. Vera).

0376-7388/$ - see front matter © 2014 Elsevier B.V. All rights reserved.
http://dx.doi.org/10.1016/j.memsci.2014.01.027

fluxes lead to lower net present values (NPV), indicating that the higher OPEX are offset by lower CAPEX since less membrane area is required, based on the results of a cost sensitivity analysis for a full-scale hollow fibre MBR. Specifically, an increase in flux from 15 to 30 l/h m^2 decreases NPV by 9%. Nevertheless, the correlation between membrane fouling and flux is influenced by hydrodynamics, cleaning protocols, feedwater characteristics and biological conditions [7]. The subsequent uncertainty has led to conservative plant designs and operation strategies. In addition, an analysis of design and operation of large MBR plants in Europe shows a broad difference between the design and operation flux [8]. For flat-sheet systems, the net fluxes are designed at 14–48 l/h m^2 (mean at 32 l/h m^2) while for the hollow-fibre modules they are 20–37 l/h m^2 (mean at 29 l/h m^2). However, for both systems the operation net flux is of about 20 l/h m^2. Therefore, the general trend is to reduce operational risk by operating at low fluxes (below the critical flux) where fouling is limited [9]. In addition, to maintain the process performance, strategies for fouling mitigation such as air scouring and physical cleaning techniques (i.e. backflushing and relaxation) have been incorporated as a standard [10,11]. Air scouring, expressed as specific aeration demand per permeate volume unit (SAD_p), takes a typical value, for full-scale facilities, between 10 and 50 N m^3/m^3 [10]. Relaxation and backflushing (only for hollow-fibre configuration) cycles with a pre-fixed duration are commonly applied for 30–130 s every 10–25 min of filtration [10]. However, inflexibility inherent of this time-based operation mode leads to a decrease in productivity when cleaning cycle is applied too often or it can promote irreversible fouling when applied too late [7].

Despite of the experience gained in the MBR operation over the last years, from a great variety of tested conditions, operation strategies are usually based on predetermined values of the key parameters (air scouring, filtration/physical cleaning sequences and permeate flux). However, these pre-set fixed values, based on general background or recommendations of membrane suppliers, lead to under-optimised systems and finally result in loss of permeate and high energy demand.

Special attention has been paid on feedback control to improve filtration process efficiency [7]. A comprehensive review of the achievements, including those related to the biological process, can be found in a recent paper [12]. Among the control systems, Smith et al. [13] have successfully validated a system for backwash initiation by permeability monitoring, automatically adjusting the backwashing frequency as a function of allowable transmembrane pressure increase in each filtration cycle, which results in a reduction of 40% in the required backwashing water. This control system was developed in a previous lab-scale study [14], which showed that membrane fouling can be significantly affected by the value of transmembrane pressure set-point (TMP_{sp}) selected and the cleaning method. However, a deeper investigation in long-term pilot experiments should be carried out in order to assess process sustainability, mainly focused on residual fouling development.

This paper assesses the sustainability of an MBR operated under controlled backwashing at supra-critical fluxes for treatment of secondary effluent. The role of backwashing flux was also investigated.

2. Material and methods

2.1. Feedwater

The pilot MBR was fed with effluent from a conventional activated sludge wastewater treatment plant whose average characteristics are given in Table 1. This is an old WWTP designed only for carbon removal. Due to the short sludge ages and oxygen deficiency in the activated sludge process, frequent episodes of sludge deflocculation or not enough sedimentation usually appear, which results in a high suspended solids concentration in the effluent.

Table 1
Feedwater main characteristics.

Parameters	Units	Mean	Range
COD	mg/l	280	13–2520
DOC	mg/l	14	9–27
$N–NH_3$	mg/l	26	1–53
$N–NO_2^-$	mg/l	4	< 1–13
$N–NO_3^-$	mg/l	2	< 1–17
Turbidity	NTU	180	10–1200
TSS	mg/l	280	33–1100

2.2. MBR

A cylindrical 220 l MBR was equipped with ZeeWeed® ZW-10 (GE Water & Process Technologies) hollow-fibre membranes of 0.04 μm rated pore diameter and 1.9 mm outer diameter, assembled vertically, which provide 0.9 m^2 of filtering surface area (Fig. 1). ZeeWeed® consists of a woven reinforcing braid on which a PVDF membrane is cast. The effluent (permeate) was extracted from the top header of the module under slight vacuum. All experiments were carried out at a constant permeate flux, registering transmembrane pressure as a function of time. Fouling was controlled by coarse bubbling of air flow and by intermittent backwashing. The unit operated in automatic cleaning initiated mode. Each filtration cycle was finished when a pre-established transmembrane pressure was reached (30 kPa), beginning the backwashing cycle immediately afterwards. A programmable logic controller (PLC) system was used to initiate and stop the backwashing by comparison of TMP set-point and instantaneous pressure values. Continuous data logging and plotting of pressure profile evolution were also performed.

Before starting the experimental period, the pilot-scale MBR was seeded with sludge from the activated sludge reactor of the WWTP and operated for over 6 months to ensure that stationary conditions were reached. In this study, the bioreactor was run at HRT values of 8.8 h without sludge removal except for sampling. In order to maintain a constant HRT independent of the permeate flux, the excess of permeate was returned to the tank. Air was supplied through the bottom, providing oxygen and stirring. The dissolved oxygen concentration was always above 1.5 mg/l in the reactor operated at 23 ± 2 °C. Suspensions were characterised by particle size, MLSS, MLVSS, biomass activity, non-flocculating microorganisms [15] and dissolved organic matter of the liquid phase. In order to determine fouling contribution of each sludge components, a filterability test in a lab filtration unit was carried out for the different sludge fractions.

2.3. Short-term flux step trials

The modified flux-step method is based on applying successive flux increments up to a maximum and back analogous, in accordance with the method of Le-Clech et al. [16] and further improved by incorporating relaxation steps for reducing the influence of fouling history [17]. Nevertheless, the modified method proposed in this work substitutes the relaxation steps for short backwashing cycles (30 s) at a fixed flux value of 60 l/h m^2, to be more similar to the conventional operation of an MBR. The results are related to the reversible fouling rate (r_f), given by the change in TMP with time ($dTMP/dt$) at each J. Residual fouling was also assessed by measuring the transmembrane

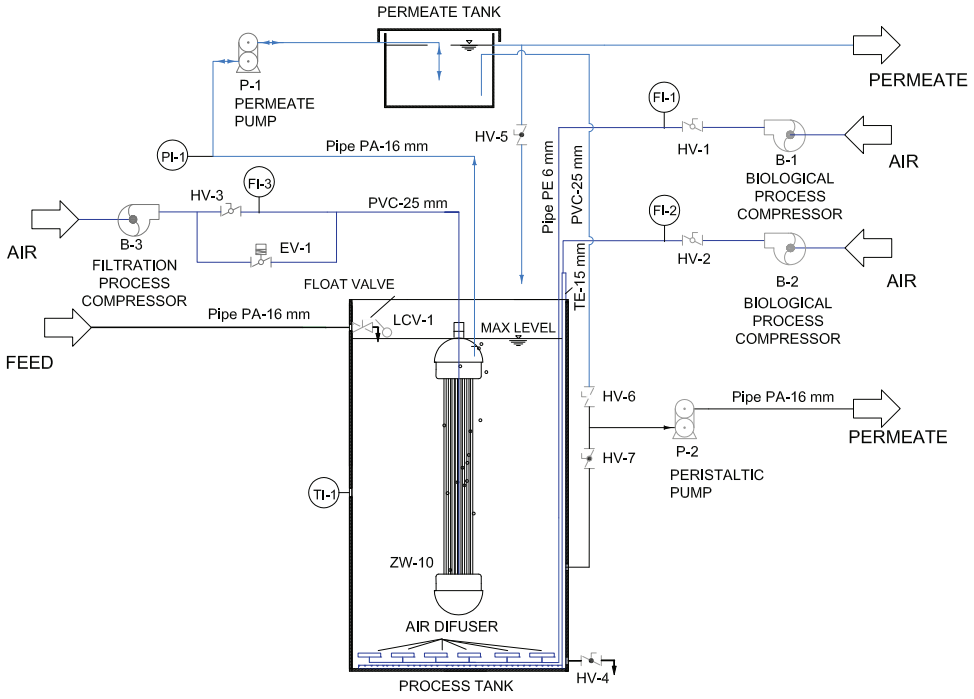

Fig. 1. Configuration of the pilot-MBR system, ZW10.

pressure after the backwashing cycle (TMP_0). The other experimental parameters were selected in accordance with [17,18]: step duration of 15 min, flux-step height of 5 l/h m^2 and a maximum flux of 100 l/h m^2.

2.4. Filterability test unit

The experiments were made in a laboratory unit equipped with ZeeWeed® ZW 1 hollow fibre membrane module similar to that used in the pilot unit with a smaller filtration area (0.047 m^2). ZW1 was operated in a closed loop, through a stirred 1.5 l tank of 21 cm water height. A magnetic drive pump was used to withdraw permeate from the membrane module. Membrane fouling was indicated by the increase of the transmembrane pressure measured by a pressure sensor. To ensure membrane cleaning, air was intermittently supplied at a frequency of 10 s on/10 s off (SAD_{mnet} = 1.12 N m^3/h m^2). Air flow-rate was controlled by a mass flow controller. The control system and the card interface were similar to the pilot system. Further details can be found elsewhere [14].

2.5. Analytical methods

Dissolved oxygen was measured using an oximeter WTW 340i. Chemical oxygen demand (COD), ammonium–nitrogen (N–NH_3), total suspended solids (TSS), mixed liquor suspended solids (MLSS), mixed liquor volatile suspended solids (MLVSS), time to filter (TTF) and turbidity were determined in conformity with the Standard Methods [19]. Analyses of nitrite–nitrogen (N–NO_2^-) and nitrate–nitrogen (N–NO_3^-) were conducted through ion chromatography using a Compact IC plus 882 device supplied by Metrohm. Dissolved organic carbon (DOC) concentration was measured with a TOC-meter (TOC-5000A, Shimadzu). The oxygen uptake rate was measured by following the dissolved concentration with a membrane oxygen electrode, in a medium without substrate ($SOUR_e$, endogenous). Microbial floc size distribution was measured by using a Malvern Mastersizer 2000 instrument (Malvern Instruments Ltd.) with a detection range of 0.02–2000 μm. In order to quantify the amount of non-flocculating microorganisms, samples of biomass were centrifuged at 1300 g for 2 min and the supernatant turbidity was then measured [15]. Sludge supernatant was obtained after settling in a 3 l cylinder for 30 min. Fractionation of the supernatant was carried out using several dead-end cell (Millipore) microfibre filters of different nominal pore sizes: 1.50, 0.45 and 0.22 μm.

3. Results and discussion

3.1. Process performance and biomass characteristics

Table 2 summarises the COD, N–NH_3 and DOC removal efficiencies and main characteristics of the microbial suspension. Ammonia, COD and DOC removal efficiency were 96%, 89% and 53% on average. Despite operating in conditions of total sludge retention, MLSS concentration stabilised between 4.1 and 7.1 g/l according to influent fluctuations (33–1100 mg TSS/l, see Table 1). In these conditions, the MLVSS/MLSS ratio remained constant throughout the experiment (77–80%), indicating no significant accumulation of inorganic matter. It is expected that microorganisms under severe substrate limitation should preferentially meet their maintenance energy requirements instead of producing additional biomass. Therefore, the “maintenance” concept introduced by Pirt [20] may be the reason for the MLSS stabilisation in the MBR operated without biomass purge. In addition, endogenous specific oxygen uptake rate ($SOUR_e$) was considerably lower than the typical values, which confirms a maintenance regime was achieved. Uniform and medium-sized flocs were also observed, with a mean d_{50} value of 43 μm. Sludge filterability, quantified as TTF, was reasonably consistent at 3.7 ± 0.5 min. Furthermore, the low quantity of small non-floculating flocs, measured as supernatant turbidity [15], showed that the hydrodynamic stress due to membrane air scouring was sufficiently low to prevent sludge deflocculation.

Finally, given the impact of soluble microbial products (SMP) on membrane fouling [7], this was routinely analysed through the measurement of the dissolved organic carbon concentration (DOC), according to Lyko et al. [21]. Results showed that SMP was 36% (on average) lower in the sludge supernatant than in the influent (Table 1),

Table 2
Bioreactor treatment performance and main characteristics of microbial suspension.

Parameter	Unit	Mean value	Range
Bioreactor treatment performance			
COD removal	%	89	
N–NH_3 removal	%	96	
DOC removal	%	53	
Permeate DOC	mg/l	6	3–16
Suspension characterisation			
MLSS	g/l	5.5	4.1–7.0
MLVSS	g/l	4.4	3.2–5.6
TTF	min	3.7	
PSD			
d_{10}	μm	17	
d_{50}	μm	43	
d_{90}	μm	92	
$SOUR_e$	mg O_2/g MLVSS h	1.66	
Supernatant turbidity	NTU	30	14–55
Supernatant DOC[a]	mg/l	9	5–34

[a] Samples were filtrated through microfibre filters with a nominal pore size of 0.45 μm

resulting in a low and relative stable concentration, attributable to the biological degradation process. Based on the concept of utilisation and biomass associated products [22], SMP production can be minimised at low substrate utilisation rates and biomass activity (i.e. maintenance conditions) while SMP biodegradation increases with sludge retention time (SRT). Nevertheless, it was found that the concentration of SMP in the supernatant was always slightly higher than that in the permeate. This confirms that the membrane retained a considerable fraction of the SMP (21%), which is expected to cause membrane fouling by entering into membrane pores or adsorbing onto the membrane surface. However, the operation at supra-critical fluxes with the associated cake layer formed on the membrane surface during filtration cycles could prevent partially this fouling, as it was reported in previous studies [23].

3.2. Critical flux determination: effect of cyclical aeration frequency

In Fig. 2, typical flux (J) and TMP profiles during short-term trial for critical flux determination are shown. Fig. 3a shows the reversible fouling rate (r_f) against J during the ascending phase. An increase of aeration frequency up to 10 s on/50 s off (net specific aeration demand, SAD_{mnet}=0.18 N m^3/h m^2) had no influence on the critical flux (J_c) of 45–50 l/h m^2. This result is consistent with other studies suggesting a threshold aeration flow value after which no improvement is achieved [16,18]. At the lowest frequency of 10 s on/100 s off (SAD_{mnet}=0.10 N m^3/h m^2), J_c decreased at 40–45 l/hm^2. If $J<J_c$, reversible fouling rates remained in the range of 0.07-0.10 Pa/s (0.04–0.06 mbar/min) for any frequency selected, lower than the upper limit (0.2 Pa/s or 0.1 mbar/min) proposed for the critical flux determination [16]. On increasing J at supra-critical values, r_f sharply increased: this could be explained by differences in particle deposition rates under diverse hydrodynamic conditions. The shear rate generated by air bubbling prevents the deposition of large particles on the membrane surface [24]. Nevertheless, at high fluxes, permeate drag forces exceed the dispersive forces and particles can deposit on the membrane wall. A similar trend in reversible fouling rate was observed for continuous and intermittent aeration at 10 s on/10 s off (SAD_{mnet}=0.55 N m^3/m^2).

From the results of the residual fouling, measured by the transmembrane pressure after backwashing (TMP_0), a critical flux value with respect to residual fouling can be determined, where above it (55 l/h m^2), the TMP_0 starts to deviate from tap water behaviour (Fig. 3b). This fact may be attributed to the severe cake fouling reached at high fluxes, which (for given conditions) cannot

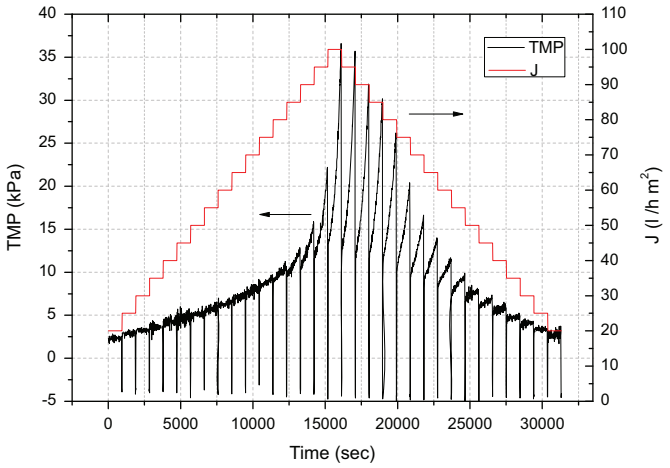

Fig. 2. Flux and TMP profiles during short-term trials; aeration frequency (on/off)=10/50 s/s; aeration flow rate=1.0 N m^3/h; t_B=30 s; and J_B=60 l/h m^2.

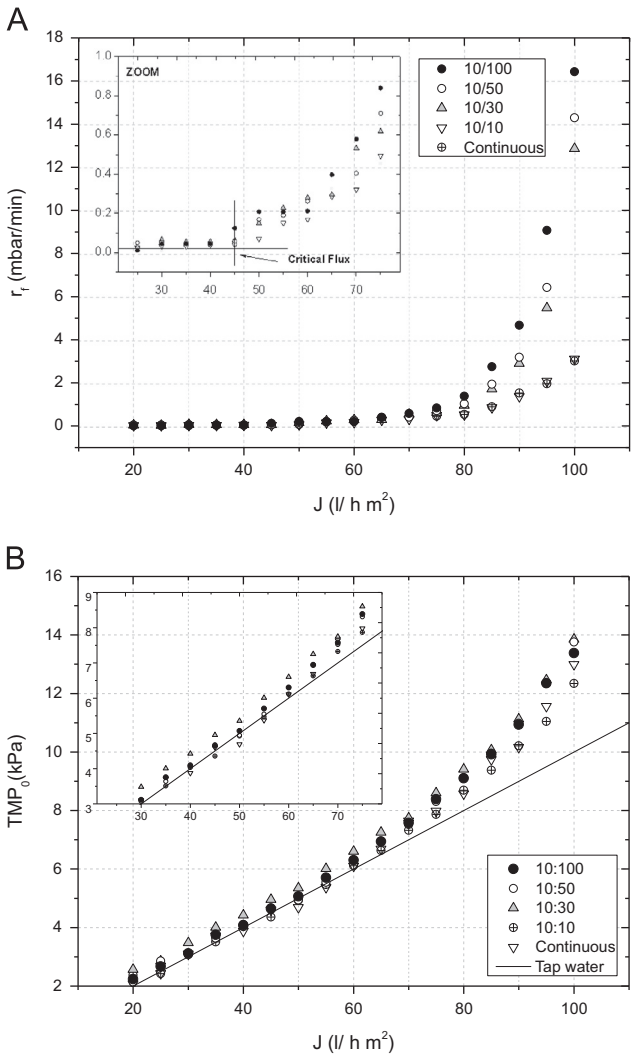

Fig. 3. Fouling rate (A) and TMP_0 (B) against permeate flux during the ascending phase of short-term trials at different aeration frequencies; t_B=30 s and J_B=60 l/h m^2.

be effectively removed by backwashing. Instead of the limitations of short-term tests to predict long-term behaviour [7], this critical flux can be used as a practical guideline for pilot-plant operation. Therefore, three supra-critical fluxes were applied (60, 70 and 80 l/h m^2) during the long-term trial.

3.3. Long-term test to assess process sustainability at supra-critical fluxes

Based on previous results [14], a value of 30 kPa was chosen for the *TMP* set-point in the long-term test. Supra-critical fluxes in the range 60–80 l/h m^2 and cyclical aeration with a frequency of 10 s on/10 s off were also selected. An important issue when operating at supra-critical fluxes is the capability of air scoring to re-disperse the cake layer detached from the membrane during the backwashing. Ye et al. [25] have reported the improvement of backwashing efficiency with the aid of air scouring. The authors concluded that the fouling material is removed from the membrane with air, thus limiting re-deposition in the subsequent filtration cycle. Therefore, in order to maximise the process performance, air flow rate was slightly increased during the filtration phase (SAD_{mnet}=1.1 N m^3/h m^2) while a constant air sparging (SAD_m =3.1 N m^3/h m^2) was applied during the backwashing phase. However, net specific aeration demand related to permeate volume (SAD_{pnet}) remained in 13.7–18.3 N m^3/m^3, which is similar to the typical full-scale values [10].

Fig. 4 shows an example of the *TMP* evolution under consecutive filtration/backwashing cycles, where each filtration phase finished when the TMP_{sp} was reached. It can be observed that the *TMP* linearly increased with elapsed time. This behaviour suggests a cake development mechanism on the membrane wall. Then, the *TMP* evolution in each filtration phase can be described by the following equation [26]:

$$TMP = TMP_0 + r_f t \quad (1)$$

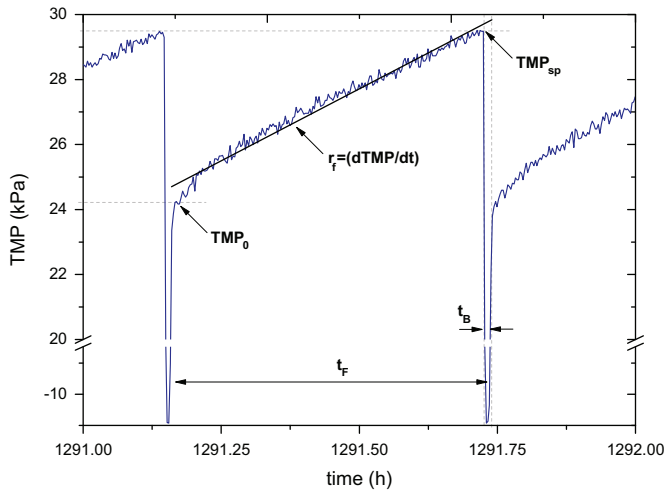

Fig. 4. Typical TMP profile of consecutive filtration and backwashing cycles in a fraction of the long-term experiment; J=70 l/h m^2; t_B=30 s; and J_B=60 l/h m^2.

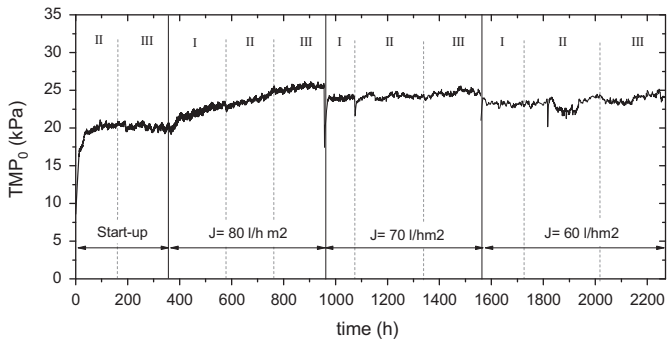

Fig. 5. TMP_0 profile for different filtration and backwashing fluxes in long-term experiment; I: J_B=40 l/h m^2; II: J_B=60 l/h m^2; and III: J_B=80 l/h m^2.

where TMP_0 is the initial transmembrane pressure, r_f the reversible fouling rate and t the elapsed time.

Resulting TMP_0 profiles, related to irremovable residual fouling by backwashing, are shown in Fig. 5. An initial sharp increase during the first 40 h (from 8.6 to 20 kPa) was followed by a slow and gradual TMP_0 rise at J=80 l/h m^2, which finally stabilised when lower fluxes (70 and 60 l/h m^2) were applied. This initial residual fouling may be due to a progressive particle accumulation in the deposit as a consequence of the experimental operating mode for backwash initiation. Accordingly, backwashing is only applied when significant fouling (significant mass deposited) is reached during the filtration phase, thus resulting in a growth in residual fouling which backwashing cannot effectively remove. This is consistent with other studies with fixed backwash intervals where increasing filtration time was observed to have a large effect on fouling resistance increase [27,28]. TMP_0 profile reflects, however, a dynamic behaviour during the first cycles, where residual fouling increased less with subsequent cycles until the amount of particle deposited and removed was balanced.

After this initial period, the backwashing was effective to remove the particle deposit during more than 2200 h of operation, even applying high permeate fluxes. Also, the lowest backwashing flux (J_B, 40 l/h m^2) has revealed as enough to achieve the desired cleaning efficiency, while upper values did not improve membrane performance. The results have shown, therefore, that once the system reached steady-state conditions, backwashing efficiency was not significantly affected by operating conditions (permeate and backwashing fluxes) and influent fluctuations (Table 1). This may due to the fact that, with this alternative strategy, the system automatically adjusts cleaning frequency to a preselected TMP_{sp}, which will determine the degree of membrane fouling allowed, and thus a stable backwashing efficiency can be achieved. In fact, it was observed a low TMP_0 increase rate (0.001-0.0033 Pa/s) at the highest flux (80 l/h m^2), but significantly lower than typical ranges for residual fouling (0.017 Pa/s) reported for full-scale MBRs [7]. It is assumed that the low TMP_0 increase rate observed can be related to the formation of a cake layer on the membrane that might act as a secondary membrane. This secondary membrane could partially prevent SMPs from entering into the membrane pores or adsorbing onto the membrane surface. This behaviour is in agreement with Hwang et al. [29] which reported that an extended filtration cycle time can increase backwashing efficiency, if the cake formed suppresses membrane pore blocking. Consistently, maintenance chemical cleanings were not necessary during the whole experimental period.

Regarding to the reversible fouling, which impacts on filtration phase duration and therefore in backwashing frequency, it is influenced by the permeate flux (Fig. 6). As expected, the obtained values are slightly higher than those frequently observed in full-scale plants (0.17-1.7 Pa/s or 0.1–1 mbar/min) operated at low fluxes [7]. Therefore,

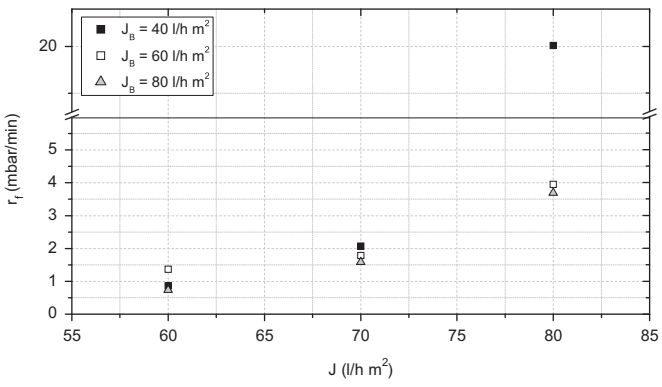

Fig. 6. Mean reversible fouling rates against permeate flux at different backwashing fluxes (long-term experiment).

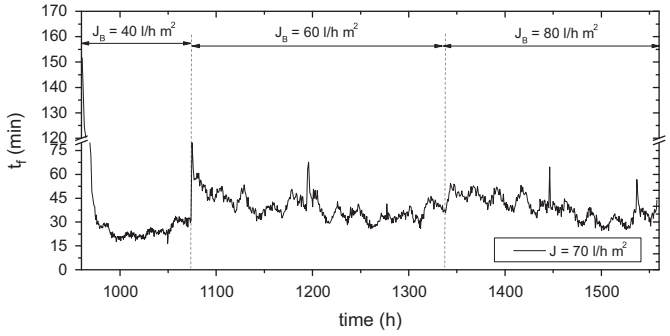

Fig. 7. Profile of the duration of filtration phase (t_f) for different backwashing fluxes at J=70 l/h m^2.

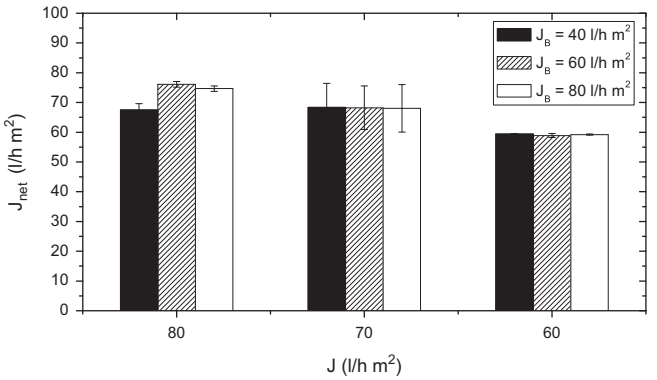

Fig. 8. Net permeate flux (J_{net}) against permeate flux for different backwashing fluxes.

controlling backwashing by TMP_{sp} has revealed as an efficient control system which allows to operate at higher permeate fluxes and to optimise the length of the filtration time without any significant increase in residual fouling. It is noticeable the high value of r_f observed at J=80 l/h m^2 and J_B=40 l/h m^2 which clearly does not fit with the general trend. This could be related to a high accumulation of solids in the vicinity of the membrane due to the deficient cake dispersion during the backwashing, which produced a higher fouling rate. However, the system was capable to automatically adjust the backwashing frequency to obtain a reasonable filtration length (4.3 min) and effectively remove the particle deposit. This dynamic cleaning strategy can be also observed in Fig. 7 where the filtration phase length changed (between 17 and 152 min) as a function of the membrane fouling.

On the other hand, membrane performance was also assessed by the net permeate flux (J_{net}) calculated as

$$J_{net} = \frac{t_F J - t_B J_B}{t_F + t_B} \quad (2)$$

where t_B and t_F are the duration of the backwashing phase and the filtration phase, respectively. Fig. 8 shows mean J_{net} as a function of the permeate flux. Although no significant effect of backwashing fluxes was found for the permeate flux, data suggest that J_{net} could be further improved by increasing J. This may be due to the larger filtration cycles obtained. The best result was obtained at the highest permeate flux (80 l/h m^2) and intermediate backwashing flux (60 l/h m^2), corresponding to a J_{net}=76 l/h m^2. This net permeate flux represents a significant improve, of about 67% of the J_{net} obtained by a conventional temporised operation at critical filtration conditions (t_F=12 min, t_B=30 s, J=J_c=50 l/h m^2 and J_B =60 l/h m^2). Also, the net flux of 76 l/h m^2 slightly improves (around 2%) the J_{net} corresponding to a temporised mode (t_F=12 min, t_B=30 s and J_B =60 l/h m^2) at the same permeate flux of 80 l/h m^2.

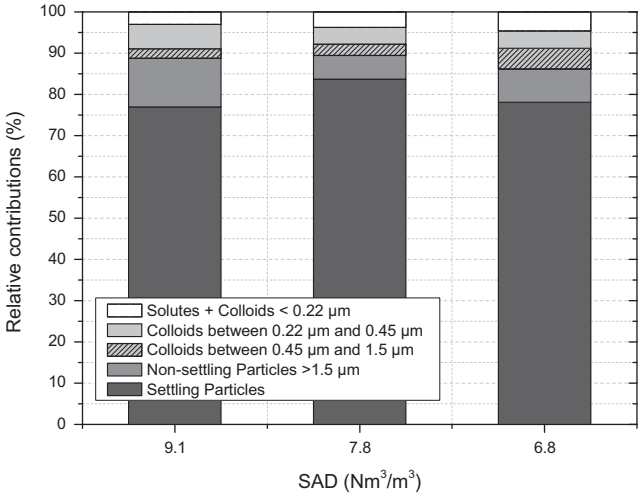

Fig. 9. Relative contributions expressed as percentage, of the different sludge fractions to fouling.

3.4. Relative contribution of different sludge fractions to cake fouling

Microbial suspension was fractionated into five components: settling particles, non-settling particles (> 1.5 μm), large colloids (0.45–1.5 μm), medium colloids (0.22–0.45 μm), and fine colloids and solutes (< 0.22 μm). This approach has been applied to assess the relative contribution of individual microbial suspension fractions to the total fouling rate. The fouling rate of each fraction was measured in the lab-scale filtration unit at the same hydrodynamic conditions of the long-term experiments (Fig. 9). Air sparging was also supplied at a similar specific air demand as that used in the pilot (SAD_{mnet}=1.12 N m^3/h m^2). Results revealed that the dominating fraction on cake membrane fouling was suspended particles (77–84% and 6–12% for settling and non-settling particles, respectively). Colloidal and soluble fractions did not have a relevant role on cake fouling (10–14%). This is because its low concentration (due to high degradation in the MBR) and the high fluxes applied, which jointly increased the particle contribution to the overall fouling. By contrast, several authors have identified colloids and solutes as the main contribution in MBRs treating raw domestic wastewater at subcritical fluxes [30]. Therefore, it is highlighted one of main advantages of the tertiary MBR operated at supra-critical fluxes: fouling control by this alternative operation mode appears to be a simple way for limiting deposition rate of suspended particles on membrane by the shear rate induced by air scouring. In addition, the deposit formed on the membrane, mainly by large particles, is effectively removed by backwashing.

4. Conclusions

The sustainability of a pilot-scale submerged aerobic membrane bioreactor as advanced treatment for secondary treated wastewater, at supercritical fluxes, was evaluated. For this purpose, an alternative backwashing strategy based on transmembrane pressure set-point (TMP_{sp}) was implemented. From this study, the following may be concluded:

- As a result of carbon substrate limited conditions (i.e. maintenance conditions), the system was successfully operated with complete sludge retention achieving a high treatment performance with a moderate liquor suspended solid concentration. In addition, MBR technology has allowed an advanced treatment without sludge production. In these conditions, the

soluble microbial products (SMP) concentration in the sludge supernatant was minimised.

- At supra-critical fluxes, an optimal membrane cyclical aeration frequency of 10 s on/ 10 s off was found, above which no improvement on membrane performance was observed.
- Sustainable process performance was observed at supra-critical fluxes (60–80 l/h m^2), providing high permeate net fluxes (59.4–76.1 l/h m^2) during more than 2250 h of operation without chemical cleaning. In these conditions, fouling is mainly caused by a cake development mechanism on the membrane wall which was effectively removed by backwashing. This cake layer could act as a secondary membrane which prevents SMPs from entering into the membrane pores or adsorbing onto the membrane surface.
- Analysis by means of sludge fractionation in lab-scale tests at similar hydrodynamic conditions indicated that the contribution of suspended solids to cake membrane fouling was about 86–89%.

Maintenance conditions in tertiary MBR could be an attractive option in terms of operational costs, due to the reduction of sludge production and the minimisation of SMPs, which is considered as an important factor affecting residual membrane fouling. This fouling requires more frequent recovery/maintenance chemical cleanings of the membrane. Since fouling is mainly caused by suspended particles, an alternative backwashing strategy based in TMP_{sp} can be implemented allowing the operation at supra-critical fluxes, and thereby obtaining high water productivity. Nevertheless, it remains to be seen if this interesting operation mode is suited for MBRs used for treatment of municipal wastewaters, as it is the main application of this technology.

Acknowledgements

The control system, funded by the N.R.C. (MINECO project CTM2011–27307), was tested for long-term validation during the MBR operation described in this paper. The authors want to express their gratitude to GE ZENON, to CANARAGUA, to EMMASA and to BALTEN for their support and also to the Water Analysis Laboratory of the ULL Chemical Engineering Department for its analytical advice. Finally, the authors would like to thank to Prof. S. Elmaleh his valuable comments and suggestions to this paper.

List of symbols

CAPEX	capital expenditure
COD	chemical oxygen demand, mg O_2/l
DOC	Dissolved organic carbon
HRT	hydraulic retention time, h
J	filtrate flux, l/h m^2
J_B	backwashing flux, l/h m^2
J_c	critical filtrate flux, l/h m^2
J_{net}	net permeate flux, l/h m^2
MBR	membrane bioreactor
MLSS	mixed liquor total suspended solids, mg/l
MLVSS	mixed liquor volatile suspended solids, mg/l
$N–NH_3$	ammonium–nitrogen, mg/l
$N–NO_2^-$	nitrite–nitrogen, mg/l
$N–NO_3^-$	nitrate–nitrogen, mg/l
NPV	net present value
OPEX	operating expenditure
PSD	pore size distribution, μm
r_f	reversible fouling rate, mbar/min
SAD_{mnet}	specific net aeration demand with respect to membrane area, N m^3/h m^2
SAD_{pnet}	specific net aeration demand with respect to permeate volume, N m^3/m^3
SMP	soluble microbial products
$SOUR_e$	specific endogenous oxygen uptake rate, mg O_2/g MLVSS h
SRT	sludge retention time, day
t	time, s
t_B	backwashing phase duration, s
t_F	filtration phase duration, min
TMP	transmembrane pressure, kPa
TMP_0	transmembrane pressure after backwashing, kPa
TMP_{sp}	transmembrane pressure set-point, kPa
TSS	total suspended solids, mg/l
TTF	time to filter, min
WWTP	wastewater treatment plant

References

[1] S. Delgado, M. Alvarez, E. Aguiar, L.E. Rodríguez-Gómez, H_2S generation in a reclaimed urban wastewater pipe. Case study: Tenerife (Spain), Water Res. 33 (2) (1999) 539.
[2] S. Delgado, M. Alvarez, L.E. Rodríguez-Gómez, S. Elmaleh, E. Aguiar, How partial nitrification could improve reclaimed wastewater transport in long pipes, Water Sci. Technol. 43 (10) (2001) 133–138.
[3] S. Judd, The status of membrane bioreactor technology, Trends Biotechnol. 26 (2007) 165–171.
[4] S. Delgado, F. Díaz, R. Villarroel, L. Vera, R. López, S. Elmaleh, Nitrification in a hollow-fibre membrane bioreactor, Desalination 146 (2002) 445–449.
[5] S. Delgado, R. Villarroel, E. González, Submerged membrane bioreactor at substrate-limited conditions: activity and biomass characteristics, Water Environ. Res. 82 (3) (2010) 202–208.
[6] B. Verrecht, T. Maere, I. Nopens, C. Brepols, S. Judd, The cost of a large-scale hollow fibre MBR, Water Res. 44 (2010) 5274–5283.
[7] A. Drews, Membrane fouling in membrane bioreactors—characterisation, contradictions, causes and cures, J. Membr. Sci. 363 (2010) 1–28.
[8] B. Lesjean, V. Ferre, E. Vonghia, H. Moeslang, Market and design considerations of the 37 larger MBR plants in Europe, Desal. Water Treat. 6 (2009) 227–233.
[9] P. Bacchin, P. Aimar, R.W. Field, Critical and sustainable fluxes: theory, experiments and applications, J. Membr. Sci. 281 (2006) 42–69.
[10] S. Judd, The MBR Book: Principles and Applications of Membrane Bioreactors for Water and Wastewater Treatment, Elsevier, Oxford, 2011.
[11] P. Le-Clech, V. Chen, A.G. Fane, Fouling in membrane bioreactors used in wastewater treatment, J. Membr. Sci. 284 (2006) 17–53.
[12] G. Ferrero, I. Rodríguez-Roda, J. Comas, Automatic control systems for submerged membrane bioreactors: a state-of-the-art review, Water Res. 46 (2012) 3421–3433.
[13] P.J. Smith, S. Vigneswaran, H.H. Ngo, R. Ben-Aim, H. Nguyen, A new approach to backwash initiation in membrane systems, J. Membr. Sci. 278 (2006) 381–389.
[14] R. Villarroel, S. Delgado, E. González, M. Morales, Physical cleaning initiation controlled by transmembrane pressure set-point in a submerged membrane bioreactor, Sep. Pur. Technol. 104 (2013) 55–63.
[15] H. Ng, S. Hermanowicz, Membrane bioreactor operation at short solids retention times: performance and biomass characteristics, Water Res. 39 (2005) 981–992.
[16] P. Le-Clech, B. Jefferson, I. Chang, S. Judd, Critical flux determination by the flux-step method in a submerged membrane bioreactor, J. Membr. Sci. 227 (2003) 83–91.
[17] P. van der Marel, A. Zwijnenburg, A. Kemperman, M. Wessling, H. Temmink, W. van der Meer, An improved flux-step method to determine the critical flux and the critical flux for irreversibility in a membrane bioreactor, J. Membr. Sci. 332 (2009) 24–29.
[18] G. Guglielmi, D. Chiarani, S.J. Judd, G. Andreottola, Flux criticality and sustainability in a hollow fibre submerged membrane bioreactor for municipal wastewater treatment, J. Membr. Sci. 289 (2007) 241–248.
[19] American Public Association/Water Environment Federation. Standard Methods for the examination of Water and Wastewater, 21 st ed. Washington, DC, USA, 2005.
[20] S. Pirt, The maintenance energy of bacteria in growing cultures, Proc. R. Soc. London 163B (1965) 224–231.
[21] S. Lyko, T. Wintgens, D. Al-Halbouni, S. Baumgarten, D. Tacke, K. Drensla, A. Janot, W. Dott, J. Pinnekamp, T. Melin, Long-term monitoring of a full-scale municipal membrane bioreactor—characterisation of foulants and operational performance, J. Membr. Sci. 317 (2008) 78–87.

[22] S.G. Lu, T. Imai, M. Ukita, M. Sekine, T. Higuchi, M. Fukagawa, A model for membrane bioreactor process based on the concept of formation and degradation of soluble microbial products, Water Res. 35 (2001) 2038–2048.
[23] V. Kuberkar, R. Davis, Modeling of fouling reduction by secondary membranes, J. Membr. Sci. 168 (2000) 243–258.
[24] J. Wu, C. He, Y. Zhang, Modeling membrane fouling in a submerged membrane bioreactor by considering the role of solid, colloidal and soluble components, J. Membr. Sci. 397–398 (2012) 102–111.
[25] Y. Ye, V. Chen, P. Le-Clech, Evolution of fouling deposition and removal on hollow fibre membrane during filtration with periodical backwash, Desalination 283 (2011) 198–205.
[26] S. Delgado, R. Villarroel, E. González, Effect of the shear intensity on fouling in submerged membrane bioreactor for wastewater treatment, J. Membr. Sci. 311 (2008) 173–181.
[27] P. Schoeberl, M. Brik, M. Bertoni, R. Braun, W. Fuchs, Optimization of operational parameters for a submerged membrane bioreactor treating dye-house wastewater, Sep. Pur. Technol. 44 (2005) 61–68.
[28] P. Gui, X. Huang, Y. Chen, Y. Qian, Effect of operational parameters on sludge accumulation on membrane surfaces in a submerged membrane bioreactor, Desalination 151 (2003) 185–194.
[29] K. Hwang, C. Chan, K. Tung, Effect of backwash on the performance of submerged membrane filtration, J. Membr. Sci. 330 (2009) 349–356.
[30] P. Le-Clech, V. Chen, T.A.G Fane, Fouling in membrane bioreactors used in wastewater treatment,, J. Membr. Sci. 284 (2006) 17–53.

ANEXO D: Application of backwashing strategy based on trasnmembrane pressure set-point in a tertiary submerged membrane bioreactor

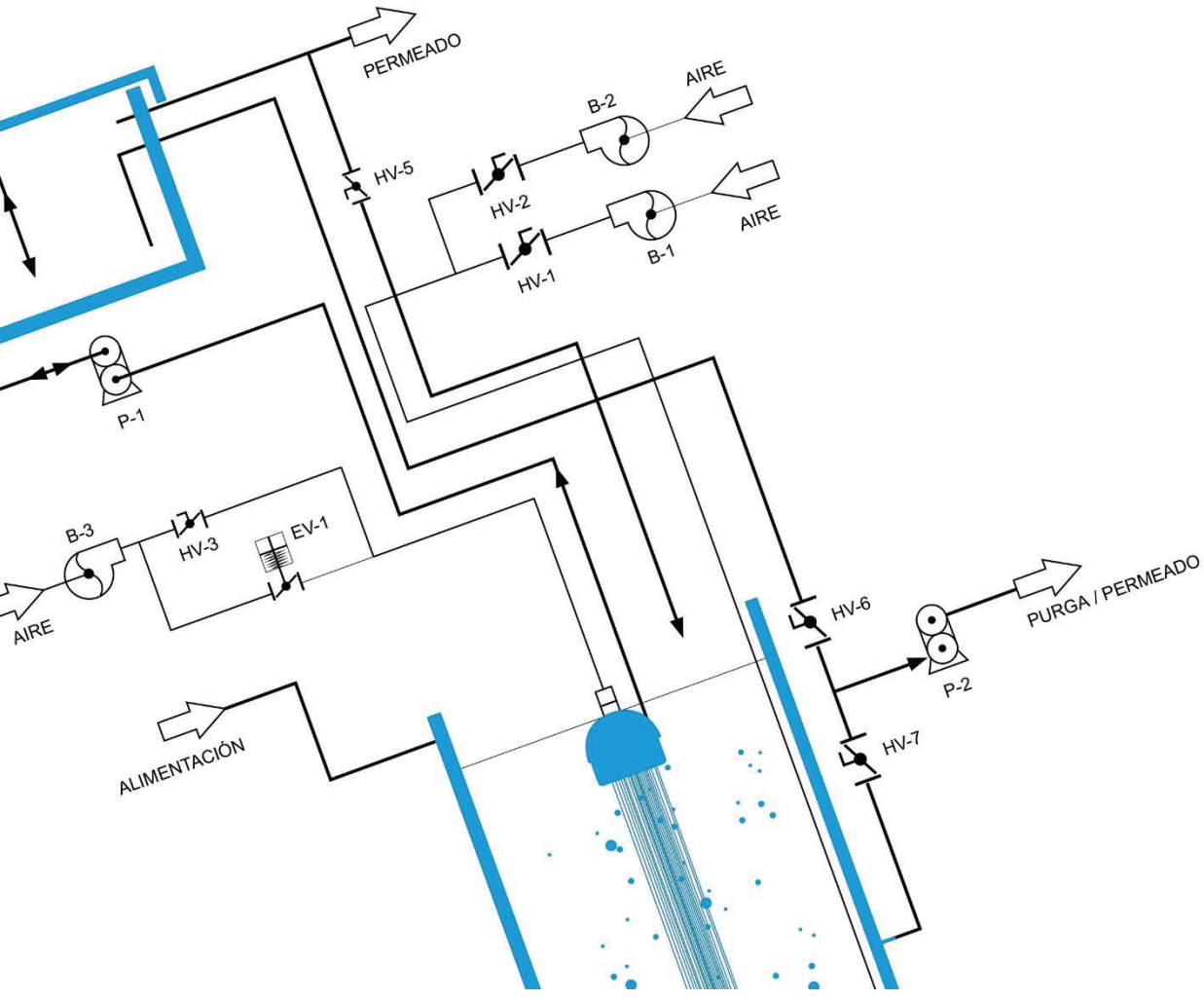

Journal of Membrane Science 470 (2014) 504–512

Contents lists available at ScienceDirect

Journal of Membrane Science

journal homepage: www.elsevier.com/locate/memsci

Application of a backwashing strategy based on transmembrane pressure set-point in a tertiary submerged membrane bioreactor

Luisa Vera *, Enrique González, Oliver Díaz, Sebastián Delgado

Department of Chemical Engineering, Faculty of Chemistry, University of La Laguna, Avenida Astrofísico Francisco Sánchez s/n., 38200 La Laguna, Spain

ARTICLE INFO

Article history:
Received 19 February 2014
Received in revised form
18 June 2014
Accepted 29 July 2014
Available online 6 August 2014

Keywords:
Submerged membrane bioreactor
Tertiary treatment
Fouling
Set-point transmembrane pressure
Wastewater reclamation

ABSTRACT

An alternative backwashing strategy to enhance water productivity in a tertiary submerged membrane bioreactor (MBR) was assayed. This strategy is based on automatically adjustment of the backwashing frequency as a function of the membrane fouling, which is expected to increase the net permeate flux produced. The effect of the key operational parameter (transmembrane pressure set-point, TMP_{sp}) on membrane fouling and process productivity was evaluated on a pilot-scale tertiary MBR. The system was successfully operated for over 4 months with complete sludge retention achieving a high treatment performance with a moderate liquor suspended solid concentration, as a result of carbon substrate limited conditions. The analysis of the membrane fouling at supra-critical filtrate flux of 70 L/(h m^2) with a specific aeration demand identical to that usual at full-scale (SAD_{pnet}=17 N m^3/m^3) showed that backwashing efficiency (described in terms of residual fouling resistance) was significantly affected by the selected TMP_{sp} value. At high TMP_{sp}, the efficiency decreased and chemical cleaning was necessary for membrane recovery. Nevertheless, moderate set-point values (30–40 kPa) provided high permeate net fluxes of 65–67 L/(h m^2) for more than 2000 h of operation, while the reversible fouling rate was not considerably influenced by TMP_{sp}. This was also confirmed by flux steps trials.

1. Introduction

Due to their well-known advantages [1,2], aerobic membrane bioreactors (MBRs) have become an attractive option for wastewater reuse, being very compact and efficient systems for achieving the highest effluent quality standards. The considerable popularity of the MBRs in the wastewater treatment market, the numerous suppliers, and the upward trend in plant size now reflect the maturity reached by this technology [3]. In fact, MBRs have been implemented in more than 200 countries [4]. Nevertheless, the main limitation to more widespread application is their high energy demand, besides awaiting new strategies to mitigate membrane fouling [5]. In addition, the uncertainty associated with fouling has led to conservative plant designs where the main operating parameters are far from being optimised [1].

As described in a previous research, aerobic MBRs can be effectively applied as an advanced treatment of secondary effluent from a wastewater treatment plant [6,7]. Delgado et al. [7] demonstrated a high conversion of ammonium to nitrate and constant COD removal efficiency in their system, regardless of the influent fluctuations. As a result of carbon substrate limited conditions, a minimal value for the carbon substrate utilisation rate was found and the system successfully operated at moderate permeate fluxes (30–32 L/(h m^2)) and low physical cleaning frequency. In these conditions, the production of soluble microbial products was minimised and higher organisms appeared.

For a submerged MBR, the operation strategy to control membrane fouling frequently includes physical cleaning through backwashing. During backwashing, permeate is used to flush the membrane backwards and it is routinely applied to hollow-fibre configuration. This technique has been successfully proved to remove reversible fouling caused by loosely packed sludge cake [8,9]. Several operating parameters such as frequency, duration and backwashing flux have been identified as crucial in fouling mitigation [10]. However, there is a gap in knowledge regarding the inter-relationships between those parameters and the permeate flux imposed. In fact, due to the complexity of the process, operation strategy is usually time-based and backwashing is commonly applied for 30–60 s every 5.8–15 min of filtration [11]. As a consequence, the systems are not optimised during the whole operational period [1].

Recently, special attention has been paid on feedback control for finding optimal operating conditions in MBRs [12]. Busch and

* Corresponding author. Tel.: +34 922318054; fax: +34 922318014.
E-mail address: luvera@ull.es (L. Vera).

http://dx.doi.org/10.1016/j.memsci.2014.07.069
0376-7388/

Marquardt [13] introduced a run-to-run process control approach, in which the manipulated variables are optimised after each filtration cycle. The manipulated variables include the permeate and backwashing fluxes, and the filtration and backwash durations. Smith et al. [14] have proposed a control system for backwash initiation by permeability monitoring, adjusting the backwashing frequency automatically as a function of the permissible increase of transmembrane pressure for each filtration cycle. This operation strategy was capable of achieving higher water productivity than the temporised mode with fixed intervals. The allowable *TMP* increase was fixed at 3% (1.5 kPa) of the maximum permissible value of 50 kPa, which is defined as the point where the fouling can still be removed by backwashing. Vargas et al. [15] used a similar strategy in which backwash is initiated when the flux drops below a predetermined fraction of the maximum value in a sequential membrane bioreactor operated at a constant *TMP*. This approach has been further developed at lab-scale in order to assess the effect of transmembrane pressure set-point (TMP_{sp}) on membrane fouling and water productivity [16]. This backwashing strategy was also validated on pilot-scale, showing that continuous operation can be maintained at supra-critical filtration fluxes without chemical cleaning at moderate TMP_{sp} (30 kPa) [17]. It is therefore desirable to identify the optimal TMP_{sp} value and its effect on membrane fouling over long-term periods in a MBR operated under real feed parameters and temperature fluctuations. This paper continues the discussion about the applicability of this alternative operation strategy, in which backwashing initiation is controlled by the TMP_{sp}. Additional flux step trials have also been carried out in order to assess the effect of TMP_{sp} on reversible fouling and threshold flux.

2. Material and methods

2.1. Feedwater

The MBR was fed with the effluent from a conventional activated sludge wastewater treatment plant. The feed water was analysed three times a week through the whole experimental period and the average characteristics are summarised in Table 1. This is a conventional WWTP designed only for carbon removal. Due to the short sludge ages and oxygen deficiency in the activated sludge process, frequent episodes of sludge de-flocculation or insufficient sedimentation usually appear, resulting in a high suspended solids concentration in the effluent.

2.2. MBR

A cylindrical 220 l MBR was equipped with ZeeWeed® ZW-10 hollow-fibre membranes (GE Water & Process Technologies) of 0.04 μm rated pore diameter, 1.9 mm external diameter and 0.9 m^2 of filtering surface area, assembled vertically (Fig. 1). ZeeWeed® consists of a woven reinforcing braid on which a PVDF membrane is cast. The effluent (permeate) was extracted from the top header of the module under slight vacuum. All experiments were carried out at constant permeate flux (70 L/(h m^2)), registering transmembrane pressure as a function of time. Membrane fouling was controlled by backwashing based on an automatic cleaning initiation mode. Each filtration phase finished when a pre-established TMP_{sp} was reached, beginning the backwashing immediately afterwards. The system was operated at 6 different TMP_{sp} (25, 30, 35, 40, 45 and 50 kPa). A programmable logic controller system was used to initiate and stop the backwashing by comparison of TMP_{sp} and instantaneous pressure values. Pressure profiles were continuously data logged and plotted. Filtration flux (J) and backwashing conditions (flux J_B and backwashing time t_B) were constant throughout the experimental period with J=70 L/(h m^2), J_B=60 L/(h m^2) and t_B=30 s.

Table 1
Feedwater main characteristics (n=63).

Parameters	Units	Mean	Range
COD	mg/L	55	12–205
DOC	mg/L	23	10.5–125.0
$N–NH_3$	mg/L	15	1.4–22.7
$N–NO_2^-$	mg/L	6	< 1–12.8
$N–NO_3^-$	mg/L	9	< 1–18.5
Turbidity	NTU	69	14–177
TSS	mg/L	156	27–316

Fouling was also controlled by intermittent coarse bubbling of air (10 s on/10 s off) supplied at 1.1 N m^3/h m^2 during the filtration phase, expressed as net aeration rate per membrane area ($SAD_{m\text{-}net}$). Nevertheless, constant air scouring during the backwashing phase was fixed at 3.1 N m^3/h m^2 in order to improve the fouling removal, on the basis of previous results [17].

The bioreactor was run at hydraulic retention time (HRT) of 8.8 h without sludge removal except for sampling. The excess of permeate was returned to the tank in order to maintain a constant HRT independent of the permeate flux. Additional air was supplied at the bottom of the bioreactor, providing oxygen and stirring. The dissolved oxygen concentration in the reactor was always above 1.5 mg/L, operated at 25 ± 2 °C. Suspensions were routinely characterised by particle size distribution, time-to-filter (TTF), MLSS, MLVSS, non-flocculating microorganisms and dissolved organic matter of the liquid phase.

Previous studies were carried out in this pilot-plant for over 3 months in order to evaluate the influence of permeate flux on membrane fouling produced with this novel operation mode based upon TMP_{sp} [17], consequently prior biomass acclimation was not required.

2.3. Short-term flux step trials

The effect of TMP_{sp} on critical flux was assessed by flux-step modified tests. The modified method is based on applying successive flux increments up to a maximum, in accordance with the method of Le-Clech et al. [18] and further improved by incorporating relaxation steps for reducing the influence of fouling history, as described by Van der Marel et al. [19]. The modified method proposed in this work substitutes the relaxation for short backwashing steps along 30 s at a fixed flux of 60 L/(h m^2). These established values are similar to those in conventional operation of MBRs. Intermittent air bubbling (10 s on/10 s off) for membrane scouring was also supplied at SAD_{mnet}=1.1 N m^3/h m^2. The other experimental parameters were selected in accordance with previous studies [19,20]: step duration of 15 min, flux-step height of 5 L/(h m^2)and a maximum flux of 70 L/(h m^2).

Results were related to reversible fouling rate (r_f), given by the derivative of the transmembrane pressure ($dTMP/dt$). On the other hand, residual fouling was assessed by measuring the transmembrane pressure after each backwashing (TMP_{if}).

2.4. Membrane cleaning protocol

After the long-term test, the fouled membrane was cleaned by a specific protocol that includes the following steps: (1) rinsing with Milli-Q water; (2) backwashing with Milli-Q water at a flux of 60 L/(h m^2); (3) chemical cleaning with a solution of sodium hypochlorite (500 mg/L) for 24 h; (4) chemical cleaning with a solution of citric acid (6000 mg/L) for 24 h; and (5) chemical cleaning with sodium hypochlorite (500 mg/L) for 24 h. After each

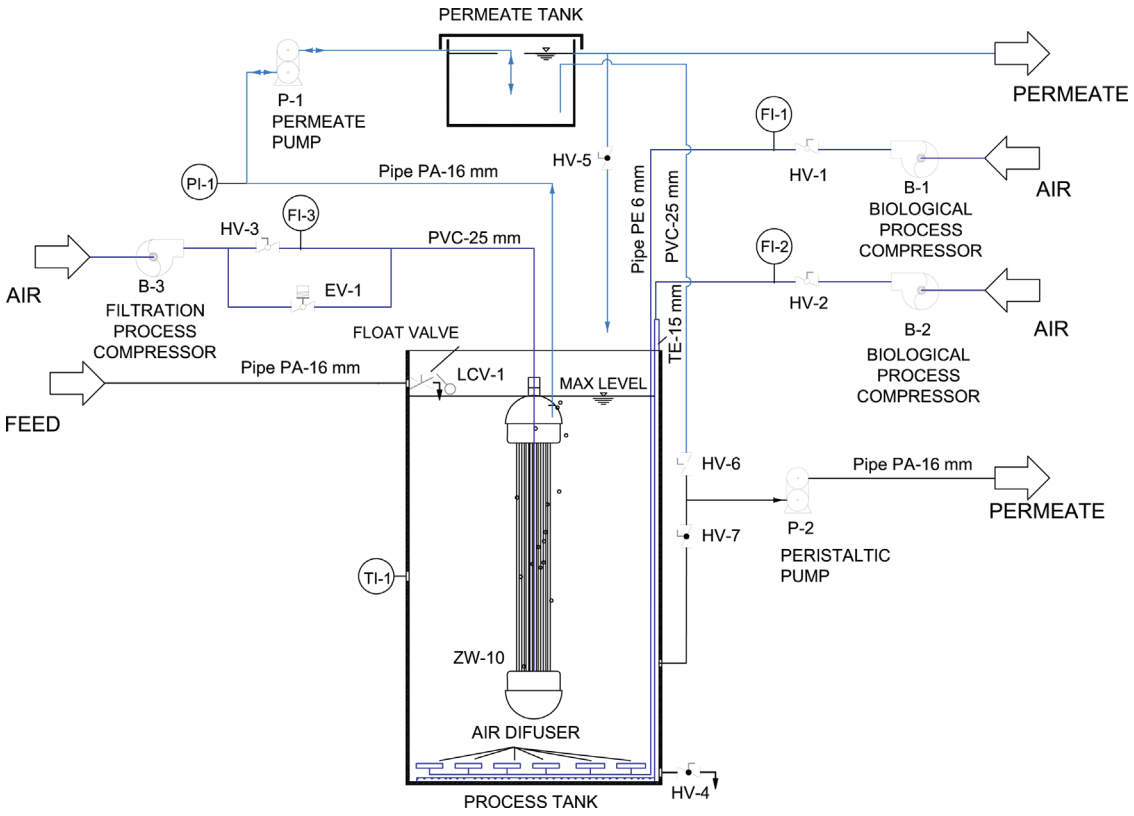

Fig. 1. Configuration of the pilot-MBR system, ZW10.

step, tap water filtration test was applied to measure the remaining resistance.

2.5. Membrane fouling characterisation

TMP evolution can be used for membrane fouling characterisation. According to the "resistance-in-series" model and disregarding the osmotic pressure term, the *TMP* can be described by

$$TMP = J\mu R_t = J\mu(R_m + R_{rdf} + R_{rvf}) \quad (1)$$

where μ is the permeate viscosity, J is the permeate flux, R_t is the total hydraulic resistance, R_m is the clean membrane resistance, R_{rdf} is the residual fouling resistance and R_{rvf} is the reversible fouling resistance.

Residual fouling is that which is not removed by backwashing. Its resistance can be separated into internal fouling resistance (R_{if}), related to internal membrane pore blocking [21] and gel or compacted particle layer that is not detached during backwashing [22], and an external fouling resistance (R_{ef}) linked to fouling layer recompression [23]:

$$R_{rdf} = R_{if} + R_{ef} \quad (2)$$

During the filtration, this external layer compresses, increasing the residual resistance, and during backwashing this layer relaxes, yielding a lower residual resistance. Therefore, just at the beginning of the filtration cycle, the initial *TMP* (TMP_i) can be described by Eq. (3):

$$TMP_i = J\mu(R_m + R_{if}) \quad (3)$$

In contrast, reversible fouling resistance R_{rvf} is generally associated with a cake development mechanism on the membrane wall [24]. According to the cake model, *TMP* linearly increases with filtration time and the slope of the straight line, the fouling rate r_f, can be used as a quantification parameter of reversible fouling [25,26]. Therefore, *TMP* evolution with elapsed time t can be described by Eq. (4):

$$TMP = TMP_0 + r_f t \quad (4)$$

where TMP_0 is the transmembrane pressure related to the residual fouling and can be defined as

$$TMP_0 = J\mu(R_m + R_{rdf}) \quad (5)$$

and the difference between TMP_i and TMP_0 called ΔTMP, is linked to the external residual fouling, R_{ef}.

Finally, another important parameter for membrane fouling characterisation can be considered, the backwashing efficiency η, which can be defined as [27]

$$\eta = \frac{R_{sp} - R_m - R_{rdf}}{R_{sp} - R_m} \times 100 \quad (6)$$

where R_{sp}, is the total hydraulic resistance at the TMP_{sp} (i.e. before backwashing), that can be estimated as the addition of several resistances: membrane itself, residual fouling and reversible cake fouling:

$$R_{sp} = R_m + R_{rdf} + R_{rvf}|_{t=t_F} \quad (7)$$

where t_F is duration of the filtration phase to reach the TMP_{sp}.

2.6. Analytical methods

Dissolved oxygen was measured using a WTW 340i. Chemical oxygen demand (COD), ammonium–nitrogen ($N–NH_3$), total suspended solids (TSS), mixed liquor suspended solids (MLSS), mixed liquor volatile suspended solids (MLVSS), time to filter (TTF) and turbidity were determined in conformity with the Standard Methods [28]. The analyses of nitrite–nitrogen ($N–NO_2^-$) and nitrate–nitrogen ($N–NO_3^-$) were conducted through ion chromatography using a Compact IC plus 882 device supplied by Metrohm. Dissolved organic carbon (DOC) concentration was

measured with a TOC-meter (TOC-5000A, Shimadzu). Microbial floc size distribution was measured by using a Malvern Mastersizer 2000 instrument with a detection range of 0.02–2000 μm. To quantify the amount of non-flocculating microorganisms, the samples of biomass were centrifuged at 1300*g* for 2 min and the supernatant turbidity was then measured [29]. The microorganism population was observed by Binocular microscopy (CME, Leica).

3. Results and discussion

3.1. Biomass characteristics and permeate quality

Table 2 summarises the main characteristics of the microbial suspension developed in the bioreactor. Despite operating with total sludge retention, moderate MLSS concentration was obtained (3.7–6.6 g/L), which is attributable to the low organic load in the feedwater (Table 1). The MLVSS/MLSS ratio remains nearly constant (69–79%) throughout the experimental period, indicating a low accumulation of inorganic particulate matter. At substrate-limited conditions, according to cellular "maintenance" concept [30] microorganisms utilise available substrates mainly for maintenance purposes instead of producing additional biomass. As a consequence, the low organic substrate utilisation rate (<0.05 kg COD/kg MLVSS d) and the long sludge retention time improved soluble microbial products (SMP) biodegradation (65% on average). This was attributable to an increase in microbial diversity, including slow-growing microorganisms [31]. As a result, a low concentration of SMP in the supernatant was observed (8.0 mg/L, expressed as equivalent DOC).

In general, the suspension also showed good filterability, quantified as TTF (270 s), with uniform and medium-sized flocs (d_{50}=47 μm). In addition, the suspension presented low quantity of small non-floculating flocs, measured as supernatant turbidity. This could be due to the presence of higher organisms like heterotroph protozoa (Fig. 2), which predate on dispersed bacteria [32].

Table 2
Characteristics of microbial suspension.

Parameter	Unit	Mean value	Range
MLSS	g/L	5.5	3.7–6.6
MLVSS	g/L	4.2	2.9–5.2
TTF	s	257	40–330
PSD			
d_{10}	μm	17	
d_{50}	μm	47	
d_{90}	μm	102	
Supernatant turbidity	NTU	28.4	14–55
Supernatant DOC[a]	mg/L	8.0	6.2–14.4

[a] Samples were filtrated through microfibre filters with a nominal pore size of 0.45 μm.

Permeate quality is presented in Table 3, where results are classified into six experimental periods according to the values of TMP_{sp} applied. Regardless of the TMP_{sp}, the permeate turbidity remained in the range 0.3–0.7 NTU, thus confirming the membrane integrity throughout the experimental period. As expected, considerable organic matter removal (56% on average for COD) and complete nitrification was always obtained in the bioreactor. Regarding SMP retention by the membrane and the associated cake layer, no considerable effect of the TMP_{sp} on the permeate DOC concentration was observed.

3.2. Effect of TMP set-point on membrane residual fouling and process productivity

In the present study, structured into six periods according to the selected TMP_{sp}, the pilot plant was run for more than 2750 h without any severe problems. However, there were two events of power shortage during the second period (912–930 h) and the fifth one (2610–2658 h).

Fig. 3A displays TMP_i profiles the residual fouling rate for each period. The general trend indicates that TMP_i increased as a function of TMP_{sp}. Each period was characterised by a sudden increase of TMP_i followed by a slower and gradual rise. This initial TMP_i increase can be related to the operating mode for backwashing initiation, which starts when the pre-fixed TMP_{sp} value (i.e. significant membrane fouling) is reached during the filtration phase. It should be noted that air scouring was continuously supplied at SAD_{mnet} of 3.1 N m^3/h m^2 during the backwashing, thus increasing this parameter by a factor of 2.8 with respect to filtration phase. Ye et al. [33] highlighted the importance of enhancing backwashing efficiency with air scouring to avoid fouling layer recompression and favouring its re-dispersion. However, this strategy seems inefficient to prevent external residual layer at the tested conditions in the present study. These results suggest a progressive consolidation of the deposit as the TMP_{sp} rises, leading to growth of internal residual fouling that cannot be removed by physical cleaning. Increasing TMP_{sp} between phases should result in longer filtration times in the first cycles, where the sharp increase in internal fouling was observed (Fig. 3B). A similar behaviour was observed after the mentioned power shortages, which can be considered as a long relaxation of the fouling layer. In fact, TMP_i rapidly increased until achieve the previous values after both power outage (Fig. 3A). Therefore, a prolonged relaxation could remove partially this fouling layer that appears during the normal operation when transmembrane pressure set-point strategy is applied. Hence, the results would support a significant part of the internal residual fouling being related to compacted particle layer. McAdam and Judd [22] indicated that the cake consolidation only occurs when the critical value of the mass deposited is reached, thus resulting in a linear increase of residual

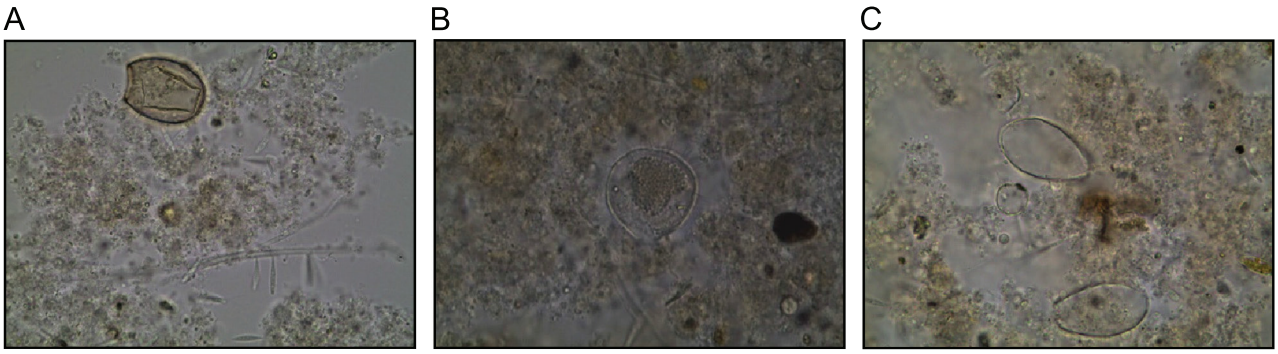

Fig. 2. Protozoan population in sludge samples (100 ×).

Table 3
Permeate main characteristics.

Parameters	Units	TMP_{sp}											
		25 kPa		30 kPa		35 kPa		40 kPa		45 kPa		50 kPa	
		Mean	Range	Mean	Range	Mean	Range	Mean	Range	Mean	Range	Mean	Range
COD	mg/L	20	15–25	32	17–42	28	18–43	25	19–36	26	12–33	23	21–25
$N–NH_3$	mg/L	0.3	0.3–0.4	0.4	0.4–0.6	0.5	0.4–0.6	0.6	0.4–1.0	0.5	0.5–0.6	0.5	0.4–0.5
$N–NO_3^-$	mg/L	36	26–43	35	24–60	36	22–42	27	5–42	27	24–30	31	29–33
Turbidity	NTU	0.5	0.4–0.6	0.6	0.4–0.7	0.5	0.4–0.7	0.4	0.3–0.5	0.6	0.5–0.6	0.5	0.4–0.5
DOC	mg/L	5.7	4.8–6.8	7.3	6.8–7.7	7.4	6.9–7.7	6.5	6.3–7.0	6.6	6.0–7.0	5.8	5.7–6.2

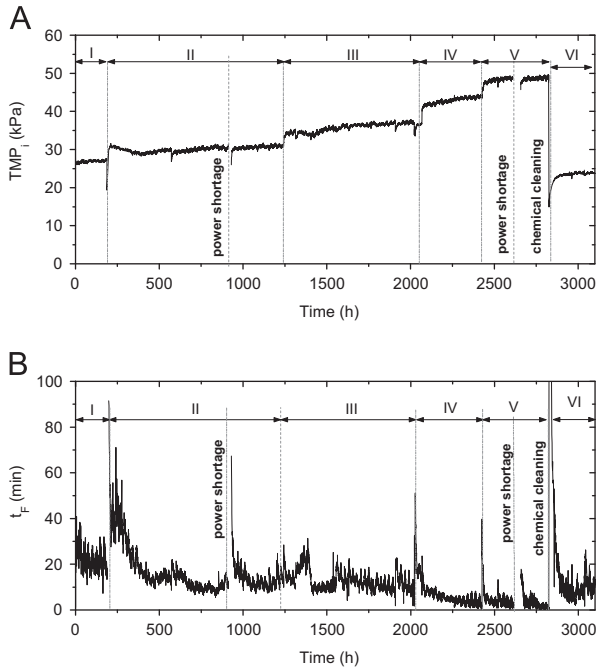

Fig. 3. TMP_i (A) and t_F (B) profile at different TMP_{sp} throughout the experimental time: (I) TMP_{sp}=30 kPa; (II) TMP_{sp}=35 kPa; (III) TMP_{sp}=40 kPa; (IV) TMP_{sp}=45 kPa; (V) TMP_{sp}=50 kPa; and (VI) TMP_{sp}=25 kPa.

fouling with filtration duration beyond this critical value. Instead, after the initial TMP_i growth at the beginning of each period, the effectiveness of the backwashing tended to stabilise the TMP_i value for each phase. This fact is reflected by the slow rates of TMP_i rise (1.8–7.2 Pa/h) which were found to be independent of the TMP_{sp}.

The TMP_{sp} increase led to a longer filtration phase (t_F) during the early cycles of each period, as previously mentioned (Fig. 3B). Then, a stabilised filtration phase length was achieved, which was significantly affected by inherent fluctuations in ambient conditions.

For the lower TMP_{sp} (25 kPa), as a consequence of the low value of the set-point, shorter stabilised filtration cycles were obtained (12 min on average). Sustainable t_F were observed at the moderate TMP_{sp} range: 22, 14 and 13 min for 30, 35 and 40 kPa, respectively. However, increasing TMP_{sp} up to 40 kPa showed a negative impact on t_F, decreasing its value below to a non-operative level (5 and 3 min on average for 45 and 50 kPa, respectively). This indicates that the backwashing efficiency to prevent the sudden increase of TMP_i at the beginning of the period, declined with TMP_{sp}. This can be attributed to the rise in fouling load to the membrane. Similar effect on backwashing efficiency has been reported by other authors after extending the filtration length (i.e. increasing the amount of fouling) with fixed backwashing intervals [34,35]. To illustrate it, averages net permeate fluxes $(J_{net})_{ave}$ and backwashing

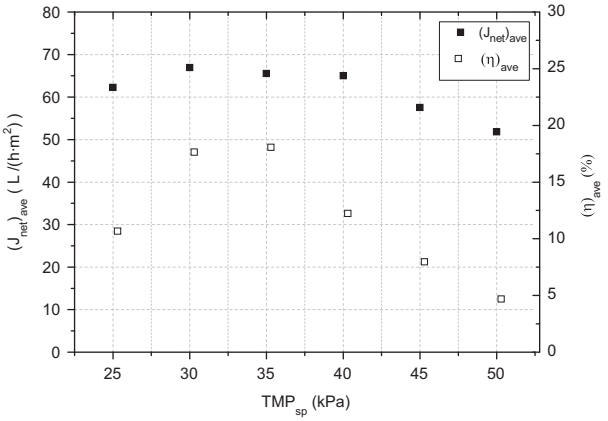

Fig. 4. $(J_{net})_{ave}$ and $(\eta)_{ave}$ against TMP_{sp}.

efficiencies $(\eta)_{ave}$ were calculated (Eqs. (8) and (9), respectively):

$$(J_{net})_{ave} = \frac{(t_F)_{ave}J - t_B J_B}{(t_F)_{ave} + t_B} \tag{8}$$

where $(t_F)_{ave}$ is the average filtration length, t_B is the duration of the backwashing phase, J is the permeate flux and J_B is the backwashing flux.

$$(\eta)_{ave} = \frac{R_{sp} - R_m - (R_{rdf})_{ave}}{R_{sp} - R_m} \times 100 \tag{9}$$

where $(R_{rdf})_{ave}$ is the average residual fouling resistance.

Fig. 4 shows average $(J_{net})_{ave}$ in each period as a function of the TMP_{sp}. At 25 kPa, the higher backwashing frequency imposed due to the low TMP_{sp} selected did not result in a high value of the backwashing efficiency. These results suggest a permanent residual fouling which cannot be completely removed by backwashing, even operating a low TMP_{sp}. Consequently, moderate set-point values (30, 35, 40 kPa) provided high water productivity (67, 66, 65 L/(h m^2)), respectively. On the other hand, increasing the selected set-point up to 40 kPa produced a significant decrease in $(J_{net})_{ave}$ due to a significant decline in average backwashing efficiency under 10%.

Finally, another aspect to analyse was the effect of the backwashing strategy on TMP_i and t_F profile during a day. Fig. 5 shows an example of the typical trend: whilst TMP_i seems to be nearly constant (varying on a 0.8% range with a mean value 36.8 kPa) (Fig. 5A), t_F showed a cyclic pattern over 24 h (Fig. 5B). Lower t_F (7–9 min) were always observed during the early hours of the early morning (0:30–7:30) which gradually increased until reaching a maximum (12–15 min) in the afternoon (12:30–19:30) starting to decline afterwards. This behaviour may be related to significant changes in sludge filterability according to fluctuations of ambient conditions. Nevertheless, a deeper research is necessary to conclude the causes for this repetitive dairy evolution.

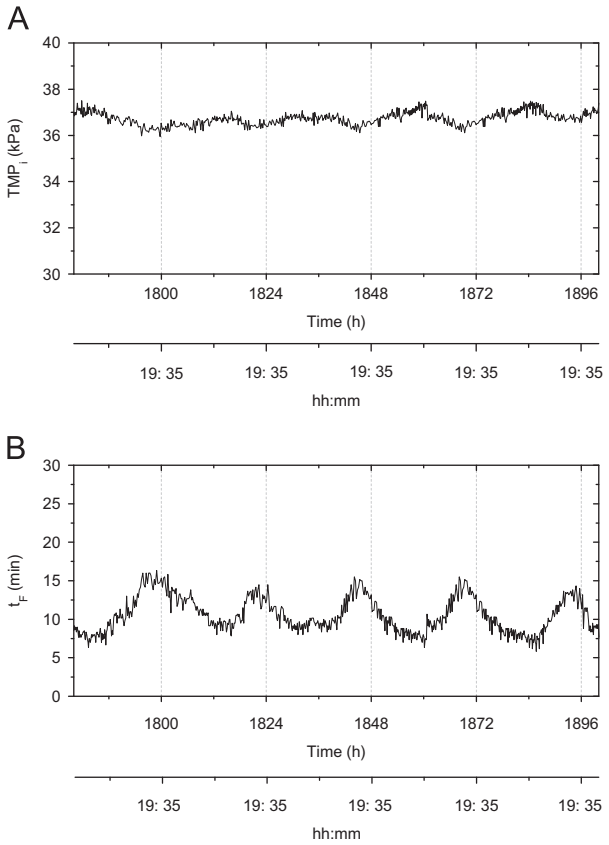

Fig. 5. TMP_i (A) and t_F (B) profile during several consecutive days; Period III: TMP_{sp}=40 kPa.

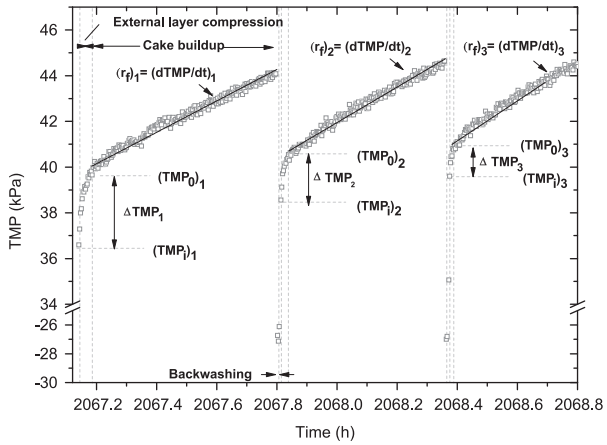

Fig. 6. *TMP* profile of consecutive filtration and backwashing cycles at the beginning of the period IV (TMP_{sp}=45 kPa).

In summary, it may be concluded that the main advantage of this backwashing strategy is that the system automatically adjusts the degree of membrane fouling allowed through backwashing frequency (i.e. filtration length) for a preselected TMP_{sp}. This allows to operate at high permeate fluxes and to optimise the length of the filtration time. Permeate net fluxes obtained at moderate TMP_{sp} represents a significant improve, of about 60–65% of the J_{net} obtained by a conventional temporised operation at critical filtration conditions (t_F=12 min, t_B=30 s, J=45 L/(h m^2) and J_B=60 L/(h m^2)) [1].

3.3. Proposed fouling mechanisms

According to the exposition developed in Section 2.5 and the results presented in previous section, a mechanism for fouling development in long-term experiments can be proposed.

As filtration proceeds, a two-step phenomenon was typically observed: a sudden increase in *TMP* followed by a linear rise (Fig. 6). A sharp fouling increase may be due to a recompression process, as it was stated in the previous section. After this transient phase, the linear *TMP* rise was assumed to be caused by a cake development mechanism on the membrane surface. As supra-critical flux was applied, it can be expected that this cake layer was mainly formed by deposition of large suspended solids which can be effectively removed by backwashing [8]. Therefore, it can be distinguished a TMP_0, corresponding to the value of *TMP* at which it starts to increase linearly, which separates reversible cake formation and residual fouling.

Also, a dynamic behaviour with consecutive filtration/backwashing cycles was typically observed at the beginning of each experimental period defined through the pre-fixed TMP_{sp} value (45 kPa in Fig. 6). An initial growth of TMP_i was observed, which was less in subsequent cycles. Accordingly, the duration of the recompression phase (associated with ΔTMP) decreased with successive cycles. This behaviour may be due to a progressive consolidation of the deposit which backwashing cannot remove. In these conditions, it is assumed that the cake layer is mainly reversible (i.e. amount of particle deposition and removal was balanced) and the resulting TMP_i increase rates were significantly lower (0.018–0.072 mbar/h) than typical ranges for residual fouling reported for full-scale MBRs (0.6 mbar/h) [26]. A reason for this finding is that the cake layer might act a secondary membrane that prevents pore blocking by SMP [36]. In addition, this hypothesis is in accordance with the relatively stable SMP concentration attributable to the degradation process, attained in the MBR due to the maintenance conditions applied. This behaviour is in agreement with Hwang et al. [9], who reported that an extended filtration cycle time can increase backwashing efficiency if the cake formed suppresses membrane pore blocking. Consistently, maintenance chemical cleanings were not necessary during the whole experimental period.

On the other hand, the effect of successive TMP_{sp} increase between steps was assessed in terms of residual fouling and reversible resistances (determined according to Section 2.5). Fig. 7 shows average fouling resistances against TMP_{sp}. It can be observed that internal fouling resistance R_{if} linearly increased with TMP_{sp} at the tested conditions. These results suggest a progressive consolidation of the deposit as the TMP_{sp} becomes higher. Both reversible resistance R_{rvf} and residual external fouling resistance R_{ef} showed near values and tended to decrease at high TMP_{sp} values (Fig. 7). This is attributable to the high level of internal fouling achieved, at 45 and 50 kPa which was able to significantly reduce the average duration of the filtration length within a cycle (5 and 3 min, respectively) and therefore, the amount of particles deposited onto the membrane. At the same time, by increasing the residual internal fouling, the pressure drop over the external layer and the cake deposit during the filtration phase was also reduced, which decreased the compression effect [37].

The results revealed that the main contribution to the overall fouling at the end of the filtration phase (i.e. at TMP_{sp}) was from internal residual fouling (varying from 58% to 96% of the total resistance), its contribution increasing with TMP_{sp}. In contrast, external residual fouling due to cake layer recompression was irrelevant (0–4%) and it only had a relevant role at low to moderate *TMPsp*of 25–40 kPa (41–9%).

3.4. Effect of TMP_{sp} on filterability of the suspension

An issue to be considered during the operation at different TMP_{sp} is the propensity to changes in reversible fouling that could

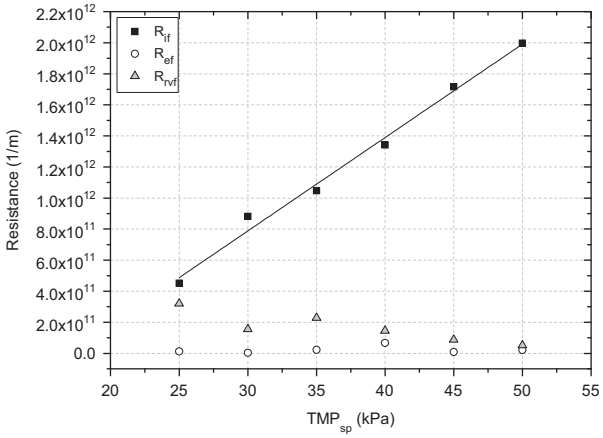

Fig. 7. Fouling resistances against TMP_{sp}; R_{if}: residual internal fouling resistance; R_{ef}: residual external fouling resistance; R_{rvf}: reversible fouling resistance.

be produced. In order to determine in situ the effect of the residual fouling achieved at different TMP_{sp} on critical fluxes, flux step trials were carried out for MBR monitoring. Fig. 8A represents TMP_i as a measure of the initial pressure observed at the beginning of each step, which consistently increased proportionally to TMP_{sp}. Fig. 8B shows the reversible fouling rates ($r_f = dTMP/dt$) against J. An exponential relationship is seem, as reported in many other studies [11,18]. Results also showed an identical critical flux of ~45 L/(h m^2) instead of the TMP_{sp} that might be an indication for the stability of the membrane performance regardless of the residual fouling history. Additionally, the identical trend suggested that particle deposition rate suggested it was not significantly affected by a compression process on the experimental conditions. Apparently, this is contrary to the results of previous studies [38,39]. The difference may be due to the high internal residual fouling levels reached in the present work, which significantly reduced the pressure drop over the cake [37].

3.5. Membrane recovery cleaning

A specific protocol that combines physical and chemical cleaning methods was developed to evaluate the nature of the residual fouling achieved at the end of the 5th period (TMP_{sp}=50 kPa). The remaining resistance after each cleaning step was evaluated by clean water tests (Fig. 9).

The resistance of the fouled membrane was initially measured. It was observed some amount of particulate matter between fibres during the visual inspection (Fig. 10A). This is a frequent operational problem (often cited as "sludging") related to local failure of membrane scouring by aeration and the subsequent dewatering of biomass within the fibres [1,2,40]. Nevertheless, after applying successive steps of physical methods (rinsed and backwashing with Milli-Q water) accompanied both by manual agitation to remove the clogged material, clean water tests revealed that the contribution to the fouled membrane resistance was low (13%) instead of the severe operating conditions imposed.

The recovery chemical cleaning (RC) included 3 sequential steps where membrane was soaked in three solutions: hypochlorite (500 mg/L), citric acid (6000 mg/L) and hypochlorite (500 mg/L). Although conventional RC sequence includes only the first two steps (hypochlorite-citric) [1], it seemed to be insufficient for a proper membrane cleaning (Fig. 10B), and an additional step of hypochlorite soaking was required. This can be attributed to the low hypochlorite concentration used in this case [1,2]. RC removed 79% of fouling resistance with a significant effect of the oxidant

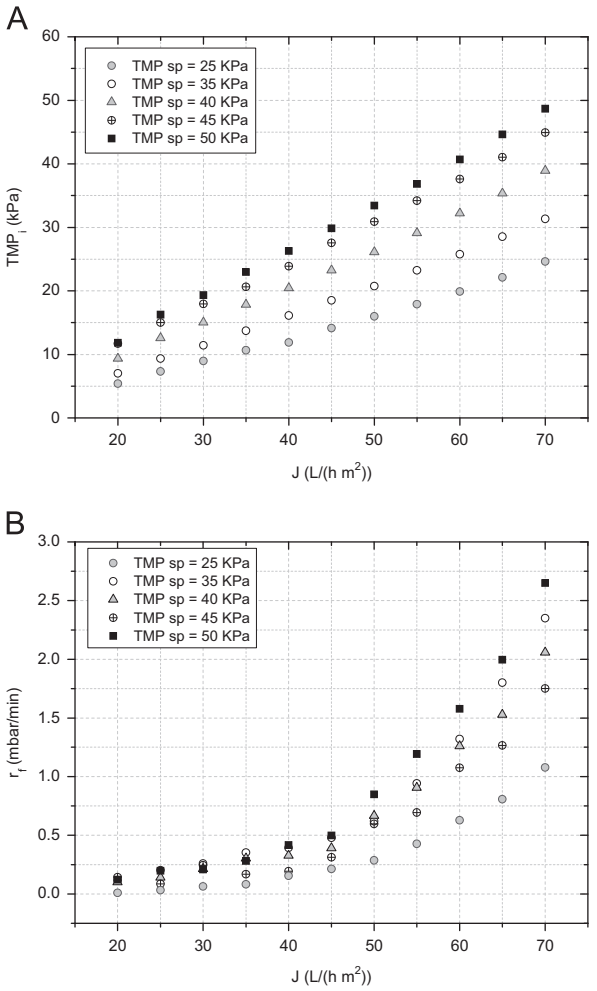

Fig. 8. TMP_i (A) and reversible fouling rate r_f (B) against permeate flux at different TMP_{sp} in the flux-step tests.

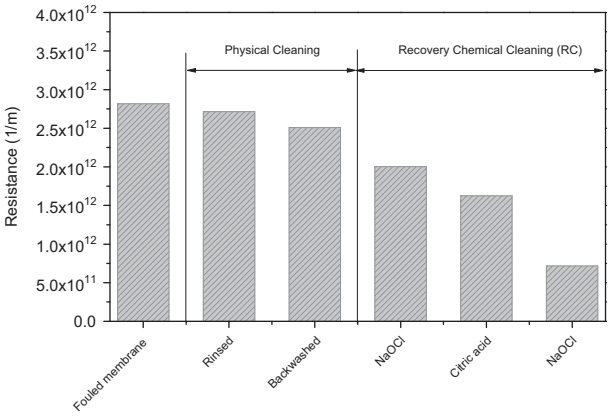

Fig. 9. Evolution of membrane resistance during the cleaning protocol.

agents (Fig. 9). After this cleaning, clean membrane resistance was successfully recovered (Fig. 10C).

4. Conclusions

- The main advantage of this backwashing strategy is that the system automatically adjusts the backwashing interval (i.e. filtration length) to a preselected transmembrane pressure set-point

Fig. 10. Membrane before physical cleaning methods (A), after first RC with hypochlorite (B) and finished the cleaned protocol (C).

(TMP_{sp}), which will determine the degree of membrane fouling allowed. However, high TMP_{sp} values (>40 kPa) during the MBR operation should be avoided in order to maintain competitive process productivity and limit residual fouling development.

- Sustainable process performance was observed at supra-critical permeate flux, with moderate TMP_{sp} (30–40 kPa), providing high permeate net fluxes J_{net} (65–67 L/h m^2). These are significantly higher than that usually obtained in conventional (temporised) operation at critical filtration conditions.
- The reversible fouling rate r_f was not significantly influenced by TMP_{sp}, as observed during in situ flux-steps trials. Therefore, an identical critical flux could be identified ($\sim$45 L/h m^2) as an indicator of the stable membrane performance instead of the residual fouling history.
- The analysis of the relative contribution of each mechanism to the overall fouling showed that the main contribution was the internal residual fouling, increasing its contribution with TMP_{sp}. In contrast, external residual fouling was insignificant and cake layer had only a relevant role at low to moderate TMP_{sp}.
- As a result of carbon substrate limited conditions, the system was successfully operated with complete sludge retention, achieving a high treatment performance with a moderate liquor suspended solid concentration. In these conditions, the soluble microbial products SMP concentration, which is considered to be an important factor affecting residual membrane fouling, was minimised.

Acknowledgements

The control system, funded by the N.R.C. (MINECO project CTM2011-27307), was tested for long-term validation during the MBR operation described in this paper. The authors want to express their gratitude to GE Water & Process Technologies and to BALTEN for their support and also to the Water Analysis Laboratory of the ULL Chemical Engineering Department for its analytical advice. In addition, we greatly appreciate the access to multi-parameter universal controller by CONVAGUA project of the Canary Agency-ACIISI sponsored by the ERDF Programme-European Commission and the Regional Canary Government.

Nomenclature

$(R_{rdf})_{ave}$	average residual fouling resistance, L/m
$(t_F)_{ave}$	average filtration phase duration, min
$(J_{net})_{ave}$	average net permeate flux, L/(h m^2)
COD	chemical oxygen demand, mg/L
ΔTMP	differential of transmembrane pressure associated with external residual fouling, kPa
d_{50}	median particle size, μm
DOC	dissolved organic carbon, mg/L
HRT	hydraulic retention time, h
J	filtrate flux, L/(h m^2)
J_B	backwashing flux, L/(h m^2)
J_{net}	net permeate flux, L/(h m^2)
MBR	membrane bioreactor
MLSS	mixed liquor total suspended solids, mg/L
MLVSS	mixed liquor volatile suspended solids, mg/L
$N–NH_3$	ammonium–nitrogen, mg/L
$N–NO_2^-$	nitrite–nitrogen, mg/L
$N–NO_3^-$	nitrate–nitrogen, mg/L
PSD	particle size distribution
RC	recovery chemical cleaning

R_{ef}	external residual fouling resistance, L/m
r_f	fouling rate, mbar/min
R_{if}	internal residual fouling resistance, L/m
R_m	clean membrane resistance, L/m
R_{rdf}	residual fouling resistance, L/m
R_{rvf}	reversible fouling resistance, L/m
R_{sp}	hydraulic resistance before the backwashing, L/m
R_t	total hydraulic resistance, L/m
SAD_{mnet}	specific net aeration demand with respect to membrane area, N m^3/h m^2
SAD_{pnet}	specific net aeration demand with respect to permeate volume, N m^3/m^3
SMP	soluble microbial products
t	elapsed time, s
t_B	backwashing phase duration, s
t_F	filtration phase duration, min
TMP	transmembrane pressure, kPa
TMP_0	transmembrane pressure associated with residual fouling, kPa
TMP_{ef}	transmembrane pressure associated with the external fouling, kPa
TMP_i	transmembrane pressure after backwashing, kPa
TMP_{sp}	transmembrane pressure set-point, kPa
TSS	total suspended solids, mg/L
TTF	time-to-filter, s

Greek letters

$(\eta)_{ave}$	average backwashing efficiency, %
η	backwashing efficiency, %
μ	permeate viscosity, Pa s

References

[1] S. Judd, The MBR Book, Principles and Applications of Membrane Bioreactors for Water and Wastewater Treatment, 2nd edition, Elsevier, Great Britain, 2010.
[2] S. Judd, The status of membrane bioreactor technology, Trends Biotechnol. 26 (2007) 165–171.
[3] A. Santos, S. Judd, The commercial status of membrane bioreactor for municipal wastewater, Sep. Sci. Technol. 45 (2010) 850–857.
[4] Icon Group Publications, The 2009–2014 World Outlook for Membrane Bioreactor (MBR) Systems for Wastewater Treatment, 2008.
[5] B. Verrecht, S. Judd, G. Guglielmi, J.W. Mulder, C. Brepols, An aeration energy model for an immersed membrane bioreactor, Water Res. 42 (2008) 4761–4770.
[6] H. Lin, F. Wang, L. Ding, H. Hong, J. Chen, X. Lu, Enhanced performance of a submerged membrane bioreactor with powdered activated carbon addition for municipal secondary effluent treatment, J. Hazard. Mater. 192 (2011) 1509–1514.
[7] S. Delgado, R. Villarroel, E. González, Submerged membrane bioreactor at substrate-limited conditions: activity and biomass characteristics, Water Environ. Res. 82 (2010) 202–208.
[8] J. Wu, P. Le-Clech, R.M. Stuetz, A.G. Fane, V. Chen, Effects of relaxation and backwashing conditions on fouling in membrane bioreactor, J. Membr. Sci. 324 (2008) 26–32.
[9] K.J. Hwang, C.S. Chan, K.L. Tung, Effect of backwash on the performance of submerged membrane filtration, J. Membr. Sci. 330 (2009) 349–356.
[10] P. Le-Clech, V. Chen, A.G. Fane, Fouling in membrane bioreactors used in wastewater treatment, J. Membr. Sci. 284 (2006) 17–53.
[11] T. Zsirai, P. Buzatu, P. Aerts, S. Judd, Efficacy of relaxation, backflushing, chemical cleaning and clogging removal for an immersed hollow fibre membrane bioreactor, Water Res. 46 (2012) 4499–4507.
[12] G. Ferrero, I. Rodríguez-Roda, J. Comas, Automatic control systems for submerged membrane bioreactors: a state-of-the-art review, Water Res. 46 (2012) 3421–3433.
[13] J. Busch, W. Marquardt, Model-based control of MF/UF filtration processes: pilot plant implementation and results, Water Sci. Technol. 59 (2009) 1713–1720.
[14] P.J. Smith, S. Vigneswaran, H.H. Ngo, R. Ben-Aim, H. Nguyen, A new approach to backwash initiation in membrane systems, J. Membr. Sci. 278 (2006) 381–389.
[15] A. Vargas, I. Moreno-Andrade, G. Buitrón, Controlled backwashing in a membrane sequencing batch reactor used for toxic wastewater treatment, J. Membr. Sci. 320 (2008) 185–190.
[16] R. Villarroel, S. Delgado, E. González, M. Morales, Physical cleaning initiation controlled by transmembrane pressure set-point in a submerged membrane bioreactor, Sep. Purif. Technol. 104 (2013) 55–63.
[17] L. Vera, E. González, O. Díaz, S. Delgado, Performance of a tertiary submerged membrane bioreactor operated at supra-critical fluxes, J. Membr. Sci. 457 (2014) 1–8. http://dx.doi.org/10.1016/j.memsci.2014.01.027.
[18] P. Le-Clech, B. Jefferson, I. Chang, S. Judd, Critical flux determination by the flux-step method in a submerged membrane bioreactor, J. Membr. Sci. 227 (2003) 83–91.
[19] P. Van der Marel, A. Zwijnenburg, A. Kemperman, M. Wessling, H. Temmink, W. van der Meer, An improved flux-step method to determine the critical flux and the critical flux for irreversibility in a membrane bioreactor, J. Membr. Sci. 332 (2009) 24–29.
[20] G. Guglielmi, D. Chiarani, S.J. Judd, G. Andreottola, Flux criticality and sustainability in a hollow fibre submerged membrane bioreactor for municipal wastewater treatment, J. Membr. Sci. 289 (2007) 241–248.
[21] T. Jiang, M.D. Kennedy, W.G.J. Van der Meer, P.A. Vanrolleghem, J.C. Schippers, The role of blocking and cake filtration in MBR fouling, Desalination 157 (2003) 335–343.
[22] E.J. McAdam, S.J. Judd, Optimisation of dead-end filtration conditions for an immersed anoxic membrane bioreactor, J. Membr. Sci. 325 (2008) 940–946.
[23] V. Diez, D. Ezquerra, J.L. Cabezas, A. García, C. Ramos, A modified method for evaluation of critical flux, fouling rate and in situ determination of resistance and compressibility in MBR under different fouling conditions, J. Membr. Sci. 453 (2014) 1–11.
[24] F. Meng, S.-R. Chae, A. Drews, M. Kraume, H.-S. Shin, F. Yang, Recent advances in membrane bioreactors (MBRs): membrane fouling and membrane material, Water Res. 43 (2009) 1489–1512.
[25] S. Delgado, R. Villarroel, E. González, Effect of the shear intensity on fouling in submerged membrane bioreactor for wastewater treatment, J. Membr. Sci. 311 (2008) 173–181.
[26] A. Drews, Membrane fouling in membrane bioreactors – characterisation, contradictions, causes and cures, J. Membr. Sci. 363 (2010) 1–28.
[27] D. Jeison, J.B. van Lier, Cake formation and consolidation: main factors governing the applicable flux in anaerobic submerged membrane bioreactors (AnSMBR) treating acidified wastewaters, Sep. Purif. Technol. 56 (2007) 71–78.
[28] American Public Health Association/Water Environment Federation, Standard Methods for the examination of Water and Wastewater, 21st ed., , 2005.
[29] H. Ng, S. Hermanowicz, Membrane bioreactor operation at short solids retention times: performance and biomass characteristics, Water Res. 39 (2005) 981–992.
[30] S. Pirt, The maintenance energy of bacteria in growing cultures, Proc. R. Soc. Lond. 163B (1965) 224–231.
[31] S.G. Lu, T. Imai, M. Ukita, M. Sekine, T. Higuchi, M. Fukagawa, A model for membrane bioreactor process based on the concept of formation and degradation of soluble microbial products, Water Res. 35 (2001) 2038–2048.
[32] Y. Wei, R. van Houten, A. Borger, D.H. Eikelboom, Y. Fan, Minimization of excess sludge production for biological wastewater treatment, Water Res. 37 (2003) 4453–4467.
[33] Y. Ye, V. Chen, P. Le-Clech, Evolution of fouling deposition and removal on hollow fibre membrane during filtration with periodical backwash, Desalination 283 (2011) 198–205.
[34] P. Schoeberl, M. Brik, M. Bertoni, R. Braun, W. Fuchs, Optimization of operational parameters for a submerged membrane bioreactor treating dyehouse wastewater, Sep. Purif. Technol. 44 (2005) 61–68.
[35] P. Gui, X. Huang, Y. Chen, Y. Qian, Effect of operational parameters on sludge accumulation on membrane surfaces in a submerged membrane bioreactor, Desalination 151 (2003) 185–194.
[36] V. Kuberkar, R. Davis, Modeling of fouling reduction by secondary membranes, J. Membr. Sci. 168 (2000) 243–258.
[37] M.K. Jørgensen, T.V. Bugge, M.L. Christensen, K. Keiding, Modeling approach to determine cake buildup and compression in a high-shear membrane bioreactor, J. Membr. Sci. 409–410 (2012) 335–345.
[38] A. Robles, M.V. Ruano, J. Ribes, A. Seco, J. Ferrer, Mathematical modeling of filtration in submerged anaerobic MBRs (SanMBRs): long-term validation, J. Membr. Sci. 446 (2013) 303–309.
[39] T.V. Bugge, K. Jørgensen, M.L. Christensen, K. Keiding, Modeling cake buildup under TMP-step filtration in a membrane bioreactor: cake compressibility is significant, Water Res. 46 (2012) 4330–4338.
[40] B. Lesjean, A. Tazi-Pain, D. Thaure, H. Moeslang, H. Buisson, Ten persistent myths and the realities of membrane bioreactor technology for municipal applications, Water Sci. Technol. 63 (2011) 32–39.

ANEXO E: Fouling analysis of a tertiary submerged membrane bioreactor operated in dead-end mode at high-fluxes

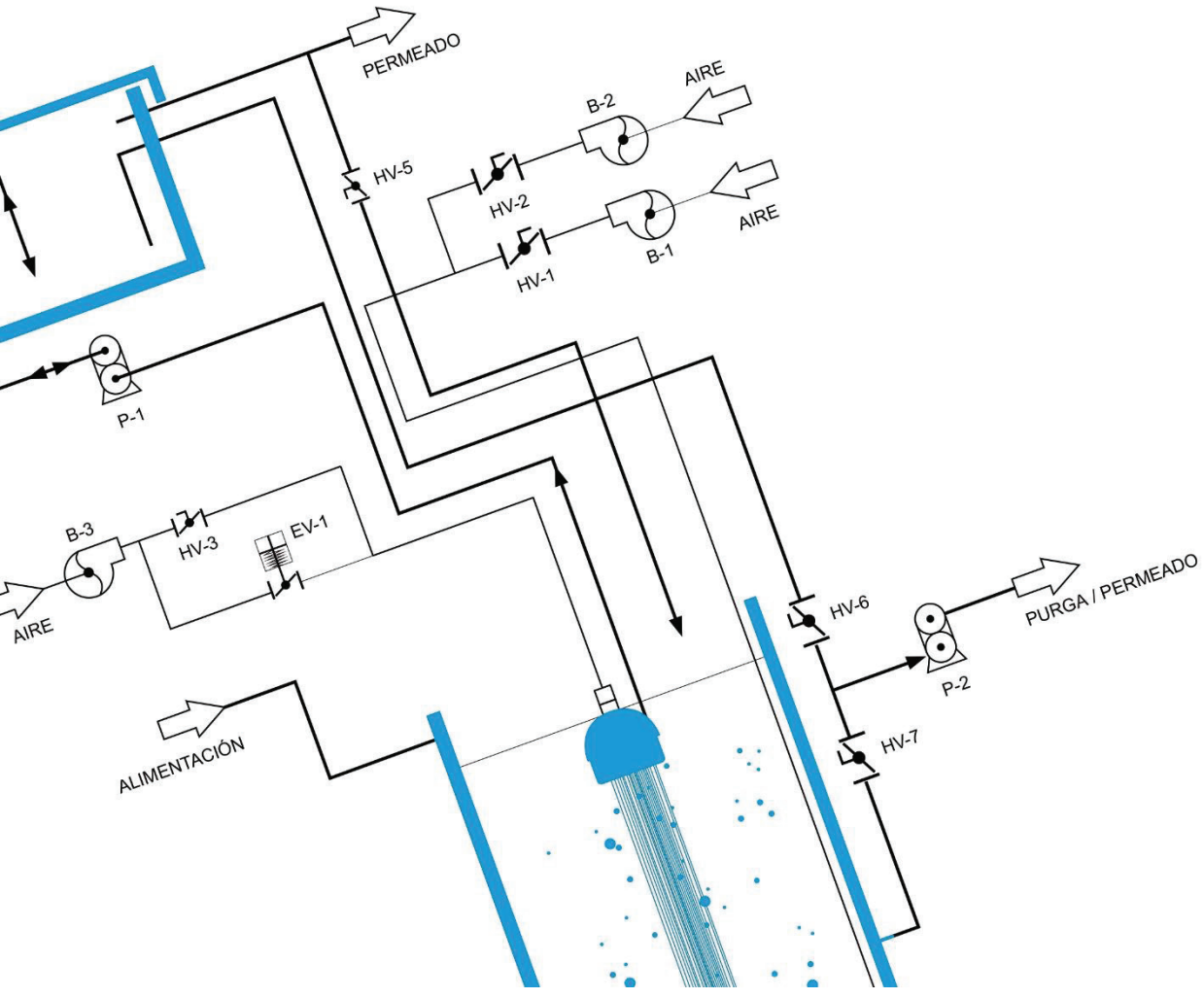

Journal of Membrane Science 493 (2015) 8–18

Contents lists available at ScienceDirect

Journal of Membrane Science

journal homepage: www.elsevier.com/locate/memsci

Fouling analysis of a tertiary submerged membrane bioreactor operated in dead-end mode at high-fluxes

Luisa Vera*, Enrique González, Oliver Díaz, Rubén Sánchez, Rafael Bohorque, Juan Rodríguez-Sevilla

Departamento de Ingeniería Química, Facultad de Ciencias- Sección de Química, Universidad de La Laguna, Av. Astrof. Fco. Sánchez s/n. 38200, La Laguna, Spain

ARTICLE INFO

Article history:
Received 5 March 2015
Received in revised form
4 June 2015
Accepted 8 June 2015
Available online 23 June 2015

Keywords:
Submerged membrane bioreactor
Tertiary treatment
Set-point transmembrane pressure
Filtration without air scouring
Empirical model of residual fouling

ABSTRACT

Fouling deposition, consolidation and reversibility were assessed in a tertiary submerged membrane bioreactor. The unit was operated in dead-end mode (i.e. without air scouring during the filtration) and with an alternative physical cleaning strategy based on *TMP* set-point initiation. Several operating parameters such as filtration and backwashing fluxes, backwash duration and the aid of air scouring during backwashing were studied. The aim of the work was to optimise membrane productivity, specific aeration demand and operative time between chemical cleanings. The membrane bioreactor was operated for over 4 months with complete sludge retention, achieving a high treatment performance with moderate suspended solids concentration (MLSS=4–8 g/L). Flux-step trials pointed to the important role of the compression process and backwashing conditions in membrane fouling reversibility. During long-term tests, while reversible fouling was described by the compressible cake build-up model, residual fouling was modelled by a non-linear expression, assuming that fouling gradually reduces the available membrane area. Based on this approach, residual fouling consistently decreased with the backwashing flux applied. Analysis of the relative contribution of the different fouling layers revealed that the fraction formed by suspended solids was the main contributor. According to the residual fouling model, optimal membrane production can be established at a filtration flux of 40 L/h m^2 and a backwashing flux of 27.5 L/h m^2, due to the low specific energy demand, low membrane area requirement and reasonable operative time (t_{op}) between chemical cleanings.

1. Introduction

Growing worldwide water supply demands and the protection of water bodies have both increased the interest in wastewater reclamation. Legislation affecting reclaimed wastewater reuse is very demanding regarding quality and health safety, which has required the application of advanced technology. Among such techniques, the use of membranes emerges as a highly efficient system to obtain high quality recycled water. In fact, low-pressure membrane filtration (microfiltration or ultrafiltration) of biologically degraded secondary effluents has been widely applied for upgrading conventional wastewater treatment plants [1]. However, in the case of old plants with poor performance of secondary clarifiers which often leads to sludge bulking, the relatively high concentration of suspended solids in secondary effluents can compromise the economic feasibility of the membrane filtration processes [2]. In this scenario, a tertiary submerged membrane bioreactor (MBR) appears to be an attractive option for advanced treatment of secondary effluent. As described in previous research [3], the tertiary MBR has demonstrated its capability of achieving high organic carbon removal and complete nitrification, regardless of high variability in the feedwater. As a consequence of the substrate-limited conditions, the microbial suspension generated in the bioreactor has suitable filtration properties (i.e. large flocs, presence of higher organisms and a low concentration of soluble microbial products). The growing interest in this technology is to be seen recently in the Aquapolo project (Sao Paulo, Brazil), the largest wastewater reuse project in the Southern Hemisphere, which includes a tertiary MBR in the treatment scheme [4].

As in all membrane processes, fouling is still the main drawback of MBRs, preventing wide application [5]. Fouling can be defined as the alteration in the membrane caused by specific physical and/or chemical interactions between the membrane and the components of the microbial suspension, which leads to membrane permeability loss. The rate and extent of fouling is typically a complex function of membrane properties, operating

* Corresponding author. Tel.: +34 922318054; fax: +34 922318014.
E-mail address: luvera@ull.es (L. Vera).

http://dx.doi.org/10.1016/j.memsci.2015.06.014
0376-7388/

conditions and microbial suspension characteristics [6]. Microbial suspension is a heterogeneous system mainly composed of salts, organic substances, colloids, cells and microbial flocs. Several mechanisms have been proposed to explain this complex phenomenon, including pore clogging, adsorption of foulants, gel or cake formation, cake layer consolidation and osmotic pressure effects [7].

In order to maintain membrane permeability, strategies for fouling mitigation such as air scouring, physical cleaning techniques (i.e. relaxation and backwashing) and chemical cleaning have been incorporated into MBR designs [5]. Based on permeability recovery by physical means, membrane fouling can be classified into two main types. The first one is known as reversible fouling (caused by loose cake deposit and possibly by pore clogging) and refers to fouling which can be removed by physical means. The second type is residual fouling, which is related to foulant adsorption, gel formation, and possibly consolidated cake deposition, and can only be removed by chemical cleaning [8].

In spite of the significant impact of fouling on membrane productivity, module lifespan and energy requirements [8], strategies for fouling control are usually based on predetermined values of the operating parameters (air scouring flow-rate and frequency, and filtration/physical cleaning sequences), which lead to an under-optimised system [5]. Air scouring has been extensively proven to be an efficient means to limit foulant deposition due to the enhancement of foulant back-transport, the shear stress induced at the membrane surface and the lateral fibre movement (in hollow fibre modules) [10]. Because of its impact on energy demand, several strategies have been implemented, mainly focused on adjusting flow rate and/or frequency of coarse air bubbles [11]. Typically, it takes a value of 12–13 Nm^3/m^3, expressed as specific aeration demand per permeate volume unit (SAD_p), for full-scale facilities [12]. Also, pulse scouring with large bubbles was recently introduced as a means to increase scouring efficiency [13]. However, air scouring is still considered the greatest energy consumer in these processes, often exceeding 50% of total energy consumption [12]. Therefore, the priority is to explore operation modes with lower energy consumption. An alternative approach could be to operate in dead-end filtration mode (i.e. without air scouring). In that case, due to absence of shear forces, foulants back-transport is significantly decreased (by ceasing the transport mechanisms of lateral migration and shear induced diffusion) and consequently, net foulants transport towards the membrane is increased. Hence, to maintain a sustainable process operation at reasonable fouling rate, filtration flux should be decreased and frequent physical cleanings should be applied. This disadvantage must be compensated by alternative physical cleaning strategies, as it is discussed below.

Conventional physical cleaning techniques include backwashing (i.e. permeate is used to flush backwards) or relaxation (ceasing filtration whilst continuing air scouring). For both methods, the key parameters generally identified are frequency and duration [6]. Additionally, another parameter influencing cleaning efficiency of backwashing is its intensity, which typically ranges between 1 and 3 times the filtration flux [14]. According to several studies of backwashing, a higher cleaning efficiency is observed with increasing backwashing flux, frequency and duration [15]. Nevertheless, given the impact of these parameters on process productivity, optimisation of backwashing conditions is still needed [16]. In this direction, a recent review study has highlighted the variety of operating trends. This is attributable to the fact that selection of appropriate cleaning protocols for a sustainable operation depends on other process variables (i.e. filtration flux, air scouring, temperature, etc.) and suspension filterability [14]. As a consequence, pre-set values of these parameters are often selected in full-scale plants [15], where the operating trend is to perform a very frequent backwashing cycle (once every 3.3–8.3 min of filtration) [17]. In recent years, several feedback control systems have been developed for physical cleaning optimisation [11]. Among them, a system has been successfully implemented for physical cleaning initiation through transmembrane pressure (*TMP*) monitoring. This automatically adjusts the backwashing frequency to a preselected *TMP* set-point, which results in a significant increase in process productivity [18]. Additionally, by selecting a moderate *TMP* set-point (30–40 kPa), effective fouling control has been achieved, allowing operation under less conservative conditions (supra-critical fluxes) [3,19].

As previously stated, dead-end operation could be an attractive option due to its lower energy demand. In fact, it has been widely used in direct ultrafiltration of secondary effluents [20]. Nevertheless, the higher quantity of suspended solids in the MBR (several orders of magnitude higher than that of a secondary effluent) significantly increases the fouling rate and limits its applicability. However, fouling rate not only depends on cake solids concentration (ω) but also on the specific cake resistance (α), which is determined by the geometrical properties of the deposit (porosity, particle diameter, etc.) [21]. Recent studies have reported significantly lower values of α for cake layers formed by microbial flocs (10^{12}–10^{13} m/kg) than that (10^{14} m/kg) obtained for gel layers mainly composed of soluble microbial products (SMP), which are considered the most important foulant in secondary effluents [22]. Therefore, highly porous aggregates with low resistances are expected to form during the filtration without air scouring of a microbial suspension. In addition, the cake layer may act as a secondary membrane that prevents residual fouling caused by pore blocking or adsorption due to SMP [23]. Another issue to be considered is the deposit reversibility, since it is known that increasing the fouling load on the membrane reduces the removal efficiency. In general, it is expected that high filtration *TMP* results in a more compact cake layer, harder to remove by physical cleaning [24]. Nevertheless, cake compressibility also depends on other factors including particle characteristics (morphology, size, etc.) and hydrodynamics of cake formation process. Accordingly, although physical cleaning strategy based on the *TMP* set-point seems to be a suitable approach to reduce residual fouling, the optimal value of TMP_{sp} is site specific. Therefore, for a given system, it is necessary an experimental evaluation of the effect of TMP_{sp} on fouling consolidation and reversibility.

The aim of this study was to investigate fouling deposition, its consolidation and reversibility in a tertiary submerged membrane bioreactor operating in dead-end mode (i.e. filtration without air scouring) during long-term trials. An alternative physical cleaning strategy based on *TMP* set-point initiation was applied. Several operating parameters such as filtration and backwashing fluxes, backwashing duration and the aid of air scouring during the backwashing were studied in order to optimise membrane productivity and the specific energy demand.

2. Material and methods

2.1. Feedwater

The pilot MBR was fed with effluent from a conventional activated sludge wastewater treatment plant whose average physico-chemical characteristics are given in Table 1. The conventional WWTP was originally designed for only carbon removal. Due to the short sludge ages and oxygen deficiency in the activated sludge process, frequent episodes of sludge de-flocculation or insufficient sedimentation usually appear, resulting in higher suspended solids and organic material concentration in the effluent.

Table 1
Main feedwater characteristics ($n=54$).

Parameters	Units	Mean	Range
COD	mg/L	230	50–770
DOC	mg/L	20	11–39
$N-NH_3$	mg/L	37	16–57
$N-NO_2^-$	mg/L	2	<1–13
$N-NO_3^-$	mg/L	2	<1–4
Turbidity	NTU	137	6–1100
TSS	mg/L	190	20–1530

2.2. MBR

The pilot plant was the same as in previous studies [3,19], where a cylindrical 220 L MBR was equipped with ZeeWeed® ZW-10 (GE Water & Process Technologies) hollow-fibre membranes with 0.04 μm rated pore diameter and 1.9 mm outer diameter, assembled vertically, which provide 0.9 m^2 of filtering surface area. ZeeWeed® consists of a woven reinforcing braid on which a PVDF membrane is cast. The effluent (permeate) was extracted from the top header of the module under a slight vacuum. All experiments were carried out at a constant permeate flux, registering transmembrane pressure as a function of time. The unit was operated in automatic cleaning initiated mode. Membrane fouling was controlled by backwashing based on this mode. Each filtration phase finished when a pre-established TMP_{sp} was reached (30 kPa), beginning the backwashing immediately afterwards. A programmable logic controller (PLC) system was used to initiate and stop the backwashing by comparison of *TMP* set-point and instantaneous pressure values. Continuous data logging and plotting of pressure profile variations were also performed.

The MBR was operated without air scouring during the filtration phase. Nevertheless, constant air scouring during the backwashing phase was fixed at 3.1 $Nm^3/h\ m^2$, on the basis of previous results [3], in order to improve fouling removal. The aim of the experiments was to assess the effect of filtration and backwashing flux on membrane fouling. For this purpose, twelve filtration tests of 250 h were carried out at different filtration fluxes (35, 45 and 55 L/h m^2) and backwashing fluxes (0, 20, 40 and 60 L/h m^2).

Before starting the experimental period, the pilot-scale MBR was seeded with sludge from the activated sludge reactor of the WWTP and operated for over 24 months. The bioreactor was run at HRT values of 8.8 h without sludge removal except for sampling. In order to maintain a constant HRT independent of the permeate flux, a fraction of permeate was returned to the tank. Additional air was supplied by fine bubble diffusers through the bottom (0.3 Nm^3/h), providing oxygen and stirring. The dissolved oxygen concentration was always above 1.5 mg/L in the reactor operated at 296 ± 2 °K °C. Suspensions were characterised according to particle size, MLSS, MLVSS, biomass activity, non-flocculating microorganisms [25] and dissolved organic matter in the liquid phase.

2.3. Short-term flux step trials

The modified flux-step method is based on applying successive flux increments up to a maximum, in accordance with the method of Le-Clech et al. [26] and further improved by incorporating relaxation steps for reducing the influence of fouling history [27]. In this study, a modified method is proposed and the relaxation steps are substituted by short backwashing cycles at a fixed flux value of 60 L/h m^2, to be more similar to the conventional operation of a MBR. Six flux step experiments were carried out at three backwashing times (15, 30 and 60 s) with and without air scouring at 3.1 $Nm^3/h\ m^2$ during the backwashing phase. The other experimental parameters were selected in accordance with previous studies [27,28]: step duration of 15 min, flux-step height of 5 L/h m^2 and a maximum flux of 70 L/h m^2. In the flux-step trials, residual fouling can be characterized by the transmembrane pressure after each backwashing (TMP_i). A critical flux value can be established when TMP_i starts to raise respect to the tap water behaviour (Fig. 1).

2.4. Membrane cleaning protocol

After each long-term test, the fouled membrane was cleaned by a specific protocol that included the following steps: (1) rinsing with Milli-Q water; (2) backwashing with Milli-Q water at a flux of 90 L/(h m^2) for 7 min and with air scouring; (3) chemical cleaning with a solution of NaOH (pH ≈ 11) for 24 h; (4) chemical cleaning with sodium hypochlorite (500 mg/L) for 24 h. After each step, a tap water filtration test was applied to measure the remaining resistance. The resulting solutions after rinsing, backwashing and desorption were collected and analysed in terms of dissolved organic carbon (DOC) and total suspended solids (TSS).

2.5. Analytical methods

Dissolved oxygen was measured using a portable dissolve oxygen meter (Oxi340i, WTW). Chemical oxygen demand (COD), total suspended solids (TSS), mixed liquor suspended solids (MLSS), mixed liquor volatile suspended solids (MLVSS), time to filter (TTF) and turbidity were determined in conformity with the Standard Methods [29]. Nitrite – nitrogen ($N-NO_2^-$) and nitrate – nitrogen ($N-NO_3^-$) were analysed by ion chromatography using a Compact IC plus 882 device supplied by Metrohm. Ammonium – nitrogen ($N-NH_3$) was analysed by the Nessler method using a DR-5000 Hach spectrophotometer. Dissolved organic carbon (DOC) concentration was measured with a TOC-meter (TOC-5000A, Shimadzu). The DOC concentration of the filtration suspension through a 0.45 μm nitrocellulose membrane filter (HA, Millipore) was assigned as the soluble microbial products (SMP). The oxygen uptake rate (SOUR) was measured in batch tests (250 ml stirred cells) by following the dissolved concentration with a membrane oxygen electrode, in a medium without substrate. Microbial floc size distribution was measured using a Malvern Mastersizer 2000 instrument with a detection range of 0.02–2000 μm. To quantify the amount of non-flocculating microorganisms, the samples of biomass were centrifuged at 1300 g for 2 min and the supernatant turbidity measured [25].

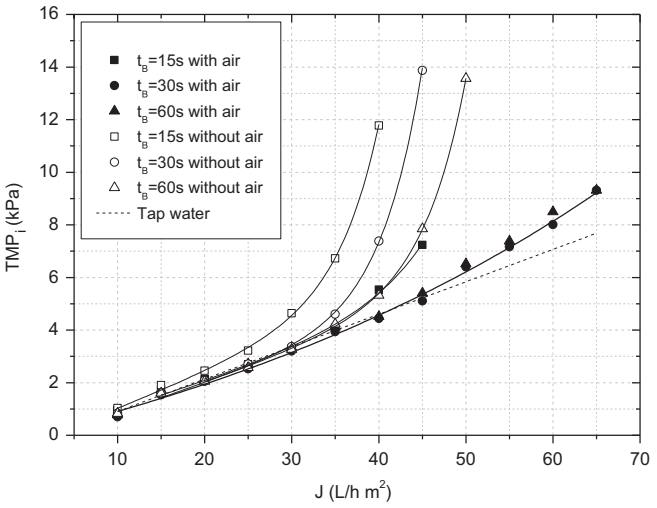

Fig. 1. TMP_i against permeate flux at different backwash conditions during the flux steps trials; $J_B=60$ L/h m^2; $t_F=$ 900 s.

2.6. Membrane fouling characterisation

TMP evolution can be used for membrane fouling characterisation. According to the "resistance-in-series" model and neglecting the osmotic pressure term, the *TMP* can be described by:

$$TMP = J \cdot \mu \cdot R_t = J \cdot \mu \cdot (R_m + R_{rdf} + R_{rvf}) \quad (1)$$

where μ is the permeate viscosity, J is the permeate flux, R_t is the total hydraulic resistance, R_m is the clean membrane resistance, R_{rdf} is the residual fouling resistance and R_{rvf} is the reversible fouling resistance.

Residual fouling is that which is not removed by backwashing. Its resistance can be separated into internal fouling resistance (R_{if}), related to internal membrane pore blocking and gel or compacted particle layer that is not detached during backwashing [30], and an external fouling resistance (R_{ef}), linked to fouling layer recompression:

$$R_{rdf} = R_{if} + R_{ef} \quad (2)$$

During the filtration, this external layer compresses, increasing the residual resistance, and during backwashing this layer relaxes, yielding a lower residual resistance. Therefore, just at the beginning of the filtration cycle, the initial *TMP* (TMP_i) can be described by Eq. (3):

$$TMP_i = J \cdot \mu \cdot (R_m + R_{if}) \quad (3)$$

In contrast, reversible fouling resistance R_{rvf} is generally associated with a cake development mechanism on the membrane wall [19]. According to the cake model, *TMP* linearly increases with filtration time and the slope of the straight line. Therefore, *TMP* evolution with elapsed time t can be described by Eq. (4):

$$TMP = TMP_0 + \mu\alpha\omega J^2 t \quad (4)$$

where TMP_0 is the transmembrane pressure related to the residual fouling, α is the specific cake resistance, ω is the solid concentration in the cake per unit filtrate volume and t *is* the elapsed time. TMP_0 can be defined as

$$TMP_0 = J \cdot \mu \cdot (R_m + R_{rdf}) \quad (5)$$

and the difference between TMP_i and TMP_0 is linked to the external residual fouling, R_{ef}.

By considering the pressure drop over the cake layer (ΔTMP_c), Eq. (4) can be rewritten as Eq. (6) [31]:

$$\Delta TMP_c = \mu\alpha\omega J^2 t \quad (6)$$

For compressible particles, α increases with *TMP*. To model it, several expressions have been proposed, including the well-known power-law expression [32]. While this expression has been found that generally represents accurately the pressure dependence of the specific resistance for most particles, its application to microbial suspensions has proved to be problematic [21]. Alternatively, a linear relationship (Eq. (7)) has often been identified for compressible cakes when filtering microbial suspensions [33]:

$$\alpha = \alpha_0 \left(1 + \frac{\Delta TMP_c}{P_a}\right) \quad (7)$$

where α_0 is the specific cake resistance at zero pressure and P_a is a characteristic pressure related to the compression effect, which usually ranges between 10 and 60 kPa for a MBR sludge, according to the studies of Jørgensen et al. [34,35,36].

On the other hand, the consolidation process induced a progressive decrease in the available membrane area for filtration. Assuming the stationary conditions were reached after 200 h operation, the local flux $(J')_{t=200}$ increased accordingly with the loss of effective area by residual fouling (Eq. (8)):

$$(J')_{t=200} = \frac{(TMP_i)_{t=200}}{TMP_i} J \quad (8)$$

where $(TMP_i)_{t=200}$ is the *TMP* at the beginning of the filtration cycle after 200 h of operation.

3. Results and discussion

3.1. Microbial suspension characteristics and permeate quality

The bioreactor treatment performance and main characteristics of the microbial suspension are summarised in Table 2. As expected, complete nitrification (98%) and high organic material removal (87% on average for COD) were obtained throughout the experimental period, regardless of fluctuations in feedwater characteristics (see Table 1). Nevertheless, there were several episodes of high particulate organic load in the feedwater, which generated relatively high F/M ratios (> 0.4 kg COD/kg MLSS d). These resulted in a sharp biomass increase (up to 8–8.6 g MLSS/L), since the system was operated with total sludge retention. Instead of these episodes, the system was able to assimilate these fluctuations obtaining a moderate concentration of biomass (6.2 g MLSS/L on average). Low accumulation of inorganic particulate matter was also found, since the MLVSS/MLSS ratio remained within the typical range of 77–89%. It is known that the biomass stabilisation achieved in MBRs operated without biomass purge is related to the "maintenance concept" introduced by Pirt [37], where microorganisms under severe substrate limitation should preferentially meet their maintenance energy requirements instead of producing additional biomass [38]. Maintenance conditions were also reflected by the low specific oxygen uptake rates ($SOUR_e$) obtained; significantly lower than the typical values of 20–40 mg O_2/g MLVSS h for a municipal activated sludge [39]. In addition, due to the maintenance level, the soluble microbial products (SMP) were minimised in the supernatant (9 mg/L, expressed as equivalent DOC [40]), consistently with previous studies [3]. Therefore, membrane fouling is expected to be mainly caused by suspended particles, and consequently soluble products should not play an important role. This is a key issue, since it is generally accepted that SMPs cause residual fouling by entering into the membrane

Table 2
Bioreactor treatment performance and main characteristics of microbial suspension.

Parameter	Unit	Mean value	Range
Bioreactor treatment performance			
COD removal	%	87	78–98[a]
$N-NH_3$ removal	%	98	94–99[a]
DOC removal	%	60	58–81[a]
Permeate *DOC*	mg/L	8	4–12[a]
Suspension characterisation			
MLSS	g/L	6.2	3.9–8.6[a]
MLVSS	g/L	5.3	3.1–7.4[a]
TTF	s	8.9	3.7–14[b]
PSD			
d_{10}	μm	20	18–22[c]
d_{50}	μm	63	55–68[c]
d_{90}	μm	183	137–204[c]
$SOUR_e$	mg O_2/g MLVSS h	1.51	0.92–2.03[b]
Supernatant turbidity	NTU	27	14–45[b]
Supernatant *DOC*[d]	mg/L	9	5–15[a]

[a] $n=54$.
[b] $n=18$.
[c] $n=12$.
[d] Samples were filtered through microfibre with a 0.45 μm nominal pore size.

pores (i.e. pore blockage) or adsorbing onto the membrane surface [7,8]. In fact, by comparing supernatant and permeate SMP concentrations, it was seen that the membrane only retained a low fraction of the SMP (11% on average).

Regarding floc morphology, medium-sized flocs were observed ($d_{50}=63\pm6$ μm) with a relatively narrow distribution (distribution spreading index of 1.29 ± 0.13). Several authors have reported that suspensions with a narrow distribution of flocs tended to form cakes with high porosity and a low specific cake resistance [41]. In addition, non-flocculating particles in the 1–10 μm range only account for 4.5% of total sludge volume, which was also confirmed by the low values of supernatant turbidity observed [25]. This can be partially attributed to the presence of higher organisms which predate on dispersed bacteria, according to previous studies [19]. Therefore, the suspension showed an excellent filterability (TTF$=8.9\pm2.9$ s).

3.2. Determination of critical flux for residual fouling: effect of backwash time and air scouring during backwash

Although the classical concept of critical flux for residual fouling is based on a mass balance between convection and diffusion transport, which leads to the formation of a residual deposit in cross-flow conditions [9], the same phenomenon can be applied to the filtration without air scouring and backwashing. In these conditions, the critical flux for residual fouling is assumed to be related to the total mass deposited and the backwashing conditions imposed. In addition, the compression process, which depends on the *TMP* applied, can result in more cohesive deposits that affect fouling reversibility [34].

Fig. 2 shows the typical flux and *TMP* profiles during a short-term trial for critical flux determination. As it shows, at the end of each filtration step a backwash was applied ($J_B=60$ L/h m^2 and $t_B=30$ s). The slope of the *TMP* against time (d*TMP*/d*t*) at each step represents the fouling rate due to fouling deposition, similar to that reported in many other studies [15,26]. For the test shown in Fig. 2 ($J_B=60$ L/h m^2 and $t_B=30$ s), different *TMP* profiles during the filtration steps can be observed below and above a critical flux, which can be identified at 40–45 L/h m^2. At sub-critical fluxes, constant and low fouling rates were obtained, while at supra-critical fluxes the fouling rate continuously increased with the elapsed time during each filtration step. Therefore it is evident that under these conditions, fouling not only depends on deposition rate (i.e. on filtration flux), but also on the mass previously deposited (filtration time) and on the actual *TMP* applied. McAdam and Judd [30] have studied fouling behaviour in an immersed anoxic membrane bioreactor operated in dead-end mode. They described the effect of the filtration flux and duration on irreversible fouling in terms of a critical deposited mass

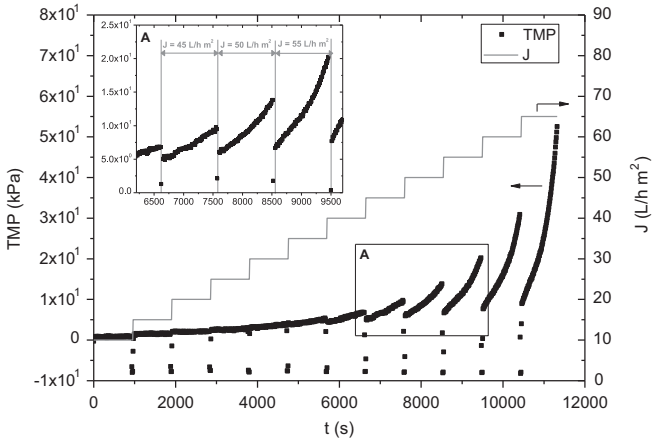

Fig. 2. Flux and *TMP* profiles during flux step trials; backwash with air scouring; $t_B=30$ s; $J_B=60$ L/h m^2; $t_F=900$ s.

that induced coagulation of the deposited cake layer. In accordance with previous studies [42], they identified the critical value at the transition between an initial low *TMP*-rise region and a second period of sharp *TMP*-rise. Therefore, once a consolidated deposit is formed it is reasonable to assume that its reversibility is related to physical cleaning conditions. Consistently with this, Jørgensen et al. [35] have reported that the critical flux for residual fouling depends on the cleaning time relative to the filtration time.

Analysing reversibility in the light of the critical flux concept, significant effects of backwashing duration and the application of air scouring during backwashing were found (Fig. 1). While tap water filtration (dotted line) shows a linear profile TMP_i vs flux, trials with microbial suspensions show a deviation from the straight-line at critical fluxes in the range of 10–45 L/h m^2, depending on backwash conditions. Without air injection during the backwash, the critical flux increased from 10 to 20 L/h m^2 while duration increased from 15 to 60 s, respectively. Higher critical values were found when air was applied (35–45 L/h m^2). Increasing backwash duration up to 60 s seems not to have a noticeable effect on the critical flux.

The higher critical fluxes observed with air scouring may be due to the lower mass deposited onto the membrane during the filtration steps. Backwash was expected to expand the deposit from the membrane and slightly disperse the expanded deposit into the bulk suspension [6]. By applying air scouring during the backwash, this dispersion process is significantly enhanced [43]. However during the flux steps without air scouring, the inefficient deposit re-dispersion induces an accumulation of mass in the convective zone near the membrane which rapidly collapses the membrane during the subsequent flux step. As a consequence, a consolidated deposit is formed. This process is expected to be more severe at high fluxes, which may explain the exponential relationship between TMP_i and filtration flux.

3.3. Fouling analysis during long-term trials.

3.3.1. Proposed fouling mechanisms based on TMP profiles

Process sustainability was investigated by assessing fouling deposition and reversibility at high filtration fluxes (35, 45 and 55 L/h m^2) with air-scouring aided backwash ($t_B=30$ s). For each flux, four backwash fluxes were tested (0, 20, 40 and 60 L/h m^2). Based on previous results [19], a moderate value of TMP_{sp} (30 kPa) was selected for these trials.

Fig. 3 shows an example of the typical *TMP* evolution during a long-term test ($J=35$ L/h m^2; $J_B=20$ L/h m^2). It can be seen that the fouling pattern (i.e. *TMP* profiles within a filtration cycle) changed with successive filtration/backwashing cycles. During the first cycles (typically corresponding to the first 25–50 h of operation, depending on experimental conditions), two phases are clearly identifiable in the *TMP* profile: an initial transient phase followed by a non-linear (concave) *TMP* rise. The initial fouling has been also observed in systems operated under high fouling load conditions with periodic filtration/backwashing cycles [43]. This behaviour has been related to a deposit recompression process in the external residual layer, which is expanded during the backwashing but not dispersed away from the convective zone of the membrane surface. Similar results have been reported by other authors on extending the filtration cycle length (i.e. increasing the amount of fouling) with fixed backwashing intervals [16,44]. Consistently, for an automatically initiated backwash, the amount of this fouling has been found to increase with the TMP_{sp} selected [19]. After the initial fouling phase, a nonlinear *TMP* rise was observed (Fig. 3), which can be described by the compressible layer buildup model [45]. In addition, this compressible layer seems to be mainly removed by the backwashing, since TMP_i did not increase considerably during the first cycles. Consequently

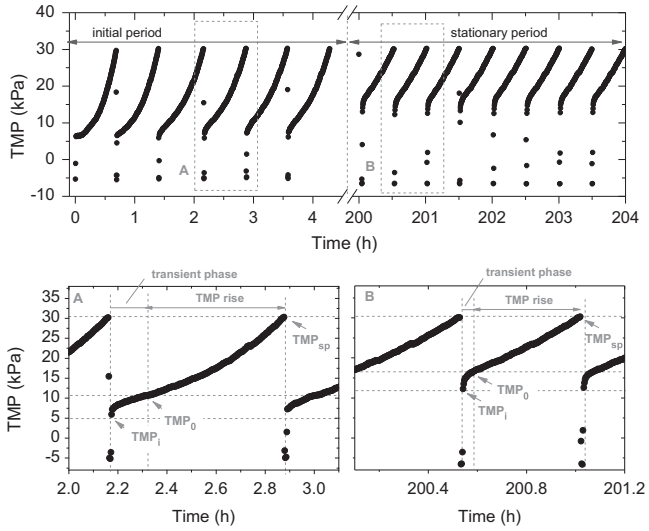

Fig. 3. Typical *TMP* profiles during initial and stationary period. J=35 L/h m^2, J_B=20 L/h m^2 and t_B=30 s.

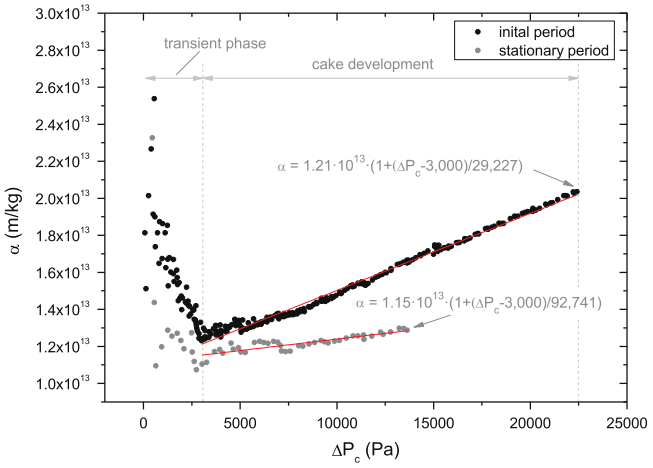

Fig. 4. Evolution of specific cake resistance with increasing pressure drop across the cake during a cycle. J=35 L/h m^2, J_B=20 L/h m^2 and t_B=30 s.

development, of a compressible cake layer on the membrane is assumed, made up mainly of large particles, which can be removed by backwashing [15,46]. Other fouling phenomena, such as solute adsorption and pore blocking, seem to have a negligible role. Due to the filtration without air scouring and the high fluxes applied, the cake formation rate is particularly enhanced and this layer might act as a secondary membrane that prevents SMP entering the membrane pores, in accordance with previous studies [47].

As previously mentioned, several changes were seen in the fouling pattern with successive filtration/backwashing cycles (Fig. 3). In the stationary period, a considerable increment in TMP_i was observed, which can be attributed to a cake consolidation process. Consolidation affects the cake properties by reducing porosity and water content, and thus reversibility is also affected [7]. Therefore, even though backwashing removed the cake layer during the initial cycles, the cake structure may have evolved to a more consolidated structure with subsequent cycles, increasing the residual fouling. Consolidation has often been observed during dead-end filtration of colloidal dispersions [42,48]. A theoretical explanation has been proposed considering a critical deposited mass that induces consolidation (i.e. residual fouling) [49]. Nevertheless, this approach does not explain the behaviour observed in the present study since the cake layer was initially completely reversible. The results suggest that cake consolidation is not only related to the deposited mass but also to the cake compressibility, which is known to be time- and *TMP*-dependent [30,36]. Probably, the differences on comparison with other studies are due to the compressibility of the cake layer formed, which is greater for activated flocs than for colloids. In fact, stabilisation of the TMP_i (i.e. consolidation) occurred when a slightly linear *TMP* rise was observed in the stationary period, which can be attributed to a lesser compressibility of the cake layer [50]. This approach can be confirmed by assessing the accuracy of the compressible cake layer model (Eq. (3)).

Fig. 4 shows the fit of α values obtained by Eq. (4) (assuming that ω is similar to suspended solid concentration in bulk suspension) to the linear expression (Eq. (7)) in both the initial and stationary periods. After the transient phase ($>$ 3000 Pa), data fitting gives an excellent correlation coefficient (R^2=0.99) for the initial period and a reasonable coefficient for the stationary period (R^2=0.77). Similar values of α_0 were found for both initial and stationary periods: 1.21×10^{13} and 1.15×10^{13} m/kg, respectively. These values are comparable with those typically found in the literature [34]. However, results indicate that the compressibility of the cake layer decreases as the operation time increases. A reason for this finding could be the higher local flux obtained in the stationary period due to the consolidation process. As layer compressibility is a time-dependent process and filtration time was considerably reduced in the stationary conditions (Fig. 3), it is reasonable to assume that the layer became less compressible. Similarly, Sioutopoulos and Karabelas [51] observed that the layer compressibility decreased with permeate flux, during the dead-end filtration of alginate-model solutions.

3.3.2. *Effect of operating parameters on stationary reversible fouling*

As also shown in Fig. 3, within each filtration cycle once the stationary period was achieved, a short transient phase (0.5–2.7 min) was generally followed by a *TMP* linear rise. In these conditions, an incompressible cake development mechanism can be assumed where reversible fouling rate r_f=d*TMP*/d*t*, ranging between 26.0 and 63.5 kPa/h, increased its value with filtration flux according to previous studies [15]. However, the fouling rates obtained in this study were far higher than those often found in full-scale MBRs operating with air scouring (0.6–6 kPa/h) [8]. This is to be expected, since aeration reduces the fouling rate by producing shear stress and lateral fiber movement [8]. However, in spite of the high fouling rate observed, the backwashing was able to remove it and, thus, a sustainable operation was attained. In fact, the mean filtration cycle length was significantly high: 21–53, 14–22 and 13–17 min for 35, 45 and 55 L/h m^2, respectively.

According to Eq. (4) and assuming α does not depend on *TMP* or *J* in the stationary period (i.e. incompressible cake model), α was determined under different backwashing conditions (Fig. 5). It should be noted that when relaxation was used, due to the high cleaning frequency and low filtration cycle length (0.67–1.99 min), the linear *TMP* rise phase is too short to be considered, and therefore α cannot be accurately determined. The results also showed that the rise in backwashing flux increased the specific resistance, which suggests that re-dispersion plays an important role in cake properties. Several authors have recorded a higher specific resistance as the suspension concentration drops and commented that this reflects more orderly tighter deposits [30,52].

3.3.3. *Effect of operating parameters on residual fouling*

As mentioned before, the TMP_i increased significantly in the first few cycles, reflecting considerable residual fouling. This internal fouling, which is not removed by backwashing, can be related to internal pore blocking [6] and a gel or compacted cake layer [24]. Although pore blocking is expected to be caused by colloids and macromolecules, some authors have pointed out that

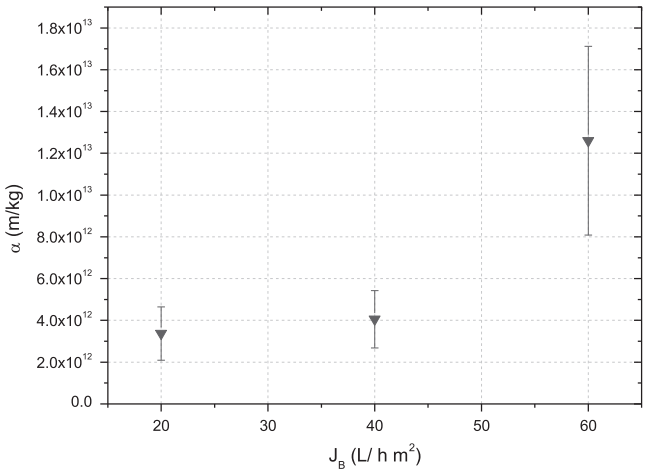

Fig. 5. Specific cake resistance, α, against backwashing flux at different filtration fluxes.

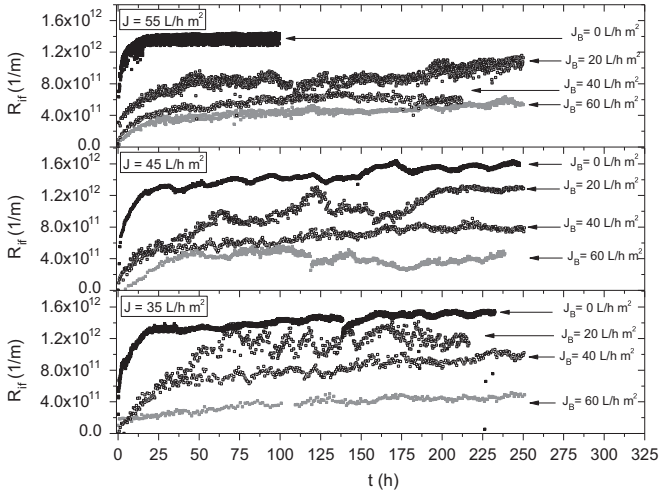

Fig. 6. R_{if} evolution at different filtration and backwashing fluxes.

cells adjacent to the membrane are exposed to a high compressive drag and will suffer great deformation [21,53]. As a consequence, these cells will be capable of blocking membrane pores. In this sense, it seems that consolidation of the cake layer and membrane pore blocking are inseparably linked, particularly in the initial period, under the tested conditions.

Fig. 6 shows the evolution of R_{if} under different operating conditions. Identical trends were observed for all filtration tests, where most of the fouling was detected in the first 25–50 h of operation followed by a slow rise. The observed variations may be related to significant changes in sludge filterability according to fluctuations in ambient conditions. It is obvious that relaxation was far less effective in preventing residual fouling than backwashing, which showed similar values. In fact, backwashing flux (J_B) decreased the residual fouling resistance, consistently with previous studies [14,15]. A roughly similar effect was observed at different filtration fluxes, where increasing J_B from 20 to 60 L/h m^2 resulted in a reduction in resistance of ~52%, ~62% and ~57%, for filtration fluxes of 55, 45 and 35 L/h m^2, respectively. Consequently, cleaning efficiency was mainly determined by backwashing flux, regardless of the imposed filtrate flux. This seems contrary to the results of previous studies where residual fouling increases with the filtrate flux applied [46]. This may be due to the system automatically adjusting the cleaning frequency to a preselected TMP_{sp}, which determines the degree of fouling allowed. As the cake-layer reversibility may be closely related to its characteristics (i.e. density and compressibility) [54], by operating under TMP_{sp} control mode, a stable backwashing efficiency can be achieved.

To summarise the effects of the operating parameters on residual fouling resistance, an overall correlation can be established. The best results were obtained with a non-linear regression of R_{if} to an empirical equation (Eq. (9)). In all cases, a reasonable accuracy of the parameters (average R^2 of 0.84 ± 0.09) was obtained. While the first term of the equation describes the sharp increase of residual fouling (i.e. initial period), the second considers the continuous R_{if} rise (i.e. stationary period).

$$R_{if} = (R_{if})_{asym}[1 - \exp(-k_c t)] + r_{if} t \quad (9)$$

where $(R_{if})_{asym}$ is the asymptotic R_{if} value during the initial period (considered after 50 h of operation), k_c is a kinetic constant and r_{if} is the residual fouling rate in the stationary period. Assuming that residual fouling gradually reduces the available membrane area, Eq. (9) suggests that the decay rate is proportional to the actual available area and to the kinetic constant, k_c. It should be noted that this decay rate is expected to be closely related to the cake consolidation rate after several filtration/cleaning cycles. Fig. 7A shows k_c against J_B at several applied J and different behaviour can be observed depending on the cleaning method used. The values for relaxation (J_B=0 L/h m^2) were significantly higher than those for backwashing, probably due to the severe fouling conditions imposed. However, the consolidation rate was not considerably affected by the filtration and backwashing fluxes under the tested conditions (k_c=0.083 ± 0.015 1/h) when backwashing was applied. $(R_{if})_{asym}$ represents the maximum available area that can be reduced by residual fouling for the given backwashing conditions. Therefore, this value is expected to depend on cleaning efficiency. Consistently, $(R_{if})_{asym}$ decreased linearly with J_B, regardless of the J imposed (Fig. 7B).

On reaching the stationary period, stable cleaning efficiencies were obtained which were not significantly affected by operating conditions (filtration and backwashing fluxes). In fact, a slight increase in the residual fouling rate (r_{if}) was noted, which ranged between 2.78×10^8 and 1.57×10^9 1/m h. These values are significantly lower than those typically found for full-scale MBRs [8].

3.4. Process productivity and specific aeration demand

Process productivity was assessed by determining the net permeate flux (J_{net}), calculated as an average during the last 50 h of the stationary period:

$$J_{net} = \frac{t_F \cdot J - t_B \cdot J_B}{t_B + t_F} \quad (10)$$

where t_B and t_F are the duration of the backwashing phase and the average duration of the filtration phase, respectively.

Fig. 8 shows J_{net} as a function of the assayed operating conditions. It is clear that relaxation (J_B=0 L/h m^2) yielded lower productivity than backwashing. This is due to the low efficiency in removing residual fouling, which resulted in a short filtration cycle length, as stated in previous sections. In contrast, backwashing obtained high productivities whose values mainly depended on the applied filtration flux. In fact, J_{net} was further improved by increasing the filtration flux (33.9 ± 0.2 L/h m^2, 42.6 ± 0.6 L/h m^2, 51.8 ± 1 L/h m^2 for 35, 45 and 55 L/h m^2, respectively). The long filtration cycles also explain the unimportant role of backwashing flux in the tested range of 20–60 L/h m^2.

Another important issue to be considered is the specific aeration demand linked to membrane cleaning (SAD_p). As previously mentioned, the system operated without air scouring and

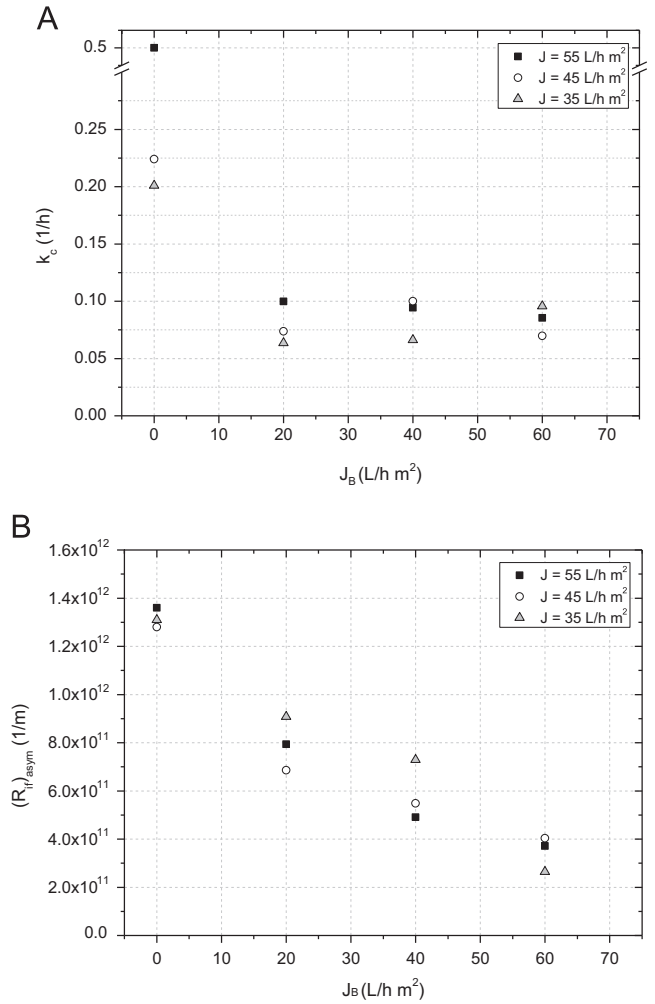

Fig. 7. Empirical parameters in Eq. (6) against backwashing flux at different filtration fluxes: (A) k_c and (B) $(R_{if})_{asym}$.

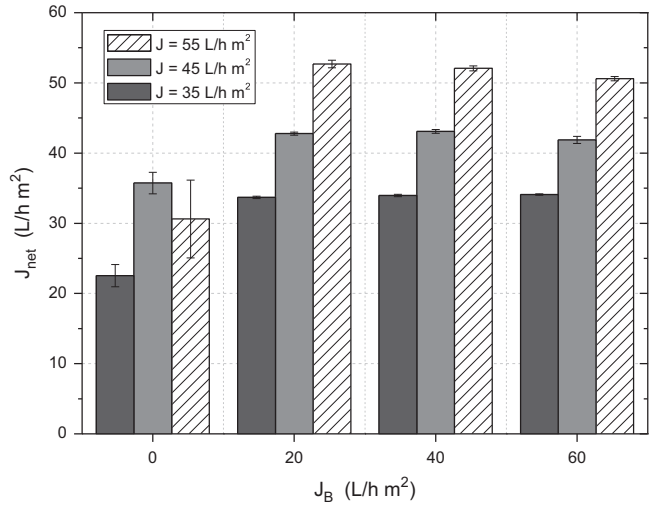

Fig. 8. J_{net} against backwashing flux at different filtration fluxes in the stationary period.

air is only supplied during the relaxation/backwashing. For relaxation, the high frequency of cleaning phases resulted in high values of SAD_p. For backwashing, SAD_p decreased with increasing J_B, achieving minimum values at 40 L/h m^2. In these conditions, SAD_p was significantly low (1–2 $Nm^3_{air}/m^3_{permeate}$) compared with those found in full-scale plants [12].

3.5. Analysis of the different fouling layers.

At the end of each filtration test, a simplified analysis of the fouling layers was carried out. The cleaning procedure separates the layers into two main fractions: cake (removed by physical means), and adsorbed material (removed by chemical means). As expected, physical methods (i.e. rinsing in tap water and subsequent application of strong backwashing at 90 L/h m^2 for 15 min) were enough to remove most of the total solids from the membrane (Table 3). Therefore, it is assumed that the reversible and consolidated cake obtained during the filtration tests can largely be removed by physical means. Assessing the cleaning efficiency in terms of resistance (Fig. 9), the cake fraction accounted for 85%, 62% and 47% of the global resistance for filtration fluxes of 35, 45 and 55 L/h m^2, respectively. Also, the filtration and backwashing conditions did not have a significant effect on the adsorbed resistance, since it was practically constant under the different conditions (from 2.26×10^{11} to 4.67×10^{11} 1/m). Consistently, these values are similar to R_{if} values obtained during the filtration tests when a backwashing flux of 60 L/h m^2 was used (Fig. 6). Therefore, results suggest that the absorbed

Table 3
Percentage of *SMP* and *TSS* reported in the membrane fouling layers at different filtration conditions.

Filtration flux (L/h m^2)	Backwashing flux (L/h m^2)	TSS (%)		SMP (%)
		Cake	Adsorbed	Cake
35	60	98	2	85
	40	96	4	76
	20	91	9	65
	0	94	6	63
45	60	98	2	68
	40	97	3	78
	20	93	7	67
	0	80	20	76
55	60	94	6	76
	40	77	23	77
	20	86	14	86
	0	84	16	86

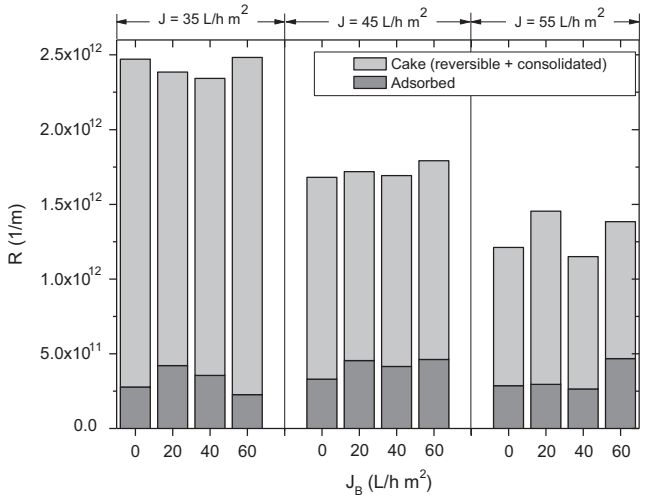

Fig. 9. Fouling resistances due to the different fouling layers under several filtration conditions.

fraction did not depend on the operating conditions and mainly comprised SMP, in accordance with previous studies [55]. However, the contribution of these foulants to the residual fouling was less, as also confirmed by the very low fouling rates observed in the stationary period (Fig. 6). In addition, it was expected that the cake layer might act as a secondary membrane, retaining SMPs. As can be observed in Table 3, the cake fraction contained much more SMP than the adsorbed fraction, consistently with other studies [56].

3.6. Optimisation of process parameters

It is generally accepted that the MBR implementation is limited by the high costs, both in capital and operating expenditure (CAPEX and OPEX). A key issue is the selection of the most appropriate filtration flux, which is determined by the classical trade-off problem: high fluxes are desirable to reduce membrane area requirement (i.e. CAPEX), however, membrane fouling increases with flux, which results in a higher energy demand and more frequent cleanings to control membrane fouling (i.e. increase OPEX).

The optimal conditions were assessed by simulating the effect of filtration and backwashing flux on specific energy demand (*SED*) (Fig. 10). These values are calculated through the equations proposed for reversible and residual fouling rates (Eqs. (4)–(9)), after 120 days of operation, which was assumed as a sustainable operative time (t_{op}) between maintenance/recovery chemical cleanings. For *SED* determination, it is only considered the equipment related to filtration process: a blower and a permeate pump. Energy consumption of the blower (W_G) and the permeate pump (W_J) was calculated by applying Eqs. (11) and (12), respectively [5]:

$$W_G = \frac{R \cdot T \cdot \lambda}{1.63 \cdot 10^5 \cdot \zeta_c \cdot (\lambda - 1)} \cdot \left[\left(\frac{P_{A2}}{P_{A1}} \right)^{1-\frac{1}{\lambda}} - 1 \right] \cdot Q_A \quad (11)$$

$$W_P = \frac{Q_p \cdot TMP}{1000 \cdot \zeta_p} \quad (12)$$

where R is gas constant, T is the air temperature, P_{A1} is the absolute inlet pressure, P_{A2} is the absolute outlet pressure, λ is the adiabatic index, Q_A is the air volumetric flow rate, Q_P is the permeate volumetric flow rate, ζ_p is the pump efficiency and ζ_c is the blower efficiency:

Then, *SED* can be defined as Eq. (13):

$$SED = \frac{W_J + W_G}{J_n \cdot A} \quad (13)$$

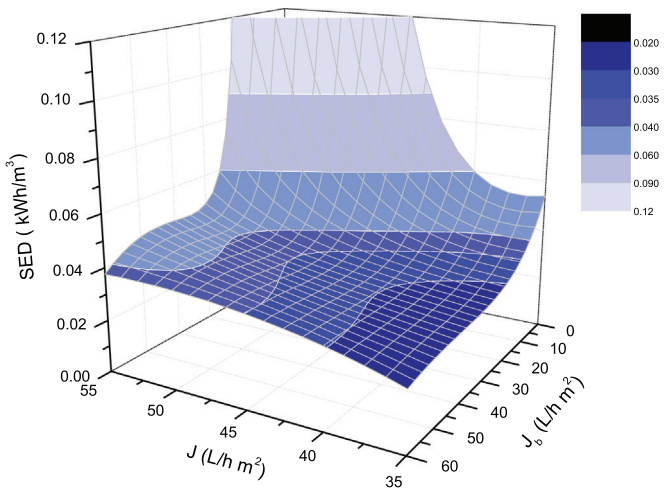

Fig. 10. Estimated specific energy demand associated with permeate suction/backwashing and module aeration (SED) against different filtration conditions.

where J_{net} is the net permeate flux and A is the membrane filtration area.

Simulation results indicated that low values of SED were achieved (0.02–0.03 kWh/m^3) when J was lower than 40–38.75 L/h m^2 and J_B was higher than 22.5–27.5 L/h m^2. For that reason it seems highly recommendable to operate at these conditions. Also, it should be noted the significant energy demand that arises from permeate pump (33–47% of total energy consumption), due to operation in dead-end filtration. When J increased above 40 L/h m^2, the significant increase of reversible fouling rate led to shorter filtration cycles and, thus, to more frequent backwashings, which both resulted in low J_{net} (Eq. (10)) and high W_G. On the other hand, it has been previously observed that backwashing flux affects the residual fouling (Section 3.3.3); this justifies the abrupt *SED* increase observed when decreasing J_B below 22.5 L/h m^2 at elevated J (0.06–0.12 kWh/m^3).

It should be noted that energy consumption depicted in Fig. 10 does not account power consumption arising from other devices including bioreactor aeration, recirculation pumps, and compressors for valve switching. This can contribute to another 0.2–0.3 kWh/m^3, according to full-scale studies [12].

Finally, another factor to be considered in order to optimize costs is the membrane area requirement. This area is inversely proportional to the net permeate flux. Hence, taken into account the operating conditions that minimize *SED* values to 0.02–0.03 kWh/m^3, a lower specific area demand (25.02 m^2 h/m^3) is obtained for the maximum J_{net} (39.97 L/h m^2, at J=40 L/h m^2 and J_B=27.5 L/h m^2). At optimum *SED* conditions, it is also observed that the specific area demand mainly depended on applied flux, while backwashing flux influence was irrelevant. Consistently, decreasing filtration flux from 40 to 35 L/h m^2 (~13%) at J_B=27.5 L/h m^2 resulted in an increase of ~14% in the specific area demand, while varying backwashing flux from 60 to 20 L/h m^2 at J=35 L/h m^2 lead to a less of 0.1% of variation in specific area demand.

4. Conclusions

- The tertiary membrane bioreactor demonstrated its capability to operate with complete sludge retention, achieving complete nitrification and high organic material removal (87% on average for COD) with moderate suspended solids concentration (MLSS=4–8 g/L). The complete retention of sludge also induced a maintenance level for the microorganisms, where the concentration of soluble microbial products (SMP) in the supernatant was minimised. Consistently, membrane fouling was mainly caused by suspended particles, with a medium size (d_{50}=63 ± 6 μm) and a relatively narrow distribution (distribution spreading index of 1.29 ± 0.13). As a result, the suspension showed an excellent filterability (TTF=8.9 ± 2.9 s).
- The *TMP* profiles during the flux-steps trials showed the important role of the compression process in cake fouling reversibility. Assessing this reversibility in terms of the critical flux, it was also found to be significantly affected by backwashing conditions (duration and application of air scouring).
- For the long-term tests, *TMP* profile can be described well by a compressible cake build-up model, where the compressibility decreased with successive filtration cycles until a stationary period was reached. During the initial period, a gradual residual fouling increase was also observed which can be attributed to cake consolidation and/or a pore-blocking mechanism.
- Evolution of residual fouling resistance was modelled by a non-linear expression, assuming that fouling gradually reduces the available membrane area. Based on this approach, the fouling resistance after the initial period decreased with the

backwashing flux applied. Consistently, the relaxation was far less effective in preventing residual fouling than backwashing. In the stationary period, similar cleaning efficiency was obtained, which was not significantly affected by the operating conditions (filtration and backwashing fluxes).

- An analysis of the relative contribution of the fouling layers to the global fouling revealed that the cake fraction (mainly formed by suspended solids) accounted for 85–47%, decreasing with the filtration flux imposed. In contrast, resistance of the adsorbed fraction remained constant and low under the tested conditions.
- Simulation results indicated that the best conditions can be established at a filtration flux of 40 L/h m^2 and a backwashing flux of 27.5 L/h m^2, due to high net permeate flux and low specific energy demand.

Acknowledgements

The control system, funded by the N.R.C. (MINECO project CTM2011-27307), was tested for long-term validation during the MBR operation described in this paper. The authors wish to express their gratitude to GE Water & Process Technologies and to BALTEN for their support, and also to the staff of the Water Analysis Laboratory of the Chemical Engineering Department at Universidad de La Laguna (ULL) for their analytical advice. In addition, we greatly appreciate access to the multi-parameter universal controller permitted by the CONVAGUA project of the Canary Agency-ACIISI, sponsored by the European Commission and the Canary Islands Regional Government. Finally, the authors thank the financial support of Canary Agency for Research, Innovation and Information Society, co-financed at 85% by European Social Fund (ESF), to ULL.

Nomenclature

$(J')_t$	local filtrate flux, L/h m^2
COD	chemical oxygen demand, mg/L
d_{50}	median particle size, μm
DOC	dissolved organic carbon, mg/L
F/M	food to microorganisms ratio, kg COD/kg MLSS d
HRT	hydraulic retention time, h
J	filtrate flux, L/h m^2
J_B	backwashing flux, L/h m^2
J_{net}	net permeate flux, L/h m^2
k_c	residual fouling kinetic constant, 1/h
MBR	membrane bioreactor
MLSS	mixed liquor total suspended solids, mg/L
MLVSS	mixed liquor volatile suspended solids, mg/L
$N-NH_3$	ammonium – nitrogen, mg/L
$N-NO_2^-$	nitrite – nitrogen, mg/L
$N-NO_3^-$	nitrate – nitrogen, mg/L
P_a	characteristic pressure related to the compression effect, kPa
P_{A1}	absolute inlet pressure in the blower, Pa
P_{A2}	absolute outlet pressure in the blower, Pa
PLC	programmable logic control
PSD	particle size distribution
PVDF	polyvinylidene fluoride
Q_A	air volumetric flow rate, Nm^3/h
Q_P	permeate volumetric flow rate, m^3/s
R	gas constant, J/mol K
R_{asym}	asymptotic internal residual fouling resistance in the initial period, 1/m
r_f	reversible fouling rate, kPa/h
R_{if}	internal residual fouling resistance, 1/m
r_{if}	residual fouling rate, 1/m h
R_m	clean membrane resistance, 1/m
SAD_p	specific net aeration demand with respect to permeate volume, Nm^3/m^3
SED	specific energy demand, kWh/m^3
SMP	soluble microbial products
$SOUR_e$	specific endogenous oxygen uptake rate, mg O_2/g MLVSS h
T	air temperature, K
t_B	backwashing phase duration, s
t_F	filtration phase duration, min
TMP	transmembrane pressure, kPa
TMP_0	transmembrane pressure associated with the beginning of the non-linear *TMP* rise phase, kPa
TMP_i	transmembrane pressure after backwashing, kPa
TMP_{sp}	transmembrane pressure set-point, kPa
t_{op}	estimated operation time, d
TSS	total suspended solids, mg/L
TTF	time-to-filter, s
W_G	energy consumption of the blower, W
W_J	energy consumption of the permeate pump, W
WWTP	wastewater treatment plant

Greek letters

α	specific deposit resistance, m/kg
α_0	specific deposit resistance at zero pressure, m/kg
ΔTMP_c	differential of transmembrane pressure across the cake, kPa
ζ_c	blower efficiency
ζ_p	pump efficiency
λ	adiabatic index
μ	permeate viscosity, Pa s
ω	solid concentration in the cake per unit filtrate volume, kg/m^3

References

[1] T. Wintgens, T. Melin, A. Schäfer, S. Khan, M. Muston, D. Bixio, C. Thoeye., The role of membrane processes in municipal wastewater reclamation and reuse, Desalination 178 (2005) 1–11.
[2] K.N. Bourgeous, J.L. Darby, G. Tchobanoglous, Ultrafiltration of wastewater: effects of particles, mode of operation, and backwash effectiveness, Water Res. 35 (2001) 77–90.
[3] L. Vera, E. González, O. Díaz, S. Delgado, Performance of a tertiary submerged membrane bioreactor operated at supra-critical fluxes, J. Membr. Sci. 457 (2014) 1–8.
[4] Koch Membrane, Case Study. Aquapolo Ambiental Water Reuse Project, 2014. ⟨http://www.kochmembrane.com/PDFs/Case-Studies/KMS-Sao-Paulo-Brazil-Case-Study.aspx⟩.
[5] S. Judd, The MBR Book, Principles and Applications of Membrane Bioreactors for Water and Wastewater Treatment, 2nd edition, Elsevier, 2010.
[6] P. Le-Clech, V. Chen, A.G. Fane, Fouling in membrane bioreactors used in wastewater treatment, J. Membr. Sci. 284 (2006) 17–53.
[7] H. Lin, M. Zhang, F. Wang, F. Meng, B. Liao, H. Hong, J. Chen, W. Gao, A critical review of extracellular polymeric substances (EPSs) in membrane bioreactors: characteristics, roles in membrane fouling and control strategies, J. Membr. Sci. 460 (2014) 110–125.
[8] A. Drews, Membrane fouling in membrane bioreactors—characterisation, contradictions, causes and cures, J. Membr. Sci. 363 (2010) 1–28.
[9] P. Bacchin, P. Aimar, R.W. Field, Critical and sustainable fluxes: theory, experiments and applications, J. Membr. Sci. 281 (2006) 42–69.
[10] Y. Wibisono, E.R. Cornelissen, A.J.B. Kemperman, W.G.J. van de Meer, K. Nijmeijer, Two-phase flow in membrane processes: a technology with a future, J. Membr. Sci. 463 (2014) 566–602.

[11] G. Ferrero, I. Rodriguez-Roda, J. Comas, Automatic control systems for submerged membrane bioreactors: a state-of-the-art review, Water Res. 46 (2012) 1–13.
[12] P. Krzeminski, J.H.J.M. van der Graaf, J.B. van Lier, Specific energy consumption of membrane bioreactor (MBR) for sewage treatment, Water Sci. Technol. 65 (2012) 380–392.
[13] J. Cumin, H. Behmann, Y. Hong, R. Bayly, 2011. Gas sparger for an immersed membrane, U.S. Patent US/2011/0049047.
[14] Z. Wang, J. Ma, C.Y. Tang, K. Kimura, Q. Wang, Membrane cleaning in membrane bioreactors: a review, J. Membr. Sci. 468 (2014) 276–307.
[15] T. Zsirai, P. Buzatu, P. Aerts, S. Judd, Efficacy of relaxation, backflushing, chemical cleaning and clogging removal for an immersed hollow fibre membrane bioreactor, Water Res. 46 (2012) 4499–4507.
[16] P. Schoeberl, M. Brik, M. Bertoni, R. Braun, W. Fuchs, Optimization of operational parameters for a submerged membrane bioreactor treating dye-house wastewater, Sep. Purif. Technol. 44 (2005) 61–68.
[17] H. Itokawa, C. Thieming, J. Pinnekamp, Design and operating experiences of municipal MBRs in Europe, Water Sci. Technol. 58 (2008) 2319–2327.
[18] R. Villarroel, S. Delgado, E. González, M. Morales, Physical cleaning initiation controlled by transmembrane pressure set-point in a submerged membrane bioreactor, Sep. Purif. Technol. 104 (2013) 55–63.
[19] L. Vera, E. González, O. Díaz, S. Delgado, Application of backwashing strategy based on transmembrane pressure set-point in a tertiary submerged membrane bioreactor, J. Membr. Sci 470 (2014) 504–512.
[20] T. Asano, F.L. Burton, H.L. Leverenz, R. Tsuchihashi, G. Tchobanoglous, Water Reuse, Issues, Technologies, and applications, 1st edition, Metcalf & Eddy, 2007.
[21] G. Foley, A review of factors affecting filter cake properties in dead-end microfiltration of microbial suspensions, J. Membr. Sci. 274 (2006) 38–46.
[22] H. Hong, M. Zhang, Y. He, J. Chen, H. Lin, Fouling mechanisms of gel layer in a submerged membrane bioreactor, Bioresour. Technol. 166 (2014) 295–302.
[23] V.T. Kuberkar, R.H. Davis, Modeling of fouling reduction by secondary membranes, J. Membr. Sci. 168 (2000) 243–258.
[24] S. Liang, T. Zhao, J. Zhang, F. Sun, C. Liu, L. Song, Determination of fouling-related critical flux in self-forming dynamic membrane bioreactors: interference of membrane compressibility, J. Membr. Sci. 390 – 391 (2012) 113–120.
[25] H. Ng, S. Hermanowicz, Membrane bioreactor operation at short solids retention times: performance and biomass characteristics, Water Res. 39 (2005) 981–992.
[26] P. Le-Clech, B. Jefferson, I. Chang, S. Judd, Critical flux determination by the flux-step method in a submerged membrane bioreactor, J. Membr. Sci. 227 (2003) 83–91.
[27] P. Van der Marel, A. Zwijnenburg, A. Kemperman, M. Wessling, H. Temmink, W. van der Meer, An improved flux-step method to determine the critical flux and the critical flux for irreversibility in a membrane bioreactor, J. Membr. Sci. 332 (2009) 24–29.
[28] G. Guglielmi, D. Chiarani, S.J. Judd, G. Andreottola, Flux criticality and sustainability in a hollow fibre submerged membrane bioreactor for municipal wastewater treatment, J. Membr. Sci. 289 (2007) 241–248.
[29] American Public Health Association, 2005.Water Environment Federation, Standard Methods for the examination of Water and Wastewater, 21st edition, Washington DC, USA.
[30] E.J. McAdam, S.J. Judd, Optimization of dead-end filtration conditions for an immersed anoxic membrane bioreactor, J. Membr. Sci. 325 (2008) 940–946.
[31] B.L. Sørensen, P.B. Sørensen, Structure compression in cake filtration, J. Environ. Eng. 123 (1997) 345–353.
[32] A. Rushton, A. S. Ward, and R. G. Holdich, Solid-Liquid Filtration and Separation Technology. VCH: Weinheim, Germany. (1996). 538 pp. ISBN 3-527-28613-6.
[33] A.A. McCarthy, P. Gilboy, P.K. Walsh, G. Foley, Characterisation of cake compressibility in dead-end microfiltration of microbial suspensions, Chem. Eng. Commun. 173 (1999) 79–90.
[34] T.V. Bugge, M.K. Jørgensen, M.L. Christensen, K. Keiding, Modeling cake buildup under TMP-step filtration in a membrane bioreactor: cake compressibility is significant, Water Res. 46 (2012) 4330–4338.
[35] M.K. Jørgensen, K. Keiding, M.L. Christensen, On the reversibility of cake buildup and compression in a membrane bioreactor, J. Membr. Sci. 455 (2014) 152–161.
[36] M.K. Jørgensen, T.V. Bugge, M.L. Christensen, K. Keiding, Modeling approach to determine cake buildup and compression in a high-shear membrane bioreactor, J. Membr. Sci. 409–410 (2012) 335–345.
[37] S. Pirt, The maintenance energy of bacteria in growing cultures, Proc. R. Soc. Lond. 163B (1965) 224–231.
[38] A. Pollice, G. Laera, M. Blonda, Biomass groth and activity in a membrane bioreactor with complete sludge retention, Water Res. 38 (2004) 1799–1808.
[39] G.H. Kristensen, P.E. JØrgensen, M. Henze, Characterization of functional microorganism groups and substrate in activated sludge and wastewater by AUR, NUR and OUR, Water Sci. Technol. 25 (1992) 43–57.
[40] S. Lyko, T. Wintgens, D. Al-Halbouni, S. Baumgarten, D. Tacke, K. Drensla, A. Janot, W. Dott, J. Pinnekamp, T. Melin, Long-term monitoring of a full-scale municipal membrane bioreactor—characterisation of foulants and operational performance, J. Membr. Sci. 317 (2008) 78–87.
[41] X. Su, Y. Tian, H. Li, C. Wang, New insights into membrane fouling based on characterization of cake sludge and bulk sludge: an especial attention to sludge aggregation, Bioresour. Technol. 128 (2013) 586–592.
[42] Y. Bessiere, N. Abidine, P. Bacchin, Low fouling conditions in dead-end filtration: evidence for a critical filtered volume and interpretation using critical osmotic pressure, J. Membr. Sci. 264 (2005) 37–47.
[43] Y. Ye, V. Chen, P. Le-Clech, Evolution of fouling deposition and removal on hollow fibre membrane during filtration with periodical backwash, Desalination 283 (2011) 198–205.
[44] P. Gui, X. Huang, Y. Chen, Y. Qian, Effect of operational parameters on sludge accumulation on membrane surfaces in a submerged membrane bioreactor, Desalination 151 (2003) 185–194.
[45] J. Kim, F.A. DiGiano, Fouling models for low-pressure membrane systems, Sep. Purif. Technol. 68 (2009) 293–304.
[46] J. Wu, P. Le-Clech, R.M. Stuetz, A.G. Fane, V. Chen, Effects of relaxation and backwashing conditions on fouling in membrane bioreactor, J. Membr. Sci. 324 (2008) 26–32.
[47] V.T. Kuberkar, R.H. Davis, Modeling of fouling reduction by secondary membranes, J. Membr. Sci. 168 (2000) 243–258.
[48] A.S. Jönsson, B. Jönsson, Ultrafiltration of colloidal dispersion—a theoretical model for the concentration polarization phenomena, J. Colloid Interface Sci. 180 (1996) 504–518.
[49] P. Harmant, P. Aimar, Coagulation of colloids in a boundary layer during cross-flow filtration, Colloids Surfaces A: Physicochem. Eng. Asp. 138 (1998) 217–230.
[50] S. Delgado, F. Díaz, L. Vera, R. Díaz, S. Elmaleh, Modelling hollow-fibre ultrafiltration of biologically treated wastewater with and without gas sparging, J. Membr. Sci. 228 (2004) 55–63.
[51] D.C. Sioutopoulos, A.J. Karabelas, The effect of permeation flux on the specific resistance of polysaccharide fouling layers developing during dead-end ultrafiltration, J. Membr. Sci. 473 (2015) 292–301.
[52] D.Y. Kwon, S. Vigneswaran, A.G. Fane, R. Ben Aim, Experimental determination of critical flux in cross-flow microfiltration, Sep. Purif. Technol. 19 (2000) 169–181.
[53] M. Meireles, C. Molle, M.J. Clifton, O. Aimar, The origin of high hydraulic resistance for filter cakes of deformable particles: cell-bed deformation or surface-layer effect? Chem. Eng. Sci. 59 (2004) 5819–5829.
[54] D. Jeison, J.B. van Lier, Cake formation and consolidation: main factors governing the applicable flux in anaerobic submerged membrane bioreactors (AnSMBR) treating acidified wastewaters, Sep. Purif. Technol. 56 (2007) 71–78.
[55] J. Wu, C. He, Y. Zhang, Modeling membrane fouling in a submerged membrane bioreactor by considering the role of solid, colloidal and soluble components, J. Membr. Sci. 397 – 398 (2012) 102–111.
[56] J. Wu, C. He, D. Bi, J. Yi, Y. Zhang, A bio-cake model for the soluble COD removal by the back-transport, adsorption and biodegradation processes in the submerged membrane bioreactor, Desalination 322 (2013) 1–12.